A COMPREHENSIVE CONCEPTUAL STUDY FOR ECONOMIC DEVELOPMENT OF THE OIL FIELDS IN KAILASHTILA AND HARIPUR

Mohammad Amirul Islam
Registration No: 169
Session: 2012-2013

Ph.D. THESIS
DEPARTMENT OF GEOLOGY
UNIVERSITY OF DHAKA
2021

A COMPREHENSIVE CONCEPTUAL STUDY FOR ECONOMIC DEVELOPMENT OF THE OIL FIELDS IN KAILASHTILA AND HARIPUR

A thesis submitted for the degree of
DOCTOR OF PHILOSOPHY
in the Department of
GEOLOGY
UNIVERSITY OF DHAKA

By
MOHAMMAD AMIRUL ISLAM
B.Sc. Engg. (Chemical), M.Sc. Engg. (Petroleum)
February 2021

Dedicated to

My

Father Late Md. Rafiqul Islam

And

Mother Mrs. Majeda Islam

CERTIFICATE

Certified that the thesis entitled "A COMPREHENSIVE CONCEPTUAL STUDY FOR ECONOMIC DEVELOPMENT OF THE OIL FIELDS IN KAILASHTILA AND HARIPUR" submitted by Mr. MOHAMMAD AMIRUL ISLAM in fulfillment of the requirements for the award of the Degree of DOCTOR OF PHILOSOPHY in GEOLOGY of the Faculty of Earth and Environmental Sciences, UNIVERSITY OF DHAKA is an original research work. No part of the thesis has been reproduced anywhere for any other degree or diploma.

Supervisor:

Dr. A S M Woobaidullah
Professor
DEPARTMENT OF GEOLOGY
UNIVERSITY OF DHAKA

Co- Supervisor:

Dr. Badrul Imam
Professor
DEPARTMENT OF GEOLOGY
UNIVERSITY OF DHAKA

DECLARATION

I hereby declare that this thesis entitled "A COMPREHENSIVE CONCEPTUAL STUDY FOR ECONOMIC DEVELOPMENT OF THE OIL FIELDS IN KAILASHTILA AND HARIPUR" has been composed by myself and all the works presented herein are my own. I further declare that this work has not been submitted anywhere for any academic degree.

February 2021

MOHAMMAD AMIRUL ISLAM
B.Sc. Engg. (Chemical), M.Sc. Engg.(Petroleum)
Registration No: 169
Session: 2012-2013

Acknowledgements

First and foremost, I would like to express my deepest gratitude to my supervisor professor Dr. A S M Woobaidullah and co-supervisor professor Dr. Badrul Imam, for their support, advice, inspiration, encouragement, patience, and warm hearts during my PhD studies. It has been very beneficial and enjoyable for me to study under their supervision. There is absolutely no doubt in my mind that without their support and constant motivation, this journey would have been an extremely difficult one for me.

MOHAMMAD AMIRUL ISLAM

Abstract

Bangladesh occupies major part of the Ganges delta Basin and has been known as a natural gas rich province. However, occurrences of oil have been known in two small oil fields, Haripur and Kailashtila. While Haripur, discovered in 1986 was on production for six years, Kailashtila, discovered in 1988, was never put under commercial production. Energy experts recommend that development of the two discovered oil fields should be carried out. This process requires preparation of oil reservoir development plans, procurement of equipment and development of skilled manpower. Oil production data and record of six years of operation in Haripur oil field and oil flowing record during drill stem test operation in Kailashtila field have testified the production capabilities of the oil reservoirs in the fields.

The present study suggests that the oil development works in these fields are terminated not because of depletion of reserves but because of not following the right procedures of the oil field development. In this study an effort has been made to prepare oil reservoir development plans on the two prospective oil fields. Comprehensive study on every aspects of oil reservoir such as seismic section, well logs, well test, core analysis, fluid analysis, fluid contacts leads to preparation of technically feasible and economically viable oil reservoir development plan.

Oil reservoir development plan includes reservoir simulation models with defined oil recovery mechanism, optimum number of oil production wells, optimum number of water injection wells and mutual positions of wells in reservoir. Finite difference reservoir simulation model (conventional reservoir simulation model) and streamline reservoir simulation model are developed from seismic section, well logs, core analysis, fluid analysis, well test, drill stem test, fluid contact and production history. Oil recovery mechanism is optimized from analysis of reservoir pressure, rock properties, fluids properties and core flood test. Streamline simulation study is performed to optimize number of oil production wells, number of water injection wells and mutual positions of wells in the reservoir. Oil production rate, well head pressure, water injection rate, water injection pressure and production period are also defined in oil reservoir development plan. Finite difference reservoir simulation study is performed to optimize oil production rate, well head pressure, water injection rate, water injection pressure and production period.

Finite difference reservoir simulation model and streamline reservoir simulation model have been constructed on oil reservoir in Haripur field. Then the oil reservoir models are validated by history matching with six years oil production data available. The reservoir has been screened to design enhanced oil recovery technique. Low salinity water (salinity 1000 ppm of NaCl) injection method has been recommended for oil reservoir to recover remaining oil. On the basis of oil recovery technique reservoir development variables have been optimized to generate reservoir development scenario. The oil reservoir has been proposed to develop with six water injection wells and two oil production wells. Streamline simulation has been run on the reservoir development scenario and observed the performance of the reservoir such as hydraulic conductivity, oil flow rate, oil flow direction, water flow rate, time of flight, water break through, water channeling and sweeping efficiency.

The Haripur oil reservoir has shown good performance under the development scenario. The reservoir model with the optimum development scenario has been considered as reservoir development plan. The optimum reservoir development plan has been simulated by finite difference reservoir simulator for duration of twenty years for economic analysis of the development plan.

Haripur oil field initially had 33 million barrels of oil and produced 0.53 million barrels of oil. Experts have predicted that there is remaining oil in the reservoir which is approximately 32.47 million barrels of oil. Six injection wells are used for water injection. Water injection pressure is 1000 psi. Well water injection rate is 300 stb/day and field water injection rate is 1800 stb/day. Two oil production wells are used for oil production. Well oil production rate is 400 stb/day and field oil production rate is 800 stb/day. Well head pressure of oil production well is 500 psi. Total oil recovery is about 5.844 million barrels within twenty years from Haripur field. Break even oil production is 2.044 million barrels of oil.

Conventional and streamline reservoir simulation models of oil reservoir in Kailashtila field have been constructed by using seismic survey, well logs, core analysis, fluid analysis, fluid contact data and drill stem test data. Reservoir simulation models have been validated by oil production data from drill stem test operation. As the oil reservoir has significant pressure to lift oil to the surface as detected from drill stem test, natural depletion mechanism has been proposed to recover oil from reservoir. A single oil production well has been placed at the center of the oil reservoir in Kailashtila field for oil reservoir development. Streamline simulation has been run on the reservoir development scenario and observed the performance of the reservoir such as hydraulic conductivity and oil flow rate. The Kailashtila oil reservoir has shown good performance under the development scenario. The Kailashtila oil reservoir model with the optimum development scenario has been considered as optimum reservoir development plan.

Twenty years oil production has been forecasted from the oil reservoir development plan by simulating the finite difference reservoir simulation model of Kailashtila oil reservoir. Experts have predicted that Kailashtila oil field initially has 94.33 million barrels of oil. A single oil production well is used for oil production. Well oil production rate is 817 stb/day. Well head pressure of oil production well is 500 psi. Total oil recovery is 5.973 million barrels from Kailashtila field. Break even oil production is 0.584 million barrels. The oil reservoir in Kailashtila field is able to produce 0.129 million barrels of additional oil than Haripur oil reservoir because Kailashtila oil reservoir contains lighter oil (42 ^{o}API) and Haripur oil reservoir contains heavier oil (28.5 ^{o}API).

In this study maximum effort has been done concentrated in seismic and well logs interpretation as well as laboratory test to minimize data uncertainty for preparing reliable oil reservoir development plans on Haripur and Kailashtila fields.

CONTENTS

Page

Page

Page

List of Figures

List of Tables

Abbreviation

API	American Petroleum Institute
DST	Drill Stem Test
EOR	Enhanced Oil Recovery
IOR	Improved Oil Recovery
LSW	Low Salinity Water
NPV	Net Present Value
PVI	Pore Volume Injected
PVT	Pressure Volume Temperature
STB	Stock Tank Barrel
USD	United State Dollar
WAG	Water Alternating Gas
STB/D	Stock Tank Barrel per Day
stb/d	Stock Tank Barrel per Day
stb/day	Stock Tank Barrel per Day
sm^3	Standard Meter Cube

Chapter 1

Introduction

1.1 Problem Statement and Importance of Research

Bangladesh has significant reserve of natural gas which meets major parts of its primary energy need. Although natural gas and oil occur in the same kind of environments in deltaic basin, Bangladesh delta basin so far has relatively small amount of oil discovered. This has led to a total dependence of the country on import of foreign oil. Therefore the need and search for more oil from local source has been an issue of the national oil exploration company. So far two small oil fields, Haripur and Kailashtila are discovered in the north eastern part of the country.

A good number of researches have been conducted on gas fields by the academic and industrial professionals. But there has been no or little wok or research on the oil reservoirs found in Bangladesh. Haripur oil field produced oil for six years after which production was suspended, while Kailashtila oil field was not put under commercial production at all.

There has been no or little work or research as to the reason of premature suspension of the Haripur oil field production or the reason for not bringing the Kailashtila oil field under production. The present research attempts to look into the oil reservoirs in these two fields from a petroleum engineering point of view and tries to find out the prospect of these fields and their production capabilities.

1.2 Study Area

The Haripur oil field and the Kailashtila oil field are located about 230 km North-East of Dhaka and 18 km from Sylhet town, and lies in the Surma basin (also known as Sylhet trough), a locally depressed HC rich basin in the northeast part of the greater Bengal Basin between the Shillong Plateau in the North and the Tripura High in the South. The location map of the Haripur field is shown in figure 1.1. Geologically the Tripura High corresponds to a folded system of Tertiary formations that plunge southward underneath the recent alluvium of the Surma river.

Geologically the oil field is housed in the NE-SW trending Sylhet anticline which is part of the Tertiary folded system covering the eastern part of the Bengal Basin. The oil is found in sandstone reservoir belonging to the Miocene Surma Group at depth of 2020- 2033 meter below the surface (Imam, 2013).

The Sylhet structure was delineated by Pakistan Petroleum Limited (PPL) through single fold seismic survey. Gas was discovered in 1955 by drilling the Sylhet-1 well which was the first gas discovery well in Bangladesh.

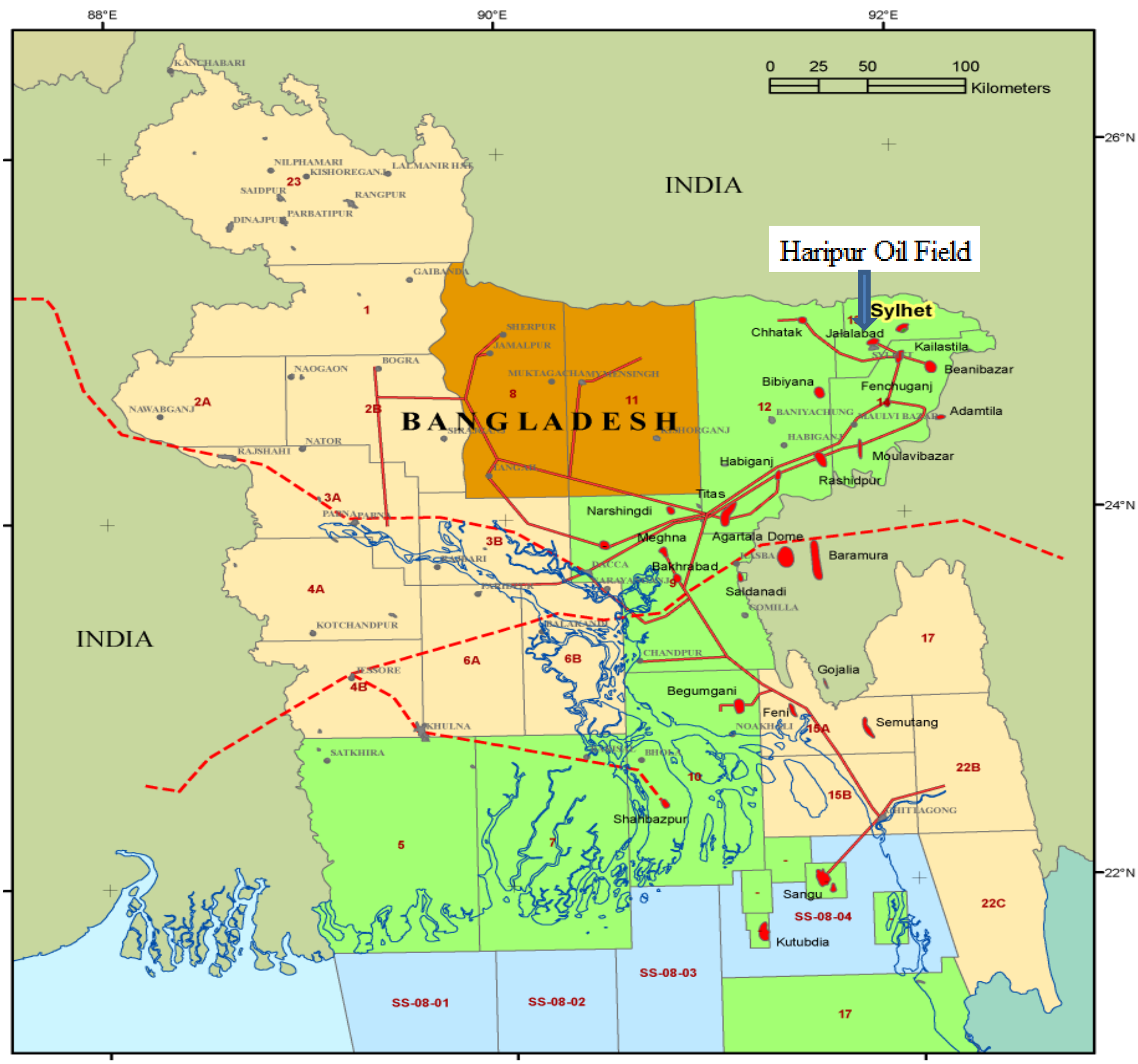

Figure 1.1: Location of Haripur oil field

Subsequently five more wells (Sylhet-2 to Sylhet-6) were drilled from 1956 to 1964. Sylhet-6 was drilled in 1964 to a depth of 1,405 m and completed as a dual producer. Sylhet-7 was drilled in 1986 as a gas development well but turned out to be the first oil discovery well. Surma-1 and the sidetracked well Surma-1A were drilled in 1989 to appraise the oil discovery.

The Kailashtila field is located 13 km south of Sylhet field and it is about 250 km north east of Dhaka. The Kailashtila field lies in the central part of the Surma Basin and on the western margin of the Tripura high. The location map of the Kailashtila field is shown in figure1.2.

Figure 1.2: Location of Kailashtilla oil field

The Kailashtila structure was delineated by Shell in 1960 on the basis of single fold analog seismic data acquired in late 1950’s. The structure is a four way dip closure. The KTL-1 was drilled in 1961 to a depth of 4138 m and encountered four gas sands. Subsequently five more wells, KTL-2 to KTL-6 were drilled since then. The upper and lower gas sands were tested in KTL-1 and KTL-6. Recently KTL-7 has been drilled to the depth of 3535 m and oil has been detected from depth 3260 m to 3270 m.

1.3 Previous Research Work

There have been some geological study on the Haripur field in previous years. Geological structure is shown in figure 1.3. The upper Bokabil (BB3) mostly represented by bluish grey thinly laminated shale, moderately hard and compacted (Hoque, 2009). Shales are interbedded occasionally with carbonaceous, micaceous, very fine grained, siltstone and sandstone (Hossain et al., 2008). Shales are firm, sticky, bluish grey clay, which is very silty and calcareous (Narender, 2004). The upper marine shale is an important marker horizon recognizable throughout this part of the Surma basin. This claystone unit is found in fairly uniform thickness and represents the final marine transgression of the Surma basin during the late Miocene (Shofiqul et al., 2015).

The middle Bokabil (BB2) is mostly represented by alternate beds of sandstone and shale. The sandstones are light bluish grey and white in color, medium to very fine grained and dark colored minerals are abundant (Chandra et al., 2010). The sandstones are generally non-calcareous. They are also micaceous and limonitic at depth.

The lower Bokabil (BB1) is mostly represented by bluish grey to dark grey colored shale, hard compact and occasionally intercalated with some sandstone and siltstone beds. The sandstones are light grey to grey in color, angular to sub angular, medium to fine grained, moderately sorted, argillaceous and occasionally very calcareous (Shamsuddin and Khan, 1991).

Bhuban formation (Middle Miocene): Since no wells of the Sylhet structure penetrated the Lower Bhuban, the thickness of this formation cannot be ascertained. This zone mainly consists of very fine to medium grained, well sorted, sub angular to sub rounded, calcareous sandstone. Interbedded grey shales are common with laminations of siltstone (Bubul et al., 2017). The palaeo-environment seems to be of persistent marine influence.

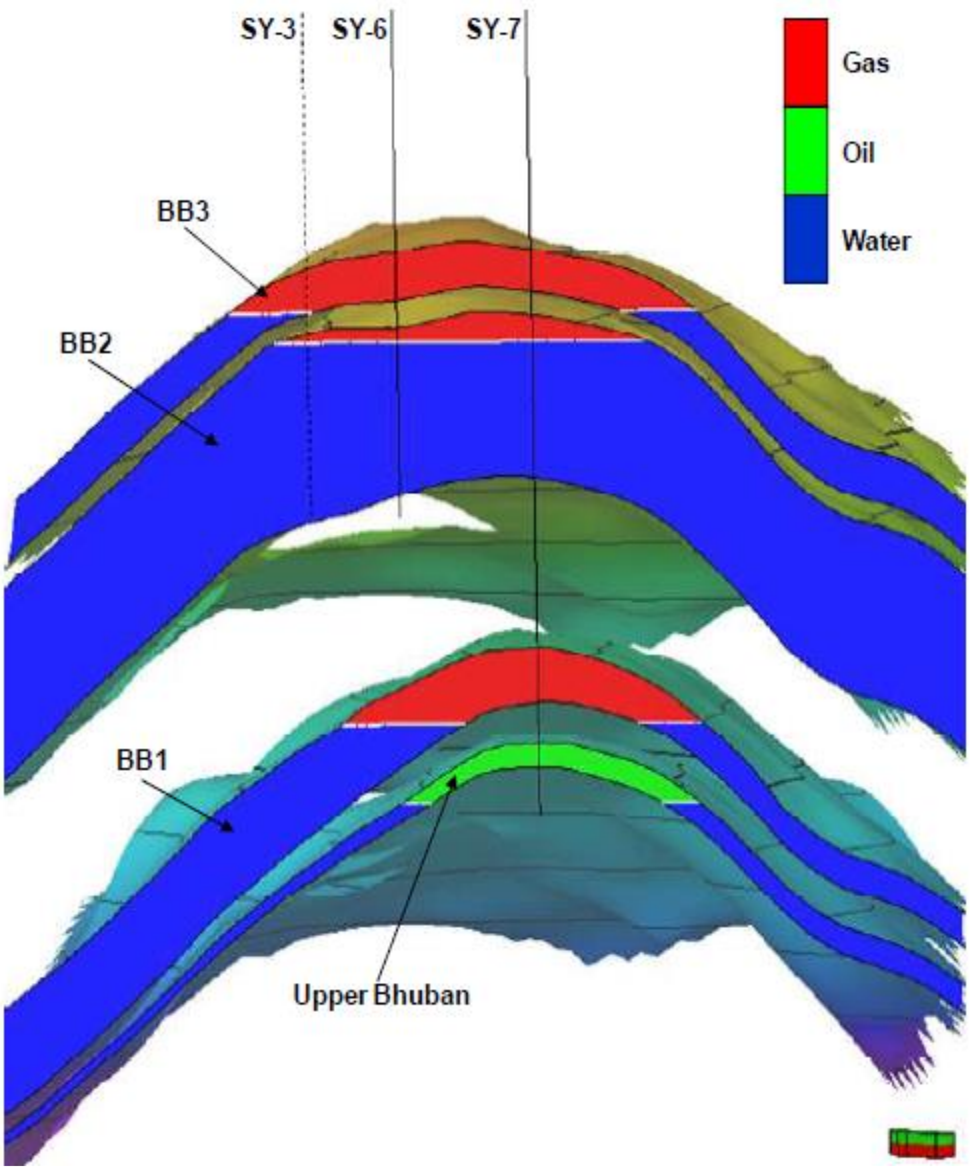

Figure 1.3: Geological structure of Haripur field (RPS Energy Report, 2009)

Reasonable degree of geological study has been performed on the Kailashtilla fields. The Kailashtilla field is located in the Surma basin which is a gas prolific tertiary basin in the northeastern part of Bangladesh (Mamud et al., 2016). Actually the Surma basin is in fact the northern extension of the Bengal basin (Afroza et al., 2019a). The deposition in the Surma basin was almost exclusively clastic sequences of deltaic to fluvial and to the lesser extent marine sandstone, siltstone and shale (Afroza et al., 2019b).

The Surma basin was formed structurally by the contemporaneous interaction of two major tectonic elements, i.e. the emerging Shillong Massif to the north and the westward moving mobile Indo-Burma fold belt (Khan et al., 1988). The tectonic movement is considered to have occurred during Neogene to the present age with the strongest period of crustal disturbance during the middle Miocene (Khanam, 2017). The primary result of this tectonics is a series of almost north-south oriented asymmetrical anticlines (Alam et al., 2003).

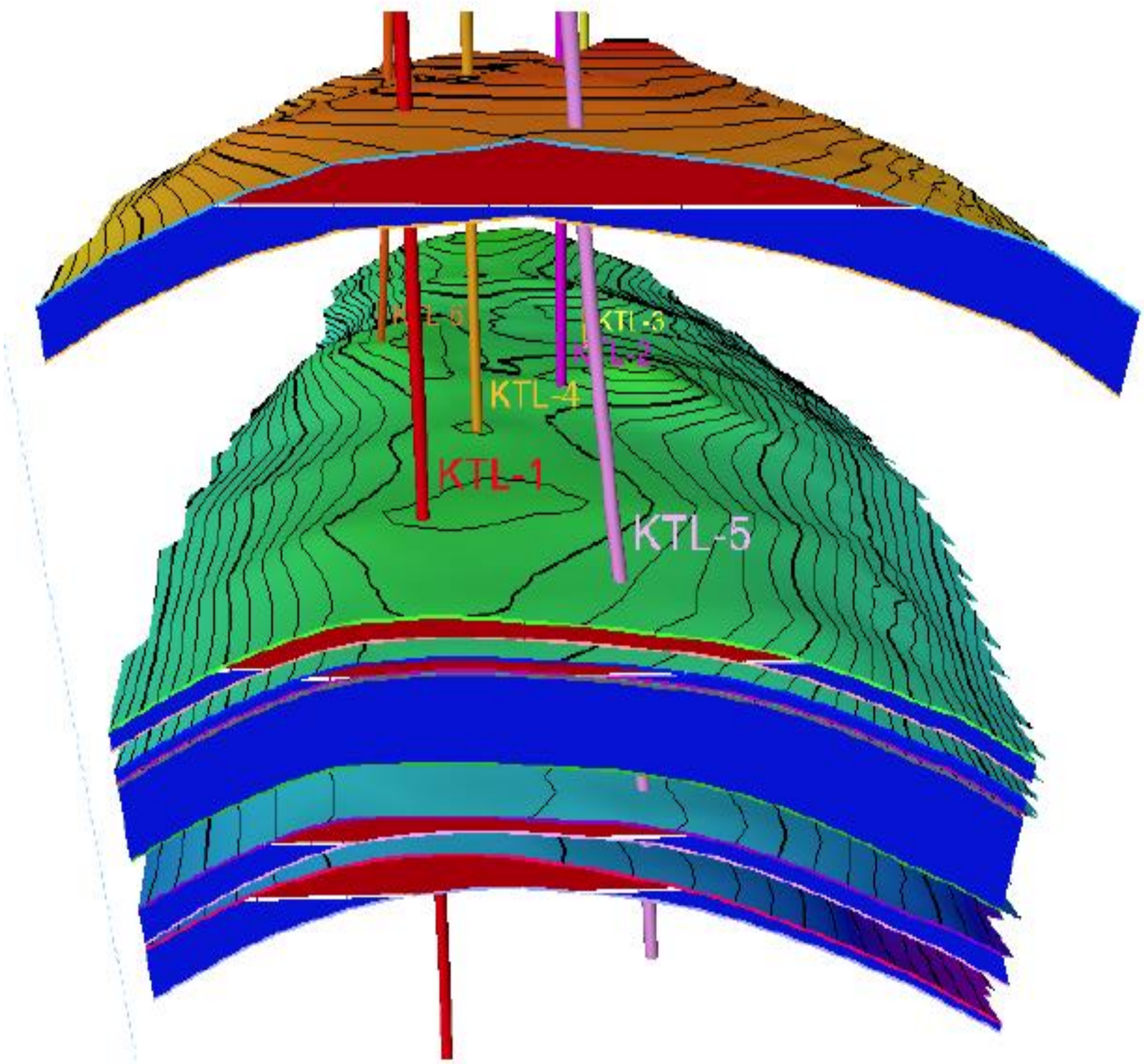

Figure 1.4: Geological structure of Kailashtilla field (RPS Energy Report, 2009)

The Kailashtilla field is an elongate asymmetrical anticline with a simple four way dip closure (Intercomp-Kanata Management Ltd., 1989). The structural trend main axis lies almost north-south with about 10 degree tilts towards northeast-southwest (Intercomp-Kanata Management Ltd., 1991). The structure lies on the northeast part of the Surma basin (Afroza et al., 2019c). The structural dip at the Kailashtilla closure is quite steep estimated to be about 11-15 degrees (Rahman et al., 2012). This indicates the strong and long duration of compression had occurred in Kailashtilla structure (Haniyum et al., 2013). The structure was first mapped by Shell in 1960 with a single fold seismic grid which acquired in the late 1950's. No fault was observed from the 2D seismic data at the Kailashtilla structure and vicinity as shown in figure 1.4. This is probably due to the low resolution of the variable quality 2D seismic data and probably more faults can be expected to be seen in a higher resolution 3D seismic dataset.

1.4 Maximizing of Oil Recovery

Primary oil recovery is mostly governed by the reservoir original pressure. Secondary and tertiary oil recoveries are mostly governed by the pressure maintenance schemes and altering reservoir rock and fluids properties. Considerable amount of oil is trapped in the pore networks of the porous media by capillary forces exist in pore scale and clay bond. To achieve maximum oil recovery the capillary forces and clay bond responsible for oil entrapment must be overcome. During last 4-5 decades different enhanced oil recovery (EOR) methods have been designed and implemented in order to efficient recovery of the oil. These methods include variety of physical, chemical and technical processes which lead to increase final oil recovery and accelerate the rate of oil recovery from the reservoirs.

The improved oil recovery (IOR) methods include all processes and procedures that affect economically increased oil recovery and cover primary, secondary, and tertiary stages of oil recovery. These recovery methods deal with both mobile and immobile oil left in the reservoir. The EOR methods mostly refer to secondary and tertiary oil recovery methods which could mobilize the immobile oil trapped in pore structure of the porous media. The most commonly applied EOR methods include but not limited to water based processes (polymer flooding, surfactant flooding, alkali/surfactant/polymer flooding), gas based processes (miscible gas injection, nitrogen (N_2) and CO_2 injection), thermal processes (in-situ combustion) and combination of these processes (water alternating gas, hot water injection, steam injection, foam injection).

1.5 New EOR Processes

Low salinity water (LSW) waterflooding has been given a great attention as new water based oil recovery process. Extensive experimental researches as well as field applications have verified the validity and potential of low salinity injection as effective and efficient oil recovery process (Skrettingland et al., 2010). The brine used in low salinity injection includes substantially lowering the salt concentration compared to the connate water of the reservoir (diluted brine) or modification of brine composition. The low salinity injection is carried out in both secondary mode and tertiary mode injections. In secondary mode, the low salinity water is injected at initial water saturation (S_{wi}), while in tertiary mode the low salinity injection follows the conventional high salinity waterflooding at residual oil saturation (S_{or}) condition.

It is well known from the literature that the low salinity environment is beneficial for the application of other well established EOR processes such as surfactant flooding and polymer flooding (Thyne and Gamage, 2011). Therefore the extension of low salinity water in combination with surfactant flooding and polymer flooding is of great interest to investigate the synergy between these different EOR methods. These combined processes which also are called hybrid EOR techniques, may lead to even higher oil recoveries than by the individual processes.

1.6 Industrial Motivation and Challenges of the Study

With the depletion of natural driving forces responsible for pushing the oil from reservoirs and declination of oil recovery after secondary stage, the emphasis is now on EOR techniques. The low saline water flooding is a type of EOR which gains the attention of researchers due to its easy to use advantages, less cost and environment friendly in nature. A good number of oil fields have successfully implemented low salinity water flooding technique for enhanced oil recovery as shown in table 1.1. The advantages of low salinity water flooding technique have motivated this research to apply this technique on Haripur and Kailashtilla fields. This study has many challenges. The main challenges are following:

- Assessment of uncertainty in seismic and well log data
- Delineation of oil reservoirs structures
- Distribution of porosity, permeability and net to gross ratio in the grid cells of reservoir
- Conduction of core flood test in laboratory

- Designing of oil recovery techniques
- Estimation of oil reserve
- Production forecasting by simulation
- Prediction of oil price

Table 1.1: Summary of field implementation of LSW (Ambia F., 2012)

Author	Reservoir	Injected Brine/ Formation Water (ppm)	Formation Damage	Incremental Oil Recovery (% OOIP)
Webb (2004)	Sandstone	3,000/ 220,000	No	20% -50%
McGuire (2005)	Sandstone <Alaska North Slope>	150-1,500 /15,000	No	13%
Robertson (2007)	Sandstone <West Semlek Reservoir> <North Semlek Reservoir> <Moran Reservoir>	10,000/60,000 3,304/42,000 7,948/128,000	No	Recovery tends to decrease as the salinity ratio increases.
Lager (2008)	Sandstone <Alaskan Oil Field>	2,600/ 16,640	No	10%
Veledder (2010)	Sandstone <Omar Oil Field> <Isa Oil Field>	2,200/ 90,000	No	10% - 15%
Seccombe (2010)	Sandstone <Endicot Oil Field>	12,000/ --	No	13%
Skrettingland (2010)	Sandstone <Snorre Oil Field>	500/50,000	No	No significant change

1.7 Oil Reservoir Development Path

International oil and gas companies follow a standard oil reservoir development path as shown in figure 1.5. During discovery phase different types of survey such as gravimetric, magnetic and seismic survey are being performed to discover the reservoir. Exploration wells are drilled at discovery and evaluation phases. Well logs and drill stem test are conducted for further evaluation of the reservoir. Geological, geocellular and simulation model of the reservoir are being constructed. Then the model is validated with production history and is used to design oil reservoir development plan. Portfolio of oil reservoir development project and project management plan are prepared. Project implementation period is 1-5 years. Production period is 15-30 years. Researches are performed in discovery, evaluation and development phases.

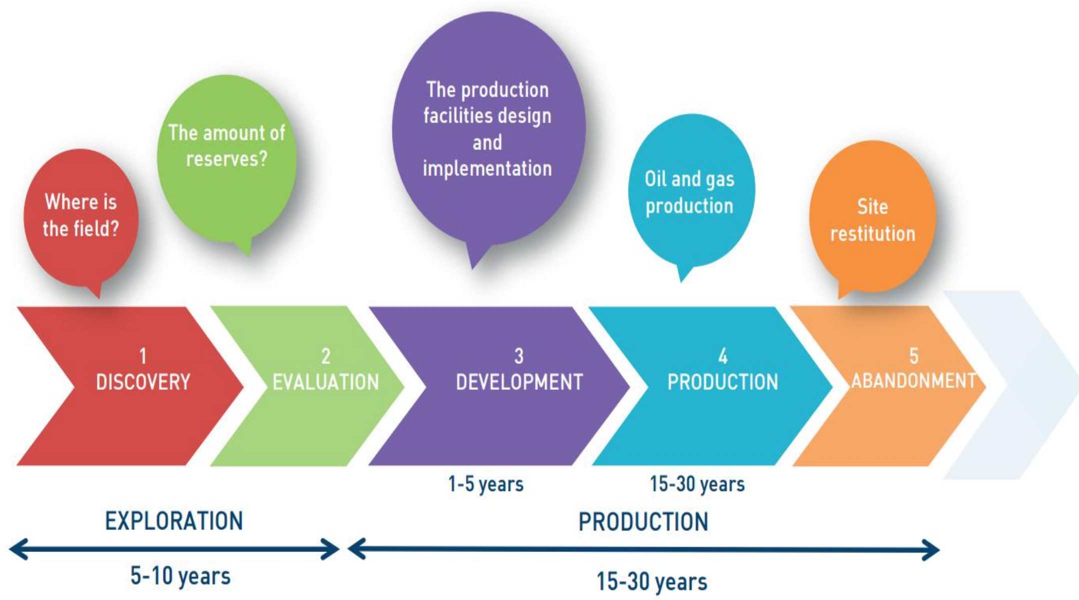

Figure 1.5: Oil reservoir development path

1.8 Aims and Objectives of Research

This research has been performed with the following aims and objectives:

- To prepare oil reservoir development plans and development project portfolios
- To develop oil reservoir simulation models using seismic, well logs, core analysis, fluid analysis, drill stem test and production data
- To validate the reservoir simulation models using production data
- To predict the dynamic characters of the reservoir at different production periods

- To generate different reservoir development scenarios
- To optimize reservoir development scenarios
- To determine net present value of the development project
- To estimate break-even point of the development project
- To evaluate the technical feasibility of the development project

1.9 Scopes of Research

The main scope of work of this research is to prepare oil reservoir development plans of oil reservoirs in Haripur and Kailashtilla fields according to the standard procedure followed by international oil and gas companies. The oil reservoir development plans are prepared by the engineers and scientists of oil and gas companies at their research centers. An oil reservoir development plan consists of finite difference and streamline reservoir simulation models with optimum reservoir development scenario.

Construct oil reservoirs structure of Haripur and Kailashtilla fields by analysis and interpretation of seismic sections and well logs. Detect the oil-water contact and gas-oil contact in oil reservoirs from well logs and DST. Distribute fluids in oil reservoirs. Perform core analysis in laboratory to determine porosity, permeability and net to gross ratio. Distribute porosity, permeability and net to gross ratio in the grid cells of the oil reservoir by sequential Gaussian simulation. Determine relative permeability and capillary pressure in laboratory. Analyze reservoir oil to determine formation volume factor, viscosity, bubble point and gas oil ratio. Estimate datum pressure and distribute pressure and water saturation in the grid cells of the oil reservoirs. Integrating all data to develop finite difference and streamline reservoir simulation models of oil reservoirs in Haripur and Kailashtilla fields.

Validation of reservoir simulation models are done by production data and DST data. Screening of reservoirs for designing oil recovery mechanisms is performed by chemical analysis of reservoir rock and fluids as well as core flood test. Streamline simulation is performed for dynamic characterization of reservoirs and determination of optimum reservoir development scenario. Finite difference simulation is performed for prediction of oil production.

1.10 Research Methodology

International oil and gas companies conduct research work for oil reservoir development in their research centers. Comprehensive research work on oil reservoir able to help for preparing an effective and efficient oil reservoir development plan and development project profile. Accordingly research methodology and procedures adopted for this study are follows.

- Analyze seismic, well logs, fluid contact and oil production data to detect oil zone in Haripur field
- Analyze oil production data of Haripur field to identify causes of oil production termination in immature stage
- Identify the drive mechanism in oil reservoir of Haripur field
- Predict remaining oil reserve
- Analyze the DST data of Kailashtilla field to detect oil zone
- Interpret seismic survey and well logs by software to delineate the structure of the oil reservoirs
- Analyze cores samples in laboratory to estimates the petrophysical properties of the oil reservoir
- Analyze fluid samples in laboratory to estimates the PVT properties of the reservoir oil
- Develop reservoir simulation model by integrating all data
- Screen reservoir to design the oil recovery technique
- Generate oil reservoir development scenarios
- Optimize reservoir development plans
- Forecast oil production by simulation
- Evaluate oil reservoirs developments projects technically and economically

1.11 Thesis Outline

An effort has been made to study the oil reservoirs in Haripur and Kailashtilla fields to prepare reservoir development plans. Appropriate reservoir development plans will enable to reduce the project investment and risk factor. Research work has been carried out as per international standard procedure to define optimum reservoir development variables such as oil recovery techniques, well placement, number of wells, production rate, injection rate and pressure. The oil development project on the basis of optimum reservoir development plans will have less uncertainty in technical and financial aspects and project implementation success will be increased. By this way this study will able to recover oil resources and contribute in economic development of Bangladesh. The main corresponding chapters of this dissertation are as following.

General introduction, problem statement and challenges of this study are presented in chapter 1. Theory of low salinity water flooding is described in chapter 2. Chapter 3 describes the oil reservoir development plan of Haripur field. A well (SY-7) in Haripur field had started oil production in December 1987 and continued oil production till July 1994. The field has produced 0.53 million barrels of oil. Oil reservoir in Haripur field had produced only 0.53 million barrels of oil during six years by natural depletion. Reservoir engineers and scientists must feel interest to investigate on the matters such as (i) What are the reasons of oil production termination in immature stage? (ii) How much oil is remaining in reservoir? (iii) How remaining oil can be recovered?

This research work has been designed to conduct detail study on every parts of the reservoir such as reservoir structure, rock, clay content, fluids, petrophysical properties, fluid contacts, hydraulic conductivity, production rate and pressure for finding out the solution of investigation. Now a day this type of work follows a systematic procedure. First of all a reservoir simulation model is being developed from seismic survey, well logs, core analysis, fluid analysis and fluids contacts data. Then history matching operation is done for validation of reservoir model.

Oil recovery technique is designed by detail screening of reservoir. Reservoir development variables under designed oil recovery technique are optimized to select the reservoir development scenario. At last reservoir development scenario is evaluated technically and economically to finalize reservoir development plan. An oil reservoir model has been developed on Haripur field and reservoir model has been validated by six years production history. Initial oil reserve is estimated as 33 million barrels. Screening of reservoir has recommended low salinity water injection for oil recovery techniques.

The optimum reservoir development variables are six water injection wells and two production wells. Simulation has been performed to evaluate the reservoir development scenario. Reservoir has shown good dynamic performance. Reservoir model with selected development scenario has been considered as reservoir development plan. Economic evaluation of development plan has been evaluated by forecasting of oil production for twenty years. Reservoir development plan is implemented as development project. Altogether 5.844 million barrel of oil can be recovered and net present value of the project is 5.8 million USD. The development project is technically feasible and economically viable.

Oil reservoir development plan of Kailashtila field has been presented in chapter 4. In 2015 well (KTL-7) has been drilled in Kailashtilla field. During second drill stem test (DST-2) operation on the KTL-7 from depth 3261 m to 3266 m significant quantities of liquid (oil and water) flow has been recorded. Interpretation of DST data has revealed the existence of oil reservoir in depth interval of 3261 m to 3266 m. Well log interpretation of KTL-7 has also shown oil sand in depth interval of 3260 m to 3270 m. This is another discovery of oil resources in Bangladesh. Exploration and production companies of Bangladesh are less interested in development of oil resources for many reasons. The main reasons are (i) there are no detail research works on these fields for oil reservoir development planning (ii) oil resource development requires intensive investment and (iii) risk factor is high in the development project.

The drill stem test describes the dynamic characteristic of the hydrocarbon bearing formation such as wellbore storage, skin effect, permeability, reservoir pressure and boundary. The wellbore storage effect and average reservoir pressure help to predict the flowing phase from the reservoir. In this chapter an effort has been made to analyze the drill stem test conducted in Kailashtilla field at the depth interval 3261 meter to 3266 meter in well KTL-7. Two sets of pressure profile have been recorded. First conditioning the well for an hour then performed drawdown following pressure buildup test. The pressure signature of the buildup period and its derivative has been plotted on semi-log and log-log coordinates to develop Horner and diagnostic plots respectively.

Wellbore storage, skin and transient flow effects have been observed in the drill stem test analysis which is an indication of the hydrocarbon bearing reservoir in the zone of interest. The value of wellbore storage effect is low which predicts the flow of liquid hydrocarbon into the well bore from the reservoir. Average pressure of the investigated zone has been estimated which is higher than the water column pressure. The higher average reservoir pressure also indicates the presence of oil reservoir.

Static and dynamic reservoir models of the oil sand in the Kailashtilla field have been constructed. Predicting the reservoir performance by dynamic model helps robust field development planning of the Kailashtilla field. Reservoir simulation study has revealed that the reservoir is able to produce oil by using its own pressure energy. Primary recovery technique has been selected to recover the oil from the Kailashtilla field in reservoir development plan. Forecasted oil production period is 20 years. Altogether 949650 standard cubic meter of oil can be recovered and net present value (NPV) of the project is 77.0 million USD. The oil reservoir development project in Kailashtilla field is technically feasible and economically viable. This study will able to contribute in the development of crude oil sector in Bangladesh. Results of twenty years simulation and economic analysis have been presented in chapter 5. States conclusions of this study and recommendations for future work have been given in chapter 6.

Chapter 2

Theory

2.1 Low Salinity Waterflooding Principles

Conventional waterflooding is a secondary recovery method in which water is injected into a reservoir to achieve additional oil recovery and supplement the natural energy (Fogden et al., 2011, Ghaoui and Lebret, 1997, Ghaoui et al., 1998 and Gringarten et al., 1979). Carll (1980) is one of the first person who reported increased oil production following accidental flooding in Pithole City, Pennsylvania. Waterflooding was first used in Pennsylvania's Bradford field in 1907 and then it was widely applied in many North American oil fields within ten years. People agreed that oil recovery by waterflooding was significantly better than that achieved by natural pressure depletion (Hajizadeh et al., 2013, Handels et al., 2007, Hiorth et al., 2010, and Honarpour et al., 1986). Many attempts have been made to understand, design, and optimize the waterflooding process. Leverett (1941), Buckley et al. (1942) and Welge (1952) are the pioneers who investigated the fundamental displacement mechanisms of water movement in porous media. Waterflooding is currently accepted worldwide as a simple, reliable, and economical technique for oil recovery, and most conventional oil reservoirs have been, are being, or will be considered for waterflooding during secondary recovery (Jiang et al., 2010, Kharaka et al., 1988, Khilar et al., 1990, Kia et al., 1987, and Korrani et al., 2013). Unquestionably, waterflooding will continue to be applied to unlock the hydrocarbon reserves left behind after primary recovery (Alagic et al., 2011, Doust et al., 2010, Earlougher, 1977, Drummond and Israelachvili, 2002, 2004).

In most waterflooding projects, especially in offshore oil fields, the injected water is normally chosen based on economic considerations and the injection water's compatibility with existing reservoir brine, so that it will not damage the formation (Alotaibi et al., 2011). Several authors, however, have reported that injecting low-salinity brine can increase oil recovery by a factor up to 40% compared with conventional high-salinity waterfloods in different sandstone reservoirs (McGuire et al., 2005, Faure et al., 1997, Fedutenko et al., 2015, Fedutenko et al., 2014).

The original findings of Low Salinity Waterflooding (LSW) were developed by Morrow and his research colleagues at the University of Wyoming in the 1990s, during their experiments to determine the interactions and effects of brine, crude oil, and mineralogy on wettability (Morrow and Bukley, 2011). Subsequently, numerous laboratory and field evaluations have proven the possibility of higher oil recovery using LSW process. LSW has a promising future since 50% of the world's conventional petroleum reservoirs are found in sandstone reservoirs, and most of these contain clay minerals, which are favorable conditions for LSW (Kozaki, 2012, Kulkarni and Rao, 2005, Lebedeva and Fogden, 2010, and Lever and Dawe, 1984). Additionally, LSW can achieve considerable low-cost recovery, with relatively simple operation compared with other chemical EOR techniques (Lever and Dawe, 1987, Li et al., 2014, Li and Nghiem, 1986, and Liegthelm et al., 2009). LSW can also be considered for secondary and tertiary recovery, or be combined with other EOR approaches such as chemical flooding (e.g. polymer or surfactant) or miscible water-alternating-gas (WAG) for a higher oil recovery factor (Marion et al., 1992, Martin, 1957, Melberg, 2010, Miller et al., 1950, and Mohammadi and Jerauld, 2012).

2.2 Industrial Motivations

Encouraged by results from laboratory experiments, LSW has been getting favorable attention from the oil and gas industry over the past two decades (Al-Shalabi et al., 2014). Several oil operators continue to promote practical research into LSW and have started to evaluate it at the field-scale (McGuire et al., 2005, Lager et al., 2008a, 2008b, Skrettingland et al., 2010, Thyne and Gamage, 2011). McGuire et al. (2005) and Lager et al. (2006, 2007) reported LSW performance in Alaska's oil fields using water injection salinity between 1,500 ppm and 3,000 ppm. Based on single-well chemical-tracer tests (SWCTT), the reported incremental LSW in these oil fields ranged from 6% to 12% OOIP. Lager et al. (2006) indicated that neither fines migration nor significant permeability reduction due to LSW was ever observed. He also achieved a 40% increase in recovery using a North Sea crude oil with a very low acid number (acid number < 0.05). Another result from the log-inject-log test, Webb et al., (2004) showed a 25-50% reduction in residual oil saturation by using LSW. Another successful LSW SWCTT test was described by Seccombe et al. (2010) in a mature offshore oil field located on the North Slope of Alaska. Additionally, historical field evidence in the Powder River basin of Wyoming reported by Robertson (2010) showed that oil recovery tended to increase by about 12.4% as the salinity of the injected brine decreases. Thyne and Gamage (2011) published a comprehensive evaluation of the effect of LSW for 26 field trials in Wyoming. LSW is also expected as an alternative improved oil-recovery method for hostile reservoirs where the conventional high salinity waterflooding and EOR technologies might fail because of a high degree of reservoir heterogeneity, high temperature, high salinity, or hardness (Dang et al., 2011a; 2011b; 2011c; 2014c).

Preliminary field-scale evaluations have demonstrated a promising future for LSW, as an emerging EOR technology; however, systematic studies of LSW are lacking (Mohan et al., 1993, Mojarad and Settari, 2007, Montes et al., 2001 and Nasralla et al., 2011a, 2011b). Further insight and mechanistic research, for a better understanding and implementation of the LSW process, is required (Ambia, 2012).

2.3 Wettability Phenomenon

Wettability is one of the most important concepts in LSW (Nasralla and Nasr, 2012, Nghiem and Rozon, 1988, 1989 and Nghiem et al., 2004a, 2004b, 2005, 2009, 2011). Wettability is defined as the tendency of one fluid to spread on, or adhere to, a solid surface in the presence of another immiscible fluid (Nguyen et al., 2012, 2014, Ozdogan et al., 2005 and Parkhurst and Appelo, 1999). When two immiscible phases are in contact with a solid surface, one phase usually attaches to the solid more strongly than the other (Peters et al., 2009, Pu et al., 2008, Pursley et al., 1973, Ramey, 1992 and Rousseau et al., 2008). The more strongly attached phase is called the wetting phase (Green and Willhite, 1998). When the fluids are water and oil, wettability is the tendency for the rock to preferentially imbibe oil, water, or both (Rueslatten et al., 1994, Ruhovets and Fertl, 1982, Ryan and Gschwend, 1994 and Shapiro and Stenby, 2000, 2002). Reservoir rock wettability is an important property which determines the success of waterflooding because it greatly influences the location, flow and distribution of the fluids in the reservoir (Puntervold, 2008). In a system at equilibrium, the wetting fluid is located on the pore walls and occupies the smallest pores, while the non-wetting fluid is located in the pore bodies (Sincock and Black, 1988, Sorbie and Collins, 2010, Soyster, 1973, Spall, 2003 and Spildo et al., 2012). This means that the aqueous phase in a water-wet reservoir will be retained by capillary forces in the smaller pores and on the walls of the larger pores, whereas the oleic phase will occupy the center of the larger pores and will form globules that might extend over many pores

(Sutanto et al., 1990, Teklu et al., 2014, Thibeau et al., 2007, Thomas et al., 1962 and Thomas and Stieber, 1975). Wettability can be evaluated by several methods including measurements of the contact angle θ or by examining the interfacial forces that exist when two immiscible fluid phases are in contact with a solid. A force balance at the line of intersection of solid, water, and oil yields:

$\sigma_{os}-\sigma_{ws}=\sigma_{ow}\cos\theta$ ……………………………………………………………..(EQ 2.1)

σ_{os} and σ_{ws} cannot be measured directly by experimental methods (Green and Willhite, 1998); therefore, contact angle, θ, is used to specify wettability (Figure 2.1). This angle is defined as the tangent to the oil-water surface in the triple-point solid-water-oil, measured through the water phase (Strand, 2005). In a system containing reservoir rock, oil and water, the solid is water-wet if $\theta < 90^o$ and oil-wet if $\theta > 90^o$. A contact angle approaching 0^o indicates a strongly water-wet system and an angle approaching 180^o indicates a strongly oil-wet rock. The rock is intermediate/neutral-wet when both fluid phases tend to wet the solid, but one phase is only slightly more attracted to the rock than the other ($\theta = 90^o$) (Green and Willhite, 1998). (Ursin, 1997) describes the relationship between contact angle and wettability as shown in Table 2.1.

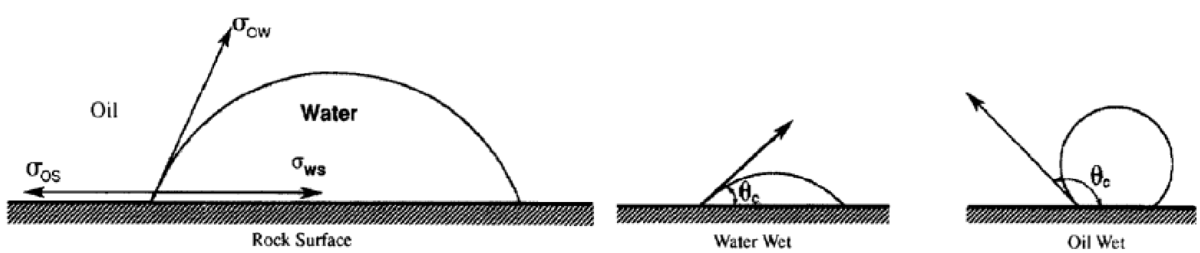

Figure 2.1: Contact angle through the water phase (Strand, 2005)

Table 2.1: Relationship between contact angle and wettability (Green and Willhite, 1998)

Contact Angle, Degree	**Wettability Preference**
0-30	Strongly water wet
30-90	Preferentially water wet
90	Natural wettability
90-150	Preferential oil wet
150-180	Strongly oil wet

Several wettability types are described in the literature, including fractional, spotted, and Dalmatian (Zeinijahromi et al., 2011). These wettability terms, which usually refer to heterogeneous reservoirs, arise from the knowledge that the many minerals that form reservoir rocks have different surface chemistry and adsorption properties, which leads to variations in wettability within a single reservoir (Anderson, 1986, and Anderson, 2006). Additionally, a mixed wettability condition is considered a type of fractional wettability (Appelo, 1994, Austad et al., 2010). Under this wettability condition, small pores and grain contacts are preferentially water-wet and contain no oil, whereas the oil-wet surface forms continuous paths through the largest pores and contains all the oil (Puntervold, 2008). Green and Willhite (1998) stated that mixed wettability results from a variation of heterogeneity in the chemical composition of the exposed rock surfaces and cementing-material surfaces in the pores.

Where the contact angle method only measures the wettability of a single solid surface, the Amott or USBM methods are used to measure the average wetting of a core sample (Anderson, 1986). The Amott method uses a sequence of imbibitions and forced displacement tests. After the core is centrifuged with brine to obtain residual oil saturation, the following determinations are made: spontaneous imbibition of oil to record the volume of water displaced, forced displacement of water by oil under centrifuge to record the volume of water displaced, spontaneous imbibition of water to record the volume of oil displaced, and forced displacement of oil by water under centrifuge to record the volume of oil displaced. The Amott method evaluates the wettability condition by calculating the ratio of the displaced volume by spontaneous imbibition, and the displaced volume by forced displacement (δo , δw):

$\delta_o=V_{wsp}/V_{wt}$ ……………………………………………………………………(EQ 2.2)

$\delta_w=V_{osp}/V_{ot}$ ……………………………………………………………………(EQ 2.3)

where V_{wsp} and V_{wt} are the water volume displaced by spontaneous imbibition and the water volume displaced by both oil imbibition and forced displacement. V_{osp} and V_{ot} are the oil volume displaced by spontaneous imbibition and the oil volume displaced by both water imbibition and forced displacement. A modification to the Amott method, referred to as the Amott-Harvey method, is commonly used. The Amott-Harvey wettability index is defined as:

$I_{a-h}= \delta_w -\delta_o= V_{osp}/V_{ot} -V_{wsp}/V_{wt}$ ……………………………………………………(EQ 2.4)

The Amott-Harvey wettability index ranges from +1 to -1, with +1 indicating strongly water wet and -1 indicating a strongly oil wet. The last method, called the USBM method, was introduced by Donaldson et al. (1969). This method, used in near-neutral wettability conditions, utilizes the following equation to determine wettability (W):

$W = \log(A_1/A_2)$ ……………………………………………………………..……(EQ 2.5)

where A1 and A2 are the areas under the water- and oil-derived capillary-pressure curves, respectively. One limitation of the USBM method is that it can only be conducted on plug-size samples (Anderson, 1986).

Wettability is found to have a large effect on key petrophysical properties such as residual saturation, relative permeability, capillary pressure, and capillary desaturation (Dang et al., 2013a, 2013b). The literature also indicates that wettability affects the relative permeability curves of the water-oil system (Tufenkji, 2007, Trantham et al., 1978, and Van et al., 2006). The location of the crossover point and the value of endpoint relative permeabilities for the wetting and non-wetting phases are functions of wettability as shown in figure 2.2. For a strongly wetted rock, the crossover point of the relative permeability curves will occur at a wetting phase saturation greater than 0.5 (Vledder et al., 2010, Wu and Bai, 2009, and Yang et al., 2007, 2009, 2011). For a neutral or mixed wet rock, the endpoint relative permeabilities are approximately equal and the crossover point will therefore be at a saturation of around 0.5 (Anderson, 2006).

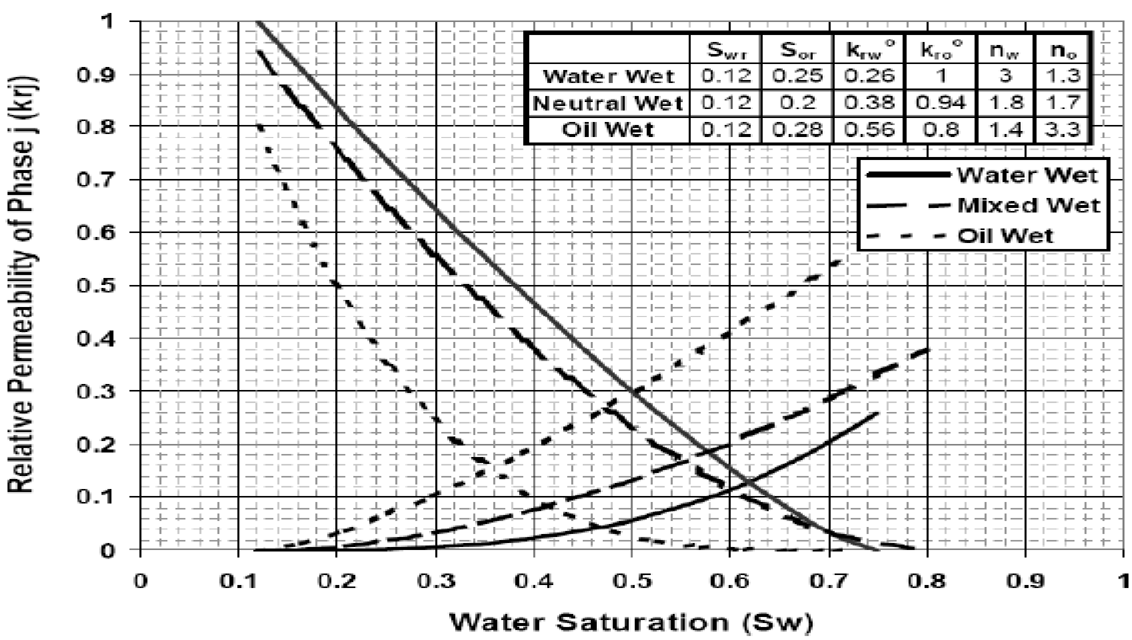

Figure 2.2: Effect of wettability on relative permeability curves (Morrow et al., 1973)

Wettability can be altered with a change in surface chemistry and adsorption properties (Yasari et al., 2013, Yousef and Ayirala, 2014 and Yousef et al., 2012). Nearly all geologic formations are completely saturated with water during deposition so are initially strongly water-wet (Verbeek and Matzakos, 2009, Zekri et al., 2011, Zolfaghari et al., 2013). During hydrocarbon migration into the water-saturated formation, the rock can either remain water-wet or its wettability can change due to the interaction of the rock with the hydrocarbon. The alteration of a formation's wettability can also be induced thermally or chemically. The primary chemicals used for wettability alteration are surfactants and/or alkali (Anderson, 2006). In addition these chemicals, a number of studies have indicated that the adsorption of divalent ions such as Ca++ and Mg++ can alter the initial wettability towards more water wetness (Suijkerbuijk et al., 2012, Mugele et al., 2014). This observation, important for LSW flooding, will be discussed later in this research.

2.4 Role of Crude Oil, Brine and Reservoir Rock on Wettability

All reservoir rocks are thought to be water-wet originally. Sedimentary rocks are formed by deposition in an aqueous environment. Most sandstone is therefore water-wet by nature. In contact with crude oil, however, the wettability of the rock surface may be altered towards more oil-wet or water-wet (Puntervold, 2008). Reservoir wettability is therefore not fixed, as often assumed. It is usually reported as a single value reflecting the initial or final wetting condition. Instead, wettability should be considered a dynamic property when, for example, low-salinity brine is injected into a reservoir (Rivet, 2009). Wetting is dependent on the crude oil/brine/rock system (COBR) (Maas et al., 2001). It can be altered when the key parameters affecting it are changed, and it can be restored when the same parameters are restored (Rivet, 2009). If the parameters are not restored, a different wetting state will exist at the new equilibrium condition. Increased oil recovery may take place during the transition from one equilibrium/wetting condition to the next.

Crude Oil

Crude oils are complex mixtures of hydrocarbons and polar organic compounds of nitrogen, sulphur and oxygen. Buckley et al. (1998) indicated that the composition of crude oil is crucial to wetting alteration in two distinct ways: (1) Polar components present in the crude oil, especially in the heavy asphaltenes and resin fractions, that exhibit surface activity and influence wetting, and (2) The oil is itself the solvent environment that influences partitioning of the surface active components between bulk oil and oil/water or oil/water/solid interfaces. Adsorption of these components onto the rock surface may result in a wetting alteration of the COBR system towards less water-wet. Later, in a low-salinity process, the oil components may desorb from the surface (Bardu et al., 2003).

Brine

Brine chemistry is another important process that affects rock wettability (Card et al., 1992). The presence of divalent cations (ions missing two electrons compared with the neutral atom), such as calcium (Ca++) and magnesium (Mg++) in the brine, can affect wettability (Anderson, 1986, Suijkerbuijk et al., 2012, Mugele et al., 2014). The salinity and pH of the brine strongly affect the surface charge of the rock and fluid interfaces, and thereby the adsorption of these divalent ions leads to modification of the original wettability. It was found that core samples with lower calcium concentration exhibit more water-wet characteristics (Sharma and Yortsos, 1987).

Reservoir Rock

The ability of different polar compounds to alter rock wettability depends on the mineral composition and surface charge of the rock material (Dang et al., 2014a). Sandstone which contains active clay minerals is necessary to obtain a favorable low-salinity effect by wettability alteration (Austad et al., 2008). Most sandstone reservoirs contain clay minerals, created by sand grains, in the pore space, the presence of which is critical to LSW effects. Numerous studies have reported that LSW has no effect without clay in the core samples (Rivet et al., 2010).

2.5 Clay Minerals

The presence of clay minerals is the crucial factor for realizing the benefits of LSW in sandstone reservoirs. Clay can be described chemically as aluminum silicates. The basic coordination units for clay minerals are tetrahedral and octahedral, with oxygen forming the corners, and a cation residing in the centre. Tetrahedral coordination means that a central cation is surrounded by four oxygens, and octahedral coordination means that a central cation is surrounded by eight oxygens (Appelo and Postma, 2005). The mineral is composed essentially of silica (Si), alumina (Al) and water. Iron (Fe) and magnesium (Mg) also frequently appear, in addition to smaller quantities of sodium (Na) and potassium (K). Typical properties of clay are fine size, large surface area, and chemical reactivity of the surface. In the clay minerals, tetrahedra and octahedra form layers that share oxygens, and stacking of the layers determines the type of clay mineral. If there is only one tetrahedral and one octahedral group in each layer, the clay is known as a 1:1 kaolinite clay; whereas, the octahedra are sandwiched between two layers of tetrahedra in the smectite or montmorillonite clay.

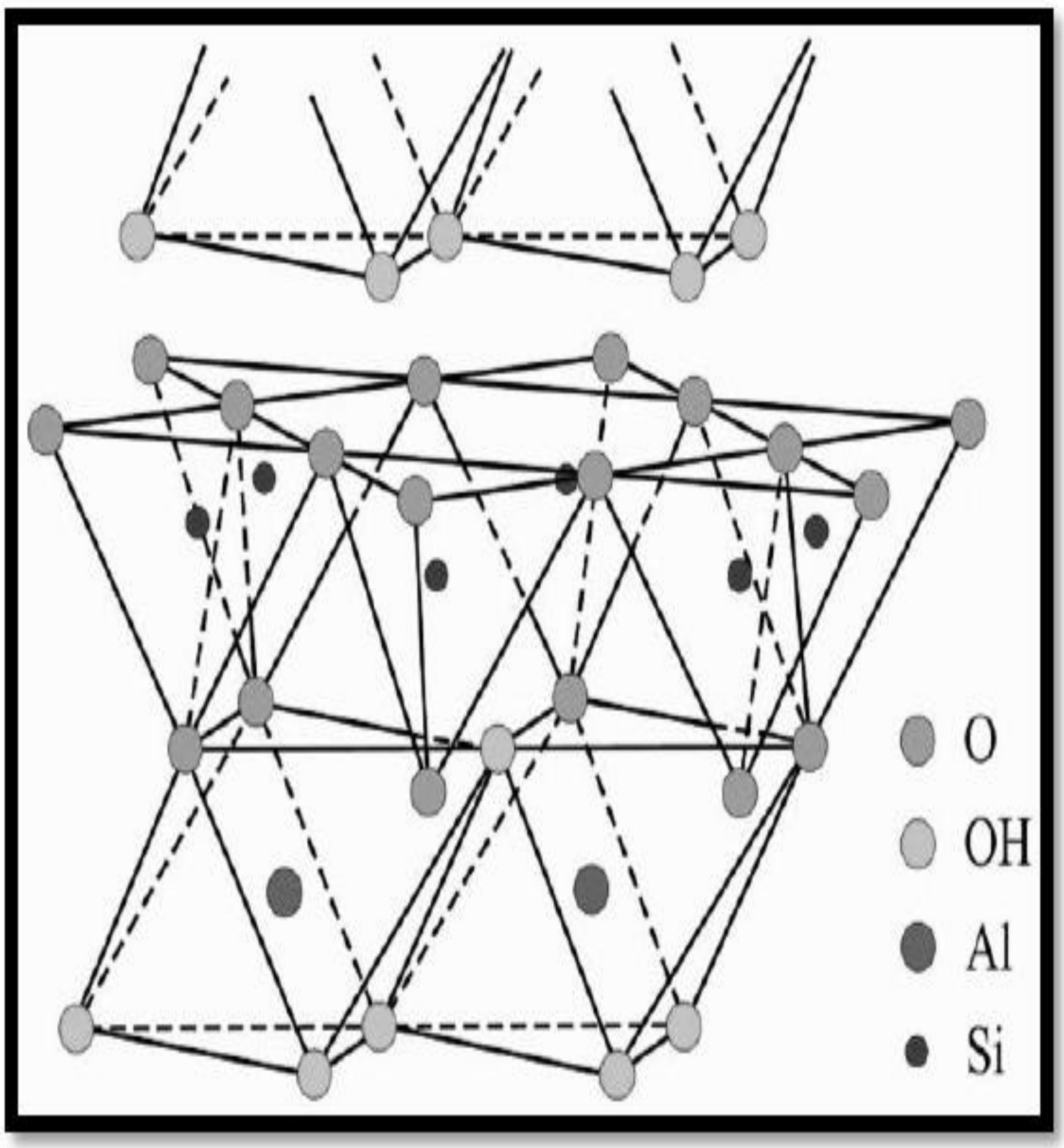

Figure 2.3: Structure of kaolinite clay mineral (Gaines and Thomas, 1953)

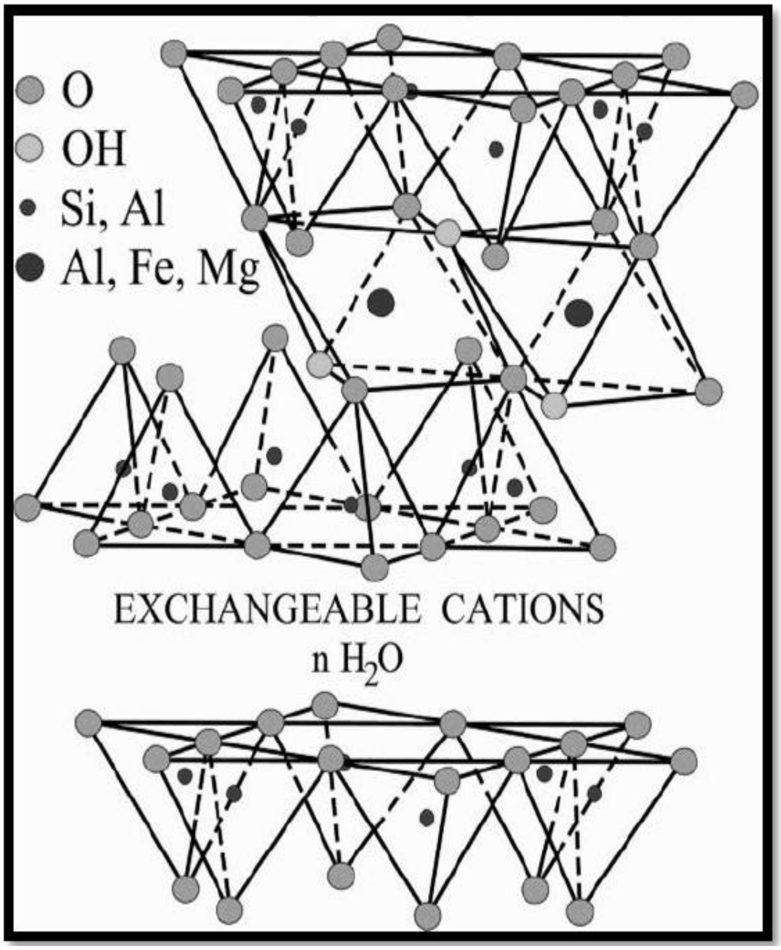

Figure 2.4: Structure of montmorillonite clay mineral (Gaines and Thomas, 1953)

One of the important properties of clay minerals in LSW is ionic exchange because of which, its surface can act as an adsorber. Ion exchange involves the replacement of one ion by another ion at a solid surface. Cation exchange capacity (CEC), which is usually expressed in meq/kg, represents the ion exchange capacity for a specified clay mineral. Clay minerals show a wide range in CEC depending on mineral structure, structural substitutions, and the specific surface of the mineral accessible to water, as shown in Table 2.2.

Similar to chemical equilibrium reactions, ion-exchange processes are characterized by equilibrium constants and exchange coefficients. Gaines and Thomas (1953) were the first to give a rigorous definition of the thermodynamic standard state of exchangeable cations. Table 2.3 provides the ion-exchange coefficients between sodium and many of the ions reported by Appelo (1994).

Table 2.2: Cation exchange capacity for various clay minerals (International Drilling Fluids, IDF, 1982)

Clay Minerals	CEC (meq/kg)
Kaolinite	30-250
Halloysite	50-100
Montmorillonite	800-1200
Vermiculite	1000-2000
Glauconite	50-400
Illite	200-500
Chlorite	100-400

Table 2.3: Ion exchange coefficients $K_{Na/I}$ (International Drilling Fluids, IDF, 1982)

Ions	$K_{Na/I}$	Ions	$K_{Na/I}$	Ions	$K_{Na/I}$
Li^{+}	1.2 (0.95-1.2)	Mg^{2+}	0.5 (0.4-0.6)	Al^{3+}	0.7 (0.5-0.9)
K^{+}	0.2 (0.15-0.25)	Ca^{2+}	0.4 (0.3-0.6)	Fe^{3+}	-
NH_4^{+}	0.25(0.2-0.3)	Sr^{2+}	0.35 (0.3-0.6)		
Rb^{+}	0.1	Ba^{2+}	0.35 (0.2-0.5)		
Cs^{+}	0.08	Mn^{2+}	0.55		
		Fe^{2+}	0.6		
		Co^{2+}	0.6		
		Ni^{2+}	0.5		
		Cu^{2+}	0.5		
		Zn^{2+}	0.4 (0.3-0.6)		
		Cd^{2+}	0.4 (0.3-0.6)		
		Pb^{2+}	0.3		

2.6 Low Salinity Waterflooding

In the 1990s, Jadhunandan and Morrow, (1995) and Yildiz et al.,(1996) published papers on the influence of brine composition on oil recovery. These preliminary studies encouraged further investigation into the optimization of waterflooding process through the simple modification of brine salinity. Numerous laboratory experiments by Morrow and his research colleagues and also researchers at BP confirmed that enhanced oil recovery can be obtained when performing tertiary low-salinity waterflood (Tang and Morrow, 1997, Morrow et al., 1998, Tang and Morrow, 1999a, Tang and Morrow, 1999b, Zhang and Morrow, 2006, Zhang et al., 2007, Buckley and Morrow, 2010, Kumar et al., 2010, Lohardjo et al, 2010, Morrow and Bukley, 2011) and also by researchers at BP (Lager et al., 2007, 2008a, 2008b, Webb et al., 2004, 2005, 2008, McGuire et al., 2005, Jerauld et al., 2008, Bazin and Labrid, 1991). The salinity in these tests was in the range of 1,000 - 5,000 ppm, and most of the coreflood tests showed positive results.

In this section, initial ideas about LSW, laboratory experimental tests, and the state-of-the-art of modeling and numerical simulation are described, along with several hypotheses of LSW mechanisms.

2.6.1 Proposed Mechanisms under Laboratory Observations

Over the past two decades, numerous LSW mechanisms have been proposed in the literature, including: (1) fines migration; (2) mineral dissolution; (3) limited release of mixed-wet particles; (4) increased pH effect and reduced interfacial tension; (5) emulsification; (6) saponification; (7) surfactant-like behavior; (8) multiple ion exchange; (9) double-layer effects; (10) salting-in effects; (11) osmotic pressure; (12) salinity shock; and (13) wettability alteration. Some of these mechanisms are related. Conflicting experimental results have led to a poor understanding of the true mechanism of LSW. This section outlines the limitations of several of the proposed concepts and mechanisms about LSW modeling.

2.6.1.1 Fines Migration

Starting a half century ago, many have tried to inject fresh water into sandstone core samples to evaluate the impact of clay content, and permeability reduction due to clay swelling. The mechanism of fines migration was initially explained using the theory of colloids (Deryaguin and Landau, 1941, Verwey and Overbeek, 1948) (DLVO).

Bernard, (1967) conducted his experiments by injecting NaCl brine and distilled water into sand packs, Berea cores, and outcrop cores from Wyoming. He found that injecting distilled water increased recovery. The recovery was accompanied by a massive increase in pressure drop in both the secondary and tertiary modes during constant-flow-rate experiments. Bernard stated that the increase in recovery was due to improved microscopic sweep efficiency induced by clay swelling and the plugging of pore throats by fines migration. Although there may be some movement of fine particles with the flow of dilute brine, several authors have reported, in their formation damage reports, that there is no catastrophic reduction in permeability when the injection brine is changed to distilled water (Jones, 1964), (Shahin et al., 2011). An important finding from comprehensive experimental studies by (Jones,1964) is that small proportions of calcium or magnesium in the formation and injected brine can significantly restrain clay blocking, and that a gradual decrease in salinity gradient also prevents permeability damage.

Tang and Morrow, (1999a) observed that fines (mainly kaolinite clay fragments) were released from the rock surface, and there was an increase of spontaneous imbibition recovery with a decrease in salinity for different sandstone cores. The authors used Berea, Bentheim, CS Reservoir, Clashach, and fired and acidized Berea cores; CS crude; and refined oil. The total dissolved solids (TDS) in 7 different brines from their experiments changed from 35,960 to 151.5 ppm. They found that the oil recovery factor increased significantly in the CS reservoir and Berea sandstone cores which had more clay content, but recovery improved only marginally in the Bentheim and Clashach cores. Oil recovery was independent of brine salinity when cores were fired and acidized to stabilize fines, and saturated with refined mineral oil rather than crude oil. From the results, they suggested that the mobilization of fines resulted from exposure of the underlying surfaces, which increased the water wetness of the system. Additionally, the released clay particles could block pore throats and divert the flow of water into non-swept pores, to improve the microscopic sweep efficiency (Valdya and Fogler, 1992).

Zhang et al., (2007) observed improved oil recovery with LSW from their spontaneous imbibition experiments using four different samples of Berea sandstone and three different crude oils, in both secondary and tertiary modes. The dependence of oil recovery on brine salinity varies in different Berea core samples, suggesting that mineralogy has a significant effect on the LSW process (Yuan and Shapiro, 2011). The lowest permeability block of Berea showed no sensitivity to salinity (Wang and Li, 2007). The lack of response was attributed to the presence of chlorite. In several cases, cores responded to low salinity brine in the secondary but not in the tertiary mode, and low-salinity effects became more dramatic as the initial water saturation increased. The authors noted that effluent pH also increased in their experiments.

Although Tang and Morrow have indicated that it is possible to have fines migration during low salinity waterflooding, (Rivet, 2009) and various BP researchers (Lager et al., 2007, 2008a, 2008b, Webb et al., 2004, 2005, 2008, McGuire et al., 2005, Jerauld et al., 2008) have carried out numerous tests indicating that LSW had higher recovery without any observations of fines migration during their experiments. Based on these results, many people have questioned the link between fines migration and incremental oil recovery.

Fines migration, in fact, occurs when the ionic strength of the injected brine is less than a critical flocculation concentration, which is strongly dependent on the relative concentration of divalent cations (Ramez et al., 2011). The differences of injected brine compositions, lithology, and minerals inside the cores tested by Morrow and the BP researchers might explain the conflicting findings (Sarma and Chen, 2008a, 2008b). The Berea sandstone used by Morrow and his staff for many of their experiments had predominantly kaolinite clay and quartz (Rezaei et al., 2009). Low-salinity brine with insufficient divalent ions might detach poorly cemented clay particles such as kaolinite, resulting in production of fines (Omekeh et al., 2012).

From the published reports, it is clear that LSW achieves additional oil recovery in the absence of fines production and migration. The fact of low-salinity response in flooding with mineral oils suggests that fines migration might contribute to the benefits of LSW in some cases but that is not the principal mechanism in LSW (Evje and Hiorth, 2011).

2.6.1.2 Saponification and Mineral Dissolution

McGuire et al. (2005) performed numerous laboratory core flood studies using Berea sandstone, and crude oil and formation brine (BPNS2, 15,000 ppm) from a BP-operated North Sea field. Experimental results showed that flooding with low-salinity water (a flood at 1,500 ppm TDS and a flood at 150 ppm TDS) increased the ultimate oil recovery to 8% and 17% of OOIP for the two floods, respectively. This represents a 30% increase in oil production compared with the high-salinity flood with 15,000 ppm formation water. In fact, an increase of pH is usually observed during LSW, as shown by the example in Figure 2.5 (McGuire et al., 2005); (Lager et al., 2006, Zhang et al., 2007). The pH level of the effluent increased from approximately 8 while flooding with 15,000 ppm formation water to a pH of approximately 10 when flooding the core with 1,500 ppm low-salinity brine. Regarding the increase in pH, the authors suggested that the EOR mechanisms of LSW appear similar to those of alkaline flooding by generating in-situ surfactants, changes in wettability, and reduction in IFT (Jensen and Radke, 1988). They also proposed the saponification mechanism of elevated pH and removal of harmful multivalent cations due to low salinity injection, as the following chemical reactions indicate:

$(RCOO)_3C_3H_5 + 3NaOH \rightarrow 3(RCOONa) + C_3H_5(OH)_3$

fat + alkali → soap + glycerol

$2(RCOONa) + Ca(HCO_3)_2 \rightarrow (RCOO)_2Ca + 2(NaHCO_3)$

soap + “hardness” → insoluble soap curd

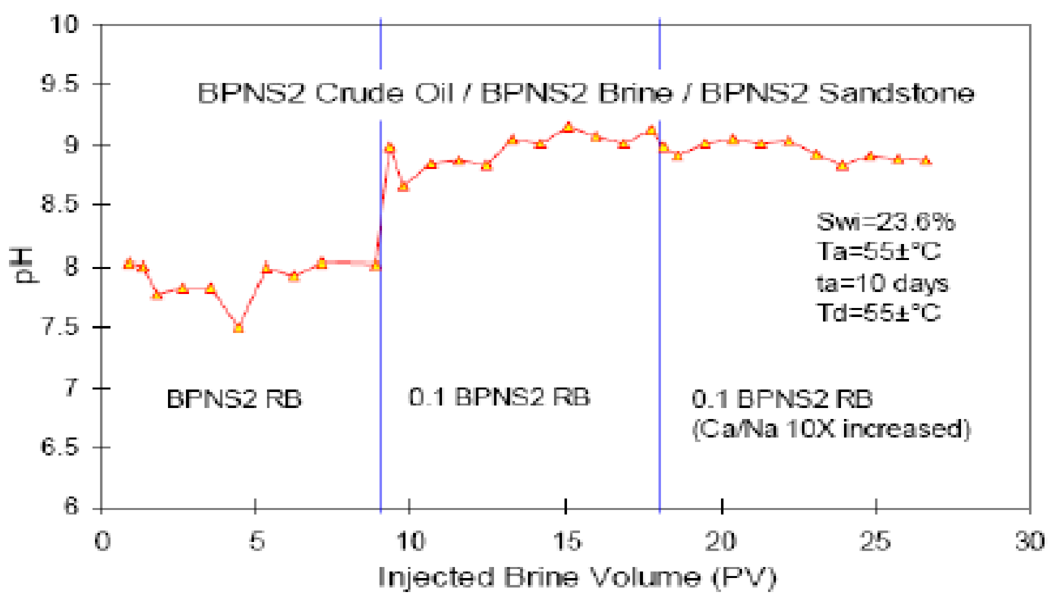

Figure 2.5: P^H Variation during a low salinity flood (McGuire et al., 2005)

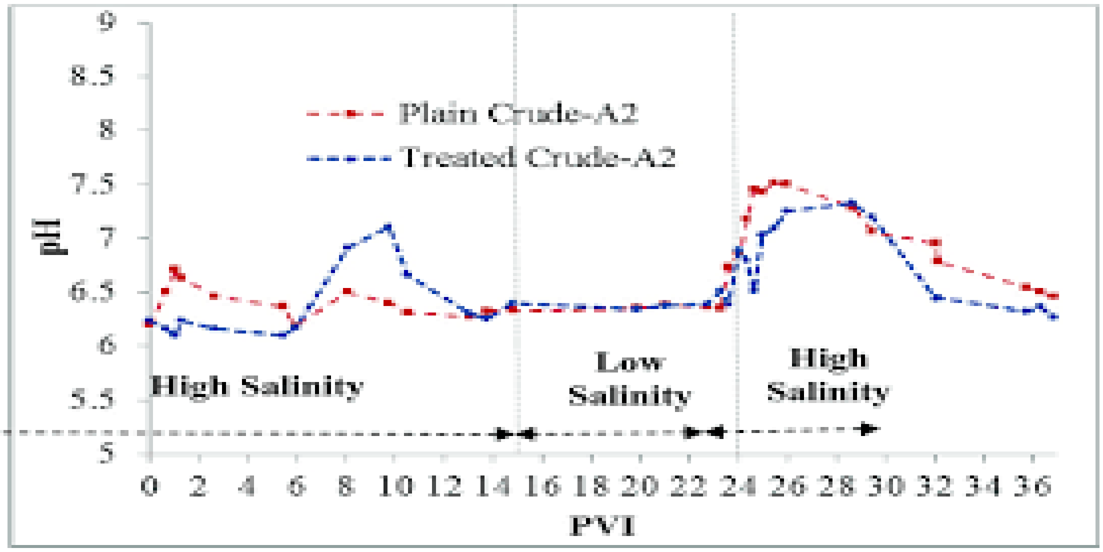

Figure 2.6: P^H variation during a low salinity flood (Lager et al., 2008a)

Based on conclusions from earlier chemical flooding research, the acid number of the crude oil should be greater than 0.2 mg KOH/g to generate enough surfactant to induce wettability reversal and/or emulsion formation in alkaline flooding (Ehrlich et al., 1974), (Jerauld and Rathmell, 1997), however, most of the crude oil samples used in the LSW experiments had an acid number less than 0.05mg KOH/g. It is difficult to conclude, therefore, that the additional oil recovery is mainly from in-situ surfactant generation. Additionally, LSW showed good performance even when it was conducted with low initial pH value (6) and final pH value of 7.5 (Rivet, 2009). This value is much lower than that typical in alkaline flooding (pH over 10).

Another fact is that the oil/water interfacial tension in LSW is not very low. Zhang et al., (2007) reported IFT of 16 dyne/cm. Buckley and Fan (2007) measured IFT values above 10 mN/m with pH<9. Since the pH from the actual tests was lower than that required to achieve saponification and emulsification, the pH mechanism may not apply to LSW. These chemical reactions are important, however, and must be considered when modeling the LSW process, since they could affect ion exchange and wettability alteration (Ehlig et al., 1990).

2.6.1.3 Desorption of the Organic Materials

Since there is a lack of evidence for the effect of in-situ surfactants. Austad et al., (2010) proposed a hypothesis of organic desorption caused by pH increase. In his statement, desorption of initially adsorbed cations onto the clay is the key process for increasing the pH of water at the clay surface. At the beginning of this process, both basic and organic materials are adsorbed onto the clay together with inorganic cations, especially Ca++ from formation water. A net desorption of cations occurs when low salinity water is injected into the reservoir. Proton H+ will be exchanged with cation Ca++ leading to a local increase in pH close to the clay surface (Carll, 1980). The local increase in pH close to the clay surface causes reactions between adsorbed basic and acidic material as in an ordinary acid-base proton transfer reaction (Austad et al., 2010). A fast reaction between OH- and the adsorbed acidic and basic material will cause desorption of organic material from the clay surface (Dang et al., 2014d). The water wetness of the rock is therefore improved. The fundamental mechanism of this theory is described by the following chemical reactions:

$\text{Clay-Ca}^{++} + \text{H2O} = \text{Clay-H}^{+} + \text{Ca}^{++} + \text{OH}^{-}$

$\text{Clay-NHR3}^{+} + \text{OH}^{-} = \text{Clay} + \text{R}_3\text{N} + \text{H}_2\text{O}$

$\text{Clay-RCOOH} + \text{OH}^{-} = \text{Clay} + \text{RCOO}^{-} + \text{H}_2\text{O}$

The concentration of H+ and OH- in the near-neutral conditions under which LSW has primarily been conducted is relatively small for these chemical processes and pH tends to increase and remains constant in many coreflood experiments and pilot tests (Lager et al., 2007, Rivet, 2009, Fjelde et al., 2012). Moreover, (Suijkerbuijk et al. 2012, Suijkerbuijk et al. 2014) found that LSW incremental oil production was observed even when substantial pH decreased during their coreflood experiments and they concluded that pH effects might just be interpreted as a result of the low salinity effect rather than its cause.

2.6.1.4 Double-Layer Effect

The double-layer, or DLVO theory, is based on the force between charged surfaces interacting through a liquid medium (Card et al., 1992). It combines the effects of the Van der Waals attraction and electrostatic repulsion (Dang et al., 2014b, 2014c, 2014e, 2015a, 2015b, 2015c, 2015d, 2015e). Low salinity brine reduces clay-clay attraction by expanding the electric double layer, resulting in more water-wet on clay surfaces, and the detachment of more oil (Sheng, 2014). However, Seilsepour and Rashidi, (2008) observed in their experiments that water film was more stable at high salinities, conflicting with the double-layer theory.

2.6.1.5 Salting-in Effect

The “salting-in” and “salting-out” theory is based on the correlation between the solubility of organic material and salt concentration (Beckner and Song, 1995, Berg et al., 2010, Bethke, 2006, Breeuwsma et al., 1986, Centilmen et al., 1999, Chen et al., 2012). Adding salt to a solution will significantly decrease the solubility of organic materials, while solubility can be increased by removing salt from water. Rezaei et al., (2009) proposed the idea of the “salting-in” effect, whereby a decrease in salinity increases the solubility of organic materials in the aqueous phase, resulting in additional oil recovery. This simple explanation, however, does not explain the dependence of clay, mineral composition, and P^H increase in LSW (Buckley et al., 1996, Alagic, 2010, Austad et al., 2008, Batycky et al., 2006, Ben-Tal and Nemirovski, 1998, 1999, 2000).

Chapter 3

Oil Reservoir Development Plan of the Haripur Field

The Haripur oil field, located about 230 km north-east of Dhaka and 18 km from Sylhet town, lies within the Surma basin between Shillong Plateau in the North and Tripura High in the South. Geologically the oil field is housed in the NE-SW trending Sylhet anticline which is part of the Tertiary folded system covering the eastern part of the Bengal Basin. The oil is found in sandstone reservoir horizon belonging to the Miocene Surma Group at depth of 6627- 6670 feet below the surface (Imam, 2013).

In 1955 drilling of Sylhet-1 well in the Sylhet structure at Haripur, a small village of Jaintapur police station in Sylhet and it was first ever gas discovery. About 35 years later in 1986 Sylhet-7 was drilled in the same structure as a gas development well. The Sylhet-7 well discovered oil horizon blow the gas zone and became the first well to discover commercial oil field named the Haripur oil field. After 07 years of more or less uninterrupted production, the well (Syl-7) ceased its production on 14th July, 1994 due to gradual decline in well head pressure (http://sgfl.org.bd/Haripur%20field.htm).

The field produced 0.53 million barrel of stock tank oil and simulation study revealed that the filed has more 33 million barrel of oil remaining in the sandston reservoir of the Bhuban Formation. An oil reservoir development plan has been prepared in Haripur field as part of oil sector development of Bangladesh.

To prepare an oil reservoir development plan engineers of oil and gas companies follow an international standard procedure. Reservoir model is developed on the real reservoir. Then reservoir model is validated by production history matching. Reservoir is screened to design oil recovery technique and optimized the reservoir development variables to generate reservoir development scenario. The valid reservoir model with reservoir development scenario is simulated to examine the reservoir performance. The valid reservoir model with the best performed reservoir development scenario is considered as reservoir development plan. Reservoir production performance is analyzed for twenty years for economic evaluation of the project. The development plan is decided for implementation when the reservoir development plan is technically feasible and economically viable. The above procedure has been followed for oil reservoir development in Haripur field.

3.1 Oil Reservoir Model Development in Haripur Field

Now a days reservoir engineers and scientists develops valid reservoir model using software from the seismic survey, well logs, well test, core analysis, fluid analysis and other laboratory tests for preparing oil reservoir development plan. Seismic survey and well logs are used for reservoir structure modeling. Well logs, well test and core analysis are used for porosity, absolute permeability and net to gross ratio (shale content, NTG) modeling. Oil formation volume factor (B_o), oil viscosity (μ_o), gas oil ratio (R_{so}) and bubble point (P_{bp}) are modeled from fluid analysis in laboratory. Oil-water relative permeability (K_{ro}, K_{rw}) and capillary pressure (P_{cow}) are modeled from laboratory test. Rock compaction is estimated from laboratory experiment. Oil-water contact and gas-oil contact are estimated from seismic section, well logs and drill stem test (DST). Also gas-oil contact is estimated from composition variation with depth experiment. Vertical flow performance (VFP) of well is modeled by software. Reservoir modeling and simulation process is shown in figure 3.1.

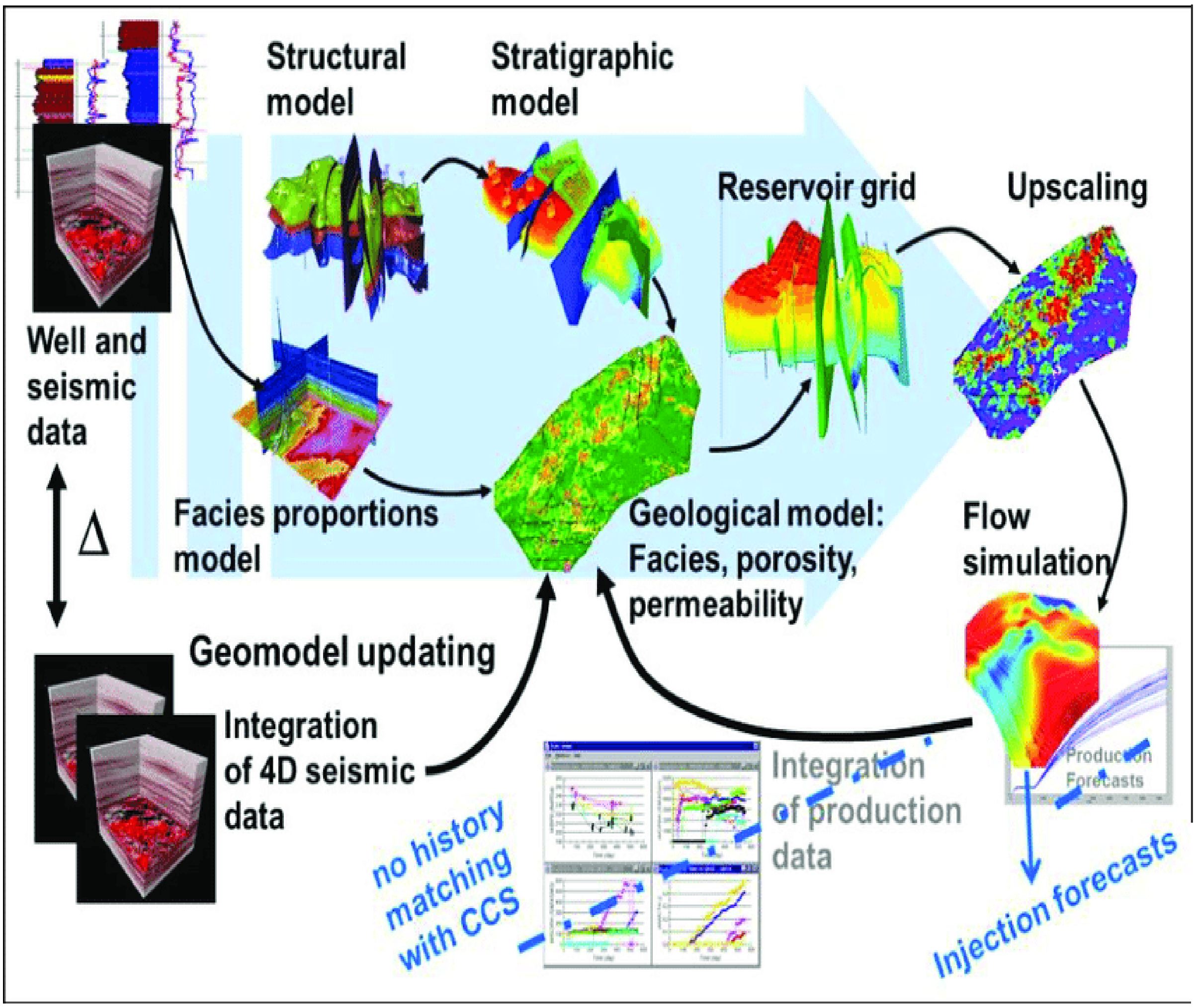

Figure 3.1: Reservoir modeling and simulation workflow

3.1.1 Structural Modeling of Oil Reservoir in Haripur Field

Two seismic horizons have been drawn in seismic sections of the field. Two well tops have been drawn in well logs interpretation. Reservoir boundaries have been determined from seismic section. By combining seismic horizons and well tops horizons of reservoir model has been generated as shown in figure 3.2.

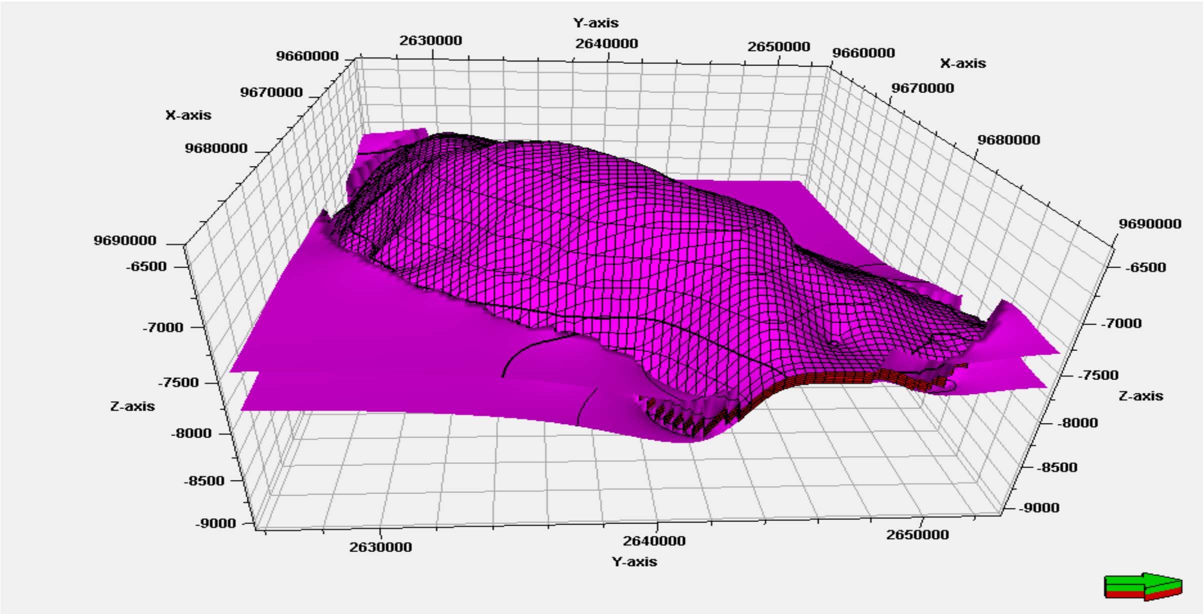

Figure 3.2: Horizons of reservoir model

Reservoir has been divided into six virtual layers as shown in figure 3.3. Each layer thickness is 20 ft.

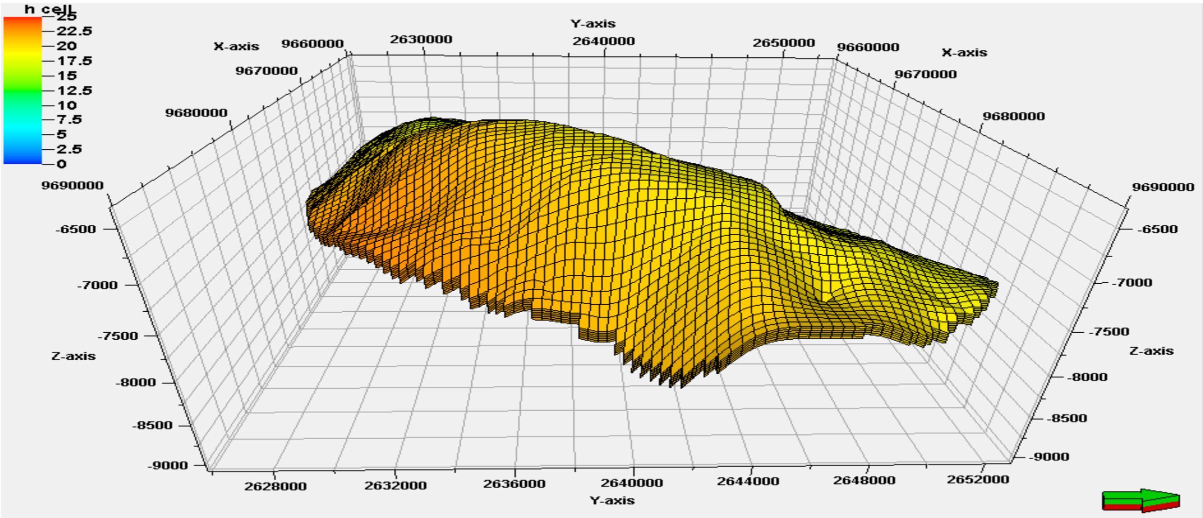

Figure 3.3: Virtual layers in reservoir model

Grid cells dimension in X direction is 320 ft as shown in figure 3.4. The cell dimension is optimized to 320 ft to reduce the number of cell in reservoir model.

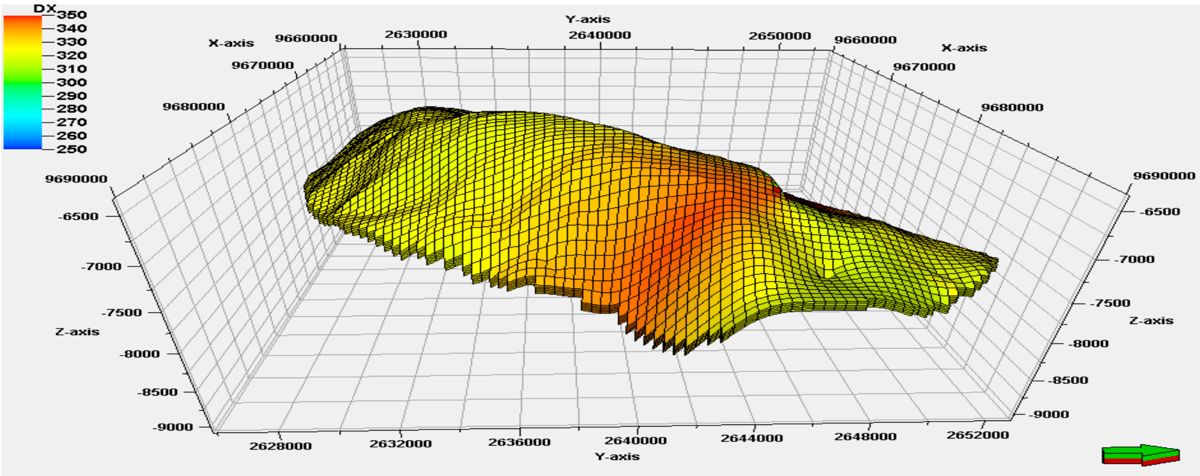

Figure 3.4: Grid cell dimension in X direction

Grid cells dimension in Y direction is 330 ft as shown in figure 3.5. The cell dimension is optimized to 330 ft to reduce the number of cell in reservoir model.

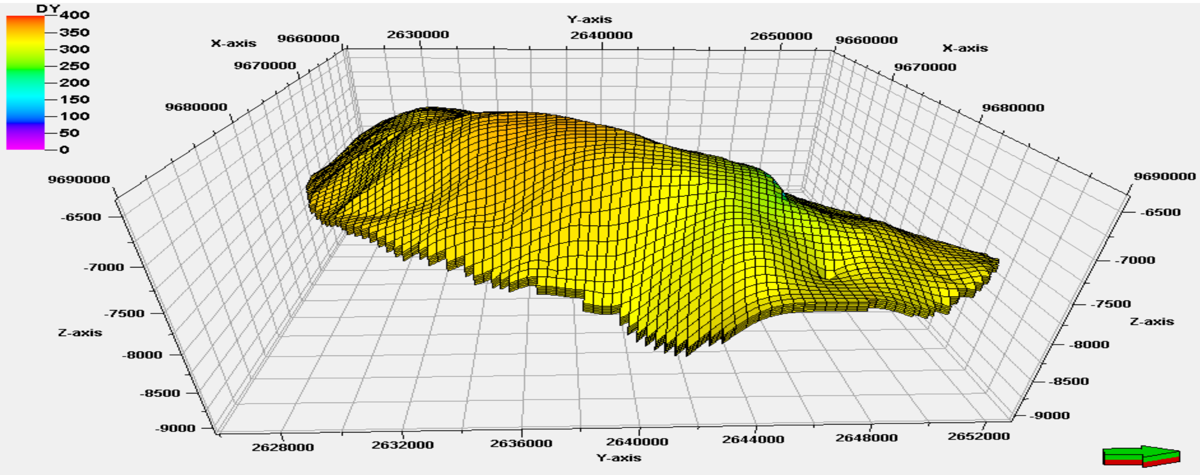

Figure 3.5: Grid cell dimension in Y direction

The 3D reservoir model has been constructed using 2D seismic survey and well logs. The model extends 30824.31 ft in east-west direction and 27670.60 ft in north-south direction. In X direction the model is divided into 94 sections and in Y direction the model is divided into 83 sections shown in table 3.1 and figure 3.5.

Table 3.1: Reservoir model dimensions

Axis	Easting-Northing	Minimum, ft	Maximum, ft	Difference, ft	Number of Grid Cell
X-X’	E-W	9659345.47	9690169.78	30824.31	94
Y-Y’	N-S	2625312.50	2652983.10	27670.60	83
Z-Z’	Depth	-9087.60	-6433.20	2654.40	6

3.1.2 Detection of Fluid Contacts in Haripur Field

In the petroleum reservoir hydrocarbon and water make oil zone and gas zone under the influence of the gravity, capillary, thermal, chemical and mechanical forces in the reservoir. In most petroleum reservoirs the gravity drives the heavier components of reservoir fluid toward deeper zones; on the other hand lighter components are driven toward upper zones, thus developing oil rim at lower zone and gas cap at upper zone coexisting at equilibrium in the reservoir. However, this is not always the case, because there are other reasons that may oppose this factor like a temperature gradient, capillary pressure, reservoir compartmentalization, reservoir filling, density overturn, and genesis processes.

Oil Water Contact (OWC)

The Oil-Water contact is at 6660 feet depth as shown in figure 3.6 which is determined by different methods such as resistivity logs, seismic data, drill stem test data and simulation (history matching with production data). At the depth of OWC the water saturation approaches to 100% and capillary pressure becomes zero.

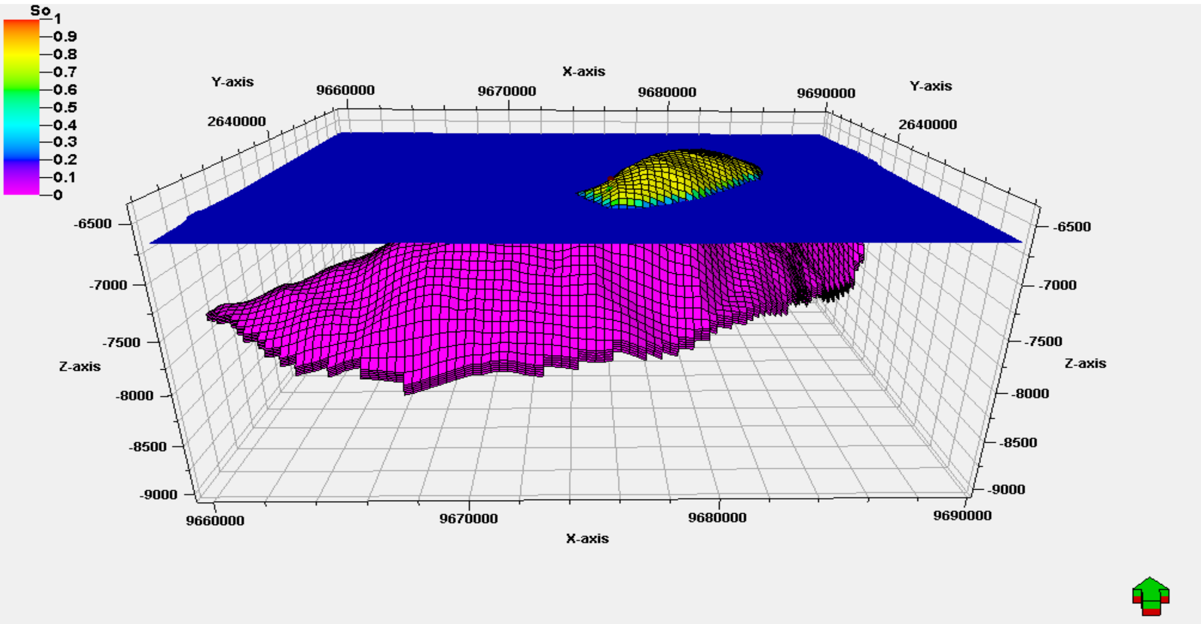

Figure 3.6: Oil water contact in 3D reservoir model

Gas Oil Contact (GOC)

Generally oil zone is rich with heavier hydrocarbon and gas zone is rich with lighter hydrocarbon. There exist a gas oil contact between these two phases which is the prime objective of the engineers' to predict. This gas-oil contact is the main information for estimation the reserve and determining recovery techniques. In this study oil rim is predicted in the Haripur oil field by simulation compositional gradient in the formation and the prediction is validated with the seven years of observed data making this outcome authentic and validate for further field development study. Saturation pressure profile is shown in figure 3.7.

Compositional gradient analysis is a proven and authentic technology to detect the gas-oil-contact (GOC) in the reservoir fluid column by collecting a reservoir fluid sample from a reference depth. In this study oil sample is collected at depth of 6660 ft and analyzed its Pressure Volume Temperature (PVT) properties with PVT cell to determine composition and API gravity. From this investigation result a compositional grading in the reservoir fluid column is modeled and detected the gas-oil-contact (GOC). The compositional grading model is validate by the seven years oil production rate and tube head pressure history matching through reservoir simulation study. Compositional grading model is shown in figure 3.8.

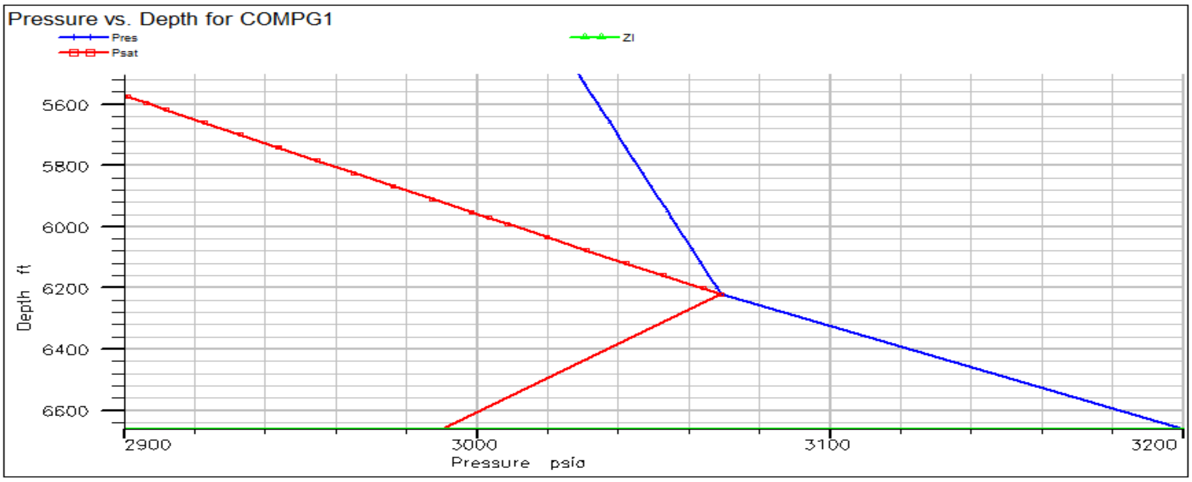

Figure 3.7: Profile of saturation pressure with depth

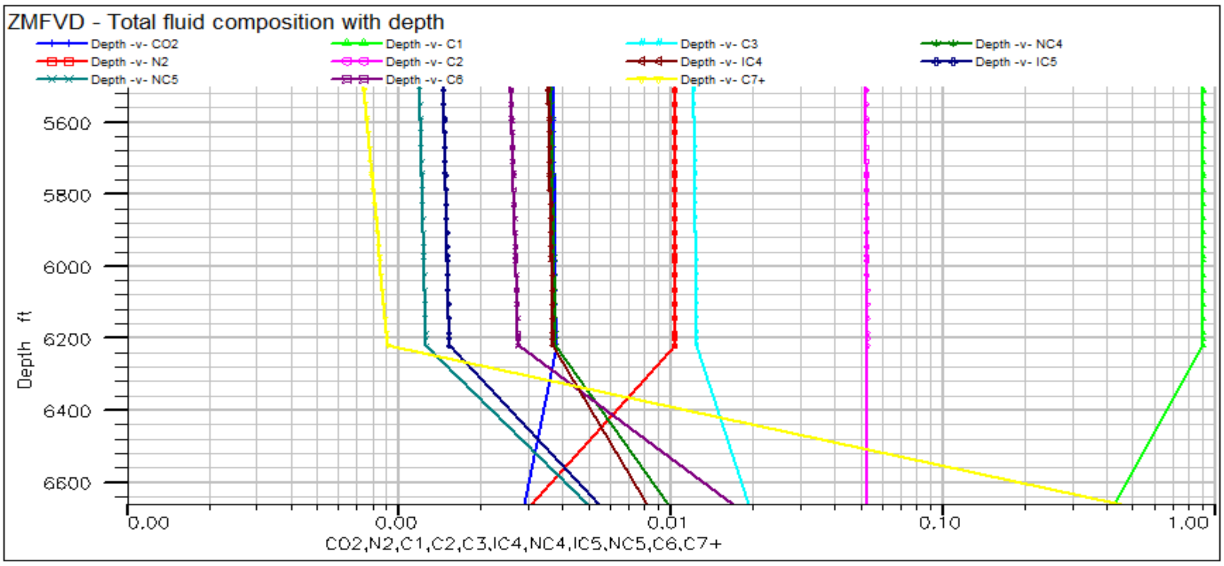

Figure 3.8: Composition variation with depth

Starting from the oil sample collected at depth 6660 ft, oil composition is estimated yielding C_1 is 41.52% and C_{7+} is 46.50%. By this reference composition at reference depth a compositional gradient model is simulated up to depth 4000 ft yielding that gas-oil-contact exists at depth 6237ft constructing an oil rim in the reservoir as shown in figure 3.9. The predicted fluid contact is inserted into a reservoir simulation model for validation of the prediction. The reservoir simulation model generate dynamic responses such as oil flow rate and tube head pressure matching with the observed data over seven years.

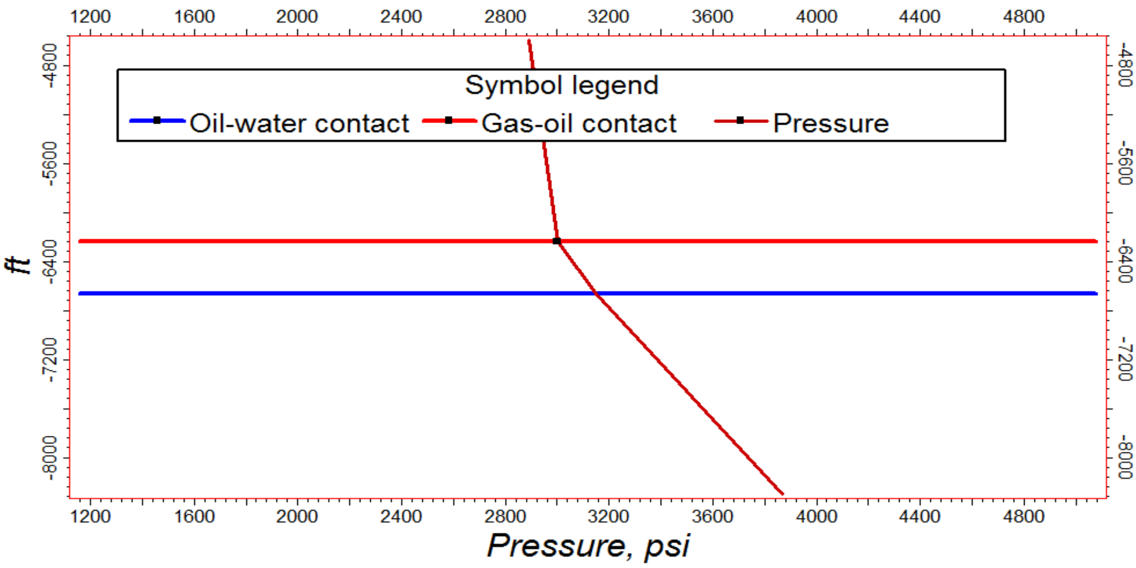

Figure 3.9: Fluid contacts in reservoir model

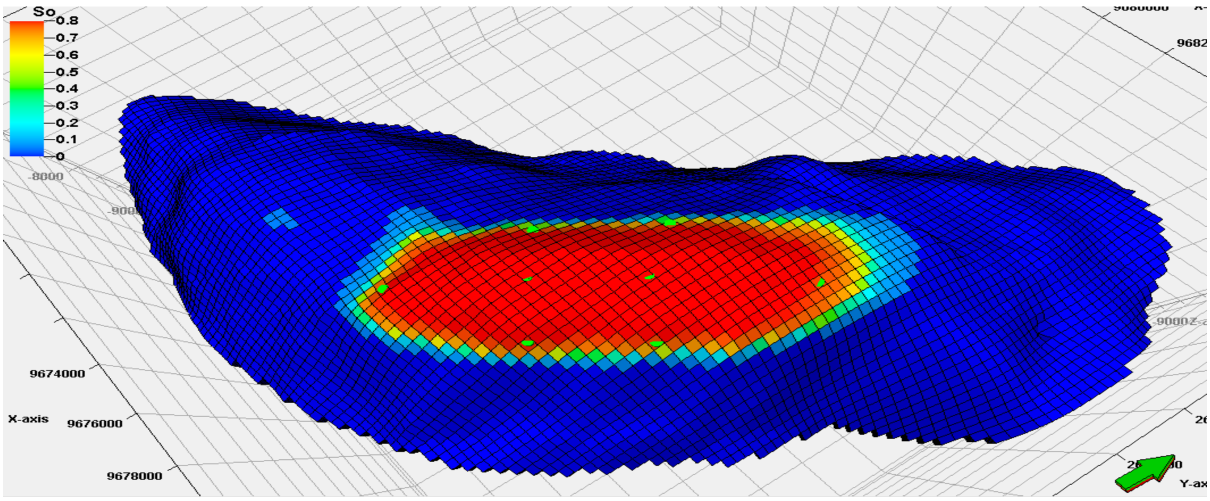

Figure 3.10: Oil zone in reservoir model

There are two zones in the reservoir model. Oil zone lays top of the water zone as shown in figure 3.10. The length of oil zone from north-east corner to south-west corner is 10912 ft and the length of oil zone from south-east corner to north-west corner is 4319 ft.

3.1.3: Petrophysical Properties Modeling in Haripur Field

Petrophysical properties of reservoir rock such as porosity, absolute permeability in X, Y and Z directions and net to gross ratio are estimated in laboratory from core analysis on core samples and from well logs. Core samples are prepared from core barrels collected from reservoir by coring operation. Core samples are tested in mercury porosimeter and gas porosimeter to measure porosity in rock samples. Absolute permeability is measured by liquid permeameter.

Porosity Measurement and Distribution:

In this project core samples have been prepared for porosity and permeability measurements. Five core plugs have been cut from core barrel in each X,Y and Z directions for porosity and permeability measurements. Altogether twenty core plugs have been prepared. Three core plugs have been tested in gas porosimeter and porosity 0.18, 0.16 and 0.19 have been found. Working principle of gas porosimeter is as shown in figure 3.11.

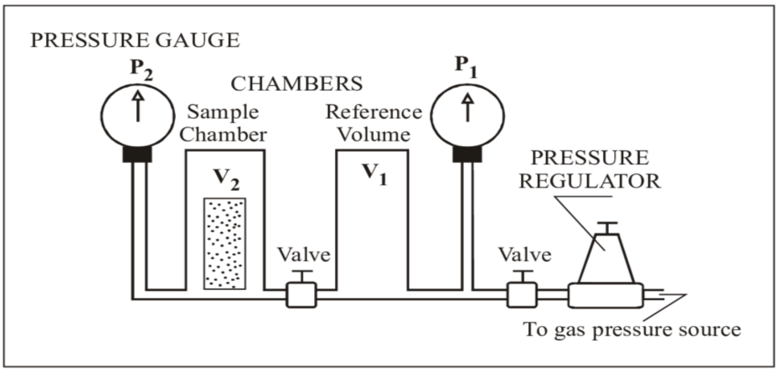

Figure 3.11: Working principle of gas porosimeter

Again three pieces of rock has been tested in mercury porosimeter and porosity 0.15, 0.14 and 0.16 have been found. Working principle of mercury porosimeter is as shown in figure 3.12. All tested values of porosity have been processed and input into petrophysical modeling software.

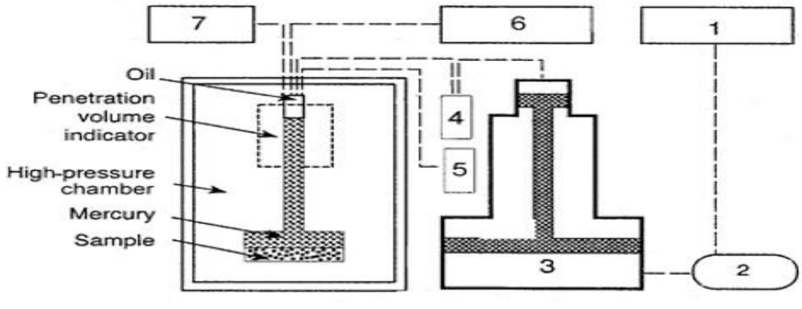

Figure 3.12: Working principle of mercury porosimeter

Porosity is also estimated from porosity logs. Porosity logs have been scaled up by averaging method along the log passed grid cells. Transformation and variogram have been made from scaled up well logs. Porosity has been distributed in all grid cells of the reservoir as shown in figure 3.13 using transformation and variogram by Sequential Gaussian Simulation (GSS) algorithm. Porosity distribution has following statistical values:

- Minimum is 0.1023
- Maximum is 0.2566
- Mean is 0.1727
- Standard Deviation is 0.0366
- Variance is 0.0013

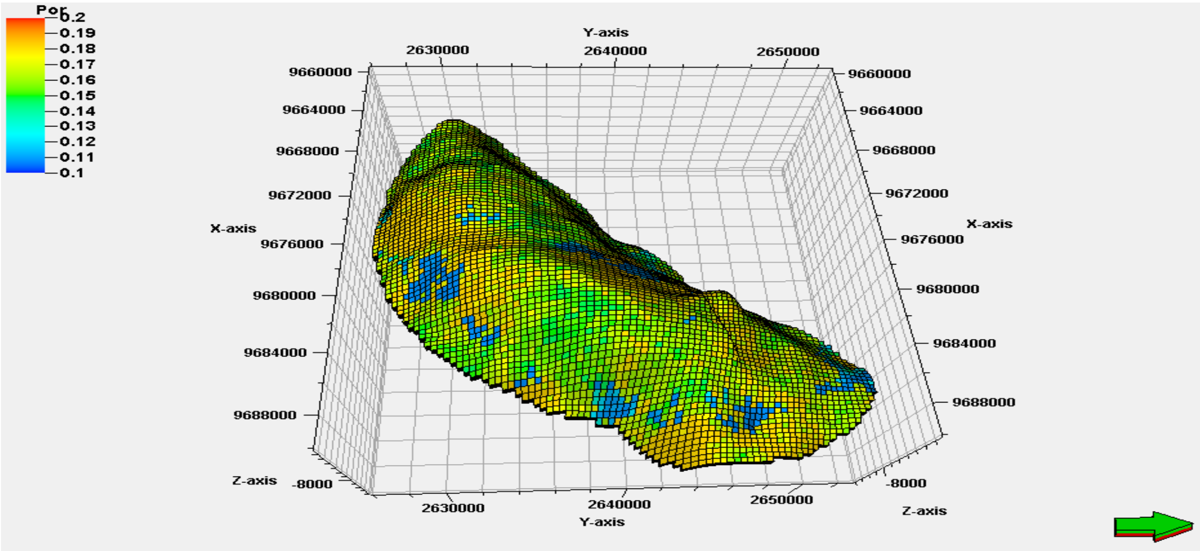

(a)

Name	Type	Min	Max	Delta	N	Mean	Std	Var	Sum
Property	Cont.	0.1023	0.2566	0.1543	297472	0.1727	0.0366	0.0013	51361.2075

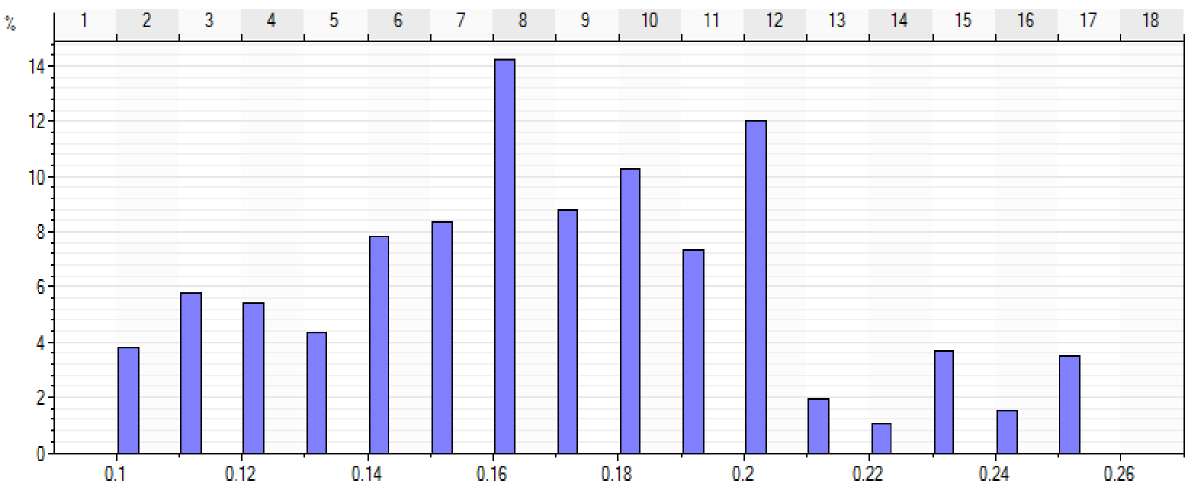

(b)

Figure 3.13: a) Porosity distribution in grid cell of reservoir model and b) statistics of porosity distribution

Permeability Measurement and Distribution:

Permeability in reservoir rock is estimated in laboratory and by deriving from well logs. Five core plugs of each three directions (X, Y and Z) have been taken for test in liquid permeameter as shown in figure 3.14. The test results are as follows:

Table 3.2: Permeability test result

Direction	Sample1 mD	Sample 2 mD	Sample 3 mD	Sample 4 mD	Sample 5 mD
X	120	125	115	110	112
Y	111	121	124	109	108
Z	100	99	120	112	121

Figure 3.14: Liquid permeameter

Permeability (in X direction) log has been derived from porosity log and scaled up by averaging method along the log passed grid cells. Transformation and variogram have been made from scaled up well logs. Permeability has been distributed in all grid cells of the reservoir as shown in figure 3.15 using transformation and variogram by Sequential Gaussian Simulation (GSS) algorithm. Permeability distribution has following statistical values:

- Minimum is 0.0 mD
- Maximum is 1052 mD
- Mean is 121 mD
- Standard Deviation is 198 mD
- Variance is 39319 mD

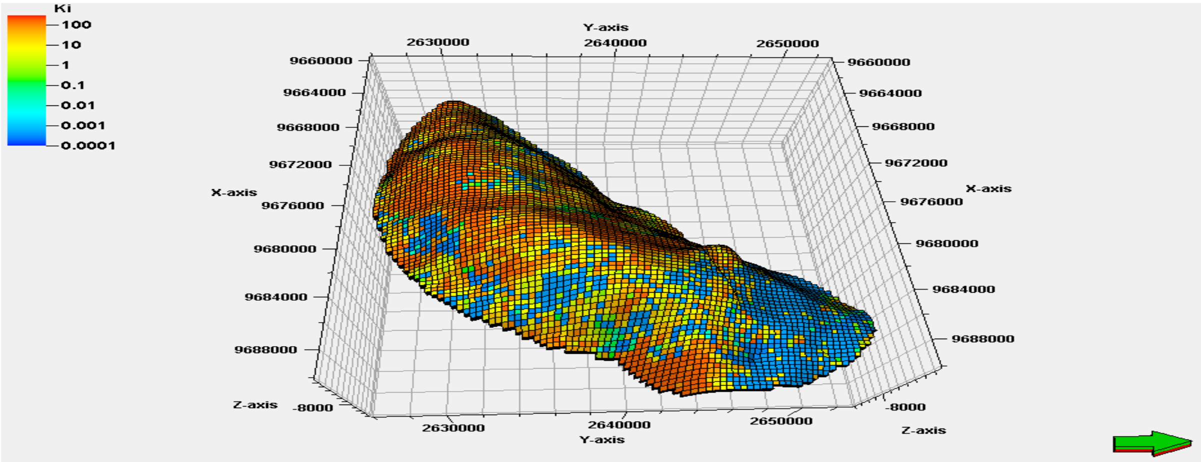

(a)

Name	Type	Min	Max	Delta	N	Mean	Std	Var	Sum
Property	Cont.	0	1052	1052	297472	121	198	39319	35945809

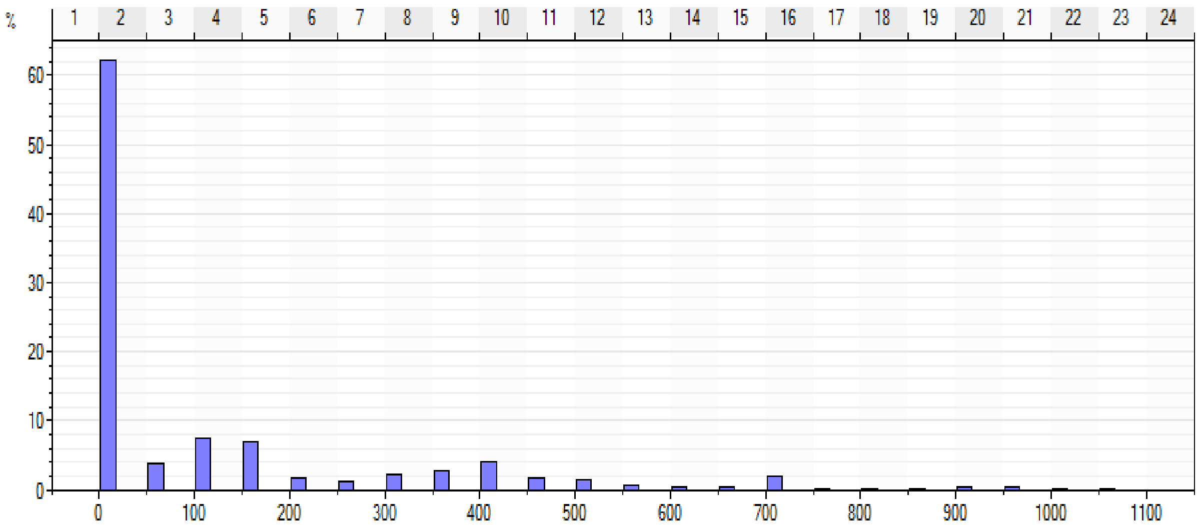

(b)

Figure 3.15: a) Distribution of absolute permeability of X direction in grid cells of reservoir model and b) statistics of permeability distribution

Similarly permeability (in Y direction) log has been derived from porosity log and scaled up by averaging method along the log passed grid cells. Transformation and variogram have been made from scaled up well logs. Permeability has been distributed in all grid cells of the reservoir as shown in figure 3.16 using transformation and variogram by Sequential Gaussian Simulation (GSS) algorithm. Permeability distribution has following statistical values:

- Minimum is 0.0 mD
- Maximum is 1052 mD
- Mean is 121 mD
- Standard Deviation is 198 mD
- Variance is 39319 mD

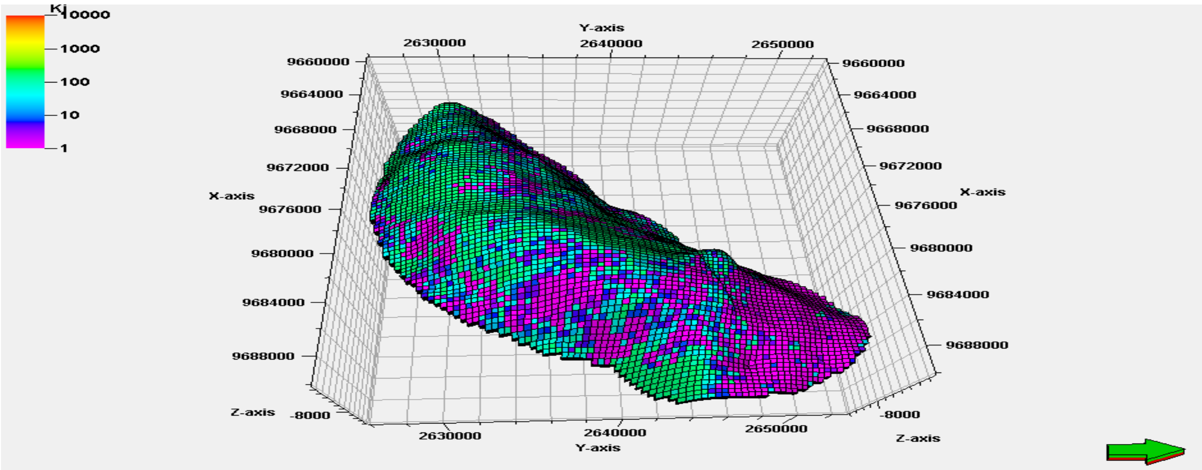

(a)

Name	Type	Min	Max	Delta	N	Mean	Std	Var	Sum
Property	Cont.	0	1052	1052	297472	121	198	39319	35945809

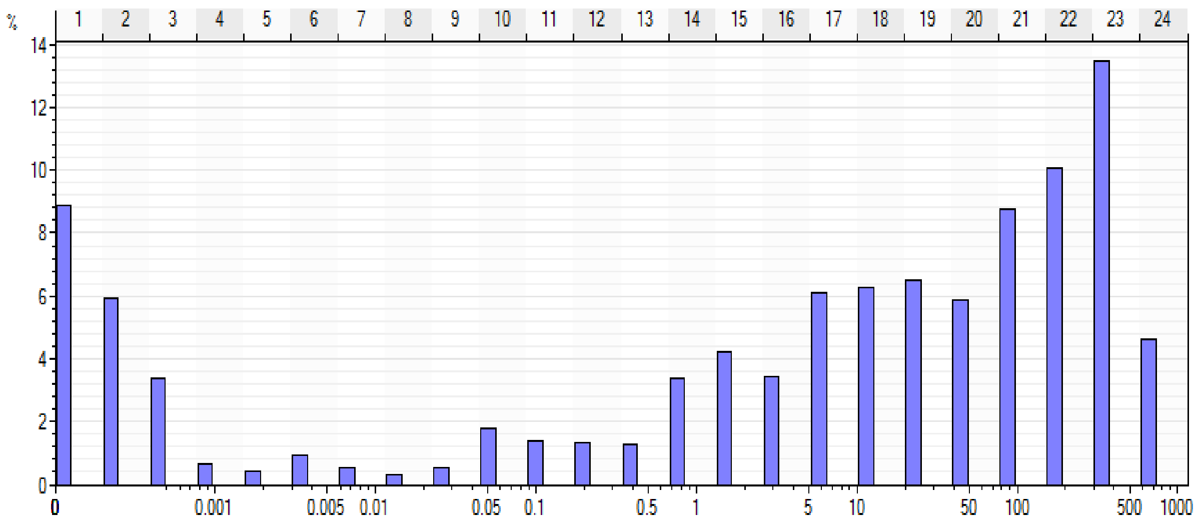

(b)

Figure 3.16: a) Distribution of absolute permeability of Y direction in grid cells of reservoir model and b) statistics of permeability distribution

Similarly permeability (in Z direction) log has been derived from porosity log and scaled up by averaging method along the log passed grid cells. Transformation and variogram have been made from scaled up well logs. Permeability has been distributed in all grid cells of the reservoir as shown in figure 3.17 using transformation and variogram by Sequential Gaussian Simulation (GSS) algorithm. Permeability distribution has following statistical values:

- Minimum is 0.0 mD
- Maximum is 1052 mD
- Mean is 121 mD
- Standard Deviation is 198 mD
- Variance is 39319 mD

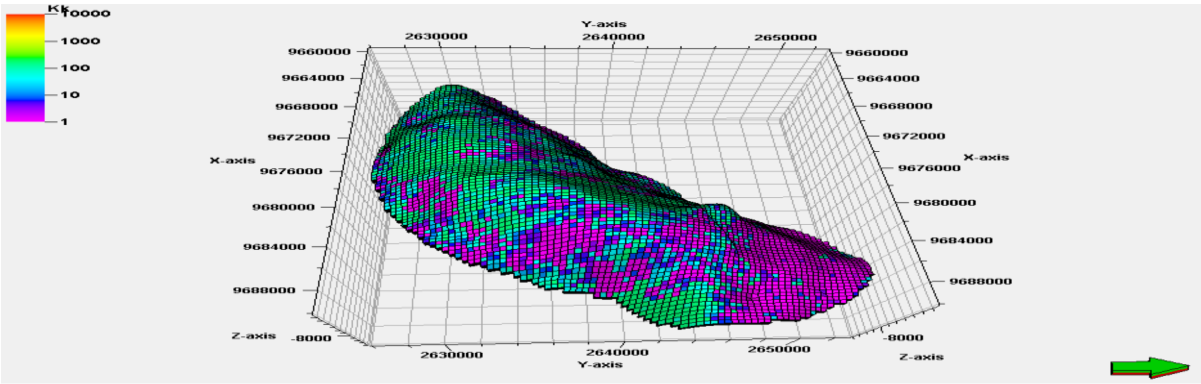

(a)

Name	Type	Min	Max	Delta	N	Mean	Std	Var	Sum
Property	Cont.	0	1052	1052	297472	121	198	39319	35945809

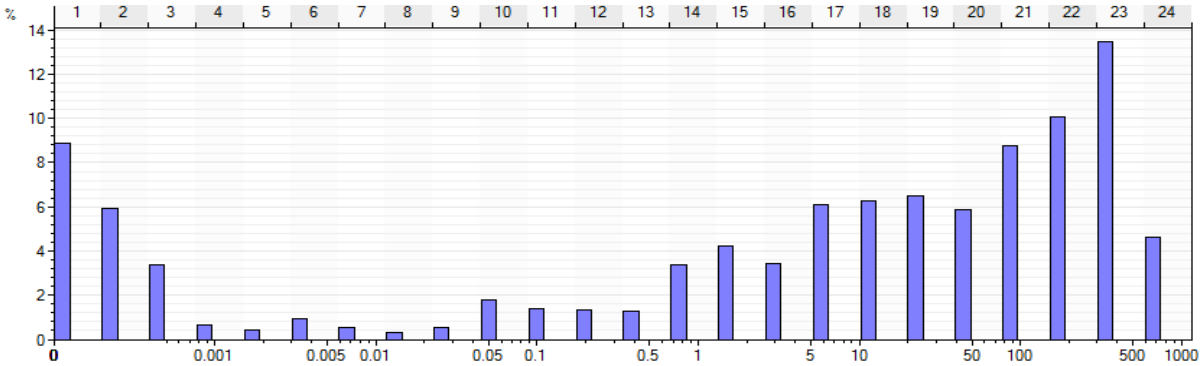

(b)

Figure 3.17: a) Distribution of absolute permeability of Z direction in grid cells of reservoir model and b) statistics of permeability distribution

Net to Gross Ratio (NTG) Measurement and Distribution:

Net to gross ratio represents the shale content in the reservoir rock. It is define as a fraction. If no shale is present in reservoir rock then its value is 1.00 and if 20% shale is present in reservoir rock by volume then its value is 0.8. Here clean sand is considered, so the net to gross ratio value is 1.0. The value of net to gross ratio has been distributed in all grid cells of the reservoir model as shown in figure 3.18.

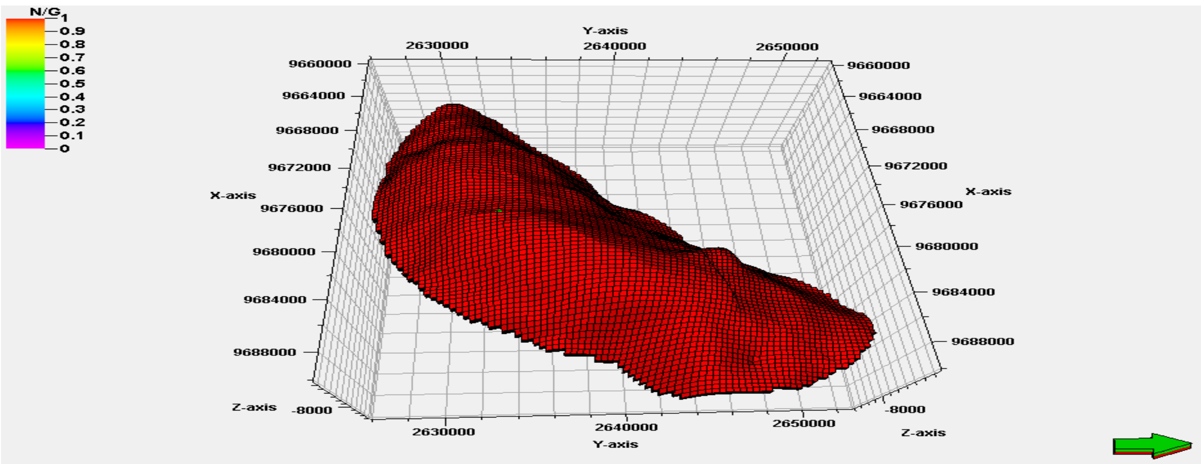

Figure 3.18: Distribution of shale content in reservoir model

3.1.4 Pressure Volume Temperature (PVT) Properties of Reservoir Fluids in Haripur Field

The reservoir has oil with dissolved gas and water. The oil zone lies above the water zone due to the hydrostatic equilibrium of the fluid phases shown in figure 3.19. Oil sample has been collected and its properties have been estimated by chromatograph and Pressure Volume Temperature (PVT) cell to model the oil by PVTi software. Reservoir water sample has collected and its properties have estimated in lab.

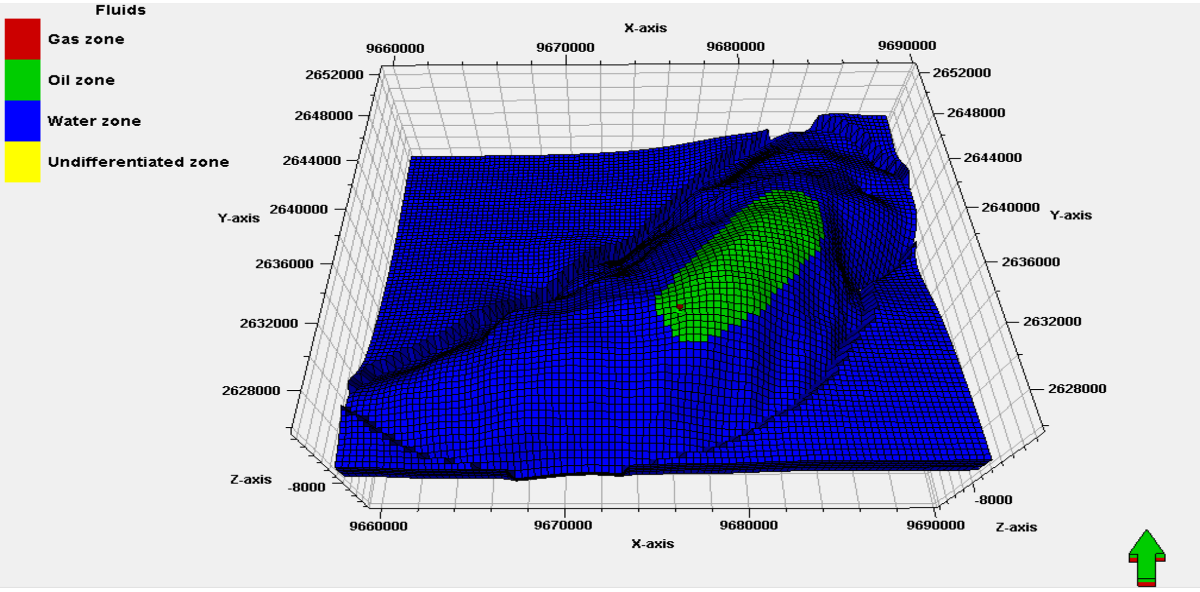

Figure 3.19: Fluid phases in reservoir

Reservoir Oil

Reservoir oil of Haripur field is shown in figure 3.20. The oil has been tested in chromatograph with Thermal Conductivity Detector (TCD) and Flame Ionization Detector (FID) as shown figure 3.21 in order to determine the composition of the reservoir oil.

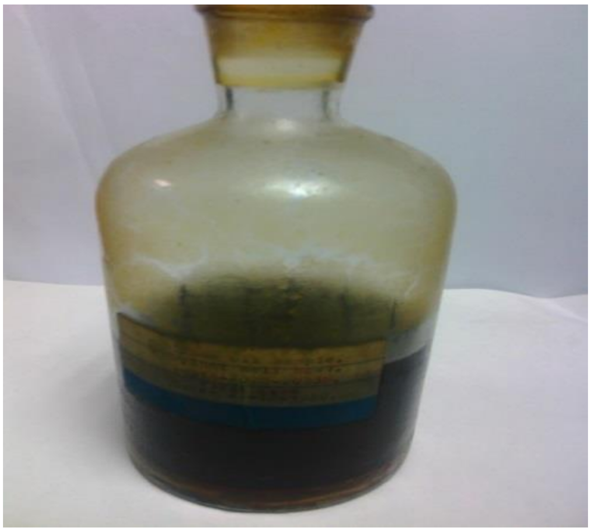

Figure 3.20: Oil sample of Haripur field

Figure 3.21: Chromatograph with TCD and FID

The chromatograph has generated two chromatograms such as chromatogram of TCD as shown in figure 3.22 and chromatogram of FID as shown figure 3.23. From these two chromatograms oil composition has been estimated for determining PVT properties of oil as shown in table 3.3.

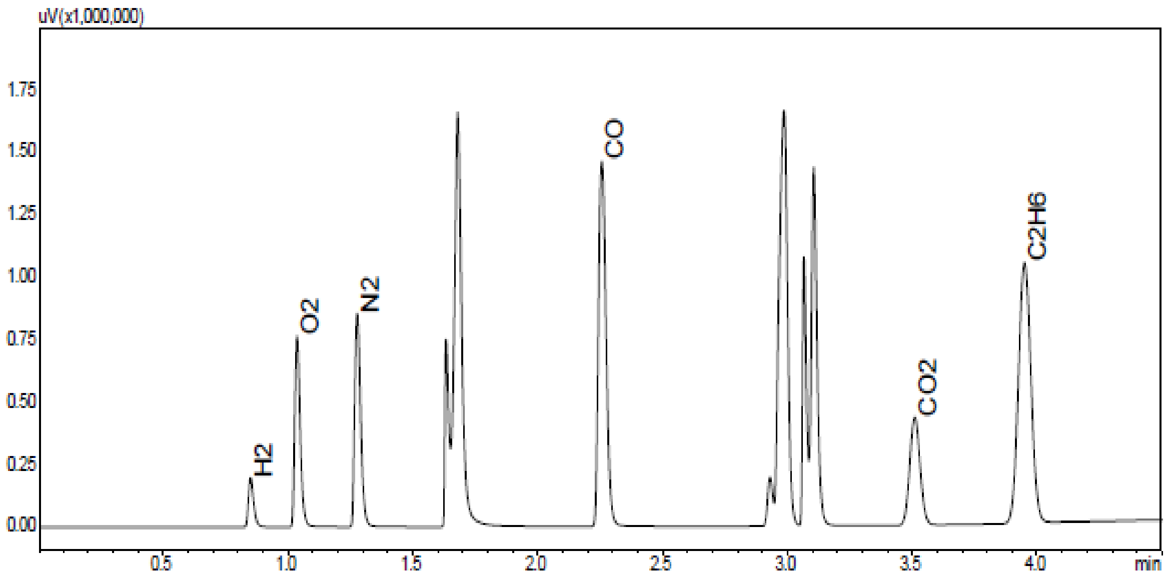

Figure 3.22: Chromatogram of TCD

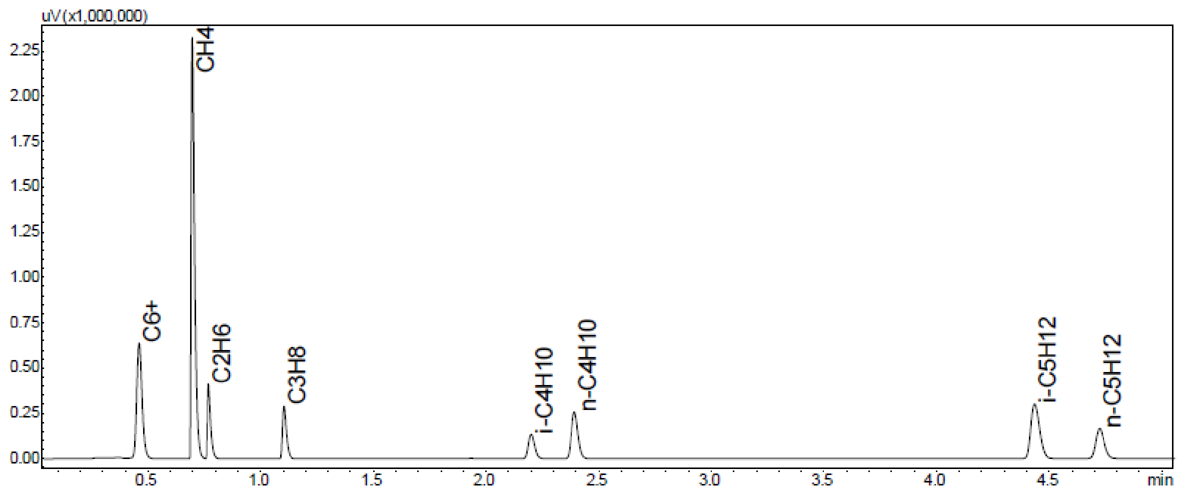

Figure 3.23: Chromatogram of FID

Table 3.3: Oil composition of Haripur field

Component	Mole %	Molecular Weight MW	Specific Gravity SG
CO_2	0.28	44.01	0.5
N_2	0.30	28.02	0.47
C_1	41.52	16.04	0.33
C_2	5.10	30.07	0.45
C_3	1.89	44.09	0.5077
iC_4	0.80	58.12	0.5613
nC_4	0.95	58.12	0.5844
iC_5	0.53	72.15	0.6274
nC_5	0.48	72.15	0.6301
C_6	1.65	86.17	0.6604
C_{7+}	46.50	220.857	0.85336

Oil sample has been tested in PVT cell as shown in figure 3.24. The laboratory experiments such as constant composition expansion (CCE) and differential liberation (DL) test have been performed in PVT cell. Oil relative volume at different pressure has been determined in CCE experiment as shown in table 3.4 and Gas Oil Ratio (GOR) has been determined in DL experiment as shown in table 3.5. The bubble point is 2989.997 psia and API gravity of oil is 28. The chromatograph estimated oil composition and PVT cell estimated CCE and DL experiments data has been inserted into PVTi software to model the oil sample. PVTi software has simulated the CCE and DL experiments and the simulated data has been matched with PVT cell data by changing Equation of State (EOS) parameters in regression analysis. After the best curve fitting, the PVTi software has generated the PVT properties of oil.

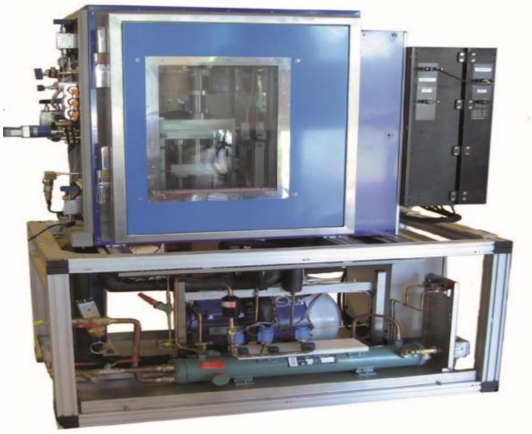

Figure 3.24: PVT Cell

Table 3.4: CCE data

Pressure	Rel Vol	Pressure	Rel Vol
PSIA	V/Vsat	PSIA	V/Vsat
5000	0.9755	2989.997 (BP)	1
4798.999	0.9776	2692.467	1.0338
4597.999	0.9798	2394.937	1.0783
4396.999	0.982	2097.407	1.1386
4195.999	0.9843	1799.877	1.2233
3994.998	0.9867	1502.346	1.3477
3793.998	0.9891	1204.816	1.5426
3592.998	0.9917	907.286	1.88
3391.998	0.9943	609.756	2.5749
3190.998	0.9971	312.226	4.6773

Table 3.5: DLE data

Pressure	GOR	Oil.re.vol	Liq_den.	Gas_Grav	Vapor Z.	Gas FVF
psia	Mscf/stb	rb/stb	lb/ft3	DL	Factor, DL	rb/Mscf
2989.997	0.5502	1.355	42.7953			
2692.467	0.4893	1.3285	43.2579	0.6266	0.9329	1.1862
2394.937	0.4311	1.3013	43.722	0.6264	0.9274	1.3257
2097.407	0.3754	1.2786	44.1888	0.627	0.9243	1.5087
1799.877	0.3219	1.2549	44.6593	0.6288	0.9239	1.7573
1502.346	0.2705	1.2319	45.1345	0.6321	0.9264	2.1109
1204.816	0.2209	1.2094	45.616	0.638	0.9318	2.6476
907.286	0.1727	1.1874	46.1058	0.6485	0.9404	3.5482
609.756	0.1256	1.1653	46.6095	0.6695	0.9522	5.346
312.226	0.0776	1.142	47.1461	0.7243	0.9677	10.6101
14.695	0	1.0934	48.045	1.2403		
14.695	0	1	52.5337			

Reservoir fluid modeling has been performed by simulating the laboratory experiments such as constant composition expansion (CCE), bubble point (BP), differential liberation (DL), multistage separator test and compositional variation with depth by two phase flash algorithms with input of the composition of reservoir oil, thermodynamic properties of pure components and binary interaction coefficient by using Peng-Robinson (PR) equation of state. The simulated experimental results have been matched with real experimental results as shown in figure 3.25. When the perfect matched has achieved by tuning the EOS parameters in regression analysis then the EOS has been used to estimate phase diagram as shown in figure 3.26. Oil formation volume factor as shown in figure 3.27, oil viscosity as shown in figure 3.28, and gas oil ratio as shown in figure 3.29 have been estimated by using EOS.

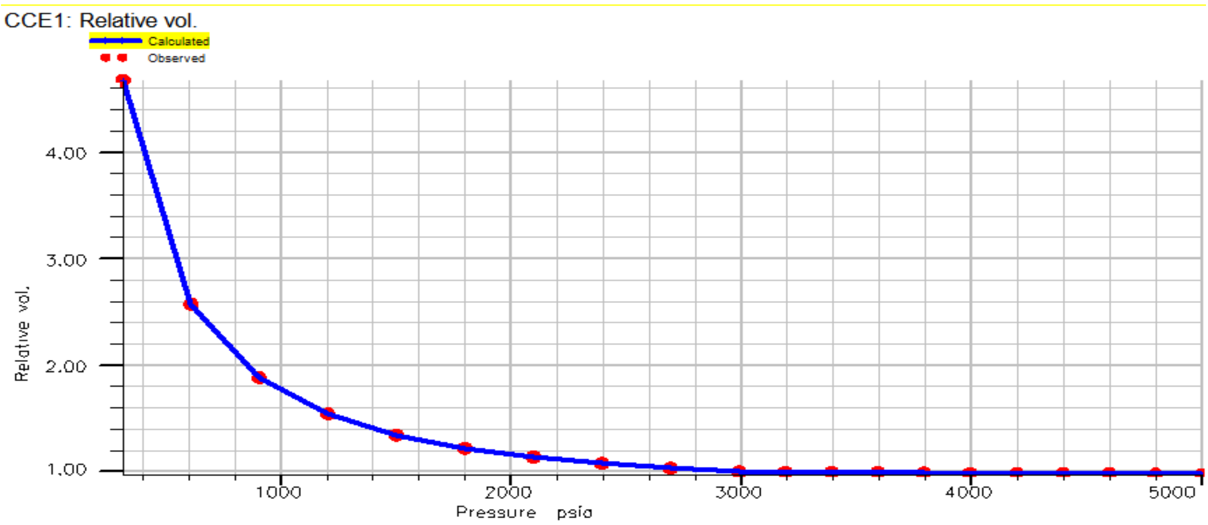

Figure 3.25: Matching of simulated and observed results

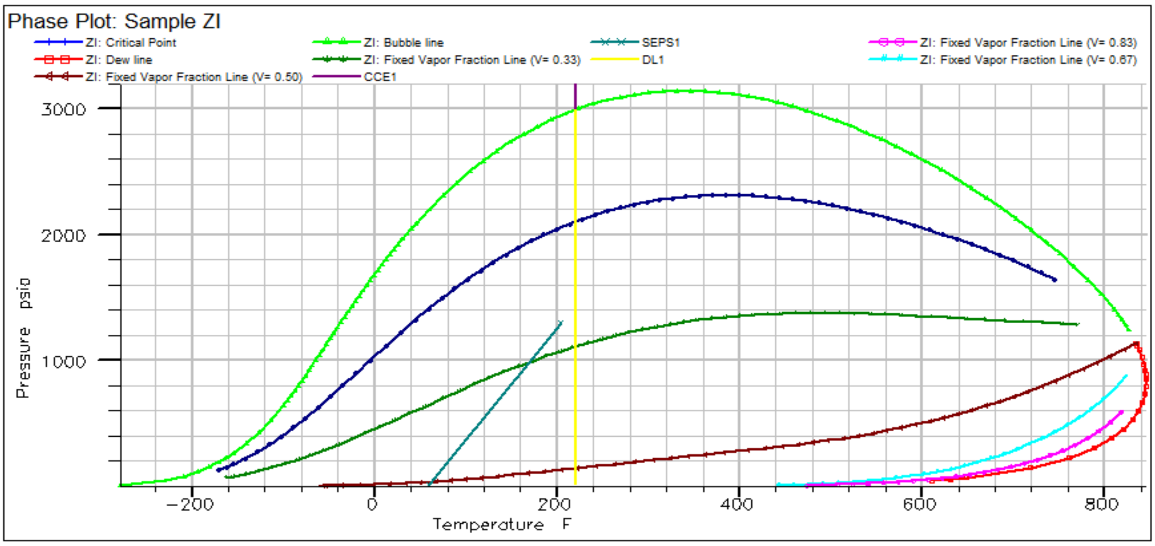

Figure 3.26: Phase diagram of oil sample

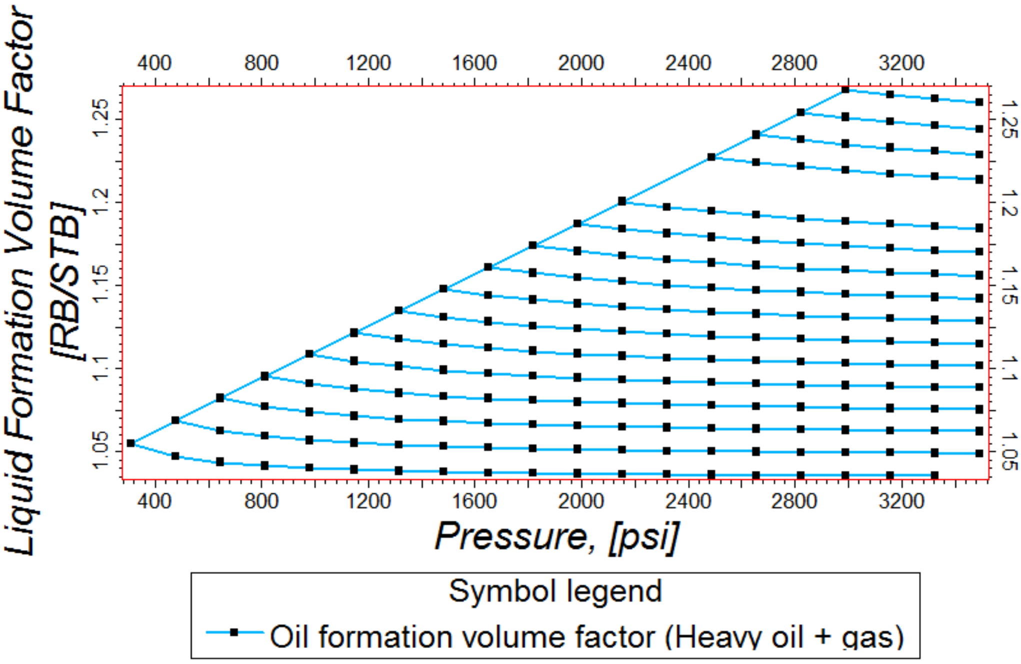

Figure 3.27: Profile of oil formation volume factor with pressure

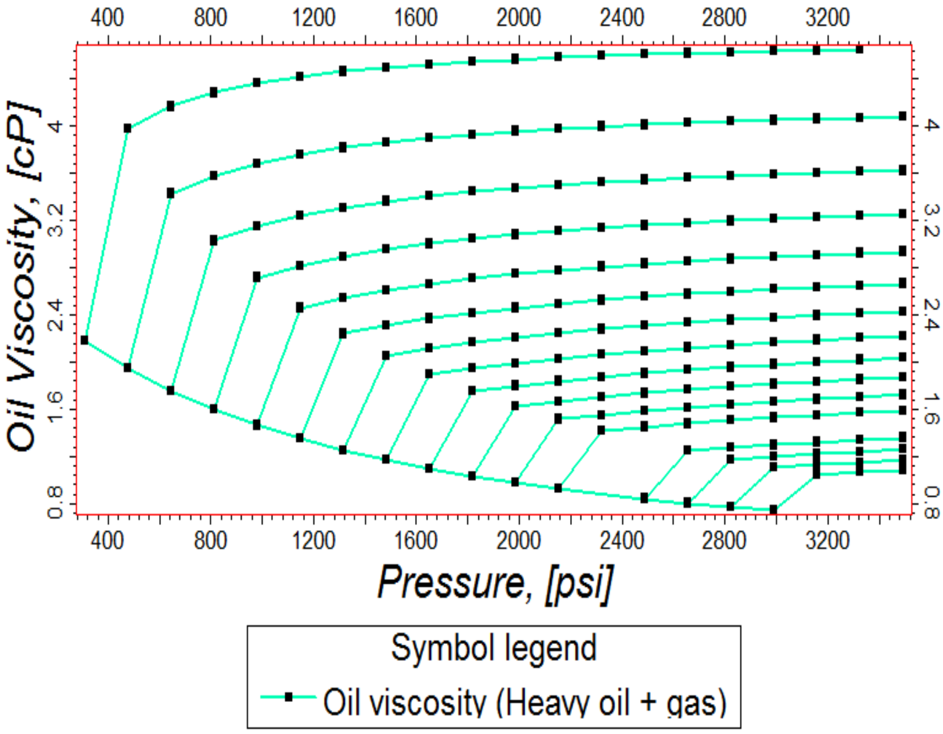

Figure 3.28: Profile of oil viscosity with pressure

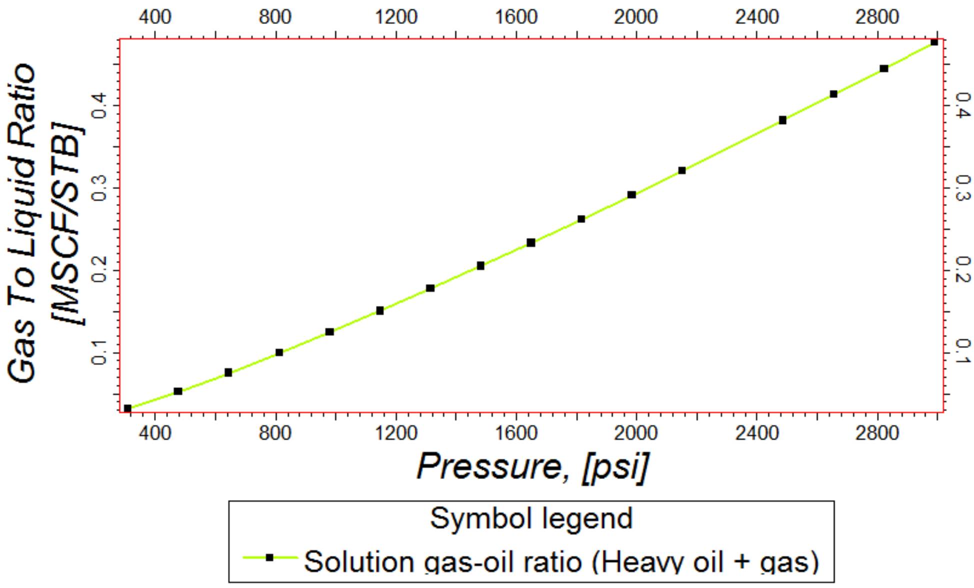

Figure 3.29: Profile of solution gas oil ratio with pressure

Reservoir Water

Physical and chemical properties of reservoir water in oil zone of Haripur field are estimated in laboratory.

The contents in water of oil reservoirs are as follows:-

- Total dissolved salts (consisting mainly of NaCl) is 1,00,000 ppm
- Solution gas (consisting mainly of methane and ethane) is 30 scf/stb

The amount of water connected with a reservoir is as important as the properties of the water, particularly in material-balance calculations where water expansion (compressibility times water volume) may contribute significantly to pressure support.

From a production point of view, Water mobility is calculated from following data

- Water saturations , Sw is 0.22
- Water viscosity, µw is 0.52 cp
- Formation volume factor (FVF), Bw is 1.0034

For surface-processing calculations following parameters are estimated

- Water composition
- Water content in the produced wellstream
- Conditions where water and hydrocarbons coexist must be defined

3.1.5: Saturation Function Properties in Haripur Field

Oil-Water relative permeability and capillary pressure have been estimated by laboratory method and mathematical model. Core plugs as shown in figure 3.30 from reservoir rock have been prepared by core plug preparation equipment. The core plugs have been used to estimate the relative permeability and capillary pressure in laboratory.

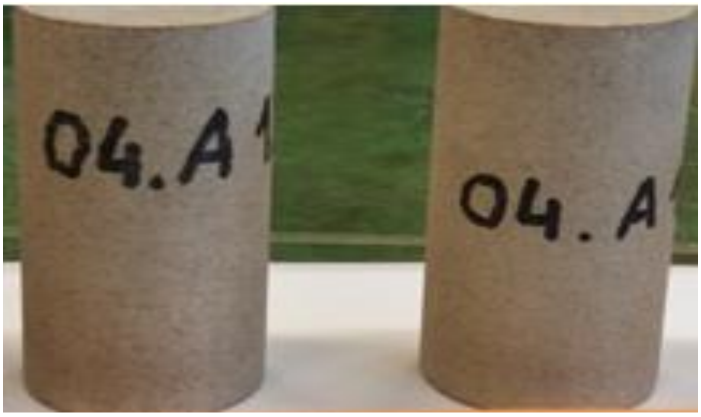

Figure 3.30: Core plugs

Relative Permeability

Oil-Water relative permeability is measured by relative permeameter as shown in figure 3.31. During the flow of reservoir oil and water through the core plug, the oil and water flow rate and pressure drop have been measures. The data found in lab test has been inserted into software to determine the relative permeability for oil and water phases.

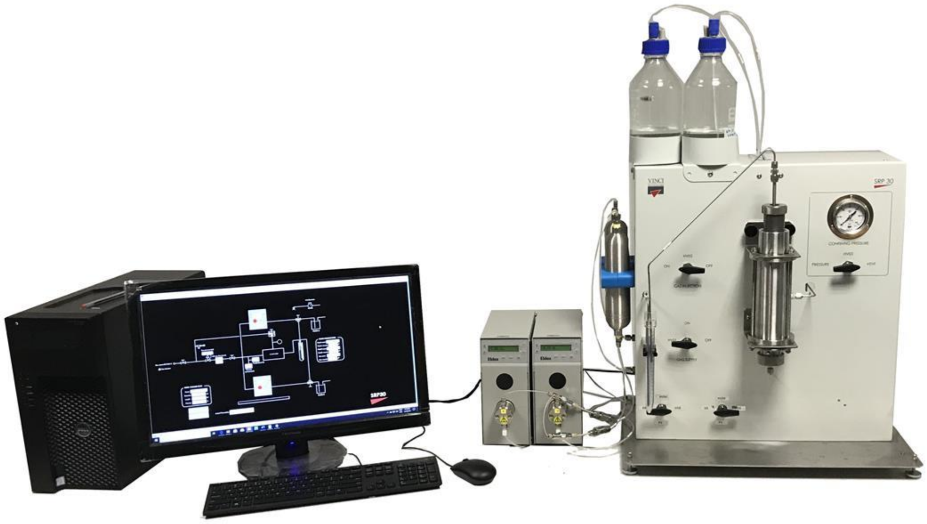

Figure 3.31: Oil water relative permeameter

Relative permeability as shown in figure 3.32 is the ability of formation to transport a fluid in the presence of other fluid. In this case there are two fluids such as oil and water are flowing through the formation. Relative permeability of oil-water in sandstone system is modeled using correlation developed by Corey.

For Oil

$$K_{ro} = K_{ro}(S_{w\min})\left[\frac{S_{w\max} - S_w - S_{orw}}{S_{w\max} - S_{wi} - S_{orw}}\right]^{C_o} \quad \ldots\ldots\ldots\ldots\ldots\ldots\ldots\ldots\ldots\ldots\ldots\ldots(EQ\ 3.1)$$

For values between S_{wmin} and (1-S_{orw}):

Where,

K_{ro} is relative permeability of oil

$K_{ro}(S_{wmin})$ is relative permeability of oil at minimum water saturation and the value is 0.9

S_{wmax} is maximum water saturation and the value is 1.00

S_w is water saturation

S_{orw} is residual oil saturation to water and the value is 0.2

S_{wi} is initial water saturation and the value is 0.2

C_o is the Corey oil exponent and the value is 3.00

For Water

$$K_{rw} = K_{rw}(S_{orw})\left[\frac{S_w - S_{wcr}}{S_{w\max} - S_{wcr} - S_{orw}}\right]^{C_w} \quad \ldots\ldots\ldots\ldots\ldots\ldots\ldots\ldots\ldots\ldots\ldots\ldots(EQ\ 3.2)$$

For values between S_{wcr} and (1-S_{orw})

Where,

K_{rw} is relative permeability of water

$K_{rw}(S_{orw})$ is relative permeability of water at residual oil saturation to water and the value is 0.8

S_w is water saturation

S_{wcr} is critical water saturation and the value is 0.22. This must be greater than or equal to S_{wmin} (minimum water saturation is 0.2)

S_{wmax} is maximum water saturation and the value is 1.00

S_{orw} is residual oil saturation to water value is 0.2
C_w is the Corey water exponent and the value is 4.00

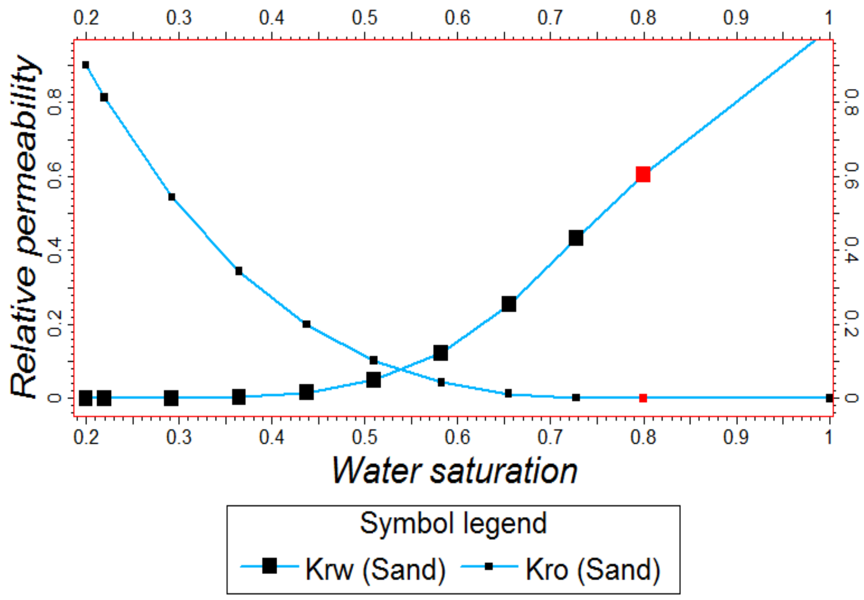

Figure 3.32: Oil water relative permeability

Capillary Pressure

Mercury capillary pressure unit as shown in figure 3.33 is used to determine the capillary pressure of the reservoir rock in laboratory. The data found in lab test inserted into software to model the capillary pressure.

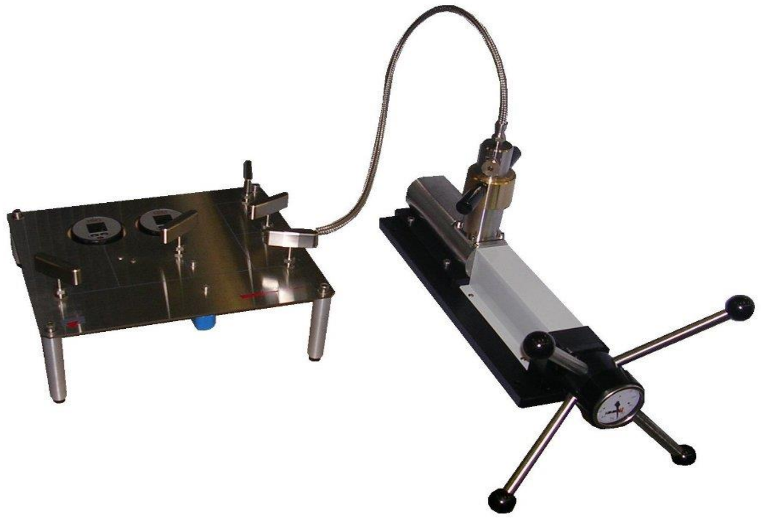

Figure 3.33: Oil water capillary pressure unit

Capillary pressure as shown in figure 3.34 is the phase pressure difference between oil phase and water phase (Pcow=Po-Pw). At oil-water contact the capillary pressure is zero and the capillary pressure increases with decreasing the depth from the contact point. To develop the capillary pressure model the following values are used.

Max Pc is Maximum capillary pressure and the value is 13 psia

Sw@Pc=0 is Water saturation when the capillary pressure is zero and the value is 0.8

Bro/Corao is Pore size distribution for oil and the value is 3.86

Bro/Coraw is Pore size distribution for water and the value is 3.86

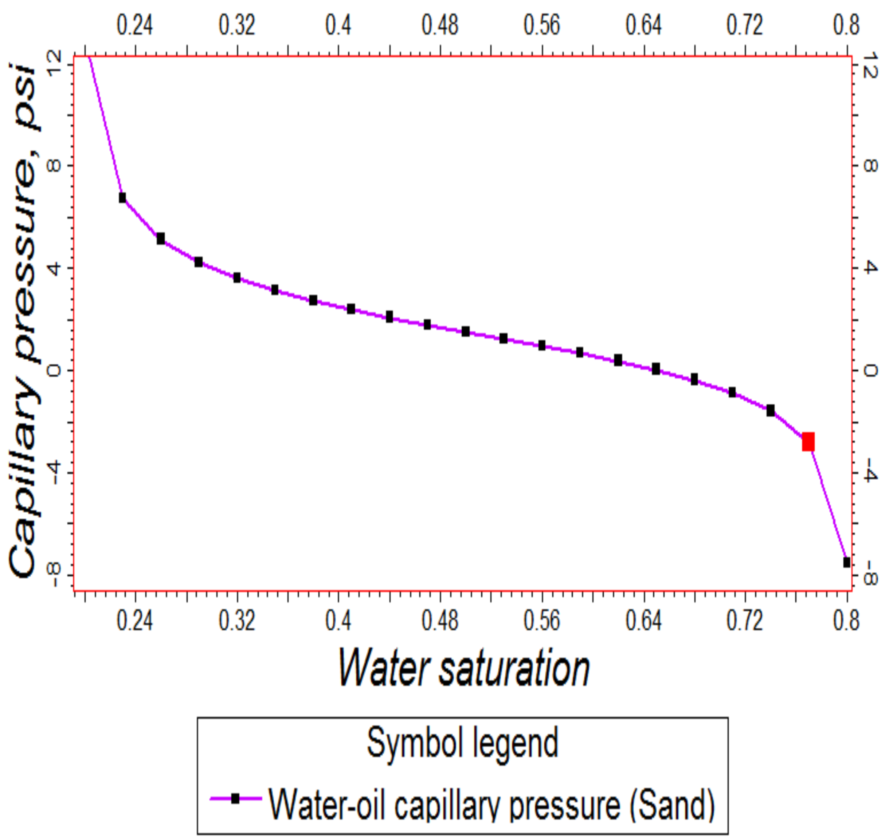

Figure 3.34: Oil water capillary pressure

The combined relative permeability and capillary pressure curve as shown in figure 3.35 is used in oil & gas industries to determine the relative permeability of oil and water along with capillary pressure at a specific water saturation value because during the oil production the water saturation increases with time.

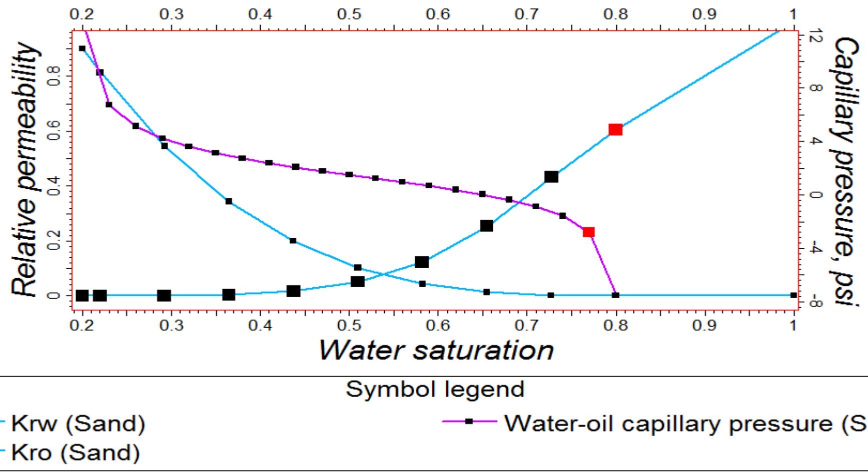

Figure 3.35: Oil water relative permeability and capillary pressure

Rock Compaction Factor

Rock Compaction factor as shown in figure 3.36 for consolidate sandstone is modeled by Newman correlation.

$C_r = \exp(5.118 - 36.26\varphi + 63.98\varphi^2) \times 10^{-6} \;\; 1/psi$ ....(EQ 3.3)

Where,

Cr is rock compressibility

Φ is porosity and the value is 0.2

Reference pressure is 6000 psia

Maximum pressure is 8000 psia

Minimum pressure is 3000 psia

During the oil production the pore pressure decreases with the time and the pore space becomes compacted this phenomenon is described by the rock compaction factor.

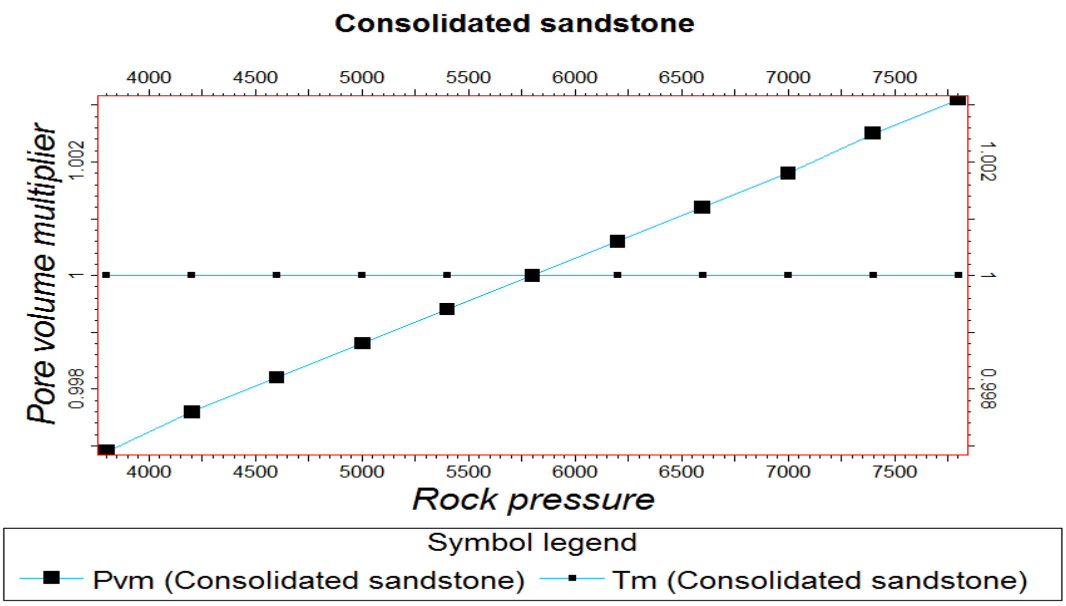

Figure 3.36: Compaction factor in consolidate sandstone

3.1.6 Initialization of Oil Reservoir Condition by Hydrostatic Equilibration in Haripur Field

Fluid pressures and saturation must be assigned in each grid cell of the reservoir model for simulation at initial condition of reservoir. Simulation start from this initial point and advances by calculating fluid pressure and saturation changes due to the production and injection over time. In this reservoir model initial condition has been designed on the basis of the following data:-

- Oil-Water Contact is at depth 6660 ft
- Gas-Oil Contact is at depth 6237 ft
- Datum Depth is 6237 ft
- Pressure at Datum is 3000 psi.

At Gas-Oil Contact (GOC) oil pressure is equal to gas pressure (P_o=P_g=3000 psi). Oil pressure below the datum depth is calculated by $P_o=P_o(GOC, Datum)+(Z-Z_{datum})\rho_o g$. Oil pressure has been estimated at Oil-Water Contact (OWC). At OWC water pressure is equal to oil pressure (Pw=Po at OWC). Water pressure at above the OWC is calculated by $P_w=P_w(OWC)-(Zowc-Z)\ \rho_w g$. Capillary pressure is difference between oil pressure and water pressure ($P_{cow}=P_o-P_w$). Capillary pressure is function of water saturation as shown in figure 3.37.

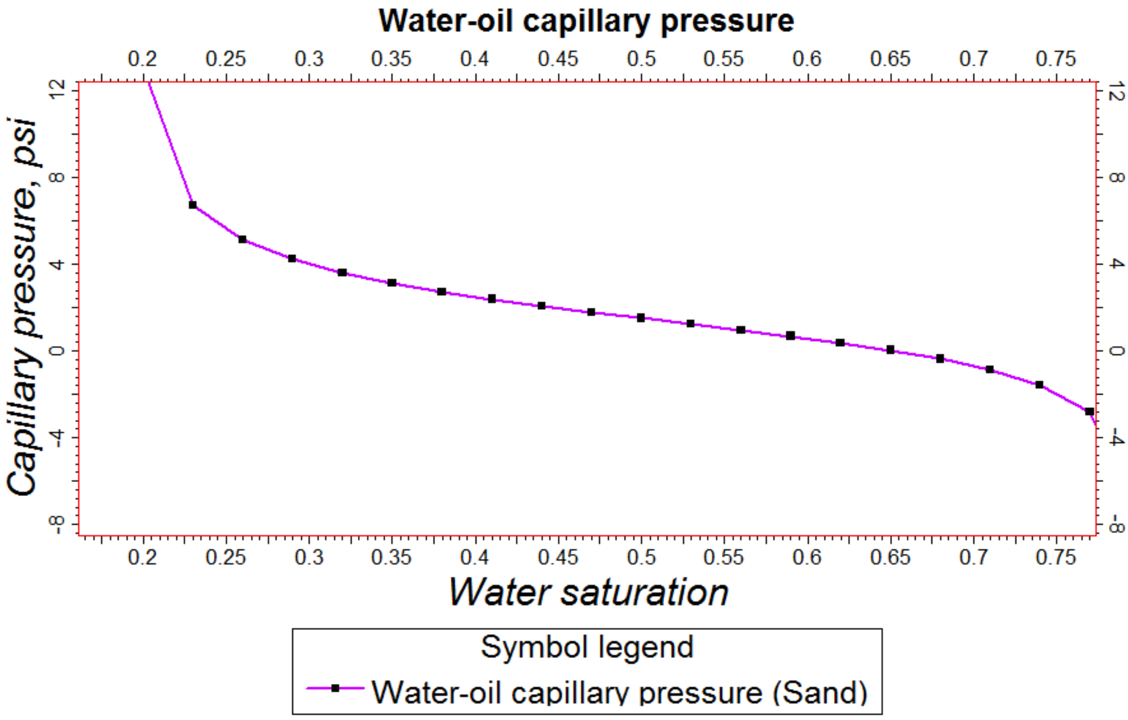

Figure 3.37: Capillary pressure

Water saturation is estimated from capillary pressure curve. For example when capillary pressure is 4 psi then water saturation is 0.28 and oil saturation is 0.72 (S_o=1-S_w). In this method oil pressure is distributed in all grid cells as shown in figure 3.38.

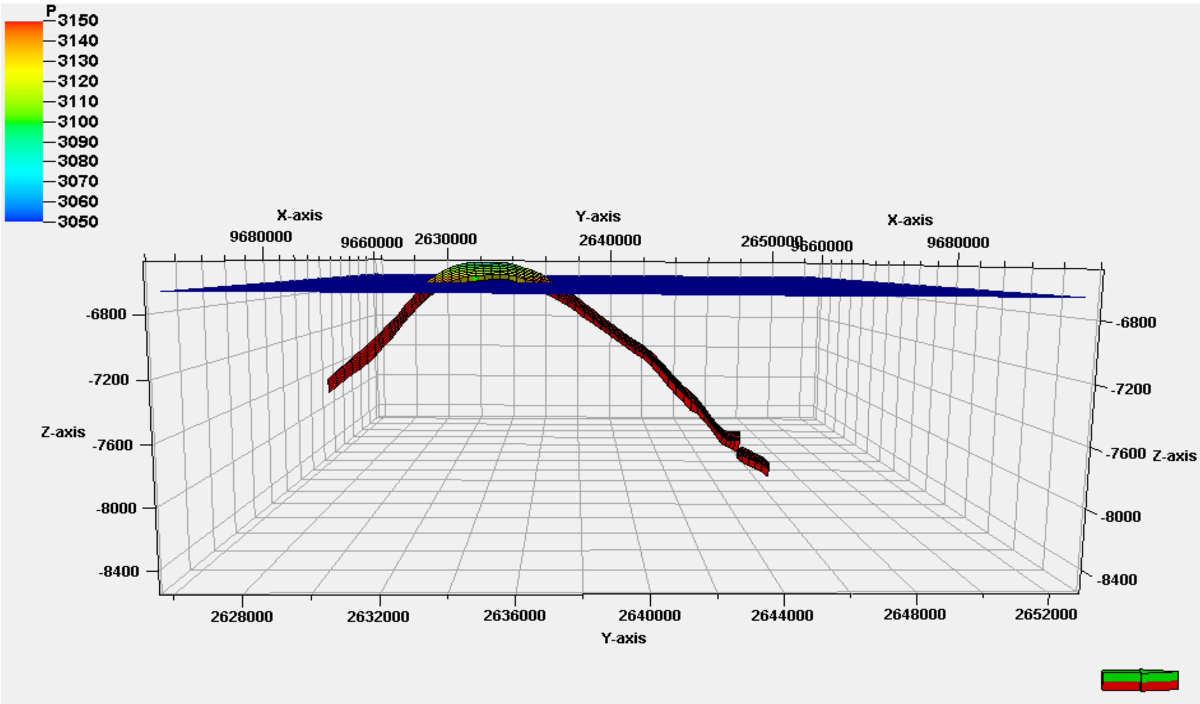

Figure 3.38: Pressure in grid cells along depth

Oil pressure has been distributed in all grid cells of the reservoir as shown in figure 3.39. Minimum pressure is 3050 psi and maximum pressure is 3150 psi.

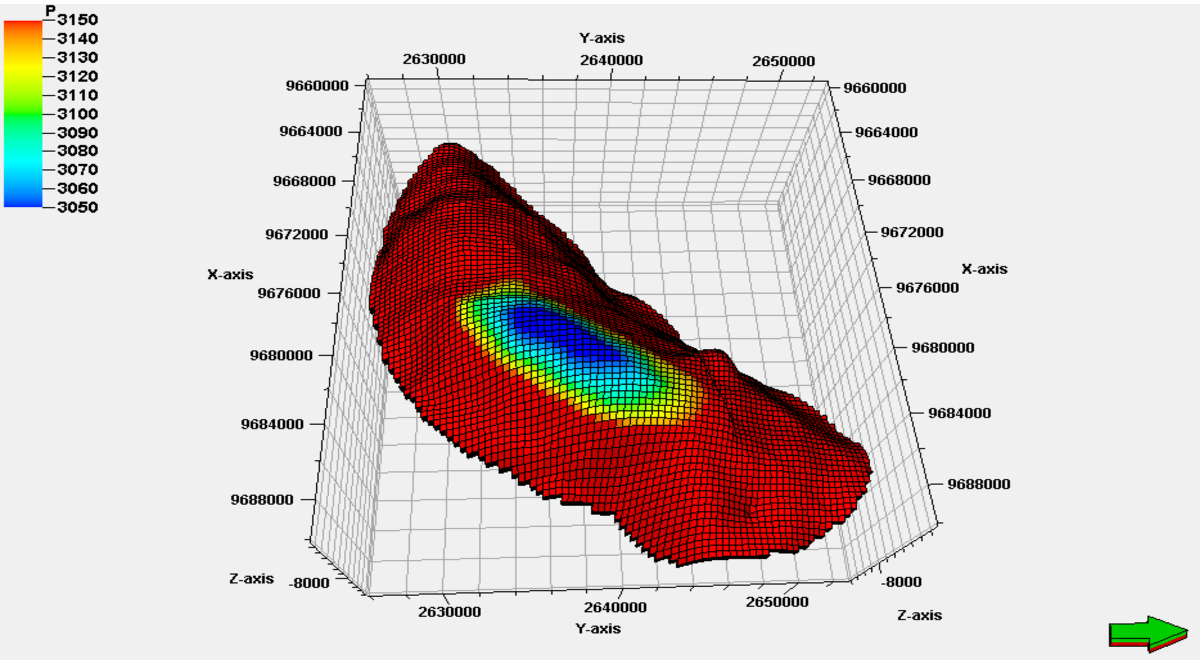

Figure 3.39: Pressure in all grid cells

Water saturation has been distributed in all grid cells of the reservoir as shown in figure 3.40. Minimum water saturation is 0.2 and maximum water saturation is 1.00 psi.

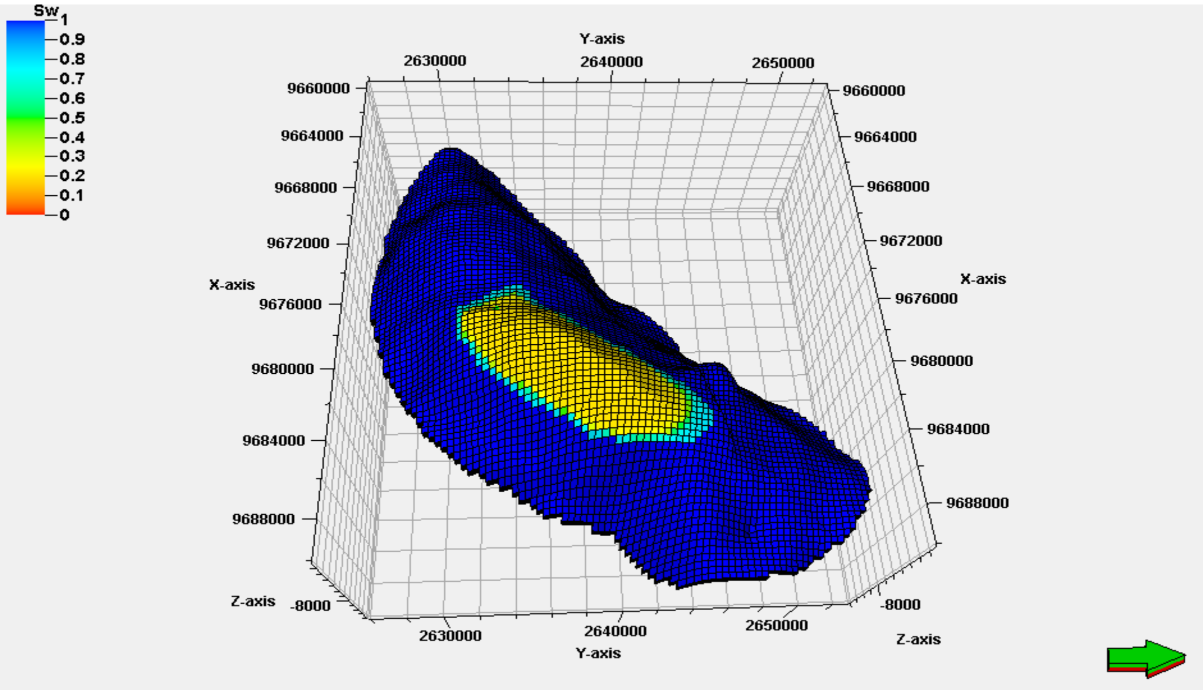

Figure 3.40: Water saturation in all grid cells

Oil saturation has been distributed in all grid cells of the reservoir as shown in figure 3.41. Minimum oil saturation is 0.2 and maximum oil saturation is 0.80 psi.

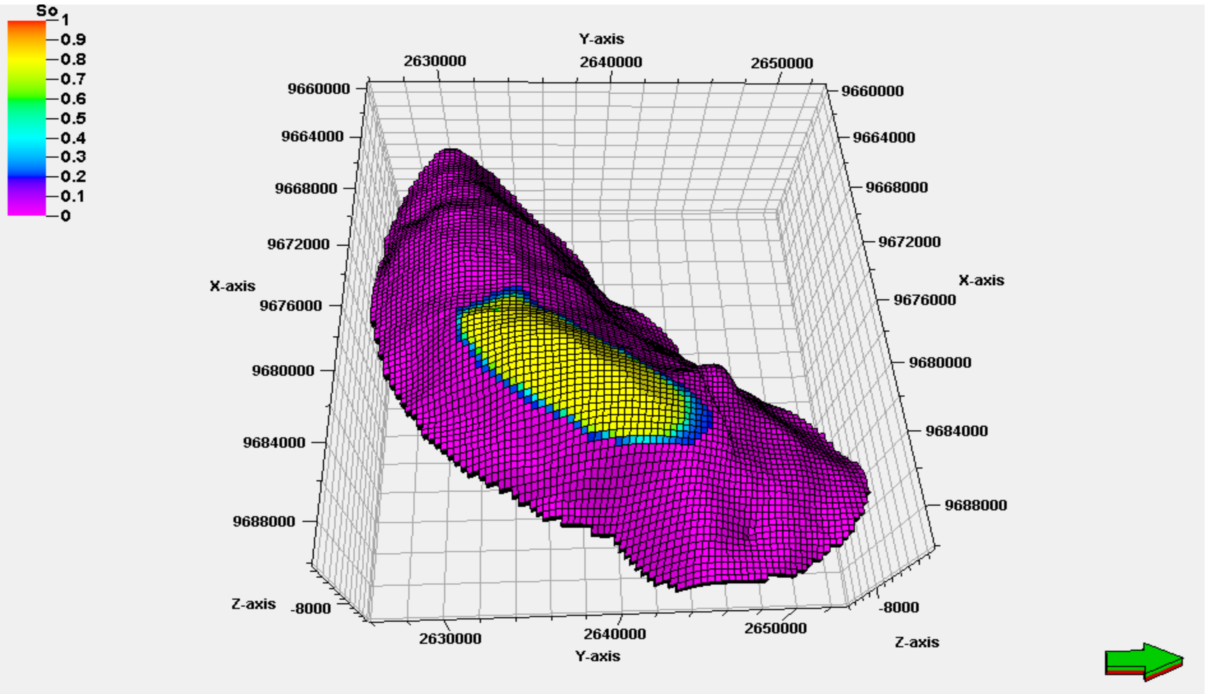

Figure 3.41: Oil saturation in all grid cells

3.1.7: Validation of Oil Reservoir Model in Haripur Field

Reservoir model for simulation purposes is constructed from systemic integration of seismic survey, well logs, fluid contact, petrophysical properties, PVT properties, hydrostatic equilibrium interpretation and analysis data. After constructing the reservoir model wells are placed in the reservoir model similar to the real field and simulate the reservoir models for real production period. The reservoir model generates production rate and pressure. The simulated production rate and pressure are matched with real production rate and pressure to validate the reservoir model. This process is called history matching. Reservoir properties such as absolute permeability, relative permeability, pressure are tuned to get perfect history matching. The reservoir model which gives perfect history matching is treated as representative of the real reservoir. Here oil reservoir in Haripur field has produced oil for seven years. Oil reservoir in Haripur field has been modeled and simulated for seven years to match the oil production rate and pressure history as shown in figure 3.42.

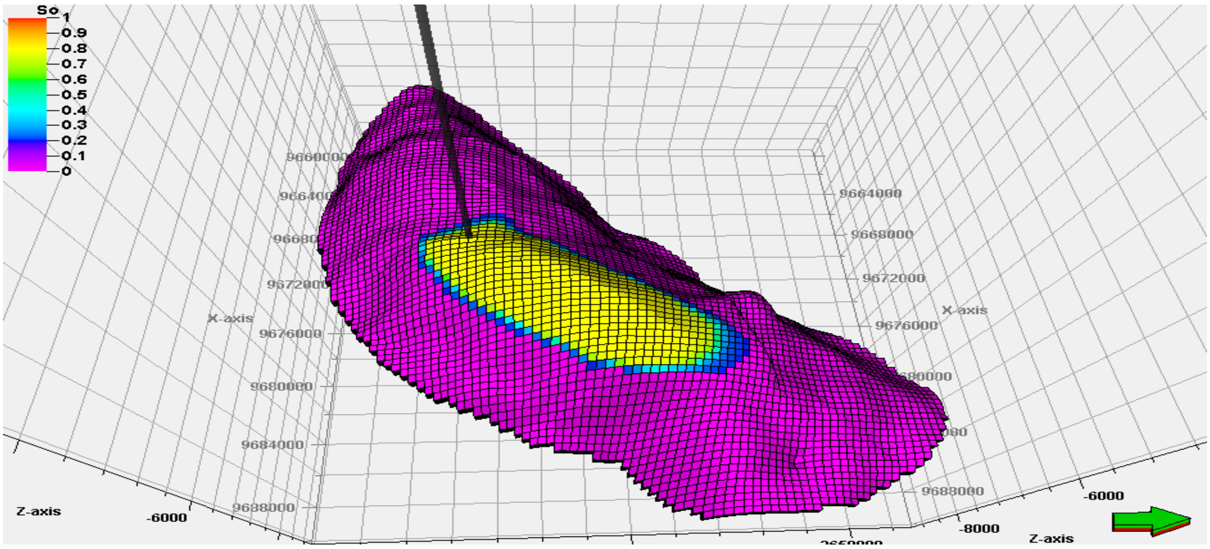

Figure 3.42: Reservoir simulation model with well SY-7

History Matching

The act of adjusting a model of a reservoir until it closely reproduces the past behavior of a reservoir. The historical production and pressures are matched as closely as possible. The accuracy of the history matching depends on the quality of the reservoir model and the quality and quantity of pressure and production data. Once a model has been history matched, it can be used to simulate future reservoir behavior with a higher degree of confidence, particularly if the adjustments are constrained by known geological properties in the reservoir.

Rate History Matching

There are production history from 01 Dec 1987 to 01 Jun 1994 by a single well and total production is 0.53 million barrel. The simulated production rate is perfectly matched with the real production rate as shown in figure 3.43.

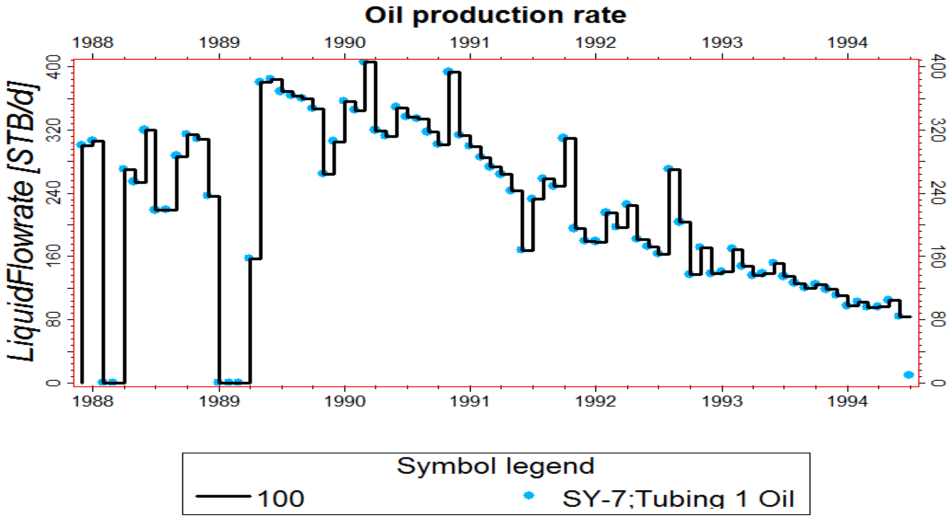

Figure 3.43: Rate history matching

Pressure History Matching

Simulated reservoir pressure does not match perfectly with the real pressure as shown in figure 3.44. The real pressure was recorded at well head. The real pressure declines gradually with the real oil production rate. Pressure and rate decline simultaneously is contradictory to production rule. When rate declines then pressure will be constant. When pressure declines then rate will be constant. In this case pressure must be constant. Well head pressure declined due to the wax formation in the production tube. So we have considered the rate history matching for validate the reservoir model. The constructed reservoir model is representative of the real reservoir and can be used for reservoir development planning.

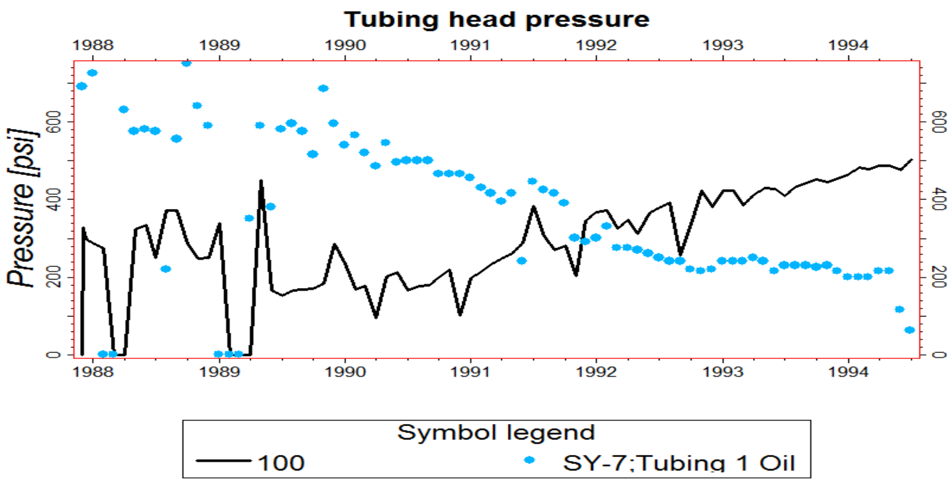

Figure 3.44: Pressure history matching

3.1.8: Oil Reserve Estimation in Haripur Field

Advances in computer technology have facilitated the widespread applications in building multimillion-cell digital geocellular models populated cell by cell with the static geological, geophysical, petrophysical, and engineering data characterizing the subsurface reservoir structure in 3D, similar to the depiction in figure 3.45.

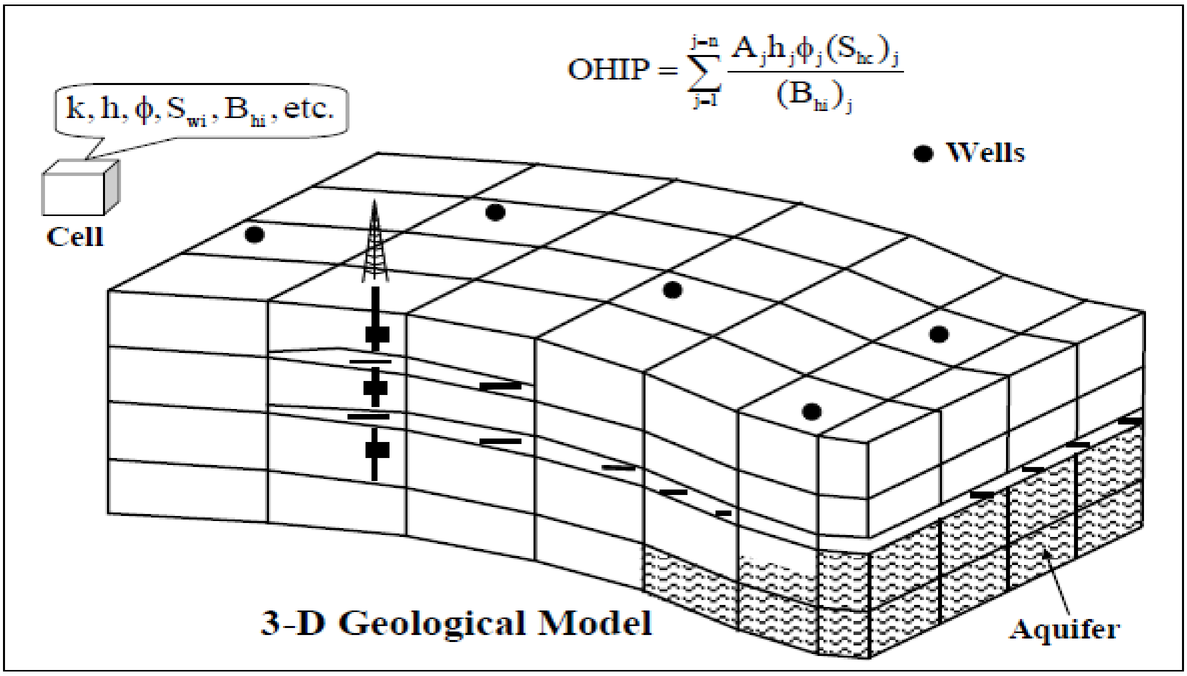

Figure 3.45: 3D geological model (http://www.spe.org)

In a gridded mapping process, the parameters in the original hydrocarbon in-place (OHIP) equation change from cell to cell, and the total OHIP is obtained by the sum of the individual values assigned to, calculated for, and/or matched for each cell. Based on early well performance, modifications to the development program including supplemental secondary and enhanced recovery projects can be designed using streamline and/or finite-difference simulation models with such multimillion-cell reservoir characterization models, including several cases of "what-if" scenarios represented by different plausible realizations. However, refinement and verification of these large geocellular models with actual analogs and thus the degree of certainty in the resulting estimates to a large extent is dependent on both the quantity and quality of geoscience, engineering, and, more importantly, the performance data. The volumes should be divided according to type of hydrocarbon, and should also be split among the deposits and reservoir units included in the plan. The calculation method for the resource estimate should be stated, and the uncertainty in the estimate should be described and quantified.

For a single grid cell

$$V_{bi} = \Delta X_i \Delta Y_i \Delta Z_i \qquad (EQ3.4)$$

$$V_{Neti} = V_b \times NTG_i \qquad (EQ3.5)$$

$$V_{pori} = V_{Neti} \times \varphi_i \qquad (EQ3.6)$$

$$V_{HCPV_{Oi}} = V_{pori} \times S_{oi} \qquad (EQ3.7)$$

$$STOIIP_i = \frac{V_{HCPV_{Oi}}}{B_{oi}} \qquad (EQ3.8)$$

Where,

Vbi=Bulk Volume in a cell

ΔXi= Cell dimension in X direction in a cell

ΔYi=Cell dimension in Y direction in a cell

ΔZi=Cell dimension in Z direction in a cell

V_{Neti}= Net volume in a cell

NTGi= Net to gross ratio in a cell

Vpori= Pore volume in a cell

φi= Porosity in a cell

V_{HCPVoi}= Hydrocarbon Pore Volume for Oil in a cell

Soi= Oil saturation in a cell

Boi= Oil formation volume factor in a cell

STOIIPi=Stock Tank Oil Initially In Place in a cell

For a zone

$$STOIIP_{zone} = \sum_{i=1}^{i=N} STOIIP_i \qquad (EQ3.9)$$

A 3-D geocellular oil reservoir model has been constructed for Haripur oil field as shown in figure 3.46 and figure 3.47. Each grid cell contains dimensions, net to gross ratio, porosity, oil saturation and oil formation volume factor data. These data are used to calculate cell stock tank oil initially in place (STOIIP) and then calculations are made for all the cells to determine reservoir STOIIP. The STOIIP calculation is absolutely dependent on the data. If data uncertainty is more the STOIIP estimation is not authenticate. To calculate authentic STOIIP the input data must be filtered and sorted. Here all input data have been filtered and sorted to estimate authentic STOIIP.

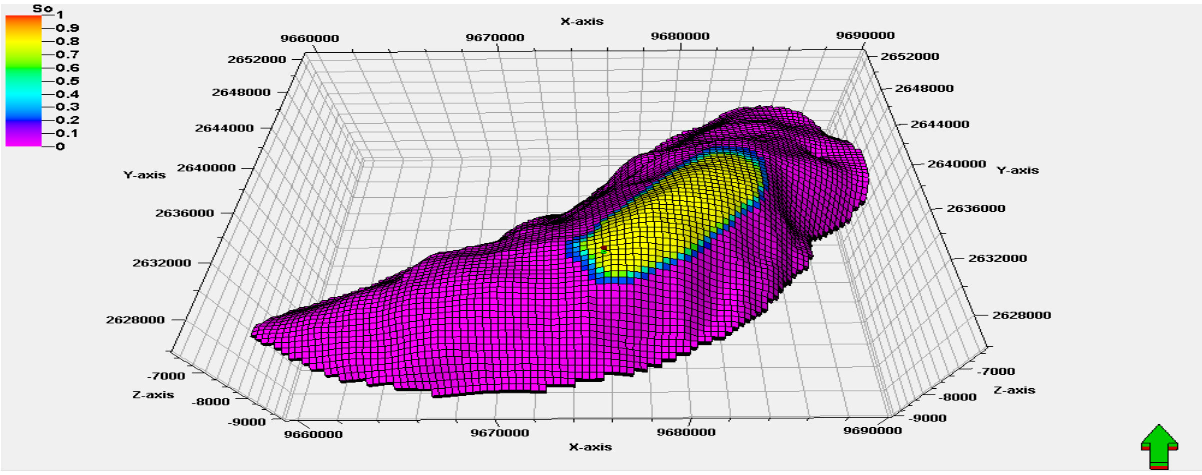

Figure 3.46: 3D geocellular oil reservoir model

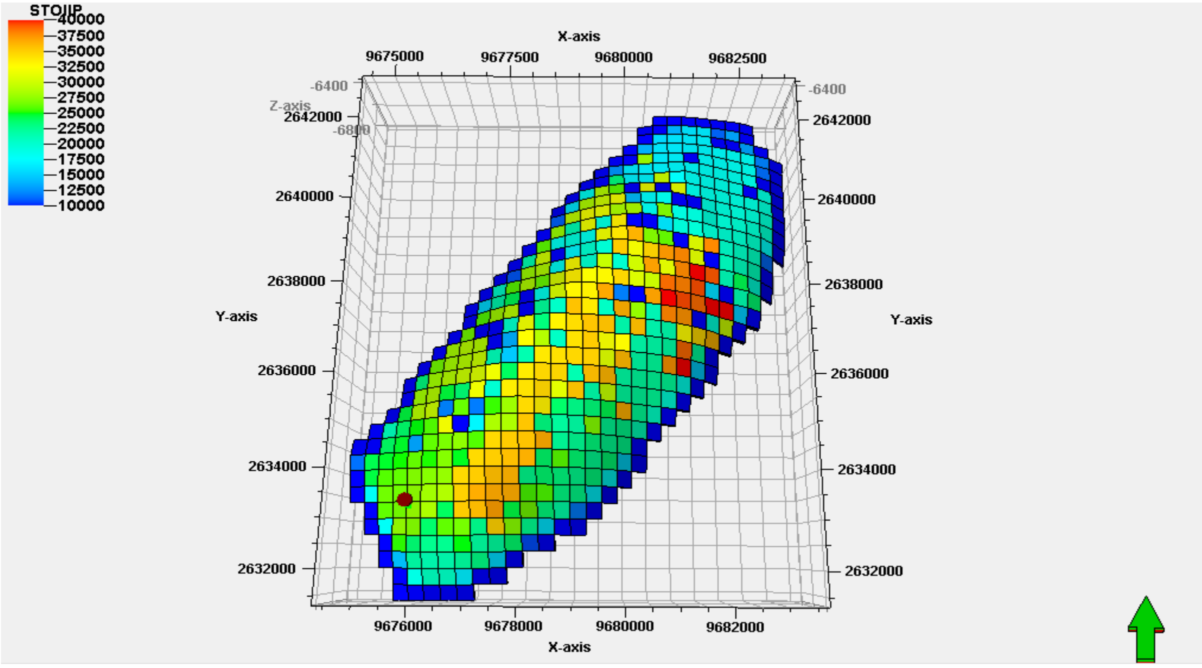

Figure 3.47: 3D geocellular oil zone model

Oil reservoir in Haripur Oil Field contains 6 simulation zones (layers) and their corresponding oil reserve is shown in table 3.6. The total initial oil reserve is 33.00 million stock tank barrel (STB). There are production history from 01 Dec 1987 to 01 Jun 1994 by a single well and total production is 0.53 million barrel. The 3-D geocellular oil reservoir model has been simulated to generate the history of the real reservoir and found the perfect history matching. After history matching volume calculation has been simulated in 3-D geocellular oil reservoir model and found total STOIIP is 33 million barrel from which 0.53 million barrel has been produced by spending reservoir own pressure energy and there is 32.47 million barrel of oil remaining in the reservoir to be produced by advanced available oil recovery techniques.

Table 3.6: Stock tank oil initially in place in Haripur oil field

Bhubon Formation Oil Zone	Bulk volume[*10^6 ft^3]	Net volume[*10^6 ft^3]	Pore volume[*10^6 RB]	HCPV oil[*10^6 RB]	STOIIP (in oil)[*10^6 STB]	GIIP (in oil)[*10^6 MSCF]
Zone 69	1066	1066	31	13	10	5
Zone 70	995	995	24	11	9	4
Zone 71	920	920	23	8	6	3
Zone 72	847	847	23	5	4	2
Zone 73	776	776	17	4	3	1
Zone 74	707	707	15	2	1	1
Total	5311	5311	133	43	33	16

The oil resources distribution framework shown in table 3.7 is developed on the basis of performed investigation on the real field. The remaining oil resources is considered as contingent resources in 3C category as to recover the oil resource it need to apply enhanced oil recovery technique such as water injection (low salinity water injection) and there are no 3D & 4D seismic data, DST data, video log, NMR log, core flood data used for reserve estimation and recovery potential so there are high uncertainty and commercial risk involved in this project. To consider the overall conditions the oil resources is treated as the contingent resources of 3C category.

Table 3.7: Estimated reserve framework

<table>
<tr><td rowspan="9">Total Petroleum Initially In Place (PIIP)
33 MMBBL</td><td rowspan="6">Discovered PIIP
33 MMBBL</td><td rowspan="3">Commercial
0.53 MMBBL</td><td colspan="3">Production, 0.53 MMBBL</td></tr>
<tr><td colspan="3">Reserve, 0.53 MMBBL</td></tr>
<tr><td>Proved
1P, 0.53 MMBBL</td><td>Probable, 2P</td><td>Possible, 3P</td></tr>
<tr><td rowspan="3">Sub-Commercial
32.47 MMBBL</td><td colspan="3">Contingent Resources, 32.47 MMBBL</td></tr>
<tr><td>1C</td><td>2C</td><td>3C
32.47 MMBBL</td></tr>
<tr><td colspan="3">Unrecoverable</td></tr>
<tr><td rowspan="3">Undiscovered PIIP</td><td colspan="4">Prospective Resources</td></tr>
<tr><td colspan="2">Low Estimate</td><td>Best Estimate</td><td>High Estimate</td></tr>
<tr><td colspan="4">Unrecoverable</td></tr>
</table>

3.1.9: Dynamic Characterization of Oil Reservoir in Haripur Field

The use of streamline technology is becoming common for reservoir flow visualization, dynamic reservoir characterization, and optimal flood management. The power of the streamlines can be exploited using both finite-difference and streamline simulators. This study covers concepts in streamline technology and its applications for reservoir characterization, reservoir management/optimization and field development strategy. The oil production rate started on 01 December 1987 with rate of 300 stb/d at tube head pressure of 690 psia and it attained its maximum rate of 405 stb/d at tube head pressure of 520 psia on 01 April 1990. Finally it terminated on 01 July 1994 with rate of 9.11 stb/d at tube head pressure of 62 psia. To observe the dynamic character of the reservoir, dynamic key attributes such as pressure, saturation, oil flow rate, time of flight, oil flow line in the reservoir are analyzed at different time of production such as initial production time, maximum production time and abandonment production time.

Reservoir Pressure

The reservoir pressure is estimated by hydrostatic equilibration method. Oil water contact is determined at 6660 ft depth where water pressure is 3177 psia. Gas Oil contact is determined by composition variation with depth at 6237 ft depth where pressure is 3000 psia. Simulator counts 6237 ft depth as datum and 3000 psia as datum pressure. From oil water contact to gas oil contact is oil column and below the oil water contact is water column. Using these data simulator estimates pressure in grid cells by following formula.

Cell Pressure=Datum Pressure+(cell depth-datum depth) x oil density x gravity

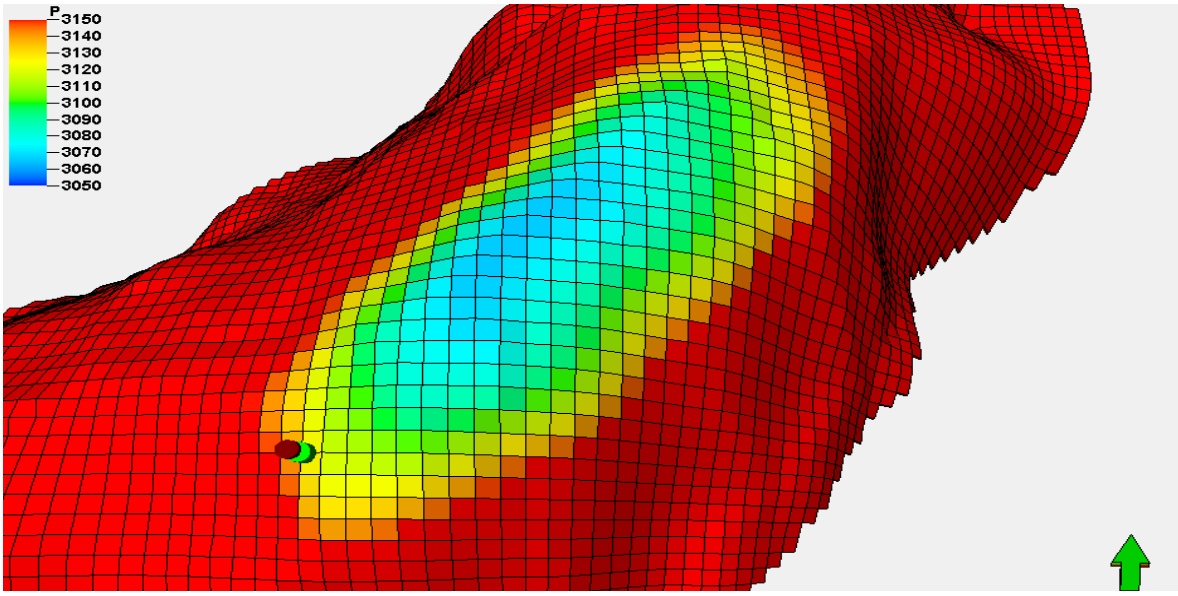

Figure 3.48: Reservoir pressure at initial production time

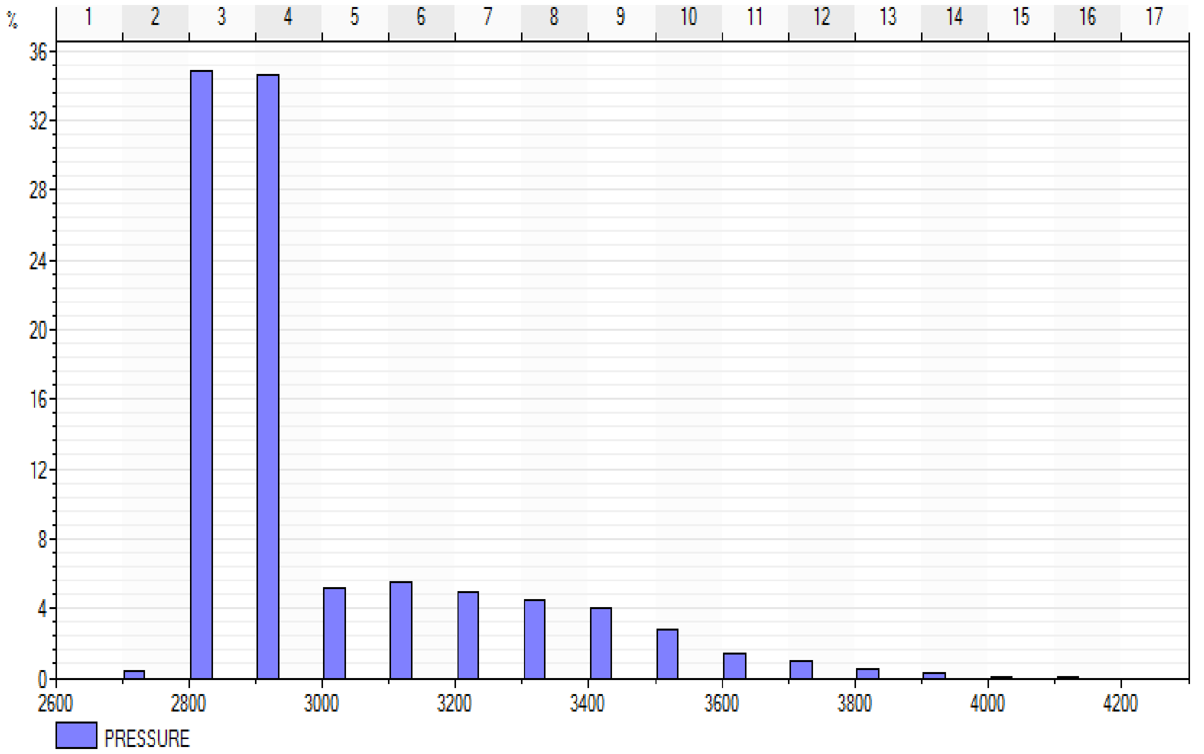

Figure 3.49: Histogram of reservoir pressure at initial production time

The pressure distribution in cell of reservoir model is shown in figure 3.48 and its histogram is shown in figure 3.49 at initial time. Average reservoir pressure is 3026 psia.

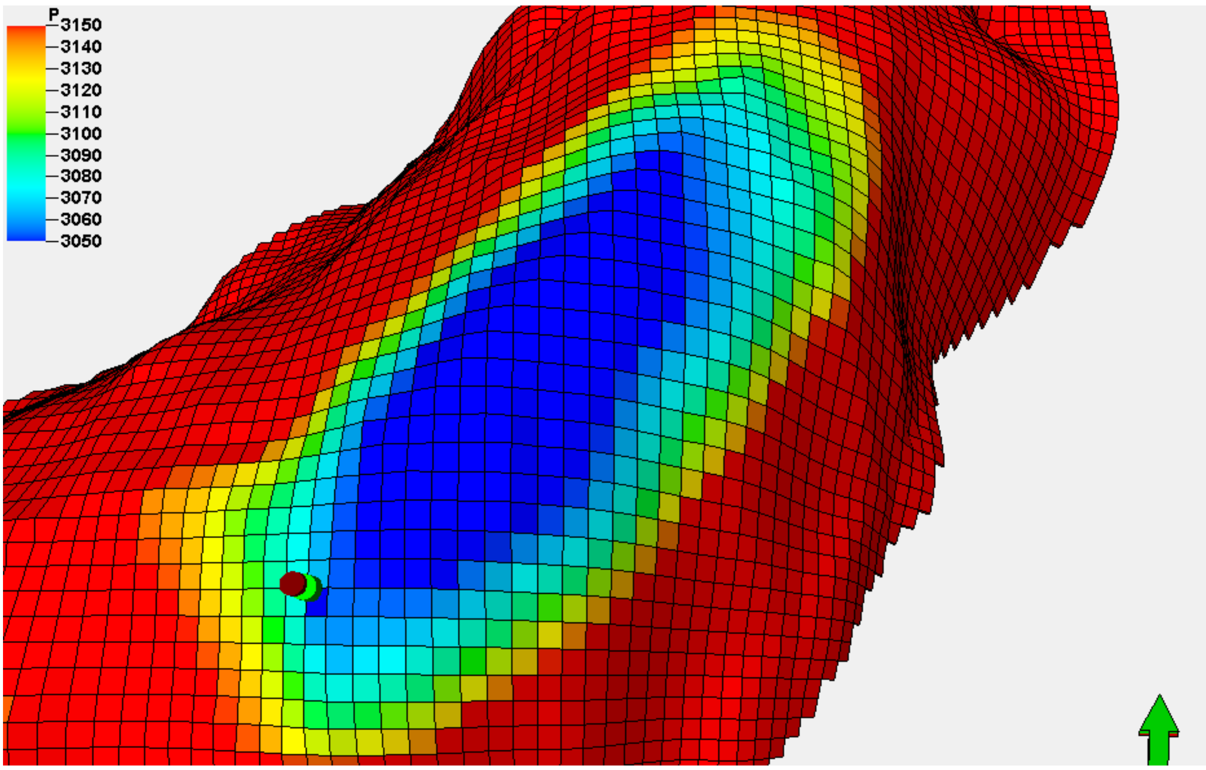

Figure 3.50: Reservoir pressure at abandonment time

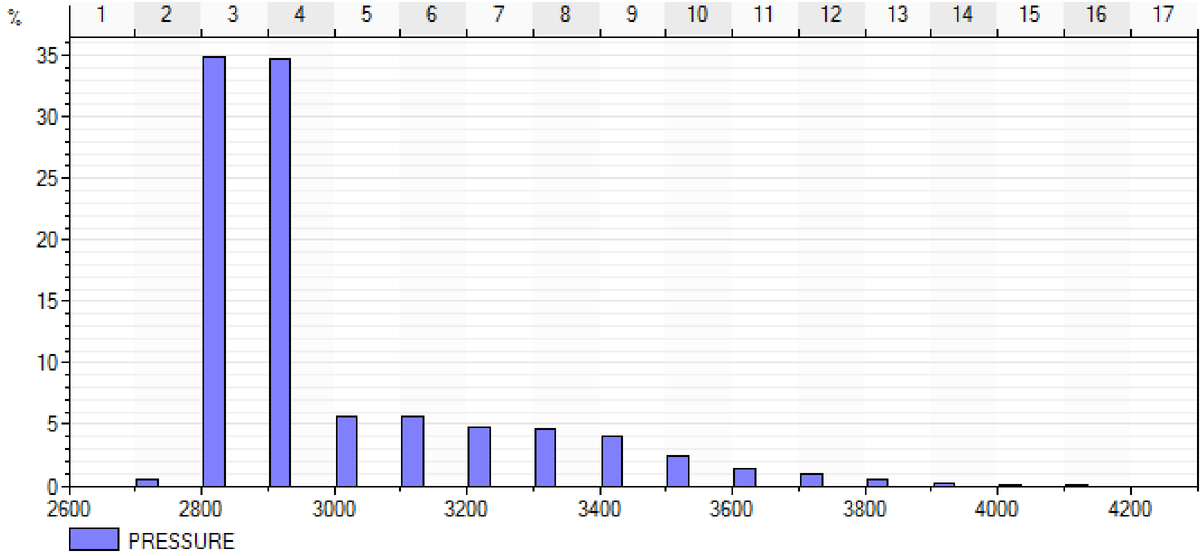

Figure 3.51: Histogram of reservoir pressure at abandonment time

The reservoir pressure at abandonment time and its histogram are shown in figure 3.50 and 3.51 respectively. The average reservoir pressure is 3022. It is observed that there is minor change in reservoir pressure during the production period. Average reservoir pressure changes only 04 psia.

Oil Saturation

Oil saturation is estimated from water saturation which is determined from resistivity log. Oil saturation at reservoir at initial and abandonment time are shown in figure 3.52 and figure 3.53 receptively. It is noticed that there is no significant changes in oil saturation during the oil production.

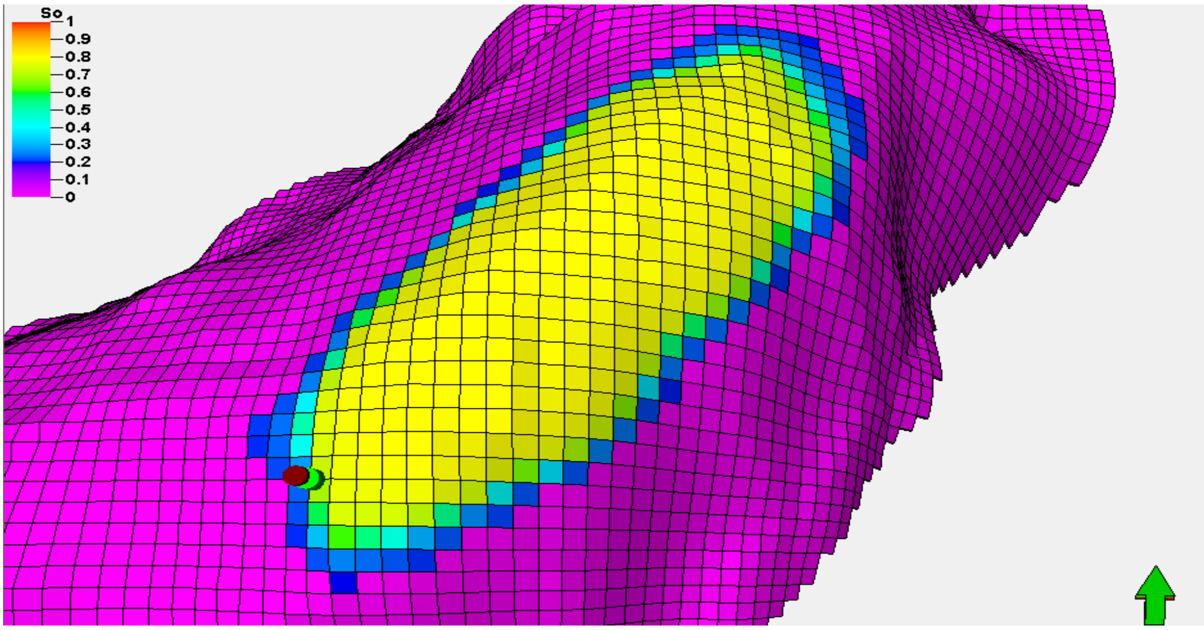

Figure 3.52: Oil saturation at initial production time

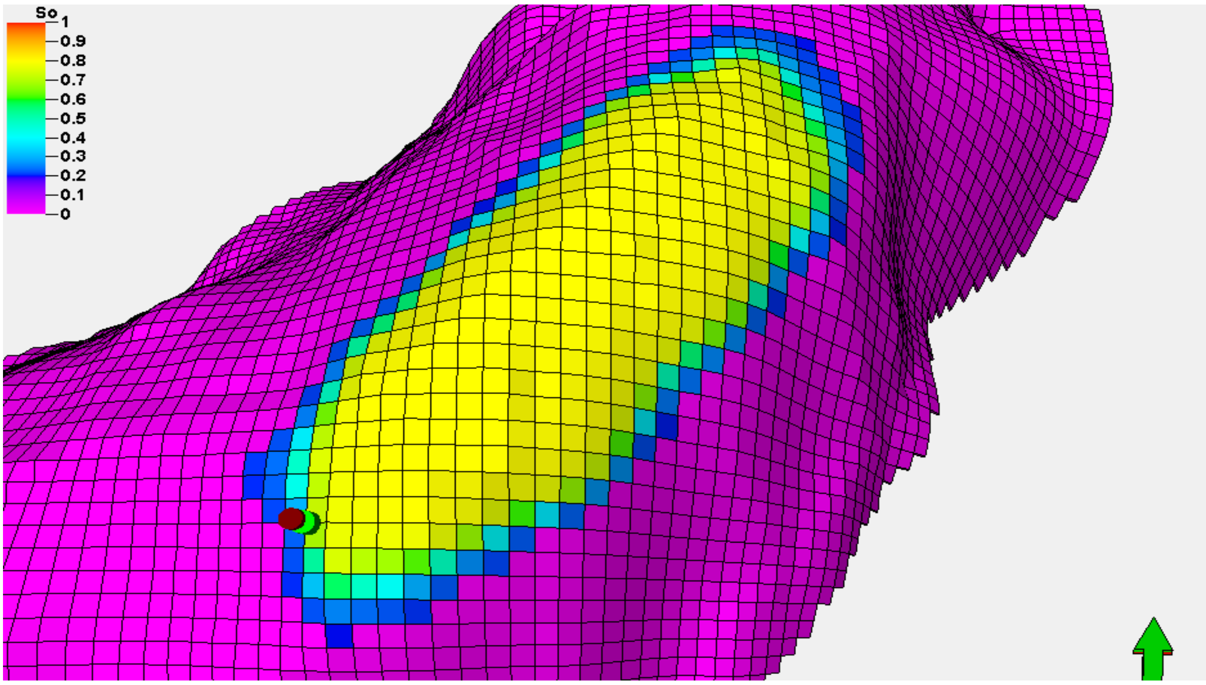

Figure 3.53: Oil saturation at abandonment time

Oil Volumetric Flow Rate inside the Reservoir.

Streamline simulation attributes oil flow rate inside the reservoir is visualized in figure 3.54, figure 3.55 and figure 3.56 for initial, maximum and abandonment time respectively.

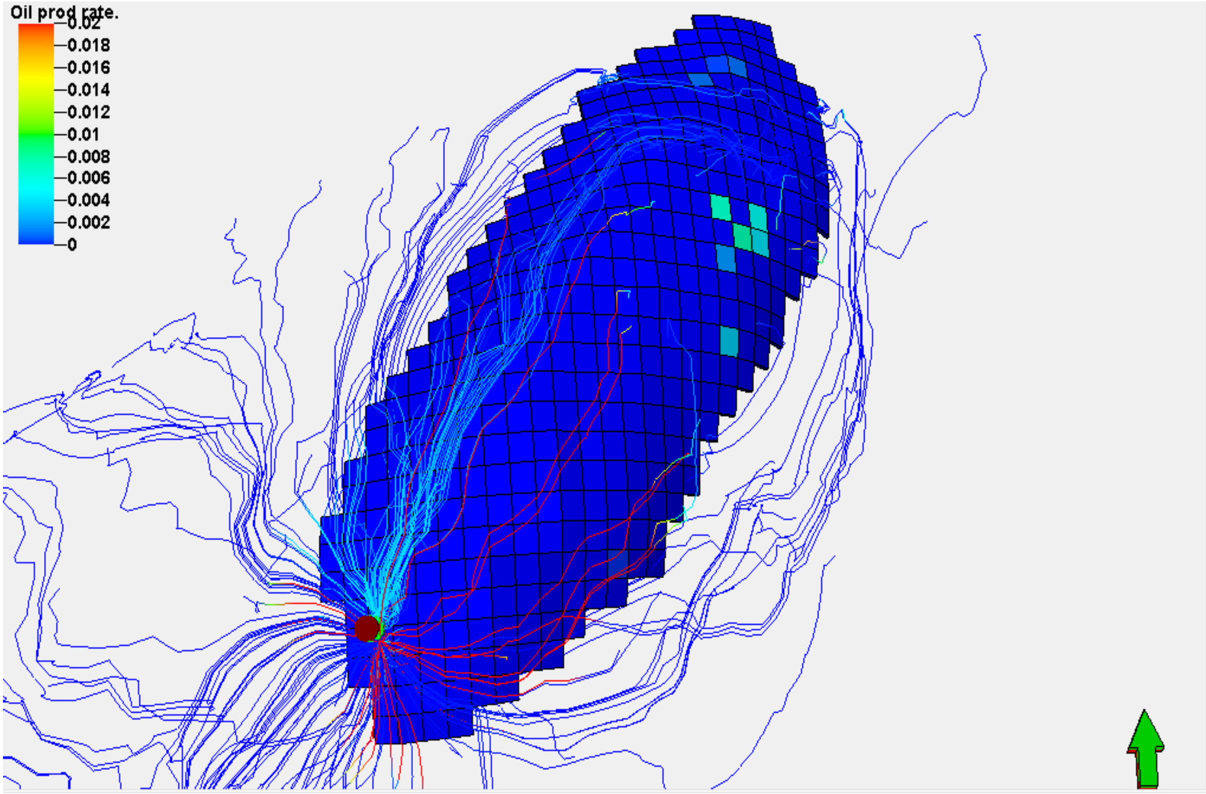

Figure 3.54: Oil production rate at initial production time

At initial time average value of oil flow rate is 0.09 STB/D. Oil flow line developed by 30% at initial time when the surface production rate is 300 STB/D and well head pressure 690 psia.

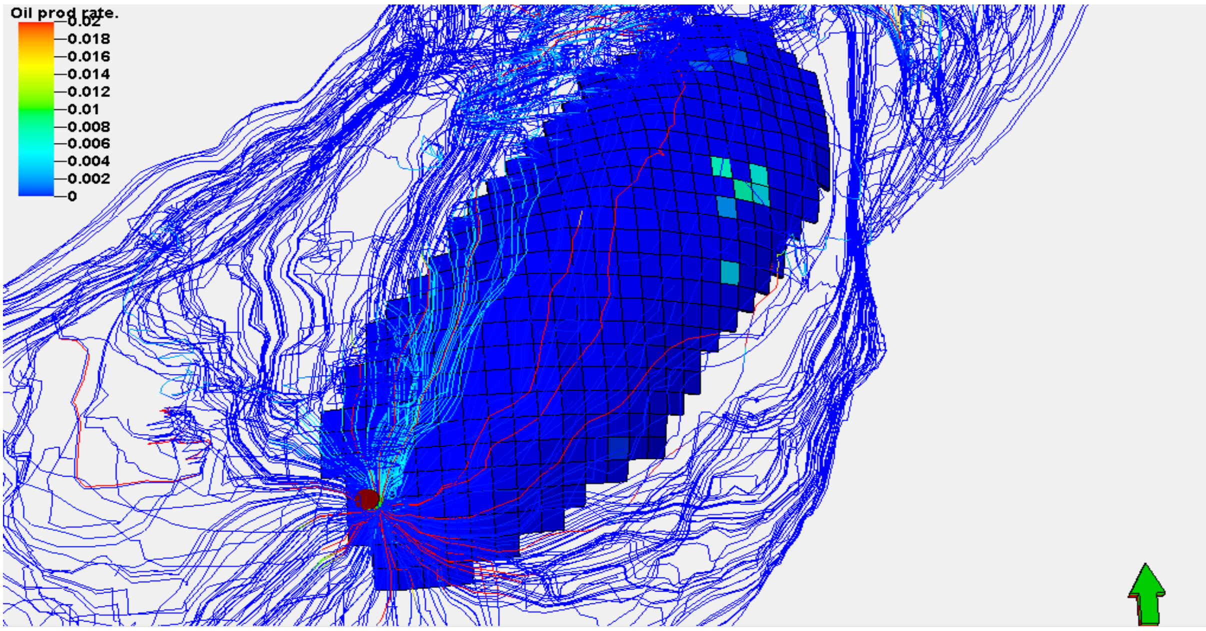

Figure 3.55: Oil production rate at maximum production time

At maximum production time average value of oil flow rate is 0.09 STB/D. Oil flow line developed by 90% at maximum production time when the surface production rate is 405 STB/D and well head pressure 520 psia.

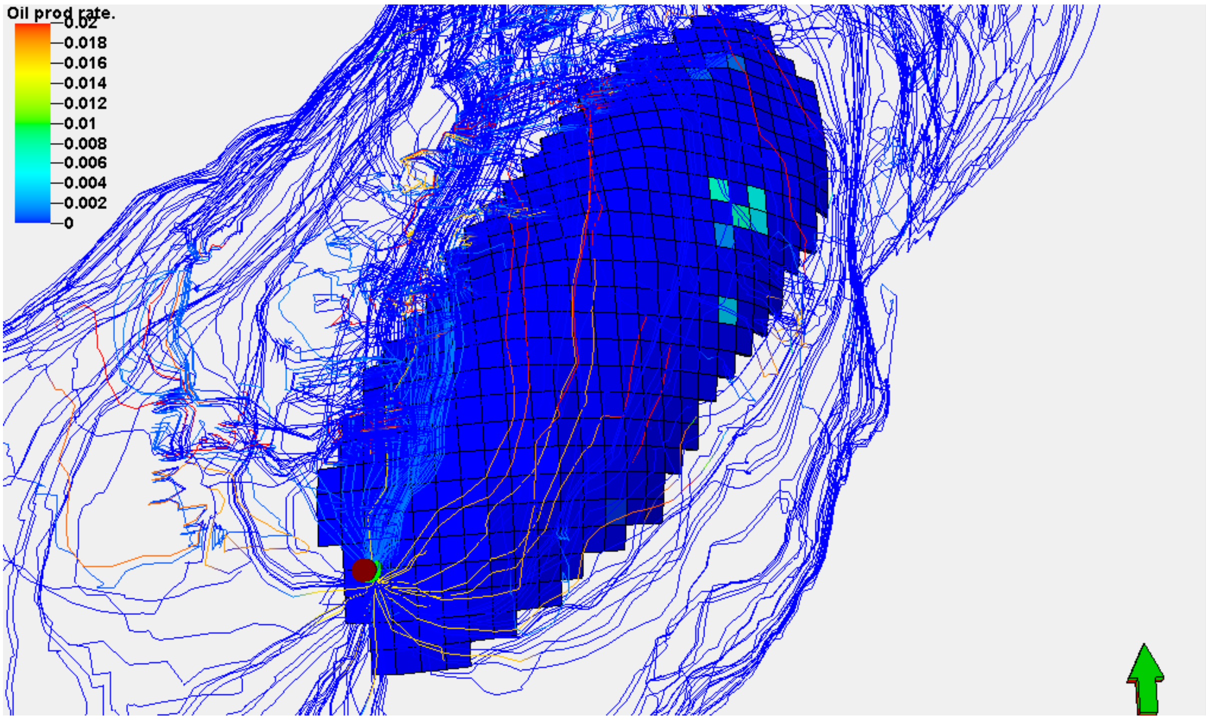

Figure 3.56: Oil production rate at abandonment time

At abandonment time average value of oil flow rate is 0.09 STB/D. Oil flow line developed by 100% at abandonment time when the surface production rate is 9.11 STB/D and well head pressure 62 psia.

Time of Flight

Another stream line simulation attribute is time of flight (end) for estimating the required time to come fluid to well act as sink from different parts of the reservoir. Time of flight (end) is shown by figure 3.57, figure 3.58 and figure 3.59 for initial, maximum and abandoned time respectively. Oil will take 1000 days to come to well bore from 2000 ft away from the well bore.

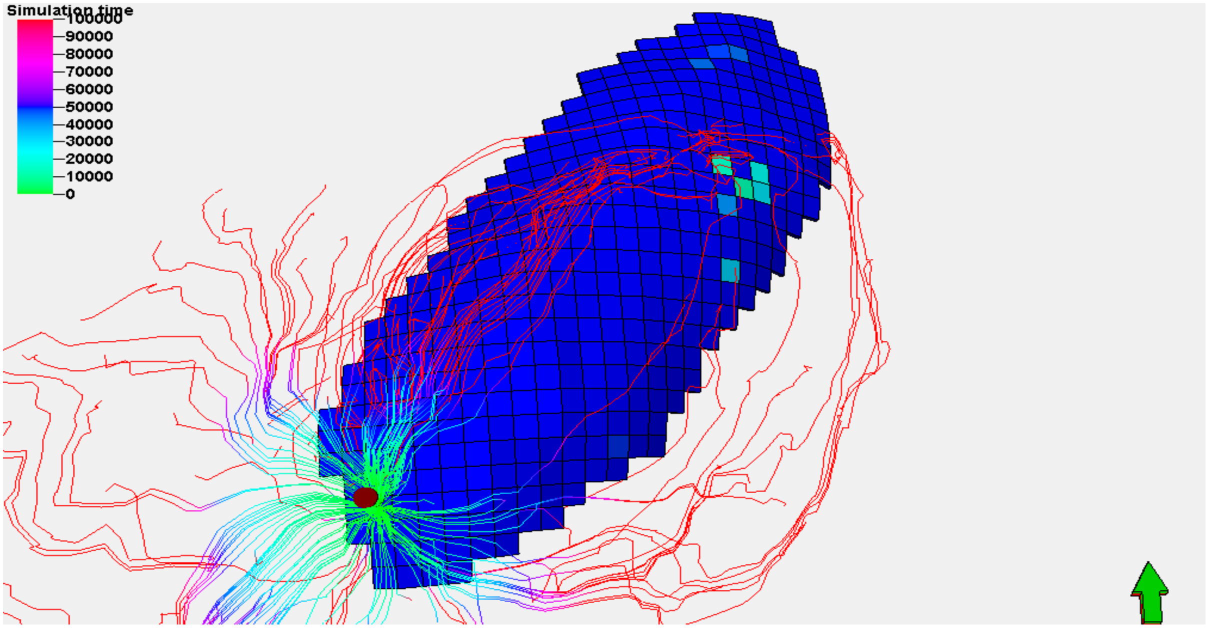

Figure 3.57: Time of flight at initial production time

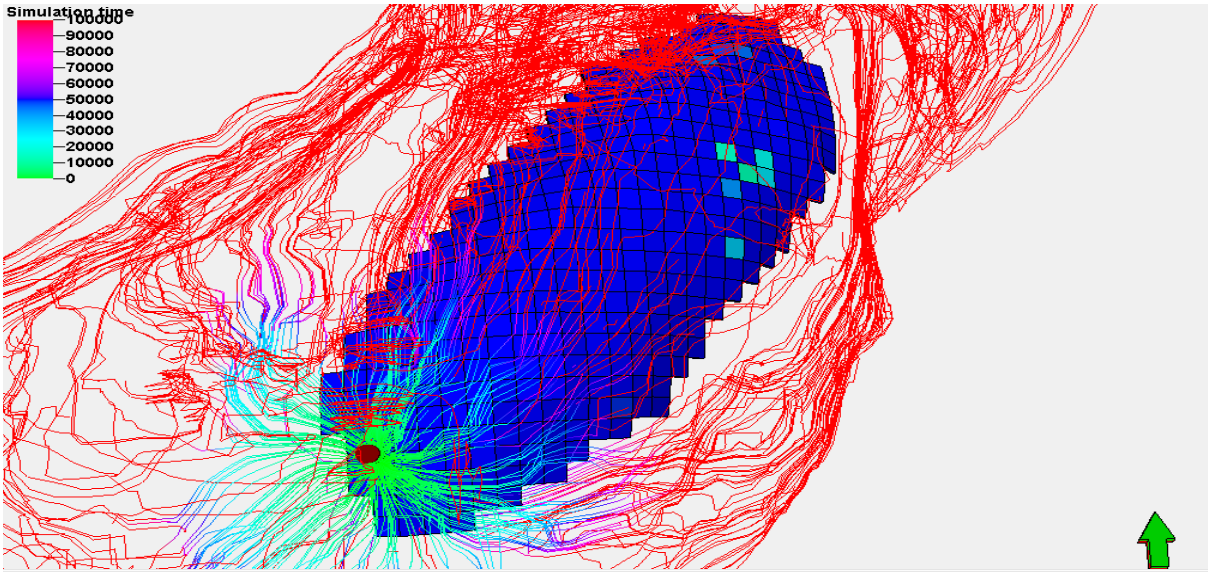

Figure 3.58: Time of flight at maximum production time

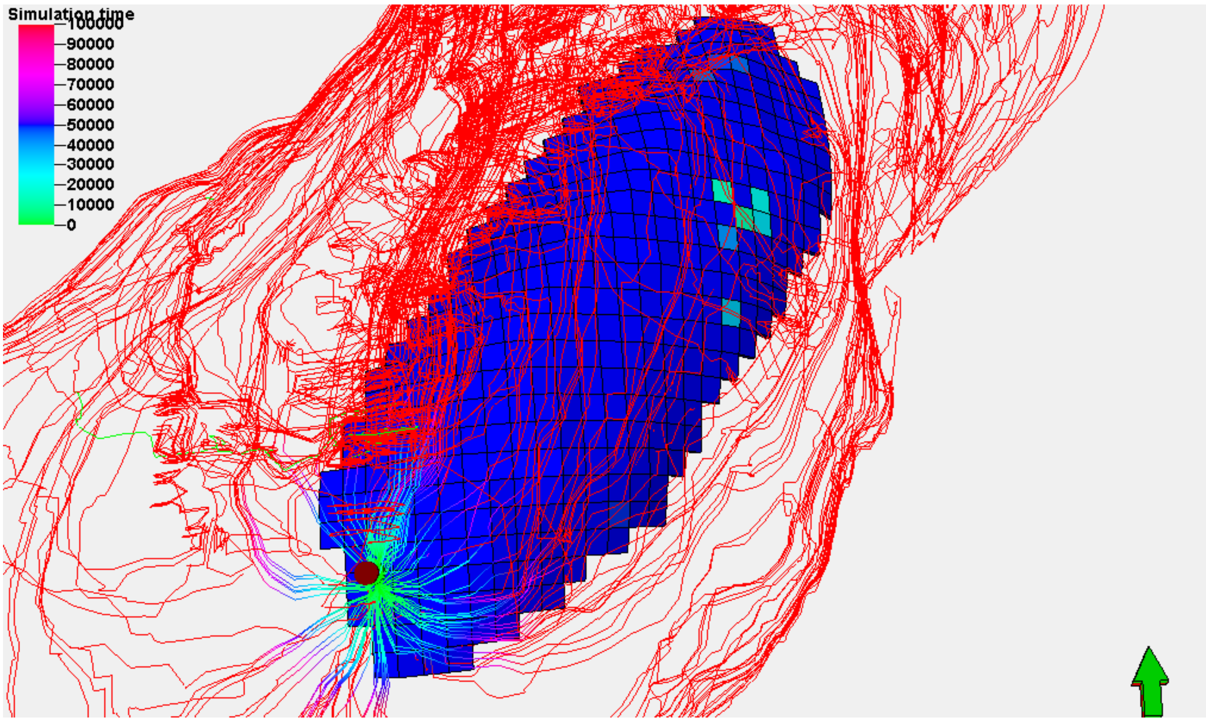

Figure 3.59: Time of flight at abandonment time

Oil Flow Direction

Streamline simulation shows oil flow direction by arrows shown in figure 3.60, figure 3.61 and figure 3.62 at initial, maximum and abandonment time respectively. In all cases a good number of flow arrow generated in the whole parts of reservoir heading to well bore.

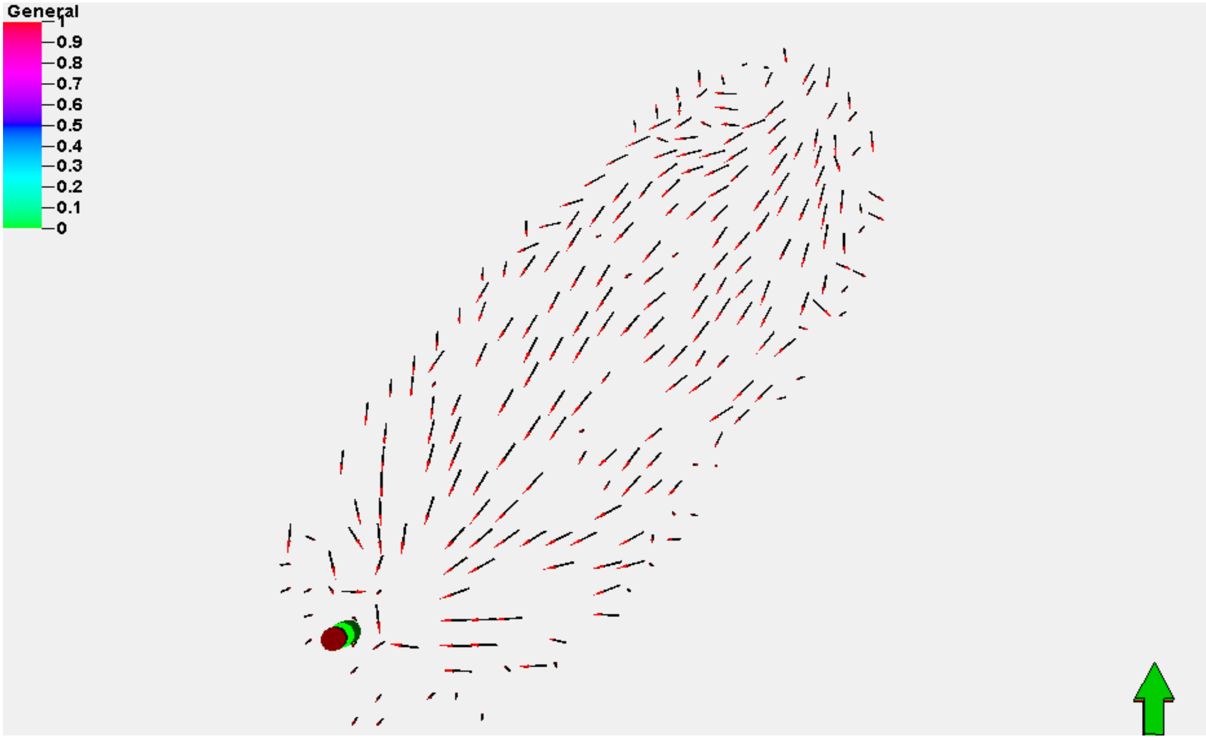

Figure 3.60: Oil flow line at initial production time

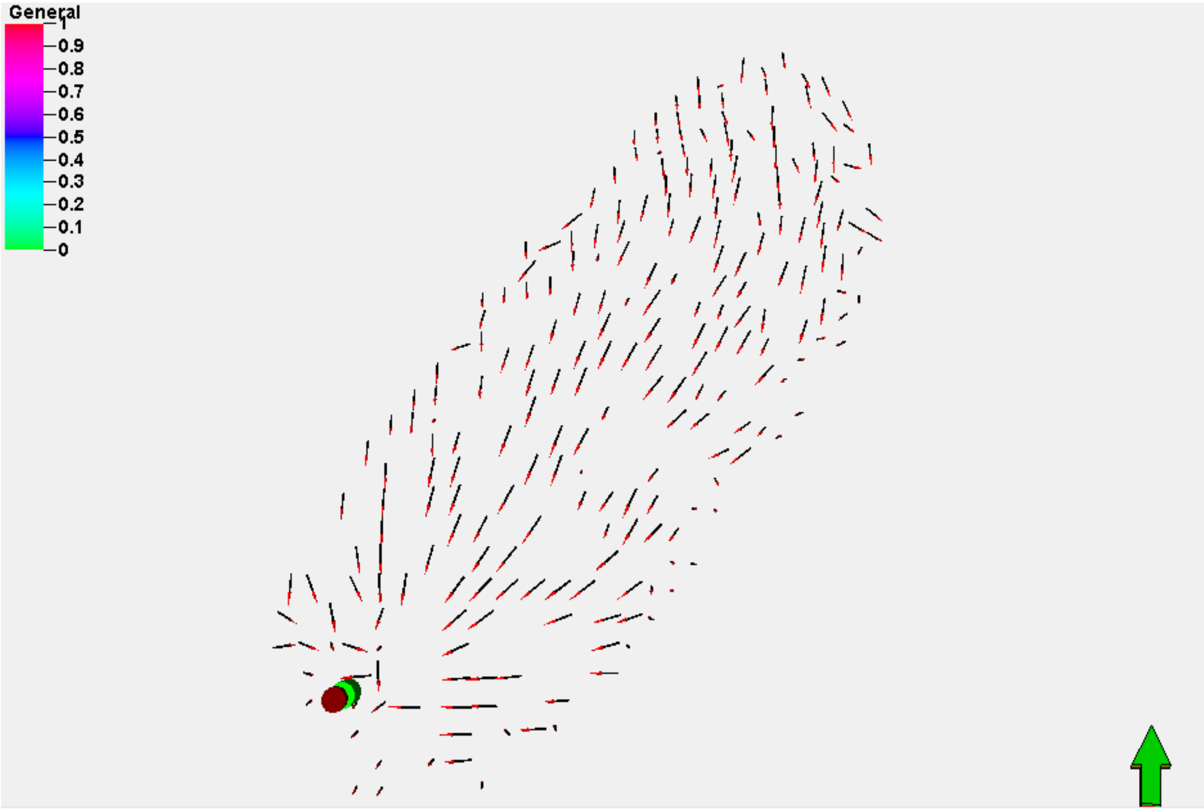

Figure 3.61: Oil flow line at maximum production time

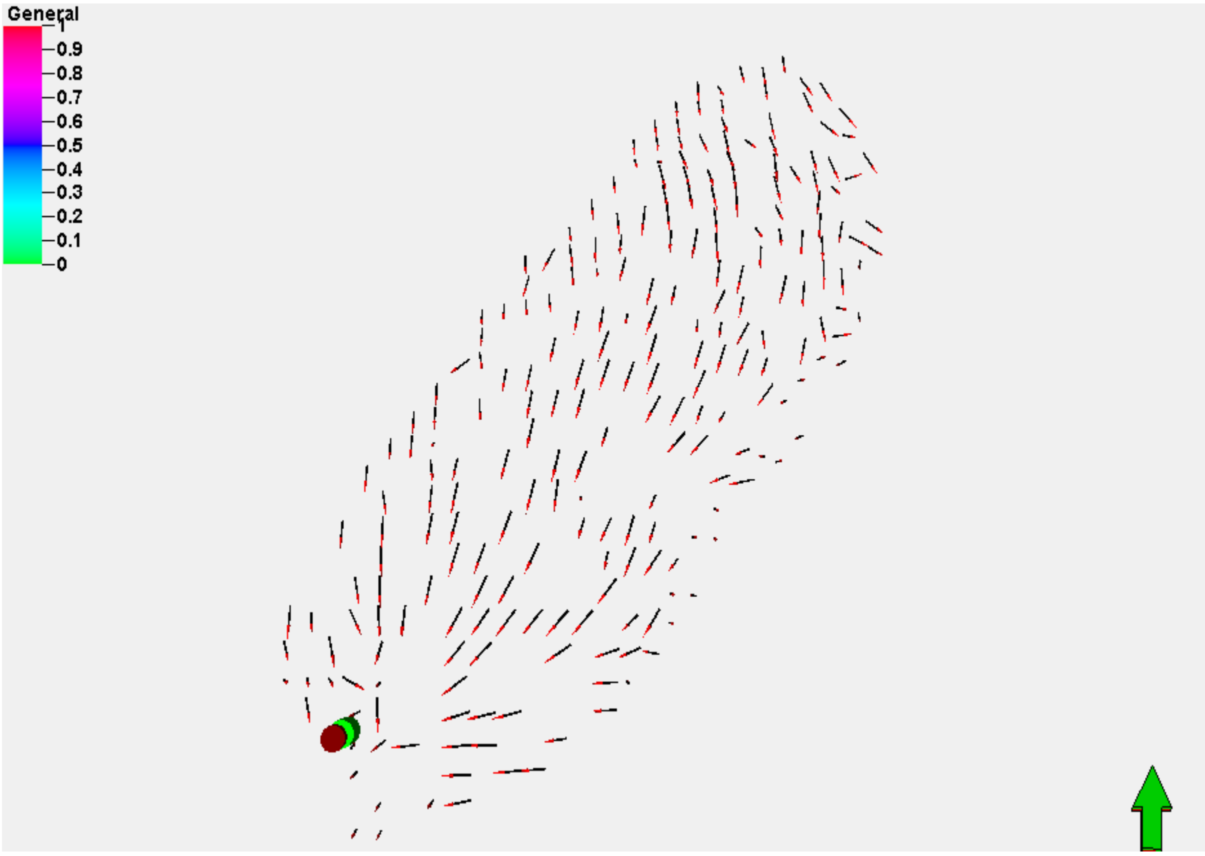

Figure 3.62: Oil flow line at abandonment time

Oil Production Optimization

Oil production started on 01 December 1987 at the rate of 300 STB/D with well head pressure 690 psia. The oil production rate is optimized as shown in figure 3.63. At well head pressure of 700 psia the optimum oil flow rate is 300 STB/D when bottom hole pressure is 2945 psia. Pressure drop in 6700 ft production tube is 2245 psia at flowing condition.

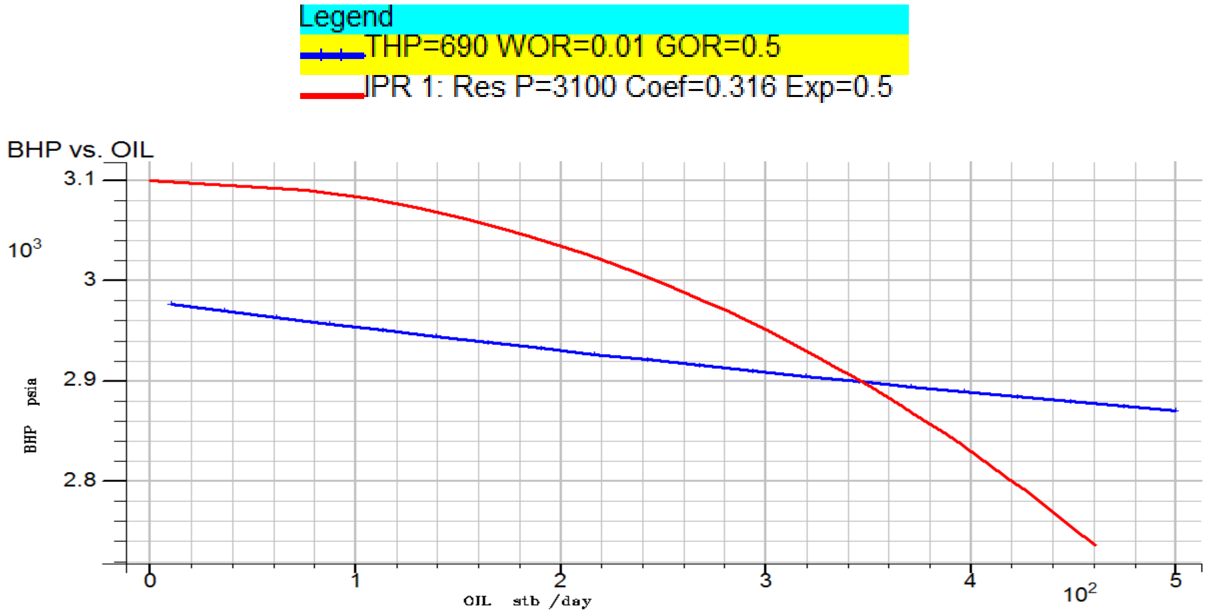

(a)

Reservoir Pressure 3100 psia

Fetkovich Coefficient 0.316

Fetkovich Exponent 0.5

IPR - VFP Curve Intersections:

IPR	VFP Curve Legend	Flow (stb /day)	BHP (psia)
1	THP=690 WOR=0.01 GOR=0.5	346.87	2899.1

(b)

Figure 3.63: a) Vertical flow performance and inflow performance relationship curves and b) Optimum BHP, THP and oil flow rate of well no. SY-7

Oil Production Rate and Tube Head Pressure Analysis

During the oil production period from 01 December 1987 to 01 July 1994 observed oil production rate and well head pressure is shown in figure 3.64. The oil production rate declines along with well head pressure. The usual trend is when oil production rate declines then well head pressure remains constant which is shown by figure 3.65. When oil production rate remains constant then well head pressure will decline which is shown by figure 3.66. The observed oil production rate and well head pressure needs to be analyzed to find out the actual fact happened during the oil production period in well No. SY-7 in Haripur Field.

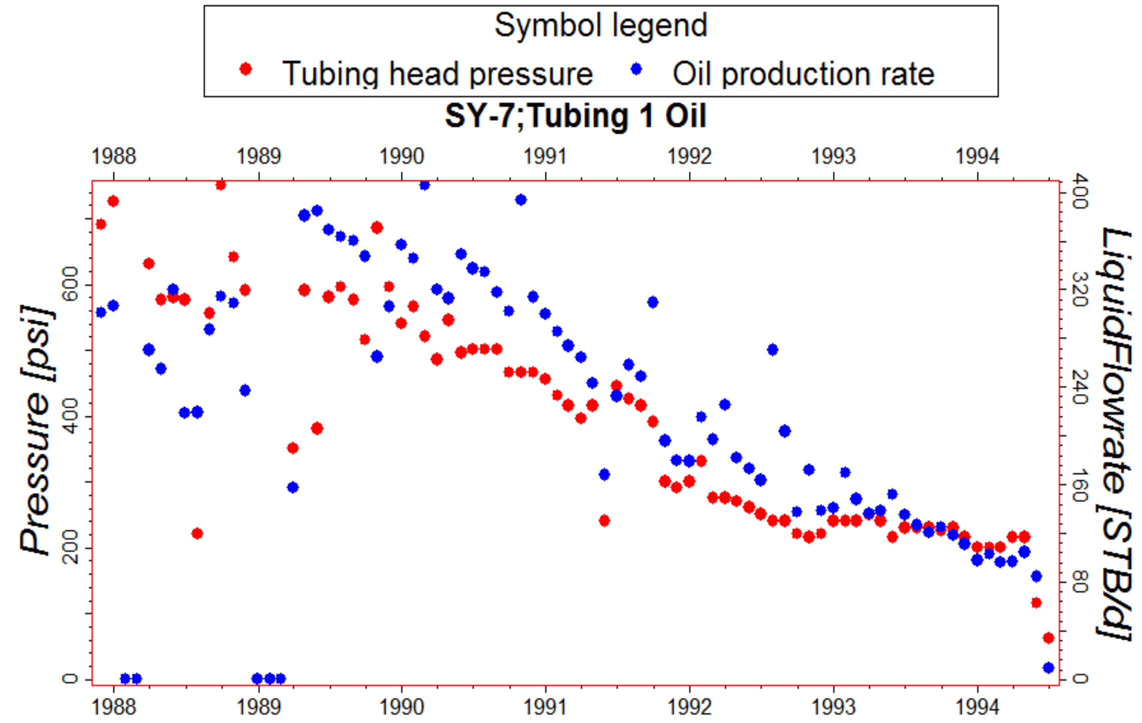

Figure 3.64: Tube head pressure and oil production rate (History 1987 to 1994)

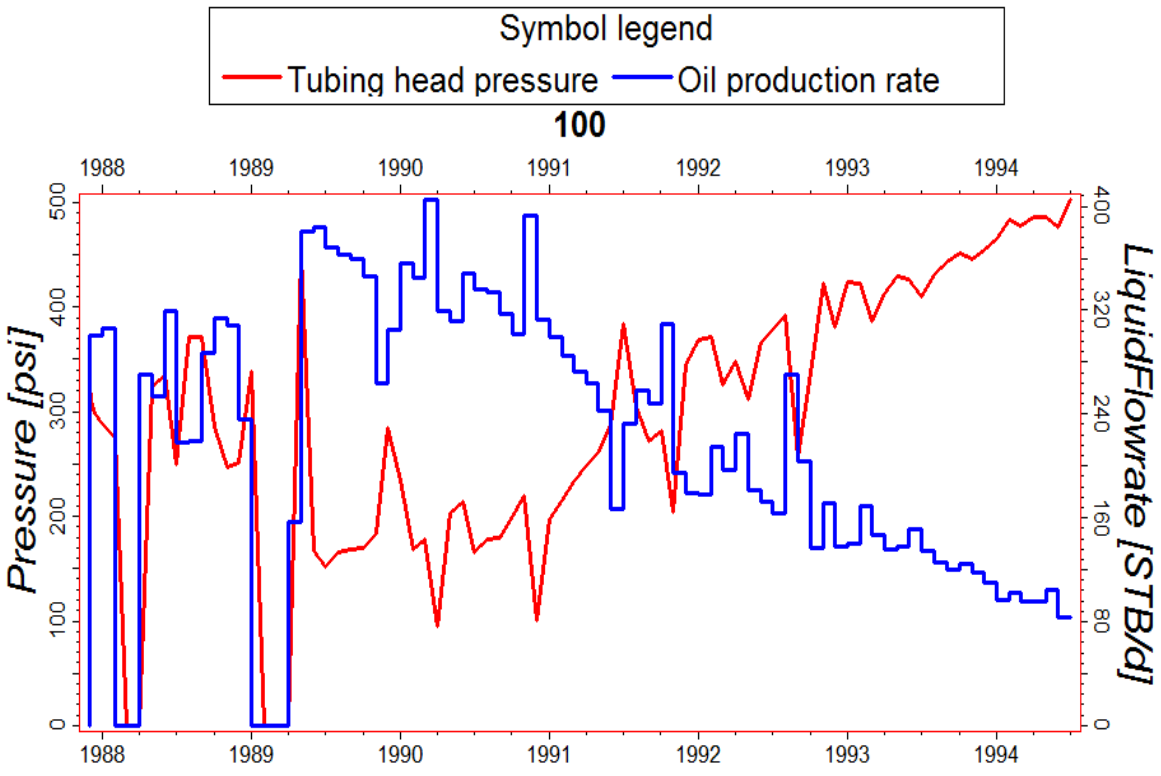

Figure 3.65: Tube head pressure and real oil production rate (Simulation 1987 to 1994)

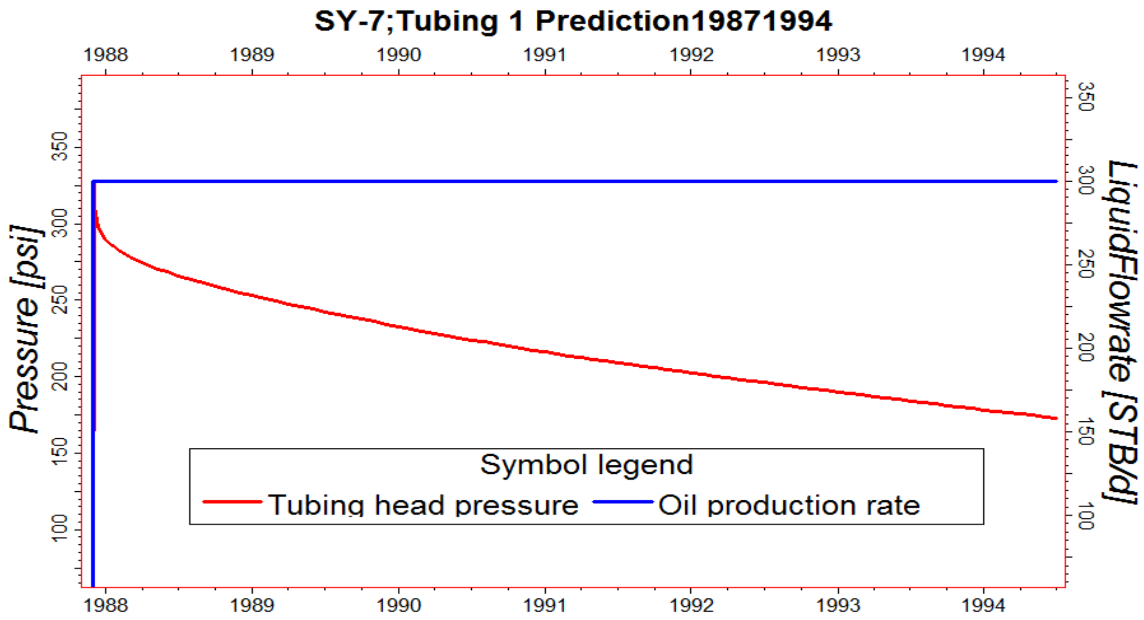

Figure 3.66: Tube head pressure and constant oil production rate (Simulation 1987 to 1994)

At abandonment day on 01 July 1994, the bottom hole pressure is 2931 psia, simulated tube head pressure is 503 psia and observed tube head pressure is 62 psia as shown in figure 3.67. Simulated pressure drop in production tubing is 2428 psia and observed pressure drop in production tubing is 2869 psia.

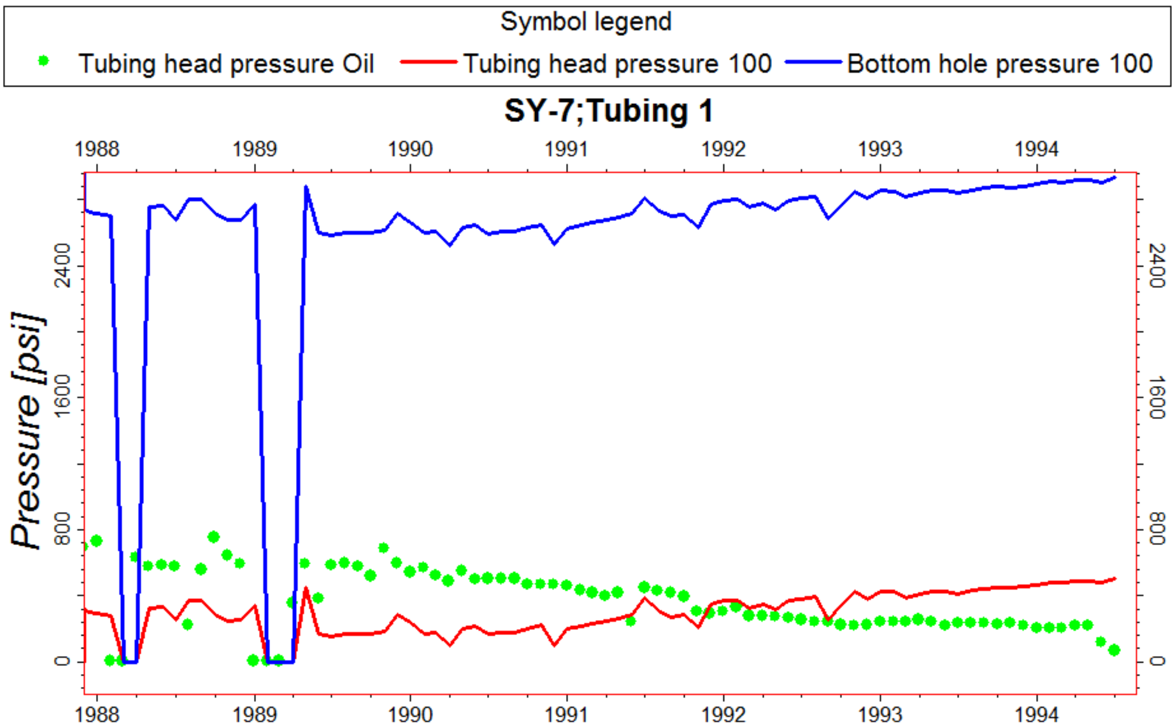

Figure 3.67: Tube head pressure and oil production rate (Simulation 1987 to 1994)

Additional pressure drop in production tubing is 441 psia. Simulated pressure drop in production tubing considers clean production tube during pressure calculation. On the other hand, observed pressure drop in production tubing showed additional 441 psia pressure drop. An investigation is required to find out the causes of additional pressure drop.

Detail investigation revealed that, there was no workover or tube cleaning operation done in this six years of oil production period. Subsequently scale and wax was deposited in production tube as shown in figure 3.68 which caused additional pressure drop in production tube. The consequence of this scale and wax deposition in production tube has terminated oil production. As standard oil well operation procedure, well must be clean in every one year and perform workover operation in every two years.

Figure 3.68: Scale and wax deposition in production tube

Water Breakthrough Analysis

At abandonment time water breakthrough is shown by figure 3.69 and 3.70 at X cross section and Y cross section respectively. There is no significant water breakthrough observed at the end of production. By the well no SY-7 the oil production may continue further but scale and wax deposition in production tube terminates the oil production.

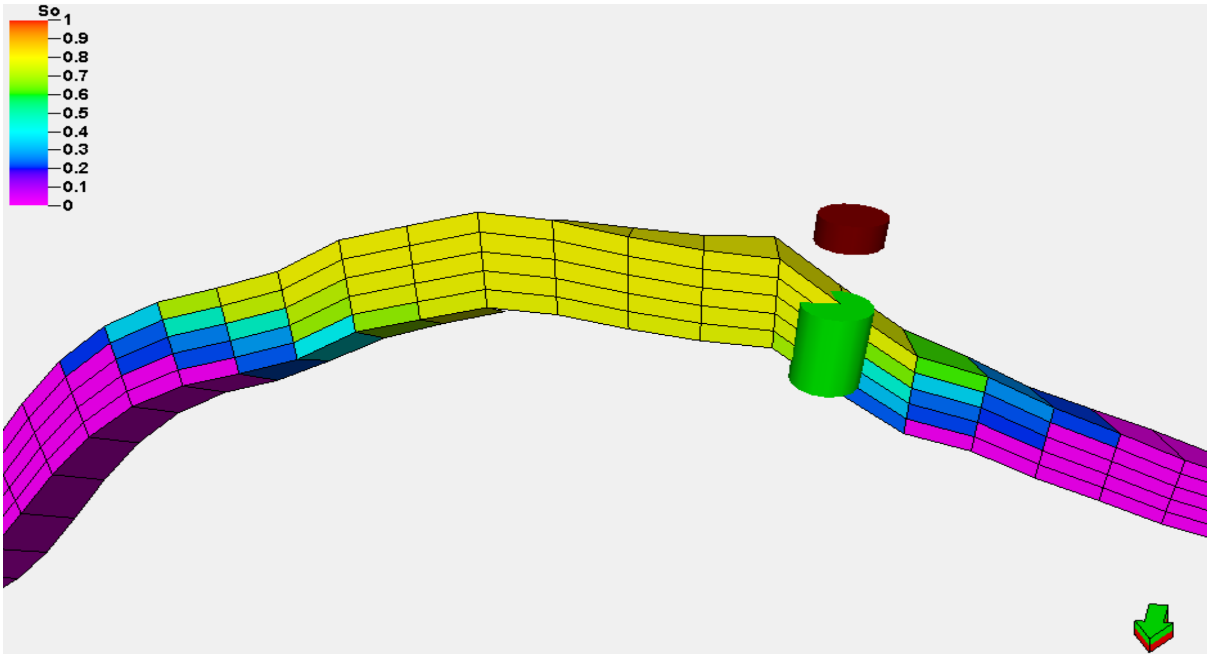

Figure 3.69: Water breakthrough at X cross section

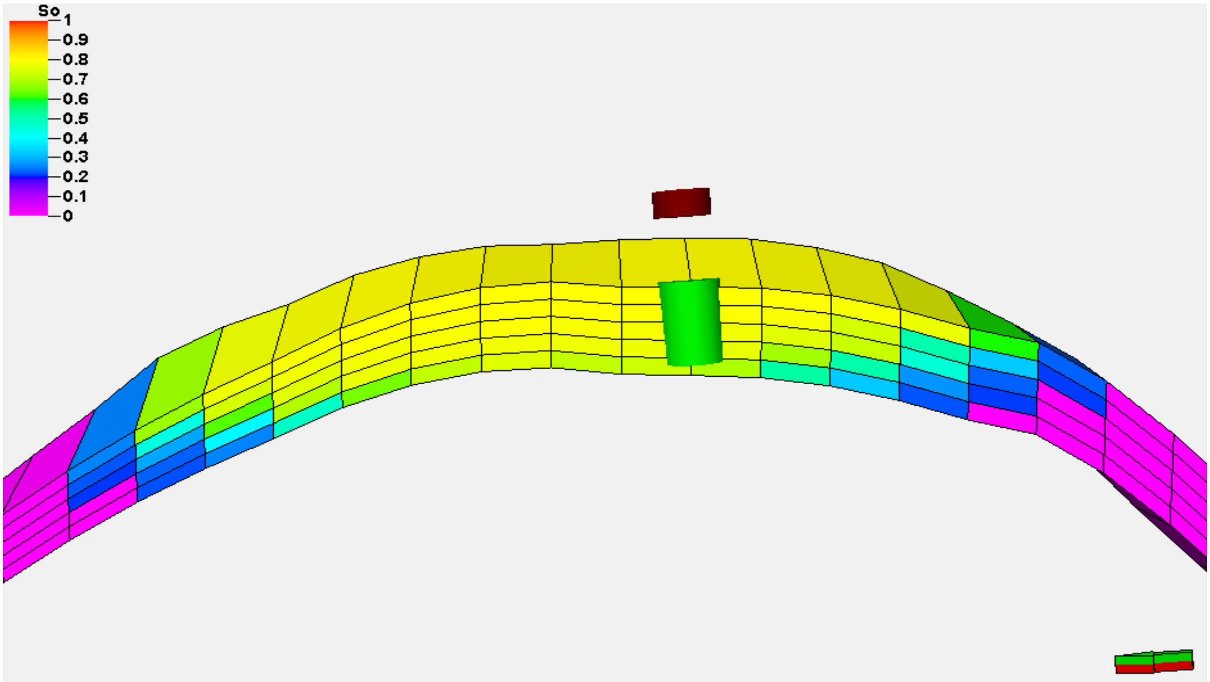

Figure 3.70: Water breakthrough at Y cross section

The reservoir dynamic performance is good as the reservoir has excellent pressure communication along with perfect oil flow lines. Lack of well cleaning and workover operation scale and wax deposited in production tube causing additional pressure drop which gradually increasing over time, finally the oil production ceased and well is abandoned. It will be worth to study the reservoir further to design oil recovery technology to produce the remaining oil from the Haripur field.

Reservoir Drive Mechanism Analysis

Drive mechanisms in oil reservoir in Haripur field during oil production period (1987 to 1994) have been determined from analysis of tube head pressure and oil production rate history from 1987 to 1994. Reservoir produces oil and gas by natural depletion using drive mechanisms also called natural drives which are followings:

- Gas cap drive
- Water drive
- Rock compaction
- Expansion of oil
- Solution gas drive
- Gravity drainage

In the case of oil reservoir in Haripur field during oil production period, it is observed that tube head pressure and oil production rate has fallen simultaneously. This occurs when reservoir has no strong drive mechanisms such as gas cap drive and water drive. Well head pressure never falls when gas cap and water drive are active. Oil has been produced by rock compaction, expansion of oil and solution gas drive. Produced oil is heavy oil which API gravity is 28.2.

3.2 Oil Recovery Technique Design in Haripur Field

When reservoir terminates production after natural depletion then engineer and scientists perform intensive work on reservoir to design remaining hydrocarbon recovery from the reservoir as energy demand is increase exponentially. There are systematic procedures to do this job in oil and gas industries. Here an effort has been made to design oil recovery technique to recover remaining oil from oil reservoir in Haripur field. There are available enhanced oil recovery methods used in oil and gas industries as shown in figure 3.71.

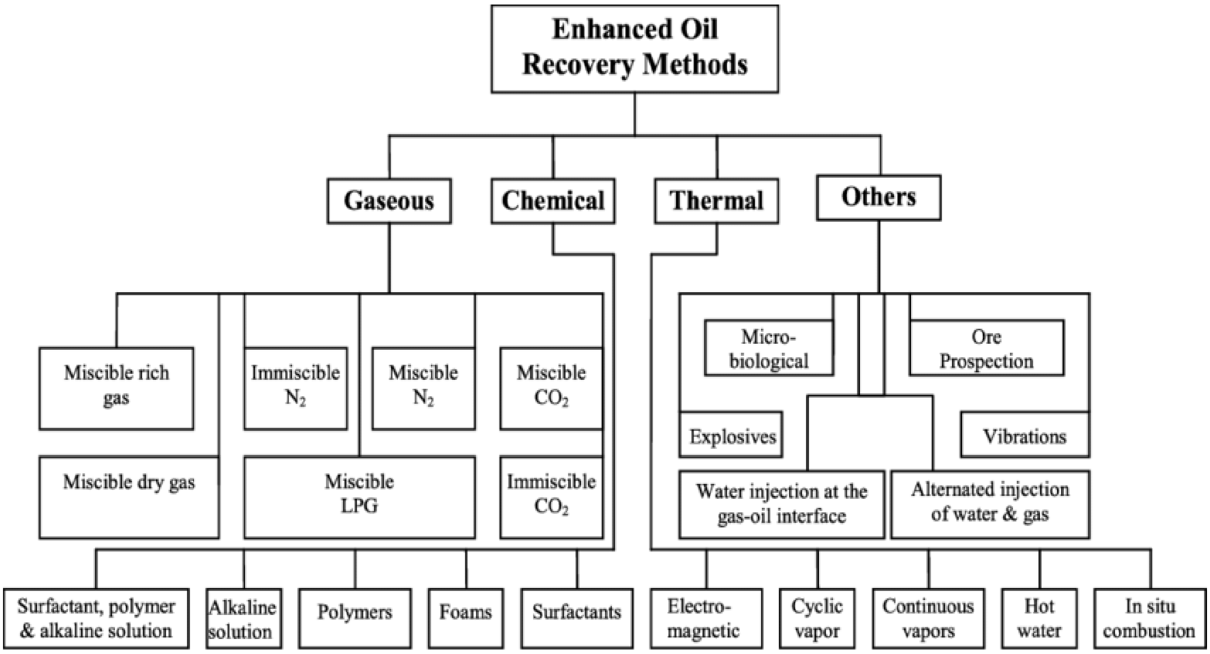

Figure 3.71: Enhanced oil recovery (EOR) methods

Low Salinity EOR

In recent years, brine-rock-oil chemistry has generated a lot of interest in relation to improving oil production from reservoirs. In carbonate reservoirs, the brine constituents have been found to be important for oil recovery. In sandstone reservoirs, the salinity and components of the brine have shown a lot of promise to improve recovery. A number of requirements have been listed as being necessary for low salinity improved recovery. These include:

- Presence of clay or some negatively charged rock surfaces.
- Polar components in the oil phase.
- Presence of formation water.
- Presence of divalent ion/multicomponent ions in the formation water.

3.2.1 Screening of Oil Reservoir in Haripur Field

Chemical properties of reservoir oil, reservoir water and reservoir rock must be estimated to design the appropriate oil recovery mechanism which is technically effective and economically viable. In light of this matter, reservoir oil, water and rock sample have been collected. Laboratory tests are performed on the reservoir oil, water and rock sample.

Reservoir Oil

Oil sample of Haripur field has been collected to estimate its chemical properties. Laboratory tests have been performed on the oil sample and acid number, base number, density, viscosity, average molecular weight and API gravity have been estimated. It has been seen that, the oil has good acid number shown in table 3.8 which indicates that reservoir oil contains significant amount of polar compounds. These polar compounds make bond with negatively charged surface (clay surface) through divalent ions such as Ca^+ and Mg^+ shown in figure 3.72.

Table 3.8: Chemical properties of reservoir oil

Oil Sample	Acid No. mg KOH/g	Base No. mg KOH/g	Density g/cc	Viscosity cp (3000 psi, 200°F)	API Gravity	Average Molecular Weight
OS-01	1.82	0.54	0.804	1.1	28.2	220.85

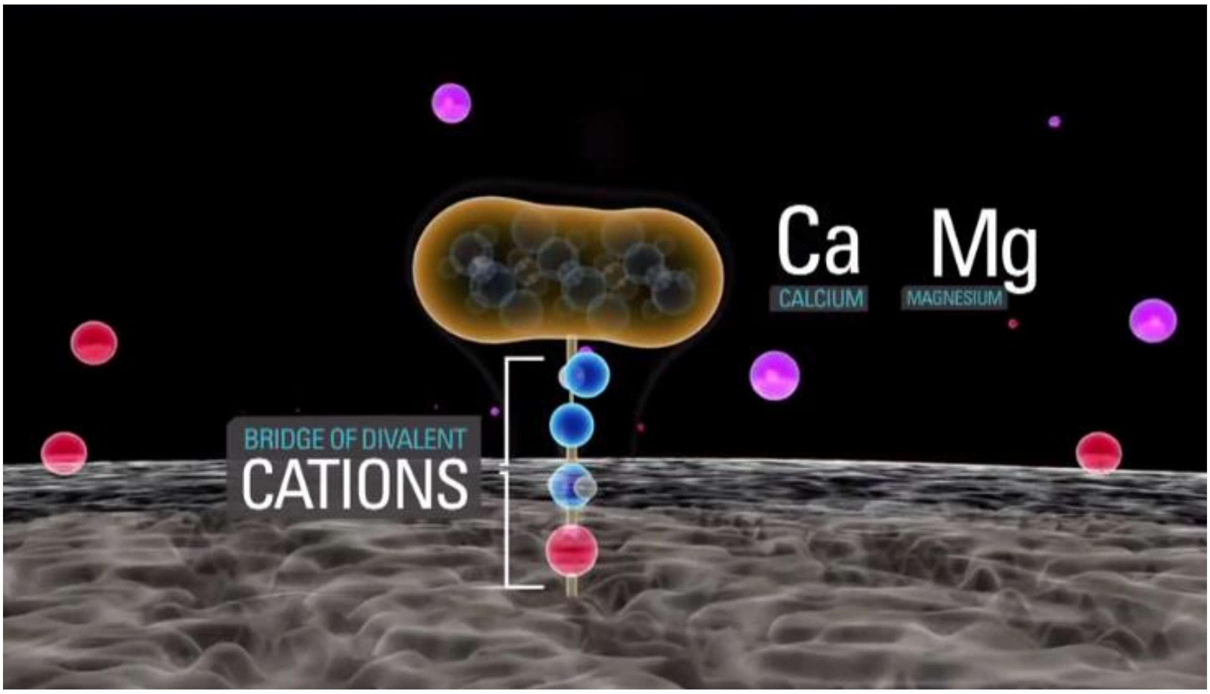

Figure 3.72: Oil bond with clay surface (Alagic E., 2010)

Reservoir Water

Reservoir water provides divalent ions for making bond between oil molecules and clay surface. In high salinity water environment the bond between oil molecules and clay surface becomes compressed due to the high concentration of Ca^{+} and Mg^{+} shown in figure 3.73. Then the bond becomes strong. The reservoir water sample has been collected and tested in laboratory. The tests results have yielded that reservoir water has significance Ca^{+} and Mg^{+} concentration and high salinity shown in table 3.9.

Table 3.9: Chemical properties of reservoir water

Water Sample	Cl^{-} mol/l	Na^{+} mol/l	Mg^{2+} mol/l	Ca^{2+} mol/l	Salinity ppm
RW-01	1.72	1.54	0.144	0.09	100,000

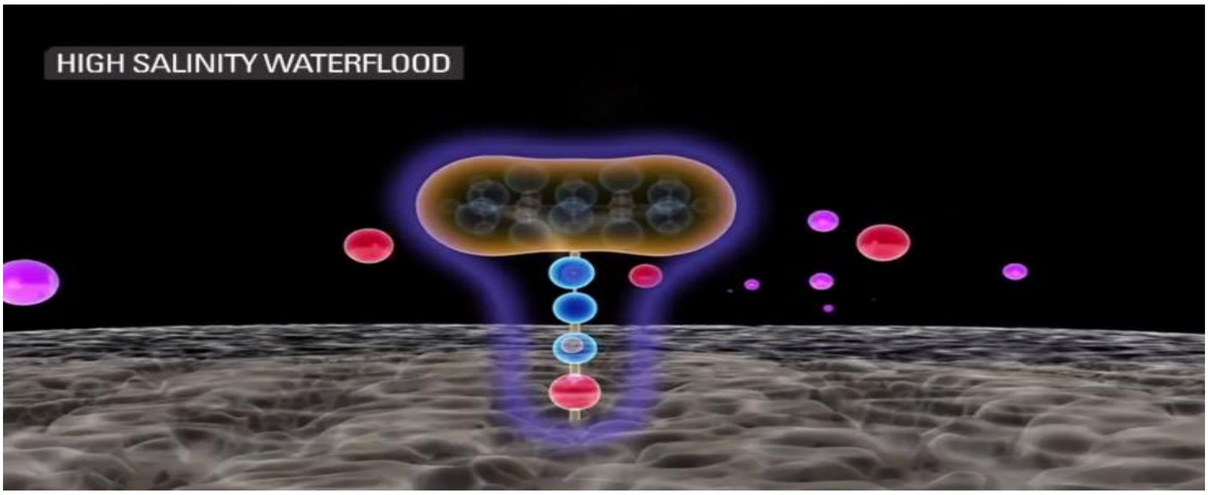

Figure 3.73: Oil bond with clay surface in high salinity water (Alagic E., 2010)

Reservoir Rock

Clay contents in reservoir rocks play important roles in oil recovery mechanism design. Reservoir rocks sample of Bhubon formation have been tested in laboratory as shown in table 3.10 to determine clay contents by Deepak et al., (2013). Bhubon formation contains important negatively charged surface clays such as Illite/Mica, Chlorite, Kaolinite and Montmorillonite in a good amount.

Table 3.10: Chemical properties of reservoir rock (Deepak et al., 2013)

Rock Sample	Illite/Mica Composition %	Chlorite Composition %	Kaolinite Composition %	Montmorillonite Composition %
RR-01	1	2	5	1

Table 3.11: Properties of clay minerals (International Drilling Fluids, IDF, 1982)

Properties	Kaolinite	Illite/Mica	Montmorillonite	Chlorite
Layer Structure	1:1	2:1	2:1	2:1:1
Particle Size (Micron)	5-0.5	Large Sheets to 0.5	2-0.1	5-0.1
Cation Exchange Capacity (CEC) (meq/100 g)	3-15	10-40	80-150	10-40
Surface Area BET-N_2 (m^2/g)	15-25	50-110	30-80	140

It has been observed that, Bhubon formation has significant quantities of negative charge surface clay. High salinity reservoir water provides divalent ions for the creation of bond between oil molecules and the clay surface. Properties of clay minerals are shown in table 3.11.

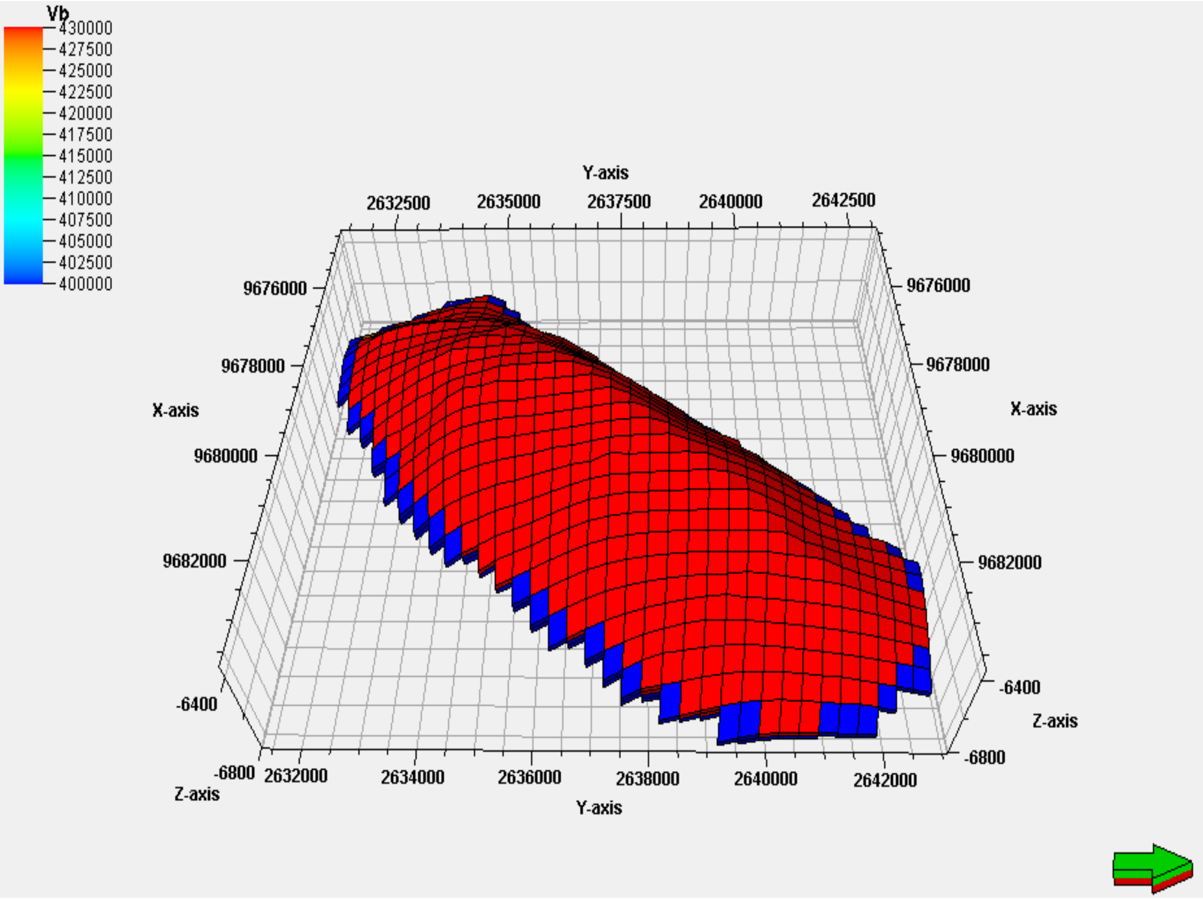

Figure 3.74: Bulk volume of reservoir rock

As reservoir rock of Haripur oil reservoir is Bhubon formation, so it is possible to quantify the amounts of oil to be bonded with clay in the Haripur oil reservoir. Reservoir bulk volume is 74370 m^3 as shown in figure 3.74 and weight of reservoir rock is 163614 ton. Cation exchange capacity of clay can exchange cation in milli equivalent. Each milli equivalent of exchange cation can bond two milli equivalent of oil. The quantities oil bonded by clay is shown in table 3.12.

Table 3.12: Quantities oil bonded by clay

Parameters	**Illite/Mica**	**Chlorite**	**Kaolinite**	**Montmorillonite**
Weight %	1	2	5	1
Clay, g	1636140000	3272280000	8180700000	1636140000
Cation Exchange Capacity (CEC) (meq/100 g)	40.00	40.00	15.00	150.00
Cation Exchange, meq	654456000	1308912000	1227105000	2454210000
Oil, meq	1308912000	2617824000	2454210000	4908420000
Oil, mg (MW=220.85)	2.89073E+11	5.78146E+11	5.42012E+11	1.08402E+12
Oil, bbl (density 0.804 gm/cc)	2261.281761	4522.563522	4239.903302	8479.806604
Total (MMbbl)				0.0195

Total oil present in reservoir is 33 million barrels as shown in figure 3.75. Total 0.0195 million barrel of oil is bonded with clay.

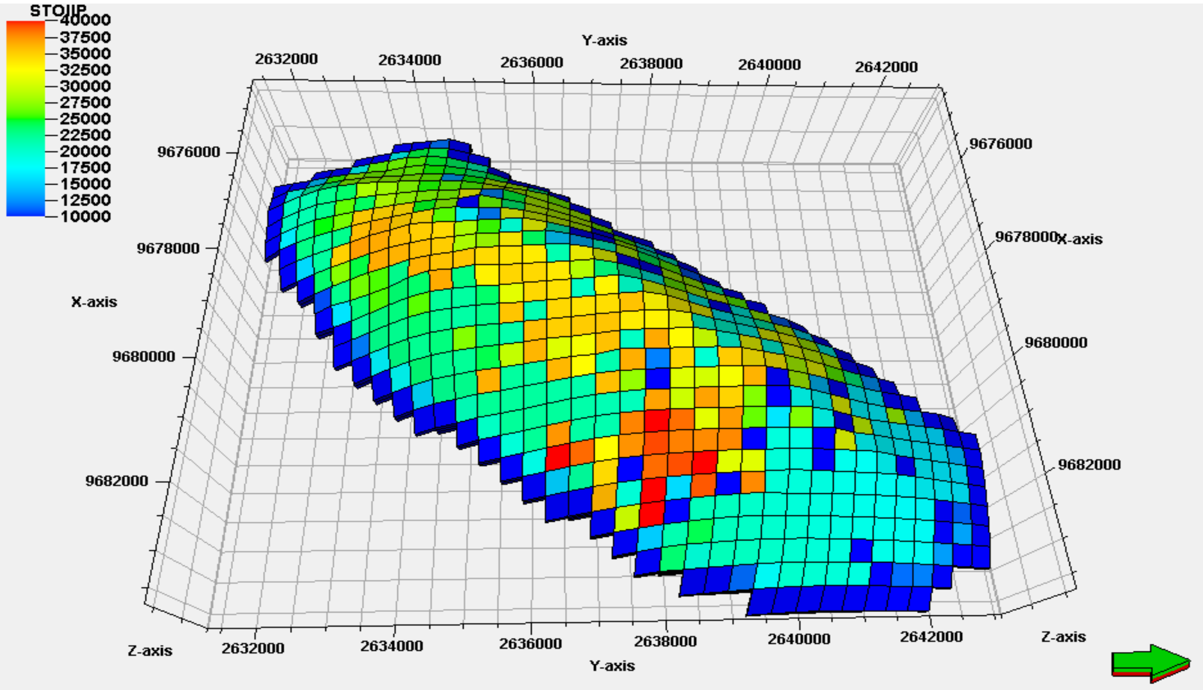

Figure 3.75: Oil in reservoir

3.2.2 Optimization of Oil Recovery Technique in Haripur Field

Analysis result of oil production period has revealed that reservoir has still good dynamic performance and oil production has terminated due to the scale and wax deposition in the production tube. Reservoir needs to be pressurized to lift oil through 6700 ft vertical production tube where 2246 psi pressure is required to produce 303 STB/D of oil as shown in figure 3.76.

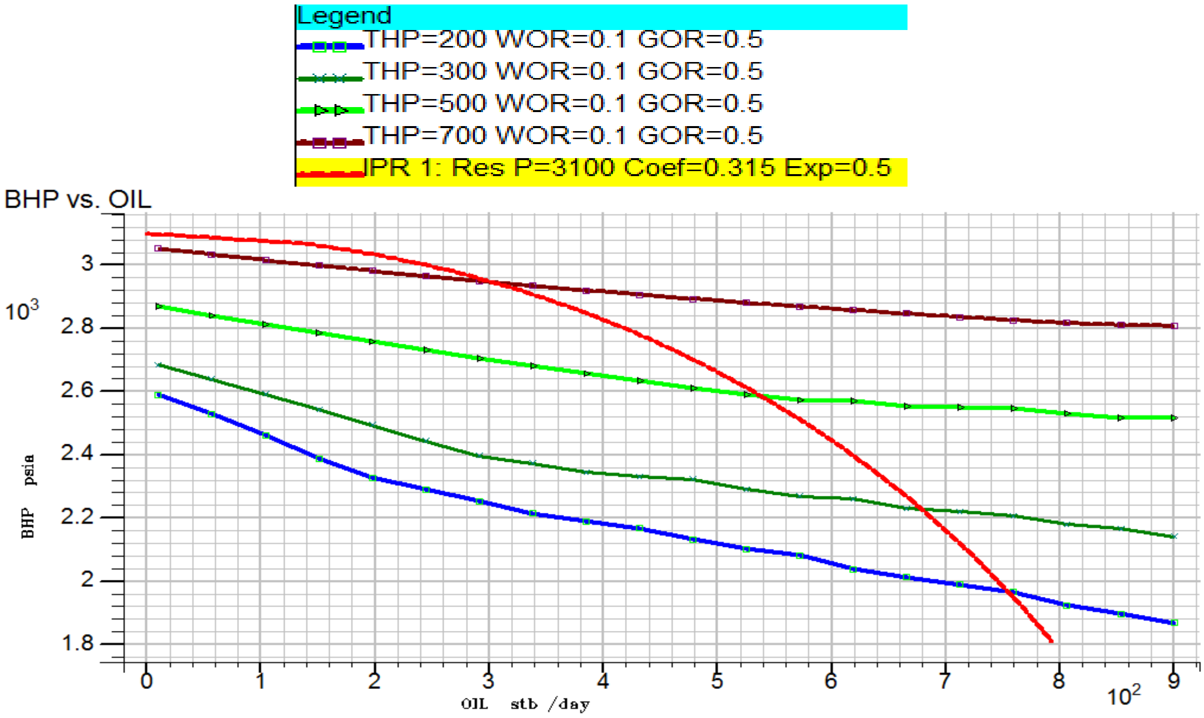

(a)

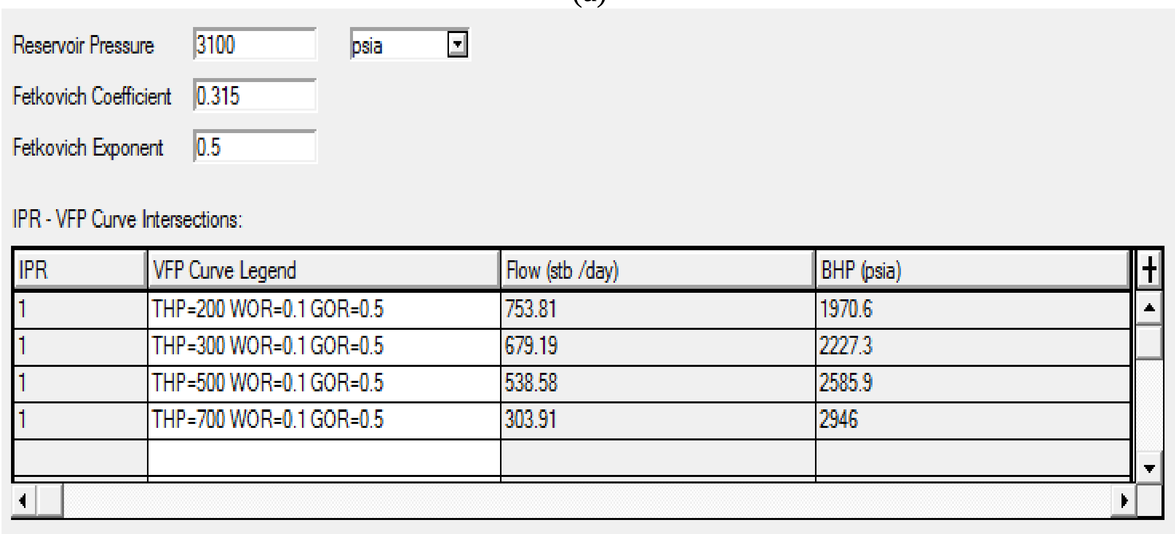

Reservoir Pressure 3100 psia

Fetkovich Coefficient 0.315

Fetkovich Exponent 0.5

IPR - VFP Curve Intersections:

IPR	VFP Curve Legend	Flow (stb /day)	BHP (psia)
1	THP=200 WOR=0.1 GOR=0.5	753.81	1970.6
1	THP=300 WOR=0.1 GOR=0.5	679.19	2227.3
1	THP=500 WOR=0.1 GOR=0.5	538.58	2585.9
1	THP=700 WOR=0.1 GOR=0.5	303.91	2946

(b)

Figure 3.76: a) Vertical flow performance and inflow performance relationship curves and b) BHP, THP and oil flow rate

On the other hand, a good quantity of oil is bonded with clay in pore space of the reservoir rock and total remaining oil reserve is only 32.47 million barrel. Oil recovery mechanism is selected in such a way that the recovery techniques pressurize the reservoir and break the bond between oil and clay, as well as economic. Oil recovery mechanism, such as low salinity water flooding, is able to meet the design requirements such as pressuring the reservoir, releasing oil from clay, low cost operation.

Low Salinity Water

In low salinity environment the bond between clay and oil expands and becomes weak. Then monovalent ion such Na^{+} displaces the divalent ions such as Ca^{++}, Mg^{++}. As a result, oil is released from clay surface shown in figure 3.77.

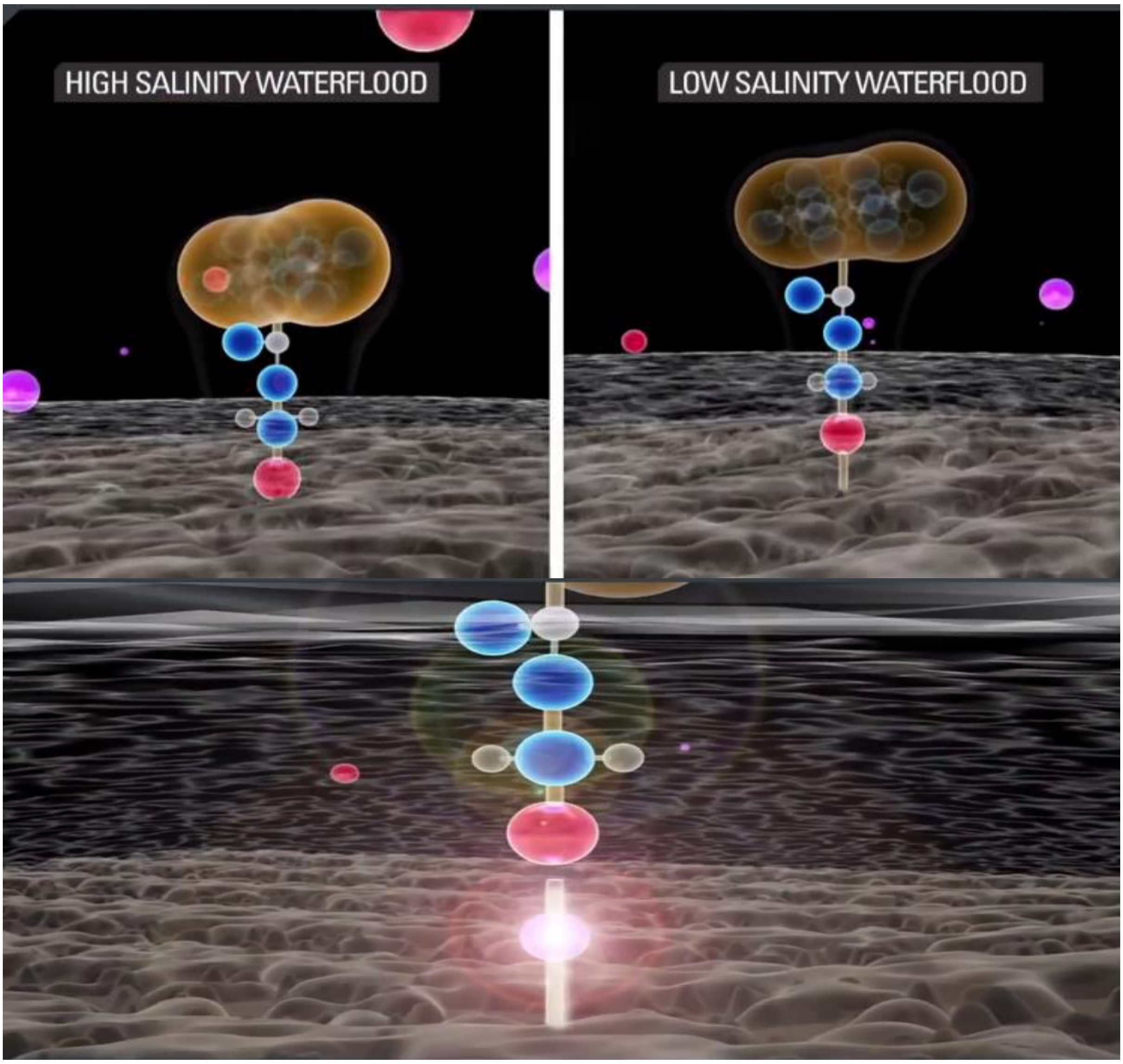

Figure 3.77: Low salinity effect (Alagic E., 2010)

High salinity water contains sufficient dissolved ions which push oil molecules to confine. Then oil molecules aggregate and form bigger oil droplets. Interfacial tension between oil and water becomes high. The bigger oil droplets are not able to flow through the narrow pore throats. On the other hand, low salinity water contains less dissolved ions which allow oil molecules to disperse into small droplets. Interfacial tension between oil and water becomes low. The small oil droplets are able to flow through the narrow pore throats.

It is important that the law salinity water must contain certain amount of monovalent ions such as Na^+ for displacing the divalent ions. Law salinity water of 500 ppm to 2000 ppm is used in industries. In light of this matter, 500 ppm, 1000 ppm, 1500 ppm, 2000 ppm and 100000 ppm NaCl solution in water have been prepared for core flood test to evaluate performance of the water solution.

Coreflood Test

From the experiment it is observed that, water of salinity 1000 ppm has yielded maximum recovery as shown in figure 3.78. 1000 ppm water solution is able to produce 15% additional oil over the 100000 ppm water solution. 500 ppm water solution is not able to produce additional oil over the 1000 ppm water solution because 500 ppm water solution has provided less monovalent ion for displacing divalent ions. The optimum salinity of water is 1000 ppm for injection in the reservoir to recover the remaining oil.

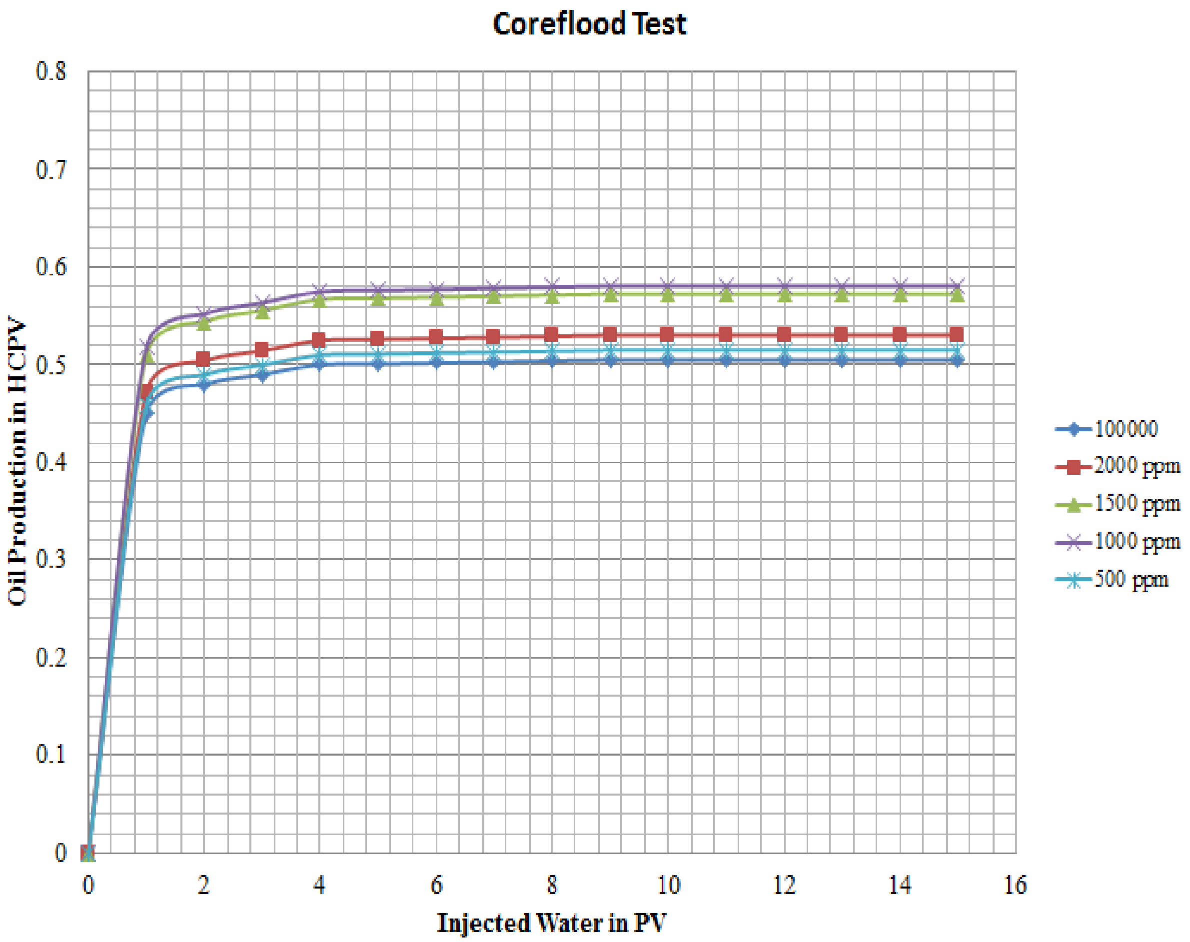

Figure 3.78: Coreflood test result

Improvement of Oil Relative Permeability

Relative permeabilities of oil-water-rock system for 100000 ppm salinity water and 1000 ppm salinity water have been estimated in laboratory. Effect of the low salinity water is to improve the oil relative permeability and reduce water relative permeability of the oil-water-rock system as shown in figure 3.79. Low salinity water injection will increase the oil flow rate and decrease the water flow rate inside the reservoir.

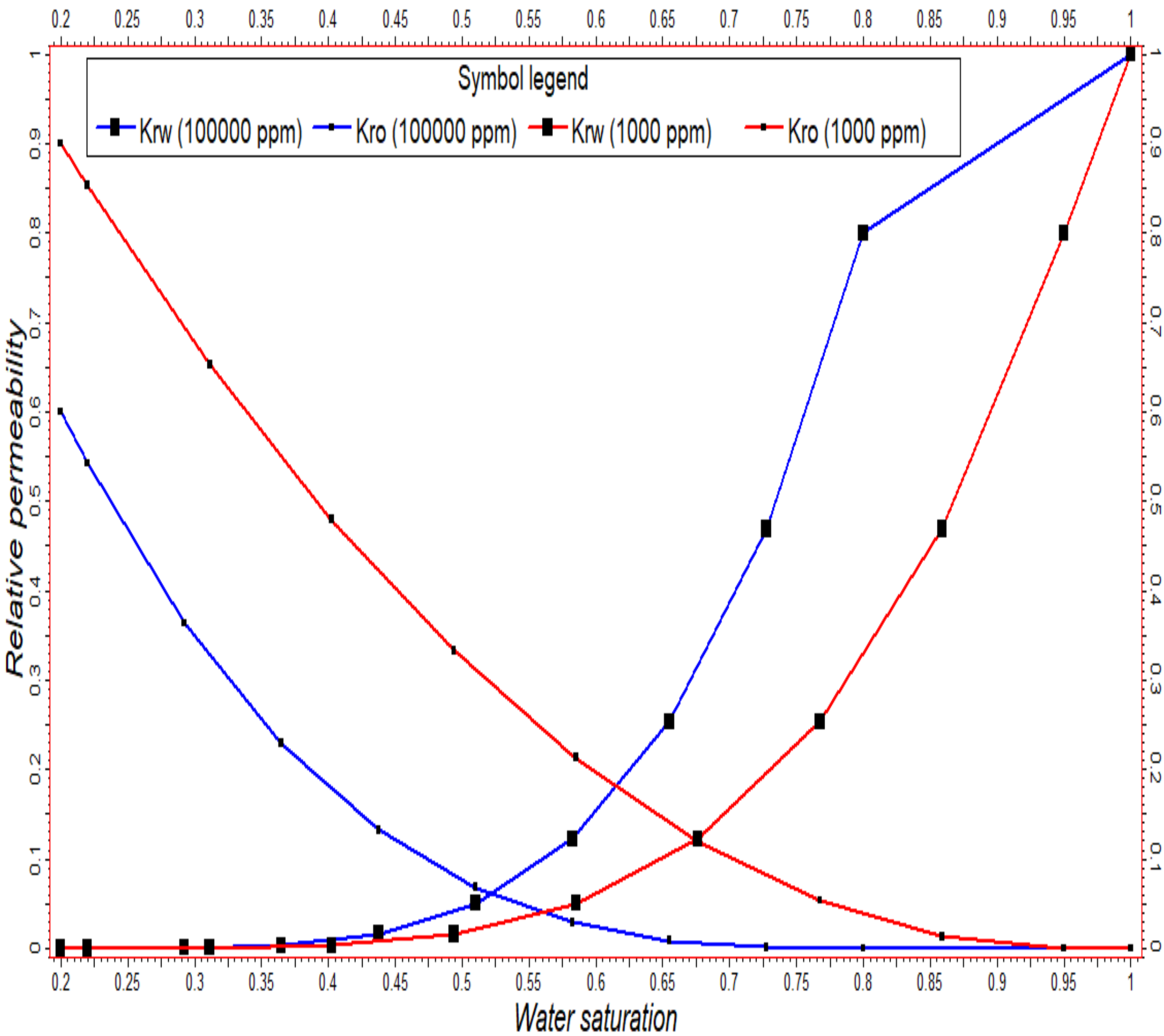

Figure 3.79: Relative permeability profile

Estimated relative permeabilities have inserted into the reservoir simulation model for observing the dynamic performance of the reservoir under different salinity water. Streamline simulation is able to show the dynamic performance of the reservoir by developing streamlines of oil flow rate, oil flow direction, water flow rate, water flow direction and time of flight among injection and production wells.

Improvement of Oil Streamline

Streamlines of oil flow rate have been generated for the 100000 ppm salinity water and 1000 ppm salinity water as shown in figure 3.80 and figure 3.81 respectively to examine dynamic behavior of oil in reservoir. When 1000 ppm salinity water has injected in the reservoir then monovalent ions displace divalent ions to release oil from clay surface.

In addition, interfacial tension between oil-water also reduces in low salinity water environment. As a result oil splits into small droplets and starts to flow through the pore space and pore throat. Streamlines of oil flow rate have become denser in 1000 ppm salinity water environment than 100000 ppm salinity water environment.

Streamlines of water flow rate have been generated for the 100000 ppm salinity water and 1000 ppm salinity water as shown in figure 3.82 and figure 3.83 respectively to examine dynamic behavior of water in reservoir. Streamlines of water flow rate have become less dense in 1000 ppm salinity water environment than 100000 ppm salinity water environment. Mobility of water has become less in 1000 ppm salinity water environment.

Water breakthrough will also be delayed in 1000 ppm salinity water environment as water has advanced less in 1000 ppm salinity water environment. It will be worthwhile to develop the reservoir with 1000 ppm salinity water injection technology.

1000 salinity water is less conductive as water mobility decreases and oil mobility increases. Water engages in sweeping oil rather than flowing through the pore space. Na^{+} ions in water is engages in displacing the Ca^{+2} and Mg^{+2} ions to free the oil from clay surface.

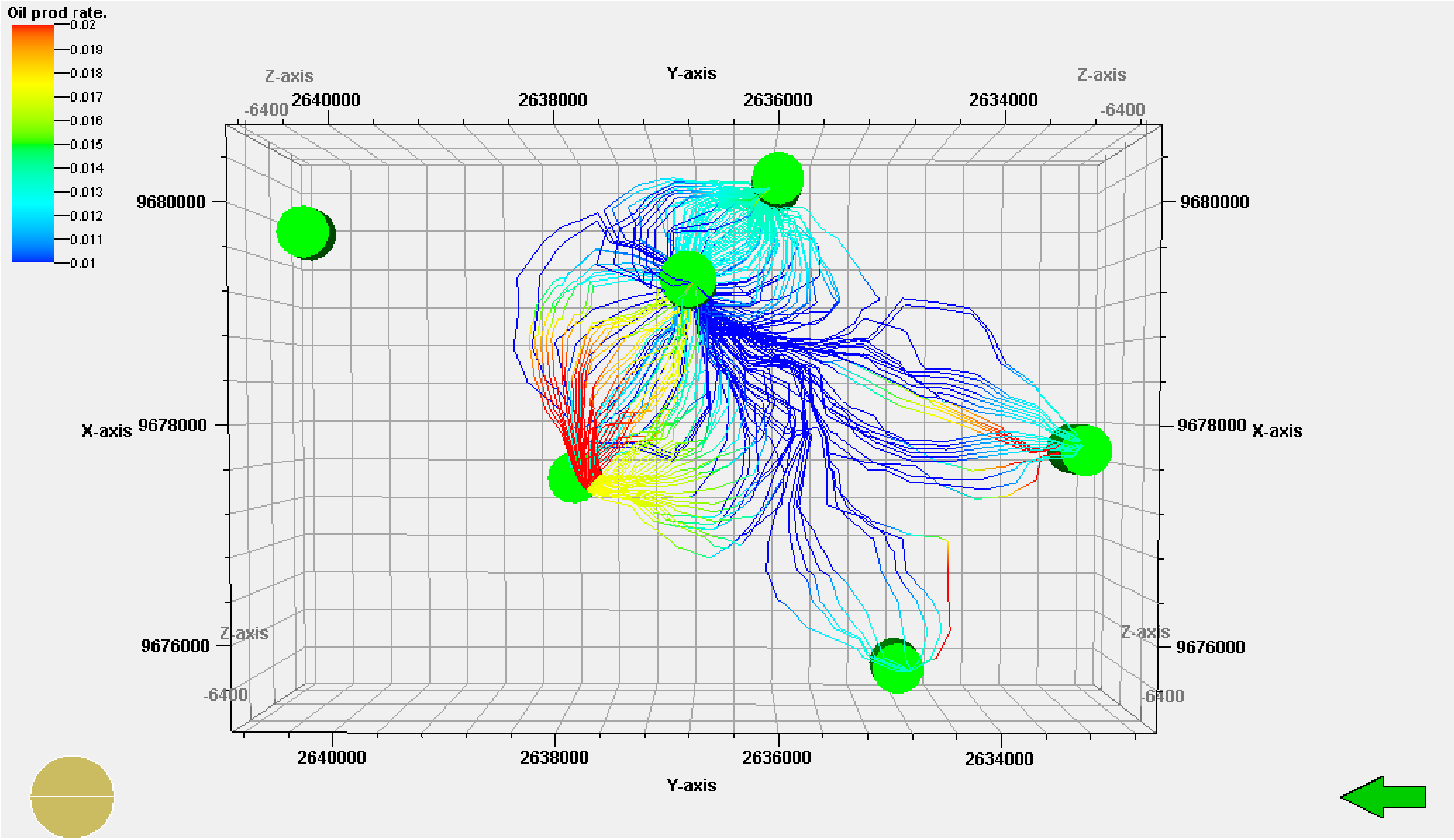

Figure 3.80: Streamline of oil flow rate at 100000 ppm salinity environment

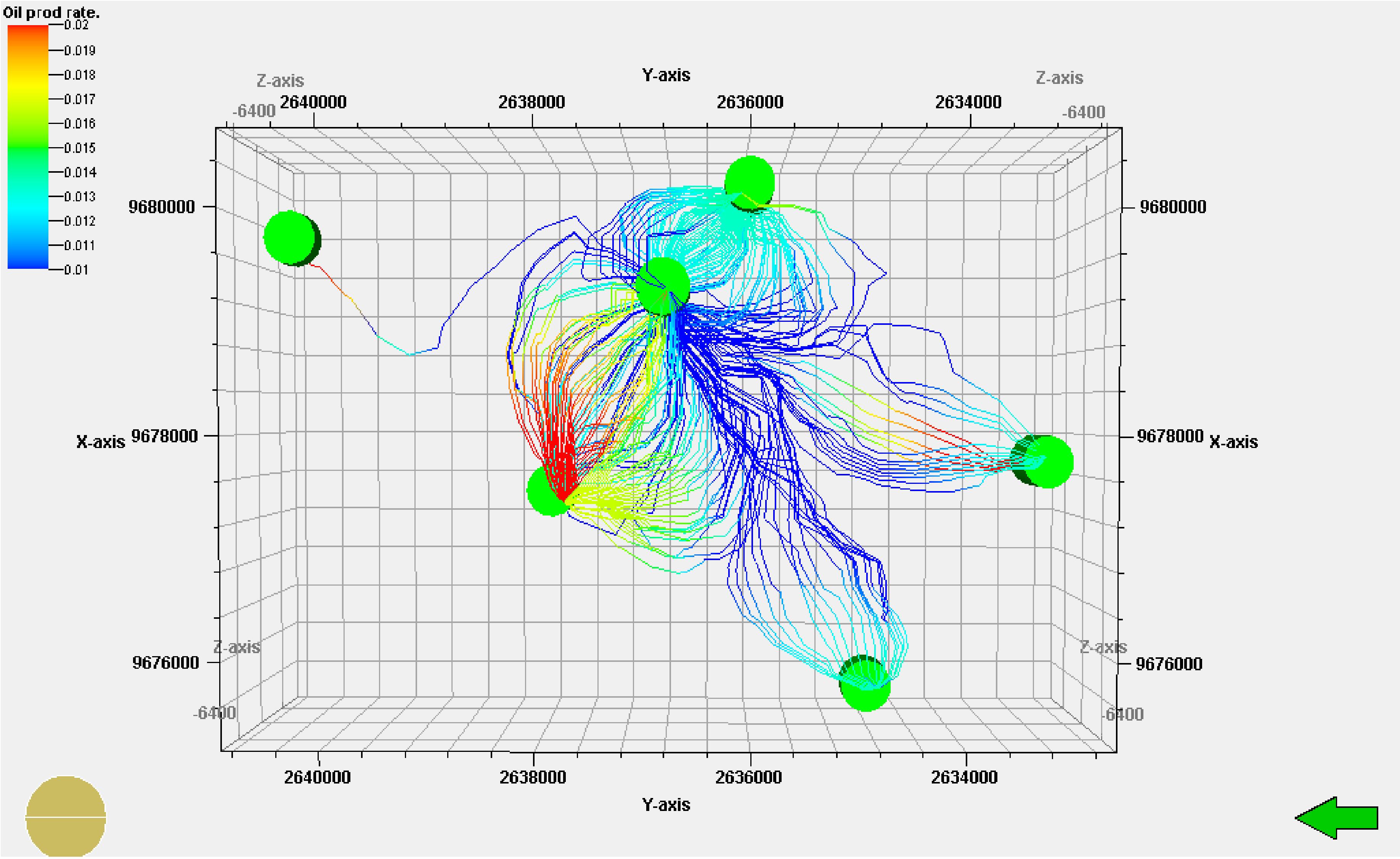

Figure 3.81: Streamline of oil flow rate at 1000 ppm salinity environment

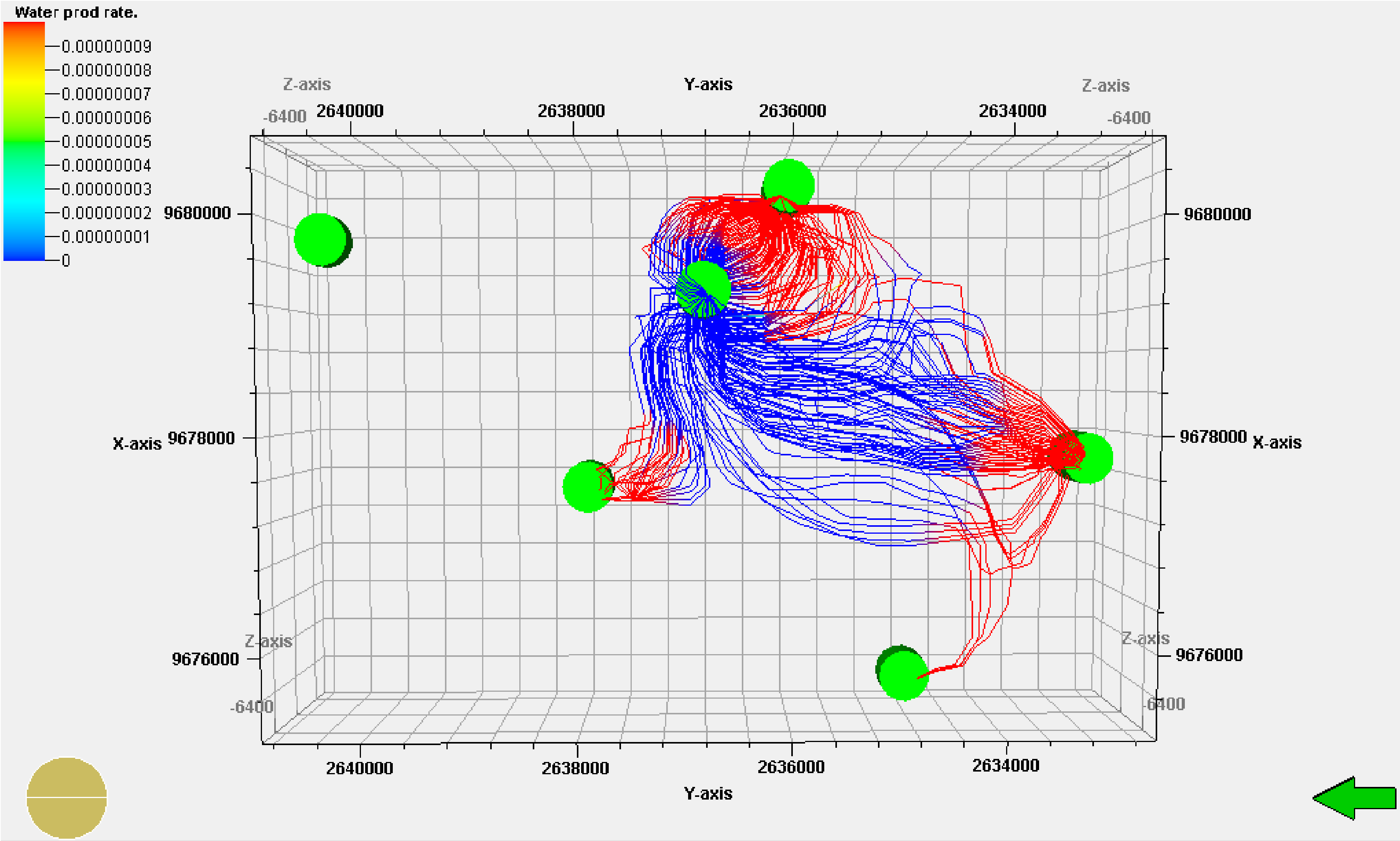

Figure 3.82: Streamline of water flow rate at 100000 ppm salinity environment

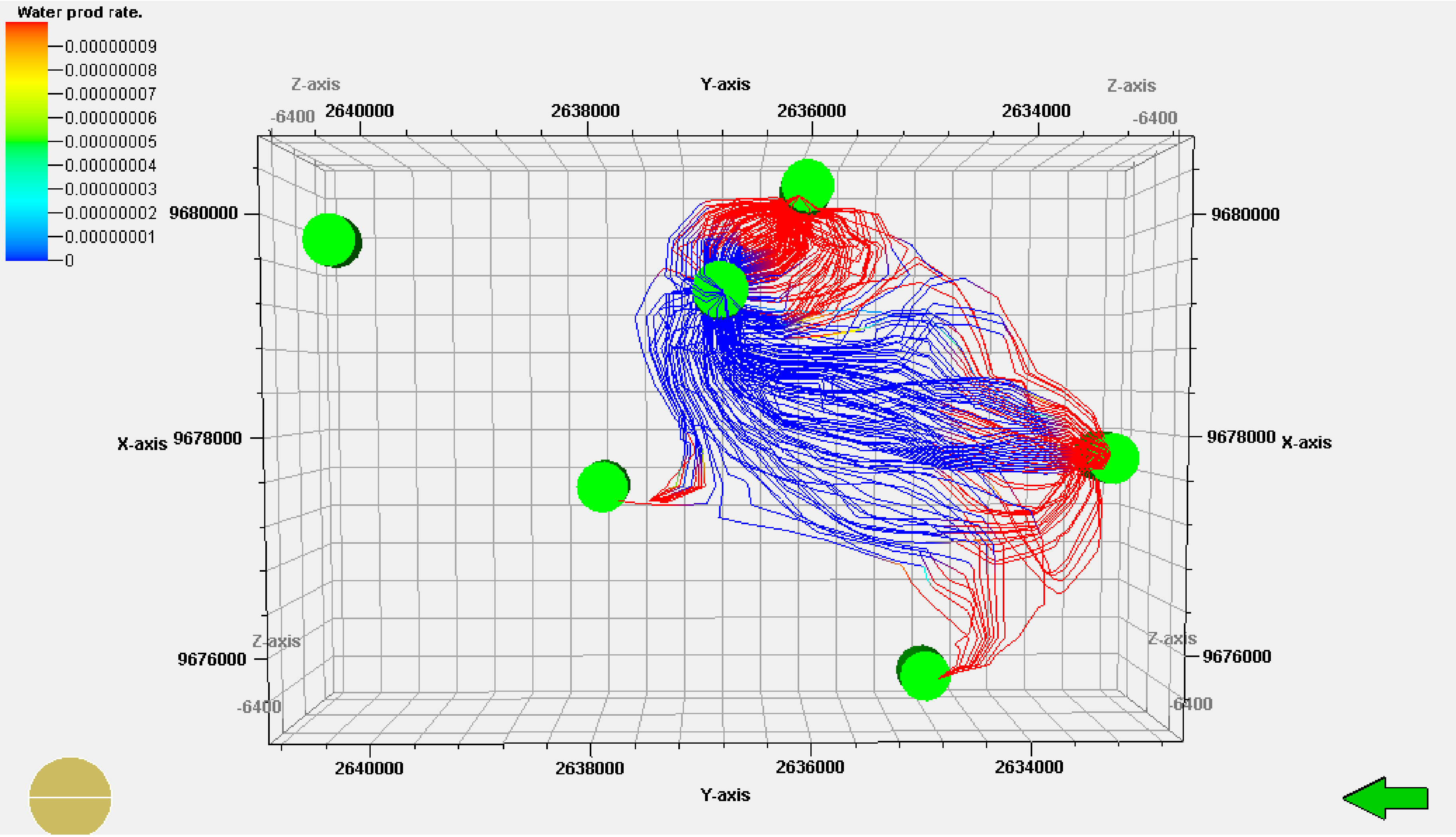

Figure 3.83: Streamline of water flow rate at 1000 ppm salinity environment

3.3 Generation of Oil Reservoir Development Scenario in Haripur Field

Preparation of reservoir development scenario is an integration of art and science. There are no specific theories for reservoir development scenario. Experts are focusing only on the maximum economic hydrocarbon recovery from reservoir by the optimum development scenario. Reservoir development variables must be optimized to furnish an appropriate reservoir development scenario. Development variables are not specific, they varies reservoir to reservoir. In this study, an effort has been done to prepare reservoir development plan for oil reservoir in Haripur field. Reservoir study has recommended that remaining 33 million barrels of oil can be recovered by low salinity water injection to pressurize the reservoir and release clay trap oil. On the basis of these information and recommendation reservoir development variables have been determined and optimized.

Reservoir Development Variables

Reservoir investigation has revealed that 1000 ppm salinity water injection method is appropriate to recover oil from the reservoir. Following reservoir development variables are needed to be optimized.

- Positions of the oil production wells in reservoir.
- Number of oil production wells.
- Positions of the water injection wells in reservoir.
- Number of water injection wells.
- Optimum oil production rate and oil pressure at tube head.
- Optimum water injection pressure and rate.

Optimization of Number and Positions of Oil Production Wells

Oil zone always lies above the water zone by the hydrostatic equilibrium as oil is lighter than the water. In this reservoir there are an oil zone and a water zone below the oil zone as shown in figure 3.84. These two zones are hydraulically connected. There is oil-water contact at the periphery of the oil zone in all direction. Oil production wells must be placed at the center of the oil zone to prolong oil production time and delay water breakthrough as injected water is advancing toward the production wells. Another consideration of oil well placement is oil well is placed in high oil saturation zone. At the center of the oil zone has high oil saturation and also away from oil water contact boundary.

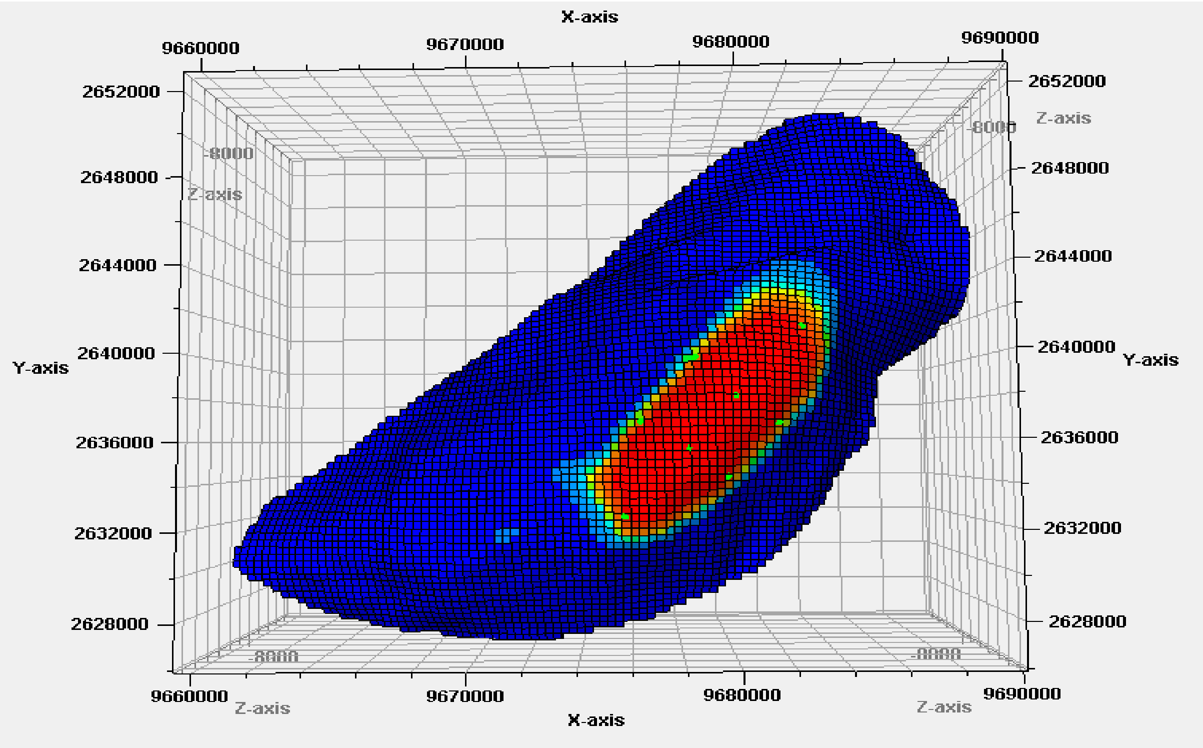

Figure 3.84: Oil reservoir model

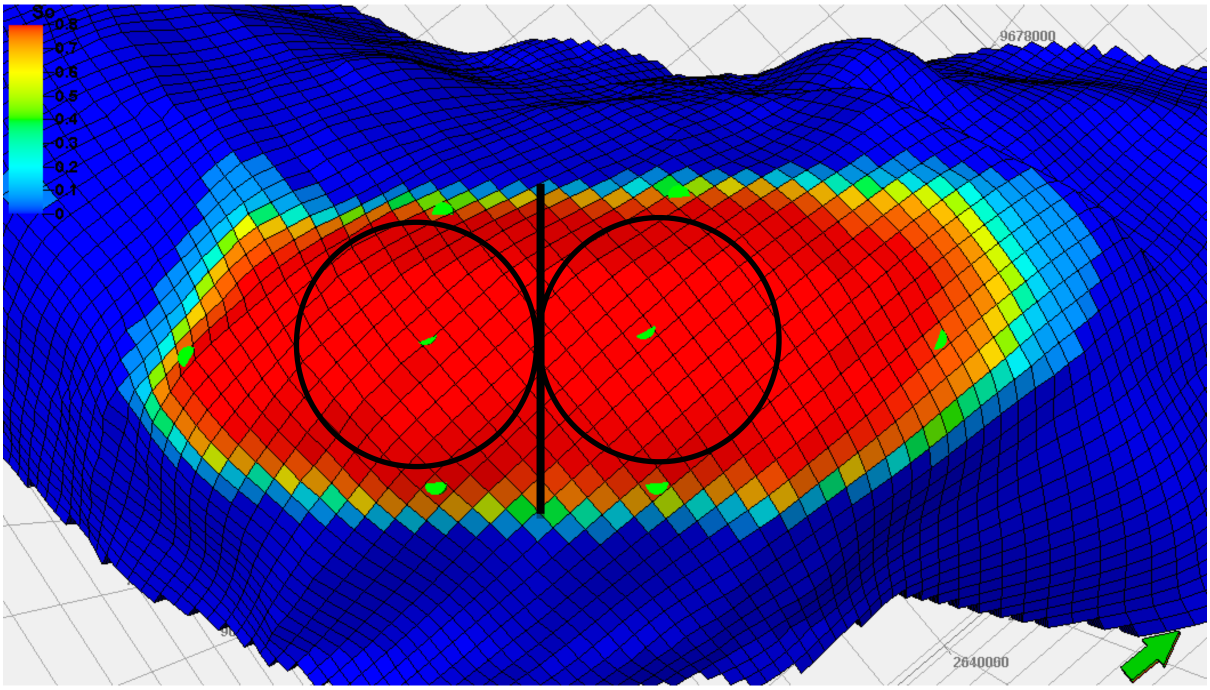

Figure 3.85: Area of oil zone

The distance of oil zone from north-east corner to south-west corner is 10912 ft and 4319 ft from south-east corner to north-west corner as shown in figure 3.85. The distance of oil zone from north-east corner to south-west corner is double of the distance from south-east corner to north-west corner. Oil zone has divided into two equal parts along north-east corner to south-west corner. Two production wells are placed in the center of two parts so that each production well is able to establish equal drainage area of equal radius in all directions.

Optimization of Number and Positions of Water Injection Wells

According to the industrial practice water is injected at the bottom boundary of the oil zone and oil is produced from crest of the oil zone to prolong oil production time and delay water breakthrough. Water injection wells are to be placed at oil-water contact. Each part of oil zone has oil-water contact at three sides. Three water injection wells are to be placed around an oil production well. Altogether six water injection wells are to be placed around two oil production wells and they are equally apart from each other as shown in figure 3.86.

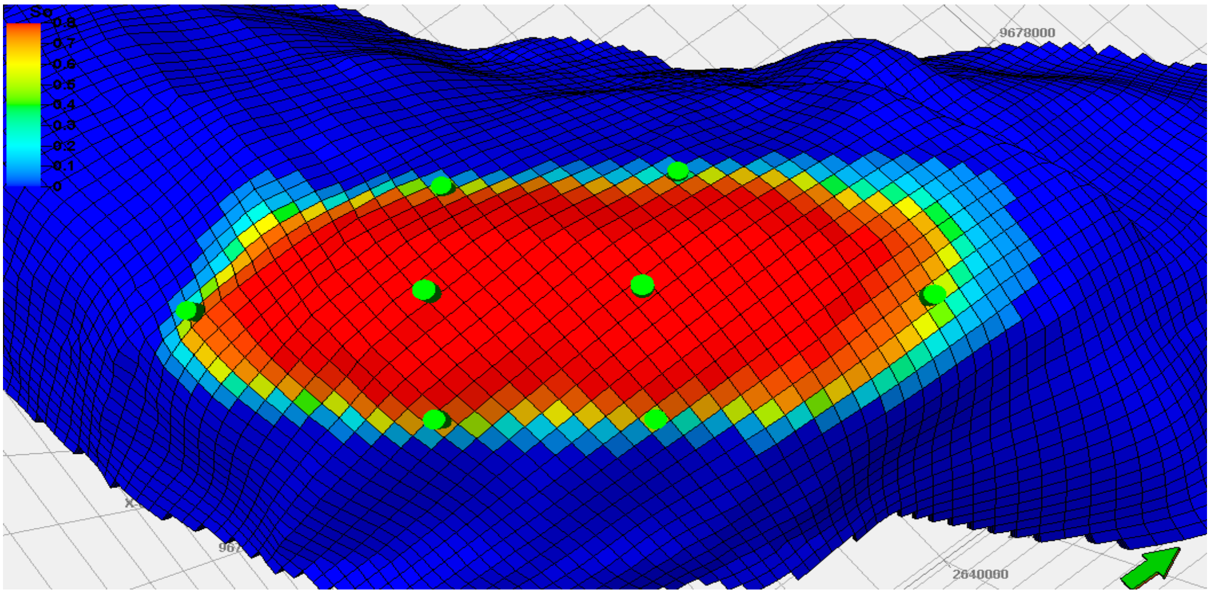

Figure 3.86: Oil production wells and water injection wells

Optimization of Oil Production Rate and Oil Pressure at Tube Head

In this reservoir bottom boundary of the oil zone is oil-water contact at depth of 6700 ft and crest of the oil zone is at depth of 6600 ft. Oil production performance is designed by VFPi software using following data to optimize oil production rate and oil pressure at tube head. Tube head pressure must be kept at minimum of 500 psi to operate the oil-gas-water separators.

Tube Data of Oil Production Well:

- Tube length is 6600 ft
- Tube diameter is 5 inch
- Tube head pressure is 500 psi

Fluids Data:

- Water Oil Ratio (WOR) is 0.001
- Gas Oil Ratio (GOR) is 0.5 MSCF/STB

Inflow Performance Relationship (IPR) Data:

- Reservoir pore pressure is 2900 psi
- Fetkovich coefficient is 0.316
- Fetkovich exponent is 0.5

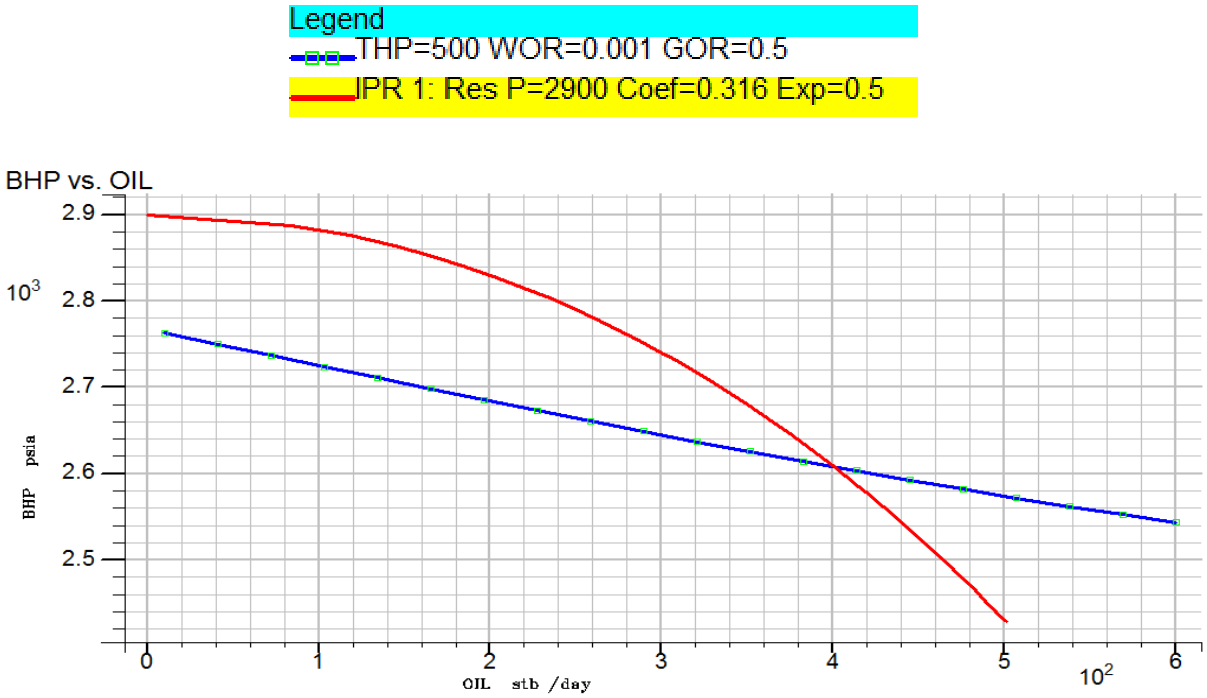

(a)

Reservoir Pressure 2900 psia

Fetkovich Coefficient 0.316

Fetkovich Exponent 0.5

IPR - VFP Curve Intersections:

IPR	VFP Curve Legend	Flow (stb /day)	BHP (psia)
1	THP=500 WOR=0.001 GOR=0.5	400.79	2607.9

(b)

Figure 3.87: a) Vertical flow performance and inflow performance relationship curves and b) Optimum BHP, THP and oil flow rate of oil production wells

The optimum oil production rate is 400.79 STB/D as shown in figure 3.87. To maintain optimum oil production rate of 422 STB/D and oil pressure of 500 psi at the tube head minimum required bottom hole pressure is 2607.9 psi.

Optimization of Water Injection Rate and Water Pressure at Tube Head

Water injection pressure and rate have been optimized by water injection performance analysis. Water is to be injected at 6700 ft depth. Water injection performance is designed by VFPi software using following data.

Tube Data of Water Injection Well:

- Tube length is 6700 ft
- Tube diameter is 5 inch

Reservoir Data:

- Reservoir pore pressure is 2900 psi
- Formation fracture pressure is 3500 psi.
- Injectivity index (II) of reservoir is 10 (stb/day)/psi.

<u>Observations of Water Injection Pressure</u>

- Water pressure in bottom hole decreases with increasing of water flow rate due to the friction loss in water injection tube.
- Injected water will not enter into formation when bottom hole water pressure becomes less than the pore pressure (oil pressure).
- On the other hand, injected water will fracture formation when bottom hole water pressure becomes more than the formation fracture pressure.
- Injection water pressure at bottomhole is slightly more than the pore pressure so that injected water can drive the oil toward the oil production wells.
- Injection water pressure at bottomhole is kept 30 to 50 psi over than the pore pressure as per oil and gas industries practice.

Water injection performance analysis has been generated for water injection pressure of 200, 400, 600, 800 and 1000 psi as shown in figure 3.88. Inflow Performance Relationship (IPR) of injected water has generated for injectivity index (II) of 10 (stb/day)/psi.

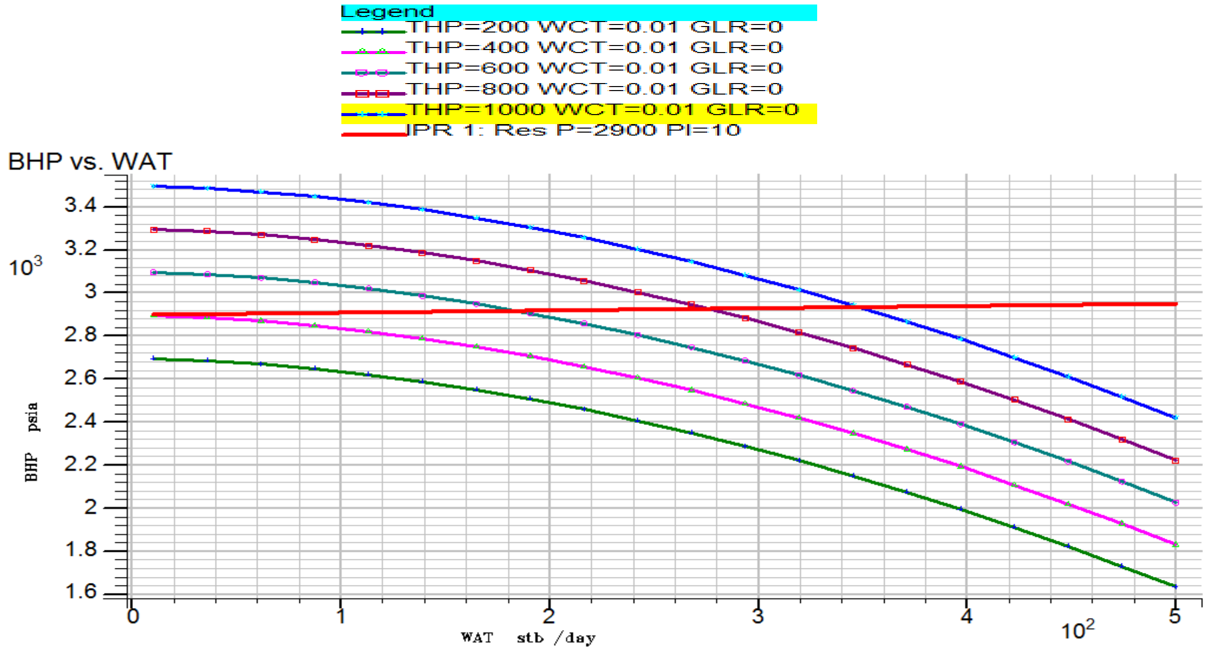

(a)

Reservoir Pressure 2900 psia

Injectivity Index 10 (stb /day) /psi

IPR - VFP Curve Intersections:

IPR	VFP Curve Legend	Flow (stb /day)	BHP (psia)
1	THP=200 WCT=0.01 GLR=0	0	0
1	THP=400 WCT=0.01 GLR=0	0	0
1	THP=600 WCT=0.01 GLR=0	183.42	2918.3
1	THP=800 WCT=0.01 GLR=0	275.54	2927.6
1	THP=1000 WCT=0.01 GLR=0	347.93	2934.8

(b)

Figure 3.88: a) Vertical flow performance and inflow performance relationship curves and b) BHP, THP and water injection rate

<u>Water Injection Pressure Optimization Criteria:</u>

- Bottom hole water pressure must be greater than the pore pressure (2900 psi) and less than the formation fracture pressure (3500 psi).
- According to the industrial practice, bottom hole water pressure is kept slightly more than the pore pressure.

Water injection by pressures of 200 psi and 400 psi will not able to inject water into reservoir because bottom hole water pressures are less than the pore pressure (2900 psi). Water injection by pressures of 600 psi, 800 psi and 1000 psi will able to inject water into reservoir because bottom hole water pressures are greater than the pore pressure (2900 psi).

Observations of Water Injection Rate:

- Injecting less quantities of water will not sweep oil properly and shows poor sweeping efficiency.
- Injecting too much quantities of water will not sweep oil. Water makes channel in the formation and flow directly to the production well without sweeping oil. This case also shows poor sweeping efficiency.

Water Injection Rate Optimization Criteria:

- Injecting such quantities of water so that water sweeps maximum oil to the production well.
- According to the industrial practice, water injection to oil production ratio is kept 2.5-7 to get maximum sweeping efficiency.

When water is injected at pressure of 600 psi, 800 psi and 1000 psi then water injection to oil production ratios are 1.373, 2.06 and 2.60 respectively. Maximum water injection rate is found when water is injected at pressure of 1000 psi. The optimum water injection rate is 347.93 stb/day and optimum water injection pressure is 1000 psi as shown in figure 3.89.

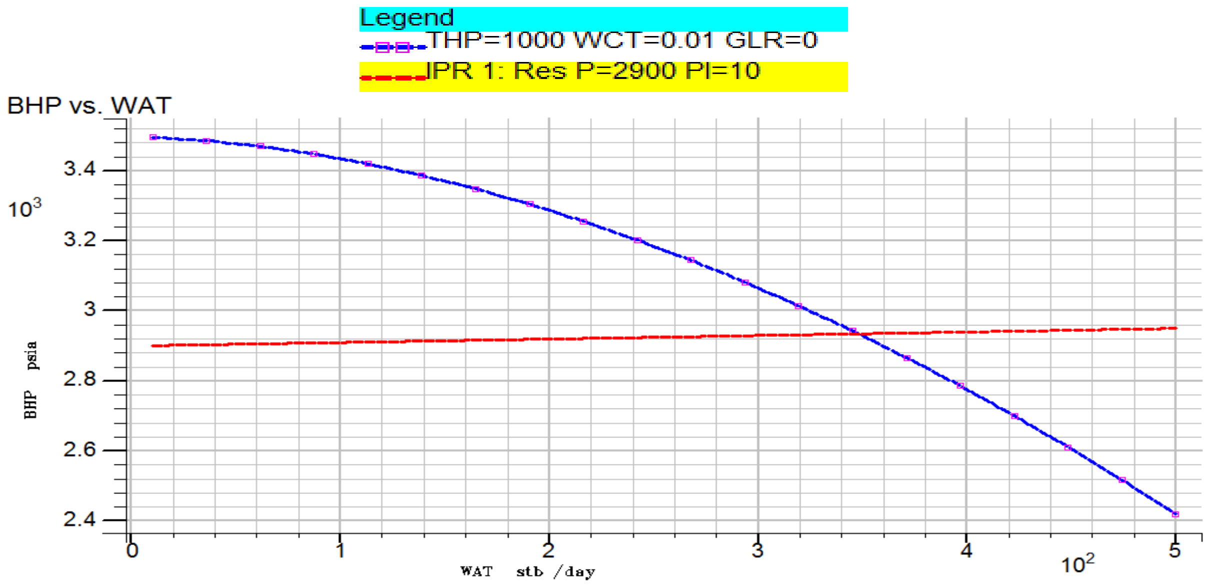

(a)

Reservoir Pressure 2900 psia

Injectivity Index 10 (stb /day) /psi

IPR - VFP Curve Intersections:

IPR	VFP Curve Legend	Flow (stb /day)	BHP (psia)
1	THP=1000 WCT=0.01 GLR=0	347.93	2934.8

(b)

Figure 3.89: a) Vertical flow performance and inflow performance relationship curves and b) Optimum BHP, THP and water injection rate

3.4 Technical Evaluation of Oil Reservoir Development Scenario in Haripur Field

According to optimum reservoir development variables two oil production wells (P1 and P2) and six water injection wells (I1, I2, I3, I4, I5 and I6) have been placed in reservoir as shown in figure 3.90. The reservoir model with development scenario has been simulated to evaluate the reservoir performance such as hydraulic connectivity among wells, fluid conductivity in pore space, oil flow rate, oil flow direction, water flow rate, time of flight, water breakthrough, sweeping efficiency, water channeling.

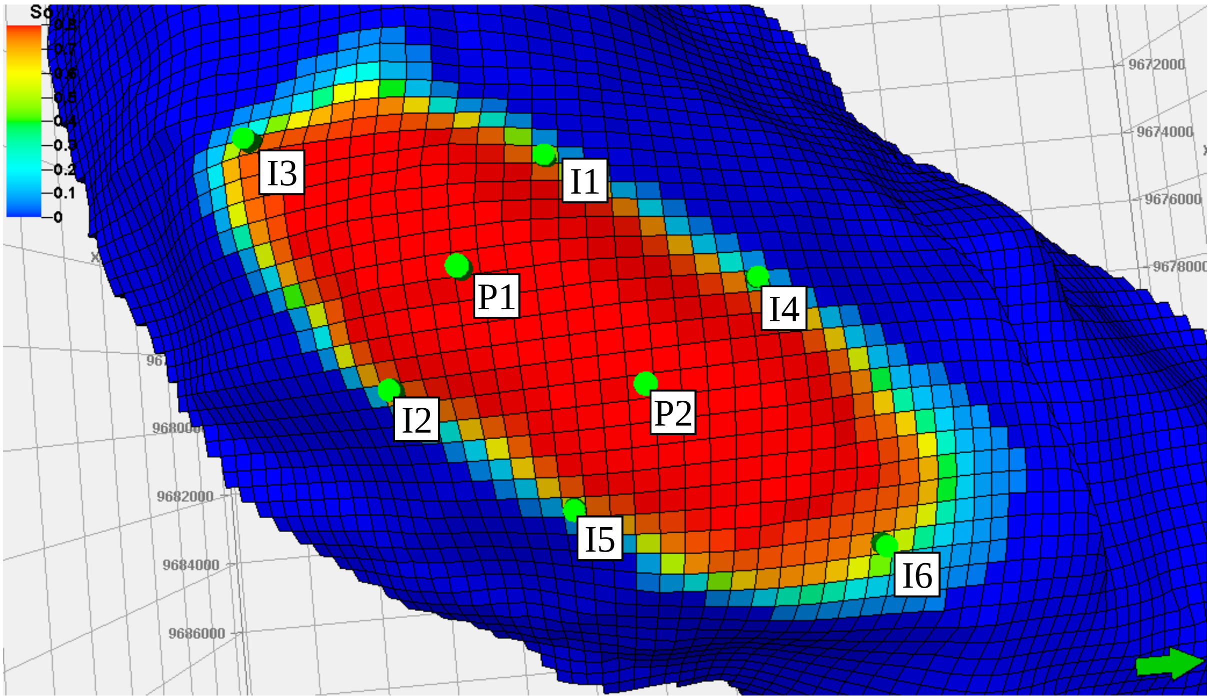

Figure 3.90: Optimum number of wells and their positions in reservoir

Distances between water injection wells and oil production wells are as following:

- P1 and I1 is 2108 ft.
- P1 and I2 is 2018 ft.
- P1 and I3 is 3837 ft.
- P2 and I4 is 2302 ft.
- P1 and I5 is 2008 ft.
- P1 and I6 is 4158 ft.
- P1 and P2 is 2957 ft.

Wells are place to maintain equal distance in north-east to south-west direction and south-east to north-west direction so that all wells are able to develop equal drainage volume.

Streamline simulation has been run on the reservoir with proposed reservoir development option. Streamline simulation has shown dynamic behaviors of the reservoir under the proposed reservoir development option. Hydraulic connectivity between wells has established in reservoir as shown in figure 3.91. Production well P1 has made connection with water injection wells I1, I2 and I3. Water injection wells I4, I5 and I6 are connected with production well P2. Hydraulic connectivity has established in whole reservoir. There is no void and unsweep space in reservoir. This reservoir development option is able to establish a good hydraulic connectivity in the entire reservoir. Also, a good network of fluid flow channels have developed in the entire reservoir through the interconnected pore spaces and pore throats between production wells and injection wells.

Streamline flux of oil flow rate has generated all over the reservoir as shown in figure 3.92. Uniform flux pattern of oil flow rate have developed between wells. Oil has started moving from every part of the reservoir. There is no stagnant oil in any part of the reservoir. Streamline of oil flow rate ranges from 0.00 STB/D to 0.04 STB/D. Average values of oil flow rate between wells are as following:

- P1 and I1 is 0.025 stb/day.
- P1 and I2 is 0.025 stb/day.
- P1 and I3 is 0.020 stb/day.
- P2 and I4 is 0.025 stb/day.
- P1 and I5 is 0.025 stb/day.
- P1 and I6 is 0.035 stb/day.

Overall average value of oil flow rate is 0.025 STB/D. Arrows of oil flow direction have generated all over the reservoir as shown in figure 3.93. Oil flows toward the two production wells from six water injection wells. There is no oil flowing in opposite direction from production wells.

Streamline Flux of water flow rate between production wells and injection wells remains zero as shown in figure 3.94. Reservoir water remains immovable. Separate water flow channel has not been established. Only reservoir oil phase is flowing through the flow channels.

Time of flight (end) express the time required to reach to production wells from injection wells by an oil particle. Simulation output has shown that maximum required time is 50000 days (164 years) as shown in figure 3.95. Oil will take 50000 days to come to production wells from distant water injection wells. Oil flow will continue for 50000 days.

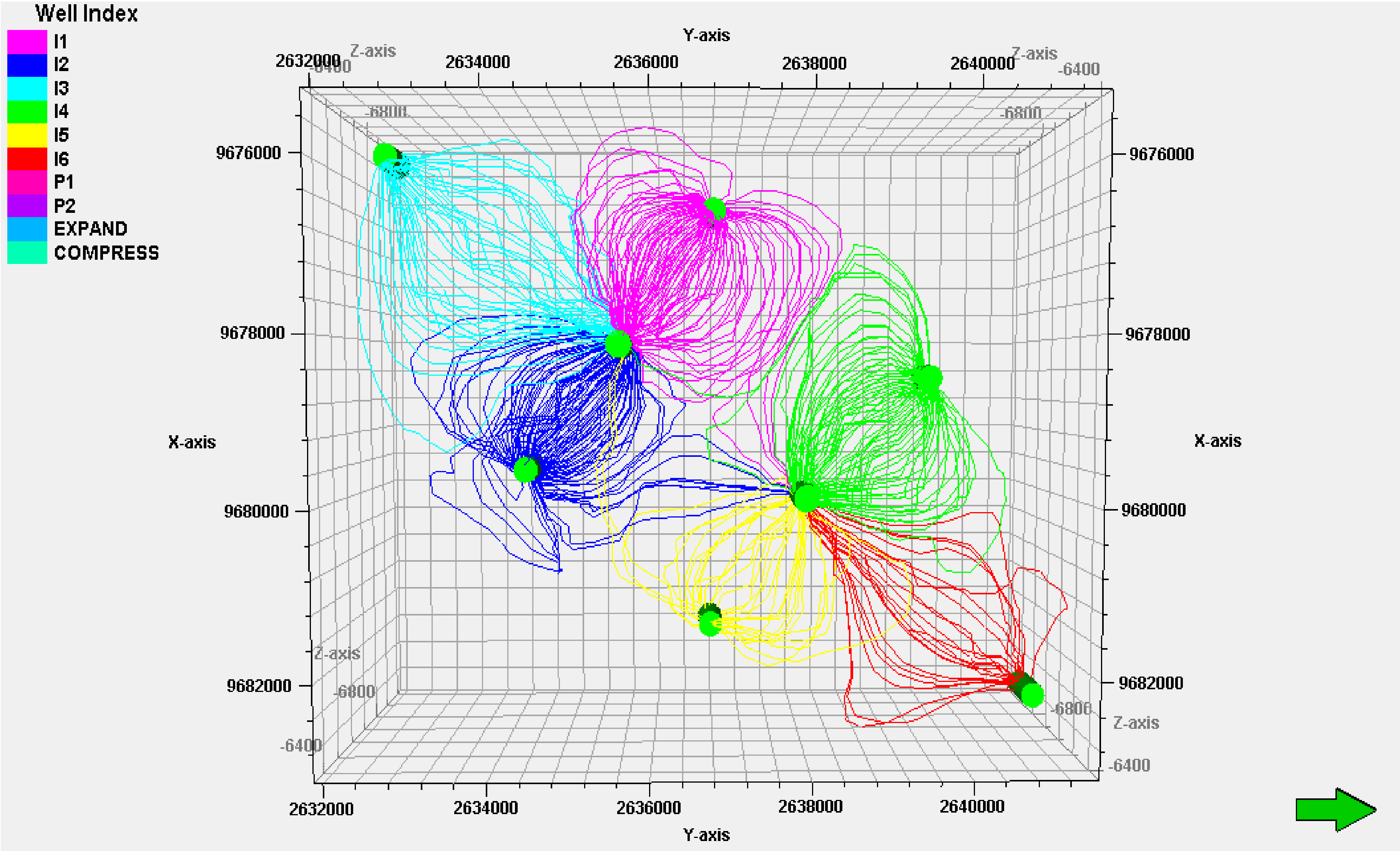

Figure 3.91: Streamline flux pattern of hydraulic connectivity

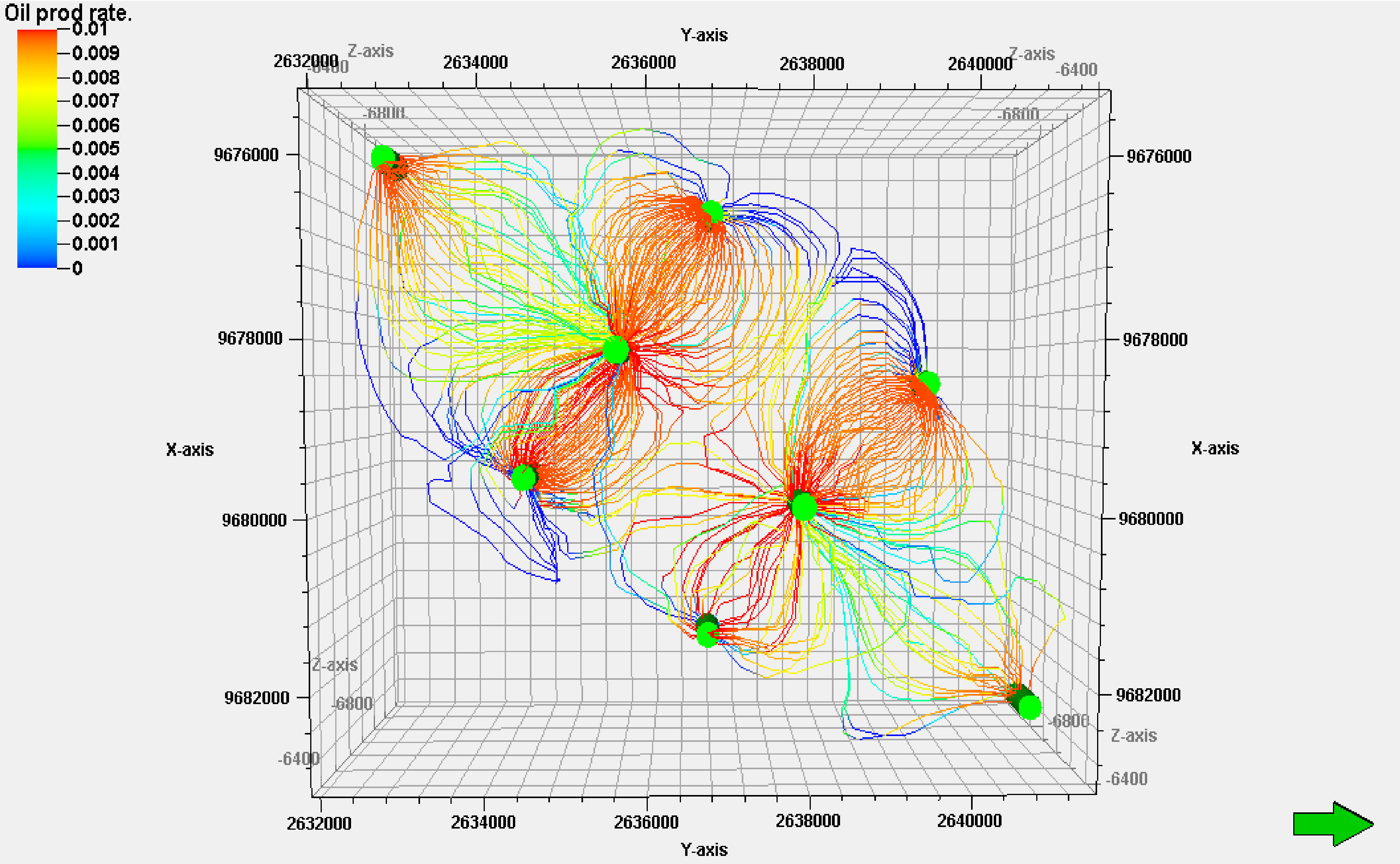

Figure 3.92: Streamline flux pattern of oil flow rate

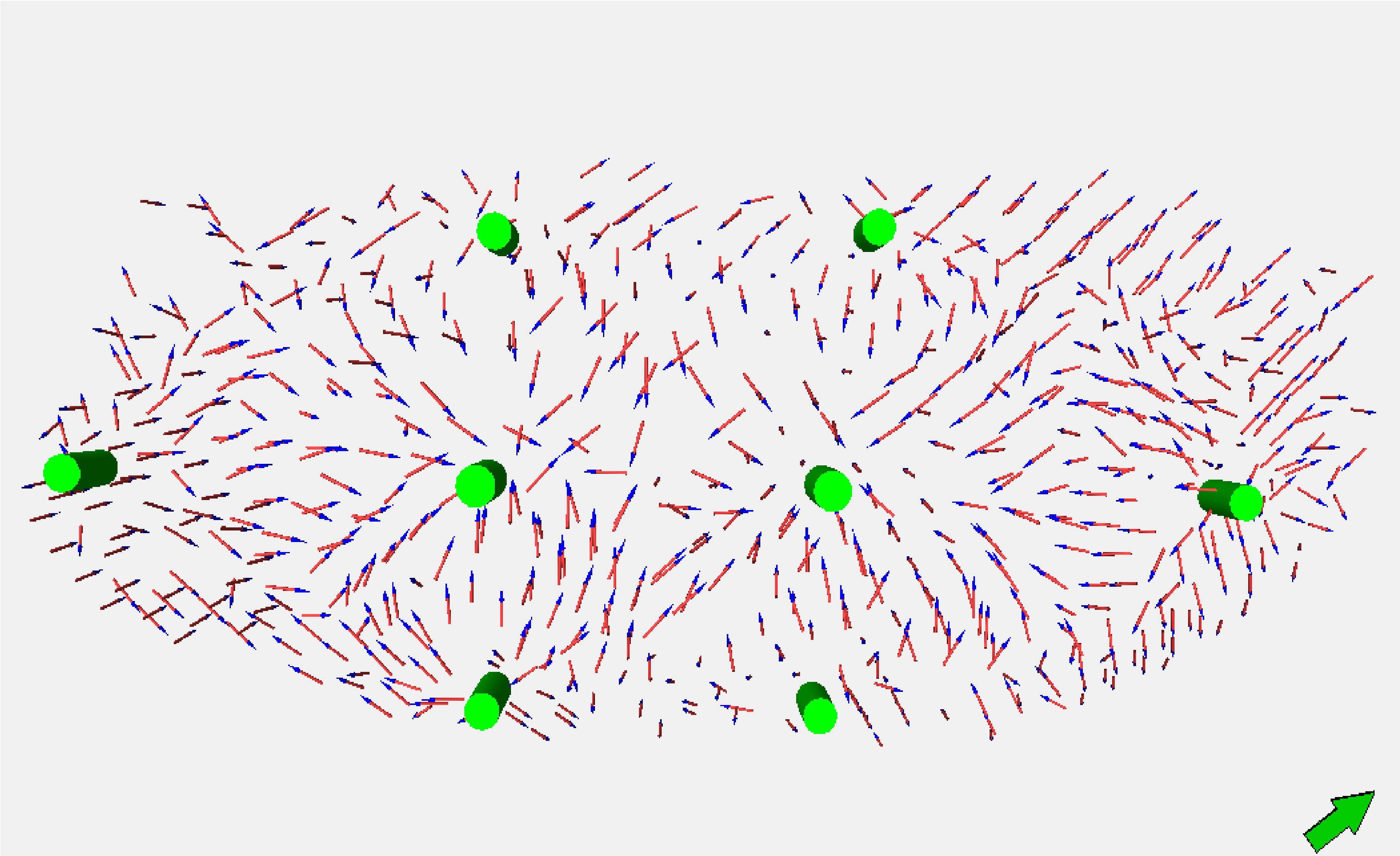

Figure 3.93: Arrows of oil flow direction

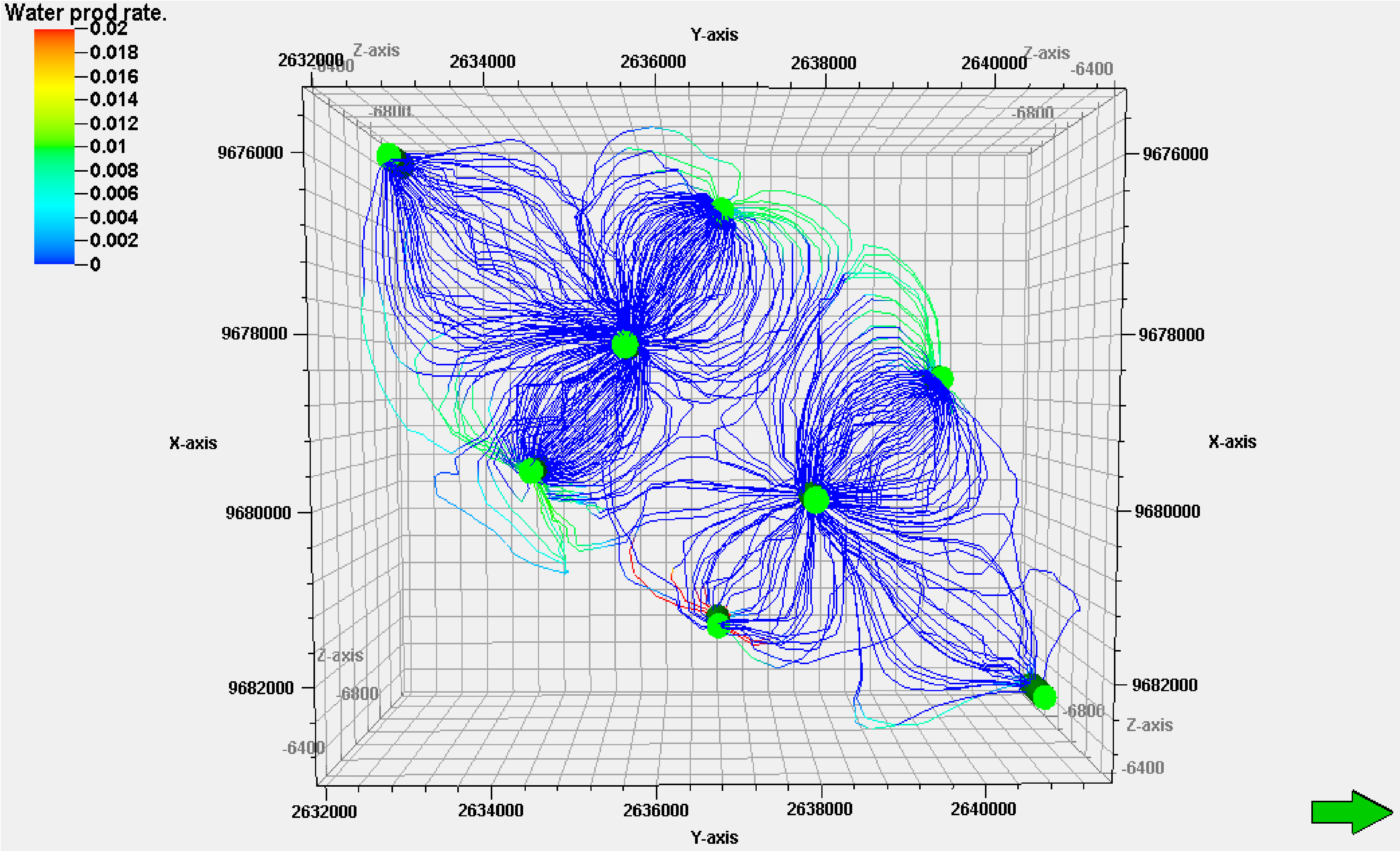

Figure 3.94: Streamline flux pattern of water flow rate

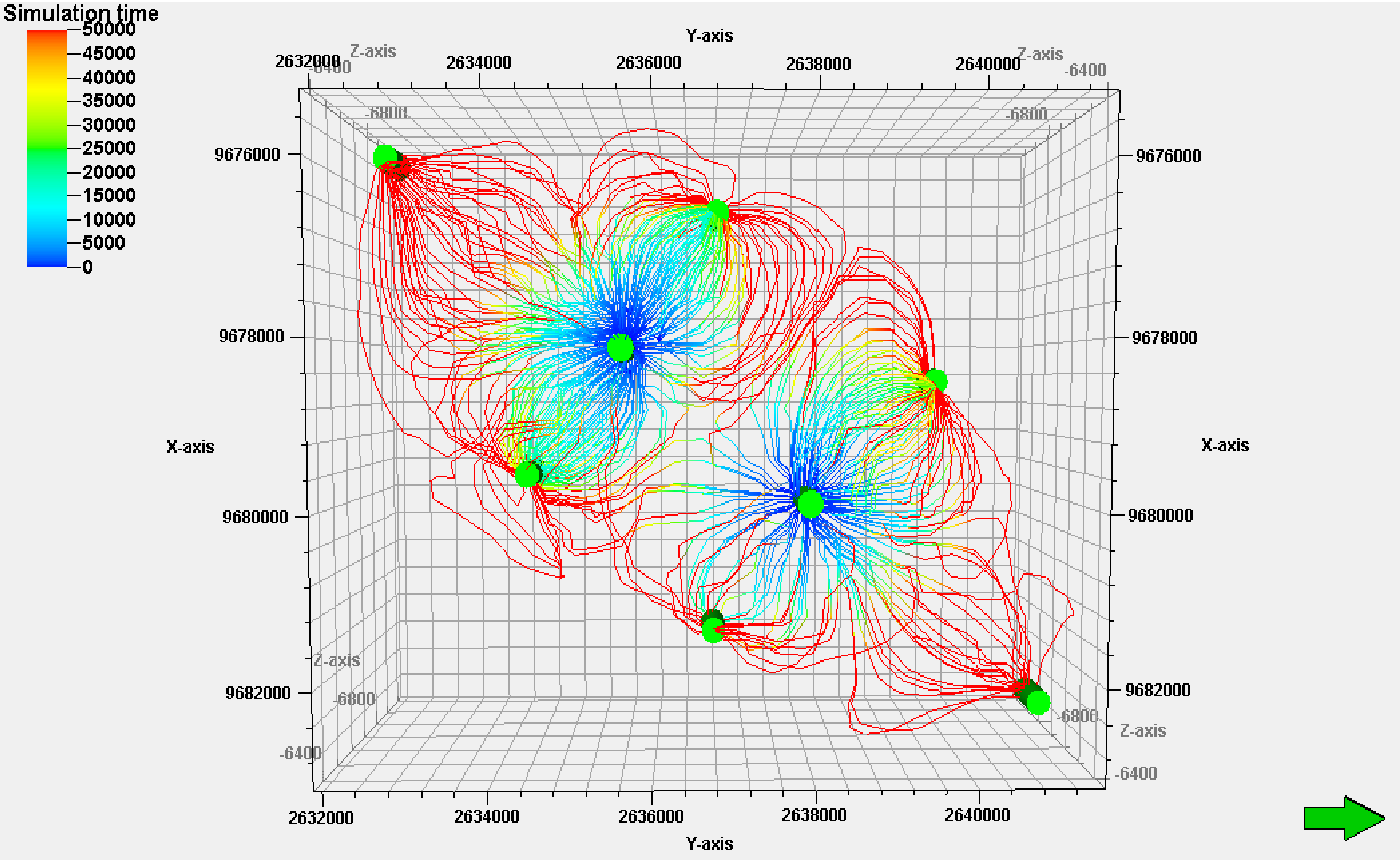

Figure 3.95: Streamline flux pattern of time of flight (End)

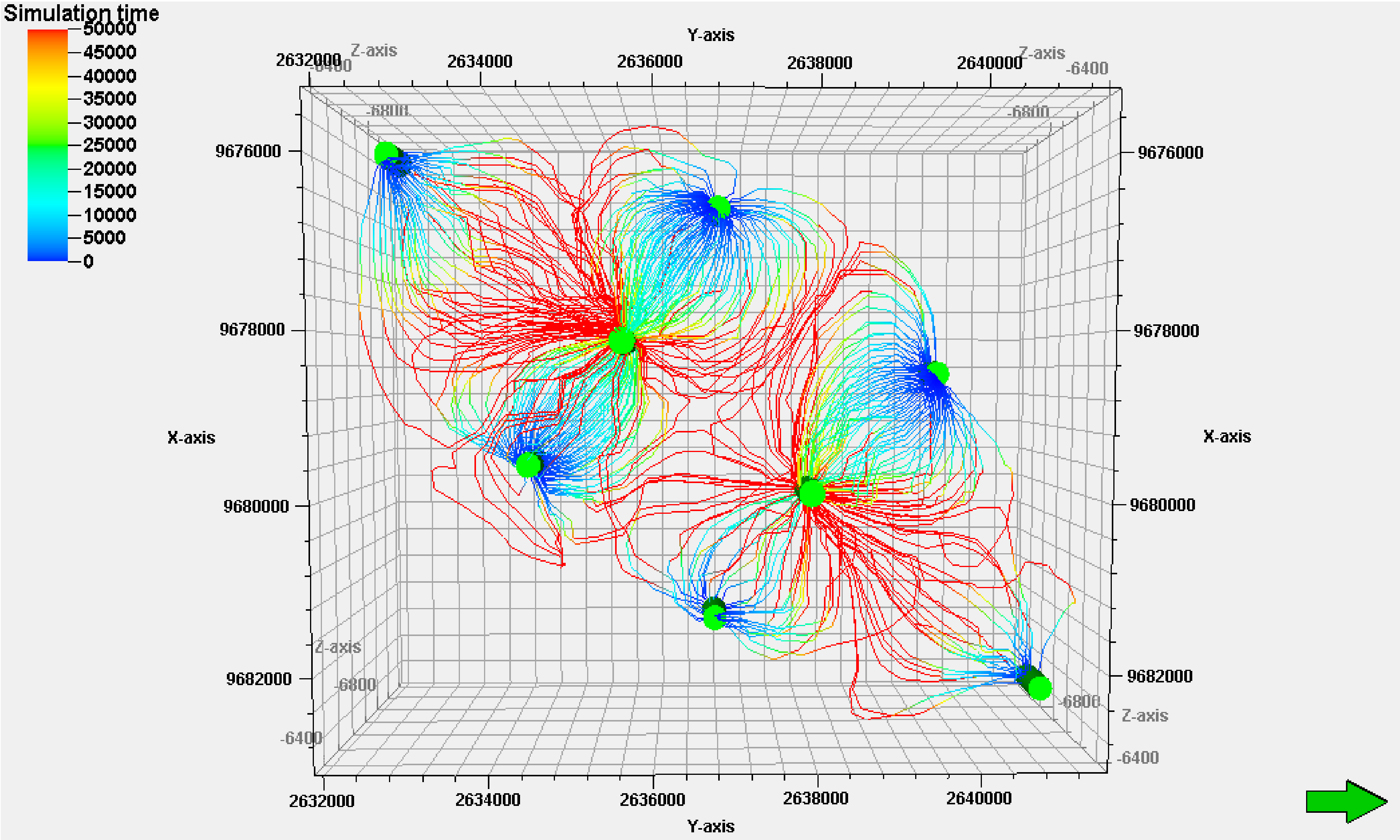

Figure 3.96: Streamline flux pattern of time of flight (Begin)

Time of flight (begin) expresses the time required to reach to production wells from injection wells by a water particle. Time of flight (begin) for water movement to production wells is shown in figure 3.96. Water of distant water injection wells will take 50000 days to come to oil production wells. Water breakthrough times of water injection wells I1, I2, I3, I4, I5 and I6 are 20000, 15000, 500000, 15000, 500000 and 500000 days respectively.

It is seen that, long time recovery strategy can be considered to this reservoir for achieving the maximum recovery. Extra infill wells drilling may provide quick recovery of oil but it will increase project expenditure and decrease overall project economic value. Oil is recovered by low salinity water injection method and six water injection wells in oil-water contact with two oil production wells in center of the oil zone is considered as oil reservoir development plan in Haripur field. Economic evaluation of oil reservoir development plan is conducted by twenty years of production forecasting. Oil reservoir development plan is implemented as Oil reservoir development project when plan is technically feasible and economically viable i.e. net present value is positive.

3.5 Oil Reservoir Development Plan in Haripur Field

After discovery of oil resources engineers and scientist provide efforts to plan for recovering oil resources from the reservoir in an economic way. To do this job enormous work is being performed by the experts to make the development plan success. A technically perfect oil reservoir development plan is able to provide revenue to the oil and gas companies. In this study, oil reservoir development plan in Haripur field has been prepared as shown in figure 3.97.

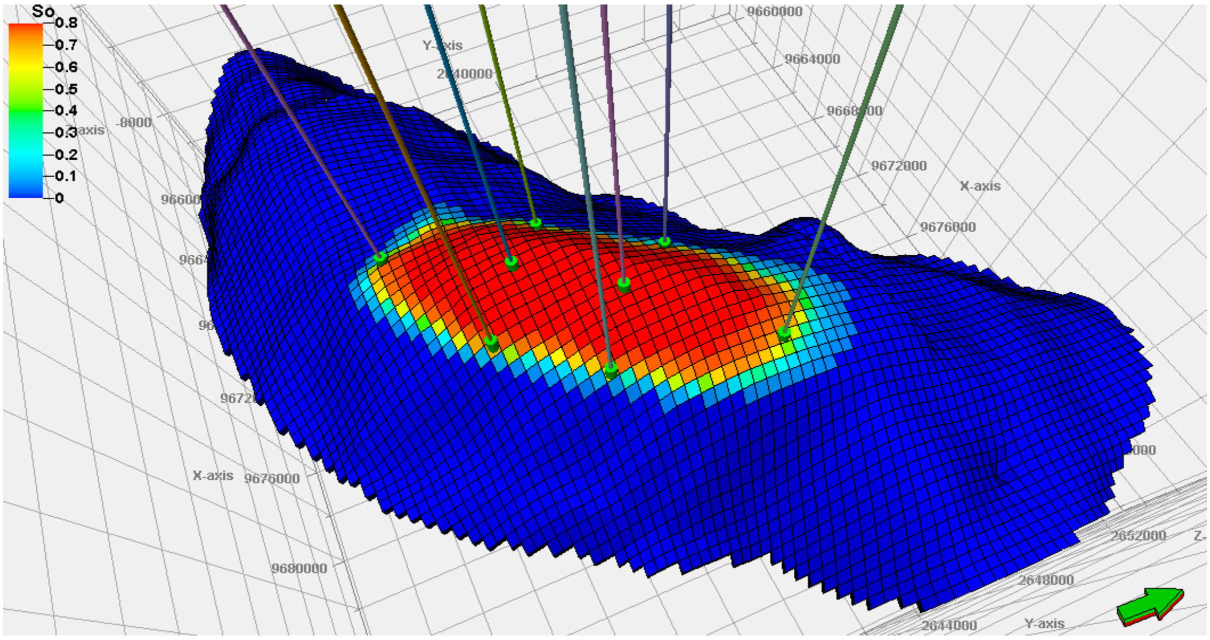

Figure 3.97: Oil reservoir development plan in Haripur field

Haripur field has produced 0.53 million barrels of oil and experts predicts there is remaining oil in the reservoir which is approximately 32.47 million barrels of oil. To recover this oil low salinity water injection method has been proposed. The oil reservoir development plan has following optimized main features:

1. Oil is recovered by low salinity water injection technique.
2. Injection water salinity is 1000 ppm of NaCl.
3. Six injection wells are used for water injection.
4. Water injection pressure is 1000 psi.
5. Well water injection rate is 300 stb/day.
6. Field water injection rate is 1800 stb/day
7. Two oil production wells are used for oil production.
8. Well oil production rate is 400 stb/day.
9. Field oil production rate is 800 stb/day
10. Well head pressure of oil production is 500 psi.

3.6 Oil Reservoir Development Project Management Plan in Haripur Field

An integrated systems project management approach can help diminish the adverse impacts on project through good project planning, organizing, scheduling, and control. The oil and gas project management experts develop the Project Management Body of Knowledge (PMBOK). On the basis of the oil reservoir development plan an oil reservoir development project management plan has been prepared. The project management body of knowledge of oil reservoir development project in Haripur field is following:-

1. Integration

- Integrative project charter
- Project scope statement
- Project management plan
- Project execution management
- Change control

2. Scope management

- Focused scope statements
- Cost/benefits analysis
- Project constraints
- Work breakdown structure
- Responsibility breakdown structure
- Change control

3. Time management
    - Schedule planning and control
    - Program Evaluation and Review Technique (PERT) and Gantt charts
    - Critical path method
    - Network models
    - Resource loading
    - Reporting
4. Cost management
    - Financial analysis
    - Cost estimating
    - Forecasting
    - Cost control
    - Cost reporting
5. Quality management
    - Total quality management
    - Quality assurance
    - Quality control
    - Cost of quality
    - Quality conformance
6. Human resources management
    - Leadership skill development
    - Team building
    - Motivation
    - Conflict management
    - Compensation
    - Organizational structures
7. Communications
    - Communication matrix
    - Communication vehicles
    - Listening and presenting skills
    - Communication barriers and facilitators
8. Risk management
    - Risk identification
    - Risk analysis

• Risk mitigation

• Contingency planning

9. Procurement and subcontracts

• Material selection

• Vendor prequalification

• Contract types

• Contract risk assessment

• Contract negotiation

• Contract change orders

Main work breakdown structure of oil reservoir development project in Haripur field is as follows:-

1. Drilling and completion of two (P1 and P2) oil production wells
2. Drilling and completion of two (I1 and I2) water injection wells
3. Drilling and completion of two (I3 and I4) water injection wells
4. Drilling and completion of two (I5 and I6) water injection wells
5. Installation and completion of following systems:-
    - Surface oil production facilities
    - Surface water injection facilities
    - water treatment plant to treat water for injection

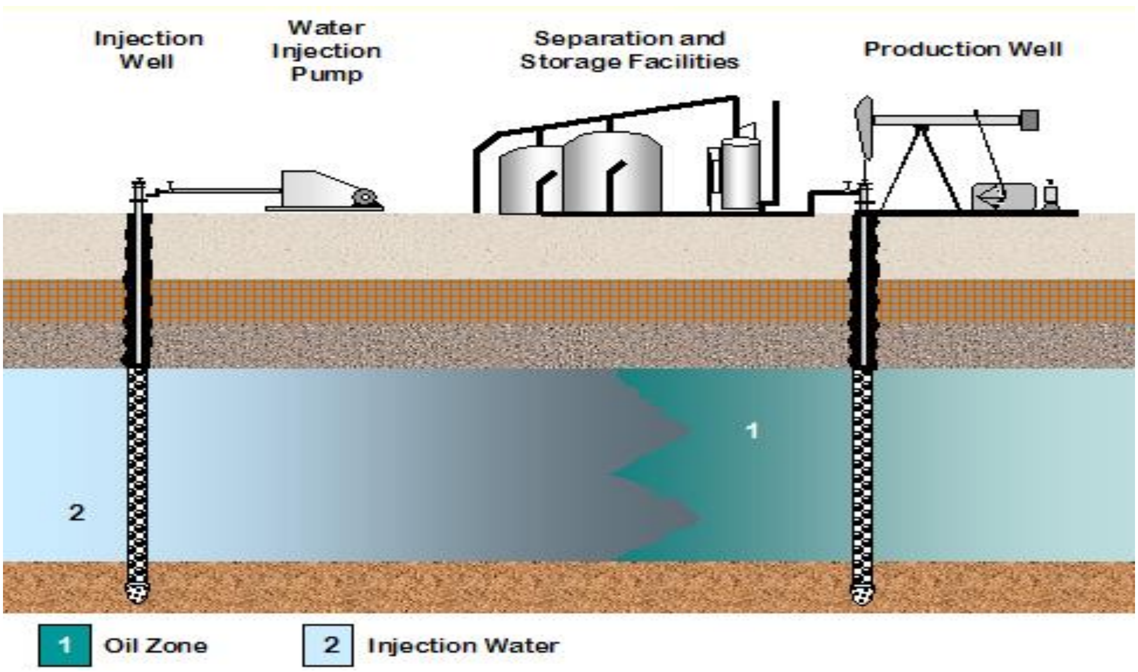

Figure 3.98: EOR by water injection method (Ambia F., 2012)

Figure 3.99: Water injection facility (Ambia F., 2012)

Finite difference reservoir simulation model (conventional reservoir simulation model) and streamline reservoir simulation model of Haripur oil reservoir have been simulated for 40 years to predict the oil flow rate and tube head pressure declining time. The oil flow rate and tube head pressure have remained constant over 40 years in oil production well No. P1 as shown in figure 3.100.

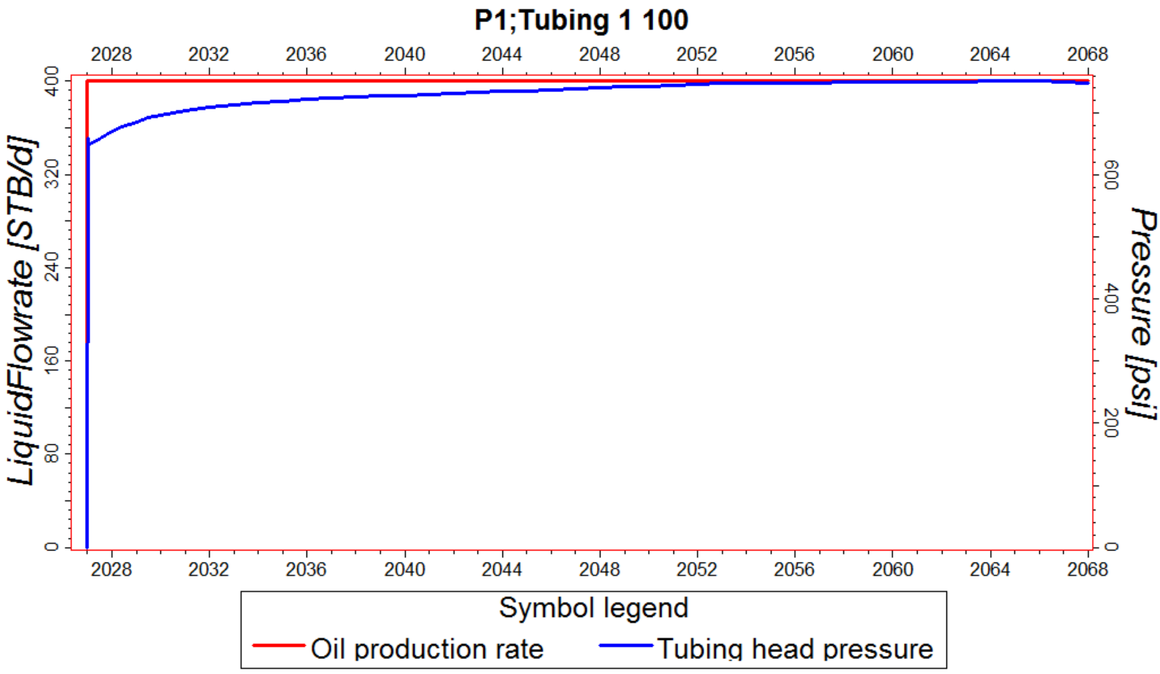

Figure 3.100: Oil flow rate and tube head pressure of well no. P1

The oil flow rate has remained constant over 40 years in oil production well No. P2 as shown in figure 3.101. The tube head pressure has started declining after 20 years from the start of oil production in oil production well No. P2 as shown in figure 3.101.

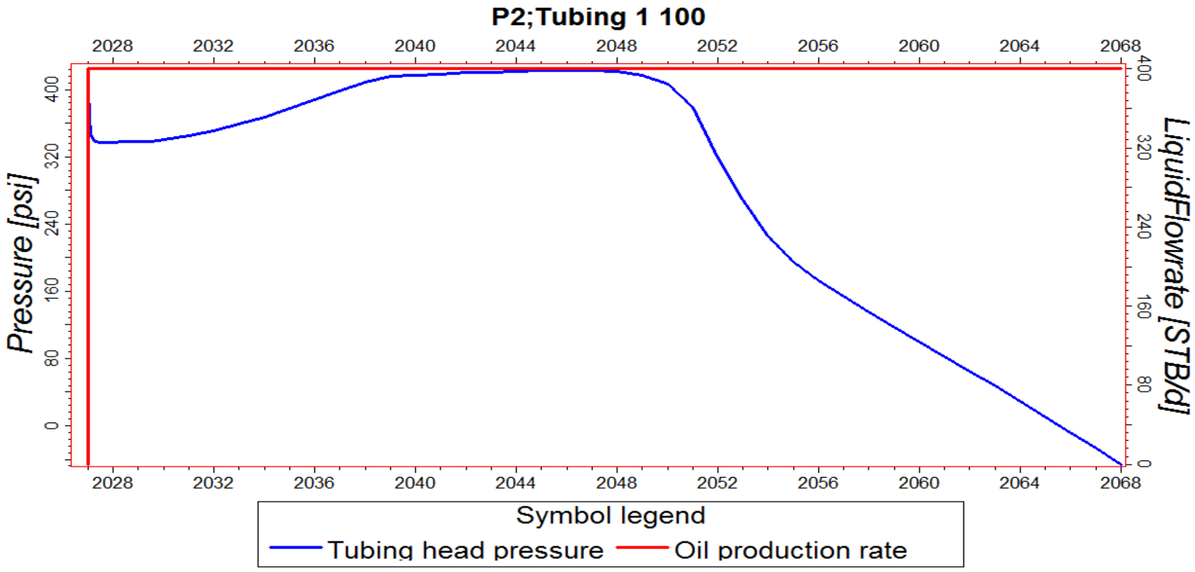

Figure 3.101: Oil flow rate and tube head pressure of well no. P2

Oil production well No.P1 and well No.P2 have been connected to the three phase separator in the oil process plant through oil gathering pipeline system to separate oil, gas and water as shown in figure 3.102. The three phase separator pressure must be maintained constant to operate the three phase separator in the oil process plant. Tube head pressure provides operating pressure to the three phase separator in the oil process plant. Tube head pressures of oil production well No.P1 and well No.P2 must be maintained constant during oil production period. Simulation has predicted that tube head pressures of oil production well No.P1 and well No.P2 have remained constant for 20 years. It is observed that oil field life is 20 years in the stage of constant oil production rate and constant tube head pressure strategy.

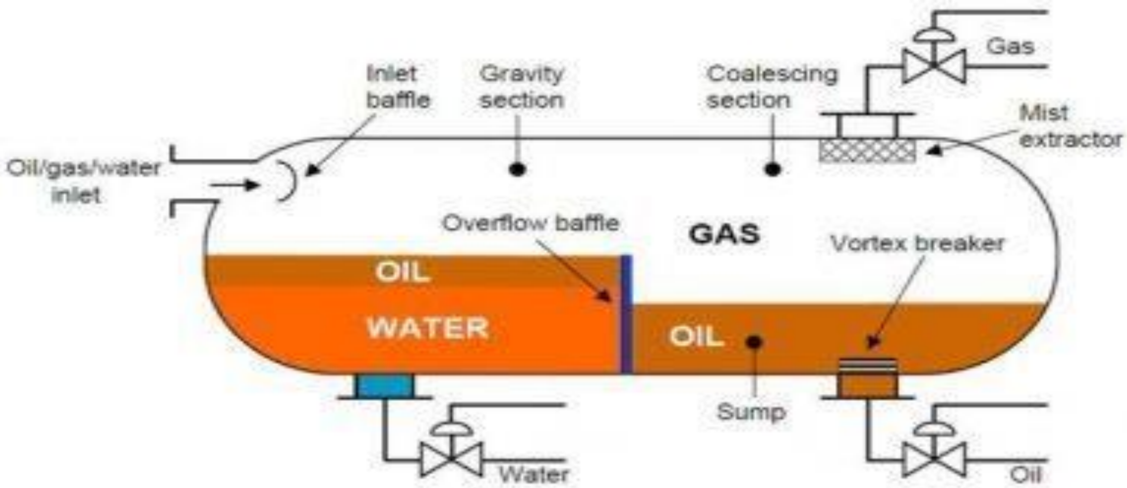

Figure 3.102: Three phase separator

The international oil and gas companies consider 15 to 25 years as commercial project life of oil reservoir development project. Commercial project life of Haripur oil reservoir development project has been considered as 20 years.

Chapter 4

Oil Reservoir Development Plan of the Kailashtila Field

The Kailashtila field is located 13 kilometers south of Sylhet field and it is about 250 kilometers northeast of Dhaka. The Kailashtila field lies in the central part of the Surma Basin. The Kailashtila structure was delineated by Shell Oil in 1960 on the basis of single fold analog seismic data acquired in late 1950's. The structure is a four way dip closure. The Kailashtila field was developed by Pakistan Shell Oil Company (PSOC) in 1961 as shown in figure 4.1.

A gas well (Kailashtila-1) was completed in June 1983 with the initial production of 30 MMSCFD. Later, three more wells namely KTL-2 (1988), KTL-3 (1988) and KTL-4 (1996) were drilled in this field. Gas of Kailashtila has a very high condensate ratio in comparison to Haripur gas field. The well KTL-5 added to the field with a production capacity of 15 MMSCFD with a condensate ratio 40 STB/MMSCF. Another well KTL-6 started producing from 8th August 2007. Production of KTL-5 ceased on 22 October 2009 due to excessive water production and reduction of well head pressure. KTL-7 was drilled in 2015. Well logs and Drill Stem Test (DST) on KTL-7 revealed that there exists oil zone between 3261 to 3266 m depth (http://sgfl.org.bd/KTL%20field.htm).

Figure 4.1: Kailashtila gas field

4.1 Detection of Oil Reservoir in Kailashtila Field

Following the drilling of well No. KTL-7, oil reservoir was detected in addition to gas reservoir through well logs including wireline logs. Drill stem test (DST) operation was performed to detect oil reservoir and characterize the dynamic behavior of the oil reservoir. An oil reservoir development plan has been attempted to prepare from the interpretation of drill stem test and well logs. Oil and gas industries use well logs attributes to record well logs data as shown in figure 4.2.

Common start depth:	2692.0000	m	Common stop depth:	3537.9000	m
Min start depth:	2692.0000	m	Max stop depth:	3537.9000	m

Log name	Property template	Global well log	Unit (File)	Unit (Petrel)	Description
AC	Sonic	Create new	us/ft	us/ft	Acoustic (F)
AT10	Resistivity	Create new	ohmm	ohm.m	AT10 (F)
AT20	Resistivity	Create new	ohmm	ohm.m	AT20 (F)
AT30	Resistivity	Create new	ohmm	ohm.m	AT30 (F)
AT60	Resistivity	Create new	ohmm	ohm.m	AT60 (F)
AT90	Resistivity	Create new	ohmm	ohm.m	AT90 (F)
CGR	Gamma ray	Create new	api	gAPI	CGR (F)
GR	Gamma ray	Create new	API	gAPI	Gamma Ray (F)
K	K factor	Create new	%	Hz	Potassium (F)
PERM	Permeability	Create new	mD	mD	Permeability (F)
POR	Porosity	Create new	%	m3/m3	Porosity (F)
SGR	Gamma ray	Create new	api	gAPI	SGR (F)
SP	Spontaneous potent	Create new	mv	mV	Spontaneous potential (F)
SW	Water saturation	Create new	mv		Water saturation (F)
CALX	General	Create new	in	in	Caliper X (F)
CALY	General	Create new	in	in	Caliper Y (F)
CNL	General	Create new	%	%	Compensated neutron (F
DEN	General	Create new	g/cm3	g/cm3	Density (F)
LSN	General	Create new	cps	cps	Long space counting (F)
PE	General	Create new	b/e	b/e	Photoelectric factor (F)
PORF	General	Create new	%	%	Porosity of flush zone (F)
PORF	General	Create new	%	%	Porosity of flush zone (F)
PORW	General	Create new	%	%	Porosity of water (F)
SH	General	Create new	%	%	Shale content (F)
SSN	General	Create new	cps	cps	Short space counting (F)
SWIR	General	Create new	%	%	Irreducible water Saturation (F
TEN_CABL	General	Create new	lbs	lbs	TEN_CABLE (F)
TH	General	Create new	ppm	ppm	Thorium (F)
U	General	Create new	ppm	ppm	Uranium (F)

Figure 4.2: Well logs attributes

4.1.1 Well Logs of KTL-7 Analysis

Well log operations have been carried out from depth 2692 m to 3537.88 m in 8.5 inch open hole of KTL-7 well. GR, SP, CALX, CALY, AT10, AT20, AT30, AT60, AT90, CN, DEN, AC logs have been recorded. S_w, PERM and PORO logs have been derived from recorded logs. A gas zone has been detected from depth 3250 m to 3260 m and below the gas zone an oil zone has been detected from depth 3260 m to 3270 m by interpretation of wireline logs as shown in figure 4.3.

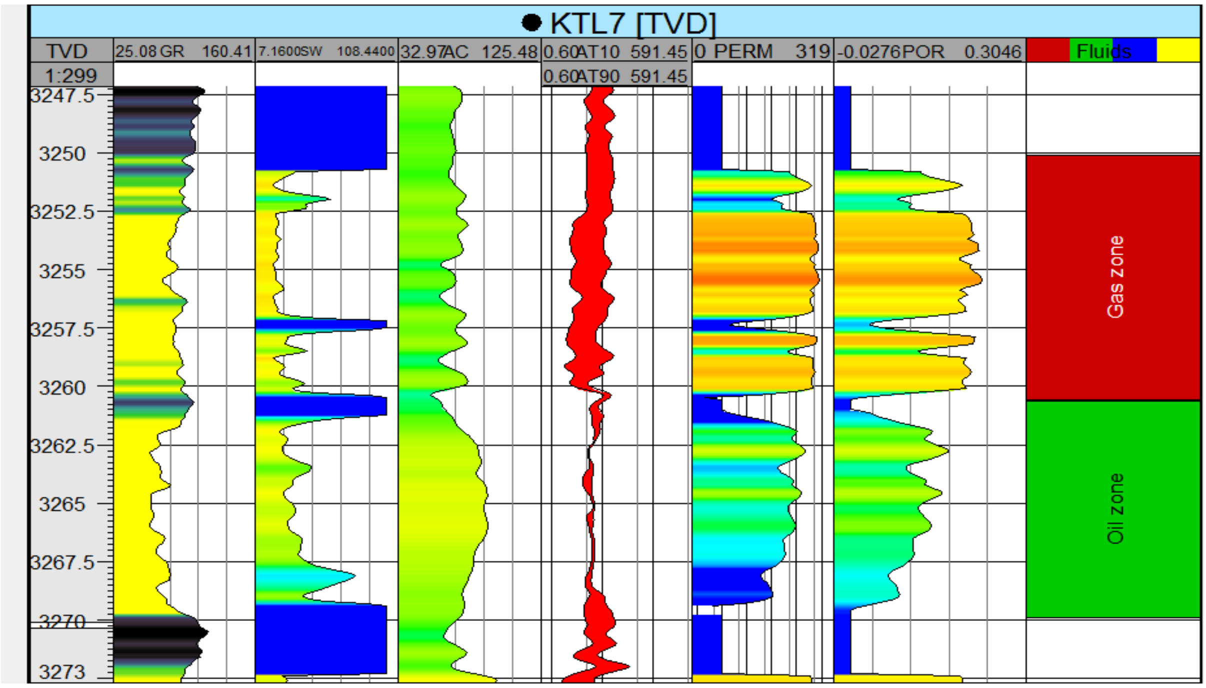

Figure 4.3: Well logs of KTL-7 (3250 m to 3270 m)

Gamma ray log (GR) has detected sandstone formation at depth interval from 3250 m to 3270 m. Resistivity logs (AT10 and AT90) are separated from each other which indicates mud filtrate invasion into the formation. As drilling mud has filtered by the formation and mud filtrate has entered into the formation so the formation is porous and permeable. During drilling operation mud (water based or oil based) does not filter by shale zone as shale is porous but not permeable and there is no separation between logs (AT10 and AT90). When drilling with water based mud then mud is filtered by porous and permeable formation and mud filtrate (water) enters into the formation. If formation contains water then mud filtrate does not change the formation resistivity along the invasion depth. Logs (AT10 and AT90) show separation that depends on the salinity contrast between mud filtrate and the formation water.

On the other hand when drilling with water based mud then mud is filtered by porous and permeable formation and mud filtrate (water) enters into the formation. IF formation contains hydrocarbon (oil and Gas) then mud filtrate changes the formation resistivity along the invasion depth as shown in figure 4.4. In this case logs (AT10 and AT90) will separate from each other. So resistivity logs operation is conducted for shallow depth of invasion (AT10 and AT20), medium depth of invasion (AT30 and AT60) and deep depth of invasion to detect flashed zone, transition zone and uninvaded zone respectively.

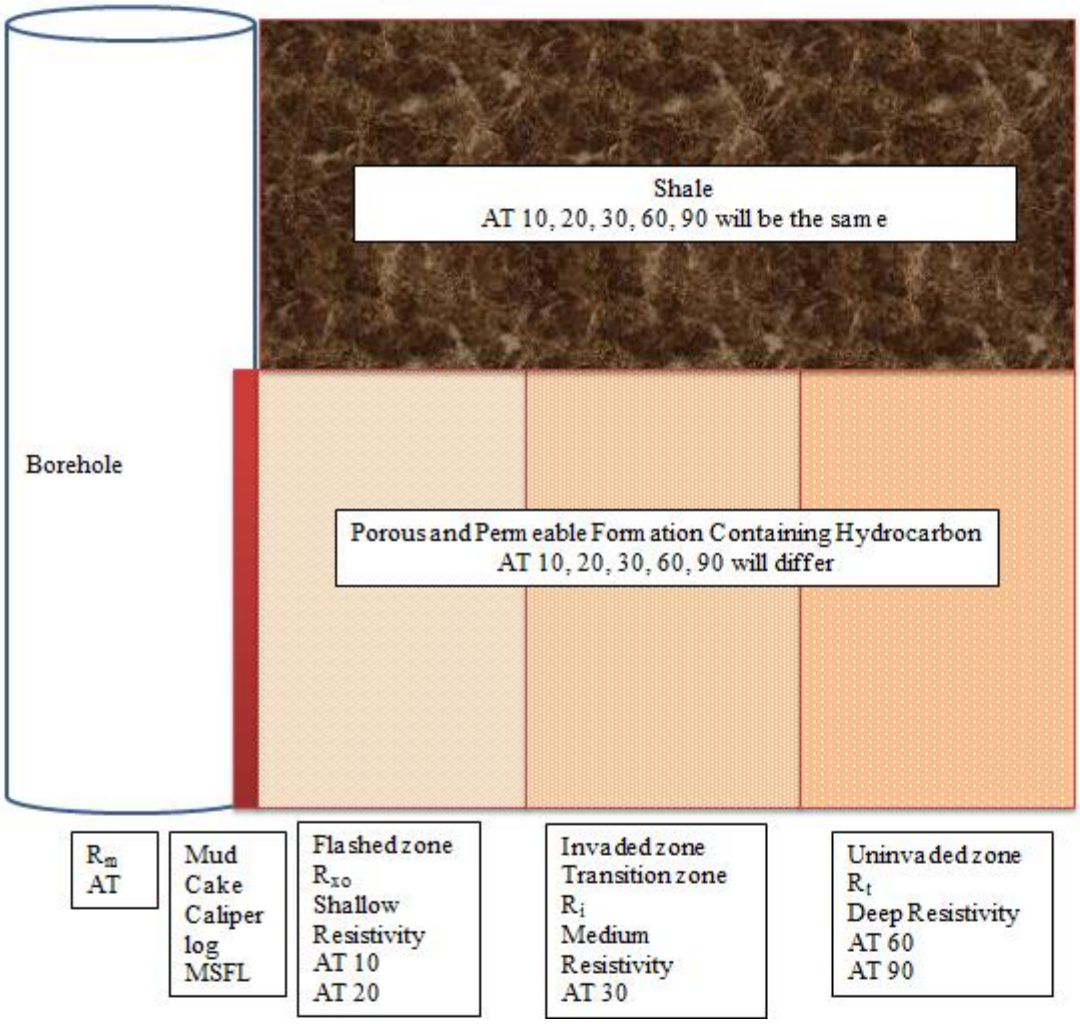

Figure 4.4: Resistivity logs of KTL-7 (AT 10, 20, 30, 60, 90)

When the formation contains water then formation resistivity is minimum. If the formation contains gas then the formation resistivity is maximum and when the formation contains oil then formation resistivity is medium. When log shows more separation between AT10 and AT90 then the formation contains gas and when log shows small separation between AT10 and AT90 then the formation contains oil.

Table 4.1: Resistivity interpretation

Depth Interval	AT10 Depth of Invasion 1 to 3 inch Flashed Zone resistivity Ωm	AT90 Depth of Invasion 12 to 15 inch Uninvaded Zone resistivity Ωm	Difference between AT10 and AT90 Ωm	Difference	Interpretation
3250 m to 3260 m	3.80	9.21	5.41	Large	Gas Zone
3260 m to 3270 m	6.40	6.73	0.33	Small	Oil Zone

Oil zone has been detected from depth 3260 m to 3270 m in KTL-7 well as shown in figure 4.5. Drill stem test has been conducted in this oil zone to assess the reservoir deliverability.

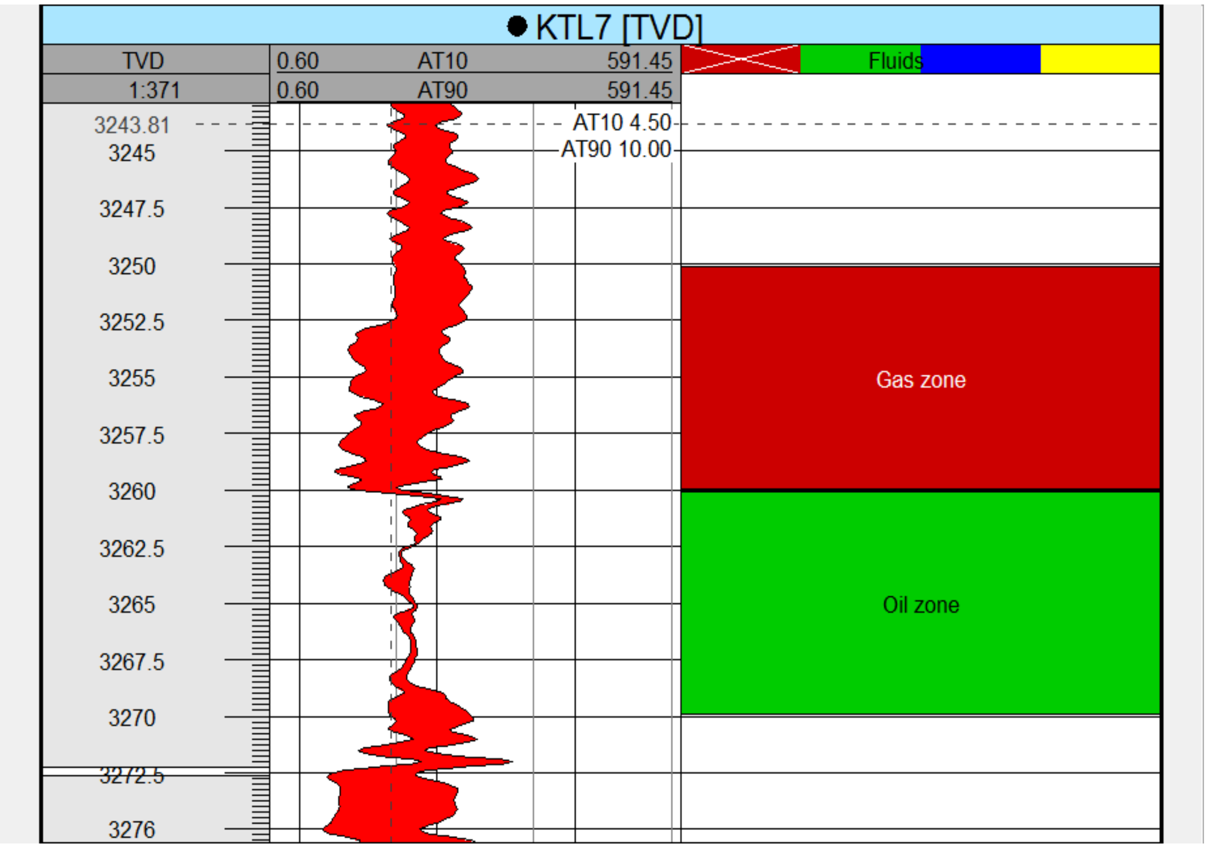

Figure 4.5: Oil zone

4.1.2 Drill Stem Test (DST) Analysis

Drill Stem Test (DST) describes the dynamic characteristic of the hydrocarbon bearing formation such as wellbore storage, skin effect, permeability, average reservoir pressure and reservoir boundary. The wellbore storage effect and average reservoir pressure help to predict the flowing phase from the reservoir.

In this study an effort has been made to analyze the DST conducted in the Kailashtilla field at the depth interval 3261 meter to 3266 meter in well KTL-7. Two sets of pressure profile have been recorded. First conditioning of the well is done for an hour and then performed drawdown following pressure buildup. The pressure signature of the buildup period and its derivatives are plotted on semi-log and log-log coordinates to develop Horner and diagnostic plots respectively. Wellbore storage, skin and transient flow effects have been observed in the DST analysis which is an indication of the hydrocarbon bearing reservoir in the zone of interest. The value of wellbore storage effect is low which predicts the flow of liquid hydrocarbon into the well bore from the reservoir. Average pressure of the investigated zone has been estimated which is higher than the water column pressure. The higher average reservoir pressure also authenticates the presence of oil reservoir.

DST interval selection

The DST interval is selected on the basis of the well log analysis. In the interval 3261 meter to 3266 meter, the log analysis shows low value of gamma ray log, high value of resistivity log with shallow and deep separation and high value of acoustic log indicating porous permeable formation with hydrocarbon bearing zone as shown in figure 4.7.

Description of DST operation

To conduct a safe and proper DST operation it is very important to design the DST string and the Bottom Hole Assembly (BHA) according to the collapse load, burst load and shear failure. The DST string and BHA are shown in Figure 4.8 where drill pipe, drill collar, crossover, pressure gauge are used.

In 2015, the DST operation commenced on 9th February at 18.00 hours and terminated on 12th February at 12.00 hours. Interval & surface pressure profile and liquid height profile are plotted over the entire test period shown in Figure 4.9.

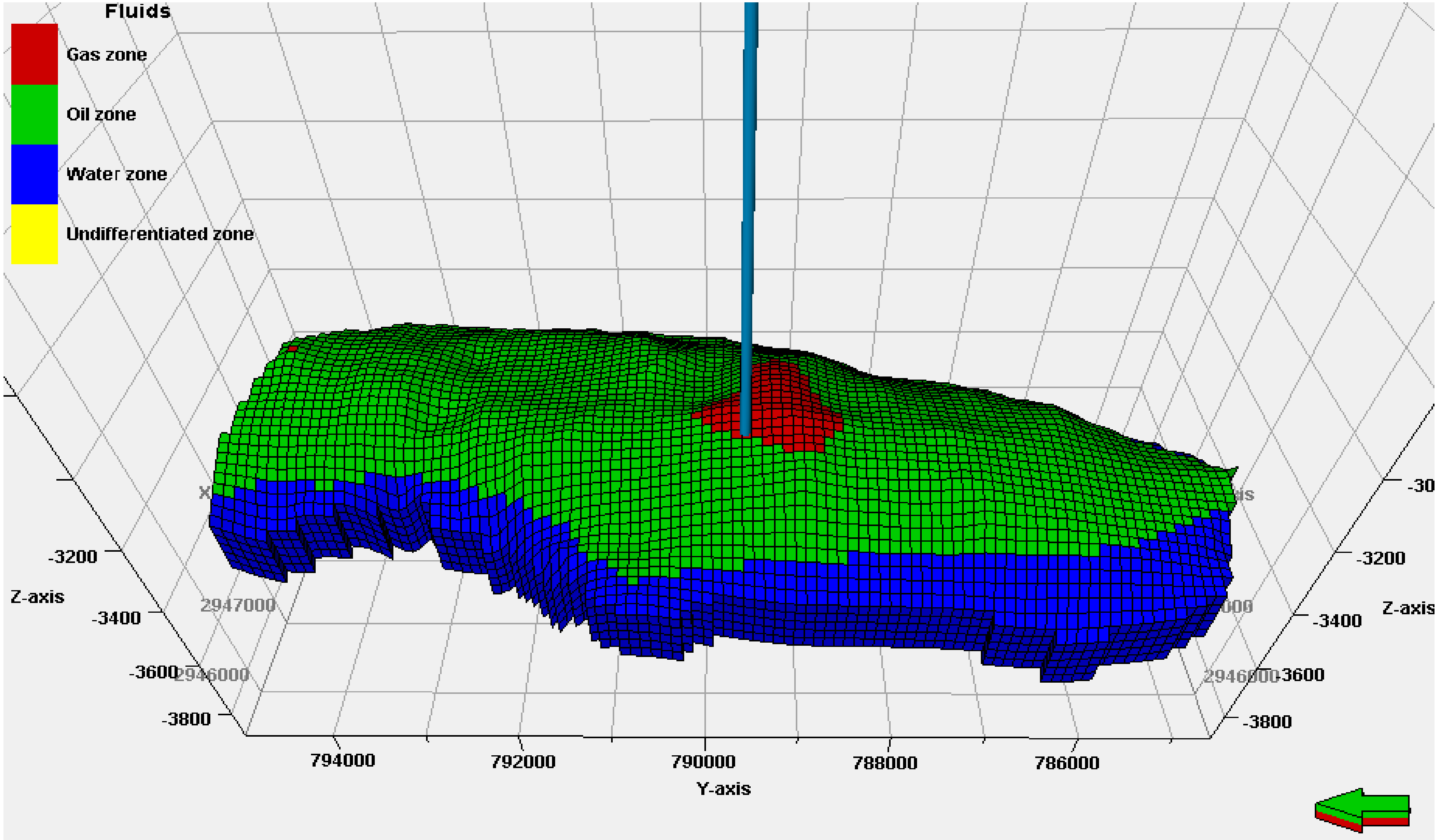

Figure 4.6: Location of well no. KTL-7 in the reservoir

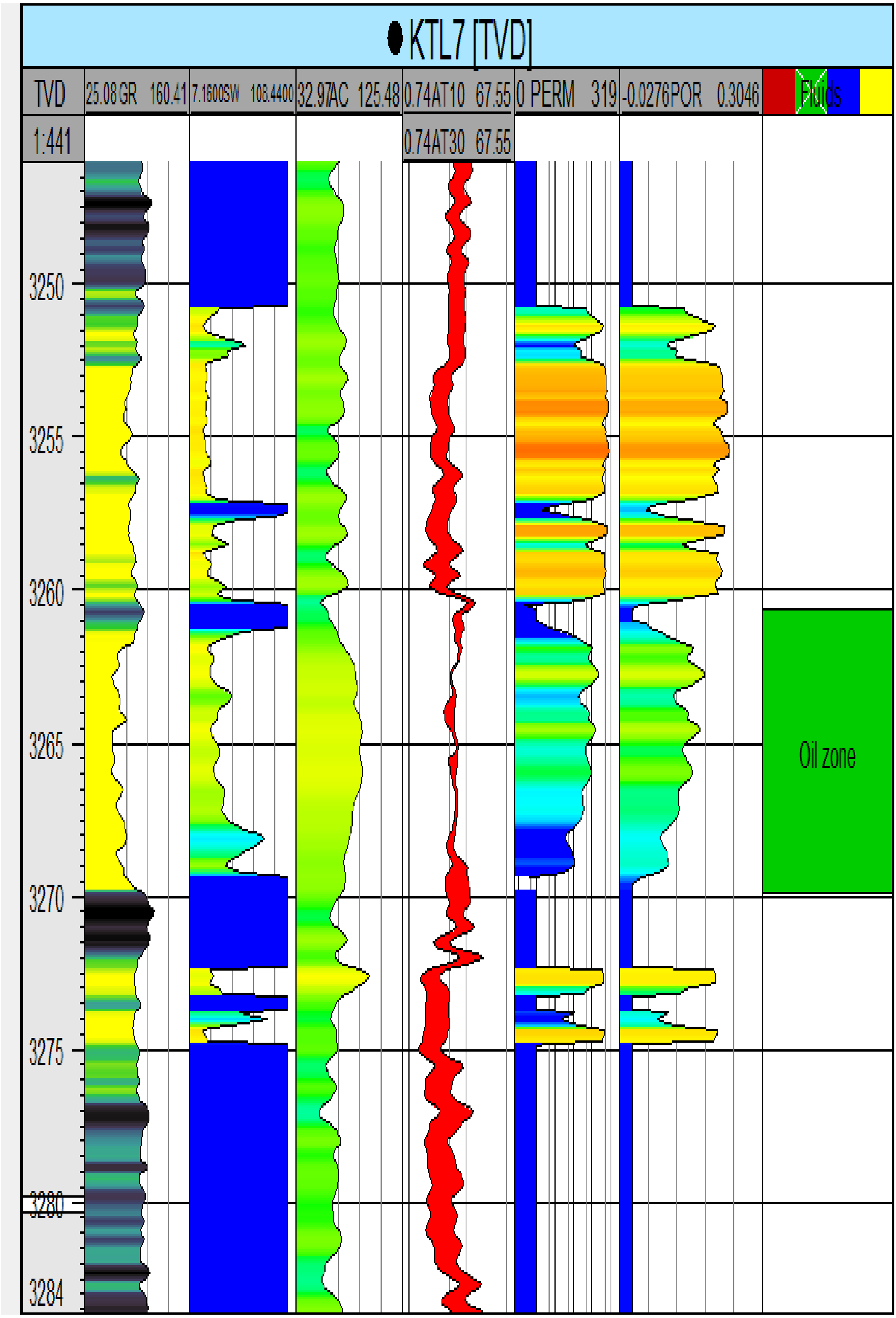

Figure 4.7: Well logs in well KTL-7 and DST interval.

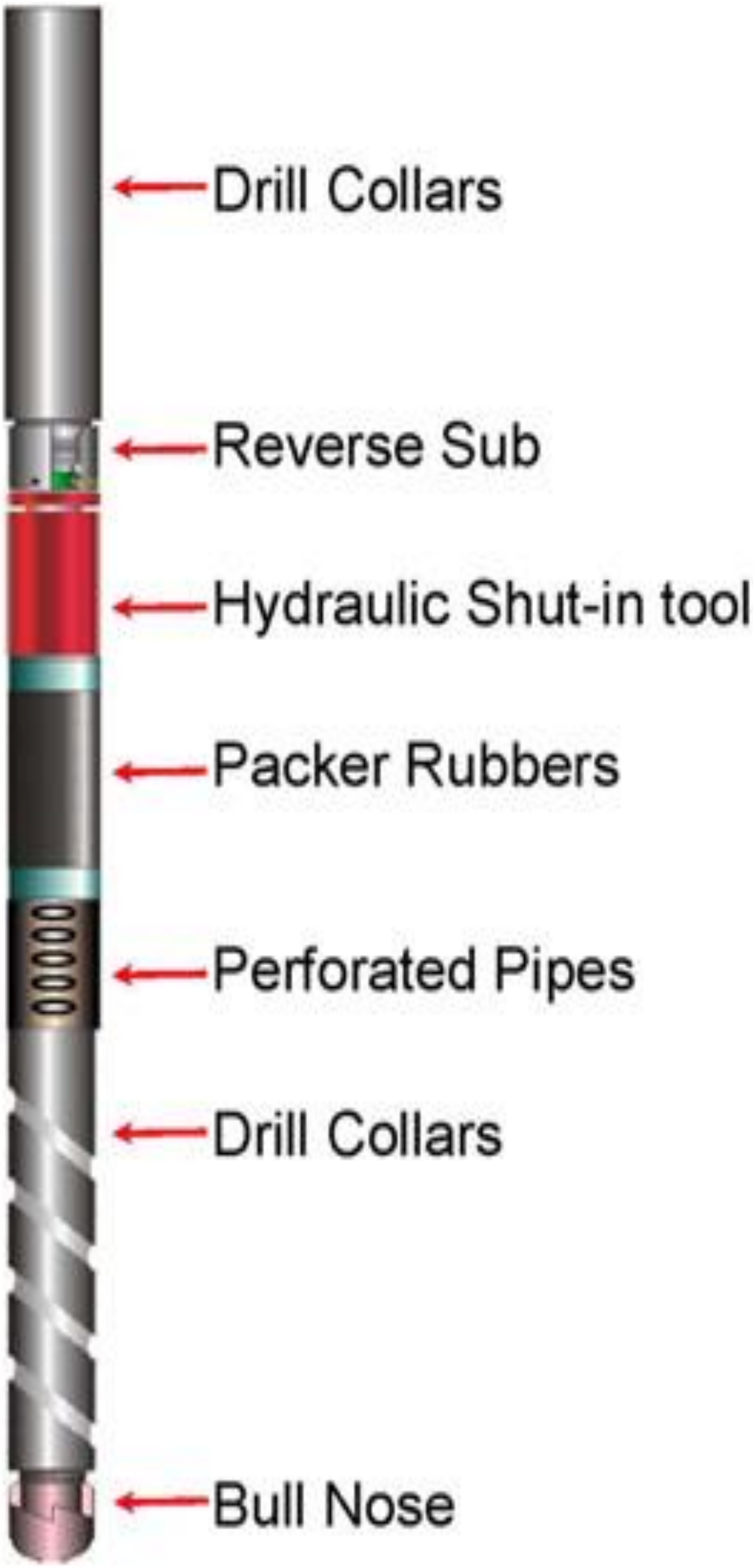

Figure 4.8: DST string and BHA for DST operation.

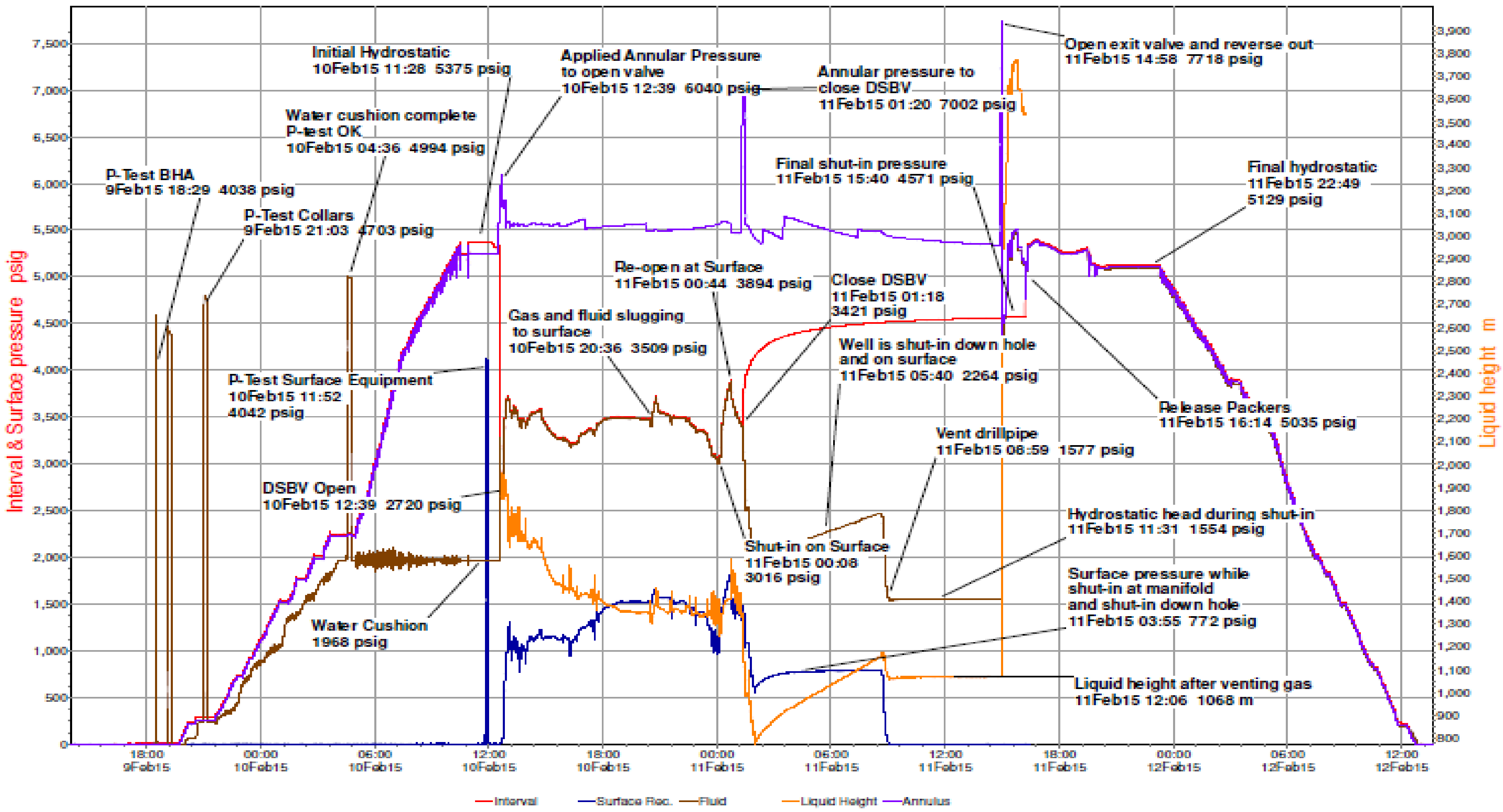

Figure 4.9: Summary of DST operation

During the total test period, first the well bore conditioning and pressure gauge calibration operation are performed in the initial hydrostatic period then started the drawdown period for 760 minutes following buildup period for 892 minutes shown in table 4.2. Four pressure gauge and temperature recorder have been installed in the test stem for recording four sets of data. Two record no. 1785 and 40914 have shown the reservoir responses in the pressure profile which have been analyzed.

Table 4.2: Summarized DST events.

	Recorder # / Depth m		Surface	1787	1788	1785	40914
event	date/time mm/dd hh:mm	duration minutes		3226.67	3226.67	3239.50	3239.50
A. Init Hydrostatic	02/10 11:18				5250	5375	5377
B. Start Flow 1	02/10 12:41	760	22	1968	6094	2723	2724
B End Flow 1	02/11 01:21		1480	3411	7047	3426	3427
C. End Shut In 1	02/11 16:12	892	5	4913	4774	4574	4575
M. End Hydrostatic	02/11 22:19			5089	5109	5128	5129

The liquid flow profile is plotted during the DST operation. It has been observed that during the DST significant quantity of liquid has flown from reservoir into wellbore in form of oil and water in an average rate 338 m^3/d shown in Figure 4.10.

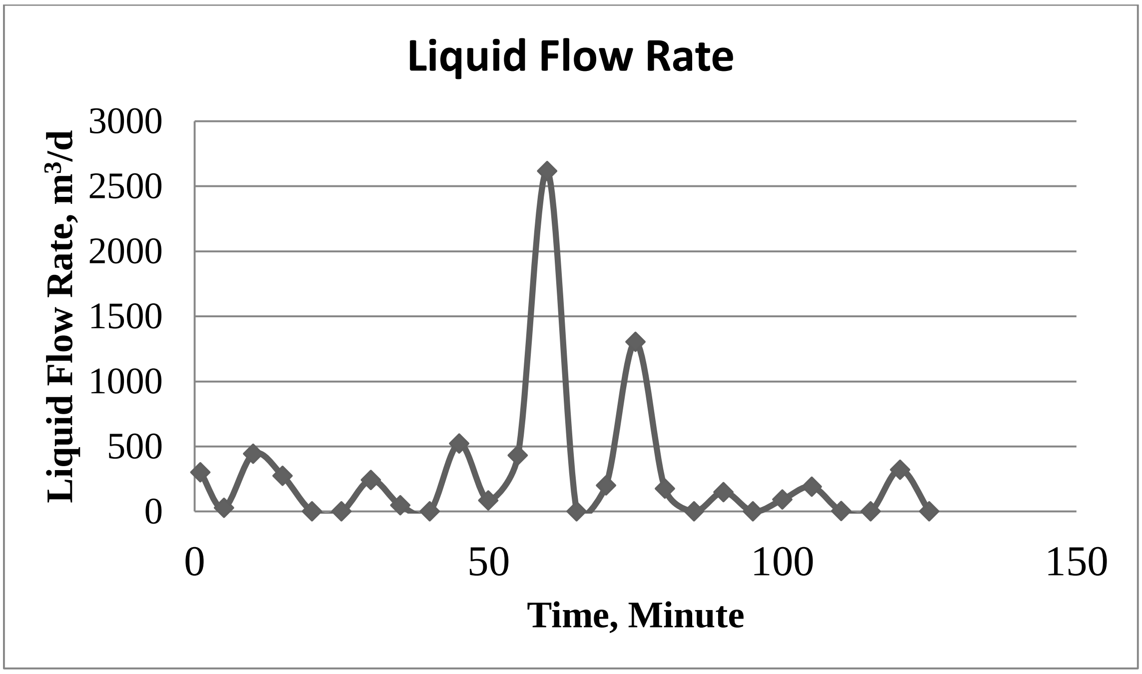

Figure 4.10: Liquid flow profile during DST

Analysis of DST data for record no. 1785

A pressure gauge is set at the depth 3239.5 meter to record the flowing pressure during the DST operation and pressure signature is recorded under the record no. 1785. In the total pressure profile of the DST there is presence of drawdown following buildup pressure signature as shown in figure 4.11 from 26.02 hours to 37.57 hours and from 37.57 hours to 53.68 hours respectively since the start of test.

The recorded total pressure data is filtered as per 300 data per cycle to remove the noise and develop the full test model of drawdown following buildup periods as shown in figure 4.12. The drawdown period (tp) persists for 11.5514 hour and pressure buildup period (Δt) exists for 16.1069 hour. The initial pressure (Pi) is 5347.53 psig and after drawdown the flowing pressure (Pwf) is 3033.92 psig following buildup period the pressure increases to 4588.57 psig.

The shut-in pressure (Pws) is plotted in Cartesian scale and the Horner time [(tp+Δt)/Δt] is plotted in log scale to build a semi-log plot of buildup test. A best fitted straight line is drawn along the data points to estimate the slope and intersection of the straight line. From the slope of the straight line permeability (k) is calculated 6.3312 millidarcy (md) and from the intersection the average reservoir pressure (p*) is calculated 4858.8 psia as shown in figure 4.13.

The buildup pressure (ΔPbu=Pws-Pwf) and its derivative [dΔPbu/d(tp+Δt)/Δt] is plotted in log scale along the Horner time [(tp+Δt)/Δt] in the same scale to build the diagnostic plot as shown in figure 4.14 where well bore storage effect, skin effect and infinite acting reservoir responses are visible clearly. The well bore storage is 0.21 bbl/psi and from the infinite acting line the permeability is 6.3312 md.

Analysis of DST data for record no. 40914

Another pressure gauge is set at the depth 3239.5 meter to record the flowing pressure during the DST operation and pressure signature is recorded under the record no. 40914. In the total pressure profile of the DST, there is presence of drawdown following buildup pressure signature as shown in figure 4.15 from 25.88 hours to 37.60 hours and from 37.60 hours to 53.59 hours respectively since the start of test.

The recorded total pressure data as shown in figure 4.15 is filtered as per 400 data per cycle to remove the noise and develop the full test model of drawdown following buildup periods as shown in figure 4.16. The drawdown period (tp) persists for 11.5986 hour and pressure buildup period (Δt) exists for 15.9848 hour. The initial pressure (Pi) is 5348.83 psig and after drawdown the flowing pressure (Pwf) is 3041.79 psig following buildup period the pressure increases to 4589.14psig.

The shut-in pressure (Pws) is plotted in Cartesian scale and the Horner time [(tp+Δt)/Δt] is plotted in log scale to build a semi-log plot of buildup test. A best fitted straight line is drawn along the data points to estimate the slope and intersection of the straight line. From the slope of the straight line permeability (k) is calculated 12.2179 millidarcy (md) and from the intersection the average reservoir pressure (p*) is calculated 4834.7 psia as shown in figure 4.17.

The buildup pressure (ΔPbu=Pws-Pwf) and its derivative [dΔPbu/d(tp+Δt)/Δt] is plotted in log scale along the Horner time [(tp+Δt)/Δt] in the same scale to build the diagnostic plot as shown in figure 4.18 where well bore storage effect, skin effect and infinite acting reservoir responses are visible clearly. The well bore storage is 0.04 bbl/psi and from the infinite acting line the permeability is 12.2179 md.

These two pressure profiles are analyzed as per the standard well test analysis technique such as semi-log and diagnostic plot analysis which reveals the existence of the petroleum reservoir of the following characteristics as shown in table 4.3.

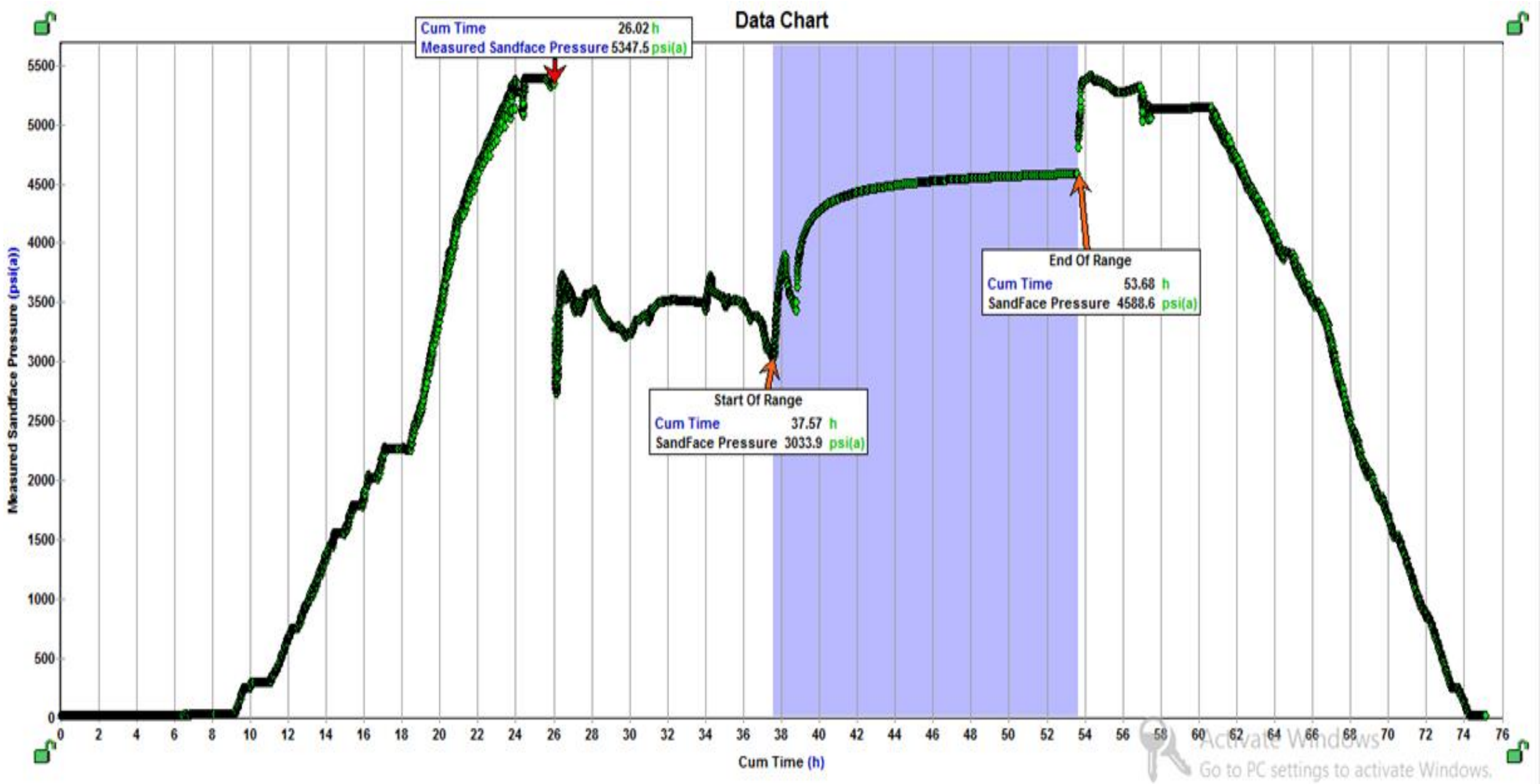

Figure 4.11: Recorded total pressure profile of DST (1785)

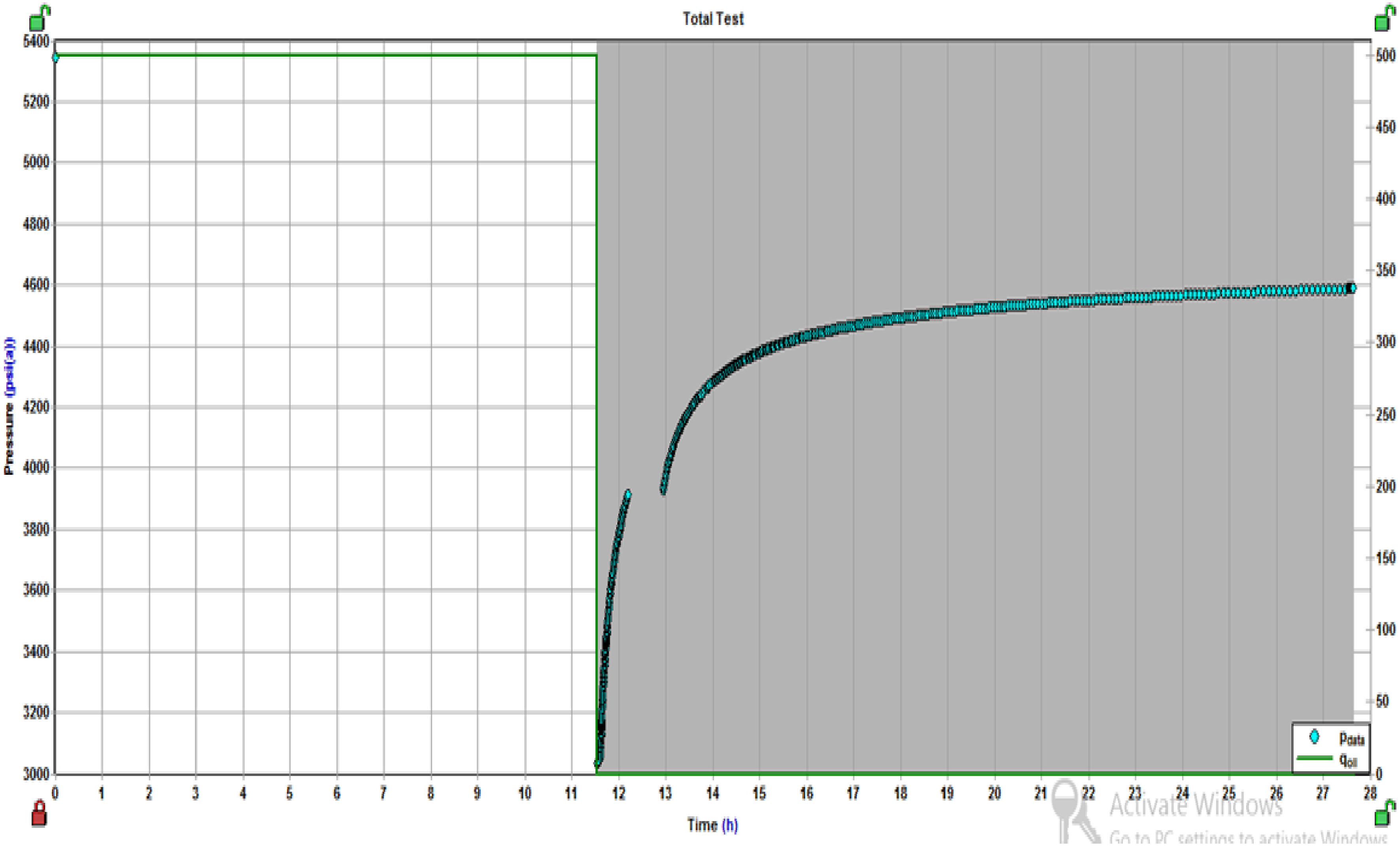

Figure 4.12: Full test model of drawdown following buildup period (1785)

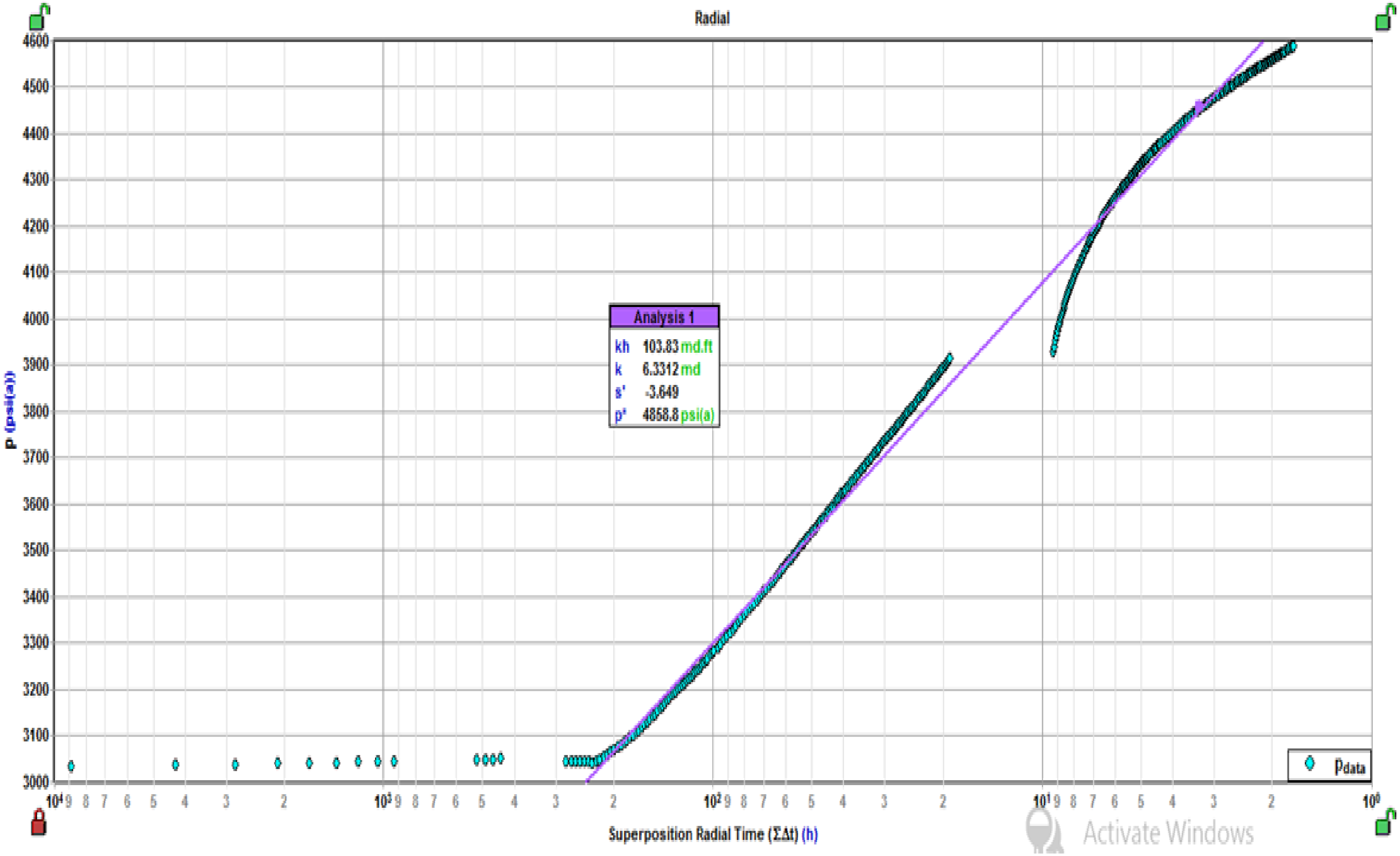

Figure 4.13: Semilog plot of buildup test (1785)

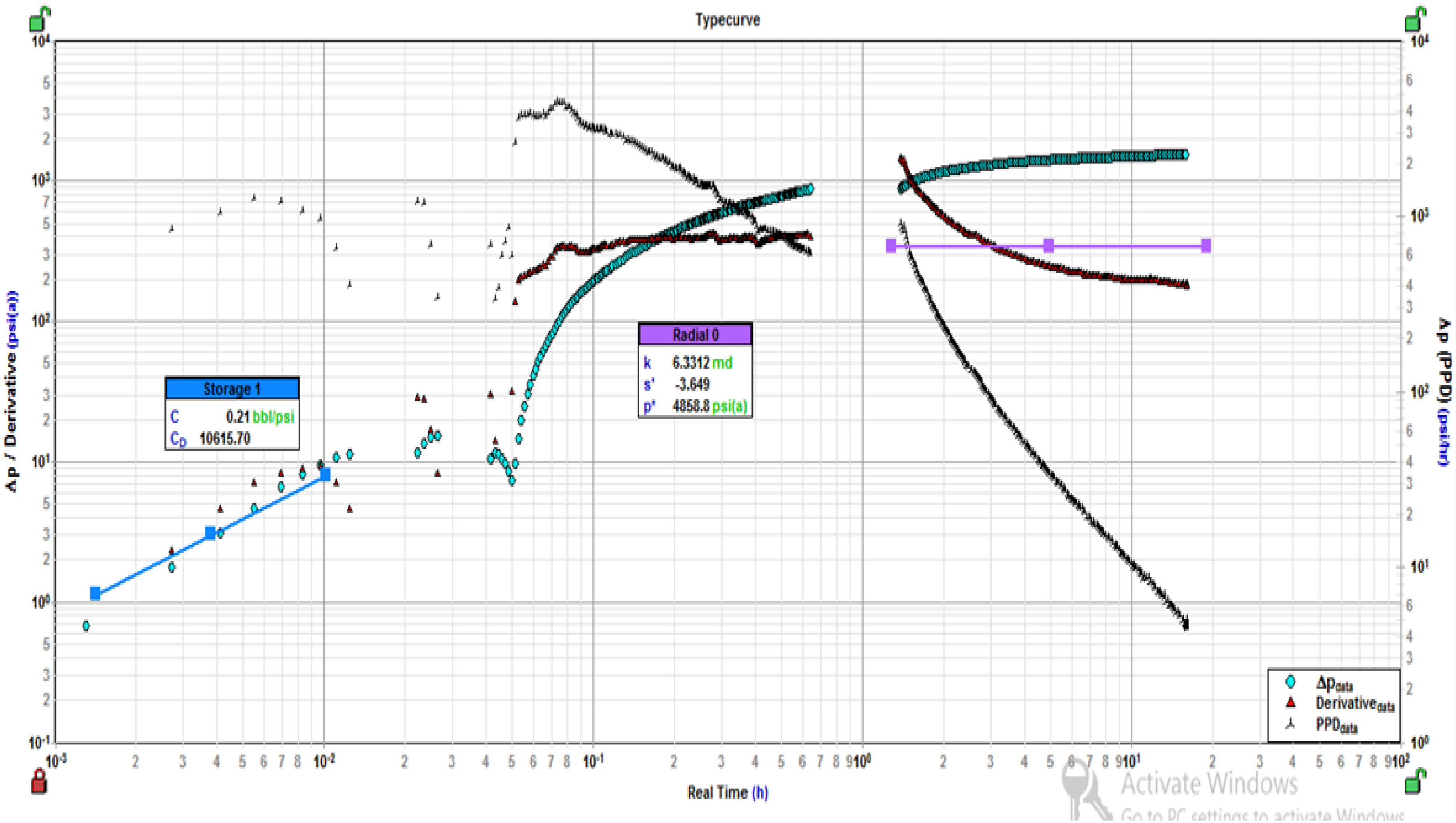

Figure 4.14: Diagnostic plot of buildup test (1785)

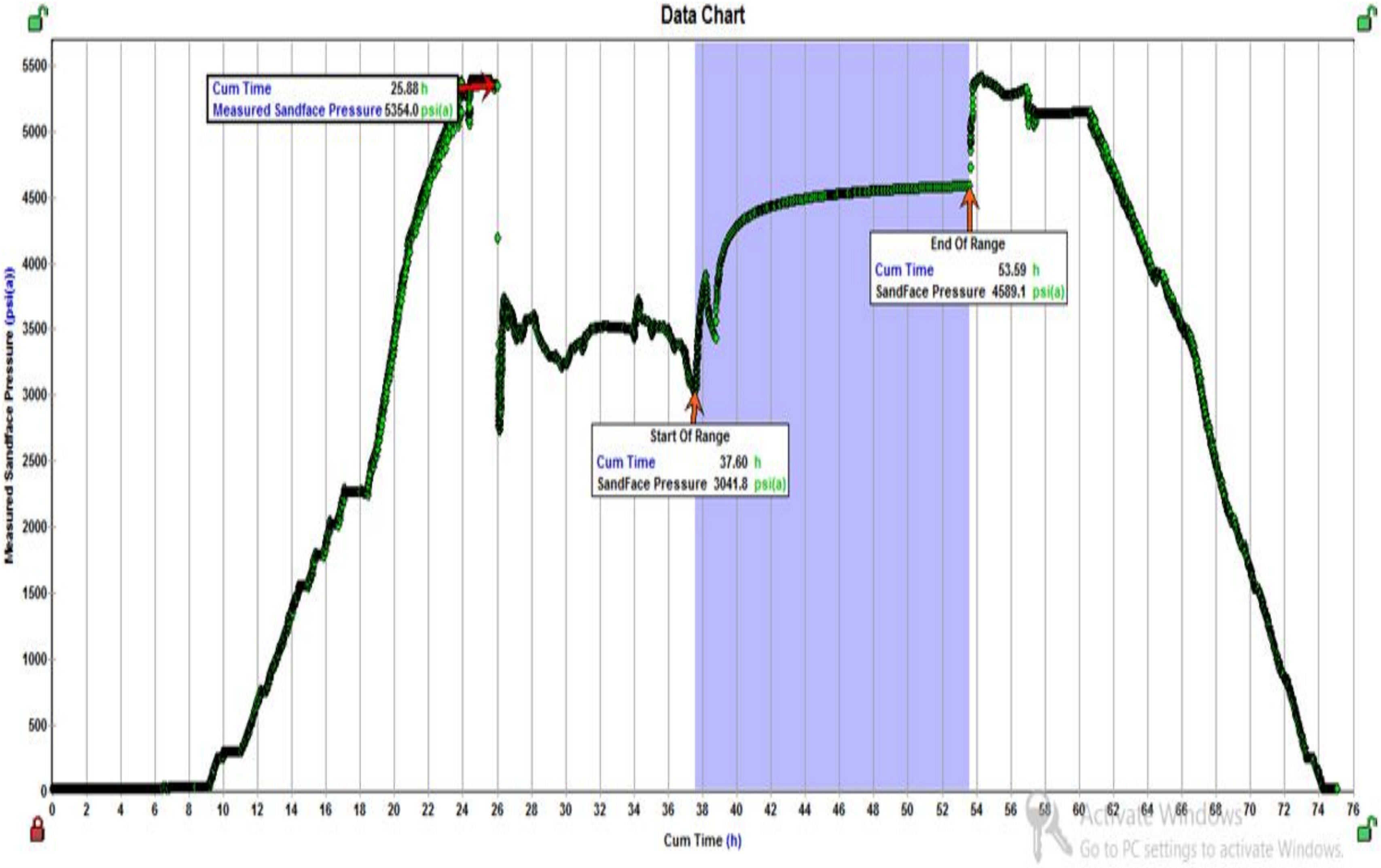

Figure 4.15: Recorded total pressure profile of DST (40914)

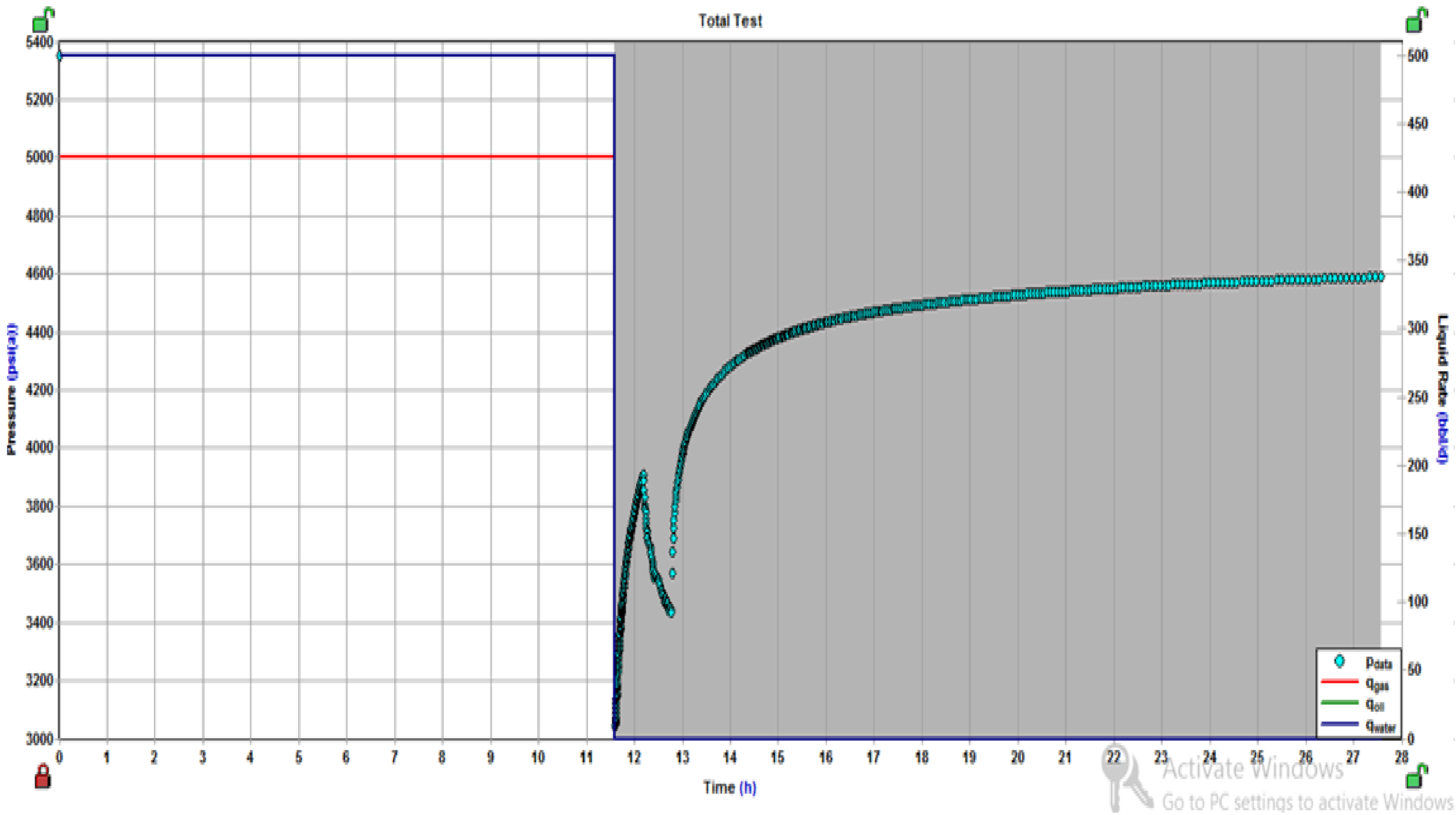

Figure 4.16: Full test model of drawdown following buildup period (40914)

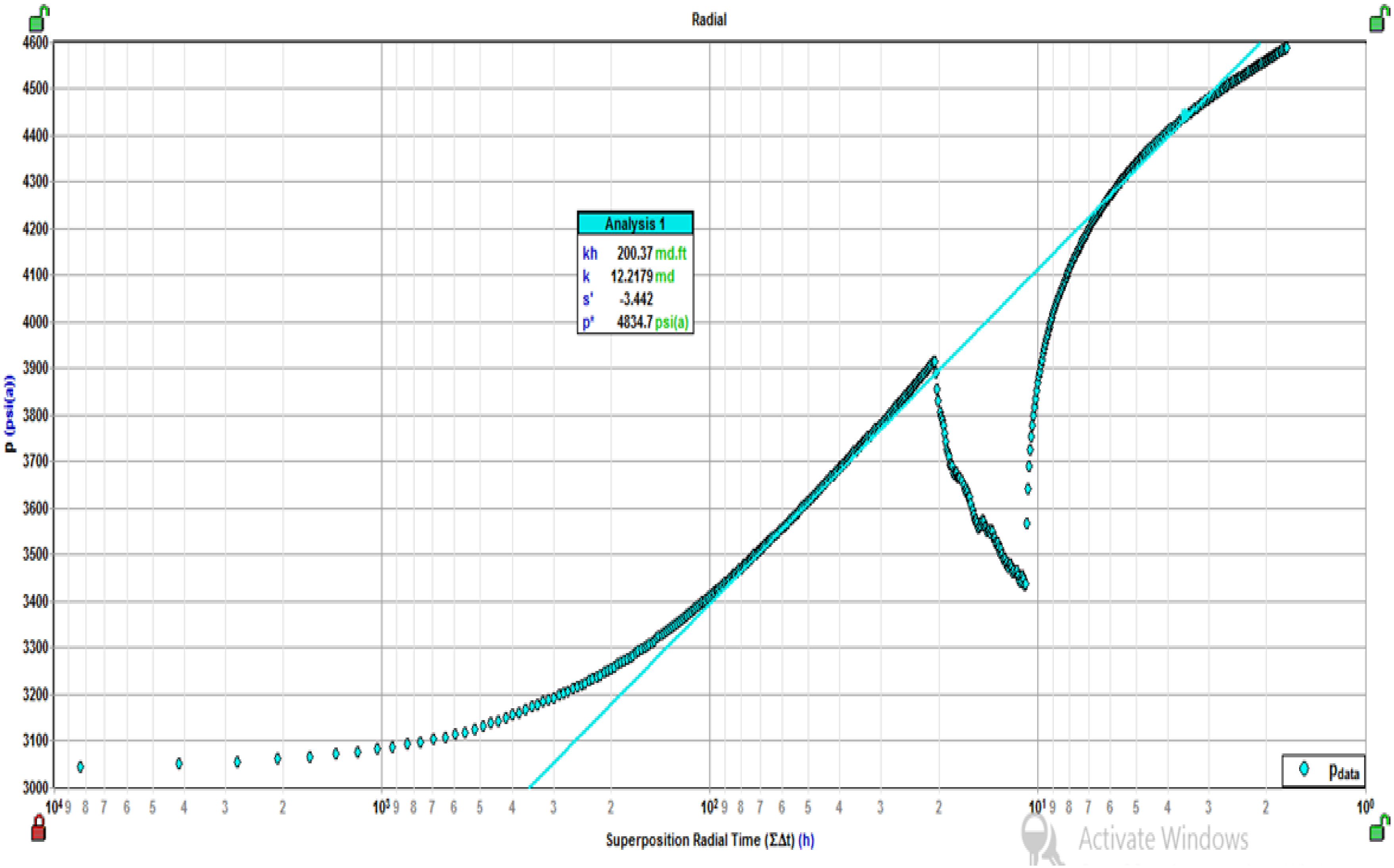

Figure 4.17: Semilog plot of buildup test (40914)

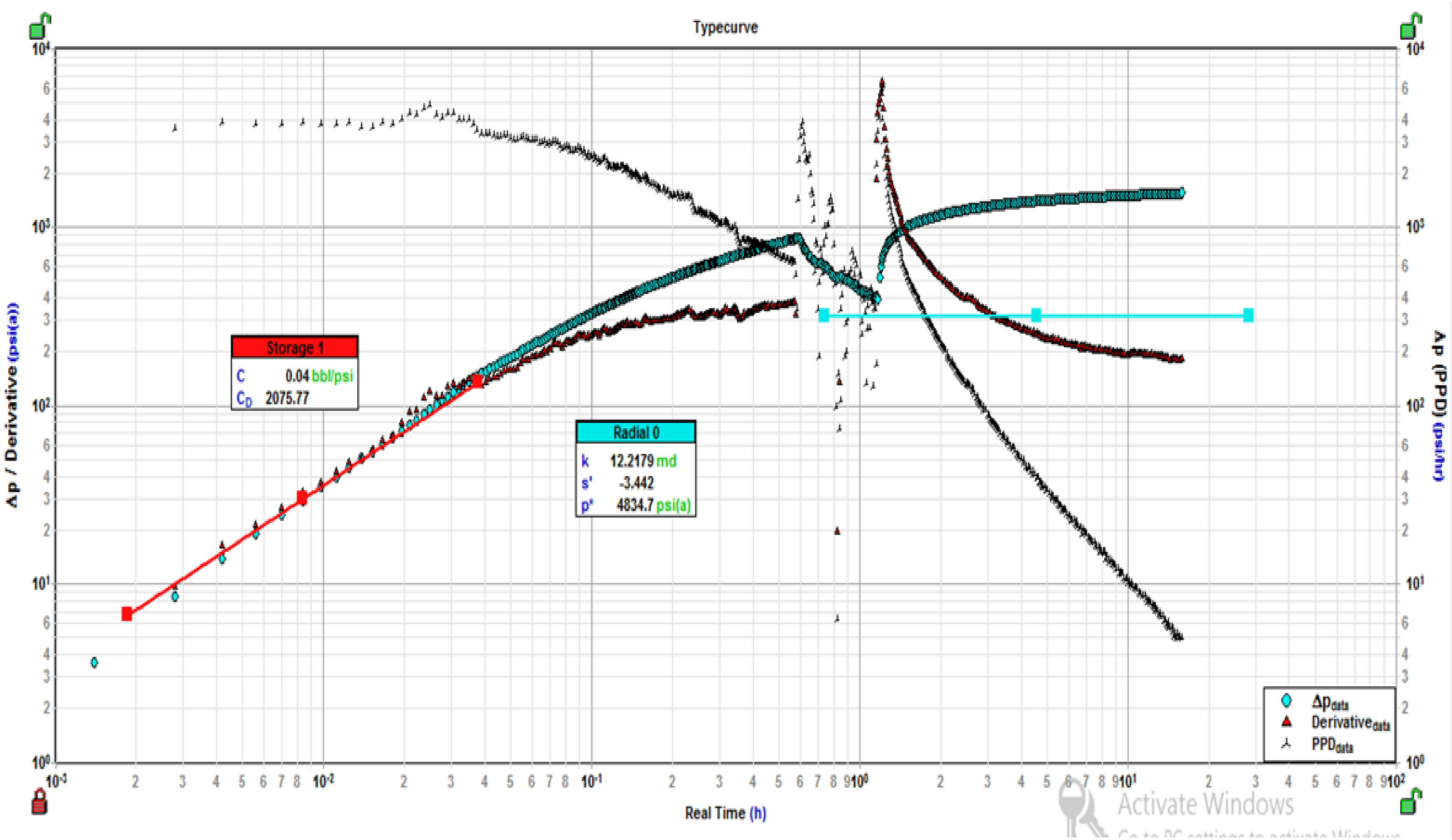

Figure 4.18: Diagnostic plot of buildup test (40914)

Table 4.3: Summary of DST interpretation

<table>
<tr><th>Parameter</th><th colspan="2">Value</th><th>Remarks</th></tr>
<tr><td>Interval</td><td colspan="2">3261 to 3266 m</td><td>Well logs indicate a porous and permeable formation</td></tr>
<tr><td rowspan="2">Effective Permeability (K), mD</td><td>Re. No. 1785</td><td>Re. No. 40914</td><td rowspan="2">Permeability is low.
Consistent with DST value.</td></tr>
<tr><td>6.3312</td><td>12.2179</td></tr>
<tr><td rowspan="2">Skin Factor (S), DL</td><td>Re. No. 1785</td><td>Re. No. 40914</td><td rowspan="2">Skin Factor is Negative.

Negative skin factor indicates fracture development near the well bore during drilling operation.</td></tr>
<tr><td>-3.649</td><td>-3.442</td></tr>
<tr><td rowspan="2">Wellbore Storage, C, bbl/psi</td><td>Re. No. 1785</td><td>Re. No. 40914</td><td rowspan="2">Wellbore Storage is low.
Low Wellbore Storage indicates that liquid has flown from reservoir into well bore.</td></tr>
<tr><td>0.21</td><td>0.04</td></tr>
<tr><td rowspan="2">Average Reservoir Pressure, P*, psia</td><td>Re. No. 1785</td><td>Re. No. 40914</td><td rowspan="2">Average Reservoir Pressure is high.
Water column pressure at depth 3266 m is 4647 psia.
Approximately 200 psi overpressure exists in the zone indicating the existence of oil.</td></tr>
<tr><td>4858.8</td><td>4834.7</td></tr>
<tr><td rowspan="2">Boundaries</td><td>Re. No. 1785</td><td>Re. No. 40914</td><td rowspan="2">No boundaries have been developed.
No interference with other wells in the field.
No fault in the drainage area.
No channel in the drainage area.
No fracture in the drainage area.</td></tr>
<tr><td>Infinite acting</td><td>Infinite acting</td></tr>
</table>

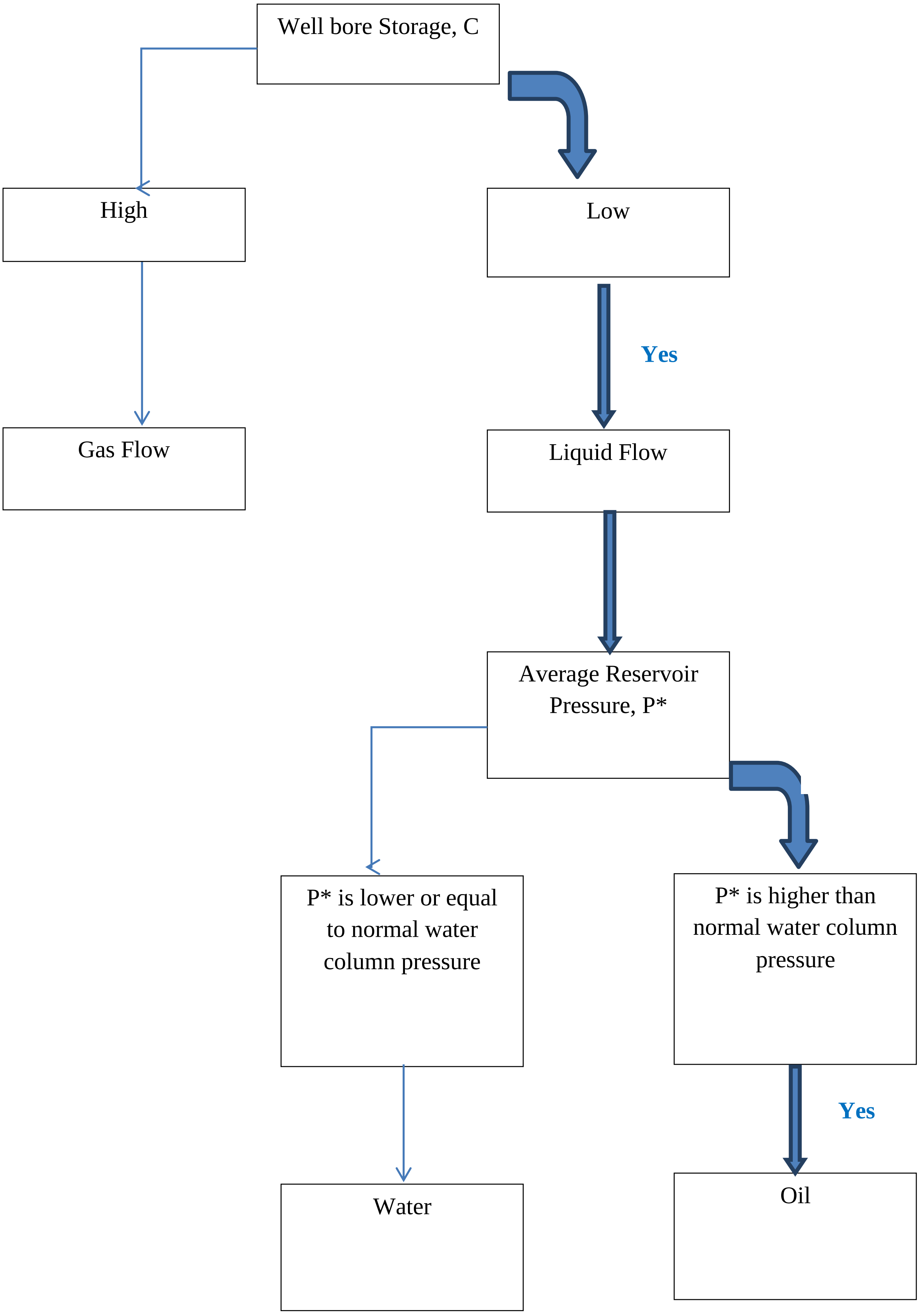

Figure 4.19: Decision flow chart on the basis of DST analysis.

The analysis of pressure signature obtained from the DST, the wellbore storage, skin factor, permeability and average reservoir pressure have been estimated and their values are analyzed to obtain the following:-

1. The flowing phase during the DST is liquid on an average rate 338 sm^3/d.
2. Although the reservoir permeability is low, the negative skin factor helps the reservoir liquid to flow into the wellbore.
3. The low value of wellbore storage provides the evidence of the presence of liquid phase that has flown into the well bore from the reservoir. There is no flow of gas phase into the wellbore from the reservoir.
4. Average reservoir pressure and water column pressure at depth 3266 m reveal the existence of the overpressure zone which is developed by the presence of hydrocarbon in liquid phase.
5. Well log analyses i.e. low value of gamma ray log and high value of resistivity log with shallow and deep resistivity separation indicates the presence of hydrocarbon as well.

From the above analysis it can be concluded that all of the investigations i.e. well logs and DST analyses are able to provide the evidence of the presence of liquid hydrocarbon (oil) in the interval 3261 to 3266 meter as shown in figure 4.19.

4.2: Oil Reservoir Model Development in Kailashtila Field

Oil reservoir model of Kailashtila field has been prepared from seismic survey, well logs of KTL-7, fluid contacts, core analysis, fluid analysis, saturation function properties analysis, and initial reservoir condition. The oil reservoir model has been validated by drill stem test data. Finally a reservoir simulation model has been developed using the reservoir simulation process as shown in figure 4.20. Reservoir simulation model includes reservoir description, fluid description, wells configuration, production facilities descriptions and production data. Reservoir description includes reservoir grid structure, grid cells dimensions, grid cells properties such as porosity, permeability, net to gross ratio, saturation, pressure. Fluid description includes formation volume factor, viscosity, compressibility, solution gas oil ratio, oil to gas ration of oil water and gas. Well description includes casing size and setting depth, tube size and depth, packer, perforation and controls valves. Production data includes flow rate and pressure of oil, water and gas. Production facilities includes separators, stock tank and valves.

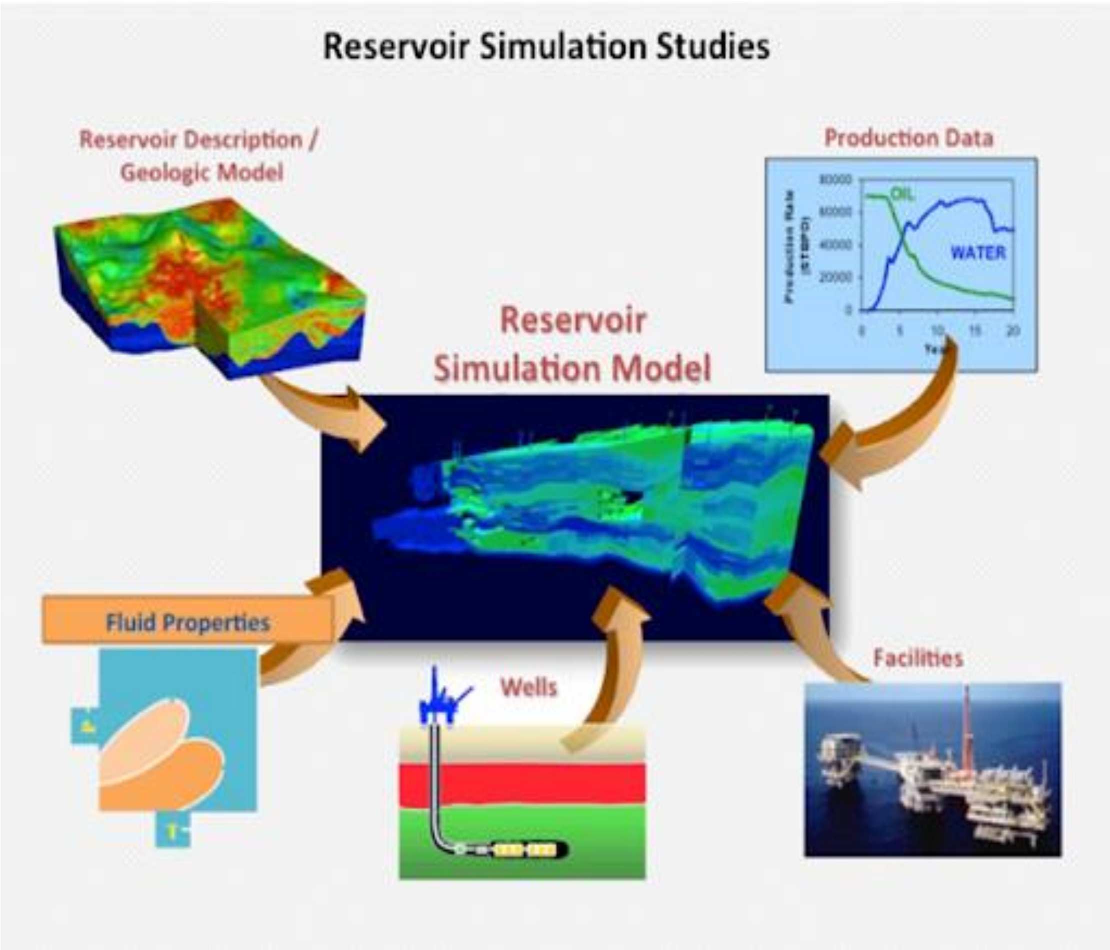

Figure 4.20: Reservoir simulation process

4.2.1 Structural Modeling of Oil Reservoir in Kailashtila Field

Oil reservoir structure in Kailashtila field has been constructed from seismic survey data and well log data of well No. KTL-7 as shown in figure 4.21. The oil reservoir structure is extended from 4388.56 m in east-west direction and 10348.59 m in north-south direction as shown in table 4.4. The reservoir has 44 grid cells in X (E-W) direction and 104 grid cells in Y (N-S) direction. Average dimension of grid cell is 99.75 m in X direction and 99.49 m in Y direction.

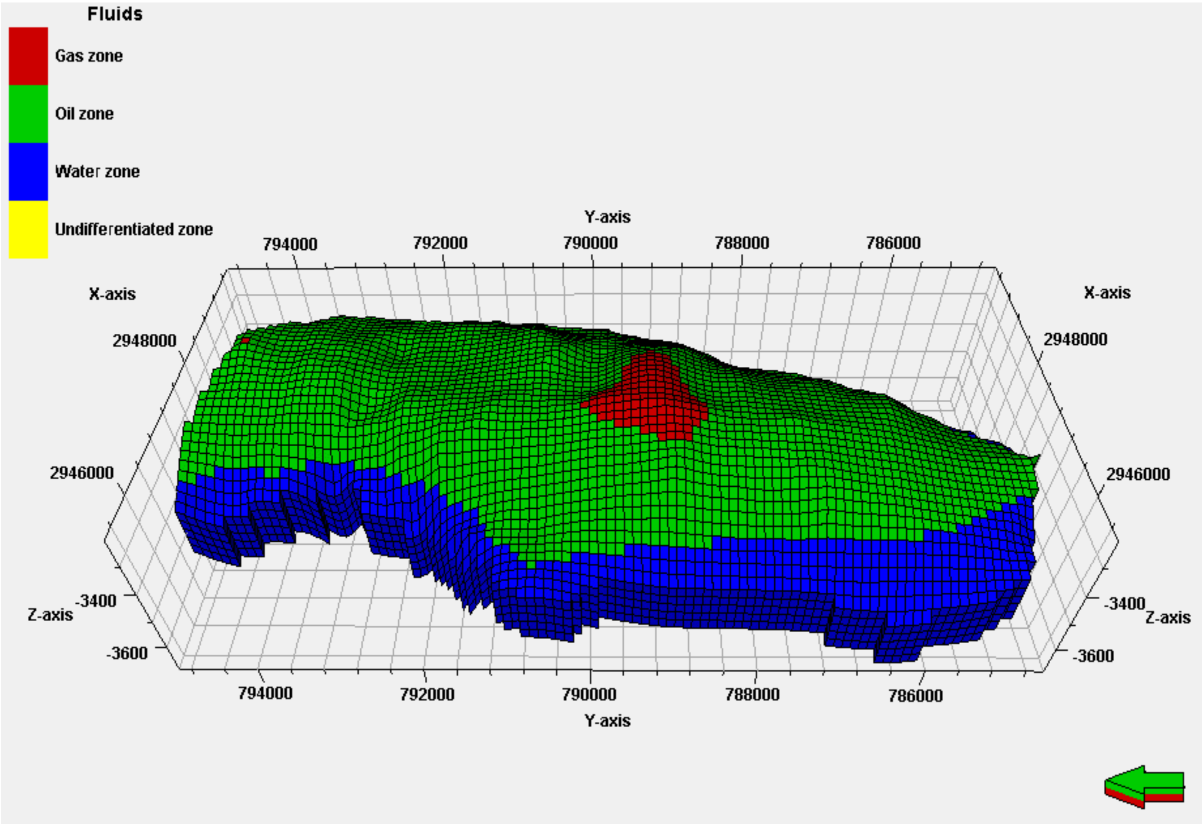

Figure 4.21: Oil Reservoir structure of Kailashtila field

Table 4.4: 3D Reservoir model dimensions

Axis	Easting-Northing	Minimum, m	Maximum, m	Difference, m	Number of Grid Cell
X-X'	E-W	2945425.39	2949813.95	4388.56	44
Y-Y'	N-S	784597.29	794945.89	10348.59	104
Z-Z'	Depth	-3636.96	-3215.16	421.80	5

4.2.2 Detection of Fluid Contacts

According to the interpretation of well log of well KTL-7 gas zone exists from 3250 m to 3260 m and oil exists from 3260 m to 3270 m along the well as shown in figure 4.22. For reservoir simulation, gas-oil contact has been placed at depth 3260 m and oil-water contact has been placed at depth 3400 m as shown in figure 4.23.

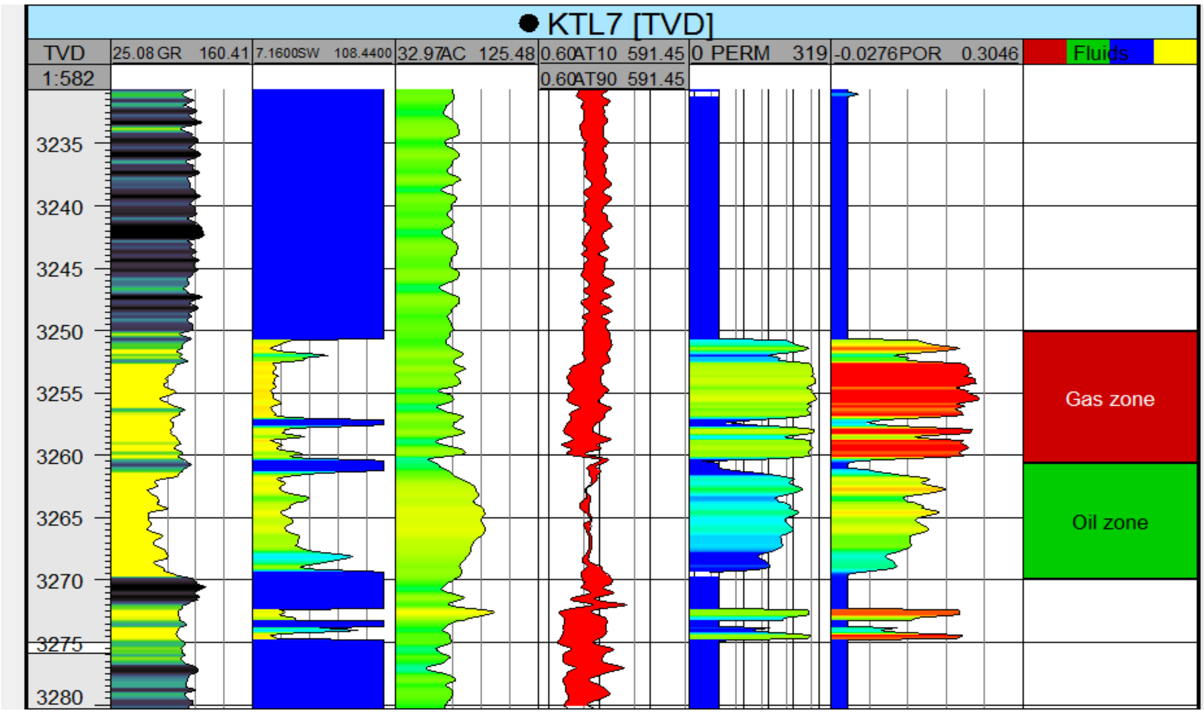

Figure 4.22: Fluid contacts in reservoir along the well KTL-7

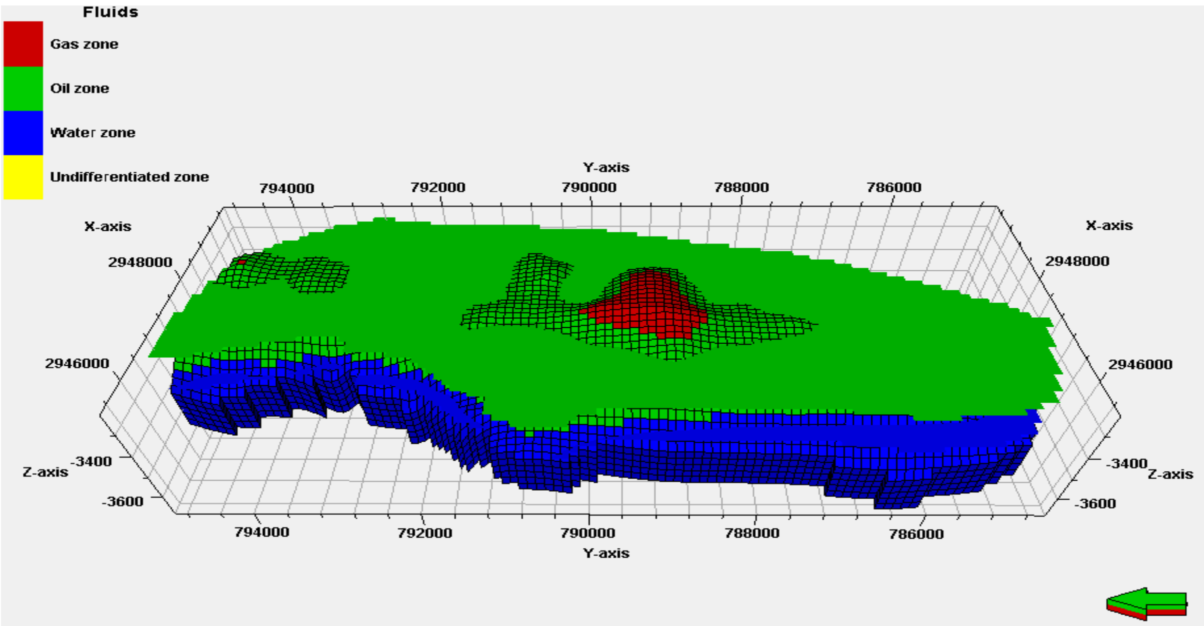

Figure 4.23: Fluid contacts in reservoir model

4.2.3 Petrophysical Properties Modeling of Kailashtila Field

Porosity has been distributed in grid cells of oil reservoir model from porosity log as shown in figure 4.24. Porosity log has been scaled up along the grid cells of the reservoir by an averaging method. Then transformation and variogram have been created from the scale up porosity log. Porosity has been distributed from transformation and variogram using sequential Gaussian simulation.

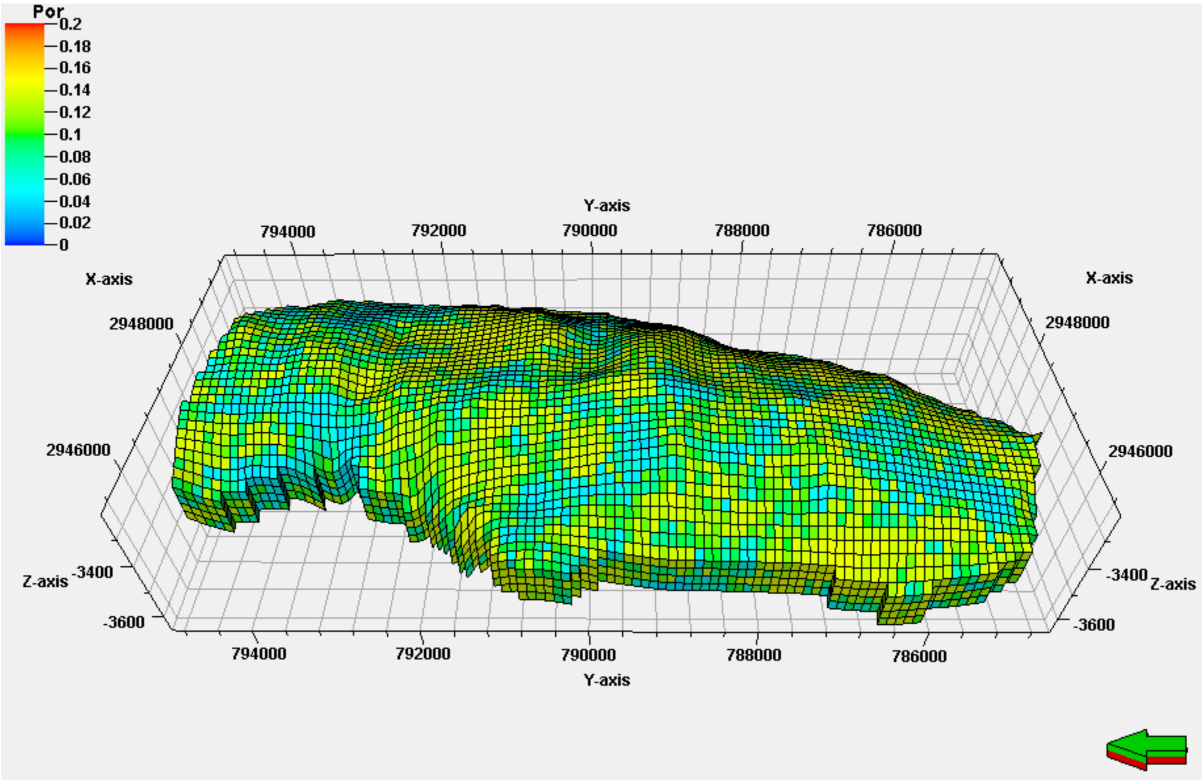

(a)

Name	Type	Min	Max	Delta	N	Mean	Std	Var	Sum
Property	Cont.	0.0396	0.1441	0.1046	12352	0.1012	0.0323	0.0010	1249.9742

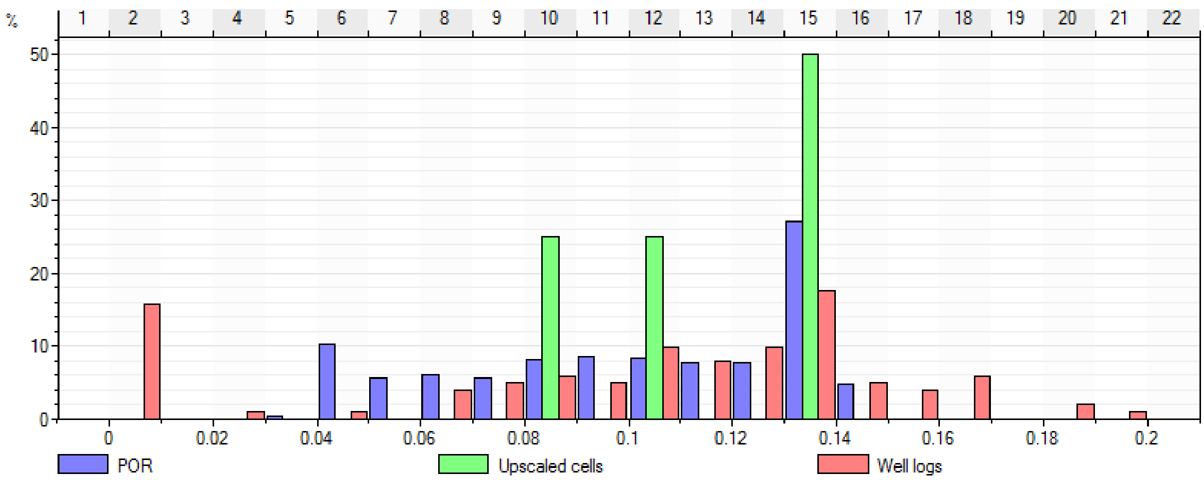

(b)

Figure 4.24: a) Porosity distribution in grid cell of reservoir model and b) statistics of porosity distribution

Reservoir simulation requires absolute permeability in X, Y and Z directions as fluid flows in X, Y and Z directions in three dimensional reservoir spaces. Fifteen core plugs have been prepared for X, Y and Z directions from core barrels. Core plugs have been tested in liquid permeameter. In X direction, minimum permeability, maximum permeability and average permeability have found 153, 200 and 180 md receptivity. Absolute permeability in X direction has been distributed in oil reservoir grid cells by normal distribution method as shown in figure 4.25.

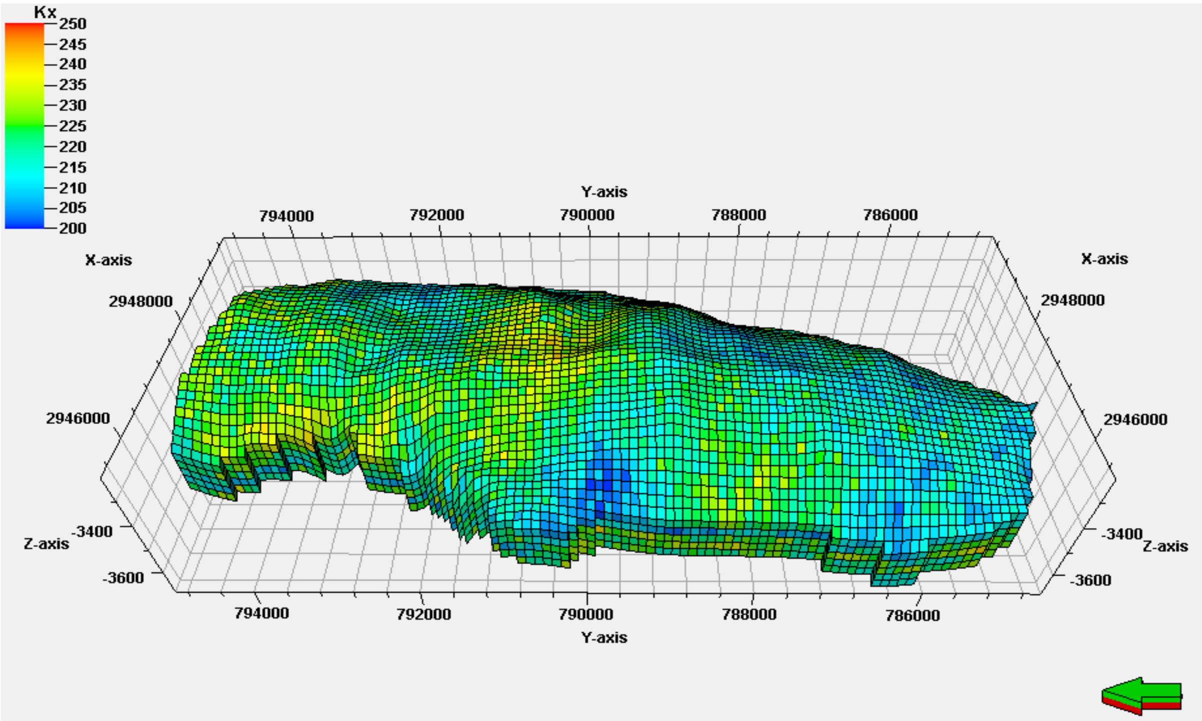

(a)

Name	Type	Min	Max	Delta	N	Mean	Std	Var
Property	Cont.	153	200	47	15440	180	8	64

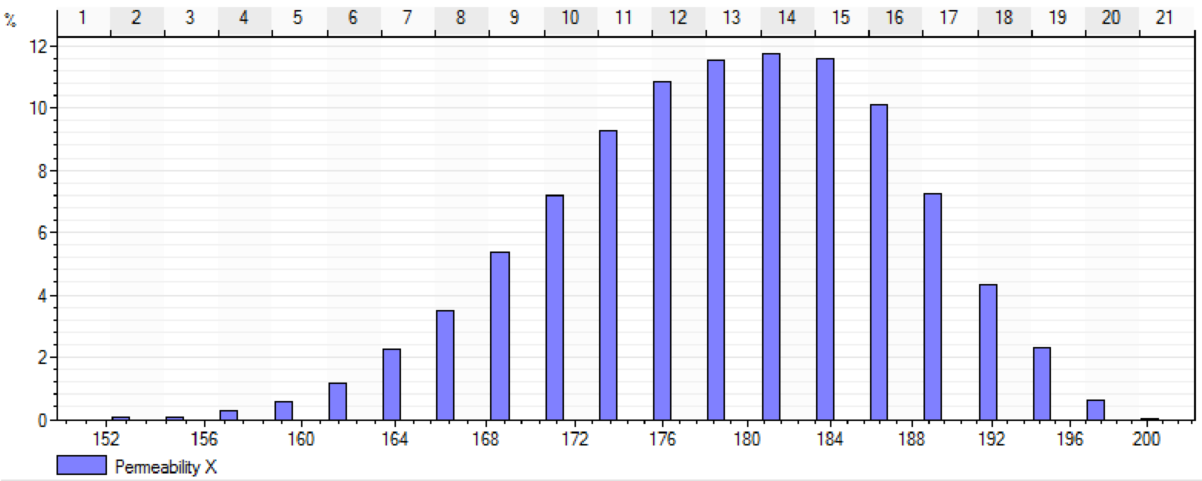

(b)

Figure 4.25: a) Distribution of absolute permeability of X direction in grid cells of reservoir model and b) statistics of permeability distribution

4.2.4 Pressure Volume Temperature (PVT) Properties of Reservoir Fluids (KTL)

Pressure volume temperature (PVT) properties such as oil formation volume factor, oil viscosity and solution gas oil ratio have been estimated in laboratory by using PVT cell. Oil sample has been collected form the Kailashtila field. Reservoir oil has charged in PVT cell and PVT cell has been operated at temperature 90 ^oC to attain the reservoir temperature.

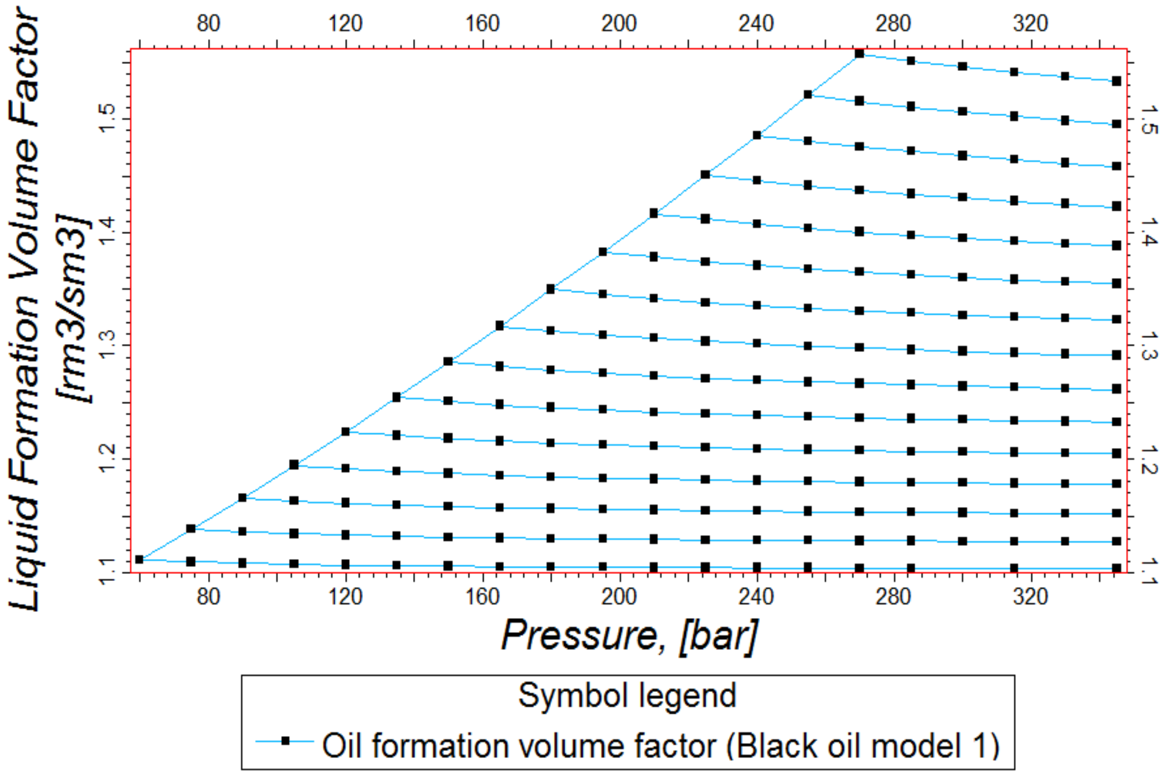

Figure 4.26: Oil formation volume factor

PVT cell has performed constant composition expansion test from pressure of 50 bar to 350 bar. Bubble point has been detected at pressure of 270 bar. Differential liberation test has been performed from pressure 270 bar to 50 bar. All the test values have been processed by the built in software of the PVT cell. Oil formation volume factor has been estimated by the PVT cell as shown in figure 4.26. PVT cell has also estimated oil viscosity at pressure from 50 bar to 350 bar as shown in figure 4.27. Solution gas oil ratio as shown in figure 4.28 has been estimated by the PVT cell from pressure 50 bar to 350 bar. Solution gas oil ratio increases with pressure as more gas dissolves in oil with pressure increase. Like this oil formation volume factor also increases with pressure increase. Oil viscosity decreases with pressure up to bubble point pressure as gas dissolves in oil reducing oil viscosity and after the bubble point pressure oil viscosity decreases with pressure due to oil compressibility.

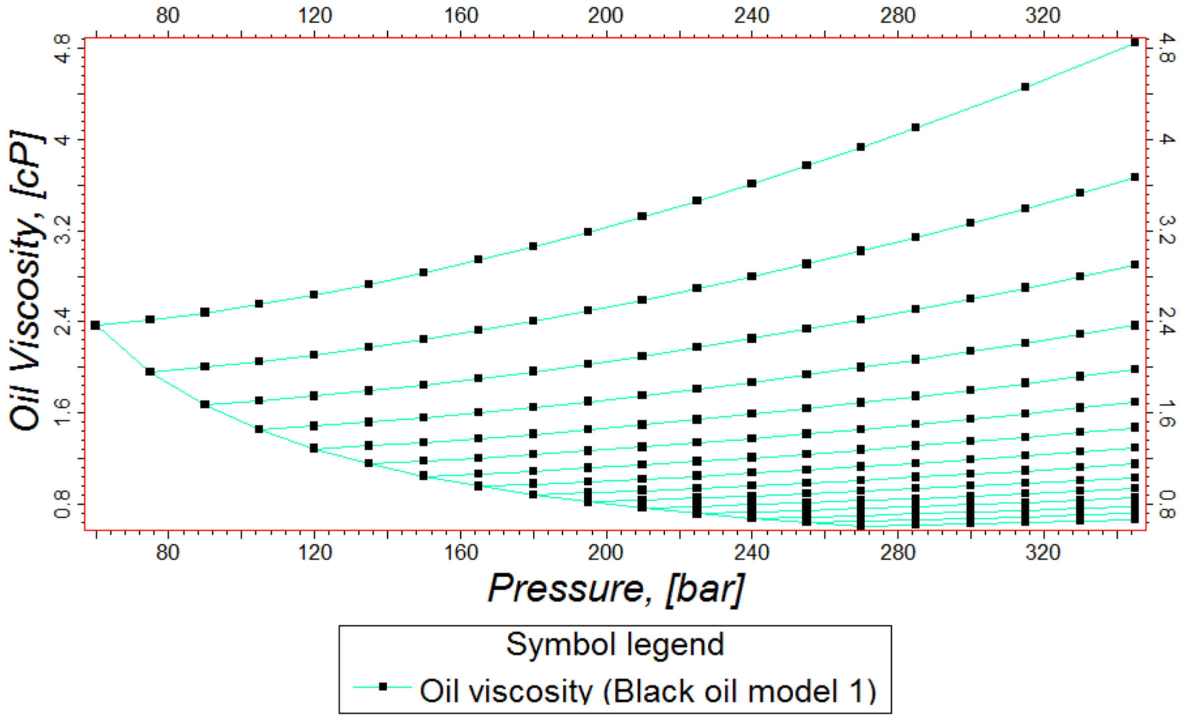

Figure 4.27: Oil viscosity

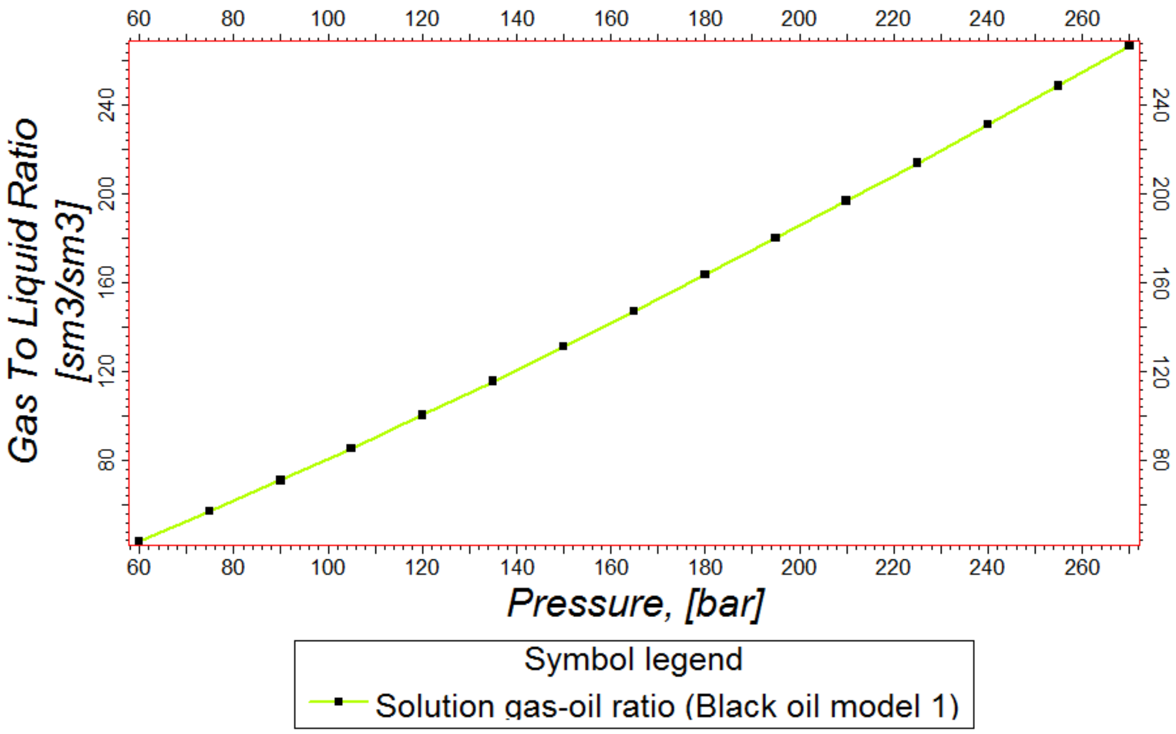

Figure 4.28: Solution gas oil ratio

4.2.5 Saturation Function Properties (KTL)

Saturation function properties such as oil-water relative permeability and capillary pressure have been estimated by relative permeameter and capillary pressure unit respectively in laboratory. Oil-water relative permeability has been measured at water saturation 0.20 to 1.00 as shown in figure 4.29. Oil-water capillary pressure has been measured at water saturation 0.20 to 1.00 as shown in figure 4.30.

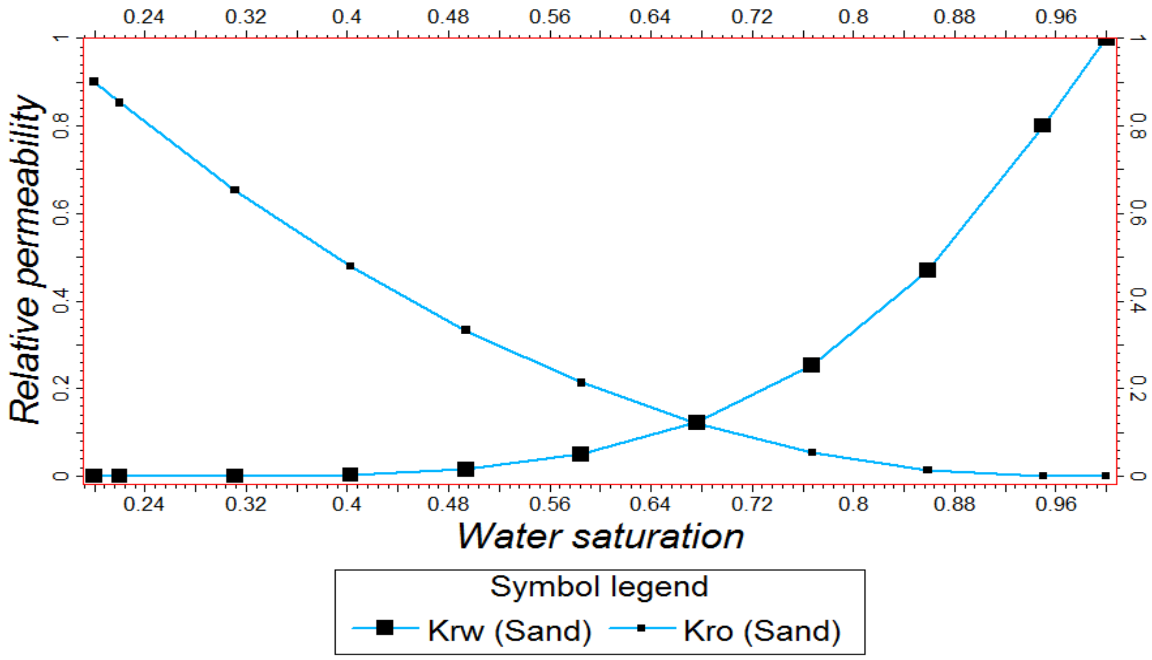

Figure 4.29: Oil water relative permeability

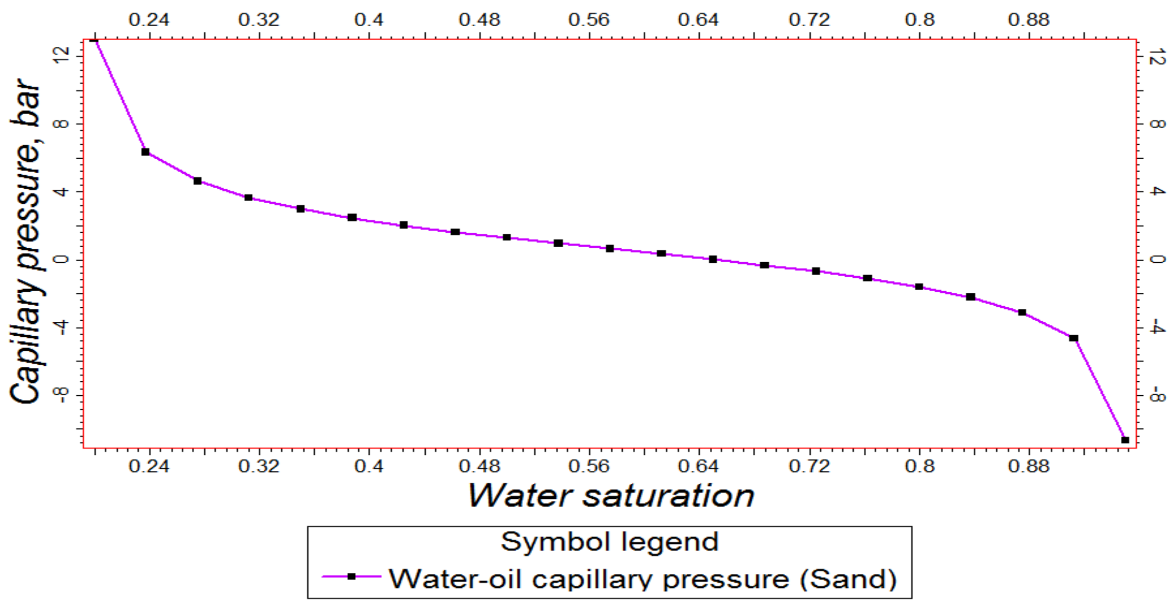

Figure 4.30: Oil water capillary pressure

4.2.6 Initialization of Reservoir Condition by Hydrostatic Equilibration (KTL)

Fluid saturation and pressure are change with time as oil, water and gas are produced from reservoir. Reservoir simulation calculates fluid saturation and pressure in each grid cell of the reservoir model in every time step. Initial pressure and saturation of each grid cell are assigned to reservoir simulation model. Initialization of reservoir condition is done by explicitly from well log analysis (water saturation and pressure) or implicitly from fluid contact (oil-water contact and gas-oil contact) and contact point pressure (Hydrostatic Equilibration). Oil reservoir model in Kailashtila field has been initialized by hydrostatic equilibration method as shown in figure 4.31. Gas-oil contact has been considered as datum and pressure at datum is 400 bar. Simulator calculates oil, water and gas pressures from this datum pressure along the reservoir depth and also estimate capillary pressure. Water saturation is function of capillary pressure. Water saturation is determined from capillary pressure along the depth. Oil saturation and gas saturation are determined from the water saturation along the depth.

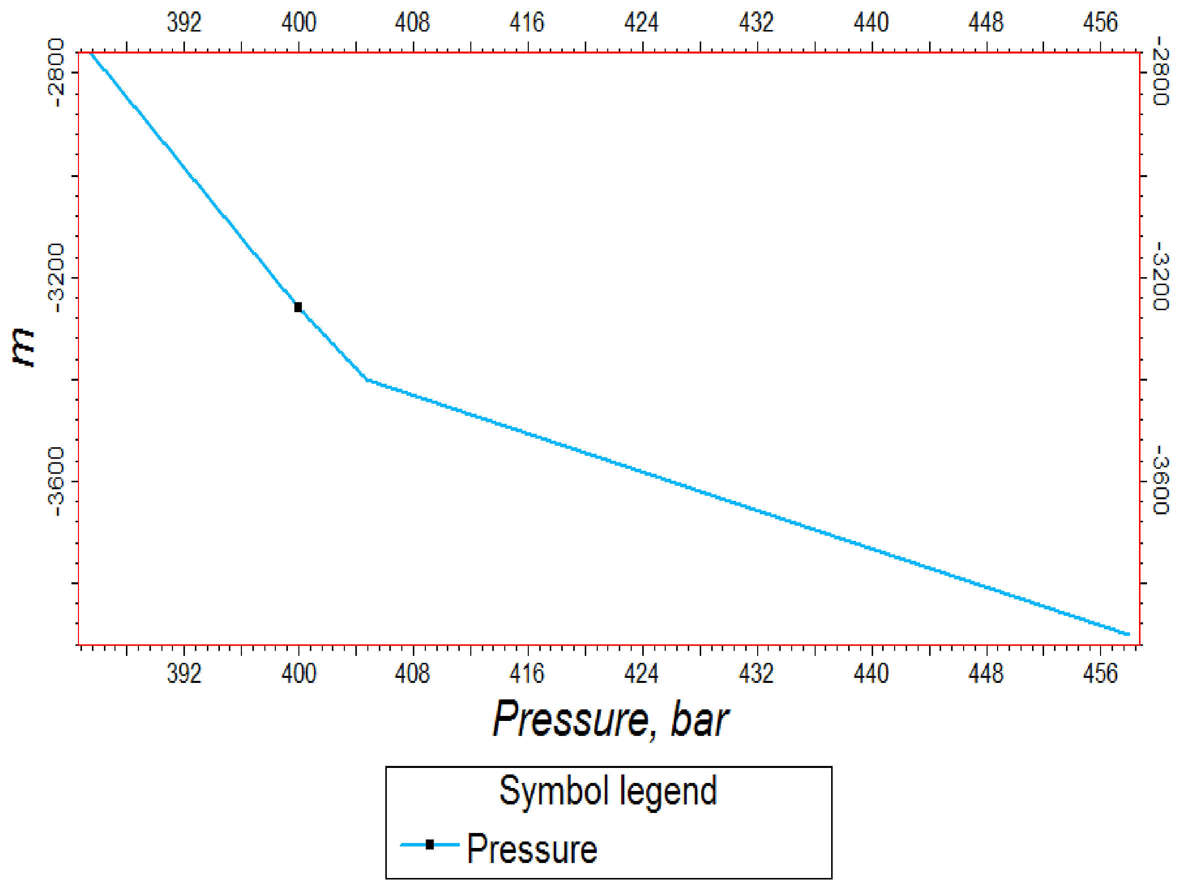

Figure 4.31: Initial condition of reservoir

4.2.7 Validation of Oil Reservoir Model (KTL)

Drill stem test has been performed on the oil reservoir of Kailashtila field. The DST has run for 125 minutes and the reservoir has delivered oil and water as liquid flow on an average rate of 338 sm^3/day (1886 STB/D) as shown in figure 4.32. From the total liquid delivery it can be said that the reservoir is able to deliver minimum 30 sm^3/day (188.6 STB/D) of oil. On the basis of the reservoir oil deliverability oil flow rate of reservoir model has been forecasted as shown in figure 4.33. It is seen that the reservoir model is able to deliver oil at a rate of 30 sm^3/day for 24 hours. This analysis has validated the reservoir model of Kailashtila field.

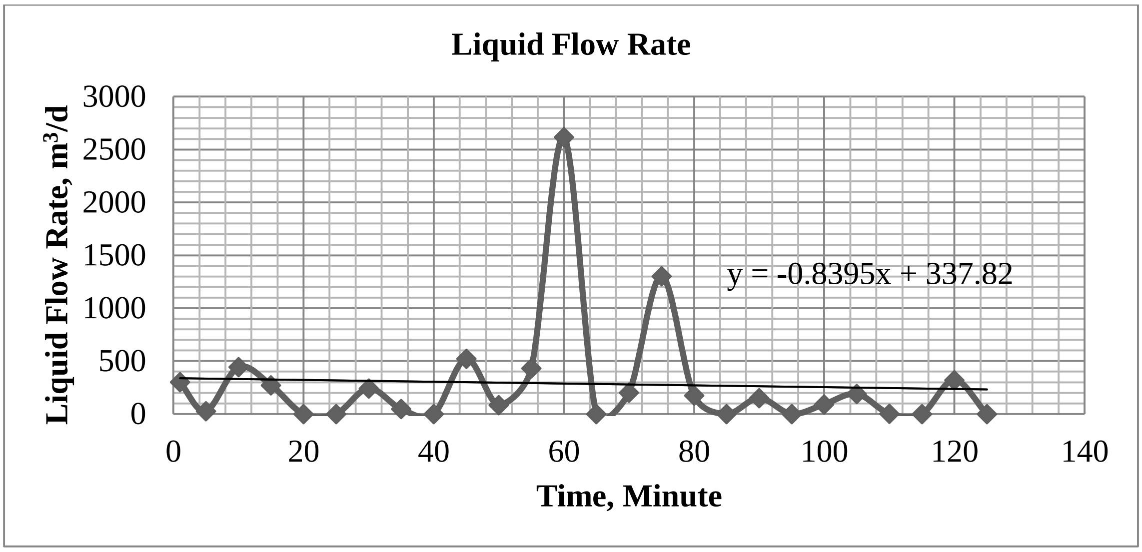

Figure 4.32: Average liquid flow profile in DST

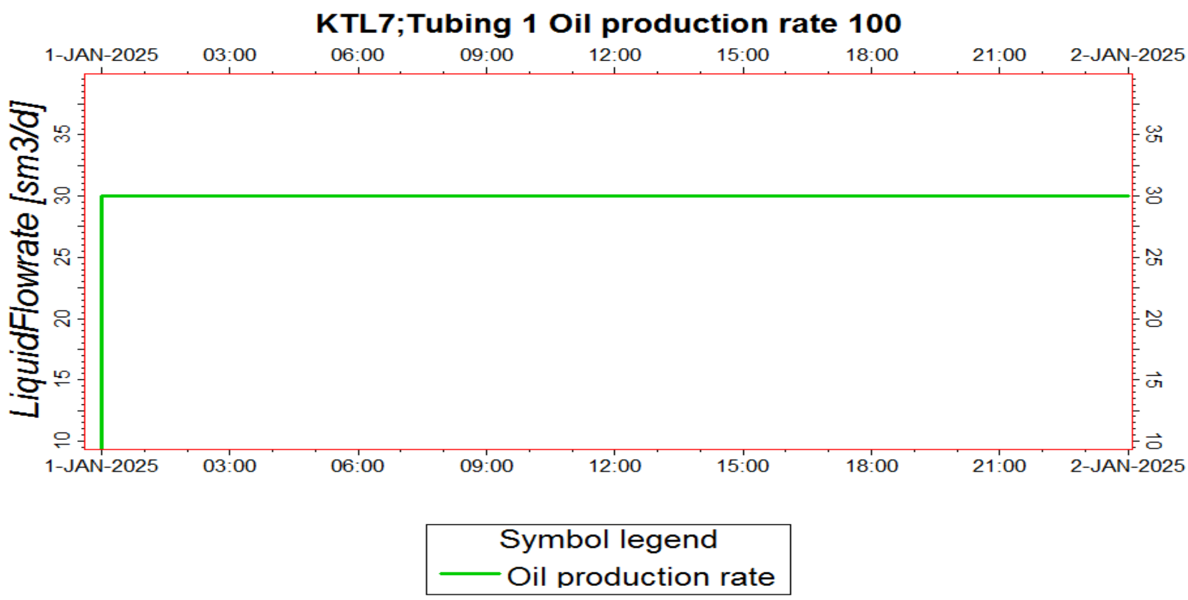

Figure 4.33: Simulated flow profile of reservoir model

4.2.8 Oil Reserve Estimation (KTL)

Oil reserve estimation is crucial task in oil and gas industries as oil reservoir development decision is totally depend on the oil reserve in the field. Authentic data of reservoir structure, fluid contact, saturation provides reliable oil reserve of less uncertainty and risk. In the Kailashtila field oil reservoir has been detected from well logs and DST which is reliable information. 3D seismic survey needs to be conducted to delineate the oil reservoir structure properly. Then estimated oil reserve will be accurate. In this case upper sand structure and boundaries has been used to delineate the oil reservoir structure of Kailashtila field. Here an analogy has been used that, in Bangladesh many fields have sand layers where upper gas sand and lower gas sand have the same structure and boundaries such as Titas Gas Field and Haripur Gas Field. On the basis of this analogy a reservoir model has been developed as shown in figure 4.34 and oil reserve has been estimated as following:

- Bulk Volume is 6165 million rm^3
- Net Volume 4974 million rm^3
- Pore Volume 402 million rm^3
- Hydrocarbon Pore Volume for Oil 15 million rm^3 (94.33 million RB)
- Stock Tank Oil Initially in Place 15 million sm^3 (94.33 million STB)

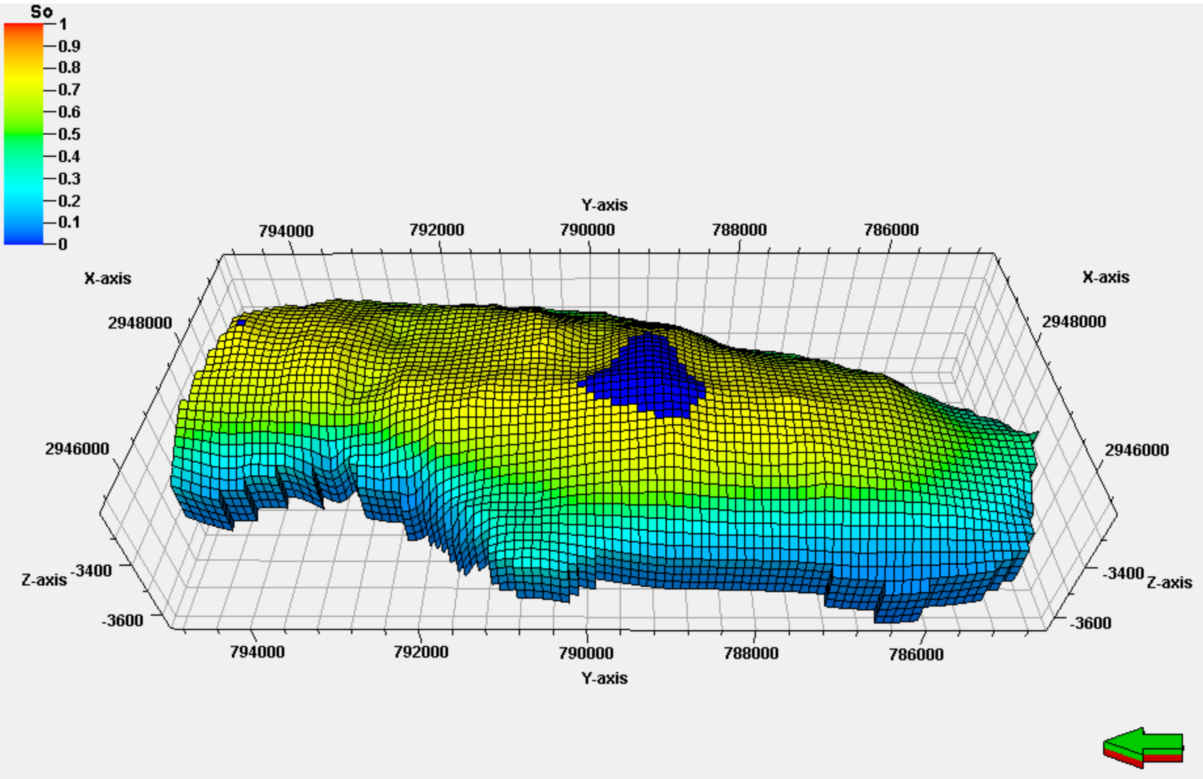

Figure 4.34: Oil saturation

4.2.9 Dynamic Characterization of Oil Reservoir (KTL)

DST operation has been performed on well no KTL-7 for 125 minutes with average liquid flow rate was 338 sm^3/day. Model well of KTL-7 has been placed in the reservoir model as shown in figure 4.35. Reservoir model has been simulated according to the DST. Dynamic characters of the reservoir such as well hydraulic connectivity, oil flow rate, oil flow direction, oil flow time, water flow rate have been evaluated for dynamic characterization of oil reservoir.

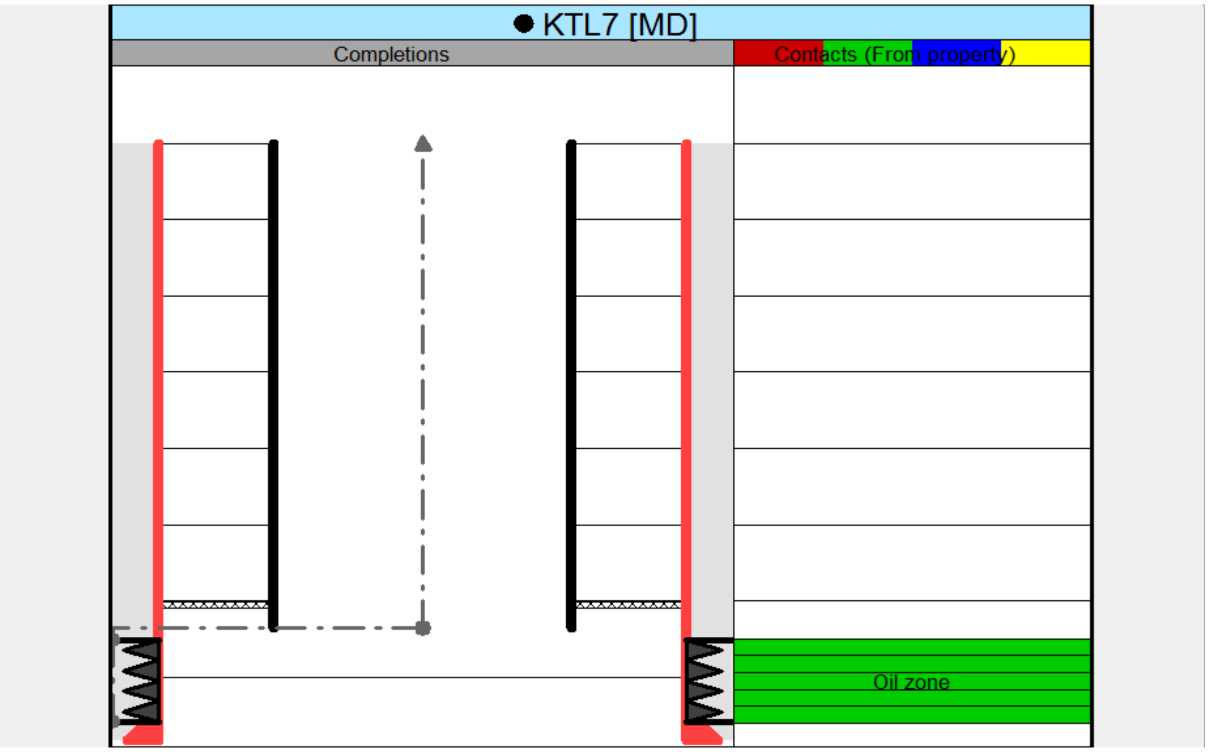

Figure 4.35: Well configuration

Hydraulic conductivity of well (KTL-7) with reservoir during DST has shown in figure 4.36. The well is able to establish a large drainage area in reservoir during the test. The well is good connected with reservoir hydraulically.

Streamline flux of oil production has shown in figure 4.37. Maximum oil production rate is 0.1 stb/day through the pore space. A good flux of oil flow pattern has been developed. Most of the oil is flowing toward the production well (KTL-7) from all parts of the reservoir as shown in figure 4.38. Oil flow direction is perfect as reservoir experts are expected. Reservoir has delivered minimum amount of water as shown in figure 4.39. Experts of oil and gas industries are expecting to produce no water from field. Here reservoir has fulfilled their expectation in terms of water production.

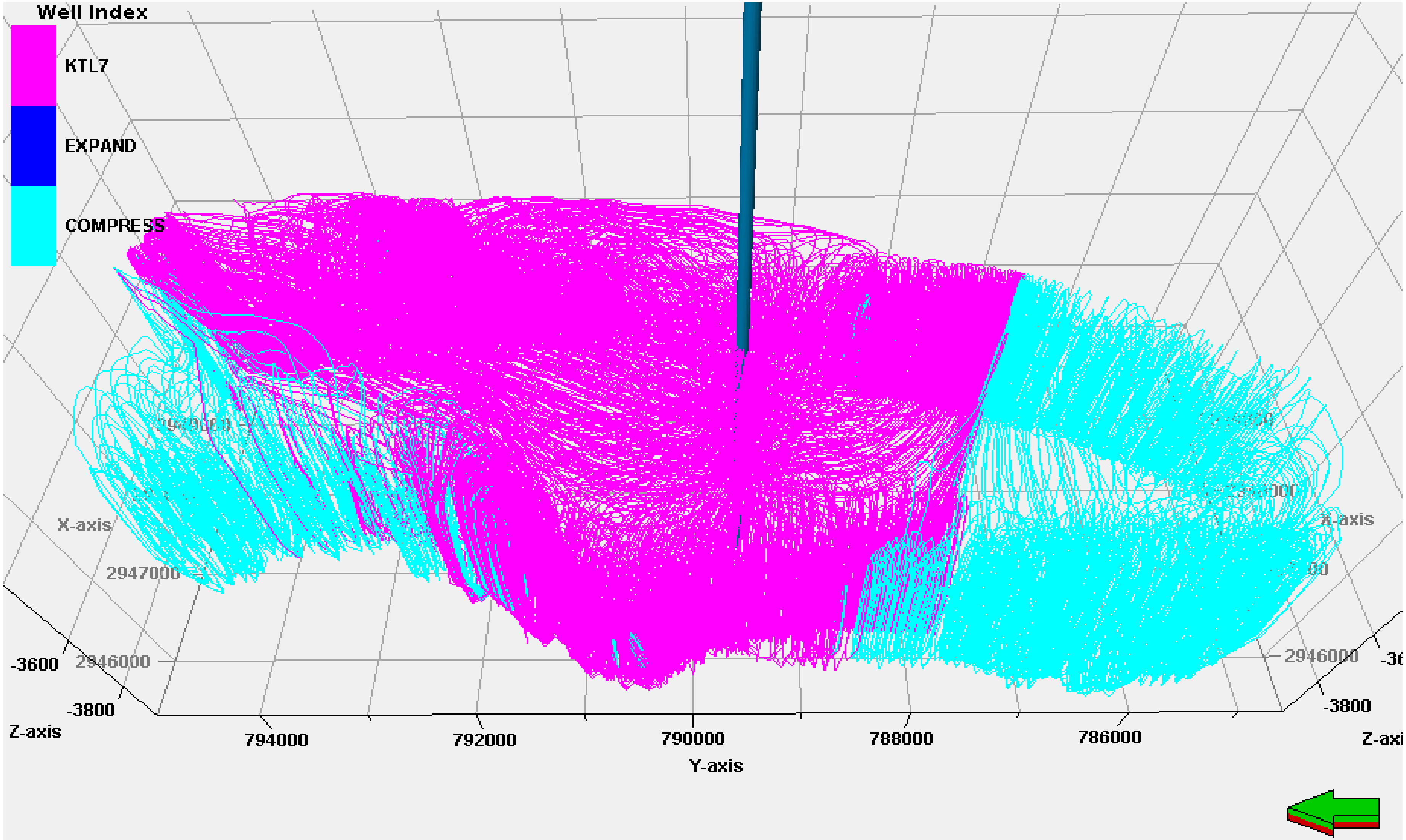

Figure 4.36: Well hydraulic connectivity with reservoir

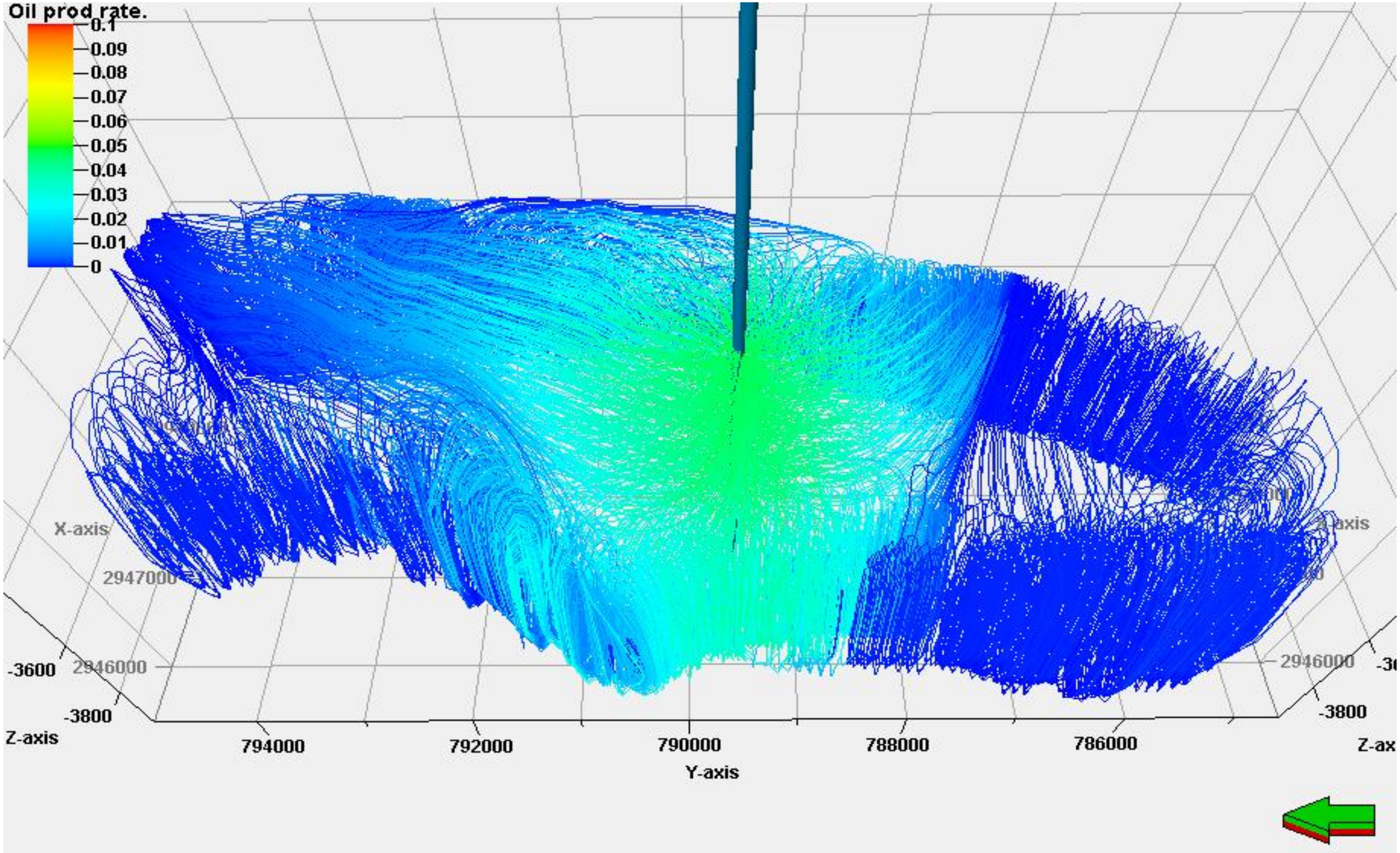

Figure 4.37: Oil production rate

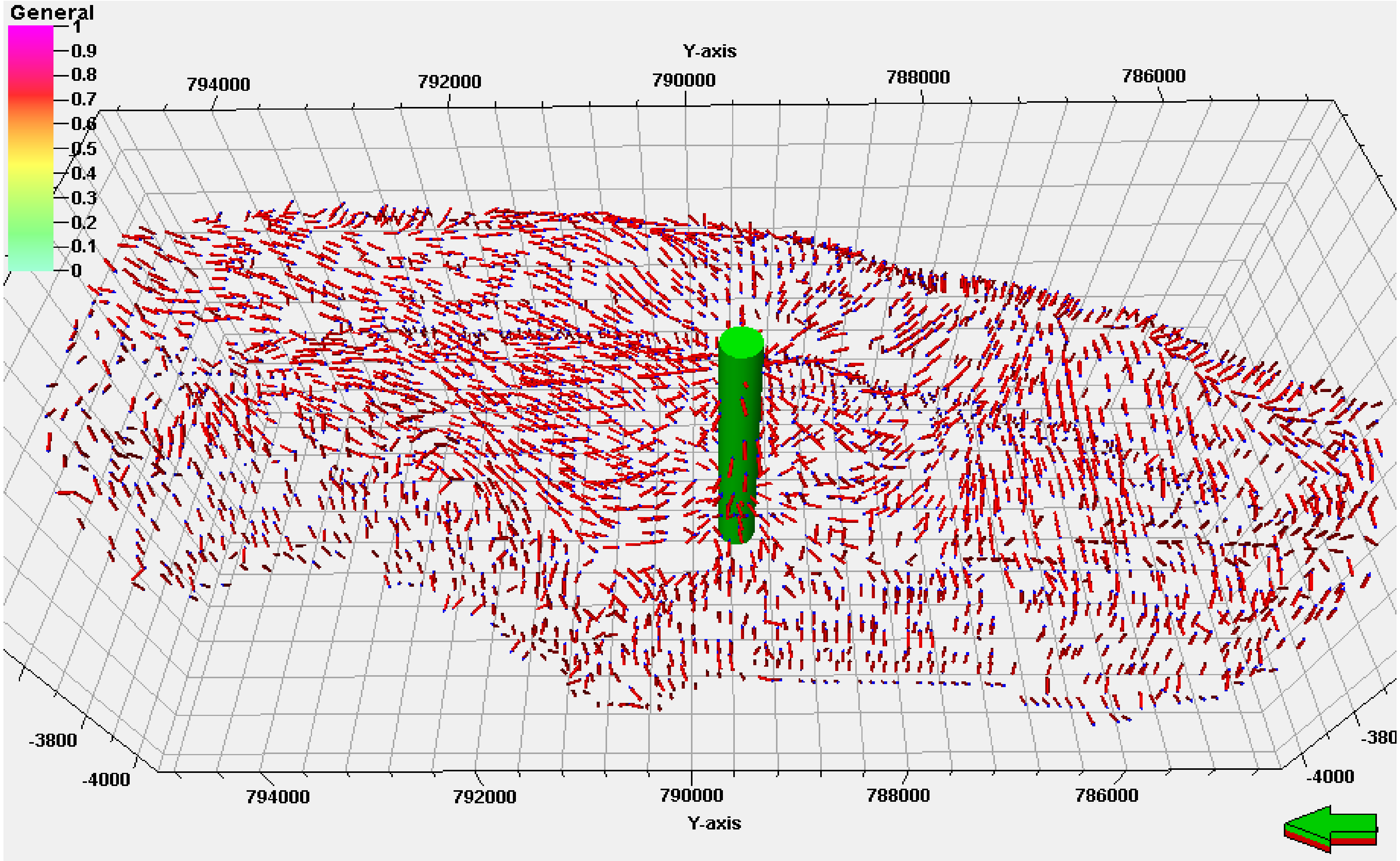

Figure 4.38: Oil flow direction

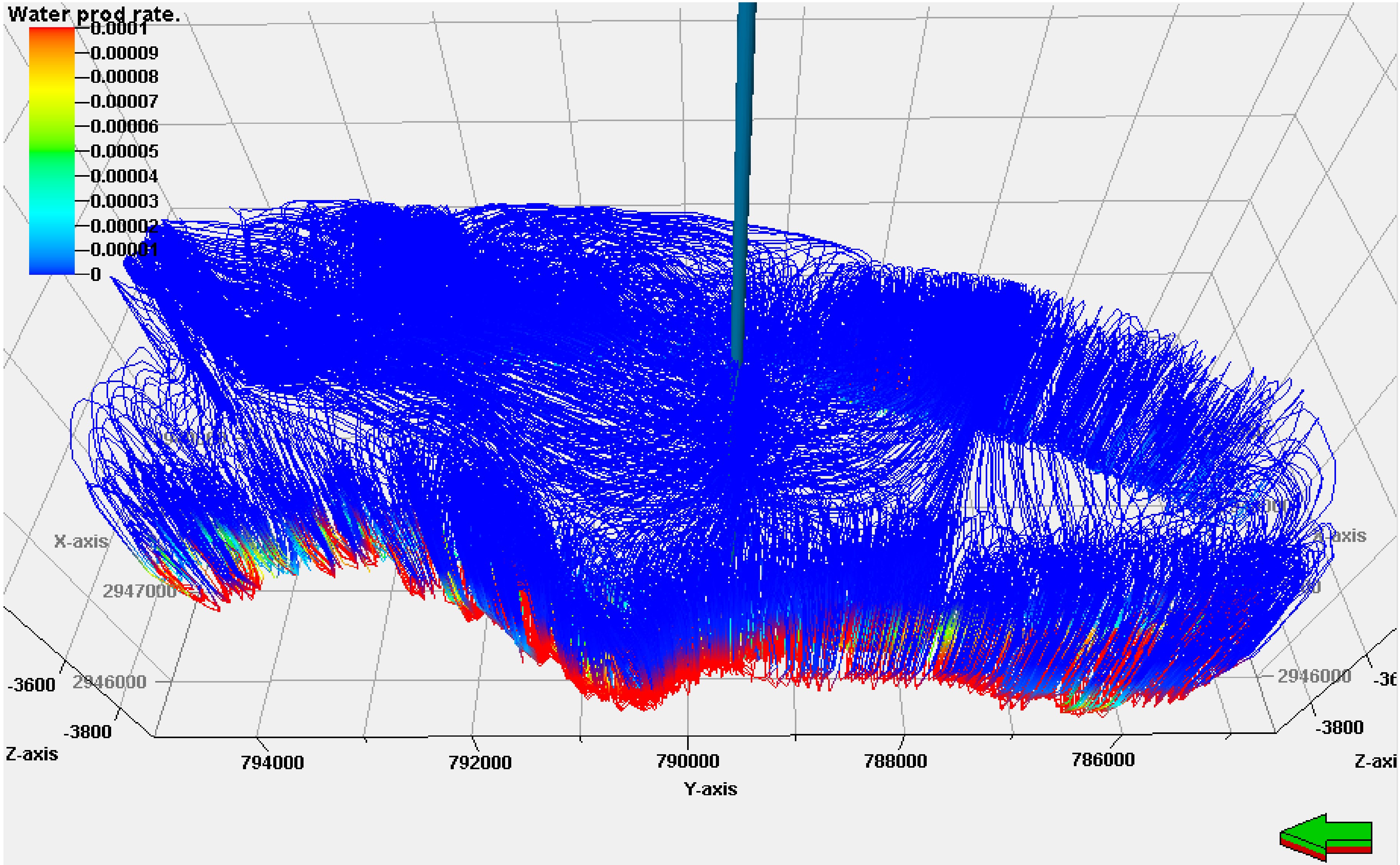

Figure 4.39: Water production rate

4.3 Designing of Oil Recovery Technique (KTL)

According to the oil recovery practices used in oil and gas industries, the oil reservoir is depleted by natural reservoir pressure energy as primary recovery technique (Figure 4.40). After natural depletion, enhanced recoveries are applied as secondary and tertiary phases. During primary recovery stage no external fluid is injected into the reservoir and no chemical is used to release trapped oil or change oil properties such as oil viscosity.

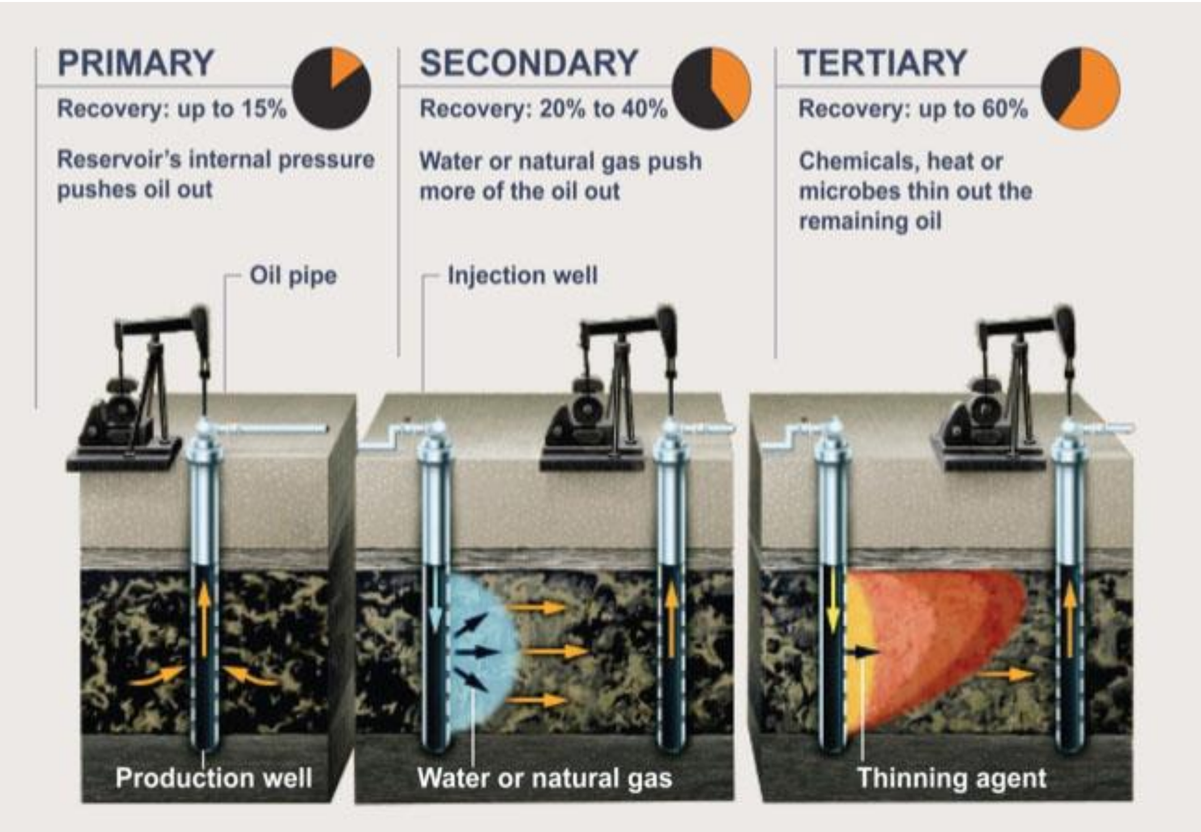

Figure 4.40: Oil recovery methods

At the secondary stage water or gas is injected to increase the reservoir pressure to lift oil to surface. At tertiary stage chemical such alkali, polymer and microorganisms are injected into the reservoir to change the oil properties which are favorable to oil flow. Oil reservoir in Kailashtila field has good enough pressure to lift the oil to surface which has been observed during the drill stem test operation. The reservoir is able to deliver maximum liquid at the rate of 2500 sm^3/day (15723 STB/D). Now it is recommended that the oil reservoir will be developed by natural depletion method. Oil production well will be drilled in the reservoir in a suitable place where well is able to establish maximum drainage area in the reservoir and able to deliver oil with maximum flow rate.

4.3.1 Screening of Oil Reservoir (KTL)

Oil reservoir is screened to design enhanced oil recovery (EOR) technique. International standard oil reservoir screening process is shown in table 4.5. At this moment natural depletion is recommended for oil reservoir in Kailashtila field. After the natural depletion the well will be screened by the process for designing enhanced oil recovery.

Table 4.5: Screening criteria for selecting of EOR candidates

	Chemical Flooding Processes				Miscible Processes	Thermal Processes	
Screening Parameters	Units	Surfactant	polymer	Alkaline	Carbon Dioxide	Steam	In Situ Combustion
Oil Gravity	°API	≥ 25	-	≤ 35	≥ 27	≤ 25	≤ 25
Oil Viscosity (μ)	Cp	≤ 30	≤ 200	≤ 200	≤ 10	≥ 20	≥ 20
Depth (D)	Feet	-	-	-	>2,300	>200< 5000	>5,000
Zone Thickness (h)	Feet	-	-	-	-	>20	>10
Temperature	°F	≤ 250	≤ 200	≤ 200	<250	-	-
Permeability, Average ($\bar{K}$)	md	≥ 20	≥ 20	≥ 20	-	-	-
Transmissibility (Kh/μ)	md-ft/Cp	-	-	-	-	100	20
Salinity of formation brine(TDS)	ppm	$\leq 200{,}000$	-	-	-	-	-
Minimum Oil Saturation at start of process	-						
In water-swept Zones(S_{orw})	fraction	≥ 20	-	-	-	-	-
Mobile(S_{or}-S_{orw})	fraction	-	≥ 10		-	-	-
Minimum Oil Content at start of process(S_{or})	B/AF	-	-	-	-	>500	>500
Rock type	-	Sandstone	-	Sandstone	Sandstone or Carbonate	Sandstone or Carbonate	Sandstone

4.3.2 Optimization of Oil Recovery Technique

It is recommended that oil will be recovered by natural depletion method by using reservoir pressure energy as the reservoir has good pressure energy which has been shown by reservoir during DST operation. Reservoir pressure is shown in figure 4.41 and oil saturation is shown in figure 4.42. Reservoir development variable such as well placement, number of wells, oil production rate will be optimized.

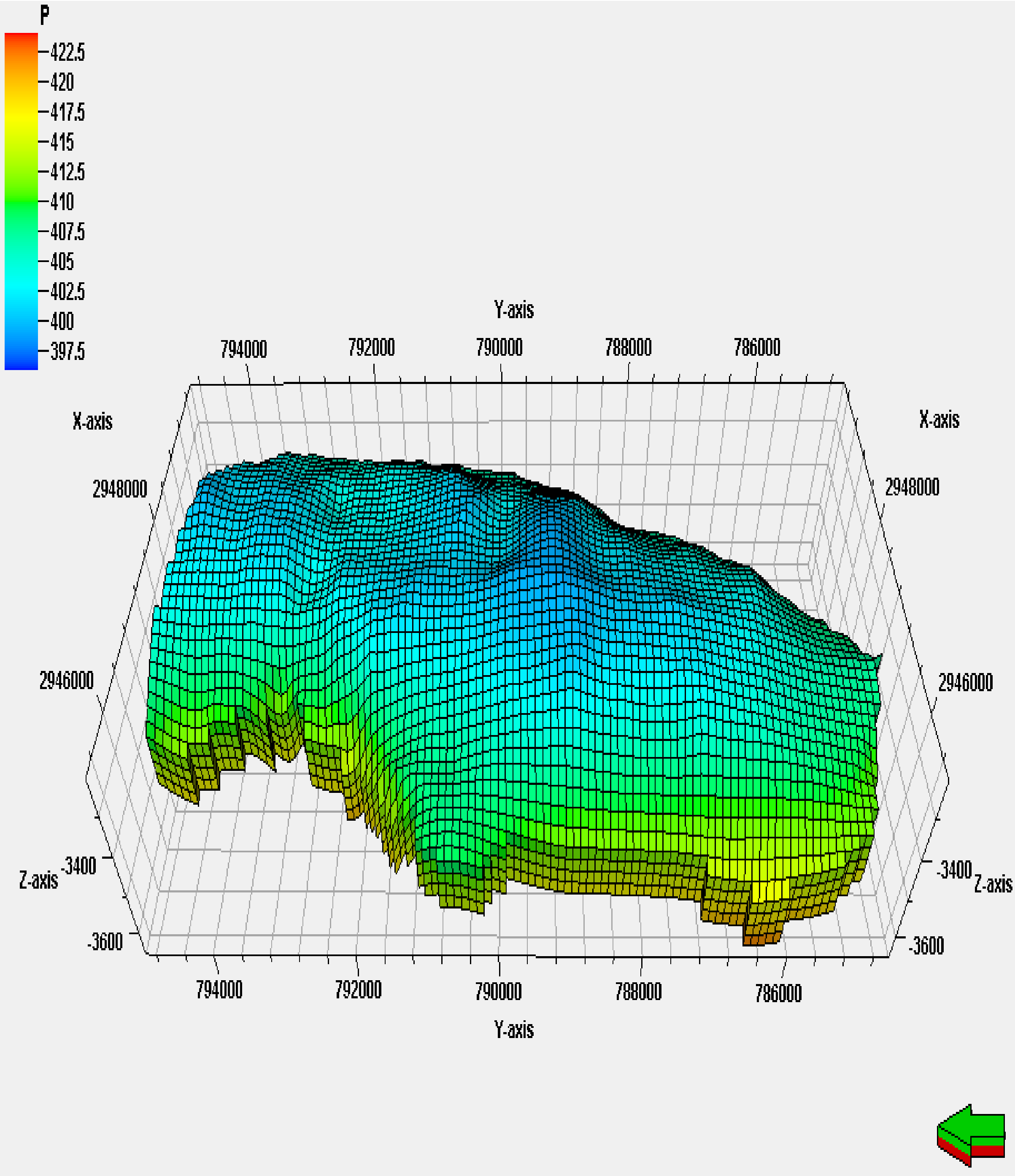

Figure 4.41: Reservoir pressure

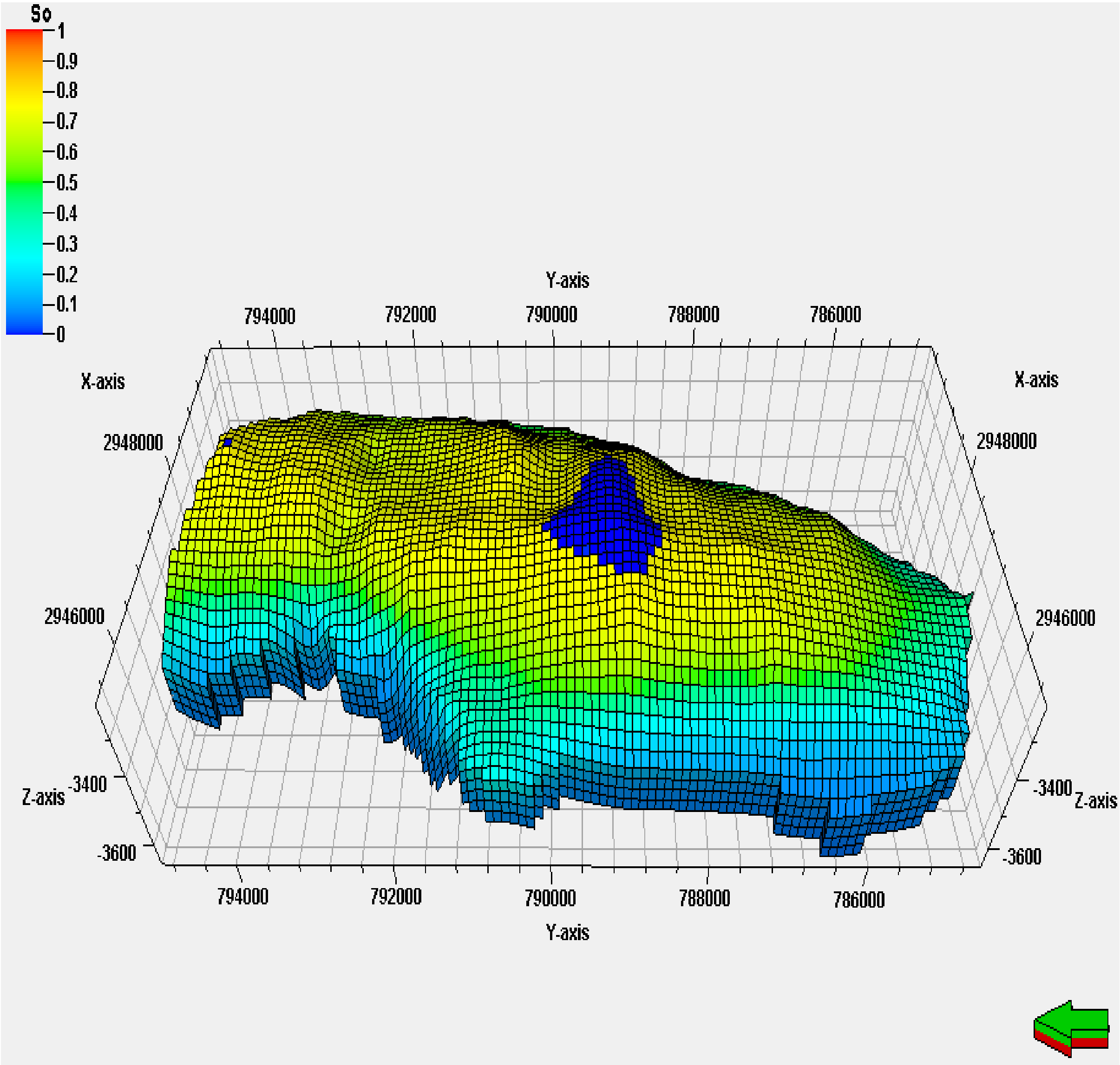

Figure 4.42: Oil saturation

4.4 Generation of Oil Reservoir Development Scenario (KTL)

There are many reservoir development scenario that can be generated using different reservoir development variables. Oil and gas industries use common reservoir development variables as follows:-

- Number of oil production wells
- Mutual positions of the oil production wells
- Oil production rate and tube head pressure
- Number of water/gas injection wells
- Mutual positions of the water/gas injection wells
- Water/gas injection rate and pressure
- Alkali/polymer/surfactant ratio in water and lean gas/CO_2/N_2 to be injected

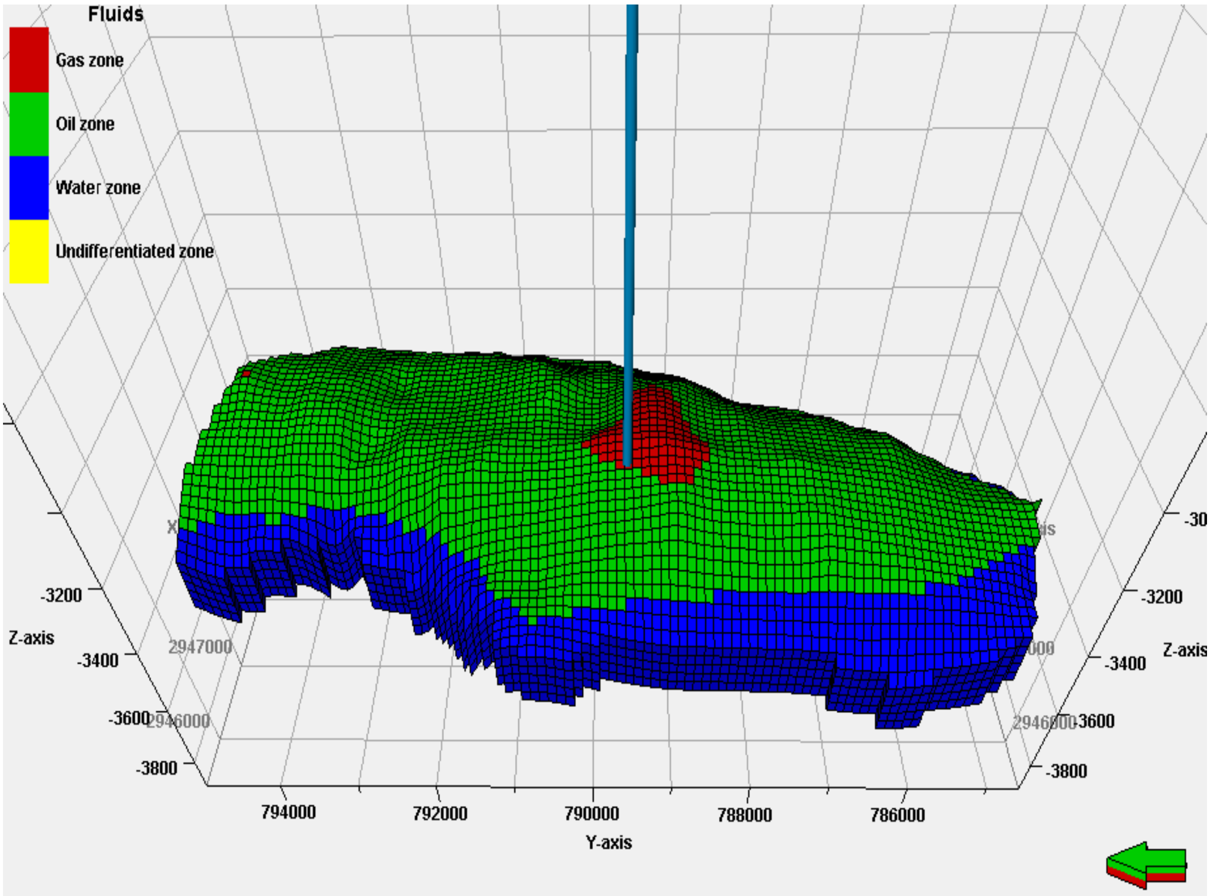

Figure 4.43: Reservoir development scenario

Oil will be recovered by natural depletion by drilling oil production wells. In this case only oil production wells need to be drilled and reservoir development variables include number of oil production wells, oil production rate and tube head pressure. A single well has been proposed in the development scenario. According to the DST, oil production rate is kept 130 sm^3/day (817 STB/D) and minimum well head pressure is maintained at 500 psi. Optimized development scenario is shown in figure 4.43.

4.5 Technical Evaluation of Oil Reservoir Development Scenario (KTL)

In the optimum reservoir development scenario a single well is drilled in center of the oil zone to prolong the oil production time and delay the water breakthrough. The reservoir model with development scenario at Kailashtila field has been simulated for the oil flow of 130 sm^3/day (817 STB/D). Reservoir dynamic performance has been evaluated. Conductivity of well with reservoir is shown in figure 4.44 and oil flow rate is shown in figure 4.45. Reservoir is able to establish good pressure communication with well in the half of the reservoir and good oil flow rate through pore space.

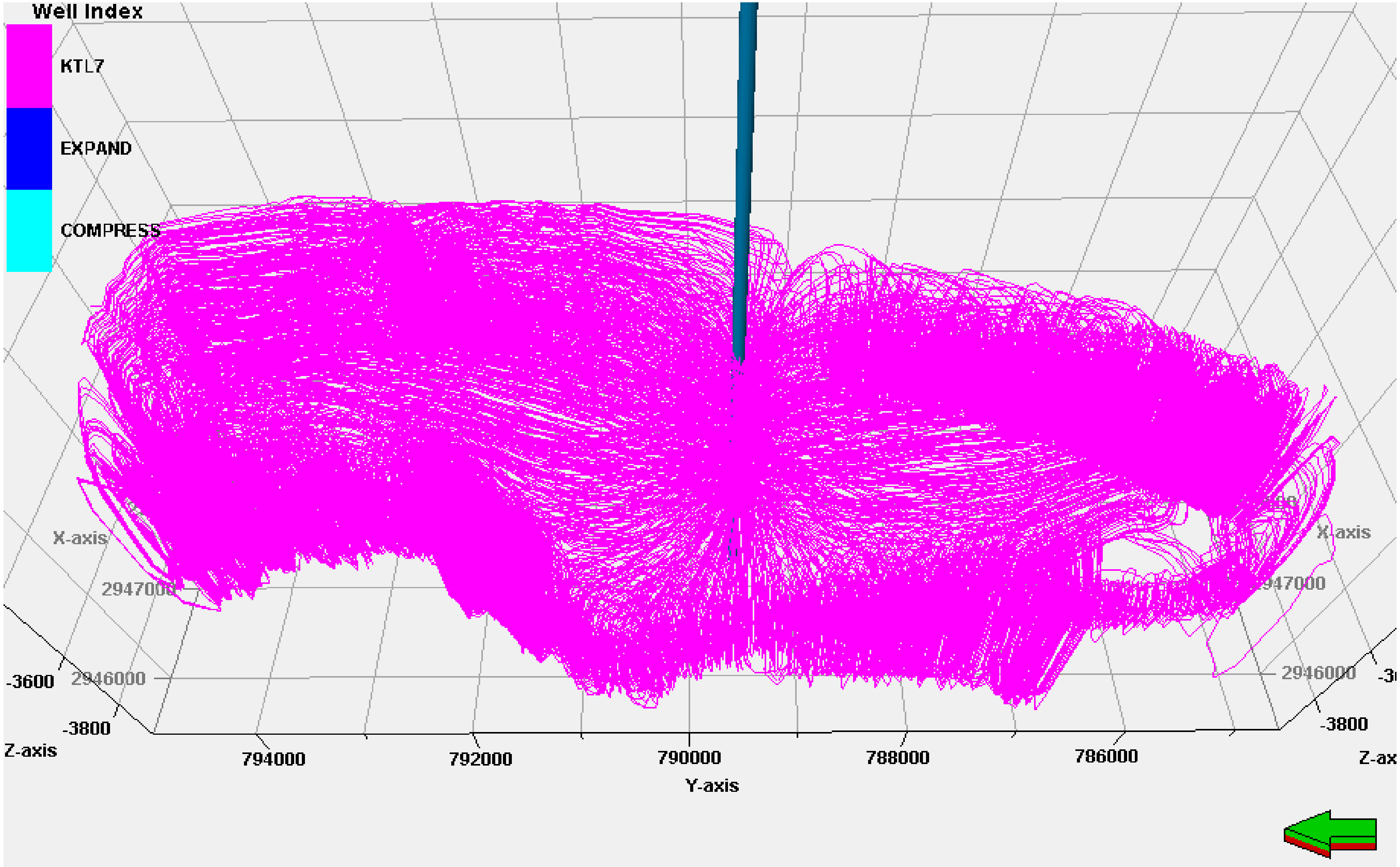

Figure 4.44: Conductivity of well with reservoir

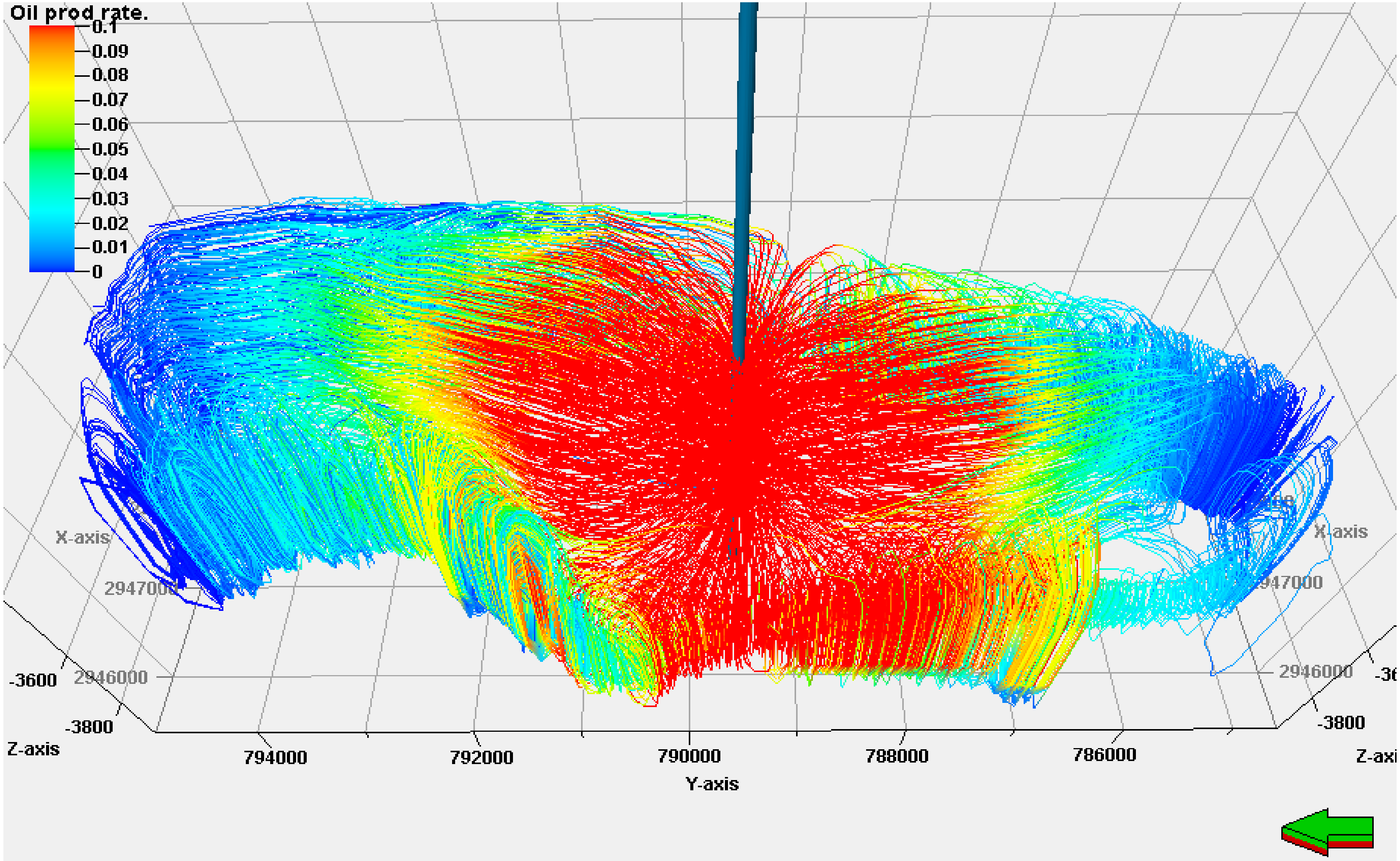

Figure 4.45: Oil production rate

4.6 Oil Reservoir Development Plan (KTL)

The reservoir development scenarios have been technically evaluated by simulating dynamic performance of the oil reservoir. The best performed reservoir model with development scenarios has been considered as oil reservoir development plan as shown in figure 4.46.

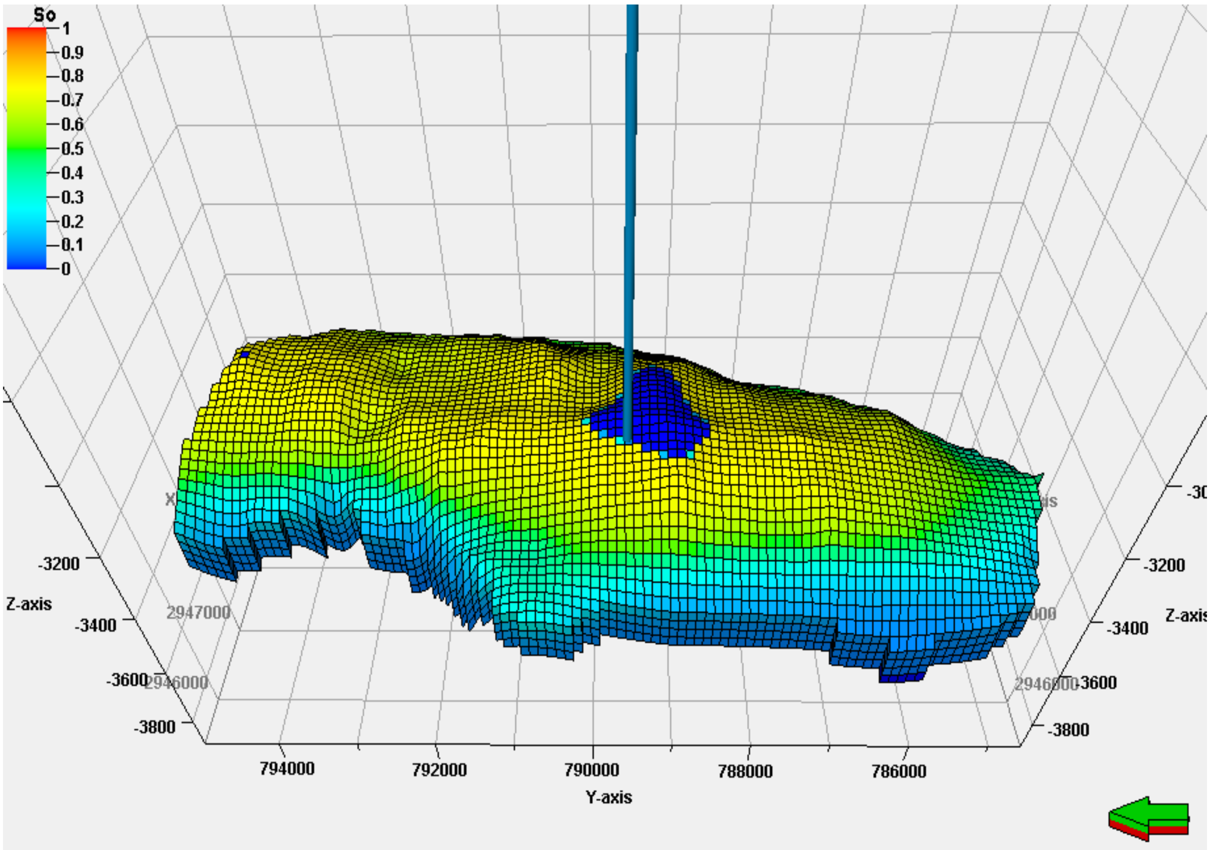

Figure 4.46: Oil reservoir development plan

Oil reservoir development plan in Kailashtila field has following features:-

- A single oil production well at the center of the oil reservoir
- Optimum oil production rate is 130 sm^3/day (817 STB/D)
- Tube head pressure is 500 psi
- Well is able to establish drainage area in half of the reservoir
- Oil production strategy is long term production.
- Pressure maintenance is not required
- Oil production by reservoir own pressure energy
- Oil is recovered by primary recovery mechanism
- Reservoir drive mechanism is solution gas drive

4.7 Oil Reservoir Development Project Management Plan in Kailashtila Field

Once oil reservoir development plan has been finalized then project management plan has to be prepared as per the international oil and gas project management guideline. Project management framework is shown in figure 4.47.

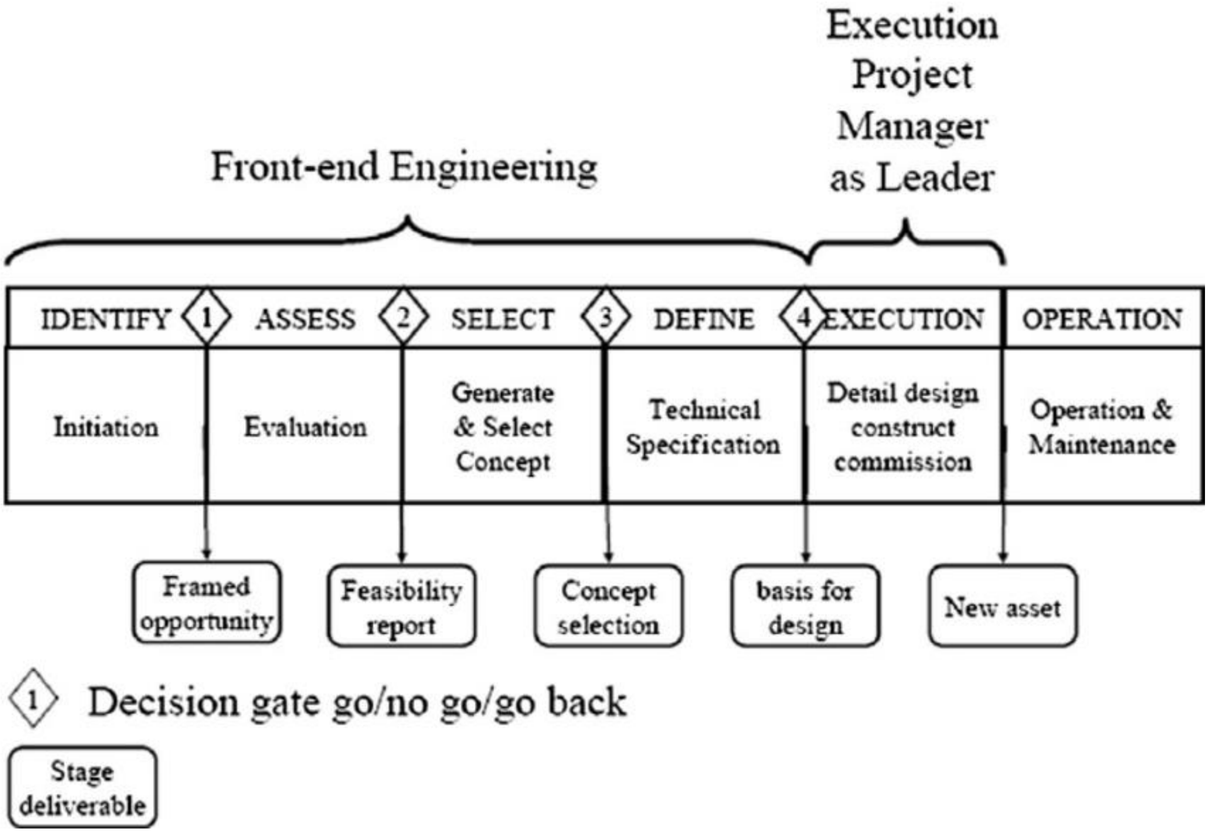

4.47: Project management framework

In addition following engineering reports are to be prepared for project management plan.

- Feasibility Analysis
- Conceptual Planning
- Early Project Planning
- Front-End Loading (FEL)
- Pre-Project Planning (PPP)
- Front-End Engineering Design (FEED)
- Front-End Engineering (FEE)
- Programming/Schematic Design
- Detailed Engineering Design
- Initial Environmental Examination (IEE)
- Environmental Impact Assessment (EIA)
- Environmental Management Plan (EMP)

Finite difference reservoir simulation model (conventional reservoir simulation model) and streamline reservoir simulation model of Kailashtila oil reservoir have been run for 25 years to predict the oil flow rate and tube head pressure declining time. It has been observed that oil flow rate and tube head pressure have started declining after 25 years from the start of production as shown in figure 4.48 and figure 4.49. The oil flow rate has remained constant and tube head pressure has slightly declined for 25 years.

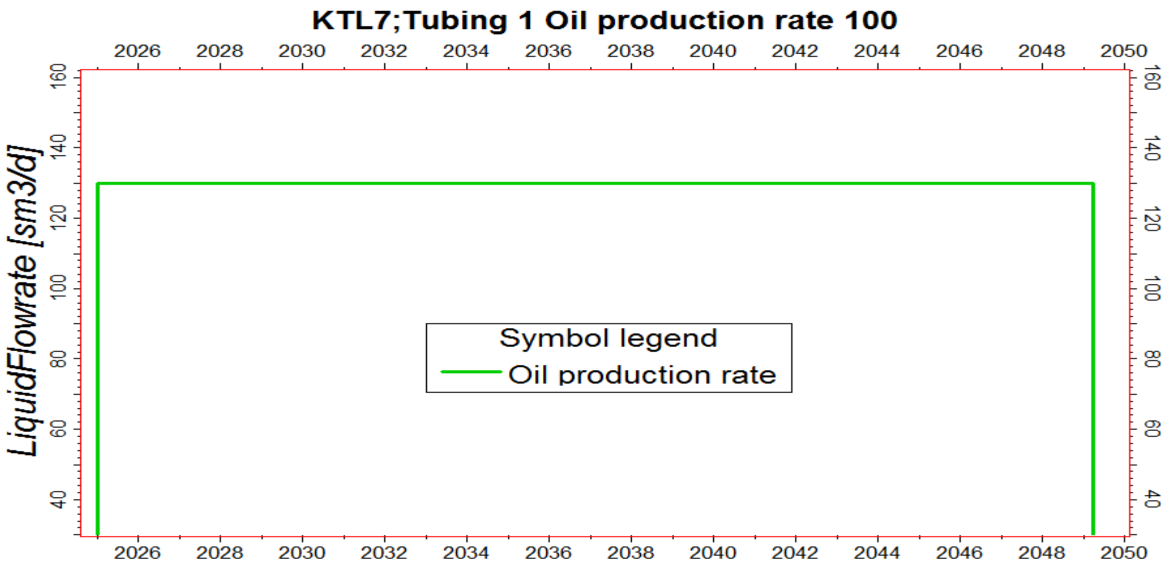

Figure 4.48: Oil flow rate of oil production well

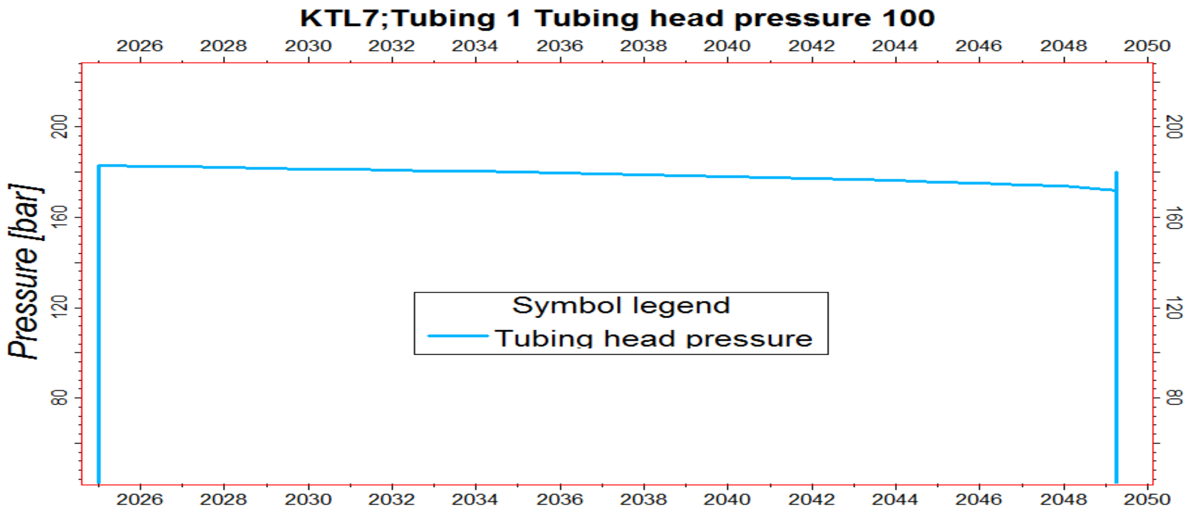

Figure 4.49: Tube head pressure of oil production well

The international oil and gas companies consider 15 to 25 years as commercial project life of oil reservoir development project. Commercial project life of Kailashtila oil reservoir development project has been considered as 20 years.

Chapter 5

Results

5.1 Haripur Oil Field

The validated reservoir model with optimized development option has been simulated for 20 (Twenty) years from 01/01/2027 to 01/01/2047. The results of the simulation along with financial analysis have been presented in this section. Streamline flux of oil flow rate has been generated at the end of 20 years simulation as shown in figure 5.1. Streamline flux density of oil flow rate after 20 years remains the same as the streamline flux density of oil flow rate at the beginning of simulation.

From streamline simulation it is observed that after 20 years of oil production overall average value of oil flow rate has decreased from 0.025 stb/day to 0.015 stb/day as oil relative permeability will be reduced. Oil saturation has been reduced due to oil production. Reduction in oil saturation has reduced oil relative permeability. Oil flow rate has decreased due to the reduction in oil relative permeability. Oil flow rate has become zero near the injection wells as injected water has advanced toward the production wells and swept entire oil. Oil production is continued by expansion of reservoir oil and sweeping by injected water.

Streamline flux of water flow rate between production wells and injection wells has been generated at the end of 20 years simulation as shown in figure 5.2. Injected water has not developed any channel to flow directly to production wells. Water breakthrough has not occurred yet. The entire injected water has taken part to sweep oil to production wells.

Oil production rate and tube head pressure of well P1 have been forecasted by the simulation as shown in figure 5.3. Reservoir is able to produce oil at a constant rate of 400 stb/day and able to maintain average well head pressure of 850 psi in the production well P1. Oil production rate remains constant and well head pressure has increased from 785 psi to 875 psi.

Oil production rate and tube head pressure of well P2 have been forecasted by the simulation as shown in figure 5.4. Reservoir is able to produce oil at a constant rate of 400 stb/day and able to maintain average well head pressure of 570 psi in the production well P2. Oil production rate remains constant and well head pressure has increased from 498 psi to 580 psi.

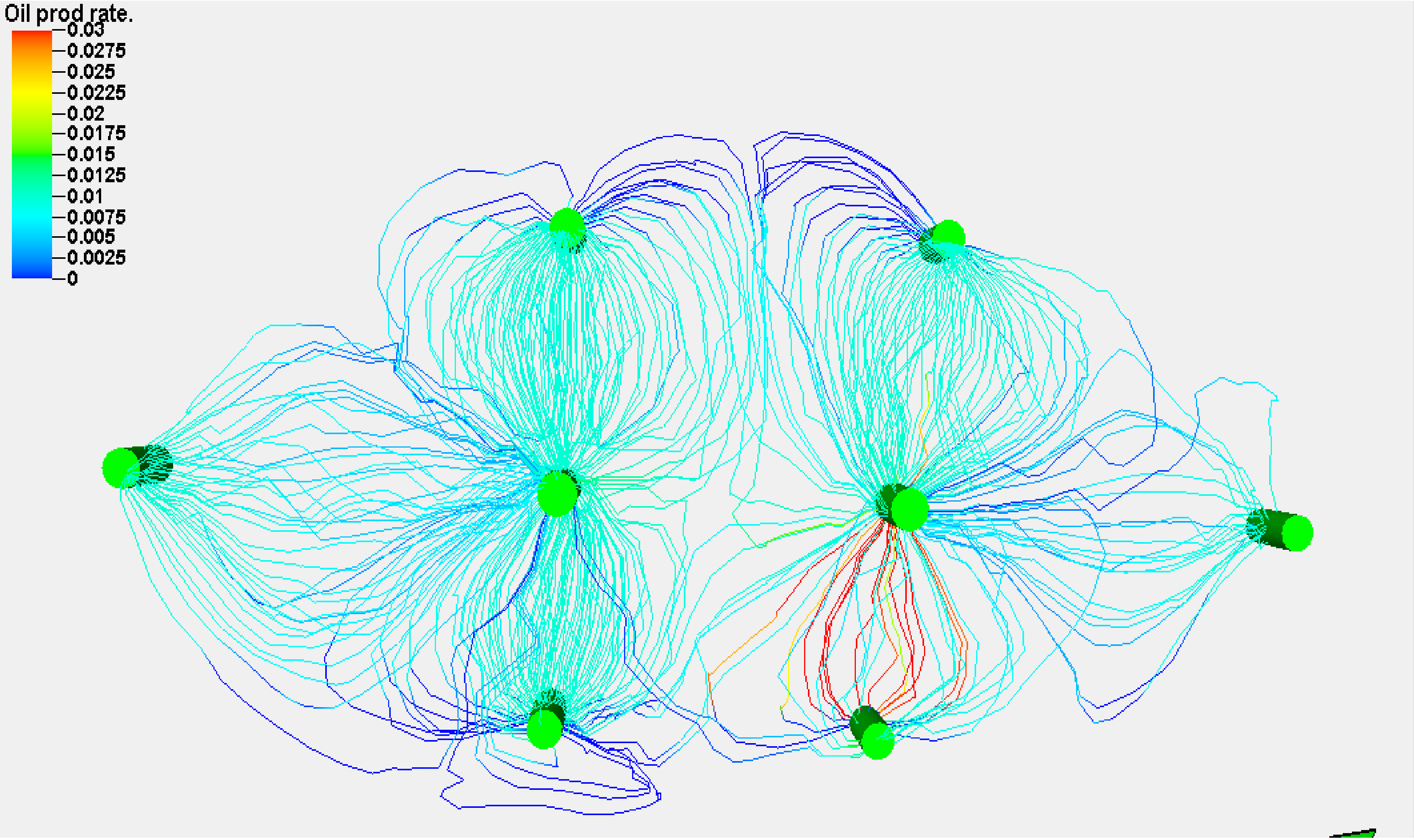

Figure 5.1: Streamline flux pattern of oil flow rate

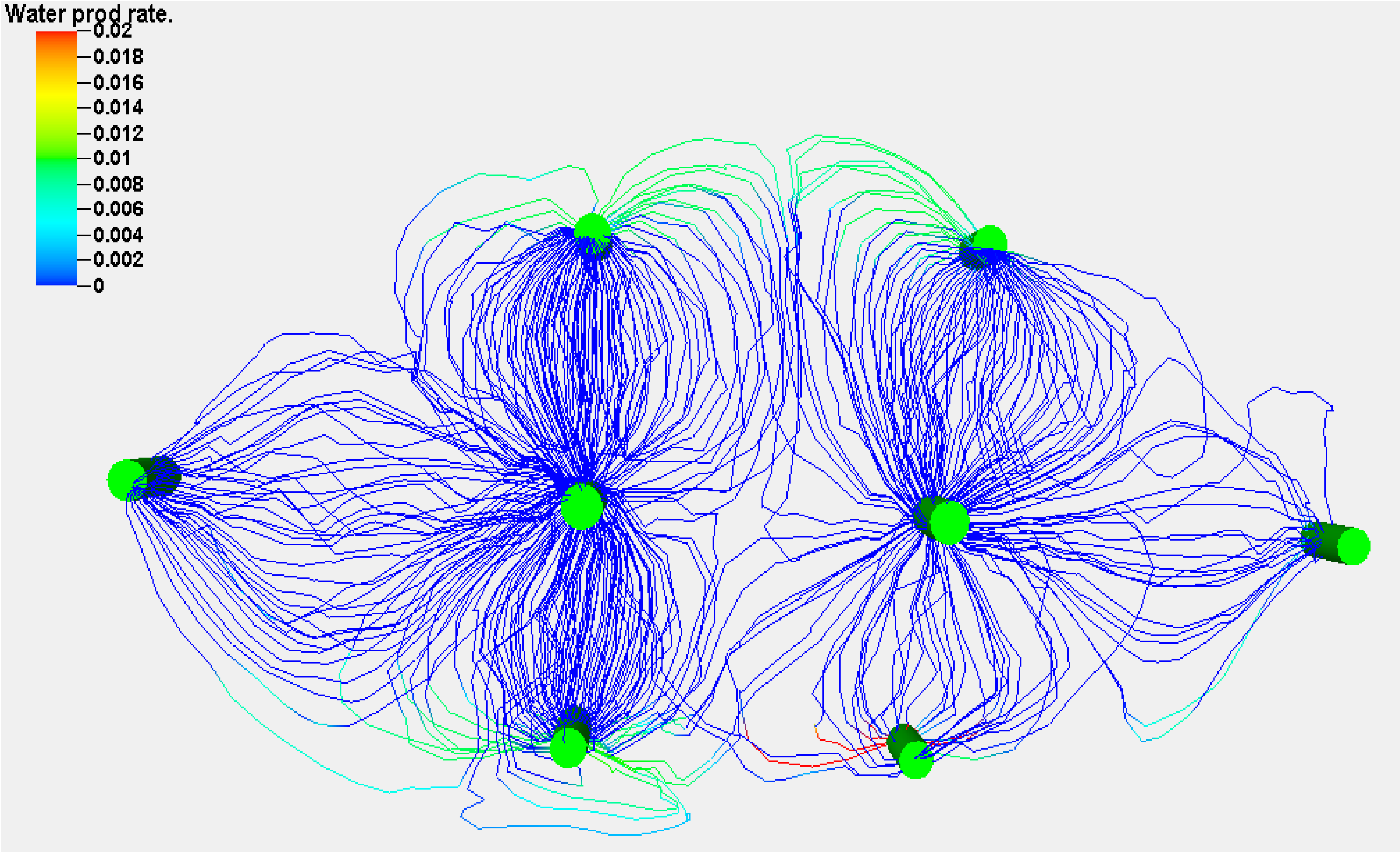

Figure 5.2: Streamline flux pattern of water flow rate

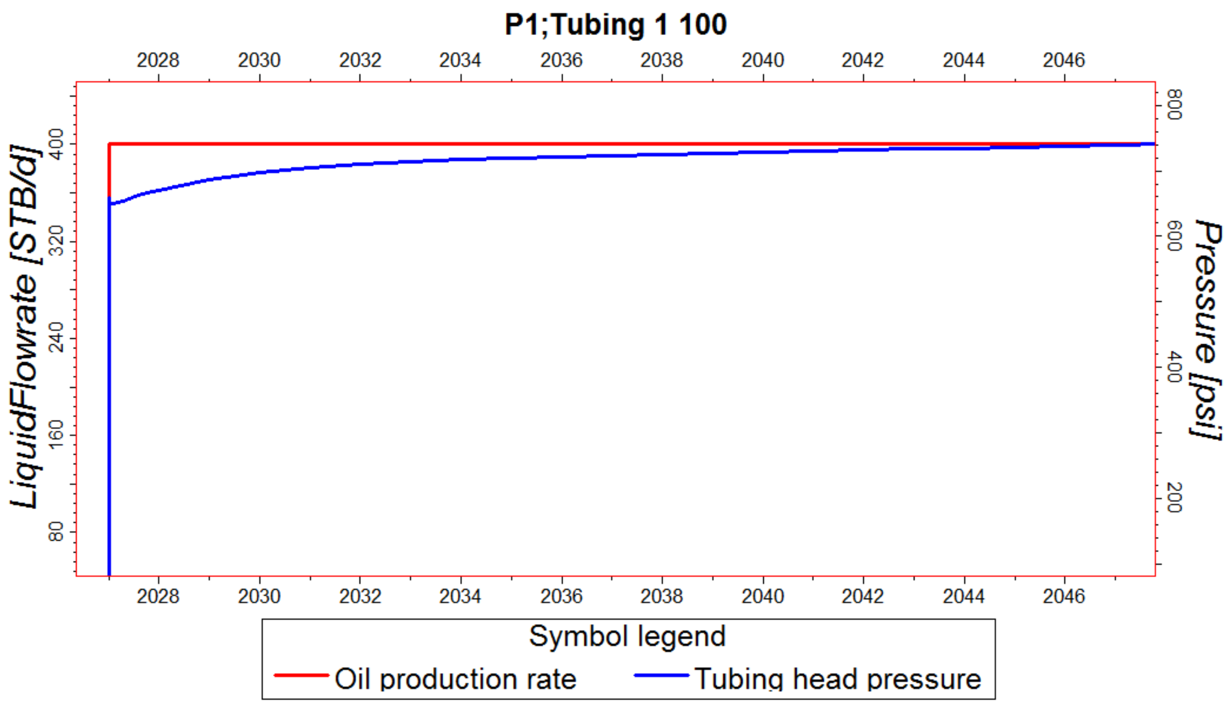

Figure 5.3: Oil production rate and tube head pressure of well no. P1

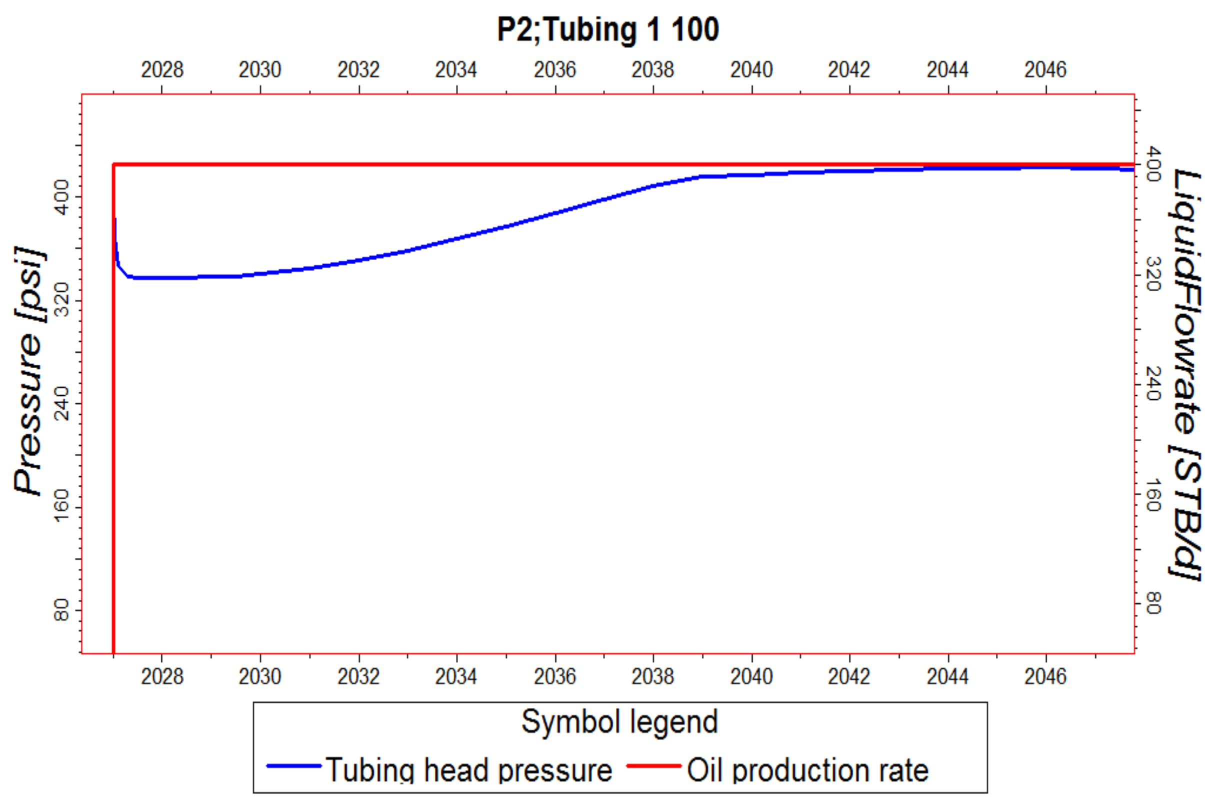

Figure 5.4: Oil production rate and tube head pressure of well no. P2

There are two production wells in this oil field according to the optimized development scenario. These two production wells provide field oil production rate as shown in figure 5.5. Field production rate remains constant at the rate of 800 stb/day.

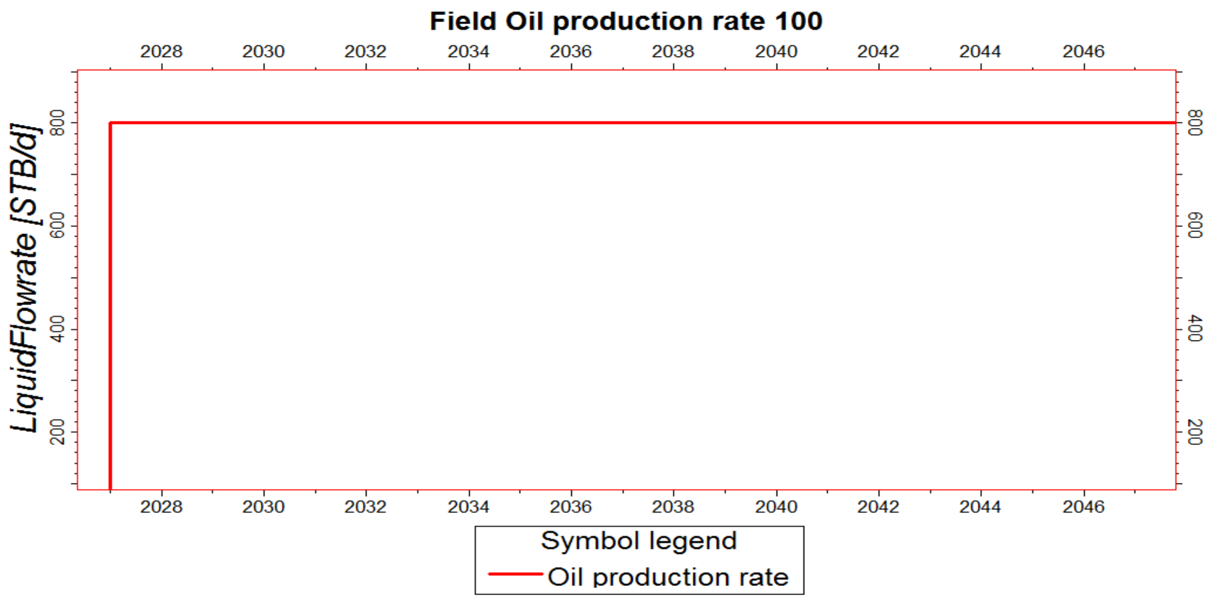

Figure 5.5: Field oil production rate

Under this development program the field is capable of producing 5.844 million barrel oil over the 20 years as shown in figure 5.6. Field cumulative oil production is increasing constantly as field oil production rate remains constant. Field cumulative oil production is rising by 292000 barrel per year.

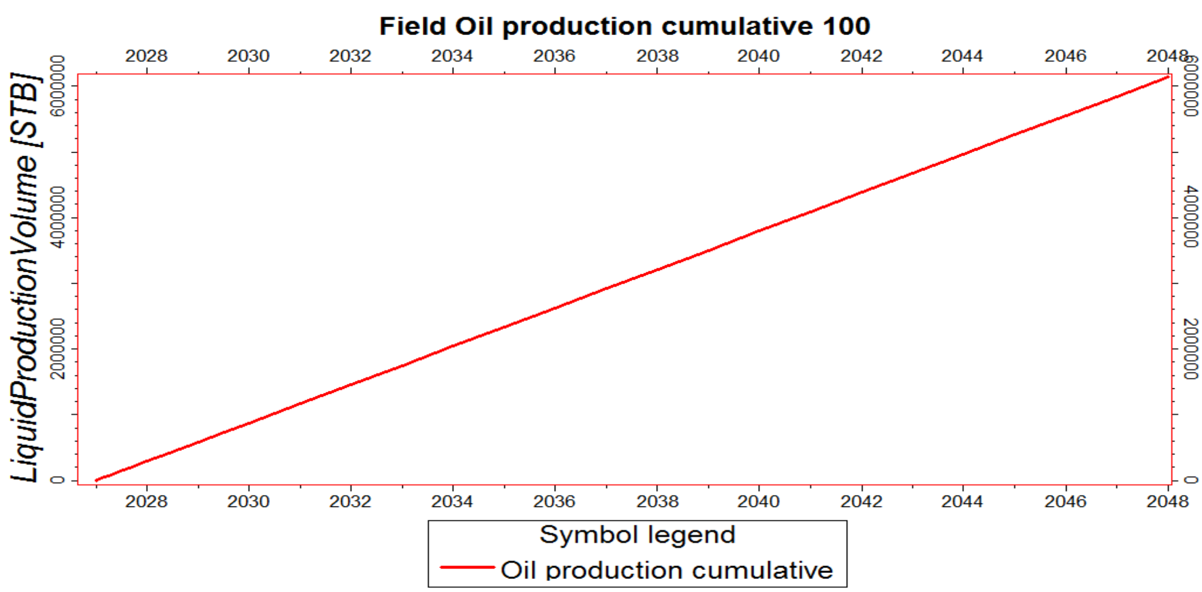

Figure 5.6: Field cumulative oil production

In this development scenario six water injection wells have been proposed. 300 barrels of water per day have been injected by each water injection well during the 20 years simulation. Altogether 1800 barrels of water per day have been injected by all water injection wells as shown in figure 5.7. Field water injection rate is maintained constant to produce oil at a constant rate over the 20 years.

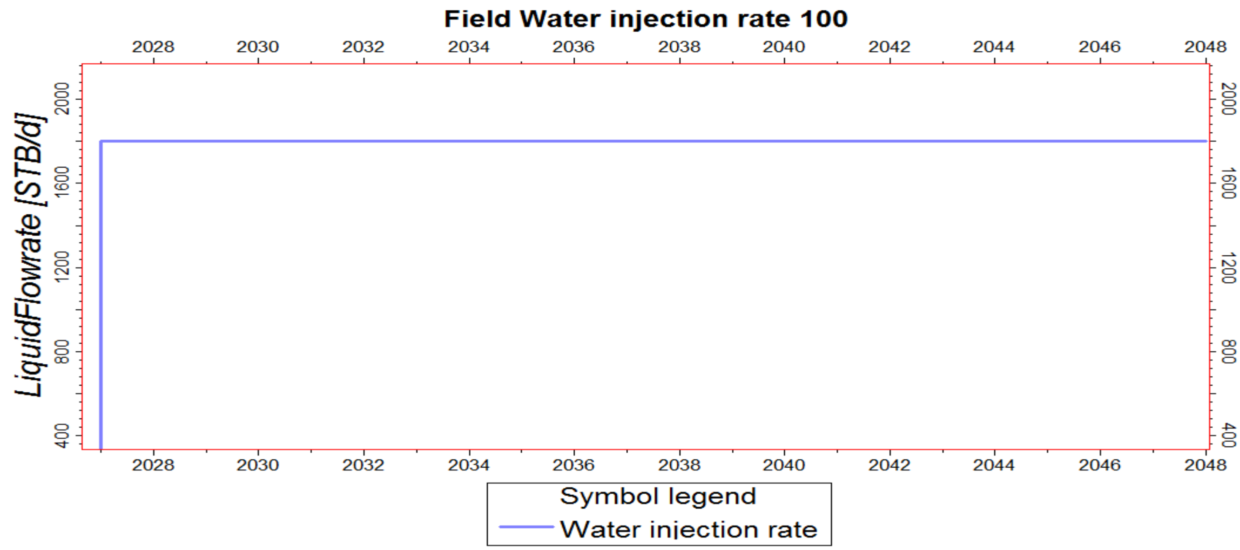

Figure 5.7: Field water injection rate

During the 20 years simulation 13.149 million barrels of water have been injected in the reservoir as shown in figure 5.8. Yearly 657000 barrels of water have been injected against the 292000 barrels of oil production.

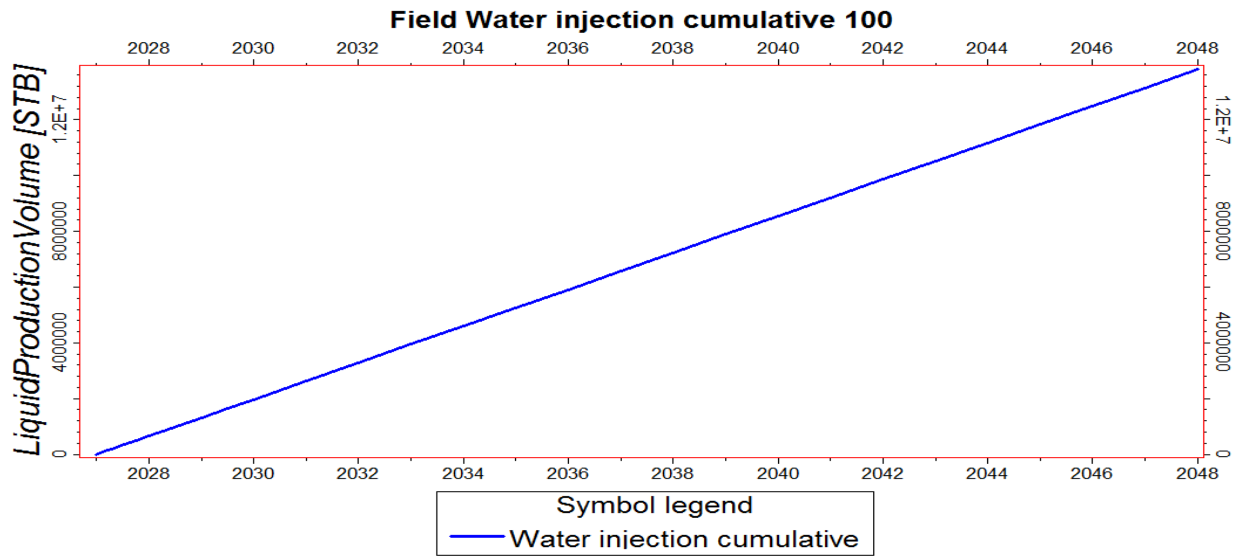

Figure 5.8: Field cumulative water injection

An amount of 0.444 barrel of oil has been produced by injection of 1 barrel of water. According to industrial practice maximum of 7 barrels of water is injected for producing 1 barrel of oil to make project economic viable. In this development project 2.25 barrels of water is injected to produce 1 barrel of oil.

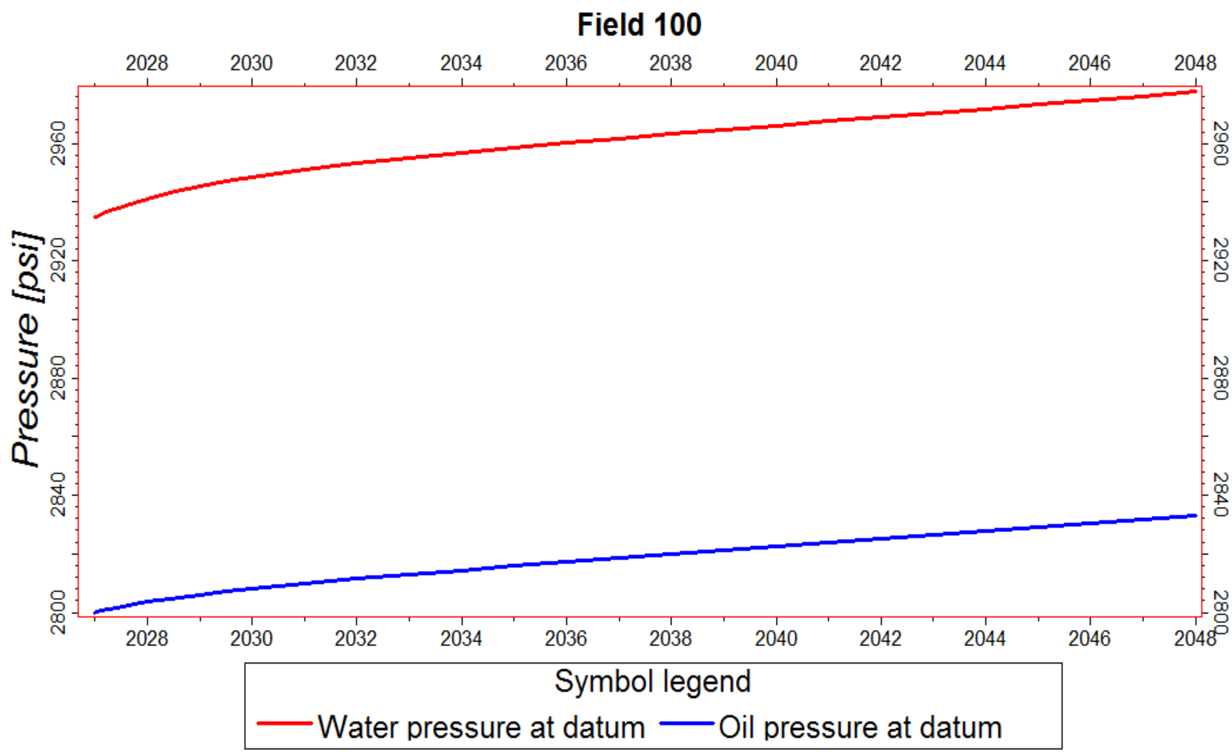

Figure 5.9: Water and oil pressure at bottom hole.

Bottom hole water pressure and bottom hole oil pressure have been simulated for 20 years as shown in figure 5.9. Bottom hole water pressure is rising from 3131.6 psi to 3173.7 psi. Bottom hole oil pressure is also rising from 3000 psi to 3032.92 psi. Pressure difference between water pressure and oil pressure is increasing from 31.6 psi to 40.7 psi. Injected water is increasing the reservoir pressure energy and reservoir is able to lift oil to surface from reservoir.

5.1.1: Economic Analysis of Haripur Oil Reservoir Development

Cost benefit analysis (CBA) has been performed to assess the economic viability of a project on the basis of technical and financial data as shown in table 5.1 and 5.2. Costs and benefits are expressed as far as possible in monetary terms so that they can be compared on an equal level. A project is assessed as economically viable if the project benefits exceed the project costs.

Table 5.1: Oil production rate and revenue

Oil Production Rate per Well	Oil Price	No. of Production Well	Yearly Total Production	Yearly Revenue
STB/Day	USD/STB	No.	STB	USD
400	50	2	292000	14600000

Table 5.2: Water injection rate and cost

Water Injection Rate per Well	No. of Injection Well	Water Injection Cost	Yearly Total Injection	Yearly Injection Cost	Total Capital Expenditure
STB/Day	No.	USD/STB	STB	USD	USD
300	6	1	657000	657000	90,000,000

Total project costs have been estimated as 90 million USD. Major costs components of the project are as following:-

- Drilling and completion of 2 oil production wells
- Drilling and completion of 6 water injection wells
- Surface oil production facilities
- Surface water injection facilities
- Water treatment plant to treat water for injection

Cash flow diagram has been determined on the basis of project expenditure schedule and oil sales revenue schedule as shown in figure 5.10. Total project expenditure (90 million USD) will be utilized within project completion period. Project task and expenditure schedule are shown in table 5.3.

Table 5.3: Gantt chart of oil reservoir development project in Haripur field

No.	**Major Task of Project**	**2022**	**2023**	**2024**	**2025**	**2026**	**Cost Million USD**
01	Drilling and completion of 2 oil production wells (P1 and P2)	↔					20
02	Drilling and completion of 2 water injection wells (I1 and I2)		↔				20
03	Drilling and completion of 2 water injection wells (I3 and I4)			↔			20
04	Drilling and completion of 2 water injection wells (I5 and I6)				↔		20
05	Installation and completion of following systems:- • Surface oil production facilities • Surface water injection facilities • water treatment plant to treat water for injection					↔	10

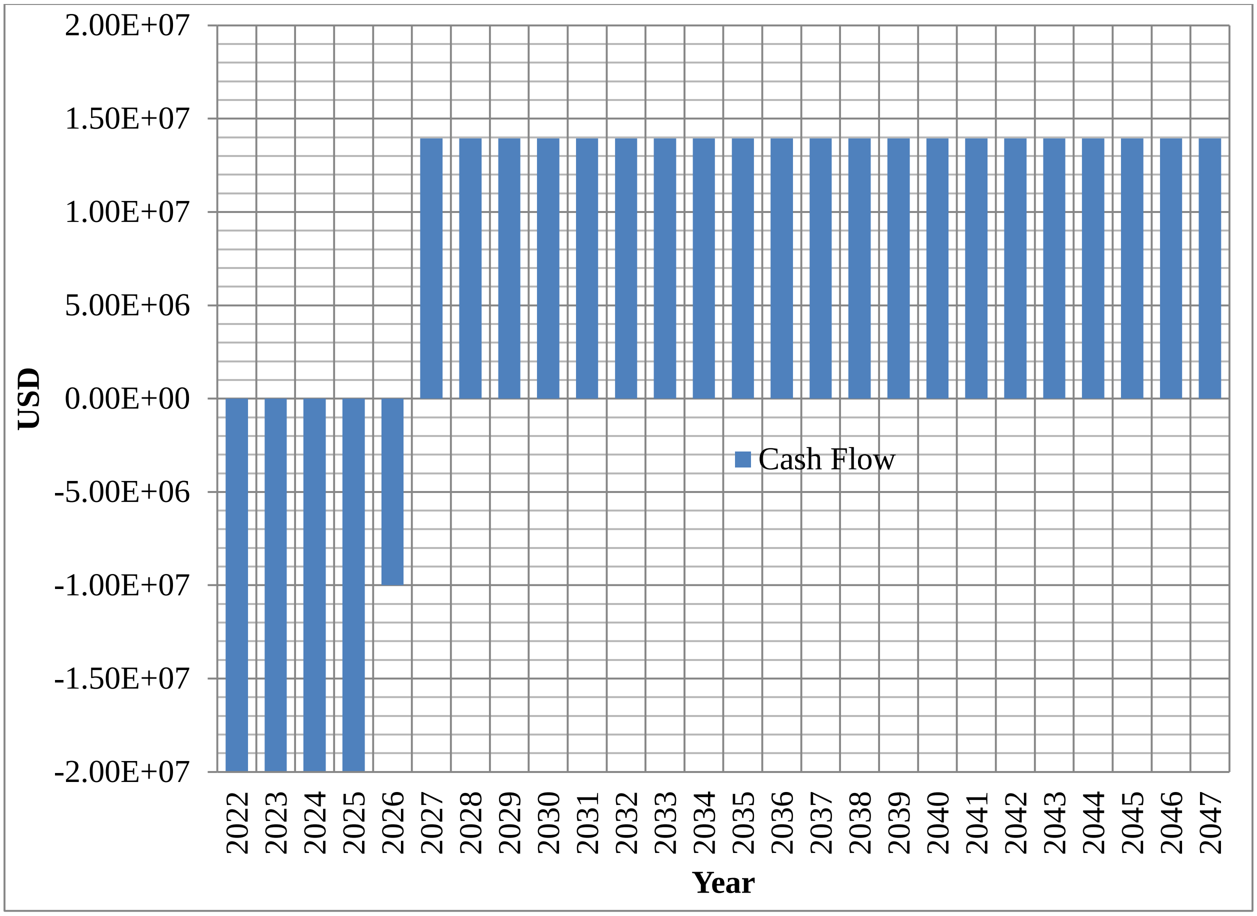

Figure 5.10: Cost and revenue profiles

Net present value (NPV) of the project has been estimated as 5.8 million USD. Net present value has been determined from the project cash flow schedule and 10% discounting rate.

Net present value (NPV) has been estimated on the following assumptions:-

- Discounting rate is 10%.
- Discounting rate includes interest on capital
- Discounting rate also includes inflation
- Uniform cash flow from sales revenue
- Uniform negative cash flow (expenditure)
- Monetary risk factor is considered
- Unavoidable circumstances are considered
- Steady state production operation

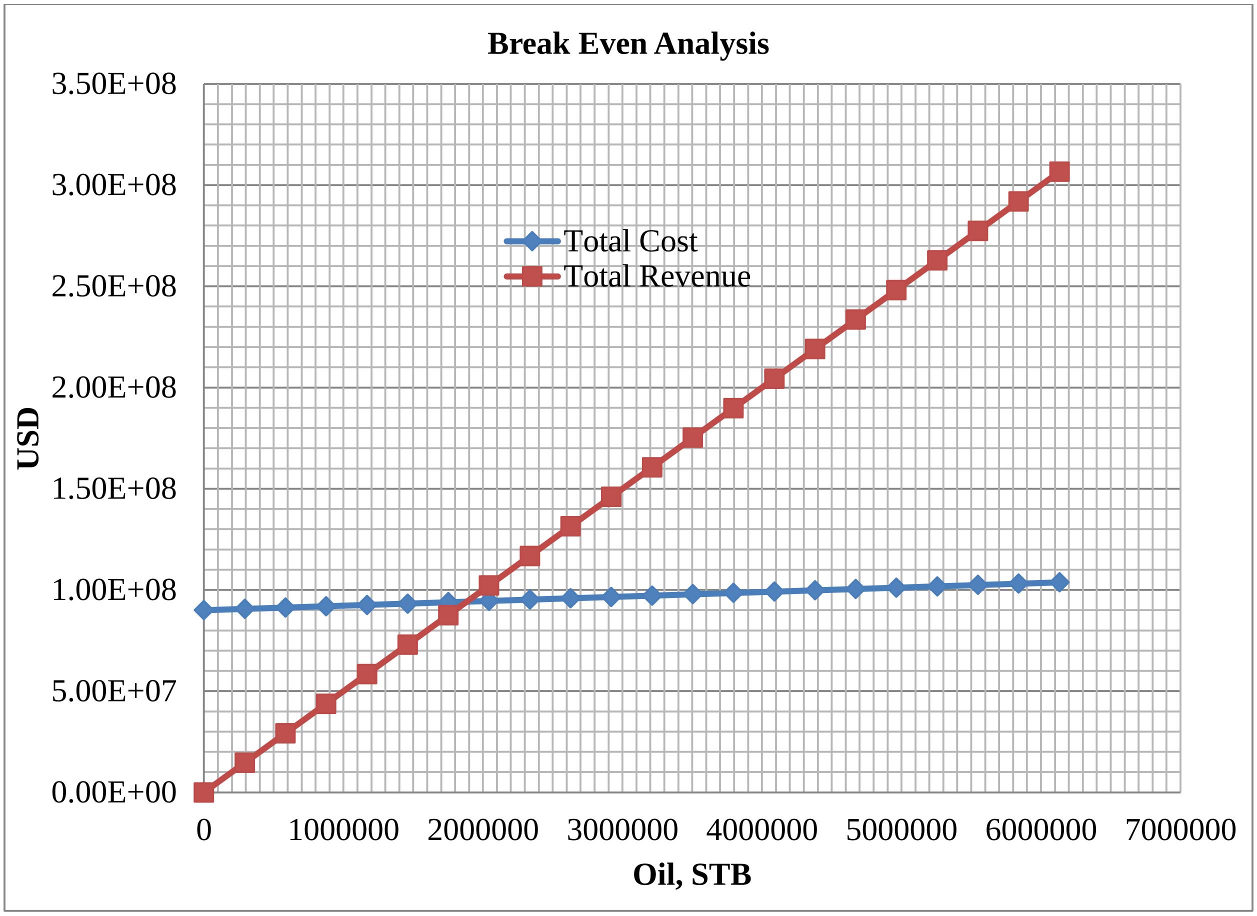

Figure 5.11: Break even analysis

Break even analysis has been performed on the project as shown in figure 5.11. Break even oil production is 2.044 million barrels. The field is able to produce 2.044 million barrels of oil within 6 years. Following assumptions have been considered in break-even analysis.

- Time value of money is not considered
- Interest rate is not considered
- Inflation is not accounted
- Oil price remains constant
- Fixed costs do not vary with time
- Uniform oil sales revenue flow
- Cost and revenue are considered against the oil production
- Contingency cost is included in the total project cost.

5.2 Kailashtila Oil Field

Oil reservoir development plan is evaluated technically and economically. Oil and gas companies expect that the field will produce 15 to 30 years for recovering the capital investment. Oil reservoir development plan has been simulated for 20 years. Simulation result has shown that the reservoir is able to produce oil at the rate of 130 sm^3/day (817 STB/D) constantly for 20 years as shown in figure 5.12 and cumulatively produce 949650 sm^3 (5.973 million STB) of oil as shown in figure 5.13.

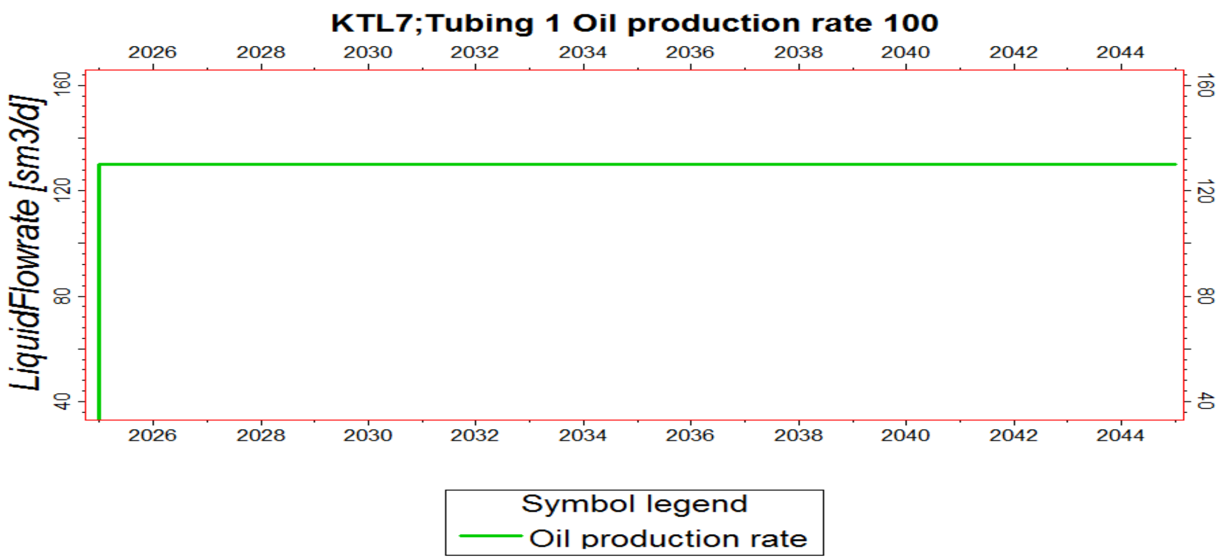

Figure 5.12: Oil production rate for 20 years

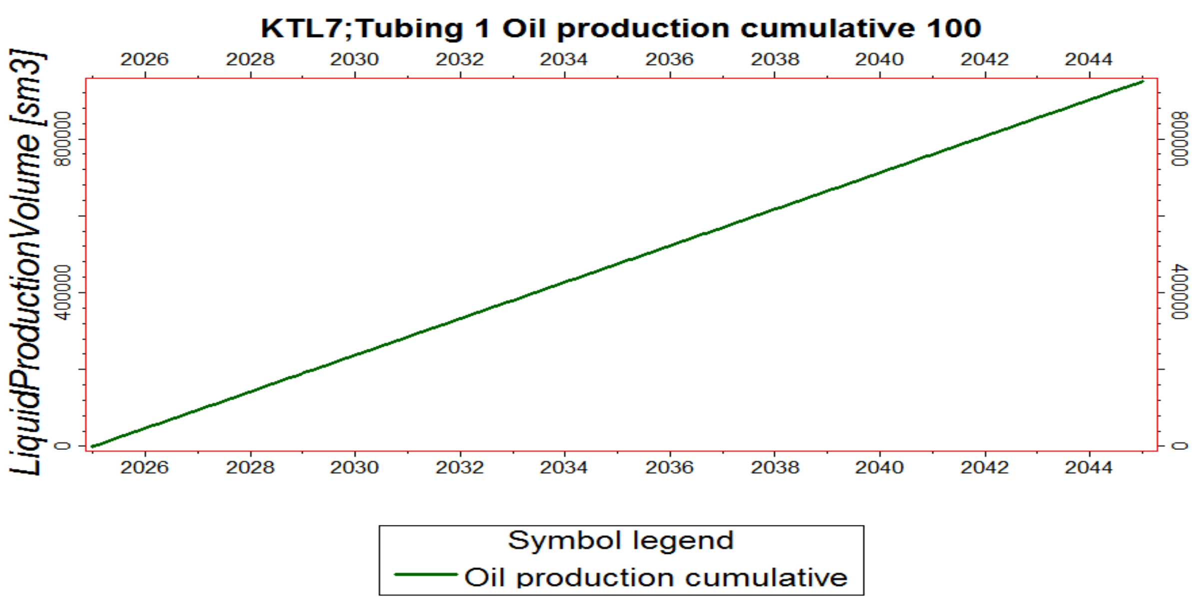

Figure 5.13: Total oil production during 20 years

Oil production pressure at well head has also been forecasted by 20 years simulation as shown in figure 5.14. Well head pressure has dropped from 133 (1928 psi) bar to 95 (1377 psi) bar after 20 years of production. Well head pressure drop is normal as usual. Bottom hole pressure has changed from 400 bar (6200 psi) to 362 bar (5311 psi) as shown in figure 5.15. Bottom hole pressure drop is also normal.

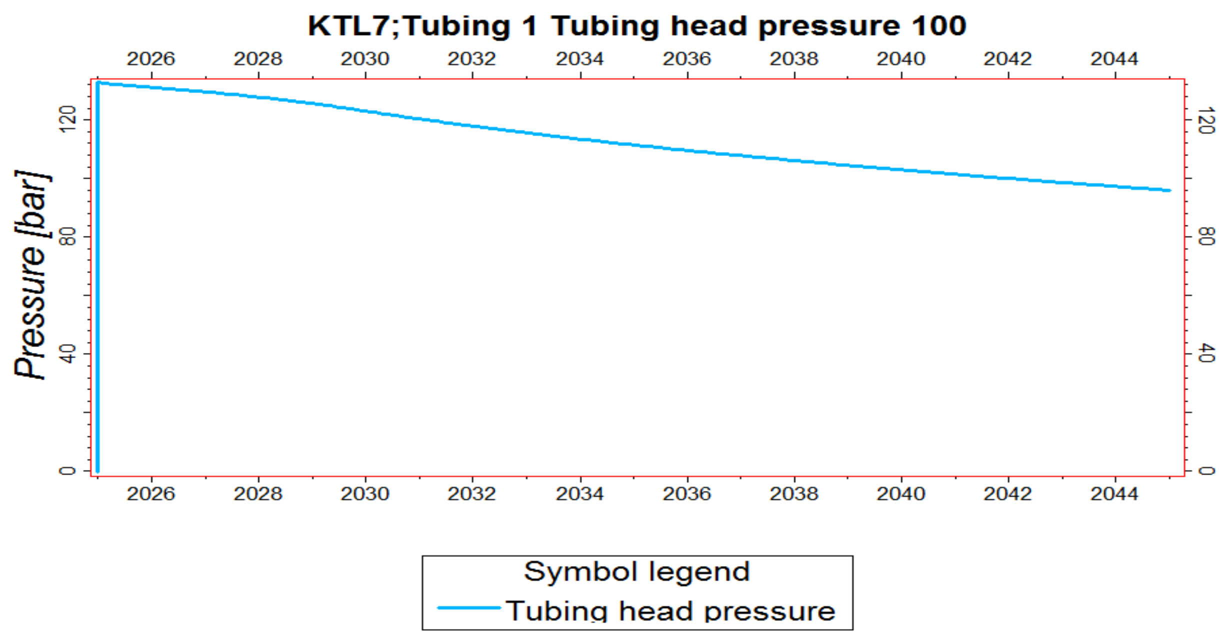

Figure 5.14: Tube head pressure

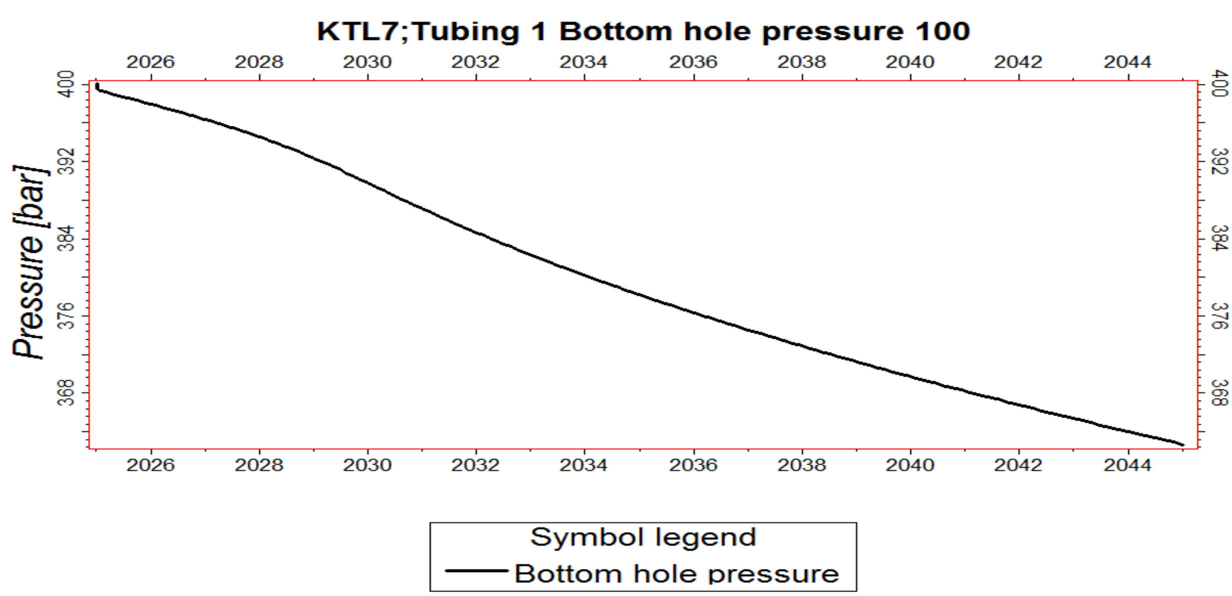

Figure 5.15: Bottom hole pressure

Pressure drop in production tube is the pressure difference between bottom hole pressure and tube head pressure. Tube pressure drop has been estimated at 260 bar (4030 psi) as shown in figure 5.16.

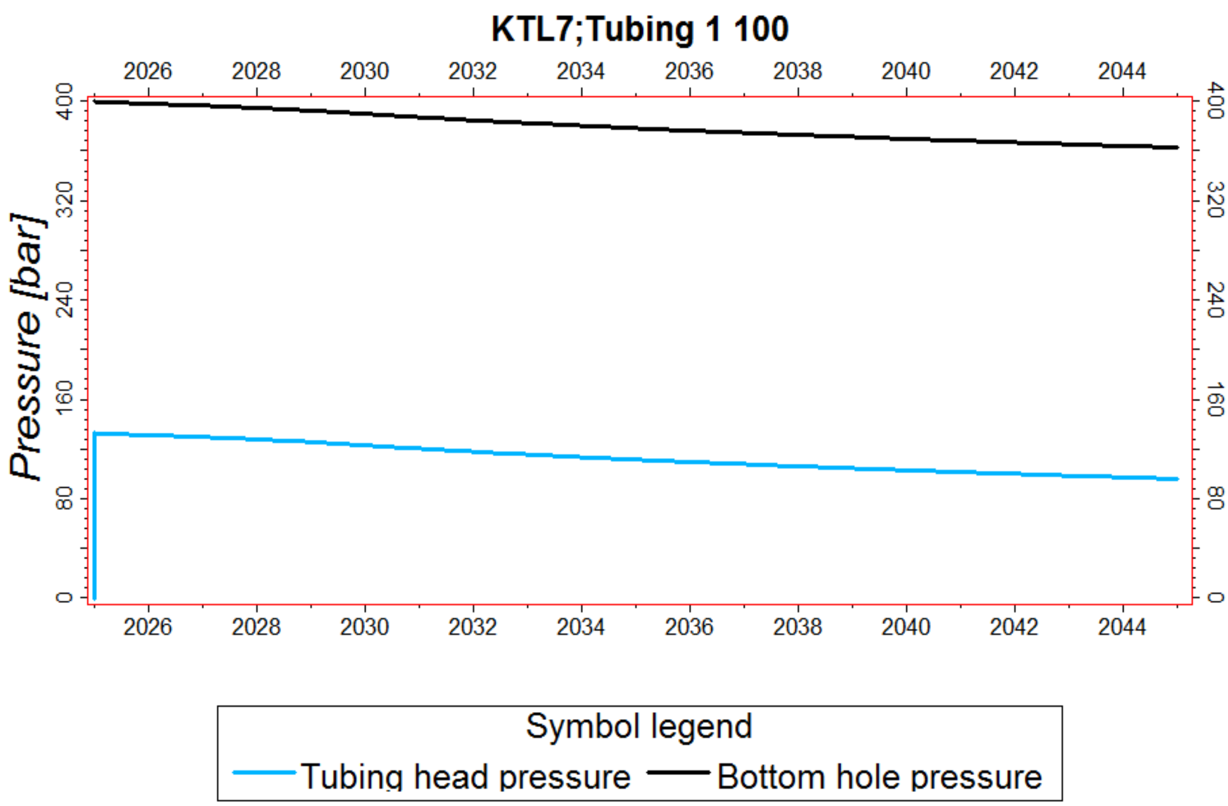

Figure 5.16: Pressure drop in tube

The well has able to establish a good hydraulic connection all over the reservoir as shown in figure 4.17. A single well is capable of draining whole of the reservoir. Oil flow rate through the pore space in the reservoir is good as shown in figure 5.18. Oil flow line has established all over the reservoir. Streamline of oil flow rate is 0.1 sm^3/day (0.63 STB/D) when oil production rate is 130 sm^3/day (817 STB/D).

Oil flow direction toward the production well is shown in figure 5.19. Oil has flown from all parts of the reservoir to the production well. Simulation time has been determined from the 20 years of simulation as shown in figure 5.20. It is seen that oil takes maximum 100000 days (274 years) to come to the production well from distant part of the reservoir.

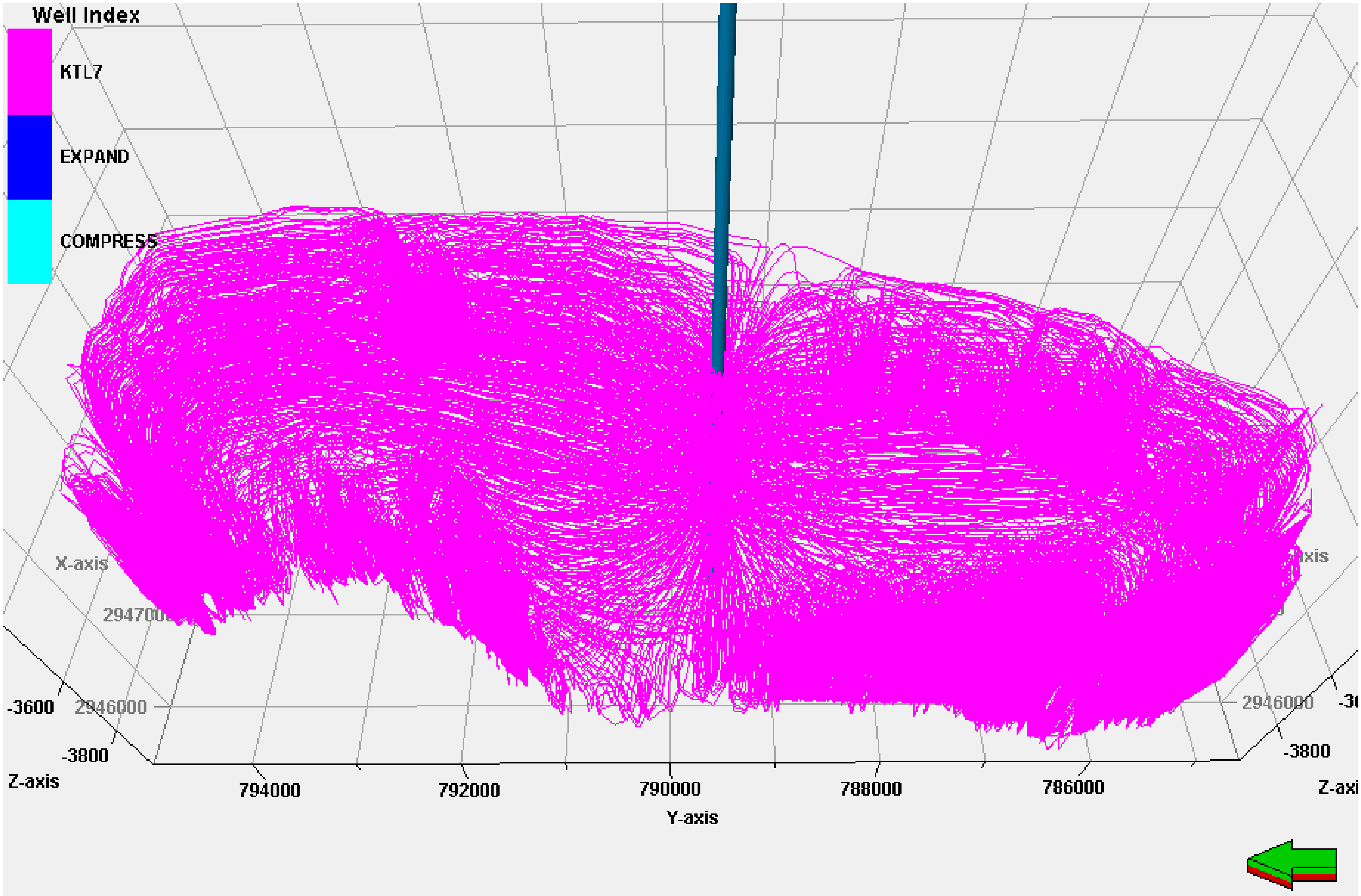

Figure 5.17: Hydraulic connectivity of well

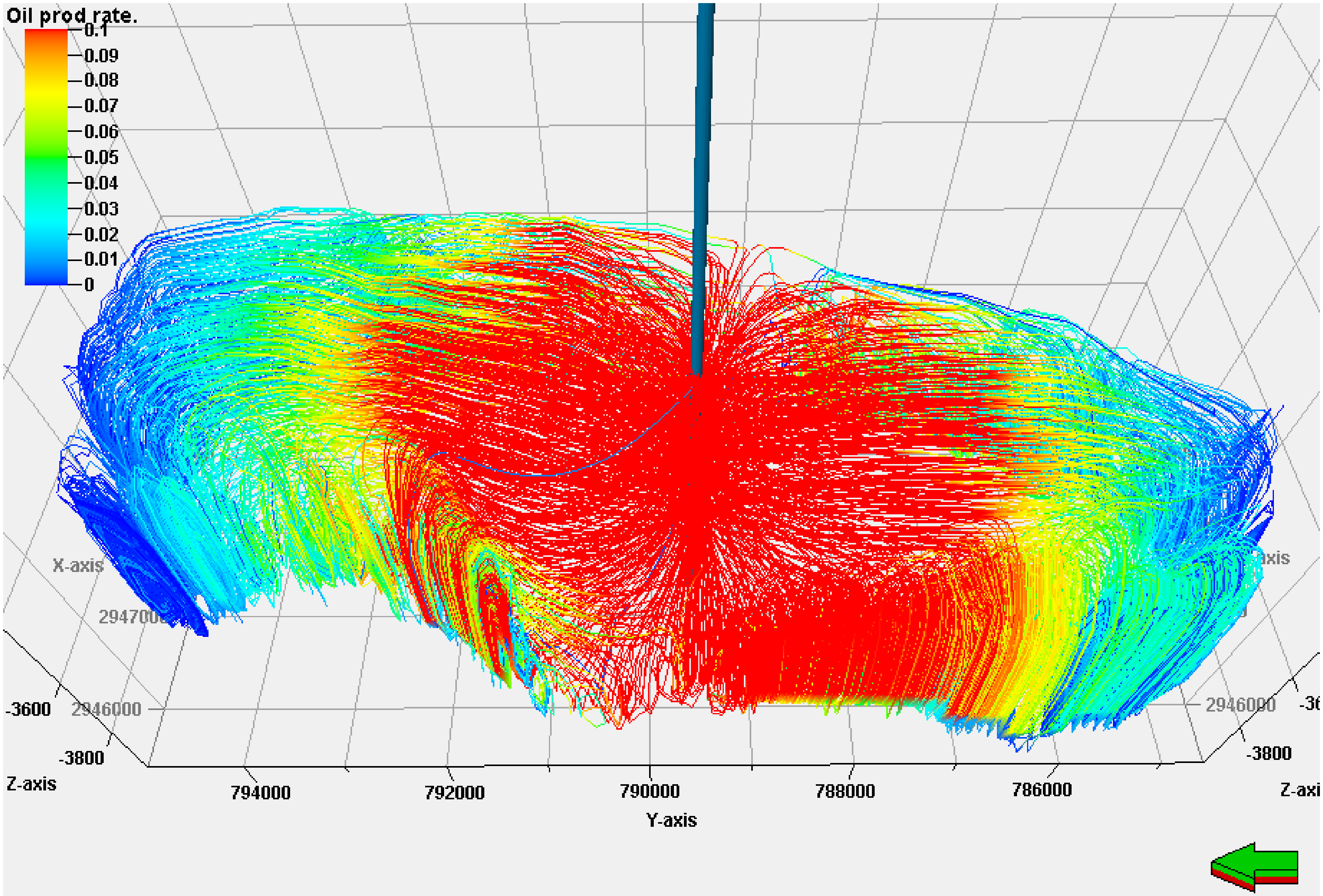

Figure 5.18: Oil flow rate in reservoir

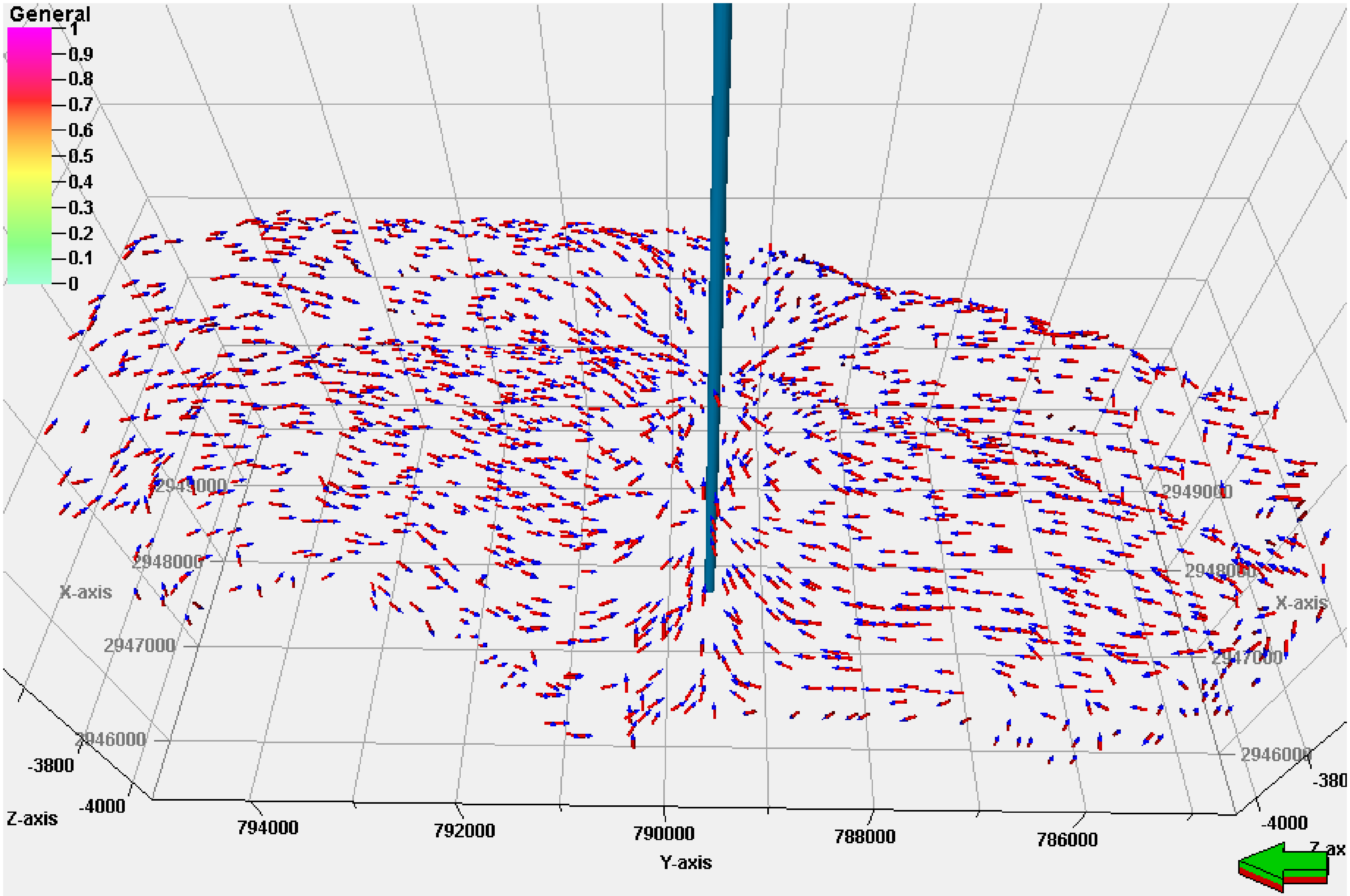

Figure 5.19: Oil flow direction

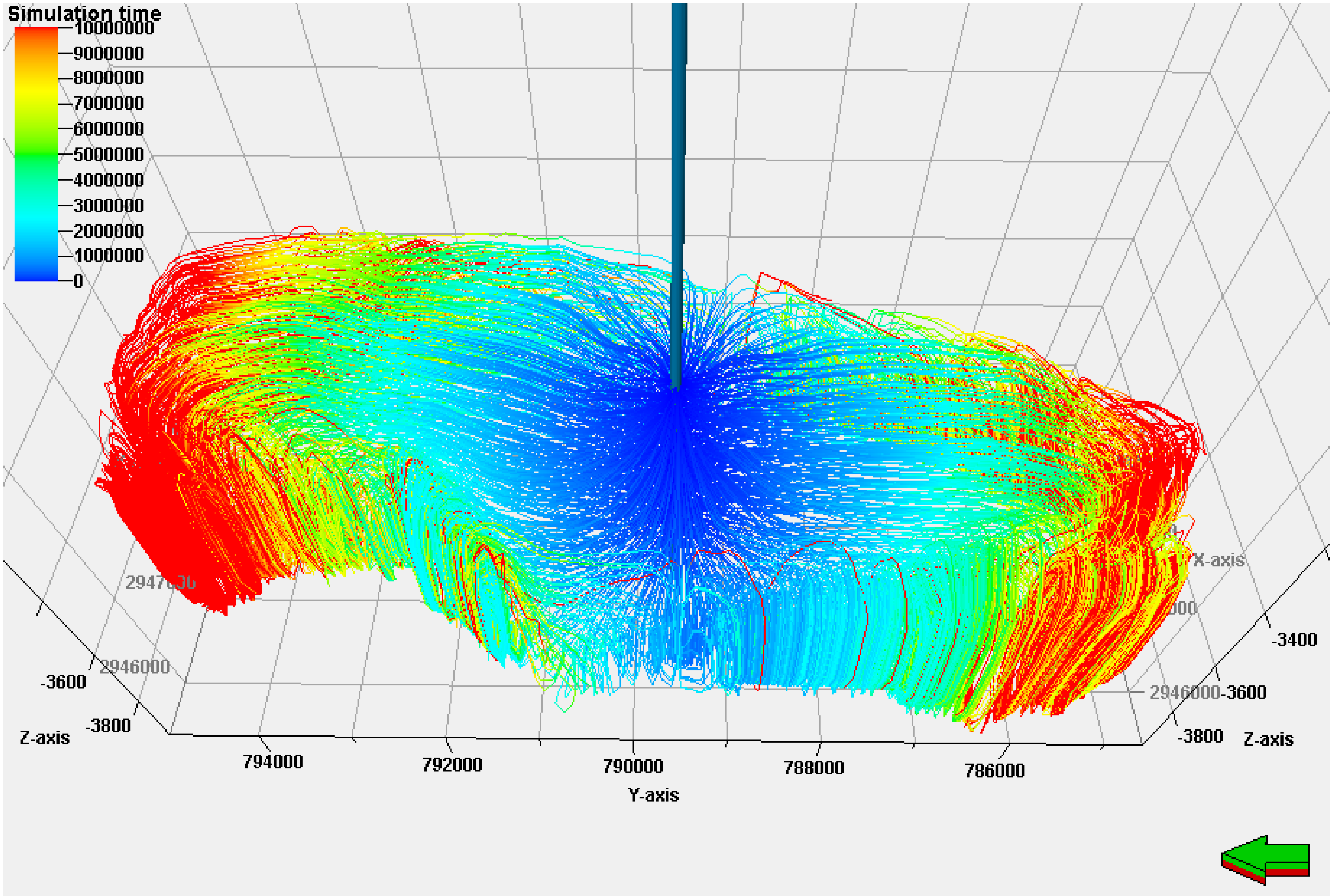

Figure 5.20: Simulation time

5.2.1: Economic Analysis of Kailashtila Oil Reservoir Development

Oil reservoir development project cash flow has been determined from project expenditure schedule as shown in figure 5.21. Net present value has also been estimated from the cash flow.

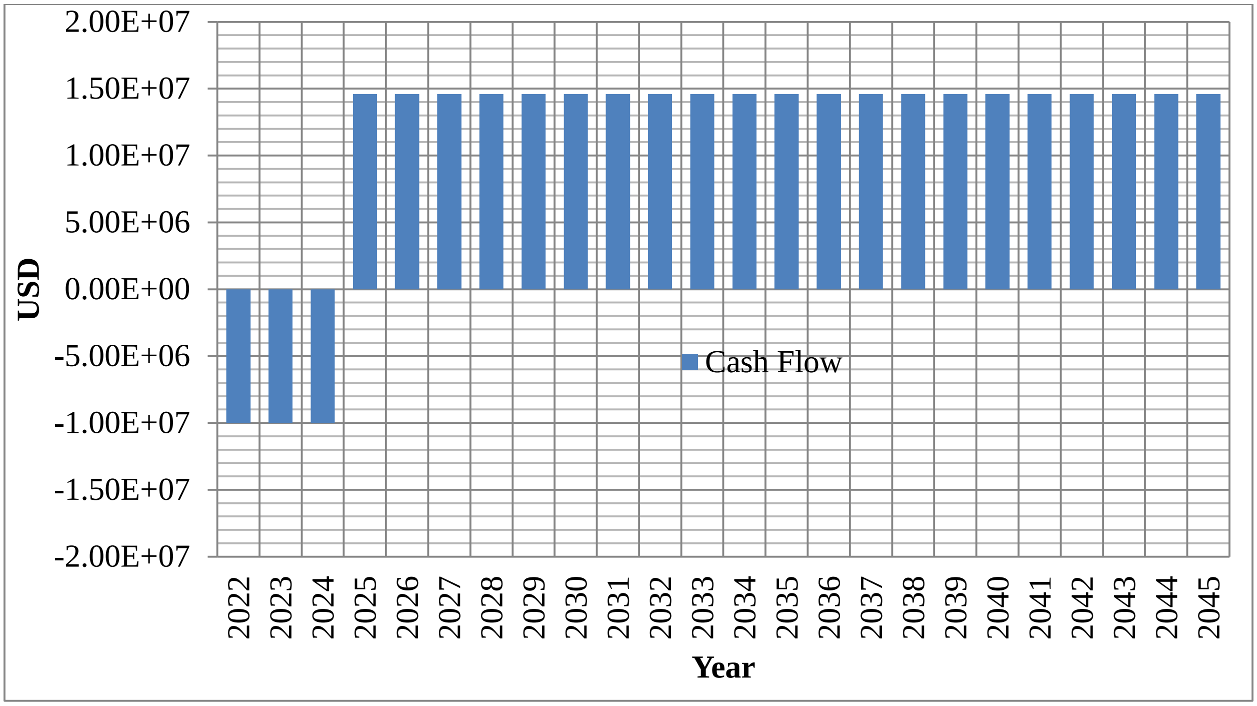

Figure 5.21: Cash flow (KTL)

Net present value of the development project is 77.0 million USD. Break even analysis has also been performed on the development project as shown in figure 5.22. Break-even point is 0.584 million STB of oil. Net present value and break even analysis have following features:

- Total project expenditure is 30 million USD
- Project expenditure is uniform in three years
- Oil sales revenue is uniform in 20 years
- Break-even point will be achieved after 3 years
- Contingency cost is included in the total project cost.
- Risk margin is considered
- Oil price is considered as the same as the international market
- Unavoidable circumstances are considered.

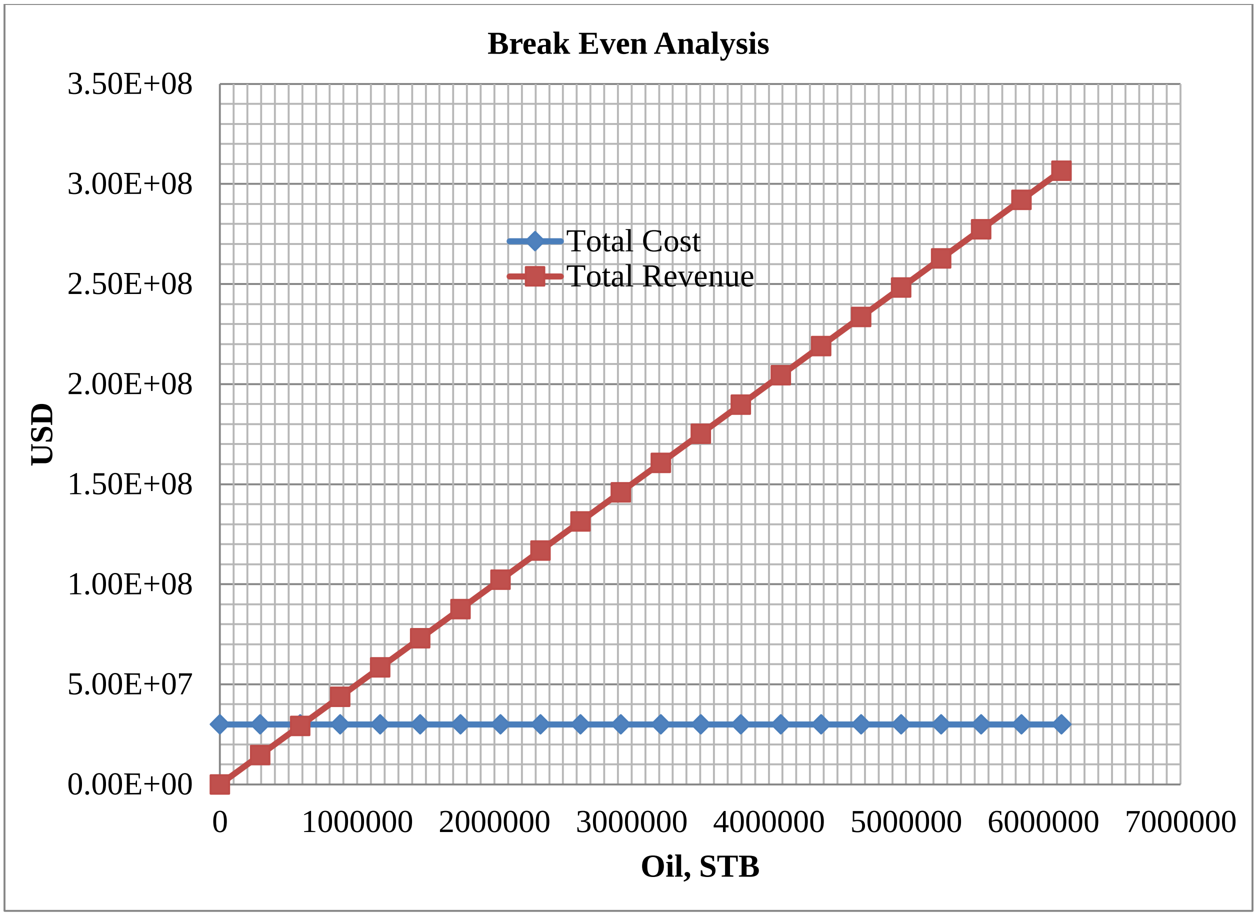

Figure 5.22: Break even analysis (KTL)

Chapter 6

Conclusions and Recommendations

6.1 Conclusions

The present research attempts to study the oil reservoirs in Haripur and Kailashtila fields from a petroleum engineering point of view and tries to find out the prospects of these fields and their production capabilities. Oil reservoir development plans are prepared from finite difference reservoir simulation model and streamline reservoir simulation model. Reservoir simulation models are validated by oil production histories. Oil reserves are estimated from valid reservoir models. Oil reservoirs are dynamically characterized from reservoir simulation models. Optimum oil recovery techniques are designed from screening of oil reservoir parameters which include chemical composition of reservoir rock, reservoir oil and reservoir water, clay content and wettability of reservoir rock, surface tension in reservoir fluids (oil-water, gas-water) pore space configuration, pore throat size, oil production rate in core flooding test and relative permeability in core flooding test. Oil reservoir development plans also includes reservoir development parameters i.e. Optimum number of oil production wells, Optimum number of water injection wells, Optimum positions of wells, Optimum oil production rate, Well head pressure, Optimum water injection rate, Optimum production period, and Total recovered oil, Recovery factor.

6.1.1 Haripur Oil Reservoir

Finite difference and streamline reservoir simulation model of the Haripur oil reservoir have been developed using seismic data, well logs data, core analysis data and fluid analysis data. The reservoir simulation models have been validated by history matching with six years of oil production data. It is evident that significant amount of oil (32.47 million STB) is still remaining in the oil reservoir of Haripur field.

Streamline simulation study of six years oil production from Haripur oil reservoir has revealed that at maximum production time, average value of oil flow rate is 0.09 stb/d. Oil flow line developed by 90% at maximum production time when the surface production rate is 405 stb/d and well head pressure 520 psia. The dynamic performance of Haripur oil reservoir was good during six years oil production period as the reservoir had excellent pressure communication along with perfect oil flow lines. Scale and wax deposited in production tube due to lack of well cleaning and workover operation. Additional pressure drop was gradually increasing over time in oil production tube and finally the oil production ceased and well was abandoned.

Six years of oil production in Haripur field is strong evidence for existence of oil reservoir in Haripur field. From the production data analysis it has been determined that oil reservoir in Haripur field produced oil by rock compaction, solution gas and oil expansion drive mechanisms.

Streamlines of oil flow rate have become denser in 1000 ppm salinity water environment than 100000 ppm salinity water environment. When 1000 ppm salinity water has been injected in the reservoir then monovalent ions displace divalent ions to release oil from clay surface. Interfacial tension between oil water also reduced in low salinity water environment. As a result oil splits into small droplets and starts to flow.

Mobility of water has become less in 1000 ppm salinity water environment. Streamlines of water flow rate have been generated for the 100000 ppm salinity water and 1000 ppm salinity water to examine dynamic behavior of water in reservoir. Streamlines of water flow rate have become less dense in 1000 ppm salinity water environment than 100000 ppm salinity water environment. Water breakthrough will also be delayed in 1000 ppm salinity water environment as water has advanced more in 100000 ppm salinity water environment. It will be worthwhile to develop the reservoir with 100000 ppm salinity water injection technology. The 1000 salinity water is less conductive as water mobility decreases and oil mobility increases. Water engages in sweeping oil rather than flowing through the pore. Na ions in water is engaged in displacing the Ca^{+2} and Mg^{+2} ions to free the oil from clay surface.

In six years, Haripur field has produced 0.53 million barrels of oil and experts predict that remaining oil in the reservoir is approximately 32.47 million barrels of oil. To recover this oil low salinity water injection method has been proposed. The oil reservoir development plan has optimized development parameters. Injection water salinity is 1000 ppm of NaCl. Six injection wells are used for water injection. Water injection pressure is 1000 psi. Well water injection rate is 300 stb/day. Field water injection rate is 1800 stb/day. Two oil production wells are used for oil production. Well oil production rate is 400 stb/day. Field oil production rate is 800 stb/day. Well head pressure of oil production is 500 psi.

The validated finite difference and streamline reservoir models with optimized development option have been simulated for 20 (Twenty) years from 01/01/2027 to 01/01/2047. Streamline flux density of oil flow rate after 20 years remains the same as the streamline flux density of oil flow rate at the beginning of simulation. Initially, overall average value of oil flow rate is 0.025 stb/day. Overall average value of oil flow rate has decreased from 0.025 stb/day to 0.015 stb/day over the 20 years as oil relative permeability has reduced. Oil saturation has been reduced due to oil production. Reduction in oil saturation has reduced oil relative permeability. Oil flow rate has been decreased due to the reduction in oil relative permeability. Oil flow rate has become zero near the injection wells as injected water has advanced toward the production wells and swept entire oil. Oil production is continued by expansion of reservoir oil and sweeping by injected water. During the 20 years simulation 13.149 million barrels of water have been injected in the reservoir to produce 5.844 million barrel oil.

6.1.2 Kailashtila Oil Reservoir

Well logs and DST analysis are able to provide the evidence of the presence of liquid hydrocarbon (oil) in the interval 3261 to 3266 meter in Kailashtila field. Finite difference and streamline reservoir simulation model of oil reservoir in Kailashtila field have been prepared from seismic survey, well logs of KTL-7, fluid contacts, core analysis, fluid analysis, saturation function properties analysis, and initial reservoir condition. The oil reservoir models have been validated by drill stem test data. Stock tank oil initially in place is 15 million sm^3 (94.33 million STB) in oil reservoir of Kailashtila field.

Streamline reservoir simulation analysis has been performed on DST operation done on well no KTL-7 for 125 minutes with average liquid flow rate was 338 sm^3/day. Model well of KTL-7 has been placed in the reservoir simulation models. Reservoir model has been simulated according to the DST. Dynamic characters of the reservoir such as well hydraulic connectivity, oil flow rate, oil flow direction, oil flow time, water flow rate have been evaluated for dynamic characterization of oil reservoir. The oil reservoir has shown good dynamic performance during DST operation.

Oil reservoir in Kailashtila field has good enough pressure to lift the oil to surface which has been observed during the drill stem test operation. The reservoir is able to deliver maximum liquid at the rate of 2500 sm^3/day (15723 STB/D). Now it is recommended that the oil reservoir will be developed by natural depletion method. One oil production well will be drilled in the reservoir in a suitable place where well is able to establish maximum drainage area in the reservoir and able to deliver oil with maximum flow rate.

A single well is drilled in center of the oil zone to prolong the oil production time and delay the water breakthrough. The streamline reservoir simulation model with development scenario at Kailashtila field has been simulated for the oil flow of 130 sm^3/day (817 STB/D). Conductivity of well with reservoir is perfect and reservoir has shown good dynamic performance in this development option. During the 20 years simulation the reservoir is able to produce 949650 sm^3 (5.973 million STB) of oil. Kailashtila oil reservoir is larger than the Haripur oil reservoir.

6.2 Recommendations

The authentication and validation of oil reservoir development plan is totally dependent on the oil reservoir simulation model. An authentic and valid oil reservoir simulation model is able to provide reliable oil reservoir development plan. The quality of oil reservoir simulation model is totally dependent on the seismic data, well log data, core analysis data and fluid analysis data. In this study reservoir structure has been constructed from the seismic and well log data. The exploration and production companies have acquired and processed the seismic and well log data. Core and fluid analyses have been performed in laboratory. Reservoir screening for EOR design has been performed in laboratory. There are several recommendations that can be drawn from this study.

Seismic data plays an important role in oil reservoir development planning. Advanced seismic survey such as 3D and 4D surveys can be carried out to delineate the oil reservoirs properly in

Haripur and Kailashtila fields. Advanced well logs such nuclear magnetic resonance (NMR) log can be carried out on the fields to detect the oil zone properly as well as to detect oil, gas and water separately.

Core analysis provides information on porosity, absolute permeability, net to gross ratio, relative permeability, capillary pressure and rock compaction factor. Advanced technologies can be applied in coring operation, core plugs preparation. Advanced equipments can be used for estimation of porosity, absolute permeability, net to gross ratio, relative permeability, capillary pressure and rock compaction factor. Reservoir oil properties such as oil formation volume factor, oil viscosity, solution gas oil ratio and bubble point pressure are estimated by PVT cell. Advanced equipment is needed for characterizing the C_{7+} components. Wax formation possibility must be examined for oil of Haripur field. Condensate banking study must be carry out in Kailashtila field. Advanced core flood test equipment is needed to perform authentic and reliable core flood test for designing appropriate EOR technique in Haripur field. Core flood test plays key role in oil recovery project. In situ core sample can be used for core flood test to observe the actual condition of oil flow in the reservoir.

References

Afroza Parvin, A. S. M. Woobaidullah, and Md Jamilur Rahman. 2019a. Sequence stratigraphic analysis of the Surma Group in X Gas Field, Surma Basin, Bengal Delta. Journal of Nepal Geological Society, 58: 39–52.

Afroza Parvin, Md. Jamilur Rahman and A.S.M. Woobaidullah. 2019b. Petroleum prospect analysis and new gas horizon detection at Fenchuganj Gas Field in the Surma Basin, Bangladesh: An application of sequence stratigraphic concept, Marine and Petroleum Geology, Elsevier, 102: 786-799.

Afroza Parvin, and A. S. M. Woobaidullah. 2019c. Incorporation of sequence stratigraphy in gas reservoir correlation: A case study, J. Asiat. Soc. Bangladesh, Sci. 45(2): 209-216.

Alagic E. 2010. Combination of Low Salinity Waterflooding with Surfactant Injection – A New Hybrid EOR Process. PhD Dissertation, University of Bergen.

Alagic E., Spildo K., Skauge A., and Solbakken, J. 2011. Effect of Crude Oil Aging on Low Salinity and Low Salinity Surfactant Injection. Journal of Petroleum Science and Engineering, 78: 220-227.

Alam M., Alam M.M., Curray J.R., Chowdhury, M.L.R., and Gani, M.R., 2003, An Overview of Sedimentary geology of the Bengal Basin in Relation to the Regional Tectonic Framework and Basin fill History. Sedimentary Geology, 155(3-4): 179–208.

Alotaibi M.B., Nasralla R.A., and Nasr-El-Din H.A. 2011. Wettability Studies Using Low Salinity Water in Sandstone Reservoirs. SPE Reservoir Evaluation & Engineering, 14(6): 713-725.

Al-Shalabi E., Sepehrnoori K., and Pope G. 2014. Geochemical Interpretation of Low Salinity Water Injection in Carbonate Oil Reservoirs. Paper SPE 169101 presented at the SPE Improved Oil Recovery Symposium, Tulsa, OK, USA, 12-16 April.

Ambia F. 2012. A Robust Optimization Tool Based on Stochastic Optimization Methods for Waterflooding Projects. Paper SPE 160907 presented at the SPE Annual Technical Conference and Exhibition, San Antonio, Texas, USA, 8-10 October.

Anderson G. A. 2006. Simulation of Chemical Floods Enhanced Oil Recovery Processes Including the Effects of Reservoir Wettability. Master’s thesis, University of Texas.

Anderson W.G. 1986. Wettability Literature Survey – Part 1: Rock/Oil/Brine Interactions and the Effects of Core Handling on Wettability. SPE Journal of Petroleum Technology, 38(11): 1125-1144.

Appelo, C.A.J. 1994. Cation and Proton Exchange, pH Variations, and Carbonate Reactions in a Freshening Aquifer. Water Resources Research Journal, 30(10): 2893-2805.

Appelo C.A.J., and Postma D. 2005. Geochemistry, Groundwater and Pollution. Balkema publisher, 2005.

Austad T., Rezaei Doust A., and Puntervold T. 2010. Chemical Mechanism of Low Salinity Water Flooding in Sandstone Reservoir. Paper SPE 129767 presented at the SPE Improved Oil Recovery Symposium, Tulsa, 24-28 April.

Austad T., Strand S., Madland M., Putervold T., and Korsnes R.I. 2008. Seawater in Chalk: An EOR and Compaction Fluid. SPE Reservoir Evaluation & Engineering, 11(4): 648-654.

Bardu O., and Kabir C.S. 2003. Well Placement Optimization in Field Development. Paper SPE 84191 presented at the 2003 SPE Annual Technical Conference and Exhibition, Denver, Colorado, USA, 5-8 October.

Batycky, R. P., M. R. Thiele, R. O. Baker and S. H. Chugh. 2006. Revisiting reservoir flood-surveillance methods using streamlines. SPEREE, 11(2): 387–394.

Bazin B., and Labrid J. 1991. Ion Exchange and Dissolution/Precipitation Modeling: Application to the Injection of Aqueous Fluids into a Reservoir Sandstone. SPE Reservoir Engineering, 6(2): 233-238.

Beckner B.L., and Song X. 1995. Field Development Planning Using Simulated Annealing-Optimal Economic Well Scheduling and Placement. Paper SPE 30650 presented at the SPE Annual Technical Conference and Exhibition, Dallas, Texas, USA, 22-25 October.

Ben-Tal A., and Nemirovski. 1998. Robust Convex Optimization. Math. Oper. Res., 23: 769-805.

Ben-Tal A., and Nemirovski. 1999. Robust Solutions of Uncertain Linear Programs. Operations Research Letters, 25(1): 1-13.

Ben-Tal A., and Nemirovski. 2000. Robust Solution of Linear Programing Problems Contaminated with Uncertain Data. Math. Programing, 88: 411-421.

Berg S., Cense A.W., Jansen E., and Bakker K. 2010. Direct Experimental Evidence of Wettability Modification by Low Salinity. Petrophysics, 51(5): 101-125.

Bernard G.G. 1967. Effect of Floodwater Salinity on Recovery of Oil from Cores Containing Clays. Paper SPE 1725: Los Angeles, California, October 26-27.

Bethke, C.M. 2006. GWB Essentials Guide. University of Illinois, May 4.

Breeuwsma A., Wosten J.H.M., Vleeshouwer J.J., Slobbe V., and Bouma J. 1986. Derivation of Land Qualities to Assess Environmental Problem from the Soil Survey. Soil Science Society of America Journal, 50: 186-190.

Buckley J.S., Liu Y., and Monsterleet S. 1998. Mechanisms of Wetting Alteration by Crude Oils. SPE Journal, 3(1): 54-61.

Buckley J.S., and Morrow N.R. 2010. Improved Oil Recovery by Low Salinity Waterflooding: A Mechanistic Review. Paper presented at 11th International Symposium on Evaluation of Wettability and Its Effect on Oil Recovery, Calgary, 6-9 September.

Buckley, J.S., Bousseau C., and Liu Y. 1996. Wetting Alteration by Brine and Crude Oil: From Contact Angles to Cores. Paper SPE 30765 presented at the SPE Annual Technical Conference & Exhibition, Dallas, USA, 22-25 October.

Buckley, S.E., and Leverett M.C. 1942. Mechanism of Fluid Displacement in Sands. Trans, AIME, 146: 107-16.

Bubul B., Pradip B., Devojit B., Vanthangliana, Parakh P., and Raghupratim R. 2017. A geological study on Upper Bhuban Formation in parts of Surma Basin. Science Vision, 17 (3): 128-147.

Card C., Nghiem L.X., Li Y-K., and Grabenstetter J. 1992. An Efficient Approach to Adaptive-Implicit Compositional Simulation with an Equation of State. SPE Reservoir Engineering, 7(2): 259-264.

Carll J.F. 1980. The Geology of the Oil Regions of Warren, Venango, Clarion and Butler Counties. Second Geological Survey of Pennsylvania, 1875(79)-268.

Centilmen A., Ertekin T., and Grader A.S. 1999. Applications of Neural Networks in Multi well Field Development. Paper SPE 56433 presented at the SPE Annual Technical Conference and Exhibition, Houston, Texas, USA, 3-6 October.

Chandra S., Kundal, and Kushwaha. 2010. Ichnology of Bhuban and Boka Bil Formations, oligocene-miocene deposits of Manipur Western Hill, Northeast India. Journal of the Geological Society of India, 76 (2010): 573–586.

Chen C., Li G., and Reynolds. 2012. Robust Constrained Optimization of Short and Long Term Net Present Value for Closed-Loop Reservoir Management. SPE Journal, 17(3): 849-864.

Dang T.Q.C., Chen Z., Ngoc T.B.N., and Bae W. 2011a. Numerical Simulation of HPAM Polymer Viscosity in Porous Media. Journal of Energy Sources, 11(1): 101-116.

Dang T.Q.C., Chen Z., Ngoc T.B.N., and Bae W. 2011b. Investigation of Surfactant Adsorption in Micellar Polymer Flooding. Journal of Energy Sources, 11(1): 151-168.

Dang T.Q.C., Chen Z., Nguyen T.B.N., and Phung H.T. 2011c. Lessons Learned and Experiences Gained in Developing the Waterflooding Concept of a Fractured Basement Granite Reservoir: A 20 Year Case Study. Journal of Canadian Petroleum Technology, 50(9-10): 10-23.

Dang T.Q.C., Nghiem, L.X., Chen, Z., and Nguyen, Q.P. 2013a. Modeling Low Salinity Waterflooding: Ion Exchange, Geochemistry and Wettability Alteration. Paper SPE 166447 presented at the 2013 SPE Annual Technical Conference and Exhibition, New Orleans, LA, USA, 30 September – 2 October.

Dang T.Q.C., Nghiem, L.X., Chen, Z., Nguyen, Q.P., and Nguyen, T.B.N. 2013b. State-of-the Art Smart Low Salinity Waterflooding for Enhanced Oil Recovery. Paper SPE 165903 presented at the 2013 SPE Asia Pacific Oil & Gas Conference and Exhibition, Jakarta, Indonesia, 22-24 October.

Dang T.Q.C., Chen Z., Ngoc T.B.N., and Bae W. 2014a. Development and Optimization of Polymer Conformance Control Technology in Mature Reservoir: Laboratory Experiment vs. Field Scale Simulation. Journal of Energy Sources: Part A, 36(11).

Dang T.Q.C., Chen Z., Ngoc T.B.N., and Bae W. 2014b. Potential of Enhanced Oil Recovery Micellar/Polymer Flooding in Heterogeneous Reservoirs. Journal of Energy Sources: Part A, 36(8).

Dang T.Q.C., Chen Z., Nguyen T.B.N., and Phung H.T. 2014c. Integrated Modeling of Naturally Fractured Basement Reservoir. International Journal of Oil, Gas, and Coal Technology, 14(1): 101-114.

Dang T.Q.C., Chen Z., Nguyen T.B.N., and Bae W. 2014d. Investigation of Polymer Adsorption in Porous Media. Petroleum Science and Technology, 31(15): 210-227.

Dang T.Q.C., Nghiem, L.X., Chen, Z., Nguyen, Q.P., and Nguyen T.B.N. 2014e. CO2 Low Salinity Water Alternating Gas: A New Promising Approach for Enhanced Oil Recovery. Paper SPE 169071 presented at the 2014 SPE Improved Oil Recovery Symposium, Tulsa, OK, USA, 12-16 April.

Dang T.Q.C., Nghiem, L.X., Nguyen, T.B.N., and Chen, Z. 2015a. Practical Concerns and Principle Guidelines for Screening, Implementation, Design, and Optimization of Low Salinity Waterflooding. Paper SPE 174008 presented at the 2015 SPE Western Regional Meeting, Garden Grove, CA, USA, 27-30 April.

Dang T.Q.C., Nghiem, L.X., Nguyen, T.B.N., Chen, Z., and Nguyen, Q.P. 2015b. Modeling and Optimization of Low Salinity Waterflooding. Paper SPE 173194 presented at the 2015 SPE Reservoir Simulation Symposium, Houston, TX, USA, 23-25 February.

Dang T.Q.C., Nghiem, L.X., Nguyen, T.B.N., and Chen, Z. 2015c. New Insights into Critical Role of Geology in Modeling and Optimization of Low Salinity Waterflooding. Paper SPE 174294 presented at the 2015 SPE EUROPEC/EAGE, Madrid, Spain, 1-4 June.

Dang T.Q.C., Nghiem, L.X., Nguyen, T.B.N., Chen, Z., and Heng L. 2015d. Modeling and Robust Optimization of CO2 Low Salinity Water Alternating Gas under Geological Uncertainties. Paper SPE 174644 presented at the SPE Asia Pacific Enhanced Oil Recovery Conference, Kuala Lumpur, Malaysia, 11-13 August.

Dang T.Q.C., Nghiem, L.X., Nguyen, T.B.N., and Chen, Z. 2015e. Field Scale Evaluation and Robust Optimization of Low Salinity Waterflooding and Hybrid Low Salinity Waterflooding under Geological Uncertainties. Paper SPE 175042 presented at the SPE Annual Technical Conference & Exhibition, Houston, TX, USA, 28-30.

Deryaguin B., and Landau L. 1941. Theory of the Stability of Strongly Charged Lyophobic Sols and of the Adhesion of Strongly Charged Particles in Solution of Electrolytes. Acta Physico Chemical URSS 14:633.

Deepak Kapoor, Soni Ashok, Goel Swati and Chaudhary Manisha, 2013, Identification of clay and other minerals, estimation of their volumes and estimation of porosity in reservoir rock of Bhuban Formation of West Tripura wells. KDMIPE, ONGC.

Donaldson E.C., Thomas R.D., and Lorenz P.B. 1969. Wettability Determination and Its Effect on Recovery Efficiency. SPEJ, 13(March 1969): 140-157.

Doust A.R., Puntervold T.P., and Austad T. 2010. A Discussion of the Low Salinity EOR Potential for a North Sea Sandstone Field. Paper SPE 134459 presented at the SPE Annual Technical Conference and Exhibition, Florence, Italy.

Drummond C., and Israelachvili J. 2002. Surface Forces and Wettability. Journal of Petroleum Science and Engineering, 33: 123-133.

Drummond C., and Israelachvili J. 2004. Fundamental Studies of Crude Oil-Surface Water Interactions and Its Relationship to Reservoir Wettability. Journal of Petroleum Science Engineering, 45: 61-68.

Earlougher R. C. Jr.1977. Advances in Well Test Analysis, Monograph Series no 5, Society of Petroleum Engineers of AIME, Dallas.

Ehlig, Economides C.A., J.A., Joseph, R.W., Ambrose Jr. and Norwood, 1990, A Modern Approach to Reservoir Testing, JPT, 1554-1563.

Ehrlich R., Hasiba H.H., and Raimondi P. 1974. Alkaline Waterflooding for Wettability Alteration – Evaluating a Potential Field Application. Journal of Petroleum Technology, 1335-1343.

Evje S., and Hiorth A. 2011. A Model for Interpretation of Brine Dependent Spontaneous Imbibition Experiments. Advances in Water Resources, 34(2011): 1627-1642.

Faure M.H., Sardin M., and Vitorge P. 1997. Release of Clay Particles from an Unconsolidated Clay-Sand Core: Experiments and Modeling. J. Contam. Hydrol. 26(1-4): 169-178.

Fedutenko E., Yang C., Card C., and Nghiem L. 2012. Forecasting SAGD Process under Geological Uncertainties Using Data-Driven Proxy Model. Paper SPE 157942 presented at the SPE Heavy Oil Conference, Calgary, Alberta, Canada, 12-14 June.

Fedutenko E., Yang C., Card C., and Nghiem L. 2014. Time-Dependent Neural Network Based Proxy Modeling of SAGD Process. Paper SPE 170085 presented at the SPE Heavy Oil Conference, Calgary, Alberta, Canada, 10-12 June.

Fjelde I., Asen S.V., and Omekeh A. 2012. Low Salinity Water Flooding Experiments and Interpretation by Simulations. Paper SPE 154142 presented at the Eighteenth SPE Improved Oil Recovery Symposium, Tulsa, OK, USA, April 14-18.

Fogden A., Kumar M., Morrow N.R., and Buckley J.S. 2011. Mobilization of Fine Particles during Flooding of Sandstones and Possible Relations to Enhanced Oil Recovery. Energy Fuels.

Gaines G.L., and Thomas H.C. 1953. Adsorption Studies on Clay Minerals. II. A Formulation of the Thermodynamic of Exchange Adsorption. J. Chem. Phys., 21(1953): 714-718.

Ghaoui E.L., and Lebret H. 1997. Robust Solution to Least-Squares Problems with Uncertain Data. SIAM J. Matrix Analysis and Applications, 18(4): 1035-1064.

Ghaoui E.L., Oustry F., and Lebret H. 1998. Robust Solutions to Uncertain Semidefinite Programs. SIAM J. Optimization, 9(1): 33-52.

Green D.W., and Willhite G.P. 1998. Enhanced Oil Recovery. Henry L. Doherty Memorial Fund of AIME, Society of Petroleum Engineers.

Gringarten, A.C., D.P. Bourdet, P.A. Landel and Kniazeff. 1979. A Comparison between Different Skin and Wellbore Storage Type-Curves for Early-Time Transient Analysis, paper SPE 8205.

Hajizadeh Y., Nghiem L., Mirzabozorg A., Yang C., Li H., and Sousa M.C. 2013. A Soft and Law-Abiding Framework for History Matching and Optimization under Uncertainty. Paper SPE 163636 presented at the SPE Reservoir Simulation Symposium, The Woodlands, Texas, USA, 18-20 February.

Handels M., Zandvliet M., Brouwer R., and Jansen J.D. 2007. Adjoint-Based Well Placement Optimization under Production Constraints. Paper SPE 105797 presented at the SPE Reservoir Simulation Symposium, Houston, Texas, USA, 26-28 February.

Haniyum Maria Khan, A.S.M. Woobaidullah, and Chowdhury Quamruzzaman. 2013. Seismic Interpretation of 2D Data over Kailashtila Gas Field, NE Bangladesh. International Journal of Emerging Technology and Advanced Engineering, 3(11): 489-496

Hiorth A., Cathles L.M., and Madland M.V. 2010. The Impact of Pore Water Chemistry on Carbonate Surface Charge and Oil Wettability. Transport in Porous Media, 85(2010): 1-21.

Honarpour M., Koederitz L., and Harvey A.H. 1986. Relative Permeability of Petroleum Reservoirs. CRC Press Inc., Boca Raton, Florida.

Hoque M. 2009. Petrography and Geochemistry of the Bhuban and Boka Bil Sandstone Formation of the Bandarban Anticline, Chittagong Hill Tracts, Bangladesh: Implications on Provenance and Tectonic Setting. Presented at the National Seminar on Deltas and Other Sedimentary Basins, Their Resource Potential & XXVI Convention. Organized By Delta Studies Institute Andhra University Visakhapatnam, India, 10-12 December

Hossain I., Moniral K., and Zakir H. 2008. Paleoenvironment of the Boka Bil Formation in the Barogang-Hari river section near Lalakhal, Jaintiapur, Sylhet, Bangladesh. Earth Evolution Sciences, 02 (2008): 3-14.

Imam, B., 2013, Energy resources of Bangladesh, Bangladesh University Grants Commission, Dhaka, 324p

Jadhunandan P.P., and Morrow N.R. 1995. Effect of Wettability on Waterflood Recovery for Crude-Oil/Brine/Rock Systems. SPE Reservoir Engineering, 10(1): 40-46.

Jensen J.A., and Radke C.J. 1988. Chromatographic Transport of Alkaline Buffers Through Reservoir Rock. SPERE, 3(3): 849-856.

Jerauld G.R., and Rathmell J.J. 1997. Wettability and Relative Permeability of Prudhoe Bay: A Case Study in Mixed-Wet Reservoirs. SPE Reservoir Engineering, 12(1): 58-65.

Jerauld G.R., Lin C.Y., Webb K.J., and Seccombe J.C. 2008. Modeling Low Salinity Waterflooding. SPE Reservoir Engineering, 11(6): 1000-1012.

Jiang H., Nuryaningsih L., and Adidharma H. 2010. The Effect of Salinity of Injection Brine on WAG Performance in Tertiary Miscible Carbon Dioxide Flooding: Experimental Study. Paper SPE 132369 presented at the Western Regional Meeting, Anaheim, CA, USA, 27-29 May.

Jones F.O. 1964. Influence of Chemical Composition of Water on Clay Blocking of Permeability. JPT, 16(4): 441-446.

Khan M.A.M., Ismail M., and Ahmed M., 1988. Geology and hydrocarbon prospects of Surma Basin, Bangladesh, Proc. 7th offshore Southeast Asia conference, Singapore, pp. 354–387.

Khanam F., 2017, Sedimentologic, Sequence Stratigraphic and Diagenetic History of the Neogene Sedimentary Succession in the Sylhet Trough, Bengal Basin, Bangladesh. PhD thesis, Jahangirnagar University, Savar, Dhaka, Bangladesh, 164p.

Kharaka Y.K., Gunter W.D., Aggarwal P.K., Perkins E.H., and DeBraal J.D. 1988. SOLMINEQ.88: A Computer Program for Geochemical Modeling of Water-Rock Interactions. US Geological Survey, Water Resources Investigation Report 88-4227, Menlo Park, CA.

Khilar K.C., Valdya R.N., and Fogler H.S. 1990. Colloidally Induced Fines Release in Porous Media. Journal of Petroleum Science and Engineering, 4(3): 213-221.

Kia S.F., Fogler H.S., Reed M.G., and Valdya R.N. 1987. Effect of Salt Composition on Clay Release in Berea Sandstones. SPE Production Engineering, 2(4): 277-283.

Korrani A.K.N., Sepehrnoori K., and Delshad M. 2013. A Novel Mechanistic Approach for Modeling Low Salinity Water Injection. Paper SPE 166523 presented at the SPE ATCE, New Orleans, Louisiana, USA, 30 September – 2 October.

Kozaki C. 2012. Efficiency of Low Salinity Polymer Flooding in Sandstone Cores. Master's Thesis, University of Texas at Austin.

Kulkarni M.M., and Rao D.N. 2005. Experimental Investigation of Miscible and Immiscible WAG Process Performance. Journal of Petroleum Science and Engineering, 48(2005): 1-20.

Kumar M., Fogden A., Morrow N.R., and Buckley J.S. 2010. Mechanisms of Improved Oil Recovery from Sandstone by Low Salinity Flooding. Paper SCA 2010-25 presented at the 24th International Symposium of Core Analysts, Halifax, Canada, 4-7 October.

Lager A., Webb K.J., and Black C.J.J. 2007. Impact of Brine Chemistry on Oil Recovery. Paper A24 presented at the 14th EAGE Symposium on Improved Oil Recovery, Cairo, 22-24 April.

Lager A., Webb K.J., Black C.J.J., Singleton M., and Sorbie K.S. 2006. Low-Salinity Oil Recovery – An Experimental Investigation. Paper SCA 2006-36 presented at the International Symposium of the Society of Core Analysts, Trondheim, Norway, 12-16 September.

Lager A., Webb K.J., Black C.J.J., Singleton M., and Sorbie K.S. 2008a. Low-Salinity Oil Recovery – An Experimental Investigation. Petrophysics 49(1): 28-35.

Lager A., Webb K.J., Collins I.R., and Richmond D.M. 2008b. LoSalTM Enhanced Oil Recovery: Evidence of Enhanced Oil Recovery at the Reservoir Scale. Paper SPE 113976 presented at the SPE/DOE Improved Oil Recovery Symposium, Tulsa, 19-23 April.

Lebedeva E.V., and Fogden A. 2010. Adhesion of Oil to Kaolinite in Water. J. Environ. Sci. Technol. 44:9470-9475.

Lever A., and Dawe R.A. 1984. Water Sensitivity and Migration of Fines in the Hopeman Sandstone. Journal of Petroleum Geology, 7(1): 97-107.

Lever A., and Dawe R.A. 1987. Clay Migration and Entrapment in Synthetic Porous Media. Mar. Pet. Geol. 4(2): 112-118.

Leverett M.C. 1941. Capillary Behavior in Porous Solids. Trans, AIME, 142: 152-69.

Li H., Yang C., Fedutenko E., and Nghiem L. 2014 Using Multiple Objective Optimization for SAGD Simulation Numerical Tuning. Paper SPE 170024 presented at the SPE Heavy Oil Conference, Calgary, Alberta, Canada, 10-12 June.

Li, Y-K., and Nghiem L.X. 1986. Phase Equilibria of Oil, Gas, and Water/Brine Mixtures from a Cubic Equation of State and Henry's Law. Can. J. Chem. Eng. 486-496.

Liegthelm D.J., Gronsveld J., Hofman J.P., Brussee N., Marcelis F., and Van der Linde H.A. 2009. Novel Waterflooding Strategy by Manipulation of Injection Brine Composition. Paper SPE 119835 presented at the EUROPEC/EAGE Annual Conference and Exhibition, Amsterdam, 8-11 June.

Loahardjo N., Xie X., and Morrow N.R. 2010. Oil Recovery by Sequential Waterflooding of Mixed-Wet Sandstone and Limestone. Energy & Fuels, 24(9): 5073-5080.

Maas J.G., and Morrow N.R. 2001. Enhanced Oil Recovery by Dilution of Injection Brine: Further Interpretations and Experimental Results. Paper SCA2001-13.

Marion D., Nur A., Yin H., and Han D. 1992. Compressional Velocity and Porosity in Sand-clay Mixtures. Geophysics, 57: 554-563.

Martin J.C. 1957. The Effects of Clay on the Displacement of Heavy Oil by Water. Paper SPE 1411: Caracas, Venezuela, October 14-16.

McGuire P.L., Chatam J.R., Paskvan F.K., Sommer D.M., and Carini F.H. 2005. Low Salinity Oil Recovery: An Exciting New EOR Opportunity for Alaska's North Slope. Paper SPE 93903 presented at the SPE Western Regional Meeting, Irvine, CA, USA, 30 March – 1 April.

Md. Lal Mamud, A. S. M. Woobaidullah, M. A. Baki, Rajib Chandra Chowdhury, Md. Zonaed Hossain Sazal, Md. Shafiqul Islam and Musabbir Ahmed Khan, 2016, Structural modeling of Fenchuganj gas field, Sylhet, Bangladesh, IJETAE, Volume 6, Issue 3, March 2016.

Melberg E. 2010. Experimental Study of Low Salinity EOR Effects from the Varg Field. Master's Thesis, University of Stavanger.

Miller, C. C., A. B., Dyes and C. A. Hutchinson, 1950, Estimation of Permeability and Reservoir Pressure from Bottom-Hole Pressure Build-up Characteristics, Trans., AIME 189, 91-104.

M.M. Rahman, A.S.M. Woobaidullah, B. Imam and M. Rahman, 2012, Evaluation of Reservoir Sands of Habiganj Gas Field on the Basis of Wireline Log Interpretation of Habiganj-7 Well, Dhaka University Journal of Earth and Environmental Sciences , 2(1): 1-8.

Mohammadi H., and Jerauld G.H. 2012. Mechanistic Modeling of the Benefit of Combining Polymer with Low Salinity Water for Enhanced Oil Recovery. Paper SPE 153161 presented at the Eighteenth SPE IOR Symposium, Tulsa, OK, USA, 14-18 April 2012.

Mohan K.K., Vaidya R.N., Reed M.G., and Fogler H.S. 1993. Water Sensitivity of Sandstones Containing Swelling and Non-Swelling Clays. Colloids Surf. A73: 237-254.

Mojarad R.S., and Settari A.T. 2007. Coupled Numerical Simulation of Reservoir Flow with Formation Plugging. Journal of Canadian Petroleum Technology, 46(3): 54-59.

Montes G., Bartolome P., and Udias A.L. 2001. The Use of Genetic Algorithms in Well Placement Optimization. Paper SPE 69439 presented at the SPE Latin American and Caribbean Petroleum Engineering Conference, Buenos Aires, Argentina, 25-28 March.

Morrow N.R., and Bukley J.S. 2011. Improved Oil Recovery by Low-Salinity Waterflooding. JPT, Distinguished Author Series, 106-112.

Morrow N.R., Cram P.J., and McCaffery F.G. 1973. Displacement Studies in Dolomite with Wettability Control by Octanoic Acid. SPE Journal, 13(04): 221-232.

Morrow N.R., Tang G.Q., Valat M., and Xie X. 1998. Prospects of Improved Oil Recovery Related to Wettability and Brine Composition. Journal of Petroleum and Engineering, 20(3-4): 267-276.

Mugele F., Siretanu I., Kumar N., Bera B., Wang L., Maestro A., Duits M., and Van Den Ende D. 2014. Charge Control and Wettability Alteration at Solid-Liquid Interfaces. Paper SPE 169143 presented at the SPE IOR conference, Tulsa, OK, USA, 12-16 April.

Narender P. 2004. Sedimentology of the Bokabil Formation of Cachar, Assam-Arakan Fold Belt, presented at the 2nd conference of the Association of Petroleum Geologists, India, 1-2 January.

Nasralla R.A., Alotaibi M.B., and Nasr-El-Din H.A. 2011. Efficiency of Oil Recovery by Low Salinity Waterflooding in Sandstone Reservoir. Paper SPE 144602 presented at the SPE Western North American Region Meeting, Alaska, USA.

Nasralla R.A., Bataweel M.A., and Nasr-El-Din H.A. 2011. Investigation of Wettability Alteration by Low Salinity Waterflooding in Sandstone Rock. Paper SPE 146322 presented at Offshore Europe Meeting, Aberdeen, UK.

Nasralla R.A., and Nasr-El-Din H.A. 2012. Double-Layer Expansion: Is it a Primary Mechanism of Improved Oil Recovery by Low Salinity Waterflooding? Paper SPE 154334 presented at the SPE Improved Oil Recovery Symposium, Tulsa, OK, USA.

Nghiem L.X., and Rozon B.J. 1988 & 1989. A Unified Approach for Handling and Solving Large Systems of Equations in Reservoir Simulation. Proceedings of the First and Second International Forum on Reservoir Simulation, Alpbach, Austria.

Nghiem L.X., Sammon P., Grabenstetter J., and Ohkuma H. 2004a. Modeling CO2 Storage in Aquifers with Fully-Coupled Geochemical EOS Compositional Simulator. Paper SPE 89474 presented at the SPE Fourteenth Symposium on Improved Oil Recovery, Tulsa, OK, USA, April 17-21.

Nghiem L.X., Sammon P., Kohse B., and Hassam, M. 2005. Modeling CO2 Storage and CO2 Advanced Recovery Processes. 8th International Forum on Reservoir Simulation, Stresa, Italy, June 20-24.

Nghiem L.X., Shrivastava V., and Kohse B. 2011. Modeling Aqueous Phase Behavior and Chemical Reactions in Compositional Simulation. Paper SPE 141417 SPE Reservoir Simulation Symposium, The Woodlands, TX, USA, February 21-23.

Nghiem L.X., Shrivastava V., Kohse B., and Sammon P. 2004b. Simulation of CO2 EOR and Sequestration Processes with a Geochemical EoS Compositional Simulator. Paper CIPC 2004-051 presented at the Petroleum Society's 5th Canadian International Conference, Calgary, AB, June 8-10.

Nghiem L.X., Yang C., Shrivastava V., Kohse B., Hassam M., Chen D., and Card C. 2009. Optimization of Residual Gas and Solubility Trapping for CO2 Sequestration in Saline Aquifers. Paper SPE 119080 presented at the SPE Reservoir Simulation Symposium, The Woodlands, TX, USA, February 2-4.

Nguyen T.B.N., Tu N.T., Bae W., Dang T.Q.C., Chung T., and Nguyen X.H. 2012. Gelation Time Optimization for an HPAM/Chromium Acetate System: The Successful Key of Conformance Control Technology. Energy Sources, Part A, 34(14): 1305-1317.

Nguyen T.B.N., Chen Z., Nghiem L.X., Dang T.Q.C., and Yang C. 2014. A New Approach for Optimization and Uncertainty Assessment of Surfactant-Polymer Flooding. Paper SPE 172003 presented at the Abu Dhabi International Petroleum Exhibition and Conference, Abu Dhabi, UAE, 10-13 November.

Omekeh A., Friis A.H., and Evje S. 2012. Modeling of Ion-Exchange and Solubility in Low Salinity Waterflooding. Paper SPE 154144 presented at the Eighteenth SPE IOR Symposium, Tulsa, OK, USA, 14-18 April 2012.

Ozdogan U., Sahni A., Yeten B., Guyaguler B., and Chen W.H. 2005. Efficient Assessment and Optimization of a Deep Water Asset Development Using Fixed Pattern Approach. Paper SPE 95792 presented at the SPE Annual Technical Conference and Exhibition, Dallas, Texas, USA, 9-12 October.

Parkhurst D.L., and Appelo C.A.J. 1999. User's Guide to PHREEQC (Version 2) – A Computer Program for Speciation, Batch-Reaction, One-Dimensional Transport, and Inverse Geochemical Calculations. U.S. Geological Survey, Water Resources Investigation Report 99-4259, Denver, Colorado.

Peters L., Arts R., Brouwer G., and Geel C. 2009. Results of the Brugge Benchmark Study for Flooding Optimisation and History Matching. Paper SPE 119094 presented at the SPE Reservoir Simulation Symposium, The Woodlands, Texas, February 2-4.

Pu H., Xie X., Yin P. and Morrow N.R., 2008. Application of coal bed methane water to oil recovery by low salinity waterflooding, Paper SPE 113410 presented at the 2008 SPE Improved Oil Recovery Symposium, Tulsa, OK, USA.

Puntervold T. 2008. Waterflooding of Carbonate Reservoirs EOR by Wettability Alteration. Doctoral Dissertation, University of Stavanger.

Pursley S.A., Healy R.N., and Sandvik E.I. 1973. A Field Test of Surfactant Flooding, Loudon, Illinois. JPT (July), 793-803

Ramez A.N., Bataweel M.A., and Nasr-El-Din H.A. 2011. Investigation of Wettability Alteration by Low Salinity. Paper SPE 146322 presented at the Offshore Europe, UK, 6-8 September.

Ramey H. J., Jr, 1992, Advances in Practical Well-Test Analysis, J. Pet. Tech. 650-659.

Rezaei Doust A., Puntervold T., Strand S., and Austad T. 2009. Smart Water as Wettability Modifier in Carbonate and Sandstone: A Discussion of Similarities/Differences in Chemical Mechanism. Energy & Fuels 23(9): 4479-4485.

Rivet S.M., Lake L.W., and Pope G.A. 2010. A Coreflood Investigation of Low Salinity Enhanced Oil Recovery. Paper SPE 134297 presented at the SPE ATCE, Florence, Italy, 19-22 September.

Rivet, S.M. 2009. Coreflooding Oil Displacements with Low Salinity Brine. Master's Thesis, University of Texas at Austin.

Robertson E.P. 2010. Oil Recovery Increases by Low Salinity Flooding: Minnelusa and Green River Formations. Paper SPE 132154 presented at the SPE Annual Technical Conference and Exhibition, Florence, Italy, 19-22 September.

Rousseau D., Latifa H., and Nabza L. 2008. Injectivity Decline from Produced Water Reinjection: New Insights on In-depth Particle-deposition Mechanisms. SPE Prod. Oper. 23(4): 525-531.

Rueslatten H.G., Hjelmeland O., and Selle O.M. 1994. Wettability of Reservoir Rocks and The Influence of Organo-metallic Compounds. North Sea Oil and Gas Reservoir III, Kluwer Academic Publishers, 317-324.

Ruhovets N., and Fertl W.H. 1982. Volumes, Types and Distribution of Clay Minerals in Reservoir Rocks Based on Well Logs. Paper SPE 10796 presented at the SPE Uncoventional Gas Recovery Symposium, Dallas, TX, USA, May, 16-18.

Ryan J.N., and Gschwend P.M. 1994. Effect of Solution Chemistry on Clay Colloid Release from an Iron Oxide-coated Aquifer Sand. Environ. Sci. Technol. 28(9): 1717-1726.

Sarma P., and Chen W. 2008a. Efficient Well Placement Optimization with Gradient-Based Algorithms and Adjoint Models. Paper SPE 112257 presented at the SPE Intelligent Energy Conference and Exhibition, Amsterdam, Netherlands, 25-27 February.

Sarma P., and Chen W. 2008b. Applications of Optimal Control Theory for Efficient Production Optimization of Realistic Reservoirs. Paper SPE 12480 presented at the IPTC conference, Kuala Lumpur, Malaysia, 3-5 December.

Seccombe J., Lager A., Jerauld G.R., Jhavier B., Buikema T., Bassler S., Denis J., Webb K., Cockin A., and Fueg E. 2010. Demonstration of Low Salinity EOR at Interwell Scale, Endicott Field, Alaska. Paper SPE 129692 presented at SPE/DOE Improved Oil Recovery Symposium, Tulsa, 24-28 April.

Seilsepour M., and Rashidi M. 2008. Prediction of Soil Cation Exchange Capacity Based on Some Soil Physical and Chemical Properties. World Applied Science Journal 3(2): 200-205.

Shahin A., Tatham R., Stoffa P., and Spikes K. 2011. Optimal Dynamic Rock-fluid Physics Template Validated by Petroelastic Reservoir Modeling. Geophysics, 76(6): 45-58.

Shamsuddin A., and Khan I., 1991. Geochemical criteria of migration of natural gases in the Miocene sediments of the Bengal Foredeep, Bangladesh. Journal of Southeast Asian Earth Sciences, 5 (4): 89-100

Shapiro, A., and Stenby, E. 2000. Factorization of Transport Coefficients in Macroporous Media. Transp. Porous Media 41(3): 305-323.

Shapiro, A., and Stenby, E. 2002. Multicomponent Adsorption: Principles and Models. In: Toth, J.(Ed), Adsorption: Theory, Modeling, and Analysis. Marcel Dekker, NY, p.375.

Sharma, M.M., and Yortsos Y.C. 1987. Fines Migration in Porous Media. AICHE J. 33(10): 1654-1662.

Sheng J.J. 2014. Critical Review of Low-Salinity Waterflooding. J. Petrol. Sci. Eng, http://dx.doi.org/10.1016/j.petrol.2014.05.026

Shofiqul I., Mosarraf H., Yeasmin N., Shahedul H., Shirin A., and Jamiul K. 2015. Geochemical Analysis of the Reservoir Rocks of Surma Basin, Bangladesh. Geosciences, 5(1): 1-7.

Sincock K.J., and Black C.J.J. 1988. Validation of Water/Oil Displacement Scaling Criteria Using Microvisualization Techniques. Paper SPE 18294 presented at the SPE Annual Technical Conference and Exhibition, Houston, TX, 2-5 October.

Skrettingland K., Holt T., Tweheyo M.T., and Skjevrak. 2010. Snorre Low Salinity Water Injection – Core Flooding Experiments and Single Well Field Pilot. Paper SPE 129877 presented at the SPE Improved Oil Recovery Symposium, Tulsa, OK, USA, 24-28 April.

Sorbie K.S., and Collins I.R. 2010. A Proposed Pore-Scale Mechanism for How Low Salinity Waterflooding Works. Paper SPE 129833 presented at the SPE IOR, Tulsa, OK, USA, 24-28 April.

Soyster A.L. 1973. Convex Programming with Set-inclusive Constraints and Applications to Inexact Linear Programming. Operations Research, 21: 1154-1157.

Spall J.C. 2003. Introduction to Stochastic Search and Optimization: Estimation, Simulation, and Control. Wiley, Hoboken, New Jersey.

Spildo K., Johannessen A.M., and Skauge A. 2012. Low Salinity Waterflood at Reduced Capillarity. Paper SPE 154236 presented at the Eighteenth SPE IOR Symposium, Tulsa, OK, USA, 14-18 April.

Strand S. 2005. Wettability Alteration in Chalk, A Study of Surface Chemistry. Doctoral Dissertation, University of Stavanger.

Suijkerbuijk B.M.J.M., Hofman J.P., Ligthelm D.J., Romanuka J., Brussee H.A., and Marcelis A.H.M. 2012. Fundamental Investigation into Wettability and Low Salinity Waterflooding by Parameter Isolation. Paper SPE 154204 presented at the Eighteenth SPE Improved Oil Recovery Symposium, Tulsa, OK, USA, April 14-18.

Suijkerbuijk B.M.J.M., Sorop T.G., Parker A.R., Masalmeh S.K., Chmuzh I.V., Karpan V.M., Volokitin Y.E., and Skripkin A.G. 2014. Low Salinity Waterflooding at West Salym: Laboratory Experiments and Field Forecasts. Paper SPE 169691 presented at the SPE EOR Conference at Oil and Gas West Asia, Muscat, Oman.

Sutanto E., Davis H.T., and Scriven L.E. 1990. Liquid Distribution in Porous Rock Examined by Cryo Scanning Electron Microscopy. Paper SPE 20518 presented at the SPE Annual Technical Conference and Exhibition, New Orleans, Louisiana, USA, 23-26 September.

Tang G.Q., and Morrow N.R. 1997. Salinity, Temperature, Oil Composition and Oil Recovery by Waterflooding. SPE Reservoir Engineering, 12(4): 269-276.

Tang G.Q., and Morrow N.R. 1999a. Influence of Brine Composition and Fines Migration on Crude Oil/Brine/Rock Interactions and Oil Recovery. Journal of Petroleum Science and Engineering, 24(2-4): 99-111.

Tang G.Q., and Morrow N.R. 1999b. Oil Recovery by Waterflooding and Imbibition – Invading Brine Cation Valency and Salinity. Paper SCA-9911 presented at the 1999 International Symposium of the Society of Core Analysis, Golden, Colorado, USA, 1-4 August.

Teklu T.W., Alameri W., Graves M.R., Kazemi H., and Alsumaiti A.M. 2014. Low Salinity Water Alternating CO2 Flooding Enhanced Oil Recovery Theory and Experiments. Paper SPE 171767 presented at the Abu Dhabi International Petroleum Exhibition and Conference, Abu Dhabi, UAE, 10-13 November.

Thibeau, S., Nghiem, L.X., and Ohkuma, H. 2007. A Modeling Study of the Role of Selected Minerals in Enhancing CO2 Mineralization during CO2 Aquifer Storage. Paper SPE 109739 presented at the SPE Annual Technical Conference and Exhibition, Anaheim, CA, USA, November 11-14.

Thomas C.E., Mahoney C.F., and Winter G.W. 1962. Water-Injection Pressure Maintenance and Waterflooding Processes. Chapter 44, Petroleum Engineering Handbook, Society of Petroleum Engineers.

Thomas E.C., and Stieber S.J. 1975. The Distribution of Shale in Sandstones and Its Effect Upon Porosity. Paper T, in 16th Annual Logging Symposium Transactions: Society of Professional Well Log Analysts.

Thyne G., and Gamage P. 2011. Evaluation of the Effect of Low Salinity Waterflooding for 26 Fields in Wyoming. Paper SPE 147410 presented at the SPE Annual Technical Conference and Exhibition, Denver, Colorado, USA, 30 October-2 November.

Tufenkji N. 2007. Colloid and Microbe Migration in Granular Environments: A Discussion of Modeling Methods. In: Frimmel, F.H., von der Kammer, F., Flemming, F.-C.(Eds.), Colloidal Transport in Porous Media. Springer-Verlag, Berlin, 119-142.

Trantham J.C., Patterson H.L., and Boneau D.F. 1978. The North Burbank Unit, Tract 97 Surfactant/Polymer Pilot – Operation and Control. JPT (July), 1068-1074

Ursin J.R., and Zolotukhin A.B. 1997. Introduction to Petroleum Reservoir Engineering. Hoyskoleforlaget AS.

Valdya R.N., and Fogler H.S. 1992. Fines Migration and Formation Damage: Influence of pH and Ion Exchange. SPE Prod. Eng, 7(4): 325-330.

Van Essen G.M., Zandvliet M.J., Van den Hof P.M.J., Bosgra O.H., and Jansen J.D. 2006. Robust Waterflooding Optimization of Multiple Geological Scenarios. Paper SPE 102913 presented at the SPE Annual Technical Conference and Exhibition, San Antonio, TX, USA, 24-27 September.

Verbeek P., and Matzakos A. 2009. Water Treatment for Flooding with Lower Salinity than Formation Water. Presentation at the Tekna Produced Water Conference, Stavanger, 11-13 January.

Verwey E.J., and Overbeek T.G. 1948. Theory of the Stability of Lyophobic Colloids. Elsvier, New York.

Vledder P., Foncesca J.C., Wells T., Gonzalez I., and Ligthelm D. 2010. Low Salinity Waterflooding: Proof of Wettability Alteration on a Field Wide Scale. Paper SPE 129564 presented at the SPE Improved Oil Recovery Symposium, Tulsa, OK, USA, 24-28 April.

Wang C., and Li G. 2007. Optimal Well Placement for Production Optimization. Paper SPE 111154 presented at the Eastern Regional Meeting, Lexington, Kentucky, USA, 17-19 October.

Webb K.J., Black C.J.J., and Al-Ajeel. 2004. Low Salinity Oil Recovery – Log-Inject-Log. Paper SPE 89379 presented at the SPE/DOE Symposium on Improved Oil Recovery, Tulsa, 17-21 April.

Webb K.J., Black C.J.J., and Edmonds I.J. 2005. Low Salinity Oil Recovery: The Role of Reservoir Condition Corefloods. Paper C18 presented at the 13th EAGE Symposium on Improved Oil Recovery, Budapest, Hungary, 25-27 April.

Webb K.J., Lager A., and Black C.J.J. 2008. Comparison of High/Low Salinity Water/Oil Relative Permeability. Presented at the International Symposium of the Society of Core Analysts, Abu Dhabi, UAE, 29 October – 2 November.

Welge J.H. 1952. A Simplified Method for Computing Oil Recoveries by Gas or Water Drive. Trans, AIME, 1952, 195: 91-98.

Wu Y.S., and Bai B. 2009. Efficient Simulation for Low Salinity Waterflooding in Porous and Fractured Reservoirs. Paper SPE 118830 presented at the SPE Reservoir Simulation Symposium, Woodlands, TX, USA, 2-4 February.

Yang C., Card C., and Nghiem L. 2009. Economic Optimization and Uncertainty Assessment of Commercial SAGD Operations. Journal of Canadian Petroleum Technology, 48(9): 33-40.

Yang C., Nghiem L., and Card C. 2007. Reservoir Model Uncertainty Quantification through Computer Assisted History Matching. Paper SPE 109825 presented at the SPE Annual Technical Conference an Exhibition, Anaheim, California, USA, 11-14 November.

Yang C., Card C., and Nghiem L. 2011. Robust Optimization of SAGD Operations under Geological Uncertainties. Paper SPE 141676 presented at the SPE Reservoir Simulation Symposium, The Woodlands, Texas, USA, 21-23 February.

Yasari E., Pishvaie M.R., Khorasheh F., Salahshoor K., and Kharrat R. 2013. Application of Multi-Criterion Robust Optimization in Water-flooding of Oil Reservoir. Journal of Petroleum Science and Engineering, 109(2013): 1-11.

Yildiz H.O., and Morrow N.R. 1996. Effect of Brine Composition on Recovery of Moutray Crude Oil by Waterflooding. Journal of Petroleum Science and Engineering, 14: 159-168.

Yousef A., and Ayirala S.C. 2014. A Novel Water Ionic Composition Optimization Technology for Smart Water Flooding Application in Carbonate Reservoirs. Paper SPE 169052 presented at the SPE IOR Symposium, Tulsa, OK, USA, 12-16 April.

Yousef A., Liu J., Blanchard G., Al-Saleh S., Al-Zahrani R., Al-Tammar H., and Al-Mulhim N. 2012. Smart Water Flooding: Industry’s First Field Test in Carbonate Reservoirs. Paper SPE 159526 presented at the SPE Annual Technical Conference and Exhibition, Texas, USA, 8-10 October.

Yuan H., and Shapiro A.A. 2011. Induced Migration of Fines During Waterflood in Communicating Layer-Cake Reservoirs. Journal of Petroleum Science and Engineering, 78(2011): 618-626.

Zeinijahromi A., Machado F., and Bedrikovetsky P. 2011. Modified Mathematical Model for Fines Migration in Oilfields. Paper SPE 143742 presented at the Brasil Offshore Conference and Exhibition, Brazil, 14-17 June.

Zekri A.Y., Nasr M.S., and Al-Arabai Z. 2011. Effect of LoSal on Wettability and Oil Recovery of Carbonate and Sandstone Formation. Paper SPE 14131 presented at the International Petroleum Technology Conference, Bangkok, Thailand, 7-9 February.

Zhang Y., and Morrow N.R. 2006. Comparison of Secondary and Tertiary Recovery with Change in Injection Brine Composition for Crude Oil/ Sandstone Combinations. Paper SPE 99757 presented at the SPE/DOE Symposium on Improved Oil Recovery, Tulsa, 22-26 April.

Zhang Y., Xie X., and Morrow N.R. 2007. Waterflood Performance by Injection of Brine with Different Salinity for Reservoir Cores. Paper SPE 109849 presented at the SPE Annual Technical Conference and Exhibition, Anaheim, CA, USA, 11-14 November.

Zolfaghari, H., Zebarjadi, A., Shahrokhi, O., and Ghazanfari, M.H. 2013. An Experimental Study of CO2 Low Salinity WAG Injection in Sandstone Heady Oil Reservoirs. Iranian Journal of Oil & Gas Science and Technology, 2(3): 37-47.

Reports:

Intercomp-Kanata Management Ltd., 1991, Gas Field Appraisal Project Geological, Geophysical and Petrophysical Report of Kailashtila Gas Field, Additional Sands, Bangladesh.

Intercomp-Kanata Management Ltd., 1989, Second Gas Development Project Summary of Introduction, Recommendations and Conclusions on Geology, Reservoir Engineering and Facilities of Kailashtila Gas Field, Bangladesh.

International Drilling Fluids, IDF, 1982

Kailashtila Geological Study Report by RPS Energy (2009)

Sylhet Geological Study Report by RPS Energy (2009)

Web Resources:

http://sgfl.org.bd/Haripur%20field.htm

http://sgfl.org.bd/KTL%20field.htm

http://www.spe.org

APPENDICES

APPENDIX A

PVT Properties Reports of Haripur Oil Sample

A1.Report on Saturation Pressure Calculation
A2.Report on Bubble Point Pressure Calculation
A3.Report on Constant Composition Expansion
A4.Report on Differential Liberation
A5.Report on Compositional Grading Experiment
A6.Report on Separators Test
A7.Oil PVT Properties Report and Gas PVT Properties Report

A1. Expt PSAT1 : Saturation Pressure Calculation

Peng-Robinson (3-Parm) on ZI with PR corr.
Lohrenz-Bray-Clark Viscosity Correlation

Specified temperature	Deg F	220.0000
Calculated bubble point pressure	PSIA	2990.0849
Observed bubble point pressure	PSIA	2990.0000

Fluid properties		Liquid	Vapour
		Calculated	Calculated
Mole Weight		118.0626	18.1805
Z-factor		1.1309	1.1309
Viscosity		0.3444	0.0188
Density	LB/FT3	42.7958	7.9236
Molar Vol	CF/LB-ML	2.7587	2.2945

Molar Distributions Components		Total, Z	Liquid,X	Vapour,Y	K-Values
Mnemonic	Number	Measured	Calculated	Calculated	Calculated
CO2	1	0.2873	0.2873	0.3823	1.3308
N2	2	0.3078	0.3078	1.0460	3.3980
C1	3	42.6014	42.6014	90.7377	2.1299
C2	4	5.2328	5.2328	5.2463	1.0026
C3	5	1.9392	1.9392	1.2314	0.6350
IC4	6	0.8208	0.8208	0.3638	0.4431
NC4	7	0.9747	0.9747	0.3707	0.3803
IC5	8	0.5438	0.5438	0.1499	0.2756
NC5	9	0.4925	0.4925	0.1226	0.2489
C6	10	1.6930	1.6930	0.2661	0.1572
C7+	11	45.1066	45.1066	0.0833	0.0018
Composition Total		100.0000	100.0000	100.0000	

A2. Expt BUBBLE1 : Bubble Point Pressure Calculation

Peng-Robinson (3-Parm) on ZI with PR corr.
Lohrenz-Bray-Clark Viscosity Correlation

Specified temperature	Deg F	220.0000
Calculated bubble point pressure	PSIA	2990.0849
Observed bubble point pressure	PSIA	2990.0000

Fluid properties		Liquid		Vapour
		Observed	Calculated	Calculated
Mole Weight			118.0626	18.1805
Z-factor			1.1309	0.9406
Viscosity			0.3444	0.0188
Density	LB/FT3	42.7953	42.7958	7.9236
Molar Vol	CF/LB-ML		2.7587	2.2945

Molar Distributions Components		Total, Z	Liquid,X	Vapour,Y	K-Values
Mnemonic	Number	Measured	Calculated	Calculated	Calculated
CO2	1	0.2873	0.2873	0.3823	1.3308
N2	2	0.3078	0.3078	1.0460	3.3980
C1	3	42.6014	42.6014	90.7377	2.1299
C2	4	5.2328	5.2328	5.2463	1.0026
C3	5	1.9392	1.9392	1.2314	0.6350
IC4	6	0.8208	0.8208	0.3638	0.4431
NC4	7	0.9747	0.9747	0.3707	0.3803
IC5	8	0.5438	0.5438	0.1499	0.2756
NC5	9	0.4925	0.4925	0.1226	0.2489
C6	10	1.6930	1.6930	0.2661	0.1572
C7+	11	45.1066	45.1066	0.0833	0.0018
Composition Total		100.0000	100.0000	100.0000	

A3. Expt CCE1 : Constant Composition Expansion

Peng-Robinson (3-Parm) on ZI with PR corr.
Lohrenz-Bray-Clark Viscosity Correlation
Density units are LB/FT3
Specific volume units are CF/LB-ML
Viscosity units are CPOISE
Surface Tension units are DYNES/CM

Specified temperature Deg F 220.0000

Liq Sat calc. is Vol oil/Vol Fluid at Sat. Vol

Pressure PSIA	Inserted Point	Rel Volume Observed	Rel Volume Calculated	Vap Mole Frn Calculated	Liq Density Calculated
5000.000		0.9755	0.9755		43.8687
4798.999		0.9776	0.9776		43.7756
4597.999		0.9798	0.9798		43.6799
4396.999		0.9820	0.9820		43.5812
4195.999		0.9843	0.9843		43.4796
3994.998		0.9867	0.9867		43.3747
3793.998		0.9891	0.9891		43.2665
3592.998		0.9917	0.9917		43.1547
3391.998		0.9943	0.9943		43.0392
3190.998		0.9971	0.9971		42.9196
2990.084	- Psat		1.0000		42.7958
2989.997		1.0000	1.0000	1.7589E-05	42.7959
2692.467		1.0338	1.0338	0.0582	43.2584
2394.937		1.0783	1.0783	0.1140	43.7244
2097.407		1.1386	1.1387	0.1676	44.1953
1799.877		1.2233	1.2233	0.2192	44.6727
1502.346		1.3477	1.3477	0.2694	45.1589
1204.816		1.5426	1.5426	0.3182	45.6571
907.286		1.8800	1.8800	0.3664	46.1728
609.756		2.5749	2.5749	0.4149	46.7171
312.226		4.6773	4.6774	0.4662	47.3198

Pressure PSIA	Inserted Point	Vap Density Calculated	Liq Z-Fac Calculated	Vap Z-Fac Calculated	Surf Tension Calculated
5000.000			1.8449		
4798.999			1.7745		
4597.999			1.7039		
4396.999			1.6331		
4195.999			1.5621		
3994.998			1.4909		
3793.998			1.4194		
3592.998			1.3477		

3391.998			1.2757		
3190.998			1.2035		
2990.084	- Psat	7.9236	1.1309	0.9406	2.9751
2989.997		7.9234	1.1309	0.9406	2.9753
2692.467		7.1828	1.0602	0.9329	3.5787
2394.937		6.4237	0.9831	0.9275	4.2916
2097.407		5.6479	0.8990	0.9246	5.1293
1799.877		4.8583	0.8071	0.9244	6.1067
1502.346		4.0592	0.7063	0.9272	7.2378
1204.816		3.2556	0.5955	0.9333	8.5350
907.286		2.4528	0.4731	0.9428	10.0090
609.756		1.6547	0.3371	0.9559	11.6720
312.226		0.8612	0.1846	0.9734	13.5484

Pressure PSIA	Inserted Point	Liq Sat Calculated	Liq Visc Calculated	Vap Visc Calculated	Liq Mole Wt Calculated
5000.000		1.0000	0.4202		118.0626
4798.999		1.0000	0.4128		118.0626
4597.999		1.0000	0.4054		118.0626
4396.999		1.0000	0.3980		118.0626
4195.999		1.0000	0.3905		118.0626
3994.998		1.0000	0.3829		118.0626
3793.998		1.0000	0.3753		118.0626
3592.998		1.0000	0.3677		118.0626
3391.998		1.0000	0.3600		118.0626
3190.998		1.0000	0.3522		118.0626
2990.084	- Psat	1.0000	0.3444	0.0188	118.0626
2989.997		1.0000	0.3444	0.0188	118.0643
2692.467		0.9804	0.3641	0.0179	124.2385
2394.937		0.9616	0.3849	0.0171	130.9147
2097.407		0.9434	0.4067	0.0163	138.1708
1799.877		0.9256	0.4296	0.0156	146.1056
1502.346		0.9082	0.4535	0.0150	154.8498
1204.816		0.8909	0.4780	0.0145	164.5857
907.286		0.8734	0.5029	0.0140	175.5923
609.756		0.8552	0.5273	0.0136	188.3650
312.226		0.8345	0.5502	0.0133	204.0791

Pressure PSIA	Inserted Point	Vap Mole Wt Calculated	Liq Mol Vol Calculated	Vap Mol Vol Calculated
5000.000			2.6913	
4798.999			2.6970	
4597.999			2.7029	
4396.999			2.7090	
4195.999			2.7154	
3994.998			2.7219	

3793.998		2.7287		
3592.998		2.7358		
3391.998		2.7431		
3190.998		2.7508		
2990.084 - Psat	18.1805	2.7587	2.2945	
2989.997	18.1805	2.7588	2.2945	
2692.467	18.1527	2.8720	2.5272	
2394.937	18.1447	2.9941	2.8246	
2097.407	18.1588	3.1264	3.2152	
1799.877	18.1990	3.2706	3.7460	
1502.346	18.2728	3.4290	4.5016	
1204.816	18.3939	3.6048	5.6499	
907.286	18.5893	3.8029	7.5790	
609.756	18.9212	4.0320	11.4348	
312.226	19.5839	4.3128	22.7393	

Molar Distributions K-Values Inserted Point	Com(1 ,CO2) Calculated	Com(2 ,N2) Calculated	Com(3 ,C1) Calculated	Com(4 ,C2) Calculated
5000.000	1.0000	1.0000	1.0000	1.0000
4798.999	1.0000	1.0000	1.0000	1.0000
4597.999	1.0000	1.0000	1.0000	1.0000
4396.999	1.0000	1.0000	1.0000	1.0000
4195.999	1.0000	1.0000	1.0000	1.0000
3994.998	1.0000	1.0000	1.0000	1.0000
3793.998	1.0000	1.0000	1.0000	1.0000
3592.998	1.0000	1.0000	1.0000	1.0000
3391.998	1.0000	1.0000	1.0000	1.0000
3190.998	1.0000	1.0000	1.0000	1.0000
2990.084 - Psat	1.3308	3.3980	2.1299	1.0026
2989.997	1.3308	3.3981	2.1300	1.0026
2692.467	1.4012	3.7470	2.2867	1.0335
2394.937	1.4907	4.1839	2.4824	1.0746
2097.407	1.6078	4.7462	2.7339	1.1304
1799.877	1.7663	5.4962	3.0691	1.2088
1502.346	1.9913	6.5449	3.5382	1.3238
1204.816	2.3325	8.1134	4.2409	1.5031
907.286	2.9050	10.7127	5.4081	1.8108
609.756	4.0486	15.8540	7.7221	2.4360
312.226	7.3988	30.8250	14.4716	4.2879

Molar Distributions K-Values Inserted Point	Com(5 ,C3) Calculated	Com(6 ,IC4) Calculated	Com(7 ,NC4) Calculated	Com(8 ,IC5) Calculated
5000.000	1.0000	1.0000	1.0000	1.0000
4798.999	1.0000	1.0000	1.0000	1.0000
4597.999	1.0000	1.0000	1.0000	1.0000

4396.999	1.0000	1.0000	1.0000	1.0000
4195.999	1.0000	1.0000	1.0000	1.0000
3994.998	1.0000	1.0000	1.0000	1.0000
3793.998	1.0000	1.0000	1.0000	1.0000
3592.998	1.0000	1.0000	1.0000	1.0000
3391.998	1.0000	1.0000	1.0000	1.0000
3190.998	1.0000	1.0000	1.0000	1.0000
2990.084 - Psat	0.6350	0.4431	0.3803	0.2756
2989.997	0.6350	0.4431	0.3803	0.2756
2692.467	0.6352	0.4329	0.3688	0.2612
2394.937	0.6394	0.4248	0.3591	0.2481
2097.407	0.6496	0.4198	0.3521	0.2368
1799.877	0.6692	0.4197	0.3491	0.2280
1502.346	0.7042	0.4276	0.3526	0.2231
1204.816	0.7662	0.4494	0.3673	0.2247
907.286	0.8823	0.4987	0.4039	0.2383
609.756	1.1316	0.6148	0.4933	0.2801
312.226	1.8936	0.9864	0.7839	0.4272

Molar Distributions K-Values Inserted Point	Com(9 ,NC5) Calculated	Com(10,C6) Calculated	Com(11,C7+) Calculated
5000.000	1.0000	1.0000	1.0000
4798.999	1.0000	1.0000	1.0000
4597.999	1.0000	1.0000	1.0000
4396.999	1.0000	1.0000	1.0000
4195.999	1.0000	1.0000	1.0000
3994.998	1.0000	1.0000	1.0000
3793.998	1.0000	1.0000	1.0000
3592.998	1.0000	1.0000	1.0000
3391.998	1.0000	1.0000	1.0000
3190.998	1.0000	1.0000	1.0000
2990.084 - Psat	0.2489	0.1572	0.0018
2989.997	0.2489	0.1572	0.0018
2692.467	0.2345	0.1445	0.0013
2394.937	0.2213	0.1329	0.0009
2097.407	0.2097	0.1224	0.0006
1799.877	0.2005	0.1135	0.0004
1502.346	0.1947	0.1066	0.0002
1204.816	0.1945	0.1027	0.0001
907.286	0.2045	0.1039	9.2305E-05
609.756	0.2382	0.1162	6.3421E-05
312.226	0.3599	0.1679	5.4478E-05

Molar Distributions Liquid, X Inserted Point	Com(1 ,CO2) Calculated	Com(2 ,N2) Calculated	Com(3 ,C1) Calculated	Com(4 ,C2) Calculated

5000.000	0.2873	0.3078	42.6014	5.2328
4798.999	0.2873	0.3078	42.6014	5.2328
4597.999	0.2873	0.3078	42.6014	5.2328
4396.999	0.2873	0.3078	42.6014	5.2328
4195.999	0.2873	0.3078	42.6014	5.2328
3994.998	0.2873	0.3078	42.6014	5.2328
3793.998	0.2873	0.3078	42.6014	5.2328
3592.998	0.2873	0.3078	42.6014	5.2328
3391.998	0.2873	0.3078	42.6014	5.2328
3190.998	0.2873	0.3078	42.6014	5.2328
2990.084 - Psat	0.2873	0.3078	42.6014	5.2328
2989.997	0.2873	0.3078	42.6005	5.2328
2692.467	0.2807	0.2654	39.6326	5.2226
2394.937	0.2721	0.2259	36.4442	5.1887
2097.407	0.2607	0.1891	33.0110	5.1209
1799.877	0.2460	0.1550	29.3064	5.0037
1502.346	0.2268	0.1234	25.3025	4.8131
1204.816	0.2017	0.0943	20.9717	4.5107
907.286	0.1692	0.0675	16.2897	4.0343
609.756	0.1268	0.0430	11.2435	3.2791
312.226	0.0721	0.0207	5.8512	2.0659

Molar Distributions Liquid, X Inserted Point	Com(5 ,C3) Calculated	Com(6 ,IC4) Calculated	Com(7 ,NC4) Calculated	Com(8 ,IC5) Calculated
5000.000	1.9392	0.8208	0.9747	0.5438
4798.999	1.9392	0.8208	0.9747	0.5438
4597.999	1.9392	0.8208	0.9747	0.5438
4396.999	1.9392	0.8208	0.9747	0.5438
4195.999	1.9392	0.8208	0.9747	0.5438
3994.998	1.9392	0.8208	0.9747	0.5438
3793.998	1.9392	0.8208	0.9747	0.5438
3592.998	1.9392	0.8208	0.9747	0.5438
3391.998	1.9392	0.8208	0.9747	0.5438
3190.998	1.9392	0.8208	0.9747	0.5438
2990.084 - Psat	1.9392	0.8208	0.9747	0.5438
2989.997	1.9392	0.8208	0.9748	0.5438
2692.467	1.9813	0.8489	1.0119	0.5682
2394.937	2.0223	0.8784	1.0515	0.5948
2097.407	2.0602	0.9092	1.0934	0.6235
1799.877	2.0908	0.9405	1.1370	0.6546
1502.346	2.1071	0.9705	1.1806	0.6877
1204.816	2.0951	0.9952	1.2205	0.7219
907.286	2.0266	1.0055	1.2472	0.7543
609.756	1.8388	0.9770	1.2342	0.7754
312.226	1.3689	0.8261	1.0840	0.7420

Molar Distributions Liquid, X Inserted	Com(9 ,NC5)	Com(10,C6)	Com(11,C7+)	Total

Point	Calculated	Calculated	Calculated	Calculated
5000.000	0.4925	1.6930	45.1066	100.0000
4798.999	0.4925	1.6930	45.1066	100.0000
4597.999	0.4925	1.6930	45.1066	100.0000
4396.999	0.4925	1.6930	45.1066	100.0000
4195.999	0.4925	1.6930	45.1066	100.0000
3994.998	0.4925	1.6930	45.1066	100.0000
3793.998	0.4925	1.6930	45.1066	100.0000
3592.998	0.4925	1.6930	45.1066	100.0000
3391.998	0.4925	1.6930	45.1066	100.0000
3190.998	0.4925	1.6930	45.1066	100.0000
2990.084 - Psat	0.4925	1.6930	45.1066	100.0000
2989.997	0.4925	1.6930	45.1074	100.0000
2692.467	0.5155	1.7817	47.8911	100.0000
2394.937	0.5405	1.8786	50.9030	100.0000
2097.407	0.5677	1.9848	54.1794	100.0000
1799.877	0.5972	2.1014	57.7673	100.0000
1502.346	0.6289	2.2295	61.7299	100.0000
1204.816	0.6623	2.3696	66.1570	100.0000
907.286	0.6951	2.5206	71.1900	100.0000
609.756	0.7201	2.6733	77.0889	100.0000
312.226	0.7020	2.7661	84.5011	100.0000

Molar Distributions	Com(1 ,CO2)	Com(2 ,N2)	Com(3 ,C1)	Com(4 ,C2)
Vapour, Y Inserted Point	Calculated	Calculated	Calculated	Calculated
5000.000				
4798.999				
4597.999				
4396.999				
4195.999				
3994.998				
3793.998				
3592.998				
3391.998				
3190.998				
2990.084 - Psat	0.3823	1.0460	90.7377	5.2463
2989.997	0.3823	1.0459	90.7376	5.2464
2692.467	0.3934	0.9944	90.6276	5.3976
2394.937	0.4056	0.9450	90.4696	5.5756
2097.407	0.4192	0.8976	90.2493	5.7887
1799.877	0.4345	0.8520	89.9457	6.0486
1502.346	0.4515	0.8079	89.5264	6.3715
1204.816	0.4706	0.7652	88.9395	6.7799
907.286	0.4915	0.7233	88.0962	7.3052
609.756	0.5136	0.6813	86.8226	7.9880
312.226	0.5336	0.6366	84.6759	8.8585

Molar Distributions Vapour, Y Inserted Point	Com(5 ,C3) Calculated	Com(6 ,IC4) Calculated	Com(7 ,NC4) Calculated	Com(8 ,IC5) Calculated
5000.000				
4798.999				
4597.999				
4396.999				
4195.999				
3994.998				
3793.998				
3592.998				
3391.998				
3190.998				
2990.084 - Psat	1.2314	0.3638	0.3707	0.1499
2989.997	1.2314	0.3638	0.3707	0.1499
2692.467	1.2585	0.3675	0.3732	0.1484
2394.937	1.2931	0.3732	0.3776	0.1476
2097.407	1.3384	0.3817	0.3850	0.1476
1799.877	1.3993	0.3948	0.3969	0.1492
1502.346	1.4838	0.4150	0.4163	0.1535
1204.816	1.6053	0.4473	0.4483	0.1622
907.286	1.7881	0.5015	0.5037	0.1798
609.756	2.0808	0.6007	0.6089	0.2172
312.226	2.5922	0.8148	0.8497	0.3169

Molar Distributions Vapour, Y Inserted Point	Com(9 ,NC5) Calculated	Com(10,C6) Calculated	Com(11,C7+) Calculated	Total Calculated
5000.000				
4798.999				
4597.999				
4396.999				
4195.999				
3994.998				
3793.998				
3592.998				
3391.998				
3190.998				
2990.084 - Psat	0.1226	0.2661	0.0833	100.0000
2989.997	0.1226	0.2661	0.0833	100.0000
2692.467	0.1209	0.2575	0.0610	100.0000
2394.937	0.1196	0.2496	0.0436	100.0000
2097.407	0.1191	0.2429	0.0305	100.0000
1799.877	0.1197	0.2384	0.0209	100.0000
1502.346	0.1225	0.2376	0.0141	100.0000
1204.816	0.1288	0.2434	0.0095	100.0000
907.286	0.1422	0.2620	0.0066	100.0000
609.756	0.1716	0.3106	0.0049	100.0000
312.226	0.2527	0.4644	0.0046	100.0000

------------------ ----------- ----------- ----------- -----------

A4. Expt DL1 : Differential Liberation

```
Peng-Robinson         (3-Parm)  on ZI       with PR corr.
Lohrenz-Bray-Clark Viscosity Correlation
Density units are                LB/FT3
Specific volume units are        CF/LB-ML
Viscosity units are              CPOISE
Surface Tension units are        DYNES/CM
Gas-Oil Ratio units are          MSCF/STB
Relative Volume units are        RB/STB
Gas FVF units are                RB/MSCF
Extracted Gas Volume units are   FT3
Oil Relative Volume units are    BBL/STB

Specified temperature            Deg F               220.0000

Relative Oil Saturated Volume (Bo(Pbub))              1.3550

GOR calc. is Gas Vol at STC/Stock Tank Oil Vol
Oil Rel Vol calc. is Stage Vol oil/Stock Tank Oil Vol
```

Pressure PSIA	Inserted Point	GOR Observed	GOR Calculated	Total RelVol Calculated
2990.084	- Psat		0.5502	1.3550
2989.997		0.5502	0.5502	1.3550
2692.467		0.4893	0.4893	1.4008
2394.937		0.4311	0.4311	1.4610
2097.407		0.3754	0.3754	1.5423
1799.877		0.3219	0.3219	1.6560
1502.346		0.2705	0.2705	1.8222
1204.816		0.2209	0.2209	2.0813
907.286		0.1727	0.1727	2.5267
609.756		0.1256	0.1255	3.4355
312.226		0.0776	0.0776	6.1560
14.695			3.2368E-16	128.5763
14.695	@ Tres			128.5763
14.695	@ Tstd			98.9929

Pressure PSIA	Inserted Point	Oil RelVol Observed	Oil RelVol Calculated	Liq Dens Observed	Liq Dens Calculated
2990.084	- Psat		1.3550		42.7958
2989.997		1.3550	1.3550	42.7953	42.7959
2692.467		1.3285	1.3285	43.2579	43.2584
2394.937		1.3013	1.3031	43.7220	43.7226
2097.407		1.2786	1.2786	44.1888	44.1894
1799.877		1.2549	1.2549	44.6593	44.6598
1502.346		1.2319	1.2319	45.1345	45.1351

1204.816	1.2094	1.2094	45.6160	45.6165
907.286	1.1874	1.1874	46.1058	46.1064
609.756	1.1653	1.1653	46.6095	46.6100
312.226	1.1420	1.1420	47.1461	47.1466
14.695	1.0934	1.0934	48.0450	48.0455
14.695 @ Tres	1.0934	1.0934	48.0450	48.0455
14.695 @ Tstd		1.0000		52.5344

Pressure PSIA	Inserted Point	Vap Dens Calculated	Gas Grav Observed	Gas Grav Calculated
2990.084	- Psat	7.9236		0.6276
2989.997		7.9234		0.6276
2692.467		7.1828	0.6266	0.6266
2394.937		6.4246	0.6264	0.6264
2097.407		5.6509	0.6270	0.6270
1799.877		4.8650	0.6288	0.6288
1502.346		4.0716	0.6321	0.6321
1204.816		3.2763	0.6380	0.6380
907.286		2.4851	0.6485	0.6485
609.756		1.7028	0.6695	0.6695
312.226		0.9283	0.7243	0.7243
14.695		0.0728	1.2403	1.2403
14.695	@ Tres	0.0728	1.2403	1.2403
14.695	@ Tstd			

Pressure PSIA	Inserted Point	Vap Z-Fac Observed	Vap Z-Fac Calculated	Liq Z-Fac Calculated	Surf Tension Calculated
2990.084	- Psat		0.9406	1.1309	2.9751
2989.997			0.9406	1.1309	2.9753
2692.467		0.9329	0.9329	1.0602	3.5787
2394.937		0.9274	0.9274	0.9830	4.2901
2097.407		0.9243	0.9243	0.8987	5.1240
1799.877		0.9239	0.9239	0.8063	6.0942
1502.346		0.9264	0.9264	0.7050	7.2132
1204.816		0.9318	0.9318	0.5935	8.4909
907.286		0.9404	0.9404	0.4704	9.9347
609.756		0.9522	0.9522	0.3338	11.5514
312.226		0.9677	0.9677	0.1815	13.3601
14.695			0.9947	0.0095	15.6737
14.695	@ Tres		0.9947	0.0095	15.6737
14.695	@ Tstd		1.0000	0.0113	

Pressure	Inserted	Gas FVF		Liq Visc	Vap Visc

PSIA	Point	Observed	Calculated	Calculated	Calculated
2990.084	- Psat		1.0769	0.3444	0.0188
2989.997			1.0769	0.3444	0.0188
2692.467		1.1862	1.1862	0.3641	0.0179
2394.937		1.3257	1.3257	0.3848	0.0171
2097.407		1.5087	1.5087	0.4064	0.0163
1799.877		1.7573	1.7573	0.4290	0.0156
1502.346		2.1109	2.1109	0.4522	0.0150
1204.816		2.6476	2.6476	0.4758	0.0145
907.286		3.5482	3.5482	0.4994	0.0140
609.756		5.3460	5.3460	0.5220	0.0136
312.226		10.6101	10.6101	0.5427	0.0131
14.695			231.7072	0.5678	0.0113
14.695	@ Tres		231.7072	0.5678	0.0113
14.695	@ Tstd		178.1076	1.5170	

Pressure	Inserted	Moles Extrac	GasVol Extrc	Liquid Sat	Vapour Sat
PSIA	Point	Calculated	Calculated	Calculated	Calculated
2990.084	- Psat			1.0000	
2989.997		1.7589E-05	0.0147	1.0000	1.4629E-05
2692.467		0.0582	48.7040	0.9484	0.0516
2394.937		0.1138	95.2104	0.9441	0.0559
2097.407		0.1670	139.7381	0.9383	0.0617
1799.877		0.2181	182.4722	0.9304	0.0696
1502.346		0.2673	223.5887	0.9190	0.0810
1204.816		0.3147	263.2715	0.9020	0.0980
907.286		0.3607	301.7568	0.8742	0.1258
609.756		0.4058	339.4751	0.8221	0.1779
312.226		0.4516	377.7839	0.6919	0.3081
14.695		0.5258	439.8450	0.0573	0.9427
14.695	@ Tres	0.5258	439.8450	1.0000	6.9441E-14
14.695	@ Tstd	0.5258	439.8450	1.0000	

Pressure	Inserted	Liq Mol Wt	Vap Mol Wt	Liq Visc	Vap Visc
PSIA	Point	Calculated	Calculated	Calculated	Calculated
2990.084	- Psat	118.0626	18.1805	0.3444	0.0188
2989.997		118.0643	18.1805	0.3444	0.0188
2692.467		124.2385	18.1527	0.3641	0.0179
2394.937		130.8935	18.1461	0.3848	0.0171
2097.407		138.0966	18.1644	0.4064	0.0163
1799.877		145.9284	18.2149	0.4290	0.0156
1502.346		154.4880	18.3114	0.4522	0.0150
1204.816		163.9016	18.4815	0.4758	0.0145
907.286		174.3435	18.7869	0.4994	0.0140
609.756		186.0998	19.3954	0.5220	0.0136

312.226	199.8860	20.9842	0.5427	0.0131
14.695	225.5320	35.9309	0.5678	0.0113
14.695 @ Tres	225.5320	35.9309	0.5678	0.0113
14.695 @ Tstd	225.5320		1.5170	

Pressure PSIA	Inserted Point	Liq Mol Vol Calculated	Vap Mol Vol Calculated
2990.084	- Psat	2.7587	2.2945
2989.997		2.7588	2.2945
2692.467		2.8720	2.5272
2394.937		2.9937	2.8244
2097.407		3.1251	3.2144
1799.877		3.2676	3.7441
1502.346		3.4228	4.4974
1204.816		3.5930	5.6410
907.286		3.7813	7.5598
609.756		3.9927	11.3902
312.226		4.2397	22.6060
14.695		4.6941	493.6760
14.695	@ Tres	4.6941	493.6760
14.695	@ Tstd	4.2930	

Molar Distributions K-Values	Inserted Point	Com(1 ,CO2) Calculated	Com(2 ,N2) Calculated	Com(3 ,C1) Calculated	Com(4 ,C2) Calculated
2990.084	- Psat	1.3308	3.3980	2.1299	1.0026
2989.997		1.3308	3.3981	2.1300	1.0026
2692.467		1.4012	3.7470	2.2867	1.0335
2394.937		1.4907	4.1835	2.4823	1.0746
2097.407		1.6078	4.7447	2.7335	1.1306
1799.877		1.7662	5.4924	3.0682	1.2092
1502.346		1.9911	6.5368	3.5361	1.3244
1204.816		2.3320	8.0969	4.2366	1.5042
907.286		2.9038	10.6788	5.3988	1.8126
609.756		4.0453	15.7772	7.7002	2.4390
312.226		7.3858	30.5978	14.4027	4.2922
14.695		146.9069	652.6025	295.0956	81.8211
14.695	@ Tres	146.9069	652.6025	295.0956	81.8211
14.695	@ Tstd	1.0000	1.0000	1.0000	1.0000

Molar Distributions K-Values	Inserted Point	Com(5 ,C3) Calculated	Com(6 ,IC4) Calculated	Com(7 ,NC4) Calculated	Com(8 ,IC5) Calculated

2990.084 - Psat	0.6350	0.4431	0.3803	0.2756
2989.997	0.6350	0.4431	0.3803	0.2756
2692.467	0.6352	0.4329	0.3688	0.2612
2394.937	0.6395	0.4249	0.3592	0.2482
2097.407	0.6499	0.4200	0.3523	0.2369
1799.877	0.6697	0.4202	0.3495	0.2283
1502.346	0.7051	0.4285	0.3534	0.2238
1204.816	0.7678	0.4508	0.3686	0.2257
907.286	0.8849	0.5010	0.4060	0.2399
609.756	1.1362	0.6189	0.4969	0.2828
312.226	1.9031	0.9949	0.7914	0.4327
14.695	34.2518	17.0526	13.4180	6.9997
14.695 @ Tres	34.2518	17.0526	13.4180	6.9997
14.695 @ Tstd	1.0000	1.0000	1.0000	1.0000

Molar Distributions K-Values Inserted Point	Com(9 ,NC5) Calculated	Com(10,C6) Calculated	Com(11,C7+) Calculated
2990.084 - Psat	0.2489	0.1572	0.0018
2989.997	0.2489	0.1572	0.0018
2692.467	0.2345	0.1445	0.0013
2394.937	0.2213	0.1329	0.0009
2097.407	0.2099	0.1225	0.0006
1799.877	0.2008	0.1137	0.0004
1502.346	0.1953	0.1070	0.0002
1204.816	0.1954	0.1033	0.0001
907.286	0.2060	0.1049	9.5174E-05
609.756	0.2407	0.1177	6.6350E-05
312.226	0.3648	0.1710	5.8010E-05
14.695	5.8398	2.5969	0.0005
14.695 @ Tres	5.8398	2.5969	0.0005
14.695 @ Tstd	1.0000	1.0000	1.0000

Molar Distributions Fluid, Z Inserted Point	Com(1 ,CO2) Calculated	Com(2 ,N2) Calculated	Com(3 ,C1) Calculated	Com(4 ,C2) Calculated
2990.084 - Psat	0.2873	0.3078	42.6014	5.2328
2989.997	0.2873	0.3078	42.6014	5.2328
2692.467	0.2873	0.3078	42.6005	5.2328
2394.937	0.2807	0.2654	39.6326	5.2226
2097.407	0.2728	0.2234	36.4440	5.1997
1799.877	0.2632	0.1824	33.0074	5.1593
1502.346	0.2514	0.1430	29.2923	5.0939
1204.816	0.2367	0.1061	25.2648	4.9921
907.286	0.2179	0.0727	20.8884	4.8343
609.756	0.1932	0.0441	16.1266	4.5843
312.226	0.1590	0.0216	10.9517	4.1619

14.695	0.1066	0.0066	5.3875	3.3197
14.695 @ Tres	0.0051	7.3772E-05	0.1321	0.2782
14.695 @ Tstd	0.0051	7.3772E-05	0.1321	0.2782

Molar Distributions Fluid, Z Inserted Point	Com(5 ,C3) Calculated	Com(6 ,IC4) Calculated	Com(7 ,NC4) Calculated	Com(8 ,IC5) Calculated
2990.084 - Psat	1.9392	0.8208	0.9747	0.5438
2989.997	1.9392	0.8208	0.9747	0.5438
2692.467	1.9392	0.8208	0.9748	0.5438
2394.937	1.9813	0.8489	1.0119	0.5682
2097.407	2.0244	0.8787	1.0517	0.5946
1799.877	2.0679	0.9104	1.0943	0.6232
1502.346	2.1106	0.9440	1.1397	0.6541
1204.816	2.1505	0.9791	1.1880	0.6877
907.286	2.1833	1.0152	1.2387	0.7240
609.756	2.2003	1.0504	1.2901	0.7629
312.226	2.1794	1.0794	1.3375	0.8036
14.695	2.0376	1.0798	1.3594	0.8403
14.695 @ Tres	0.3706	0.3405	0.5073	0.4639
14.695 @ Tstd	0.3706	0.3405	0.5073	0.4639

Molar Distributions Fluid, Z Inserted Point	Com(9 ,NC5) Calculated	Com(10,C6) Calculated	Com(11,C7+) Calculated	Total Calculated
2990.084 - Psat	0.4925	1.6930	45.1066	100.0000
2989.997	0.4925	1.6930	45.1066	100.0000
2692.467	0.4925	1.6930	45.1074	100.0000
2394.937	0.5155	1.7817	47.8911	100.0000
2097.407	0.5403	1.8778	50.8925	100.0000
1799.877	0.5672	1.9823	54.1425	100.0000
1502.346	0.5965	2.0962	57.6782	100.0000
1204.816	0.6282	2.2209	61.5459	100.0000
907.286	0.6627	2.3577	65.8051	100.0000
609.756	0.7001	2.5084	70.5397	100.0000
312.226	0.7397	2.6749	75.8913	100.0000
14.695	0.7777	2.8574	82.2274	100.0000
14.695 @ Tres	0.4700	2.3499	95.0823	100.0000
14.695 @ Tstd	0.4700	2.3499	95.0823	100.0000

Molar Distributions Liquid, X Inserted Point	Com(1 ,CO2) Calculated	Com(2 ,N2) Calculated	Com(3 ,C1) Calculated	Com(4 ,C2) Calculated
2990.084 - Psat	0.2873	0.3078	42.6014	5.2328

2989.997	0.2873	0.3078	42.6005	5.2328
2692.467	0.2807	0.2654	39.6326	5.2226
2394.937	0.2728	0.2234	36.4440	5.1997
2097.407	0.2632	0.1824	33.0074	5.1593
1799.877	0.2514	0.1430	29.2923	5.0939
1502.346	0.2367	0.1061	25.2648	4.9921
1204.816	0.2179	0.0727	20.8884	4.8343
907.286	0.1932	0.0441	16.1266	4.5843
609.756	0.1590	0.0216	10.9517	4.1619
312.226	0.1066	0.0066	5.3875	3.3197
14.695	0.0051	7.3772E-05	0.1321	0.2782
14.695 @ Tres	0.0051	7.3772E-05	0.1321	0.2782
14.695 @ Tstd	0.0051	7.3772E-05	0.1321	0.2782

Molar Distributions Liquid, X Inserted Point	Com(5 ,C3) Calculated	Com(6 ,IC4) Calculated	Com(7 ,NC4) Calculated	Com(8 ,IC5) Calculated
2990.084 - Psat	1.9392	0.8208	0.9747	0.5438
2989.997	1.9392	0.8208	0.9748	0.5438
2692.467	1.9813	0.8489	1.0119	0.5682
2394.937	2.0244	0.8787	1.0517	0.5946
2097.407	2.0679	0.9104	1.0943	0.6232
1799.877	2.1106	0.9440	1.1397	0.6541
1502.346	2.1505	0.9791	1.1880	0.6877
1204.816	2.1833	1.0152	1.2387	0.7240
907.286	2.2003	1.0504	1.2901	0.7629
609.756	2.1794	1.0794	1.3375	0.8036
312.226	2.0376	1.0798	1.3594	0.8403
14.695	0.3706	0.3405	0.5073	0.4639
14.695 @ Tres	0.3706	0.3405	0.5073	0.4639
14.695 @ Tstd	0.3706	0.3405	0.5073	0.4639

Molar Distributions Liquid, X Inserted Point	Com(9 ,NC5) Calculated	Com(10,C6) Calculated	Com(11,C7+) Calculated	Total Calculated
2990.084 - Psat	0.4925	1.6930	45.1066	100.0000
2989.997	0.4925	1.6930	45.1074	100.0000
2692.467	0.5155	1.7817	47.8911	100.0000
2394.937	0.5403	1.8778	50.8925	100.0000
2097.407	0.5672	1.9823	54.1425	100.0000
1799.877	0.5965	2.0962	57.6782	100.0000
1502.346	0.6282	2.2209	61.5459	100.0000
1204.816	0.6627	2.3577	65.8051	100.0000
907.286	0.7001	2.5084	70.5397	100.0000
609.756	0.7397	2.6749	75.8913	100.0000
312.226	0.7777	2.8574	82.2274	100.0000
14.695	0.4700	2.3499	95.0823	100.0000
14.695 @ Tres	0.4700	2.3499	95.0823	100.0000

14.695 @ Tstd	0.4700	2.3499	95.0823	100.0000

Molar Distributions Vapour, Y Inserted Point	Com(1 ,CO2) Calculated	Com(2 ,N2) Calculated	Com(3 ,C1) Calculated	Com(4 ,C2) Calculated
2990.084 - Psat	0.3823	1.0460	90.7377	5.2463
2989.997	0.3823	1.0459	90.7376	5.2464
2692.467	0.3934	0.9944	90.6276	5.3976
2394.937	0.4067	0.9346	90.4650	5.5877
2097.407	0.4232	0.8653	90.2267	5.8329
1799.877	0.4440	0.7853	89.8741	6.1595
1502.346	0.4712	0.6934	89.3396	6.6118
1204.816	0.5081	0.5885	88.4949	7.2718
907.286	0.5610	0.4705	87.0646	8.3096
609.756	0.6434	0.3404	84.3310	10.1510
312.226	0.7872	0.2012	77.5941	14.2490
14.695	0.7551	0.0481	38.9851	22.7640
14.695 @ Tres	0.7551	0.0481	38.9851	22.7640
14.695 @ Tstd				

Molar Distributions Vapour, Y Inserted Point	Com(5 ,C3) Calculated	Com(6 ,IC4) Calculated	Com(7 ,NC4) Calculated	Com(8 ,IC5) Calculated
2990.084 - Psat	1.2314	0.3638	0.3707	0.1499
2989.997	1.2314	0.3638	0.3707	0.1499
2692.467	1.2585	0.3675	0.3732	0.1484
2394.937	1.2945	0.3733	0.3778	0.1476
2097.407	1.3438	0.3824	0.3855	0.1477
1799.877	1.4135	0.3966	0.3984	0.1494
1502.346	1.5163	0.4195	0.4198	0.1539
1204.816	1.6762	0.4577	0.4566	0.1634
907.286	1.9471	0.5263	0.5237	0.1830
609.756	2.4762	0.6681	0.6647	0.2272
312.226	3.8777	1.0744	1.0758	0.3636
14.695	12.6943	5.8064	6.8069	3.2469
14.695 @ Tres	12.6943	5.8064	6.8069	3.2469
14.695 @ Tstd				

Molar Distributions Vapour, Y Inserted Point	Com(9 ,NC5) Calculated	Com(10,C6) Calculated	Com(11,C7+) Calculated	Total Calculated
2990.084 - Psat	0.1226	0.2661	0.0833	100.0000
2989.997	0.1226	0.2661	0.0833	100.0000
2692.467	0.1209	0.2575	0.0610	100.0000

2394.937	0.1196	0.2496	0.0436	100.0000
2097.407	0.1191	0.2429	0.0305	100.0000
1799.877	0.1198	0.2383	0.0210	100.0000
1502.346	0.1227	0.2376	0.0142	100.0000
1204.816	0.1295	0.2437	0.0097	100.0000
907.286	0.1442	0.2631	0.0067	100.0000
609.756	0.1780	0.3149	0.0050	100.0000
312.226	0.2838	0.4885	0.0048	100.0000
14.695	2.7449	6.1023	0.0459	100.0000
14.695 @ Tres	2.7449	6.1023	0.0459	100.0000
14.695 @ Tstd				

A5. Expt COMPG1 : Compositional Grading Experiment

Peng-Robinson (3-Parm) on ZI with PR corr.
Lohrenz-Bray-Clark Viscosity Correlation

Reference temperature	Deg F	220.0000
Reference pressure	PSIA	3200.0000
Reference depth	FEET	6660.105

Viscosity units are	CPOISE
Pressure units are	PSIA
Specific volume units are	CF/LB-ML
Density units are	LB/FT3

Depths FEET	Inserted Point	Pressure Calculated	Psat Calculated	Mole Weight Calculated	Density Calculated
229.655	- dusr	2753.5629	1724.7574	17.6805	7.0924
269.432	- dins	2755.5236	1732.6974	17.6830	7.0984
308.802	- dins	2757.4659	1740.5610	17.6855	7.1044
348.172	- dins	2759.4097	1748.4297	17.6880	7.1103
387.542	- dins	2761.3552	1756.3035	17.6905	7.1162
426.912	- dins	2763.3024	1764.1827	17.6930	7.1222
459.310	- dusr	2764.9059	1770.6707	17.6951	7.1271
469.563	- dins	2765.4136	1772.7248	17.6957	7.1286
508.933	- dins	2767.3641	1780.6158	17.6983	7.1346
548.303	- dins	2769.3163	1788.5126	17.7008	7.1406
587.673	- dins	2771.2701	1796.4155	17.7034	7.1466
627.044	- dins	2773.2255	1804.3246	17.7059	7.1526
666.414	- dins	2775.1826	1812.2401	17.7085	7.1586
688.965	- dusr	2776.3043	1816.7770	17.7100	7.1620
705.784	- dins	2777.1413	1820.1621	17.7111	7.1646
745.154	- dins	2779.1017	1828.0907	17.7137	7.1706
784.524	- dins	2781.0637	1836.0263	17.7163	7.1766
823.894	- dins	2783.0273	1843.9688	17.7189	7.1827
866.545	- dins	2785.1565	1852.5813	17.7217	7.1892
905.915	- dins	2787.1236	1860.5390	17.7243	7.1953
918.620	- dusr	2787.7588	1863.1086	17.7252	7.1973
945.285	- dins	2789.0924	1868.5041	17.7270	7.2014
984.655	- dins	2791.0628	1876.4769	17.7296	7.2075
1024.025	- dins	2793.0349	1884.4575	17.7323	7.2135
1063.395	- dins	2795.0087	1892.4460	17.7350	7.2196
1102.765	- dins	2796.9841	1900.4426	17.7376	7.2258
1142.135	- dins	2798.9612	1908.4475	17.7403	7.2319
1148.275	- dusr	2799.2697	1909.6967	17.7407	7.2328
1181.505	- dins	2800.9400	1916.4609	17.7430	7.2380
1220.876	- dins	2802.9205	1924.4827	17.7457	7.2442
1263.526	- dins	2805.0679	1933.1830	17.7487	7.2508
1302.897	- dins	2807.0518	1941.2232	17.7514	7.2570
1342.267	- dins	2809.0375	1949.2725	17.7542	7.2631
1377.931	- dusr	2810.8377	1956.5720	17.7566	7.2687
1381.637	- dins	2811.0248	1957.3310	17.7569	7.2693

1421.007 - dins	2813.0139	1965.3987	17.7597	7.2755
1460.377 - dins	2815.0046	1973.4760	17.7624	7.2817
1499.747 - dins	2816.9970	1981.5629	17.7652	7.2879
1539.117 - dins	2818.9912	1989.6596	17.7680	7.2941
1578.487 - dins	2820.9870	1997.7663	17.7708	7.3004
1607.586 - dusr	2822.4632	2003.7645	17.7729	7.3050
1617.857 - dins	2822.9845	2005.8830	17.7737	7.3066
1660.508 - dins	2825.1504	2014.6877	17.7767	7.3134
1699.878 - dins	2827.1515	2022.8260	17.7796	7.3197
1739.248 - dins	2829.1544	2030.9748	17.7824	7.3259
1778.618 - dins	2831.1589	2039.1343	17.7853	7.3322
1817.988 - dins	2833.1651	2047.3047	17.7882	7.3385
1837.241 - dusr	2834.1469	2051.3041	17.7896	7.3416
1857.359 - dins	2835.1731	2055.4860	17.7910	7.3448
1896.729 - dins	2837.1828	2063.6785	17.7939	7.3511
1936.099 - dins	2839.1942	2071.8824	17.7969	7.3575
1975.469 - dins	2841.2074	2080.0977	17.7998	7.3638
2014.839 - dins	2843.2223	2088.3246	17.8027	7.3702
2057.490 - dins	2845.4071	2097.2503	17.8059	7.3771
2066.896 - dusr	2845.8892	2099.2207	17.8066	7.3786
2096.860 - dins	2847.4256	2105.5019	17.8089	7.3834
2136.230 - dins	2849.4459	2113.7655	17.8118	7.3898
2175.600 - dins	2851.4679	2122.0414	17.8148	7.3962
2214.970 - dins	2853.4917	2130.3296	17.8178	7.4026
2254.340 - dins	2855.5172	2138.6304	17.8208	7.4090
2293.710 - dins	2857.5445	2146.9438	17.8239	7.4155
2296.551 - dusr	2857.6908	2147.5443	17.8241	7.4159
2333.080 - dins	2859.5735	2155.2701	17.8269	7.4219
2372.450 - dins	2861.6043	2163.6094	17.8299	7.4284
2411.820 - dins	2863.6369	2171.9618	17.8330	7.4348
2454.471 - dins	2865.8408	2181.0253	17.8363	7.4419
2493.841 - dins	2867.8771	2189.4056	17.8394	7.4484
2526.207 - dusr	2869.5524	2196.3050	17.8420	7.4537
2533.212 - dins	2869.9151	2197.7995	17.8425	7.4549
2572.582 - dins	2871.9550	2206.2072	17.8457	7.4614
2611.952 - dins	2873.9966	2214.6288	17.8488	7.4679
2651.322 - dins	2876.0400	2223.0645	17.8519	7.4744
2690.692 - dins	2878.0851	2231.5144	17.8551	7.4810
2730.062 - dins	2880.1321	2239.9788	17.8583	7.4876
2755.862 - dusr	2881.4745	2245.5335	17.8604	7.4919
2769.432 - dins	2882.1809	2248.4577	17.8615	7.4941
2808.802 - dins	2884.2315	2256.9513	17.8647	7.5007
2851.453 - dins	2886.4550	2266.1695	17.8682	7.5079
2890.823 - dins	2888.5093	2274.6943	17.8714	7.5145
2930.193 - dins	2890.5655	2283.2343	17.8746	7.5211
2969.563 - dins	2892.6234	2291.7897	17.8779	7.5278
2985.517 - dusr	2893.4579	2295.2610	17.8792	7.5305
3008.933 - dins	2894.6832	2300.3606	17.8812	7.5344
3048.303 - dins	2896.7448	2308.9473	17.8845	7.5411
3087.674 - dins	2898.8083	2317.5497	17.8878	7.5478
3127.044 - dins	2900.8735	2326.1683	17.8911	7.5545
3166.414 - dins	2902.9406	2334.8030	17.8944	7.5612
3205.784 - dins	2905.0095	2343.4541	17.8978	7.5679
3215.172 - dusr	2905.5032	2345.5194	17.8986	7.5695

3248.435	- dins	2907.2530	2352.8447	17.9015	7.5752
3287.805	- dins	2909.3257	2361.5304	17.9048	7.5820
3327.175	- dins	2911.4004	2370.2329	17.9082	7.5887
3366.545	- dins	2913.4768	2378.9525	17.9117	7.5955
3405.915	- dins	2915.5552	2387.6894	17.9151	7.6023
3444.827	- dusr	2917.6112	2396.3417	17.9185	7.6090
3445.285	- dins	2917.6354	2396.4436	17.9186	7.6091
3484.655	- dins	2919.7174	2405.2153	17.9220	7.6159
3524.025	- dins	2921.8013	2414.0048	17.9255	7.6228
3563.395	- dins	2923.8871	2422.8123	17.9290	7.6296
3602.765	- dins	2925.9748	2431.6378	17.9325	7.6365
3642.135	- dins	2928.0643	2440.4815	17.9361	7.6434
3674.482	- dusr	2929.7826	2447.7615	17.9390	7.6490
3684.786	- dins	2930.3301	2450.0831	17.9399	7.6508
3724.156	- dins	2932.4236	2458.9654	17.9435	7.6578
3763.527	- dins	2934.5190	2467.8666	17.9471	7.6647
3802.897	- dins	2936.6163	2476.7868	17.9507	7.6716
3842.267	- dins	2938.7154	2485.7262	17.9544	7.6786
3881.637	- dins	2940.8165	2494.6849	17.9580	7.6855
3904.138	- dusr	2942.0182	2499.8138	17.9601	7.6895
3921.007	- dins	2942.9195	2503.6632	17.9617	7.6925
3960.377	- dins	2945.0244	2512.6612	17.9654	7.6995
3999.747	- dins	2947.1312	2521.6792	17.9691	7.7066
4039.117	- dins	2949.2399	2530.7172	17.9728	7.7136
4081.768	- dins	2951.5266	2540.5313	17.9769	7.7212
4121.138	- dins	2953.6393	2549.6119	17.9806	7.7283
4133.793	- dusr	2954.3188	2552.5350	17.9818	7.7306
4160.508	- dins	2955.7540	2558.7132	17.9844	7.7354
4199.878	- dins	2957.8706	2567.8353	17.9882	7.7425
4239.248	- dins	2959.9892	2576.9786	17.9920	7.7496
4278.618	- dins	2962.1097	2586.1431	17.9959	7.7567
4317.989	- dins	2964.2322	2595.3292	17.9998	7.7639
4357.359	- dins	2966.3566	2604.5369	18.0036	7.7711
4363.448	- dusr	2966.6854	2605.9630	18.0043	7.7722
4396.729	- dins	2968.4830	2613.7665	18.0076	7.7783
4436.099	- dins	2970.6114	2623.0183	18.0115	7.7855
4478.750	- dins	2972.9194	2633.0662	18.0158	7.7933
4518.120	- dins	2975.0518	2642.3646	18.0197	7.8005
4557.490	- dins	2977.1863	2651.6858	18.0237	7.8078
4563.990	- dusr	2977.5389	2653.2270	18.0244	7.8090
4593.103	- dusr	2979.1188	2660.1373	18.0274	7.8144
4596.860	- dins	2979.3228	2661.0299	18.0278	7.8151
4636.230	- dins	2981.4612	2670.3972	18.0318	7.8223
4675.600	- dins	2983.6016	2679.7879	18.0359	7.8297
4714.970	- dins	2985.7441	2689.2021	18.0400	7.8370
4754.340	- dins	2987.8885	2698.6402	18.0441	7.8443
4793.710	- dins	2990.0350	2708.1024	18.0482	7.8517
4822.758	- dusr	2991.6200	2715.0992	18.0513	7.8572
4833.080	- dins	2992.1835	2717.5887	18.0524	7.8591
4875.731	- dins	2994.5133	2727.8933	18.0569	7.8671
4915.101	- dins	2996.6660	2737.4309	18.0611	7.8745
4954.471	- dins	2998.8207	2746.9935	18.0653	7.8820
4993.842	- dins	3000.9775	2756.5813	18.0696	7.8895
5033.212	- dins	3003.1363	2766.1945	18.0739	7.8969

5052.414	- dusr	3004.1900	2770.8924	18.0760	7.9006
5072.582	- dins	3005.2972	2775.8334	18.0782	7.9044
5111.952	- dins	3007.4601	2785.4981	18.0825	7.9120
5151.322	- dins	3009.6251	2795.1890	18.0869	7.9195
5190.692	- dins	3011.7921	2804.9062	18.0913	7.9271
5230.062	- dins	3013.9613	2814.6501	18.0957	7.9347
5272.713	- dins	3016.3135	2825.2364	18.1005	7.9429
5282.069	- dusr	3016.8298	2827.5627	18.1015	7.9447
5312.083	- dins	3018.4869	2835.0365	18.1050	7.9505
5351.453	- dins	3020.6625	2844.8640	18.1094	7.9582
5390.823	- dins	3022.8401	2854.7192	18.1140	7.9659
5430.193	- dins	3025.0199	2864.6022	18.1185	7.9736
5469.563	- dins	3027.2017	2874.5135	18.1231	7.9813
5508.933	- dins	3029.3857	2884.4531	18.1277	7.9890
5511.724	- dusr	3029.5406	2885.1587	18.1280	7.9896
5548.304	- dins	3031.5718	2894.4214	18.1323	7.9968
5587.674	- dins	3033.7600	2904.4187	18.1370	8.0046
5595.082	- dusr	3034.1720	2906.3032	18.1379	8.0060
5627.044	- dins	3035.9503	2914.4452	18.1417	8.0124
5669.695	- dins	3038.3256	2925.3406	18.1468	8.0208
5709.065	- dins	3040.5204	2935.4288	18.1516	8.0287
5741.379	- dusr	3042.3235	2943.7316	18.1555	8.0352
5748.435	- dins	3042.7174	2945.5472	18.1563	8.0366
5787.805	- dins	3044.9165	2955.6959	18.1612	8.0445
5827.175	- dins	3047.1178	2965.8753	18.1660	8.0524
5866.545	- dins	3049.3212	2976.0856	18.1709	8.0604
5905.915	- dins	3051.5269	2986.3271	18.1758	8.0683
5945.285	- dins	3053.7347	2996.6001	18.1807	8.0763
5971.034	- dusr	3055.1798	3003.3362	18.1840	8.0816
5984.655	- dins	3055.9447	3006.9050	18.1857	8.0844
6024.025	- dins	3058.1569	3017.2420	18.1907	8.0924
6066.676	- dins	3060.5559	3028.4770	18.1962	8.1012
6106.046	- dins	3062.7727	3038.8819	18.2013	8.1093
6145.416	- dins	3064.9918	3049.3199	18.2064	8.1174
6184.786	- dins	3067.2130	3059.7913	18.2115	8.1255
6200.689	- dusr	3068.1109	3064.0306	18.2136	8.1288
6220.076	- DGOC	3069.2059	3069.2059	18.2162	5.8906
6660.105	- DREF	3200.0000	2990.0849	118.0626	42.9250

Depths FEET	Inserted Point	Viscosity Calculated	Z-Factor Calculated	Specific Vol Calculated
229.655	- dusr	0.0179	0.9411	2.4929
269.432	- dins	0.0179	0.9411	2.4911
308.802	- dins	0.0179	0.9411	2.4894
348.172	- dins	0.0179	0.9411	2.4877
387.542	- dins	0.0179	0.9412	2.4859
426.912	- dins	0.0179	0.9412	2.4842
459.310	- dusr	0.0179	0.9412	2.4828
469.563	- dins	0.0180	0.9412	2.4823
508.933	- dins	0.0180	0.9412	2.4806

548.303 - dins	0.0180	0.9412	2.4789
587.673 - dins	0.0180	0.9412	2.4772
627.044 - dins	0.0180	0.9412	2.4755
666.414 - dins	0.0180	0.9412	2.4737
688.965 - dusr	0.0180	0.9412	2.4728
705.784 - dins	0.0180	0.9412	2.4720
745.154 - dins	0.0180	0.9412	2.4703
784.524 - dins	0.0180	0.9413	2.4686
823.894 - dins	0.0180	0.9413	2.4669
866.545 - dins	0.0180	0.9413	2.4650
905.915 - dins	0.0180	0.9413	2.4633
918.620 - dusr	0.0180	0.9413	2.4628
945.285 - dins	0.0180	0.9413	2.4616
984.655 - dins	0.0180	0.9413	2.4599
1024.025 - dins	0.0180	0.9413	2.4582
1063.395 - dins	0.0180	0.9413	2.4565
1102.765 - dins	0.0181	0.9413	2.4548
1142.135 - dins	0.0181	0.9414	2.4531
1148.275 - dusr	0.0181	0.9414	2.4528
1181.505 - dins	0.0181	0.9414	2.4514
1220.876 - dins	0.0181	0.9414	2.4497
1263.526 - dins	0.0181	0.9414	2.4478
1302.897 - dins	0.0181	0.9414	2.4461
1342.267 - dins	0.0181	0.9414	2.4444
1377.931 - dusr	0.0181	0.9414	2.4429
1381.637 - dins	0.0181	0.9414	2.4427
1421.007 - dins	0.0181	0.9414	2.4410
1460.377 - dins	0.0181	0.9414	2.4393
1499.747 - dins	0.0181	0.9415	2.4376
1539.117 - dins	0.0181	0.9415	2.4359
1578.487 - dins	0.0181	0.9415	2.4342
1607.586 - dusr	0.0181	0.9415	2.4330
1617.857 - dins	0.0181	0.9415	2.4325
1660.508 - dins	0.0181	0.9415	2.4307
1699.878 - dins	0.0182	0.9415	2.4290
1739.248 - dins	0.0182	0.9415	2.4273
1778.618 - dins	0.0182	0.9415	2.4256
1817.988 - dins	0.0182	0.9415	2.4239
1837.241 - dusr	0.0182	0.9416	2.4231
1857.359 - dins	0.0182	0.9416	2.4223
1896.729 - dins	0.0182	0.9416	2.4206
1936.099 - dins	0.0182	0.9416	2.4189
1975.469 - dins	0.0182	0.9416	2.4172
2014.839 - dins	0.0182	0.9416	2.4155
2057.490 - dins	0.0182	0.9416	2.4137
2066.896 - dusr	0.0182	0.9416	2.4133
2096.860 - dins	0.0182	0.9416	2.4120
2136.230 - dins	0.0182	0.9416	2.4103
2175.600 - dins	0.0182	0.9416	2.4086
2214.970 - dins	0.0182	0.9417	2.4070
2254.340 - dins	0.0183	0.9417	2.4053
2293.710 - dins	0.0183	0.9417	2.4036
2296.551 - dusr	0.0183	0.9417	2.4035
2333.080 - dins	0.0183	0.9417	2.4019

2372.450 - dins	0.0183	0.9417	2.4002
2411.820 - dins	0.0183	0.9417	2.3986
2454.471 - dins	0.0183	0.9417	2.3968
2493.841 - dins	0.0183	0.9417	2.3951
2526.207 - dusr	0.0183	0.9417	2.3937
2533.212 - dins	0.0183	0.9417	2.3934
2572.582 - dins	0.0183	0.9418	2.3917
2611.952 - dins	0.0183	0.9418	2.3901
2651.322 - dins	0.0183	0.9418	2.3884
2690.692 - dins	0.0183	0.9418	2.3867
2730.062 - dins	0.0183	0.9418	2.3851
2755.862 - dusr	0.0183	0.9418	2.3840
2769.432 - dins	0.0183	0.9418	2.3834
2808.802 - dins	0.0184	0.9418	2.3817
2851.453 - dins	0.0184	0.9418	2.3799
2890.823 - dins	0.0184	0.9418	2.3783
2930.193 - dins	0.0184	0.9419	2.3766
2969.563 - dins	0.0184	0.9419	2.3749
2985.517 - dusr	0.0184	0.9419	2.3742
3008.933 - dins	0.0184	0.9419	2.3733
3048.303 - dins	0.0184	0.9419	2.3716
3087.674 - dins	0.0184	0.9419	2.3699
3127.044 - dins	0.0184	0.9419	2.3683
3166.414 - dins	0.0184	0.9419	2.3666
3205.784 - dins	0.0184	0.9419	2.3650
3215.172 - dusr	0.0184	0.9419	2.3646
3248.435 - dins	0.0184	0.9419	2.3632
3287.805 - dins	0.0184	0.9420	2.3615
3327.175 - dins	0.0184	0.9420	2.3598
3366.545 - dins	0.0185	0.9420	2.3582
3405.915 - dins	0.0185	0.9420	2.3565
3444.827 - dusr	0.0185	0.9420	2.3549
3445.285 - dins	0.0185	0.9420	2.3549
3484.655 - dins	0.0185	0.9420	2.3532
3524.025 - dins	0.0185	0.9420	2.3516
3563.395 - dins	0.0185	0.9420	2.3499
3602.765 - dins	0.0185	0.9420	2.3483
3642.135 - dins	0.0185	0.9420	2.3466
3674.482 - dusr	0.0185	0.9421	2.3453
3684.786 - dins	0.0185	0.9421	2.3448
3724.156 - dins	0.0185	0.9421	2.3432
3763.527 - dins	0.0185	0.9421	2.3415
3802.897 - dins	0.0185	0.9421	2.3399
3842.267 - dins	0.0185	0.9421	2.3382
3881.637 - dins	0.0186	0.9421	2.3366
3904.138 - dusr	0.0186	0.9421	2.3357
3921.007 - dins	0.0186	0.9421	2.3349
3960.377 - dins	0.0186	0.9421	2.3333
3999.747 - dins	0.0186	0.9421	2.3317
4039.117 - dins	0.0186	0.9421	2.3300
4081.768 - dins	0.0186	0.9422	2.3282
4121.138 - dins	0.0186	0.9422	2.3266
4133.793 - dusr	0.0186	0.9422	2.3261
4160.508 - dins	0.0186	0.9422	2.3250

4199.878 - dins	0.0186	0.9422	2.3233
4239.248 - dins	0.0186	0.9422	2.3217
4278.618 - dins	0.0186	0.9422	2.3200
4317.989 - dins	0.0186	0.9422	2.3184
4357.359 - dins	0.0187	0.9422	2.3168
4363.448 - dusr	0.0187	0.9422	2.3165
4396.729 - dins	0.0187	0.9422	2.3151
4436.099 - dins	0.0187	0.9422	2.3135
4478.750 - dins	0.0187	0.9422	2.3117
4518.120 - dins	0.0187	0.9423	2.3101
4557.490 - dins	0.0187	0.9423	2.3084
4563.990 - dusr	0.0187	0.9423	2.3082
4593.103 - dusr	0.0187	0.9423	2.3070
4596.860 - dins	0.0187	0.9423	2.3068
4636.230 - dins	0.0187	0.9423	2.3052
4675.600 - dins	0.0187	0.9423	2.3035
4714.970 - dins	0.0187	0.9423	2.3019
4754.340 - dins	0.0187	0.9423	2.3003
4793.710 - dins	0.0187	0.9423	2.2986
4822.758 - dusr	0.0187	0.9423	2.2974
4833.080 - dins	0.0188	0.9423	2.2970
4875.731 - dins	0.0188	0.9423	2.2952
4915.101 - dins	0.0188	0.9423	2.2936
4954.471 - dins	0.0188	0.9423	2.2920
4993.842 - dins	0.0188	0.9424	2.2903
5033.212 - dins	0.0188	0.9424	2.2887
5052.414 - dusr	0.0188	0.9424	2.2879
5072.582 - dins	0.0188	0.9424	2.2871
5111.952 - dins	0.0188	0.9424	2.2855
5151.322 - dins	0.0188	0.9424	2.2838
5190.692 - dins	0.0188	0.9424	2.2822
5230.062 - dins	0.0188	0.9424	2.2806
5272.713 - dins	0.0188	0.9424	2.2788
5282.069 - dusr	0.0188	0.9424	2.2784
5312.083 - dins	0.0189	0.9424	2.2772
5351.453 - dins	0.0189	0.9424	2.2756
5390.823 - dins	0.0189	0.9424	2.2739
5430.193 - dins	0.0189	0.9424	2.2723
5469.563 - dins	0.0189	0.9424	2.2707
5508.933 - dins	0.0189	0.9424	2.2691
5511.724 - dusr	0.0189	0.9424	2.2690
5548.304 - dins	0.0189	0.9424	2.2675
5587.674 - dins	0.0189	0.9424	2.2658
5595.082 - dusr	0.0189	0.9424	2.2655
5627.044 - dins	0.0189	0.9425	2.2642
5669.695 - dins	0.0189	0.9425	2.2625
5709.065 - dins	0.0189	0.9425	2.2608
5741.379 - dusr	0.0190	0.9425	2.2595
5748.435 - dins	0.0190	0.9425	2.2592
5787.805 - dins	0.0190	0.9425	2.2576
5827.175 - dins	0.0190	0.9425	2.2560
5866.545 - dins	0.0190	0.9425	2.2544
5905.915 - dins	0.0190	0.9425	2.2527
5945.285 - dins	0.0190	0.9425	2.2511

5971.034 - dusr	0.0190	0.9425	2.2501
5984.655 - dins	0.0190	0.9425	2.2495
6024.025 - dins	0.0190	0.9425	2.2479
6066.676 - dins	0.0190	0.9425	2.2461
6106.046 - dins	0.0190	0.9425	2.2445
6145.416 - dins	0.0190	0.9425	2.2429
6184.786 - dins	0.0191	0.9425	2.2413
6200.689 - dusr	0.0191	0.9425	2.2406
6220.076 - DGOC	0.0166	1.3013	3.0924
6660.105 - DREF	0.3526	1.2067	2.7504

Molar Distributions Fluid, Z Inserted Point	Com(1 ,CO2) Calculated	Com(2 ,N2) Calculated	Com(3 ,C1) Calculated	Com(4 ,C2) Calculated
229.655 - dusr	0.3190	1.0107	92.0102	4.7510
269.432 - dins	0.3194	1.0109	92.0027	4.7542
308.802 - dins	0.3197	1.0111	91.9952	4.7574
348.172 - dins	0.3201	1.0113	91.9877	4.7606
387.542 - dins	0.3204	1.0115	91.9801	4.7639
426.912 - dins	0.3208	1.0116	91.9726	4.7671
459.310 - dusr	0.3211	1.0118	91.9664	4.7698
469.563 - dins	0.3212	1.0118	91.9644	4.7706
508.933 - dins	0.3215	1.0120	91.9569	4.7738
548.303 - dins	0.3219	1.0122	91.9493	4.7771
587.673 - dins	0.3223	1.0124	91.9417	4.7803
627.044 - dins	0.3226	1.0126	91.9341	4.7836
666.414 - dins	0.3230	1.0128	91.9265	4.7868
688.965 - dusr	0.3232	1.0129	91.9221	4.7887
705.784 - dins	0.3233	1.0129	91.9189	4.7901
745.154 - dins	0.3237	1.0131	91.9112	4.7933
784.524 - dins	0.3241	1.0133	91.9036	4.7966
823.894 - dins	0.3244	1.0135	91.8959	4.7998
866.545 - dins	0.3248	1.0137	91.8876	4.8034
905.915 - dins	0.3252	1.0139	91.8799	4.8066
918.620 - dusr	0.3253	1.0139	91.8774	4.8077
945.285 - dins	0.3255	1.0140	91.8722	4.8099
984.655 - dins	0.3259	1.0142	91.8644	4.8131
1024.025 - dins	0.3263	1.0144	91.8567	4.8164
1063.395 - dins	0.3266	1.0146	91.8489	4.8197
1102.765 - dins	0.3270	1.0147	91.8412	4.8230
1142.135 - dins	0.3274	1.0149	91.8334	4.8263
1148.275 - dusr	0.3274	1.0150	91.8322	4.8268
1181.505 - dins	0.3277	1.0151	91.8256	4.8295
1220.876 - dins	0.3281	1.0153	91.8178	4.8328
1263.526 - dins	0.3285	1.0155	91.8093	4.8364
1302.897 - dins	0.3289	1.0156	91.8015	4.8397
1342.267 - dins	0.3292	1.0158	91.7936	4.8430
1377.931 - dusr	0.3296	1.0160	91.7865	4.8460
1381.637 - dins	0.3296	1.0160	91.7857	4.8463
1421.007 - dins	0.3300	1.0162	91.7778	4.8496

1460.377 - dins	0.3303	1.0163	91.7699	4.8529
1499.747 - dins	0.3307	1.0165	91.7620	4.8562
1539.117 - dins	0.3311	1.0167	91.7541	4.8595
1578.487 - dins	0.3314	1.0169	91.7461	4.8628
1607.586 - dusr	0.3317	1.0170	91.7403	4.8653
1617.857 - dins	0.3318	1.0170	91.7382	4.8661
1660.508 - dins	0.3322	1.0172	91.7295	4.8697
1699.878 - dins	0.3326	1.0174	91.7216	4.8730
1739.248 - dins	0.3329	1.0176	91.7136	4.8764
1778.618 - dins	0.3333	1.0177	91.7055	4.8797
1817.988 - dins	0.3337	1.0179	91.6975	4.8830
1837.241 - dusr	0.3339	1.0180	91.6936	4.8847
1857.359 - dins	0.3341	1.0181	91.6894	4.8864
1896.729 - dins	0.3344	1.0182	91.6814	4.8897
1936.099 - dins	0.3348	1.0184	91.6733	4.8930
1975.469 - dins	0.3352	1.0186	91.6652	4.8964
2014.839 - dins	0.3355	1.0188	91.6571	4.8997
2057.490 - dins	0.3360	1.0189	91.6483	4.9034
2066.896 - dusr	0.3360	1.0190	91.6463	4.9042
2096.860 - dins	0.3363	1.0191	91.6401	4.9067
2136.230 - dins	0.3367	1.0193	91.6319	4.9101
2175.600 - dins	0.3371	1.0194	91.6238	4.9134
2214.970 - dins	0.3375	1.0196	91.6156	4.9168
2254.340 - dins	0.3378	1.0198	91.6074	4.9202
2293.710 - dins	0.3382	1.0199	91.5991	4.9235
2296.551 - dusr	0.3382	1.0199	91.5985	4.9238
2333.080 - dins	0.3386	1.0201	91.5909	4.9269
2372.450 - dins	0.3390	1.0203	91.5826	4.9303
2411.820 - dins	0.3393	1.0204	91.5743	4.9336
2454.471 - dins	0.3398	1.0206	91.5653	4.9373
2493.841 - dins	0.3401	1.0208	91.5570	4.9407
2526.207 - dusr	0.3404	1.0209	91.5502	4.9435
2533.212 - dins	0.3405	1.0209	91.5487	4.9441
2572.582 - dins	0.3409	1.0211	91.5403	4.9475
2611.952 - dins	0.3413	1.0213	91.5320	4.9509
2651.322 - dins	0.3417	1.0214	91.5236	4.9543
2690.692 - dins	0.3420	1.0216	91.5152	4.9577
2730.062 - dins	0.3424	1.0217	91.5068	4.9611
2755.862 - dusr	0.3427	1.0218	91.5012	4.9633
2769.432 - dins	0.3428	1.0219	91.4983	4.9645
2808.802 - dins	0.3432	1.0221	91.4899	4.9679
2851.453 - dins	0.3436	1.0222	91.4807	4.9716
2890.823 - dins	0.3440	1.0224	91.4722	4.9750
2930.193 - dins	0.3444	1.0225	91.4637	4.9784
2969.563 - dins	0.3448	1.0227	91.4552	4.9819
2985.517 - dusr	0.3449	1.0228	91.4517	4.9832
3008.933 - dins	0.3451	1.0229	91.4466	4.9853
3048.303 - dins	0.3455	1.0230	91.4381	4.9887
3087.674 - dins	0.3459	1.0232	91.4295	4.9921
3127.044 - dins	0.3463	1.0233	91.4209	4.9956
3166.414 - dins	0.3467	1.0235	91.4123	4.9990
3205.784 - dins	0.3471	1.0236	91.4036	5.0025
3215.172 - dusr	0.3472	1.0237	91.4016	5.0033
3248.435 - dins	0.3475	1.0238	91.3942	5.0062

3287.805 - dins	0.3479	1.0240	91.3856	5.0097
3327.175 - dins	0.3483	1.0241	91.3769	5.0131
3366.545 - dins	0.3487	1.0243	91.3681	5.0166
3405.915 - dins	0.3490	1.0244	91.3594	5.0200
3444.827 - dusr	0.3494	1.0246	91.3508	5.0235
3445.285 - dins	0.3494	1.0246	91.3507	5.0235
3484.655 - dins	0.3498	1.0247	91.3419	5.0270
3524.025 - dins	0.3502	1.0249	91.3331	5.0304
3563.395 - dins	0.3506	1.0250	91.3243	5.0339
3602.765 - dins	0.3510	1.0252	91.3154	5.0374
3642.135 - dins	0.3514	1.0253	91.3066	5.0409
3674.482 - dusr	0.3517	1.0254	91.2993	5.0438
3684.786 - dins	0.3518	1.0255	91.2970	5.0447
3724.156 - dins	0.3522	1.0256	91.2881	5.0482
3763.527 - dins	0.3526	1.0258	91.2792	5.0517
3802.897 - dins	0.3530	1.0259	91.2702	5.0552
3842.267 - dins	0.3534	1.0261	91.2613	5.0587
3881.637 - dins	0.3538	1.0262	91.2523	5.0622
3904.138 - dusr	0.3540	1.0263	91.2471	5.0642
3921.007 - dins	0.3542	1.0264	91.2433	5.0657
3960.377 - dins	0.3546	1.0265	91.2343	5.0692
3999.747 - dins	0.3550	1.0266	91.2252	5.0727
4039.117 - dins	0.3554	1.0268	91.2161	5.0762
4081.768 - dins	0.3558	1.0269	91.2063	5.0801
4121.138 - dins	0.3562	1.0271	91.1972	5.0836
4133.793 - dusr	0.3563	1.0271	91.1943	5.0847
4160.508 - dins	0.3566	1.0272	91.1881	5.0871
4199.878 - dins	0.3570	1.0274	91.1789	5.0907
4239.248 - dins	0.3574	1.0275	91.1697	5.0942
4278.618 - dins	0.3578	1.0276	91.1605	5.0977
4317.989 - dins	0.3582	1.0278	91.1513	5.1013
4357.359 - dins	0.3586	1.0279	91.1421	5.1049
4363.448 - dusr	0.3587	1.0279	91.1406	5.1054
4396.729 - dins	0.3590	1.0280	91.1328	5.1084
4436.099 - dins	0.3594	1.0282	91.1235	5.1120
4478.750 - dins	0.3598	1.0283	91.1134	5.1158
4518.120 - dins	0.3602	1.0285	91.1041	5.1194
4557.490 - dins	0.3606	1.0286	91.0947	5.1230
4563.990 - dusr	0.3607	1.0286	91.0932	5.1236
4593.103 - dusr	0.3610	1.0287	91.0862	5.1262
4596.860 - dins	0.3611	1.0287	91.0853	5.1266
4636.230 - dins	0.3615	1.0289	91.0759	5.1301
4675.600 - dins	0.3619	1.0290	91.0665	5.1337
4714.970 - dins	0.3623	1.0291	91.0570	5.1373
4754.340 - dins	0.3627	1.0293	91.0475	5.1409
4793.710 - dins	0.3631	1.0294	91.0380	5.1445
4822.758 - dusr	0.3634	1.0295	91.0310	5.1472
4833.080 - dins	0.3635	1.0295	91.0285	5.1481
4875.731 - dins	0.3639	1.0297	91.0181	5.1520
4915.101 - dins	0.3643	1.0298	91.0086	5.1556
4954.471 - dins	0.3647	1.0299	90.9990	5.1593
4993.842 - dins	0.3652	1.0300	90.9893	5.1629
5033.212 - dins	0.3656	1.0302	90.9797	5.1665
5052.414 - dusr	0.3658	1.0302	90.9749	5.1683

5072.582 - dins	0.3660	1.0303	90.9700	5.1701
5111.952 - dins	0.3664	1.0304	90.9603	5.1738
5151.322 - dins	0.3668	1.0305	90.9505	5.1774
5190.692 - dins	0.3672	1.0307	90.9407	5.1811
5230.062 - dins	0.3676	1.0308	90.9310	5.1847
5272.713 - dins	0.3681	1.0309	90.9203	5.1887
5282.069 - dusr	0.3682	1.0309	90.9180	5.1895
5312.083 - dins	0.3685	1.0310	90.9105	5.1923
5351.453 - dins	0.3689	1.0311	90.9006	5.1960
5390.823 - dins	0.3693	1.0313	90.8907	5.1996
5430.193 - dins	0.3697	1.0314	90.8807	5.2033
5469.563 - dins	0.3701	1.0315	90.8708	5.2070
5508.933 - dins	0.3705	1.0316	90.8608	5.2107
5511.724 - dusr	0.3706	1.0316	90.8601	5.2109
5548.304 - dins	0.3710	1.0317	90.8508	5.2144
5587.674 - dins	0.3714	1.0318	90.8407	5.2181
5595.082 - dusr	0.3715	1.0319	90.8388	5.2188
5627.044 - dins	0.3718	1.0320	90.8307	5.2218
5669.695 - dins	0.3722	1.0321	90.8197	5.2258
5709.065 - dins	0.3727	1.0322	90.8096	5.2295
5741.379 - dusr	0.3730	1.0323	90.8012	5.2325
5748.435 - dins	0.3731	1.0323	90.7994	5.2332
5787.805 - dins	0.3735	1.0324	90.7892	5.2369
5827.175 - dins	0.3739	1.0325	90.7790	5.2406
5866.545 - dins	0.3743	1.0326	90.7687	5.2443
5905.915 - dins	0.3748	1.0327	90.7584	5.2481
5945.285 - dins	0.3752	1.0328	90.7481	5.2518
5971.034 - dusr	0.3755	1.0329	90.7413	5.2543
5984.655 - dins	0.3756	1.0329	90.7377	5.2556
6024.025 - dins	0.3760	1.0330	90.7274	5.2593
6066.676 - dins	0.3765	1.0332	90.7161	5.2634
6106.046 - dins	0.3769	1.0333	90.7056	5.2671
6145.416 - dins	0.3773	1.0334	90.6951	5.2709
6184.786 - dins	0.3777	1.0335	90.6846	5.2747
6200.689 - dusr	0.3779	1.0335	90.6803	5.2762
6220.076 - DGOC	0.3781	1.0336	90.6752	5.2780
6660.105 - DREF	0.2873	0.3078	42.6014	5.2328

Molar Distributions Fluid, Z Inserted Point	Com(5 ,C3) Calculated	Com(6 ,IC4) Calculated	Com(7 ,NC4) Calculated	Com(8 ,IC5) Calculated
229.655 - dusr	1.0069	0.2674	0.2716	0.1002
269.432 - dins	1.0083	0.2679	0.2722	0.1005
308.802 - dins	1.0097	0.2685	0.2728	0.1008
348.172 - dins	1.0110	0.2690	0.2734	0.1011
387.542 - dins	1.0124	0.2696	0.2739	0.1013
426.912 - dins	1.0138	0.2702	0.2745	0.1016
459.310 - dusr	1.0150	0.2706	0.2750	0.1018
469.563 - dins	1.0153	0.2708	0.2751	0.1019
508.933 - dins	1.0167	0.2713	0.2757	0.1022
548.303 - dins	1.0181	0.2719	0.2763	0.1025

587.673 - dins	1.0195	0.2724	0.2769	0.1027
627.044 - dins	1.0209	0.2730	0.2774	0.1030
666.414 - dins	1.0223	0.2736	0.2780	0.1033
688.965 - dusr	1.0231	0.2739	0.2784	0.1035
705.784 - dins	1.0237	0.2741	0.2786	0.1036
745.154 - dins	1.0251	0.2747	0.2792	0.1039
784.524 - dins	1.0265	0.2753	0.2798	0.1041
823.894 - dins	1.0279	0.2758	0.2804	0.1044
866.545 - dins	1.0295	0.2765	0.2810	0.1047
905.915 - dins	1.0309	0.2770	0.2816	0.1050
918.620 - dusr	1.0313	0.2772	0.2818	0.1051
945.285 - dins	1.0323	0.2776	0.2822	0.1053
984.655 - dins	1.0337	0.2782	0.2828	0.1056
1024.025 - dins	1.0351	0.2788	0.2834	0.1059
1063.395 - dins	1.0366	0.2793	0.2840	0.1062
1102.765 - dins	1.0380	0.2799	0.2846	0.1065
1142.135 - dins	1.0394	0.2805	0.2852	0.1068
1148.275 - dusr	1.0396	0.2806	0.2853	0.1068
1181.505 - dins	1.0408	0.2811	0.2858	0.1071
1220.876 - dins	1.0423	0.2817	0.2864	0.1073
1263.526 - dins	1.0438	0.2823	0.2870	0.1077
1302.897 - dins	1.0453	0.2829	0.2876	0.1080
1342.267 - dins	1.0467	0.2835	0.2882	0.1083
1377.931 - dusr	1.0480	0.2840	0.2888	0.1085
1381.637 - dins	1.0482	0.2840	0.2888	0.1086
1421.007 - dins	1.0496	0.2846	0.2895	0.1089
1460.377 - dins	1.0510	0.2852	0.2901	0.1091
1499.747 - dins	1.0525	0.2858	0.2907	0.1094
1539.117 - dins	1.0539	0.2864	0.2913	0.1097
1578.487 - dins	1.0554	0.2870	0.2919	0.1100
1607.586 - dusr	1.0565	0.2875	0.2924	0.1103
1617.857 - dins	1.0569	0.2876	0.2925	0.1104
1660.508 - dins	1.0584	0.2883	0.2932	0.1107
1699.878 - dins	1.0599	0.2889	0.2938	0.1110
1739.248 - dins	1.0614	0.2895	0.2944	0.1113
1778.618 - dins	1.0628	0.2901	0.2951	0.1116
1817.988 - dins	1.0643	0.2907	0.2957	0.1119
1837.241 - dusr	1.0650	0.2910	0.2960	0.1121
1857.359 - dins	1.0658	0.2913	0.2963	0.1122
1896.729 - dins	1.0672	0.2919	0.2969	0.1125
1936.099 - dins	1.0687	0.2925	0.2976	0.1128
1975.469 - dins	1.0702	0.2931	0.2982	0.1131
2014.839 - dins	1.0717	0.2937	0.2988	0.1134
2057.490 - dins	1.0733	0.2944	0.2995	0.1138
2066.896 - dusr	1.0736	0.2945	0.2997	0.1139
2096.860 - dins	1.0748	0.2950	0.3001	0.1141
2136.230 - dins	1.0763	0.2956	0.3008	0.1144
2175.600 - dins	1.0778	0.2962	0.3014	0.1147
2214.970 - dins	1.0792	0.2968	0.3021	0.1150
2254.340 - dins	1.0807	0.2974	0.3027	0.1154
2293.710 - dins	1.0822	0.2981	0.3033	0.1157
2296.551 - dusr	1.0823	0.2981	0.3034	0.1157
2333.080 - dins	1.0837	0.2987	0.3040	0.1160
2372.450 - dins	1.0852	0.2993	0.3046	0.1163

2411.820 - dins	1.0868	0.2999	0.3053	0.1166
2454.471 - dins	1.0884	0.3006	0.3060	0.1170
2493.841 - dins	1.0899	0.3013	0.3066	0.1173
2526.207 - dusr	1.0911	0.3018	0.3072	0.1176
2533.212 - dins	1.0914	0.3019	0.3073	0.1176
2572.582 - dins	1.0929	0.3025	0.3079	0.1180
2611.952 - dins	1.0944	0.3031	0.3086	0.1183
2651.322 - dins	1.0960	0.3038	0.3093	0.1186
2690.692 - dins	1.0975	0.3044	0.3099	0.1189
2730.062 - dins	1.0990	0.3051	0.3106	0.1193
2755.862 - dusr	1.1000	0.3055	0.3110	0.1195
2769.432 - dins	1.1006	0.3057	0.3112	0.1196
2808.802 - dins	1.1021	0.3063	0.3119	0.1199
2851.453 - dins	1.1037	0.3070	0.3126	0.1203
2890.823 - dins	1.1053	0.3077	0.3133	0.1206
2930.193 - dins	1.1068	0.3083	0.3140	0.1210
2969.563 - dins	1.1084	0.3090	0.3146	0.1213
2985.517 - dusr	1.1090	0.3092	0.3149	0.1214
3008.933 - dins	1.1099	0.3096	0.3153	0.1216
3048.303 - dins	1.1115	0.3103	0.3160	0.1220
3087.674 - dins	1.1130	0.3109	0.3167	0.1223
3127.044 - dins	1.1146	0.3116	0.3173	0.1226
3166.414 - dins	1.1161	0.3122	0.3180	0.1230
3205.784 - dins	1.1177	0.3129	0.3187	0.1233
3215.172 - dusr	1.1181	0.3130	0.3189	0.1234
3248.435 - dins	1.1194	0.3136	0.3194	0.1237
3287.805 - dins	1.1209	0.3143	0.3201	0.1240
3327.175 - dins	1.1225	0.3149	0.3208	0.1244
3366.545 - dins	1.1241	0.3156	0.3215	0.1247
3405.915 - dins	1.1257	0.3163	0.3222	0.1251
3444.827 - dusr	1.1272	0.3169	0.3229	0.1254
3445.285 - dins	1.1272	0.3169	0.3229	0.1254
3484.655 - dins	1.1288	0.3176	0.3236	0.1258
3524.025 - dins	1.1304	0.3183	0.3243	0.1261
3563.395 - dins	1.1320	0.3189	0.3250	0.1265
3602.765 - dins	1.1336	0.3196	0.3257	0.1268
3642.135 - dins	1.1352	0.3203	0.3264	0.1272
3674.482 - dusr	1.1365	0.3208	0.3269	0.1275
3684.786 - dins	1.1369	0.3210	0.3271	0.1276
3724.156 - dins	1.1385	0.3217	0.3278	0.1279
3763.527 - dins	1.1401	0.3224	0.3285	0.1283
3802.897 - dins	1.1417	0.3231	0.3292	0.1287
3842.267 - dins	1.1433	0.3237	0.3299	0.1290
3881.637 - dins	1.1449	0.3244	0.3307	0.1294
3904.138 - dusr	1.1458	0.3248	0.3311	0.1296
3921.007 - dins	1.1465	0.3251	0.3314	0.1297
3960.377 - dins	1.1481	0.3258	0.3321	0.1301
3999.747 - dins	1.1497	0.3265	0.3328	0.1305
4039.117 - dins	1.1514	0.3272	0.3335	0.1308
4081.768 - dins	1.1531	0.3279	0.3343	0.1312
4121.138 - dins	1.1548	0.3286	0.3350	0.1316
4133.793 - dusr	1.1553	0.3289	0.3353	0.1317
4160.508 - dins	1.1564	0.3293	0.3357	0.1320
4199.878 - dins	1.1580	0.3300	0.3365	0.1323

4239.248 - dins	1.1597	0.3307	0.3372	0.1327
4278.618 - dins	1.1613	0.3314	0.3379	0.1331
4317.989 - dins	1.1629	0.3322	0.3387	0.1335
4357.359 - dins	1.1646	0.3329	0.3394	0.1338
4363.448 - dusr	1.1648	0.3330	0.3395	0.1339
4396.729 - dins	1.1662	0.3336	0.3401	0.1342
4436.099 - dins	1.1679	0.3343	0.3409	0.1346
4478.750 - dins	1.1697	0.3351	0.3417	0.1350
4518.120 - dins	1.1713	0.3358	0.3424	0.1354
4557.490 - dins	1.1730	0.3365	0.3432	0.1358
4563.990 - dusr	1.1733	0.3366	0.3433	0.1358
4593.103 - dusr	1.1745	0.3371	0.3438	0.1361
4596.860 - dins	1.1747	0.3372	0.3439	0.1361
4636.230 - dins	1.1763	0.3379	0.3447	0.1365
4675.600 - dins	1.1780	0.3387	0.3454	0.1369
4714.970 - dins	1.1797	0.3394	0.3462	0.1373
4754.340 - dins	1.1813	0.3401	0.3469	0.1377
4793.710 - dins	1.1830	0.3408	0.3477	0.1381
4822.758 - dusr	1.1843	0.3414	0.3482	0.1384
4833.080 - dins	1.1847	0.3416	0.3484	0.1385
4875.731 - dins	1.1865	0.3424	0.3493	0.1389
4915.101 - dins	1.1882	0.3431	0.3500	0.1393
4954.471 - dins	1.1899	0.3438	0.3508	0.1397
4993.842 - dins	1.1916	0.3446	0.3516	0.1401
5033.212 - dins	1.1933	0.3453	0.3523	0.1405
5052.414 - dusr	1.1942	0.3457	0.3527	0.1407
5072.582 - dins	1.1950	0.3461	0.3531	0.1409
5111.952 - dins	1.1967	0.3468	0.3539	0.1413
5151.322 - dins	1.1984	0.3475	0.3547	0.1417
5190.692 - dins	1.2002	0.3483	0.3554	0.1421
5230.062 - dins	1.2019	0.3490	0.3562	0.1425
5272.713 - dins	1.2037	0.3499	0.3571	0.1429
5282.069 - dusr	1.2042	0.3500	0.3572	0.1430
5312.083 - dins	1.2055	0.3506	0.3578	0.1433
5351.453 - dins	1.2072	0.3514	0.3586	0.1437
5390.823 - dins	1.2089	0.3521	0.3594	0.1442
5430.193 - dins	1.2107	0.3529	0.3602	0.1446
5469.563 - dins	1.2124	0.3537	0.3610	0.1450
5508.933 - dins	1.2142	0.3544	0.3618	0.1454
5511.724 - dusr	1.2143	0.3545	0.3619	0.1454
5548.304 - dins	1.2159	0.3552	0.3626	0.1458
5587.674 - dins	1.2177	0.3560	0.3634	0.1462
5595.082 - dusr	1.2180	0.3561	0.3636	0.1463
5627.044 - dins	1.2194	0.3567	0.3642	0.1466
5669.695 - dins	1.2213	0.3576	0.3651	0.1471
5709.065 - dins	1.2231	0.3583	0.3659	0.1475
5741.379 - dusr	1.2245	0.3590	0.3666	0.1479
5748.435 - dins	1.2248	0.3591	0.3667	0.1479
5787.805 - dins	1.2266	0.3599	0.3675	0.1484
5827.175 - dins	1.2284	0.3607	0.3683	0.1488
5866.545 - dins	1.2302	0.3615	0.3692	0.1492
5905.915 - dins	1.2319	0.3623	0.3700	0.1497
5945.285 - dins	1.2337	0.3631	0.3708	0.1501
5971.034 - dusr	1.2349	0.3636	0.3713	0.1504

5984.655 - dins	1.2355	0.3638	0.3716	0.1505
6024.025 - dins	1.2373	0.3646	0.3724	0.1510
6066.676 - dins	1.2393	0.3655	0.3733	0.1514
6106.046 - dins	1.2411	0.3663	0.3742	0.1519
6145.416 - dins	1.2429	0.3671	0.3750	0.1523
6184.786 - dins	1.2447	0.3679	0.3759	0.1528
6200.689 - dusr	1.2454	0.3682	0.3762	0.1529
6220.076 - DGOC	1.2463	0.3686	0.3766	0.1531
6660.105 - DREF	1.9392	0.8208	0.9747	0.5438

Molar Distributions Fluid, Z Inserted Point	Com(9 ,NC5) Calculated	Com(10,C6) Calculated	Com(11,C7+) Calculated	Total Calculated
229.655 - dusr	0.0816	0.1637	0.0176	100.0000
269.432 - dins	0.0819	0.1643	0.0178	100.0000
308.802 - dins	0.0821	0.1648	0.0179	100.0000
348.172 - dins	0.0823	0.1654	0.0181	100.0000
387.542 - dins	0.0825	0.1659	0.0183	100.0000
426.912 - dins	0.0828	0.1665	0.0185	100.0000
459.310 - dusr	0.0830	0.1669	0.0187	100.0000
469.563 - dins	0.0830	0.1671	0.0187	100.0000
508.933 - dins	0.0832	0.1676	0.0189	100.0000
548.303 - dins	0.0835	0.1682	0.0191	100.0000
587.673 - dins	0.0837	0.1687	0.0193	100.0000
627.044 - dins	0.0839	0.1693	0.0195	100.0000
666.414 - dins	0.0842	0.1699	0.0197	100.0000
688.965 - dusr	0.0843	0.1702	0.0199	100.0000
705.784 - dins	0.0844	0.1704	0.0200	100.0000
745.154 - dins	0.0846	0.1710	0.0202	100.0000
784.524 - dins	0.0849	0.1715	0.0204	100.0000
823.894 - dins	0.0851	0.1721	0.0206	100.0000
866.545 - dins	0.0854	0.1727	0.0208	100.0000
905.915 - dins	0.0856	0.1733	0.0211	100.0000
918.620 - dusr	0.0857	0.1735	0.0211	100.0000
945.285 - dins	0.0858	0.1739	0.0213	100.0000
984.655 - dins	0.0861	0.1745	0.0215	100.0000
1024.025 - dins	0.0863	0.1750	0.0217	100.0000
1063.395 - dins	0.0865	0.1756	0.0220	100.0000
1102.765 - dins	0.0868	0.1762	0.0222	100.0000
1142.135 - dins	0.0870	0.1768	0.0224	100.0000
1148.275 - dusr	0.0871	0.1769	0.0225	100.0000
1181.505 - dins	0.0873	0.1774	0.0227	100.0000
1220.876 - dins	0.0875	0.1780	0.0229	100.0000
1263.526 - dins	0.0878	0.1786	0.0232	100.0000
1302.897 - dins	0.0880	0.1792	0.0234	100.0000
1342.267 - dins	0.0883	0.1798	0.0237	100.0000
1377.931 - dusr	0.0885	0.1803	0.0239	100.0000
1381.637 - dins	0.0885	0.1804	0.0239	100.0000
1421.007 - dins	0.0888	0.1810	0.0242	100.0000
1460.377 - dins	0.0890	0.1816	0.0244	100.0000
1499.747 - dins	0.0892	0.1822	0.0247	100.0000

1539.117 - dins	0.0895	0.1828	0.0250	100.0000
1578.487 - dins	0.0897	0.1834	0.0252	100.0000
1607.586 - dusr	0.0899	0.1839	0.0254	100.0000
1617.857 - dins	0.0900	0.1840	0.0255	100.0000
1660.508 - dins	0.0903	0.1847	0.0258	100.0000
1699.878 - dins	0.0905	0.1853	0.0261	100.0000
1739.248 - dins	0.0908	0.1859	0.0263	100.0000
1778.618 - dins	0.0910	0.1866	0.0266	100.0000
1817.988 - dins	0.0913	0.1872	0.0269	100.0000
1837.241 - dusr	0.0914	0.1875	0.0270	100.0000
1857.359 - dins	0.0915	0.1878	0.0272	100.0000
1896.729 - dins	0.0918	0.1884	0.0275	100.0000
1936.099 - dins	0.0920	0.1891	0.0278	100.0000
1975.469 - dins	0.0923	0.1897	0.0281	100.0000
2014.839 - dins	0.0926	0.1903	0.0284	100.0000
2057.490 - dins	0.0928	0.1910	0.0287	100.0000
2066.896 - dusr	0.0929	0.1912	0.0288	100.0000
2096.860 - dins	0.0931	0.1917	0.0290	100.0000
2136.230 - dins	0.0934	0.1923	0.0293	100.0000
2175.600 - dins	0.0936	0.1929	0.0296	100.0000
2214.970 - dins	0.0939	0.1936	0.0299	100.0000
2254.340 - dins	0.0941	0.1942	0.0303	100.0000
2293.710 - dins	0.0944	0.1949	0.0306	100.0000
2296.551 - dusr	0.0944	0.1949	0.0306	100.0000
2333.080 - dins	0.0947	0.1955	0.0309	100.0000
2372.450 - dins	0.0949	0.1962	0.0313	100.0000
2411.820 - dins	0.0952	0.1969	0.0316	100.0000
2454.471 - dins	0.0955	0.1976	0.0320	100.0000
2493.841 - dins	0.0957	0.1982	0.0323	100.0000
2526.207 - dusr	0.0960	0.1988	0.0326	100.0000
2533.212 - dins	0.0960	0.1989	0.0326	100.0000
2572.582 - dins	0.0963	0.1996	0.0330	100.0000
2611.952 - dins	0.0966	0.2002	0.0334	100.0000
2651.322 - dins	0.0968	0.2009	0.0337	100.0000
2690.692 - dins	0.0971	0.2016	0.0341	100.0000
2730.062 - dins	0.0974	0.2023	0.0344	100.0000
2755.862 - dusr	0.0976	0.2027	0.0347	100.0000
2769.432 - dins	0.0976	0.2029	0.0348	100.0000
2808.802 - dins	0.0979	0.2036	0.0352	100.0000
2851.453 - dins	0.0982	0.2044	0.0356	100.0000
2890.823 - dins	0.0985	0.2051	0.0360	100.0000
2930.193 - dins	0.0988	0.2058	0.0364	100.0000
2969.563 - dins	0.0990	0.2064	0.0368	100.0000
2985.517 - dusr	0.0992	0.2067	0.0369	100.0000
3008.933 - dins	0.0993	0.2071	0.0372	100.0000
3048.303 - dins	0.0996	0.2078	0.0376	100.0000
3087.674 - dins	0.0999	0.2085	0.0380	100.0000
3127.044 - dins	0.1002	0.2092	0.0384	100.0000
3166.414 - dins	0.1004	0.2100	0.0388	100.0000
3205.784 - dins	0.1007	0.2107	0.0392	100.0000
3215.172 - dusr	0.1008	0.2108	0.0393	100.0000
3248.435 - dins	0.1010	0.2114	0.0397	100.0000
3287.805 - dins	0.1013	0.2122	0.0401	100.0000
3327.175 - dins	0.1016	0.2129	0.0405	100.0000

3366.545 - dins	0.1019	0.2136	0.0410	100.0000
3405.915 - dins	0.1022	0.2143	0.0414	100.0000
3444.827 - dusr	0.1025	0.2150	0.0419	100.0000
3445.285 - dins	0.1025	0.2150	0.0419	100.0000
3484.655 - dins	0.1028	0.2158	0.0423	100.0000
3524.025 - dins	0.1031	0.2165	0.0428	100.0000
3563.395 - dins	0.1033	0.2172	0.0432	100.0000
3602.765 - dins	0.1036	0.2180	0.0437	100.0000
3642.135 - dins	0.1039	0.2187	0.0442	100.0000
3674.482 - dusr	0.1042	0.2193	0.0446	100.0000
3684.786 - dins	0.1043	0.2195	0.0447	100.0000
3724.156 - dins	0.1045	0.2203	0.0452	100.0000
3763.527 - dins	0.1048	0.2210	0.0457	100.0000
3802.897 - dins	0.1051	0.2218	0.0462	100.0000
3842.267 - dins	0.1054	0.2225	0.0467	100.0000
3881.637 - dins	0.1057	0.2233	0.0472	100.0000
3904.138 - dusr	0.1059	0.2237	0.0475	100.0000
3921.007 - dins	0.1060	0.2240	0.0477	100.0000
3960.377 - dins	0.1063	0.2248	0.0482	100.0000
3999.747 - dins	0.1066	0.2256	0.0487	100.0000
4039.117 - dins	0.1069	0.2263	0.0493	100.0000
4081.768 - dins	0.1073	0.2272	0.0499	100.0000
4121.138 - dins	0.1076	0.2279	0.0504	100.0000
4133.793 - dusr	0.1077	0.2282	0.0506	100.0000
4160.508 - dins	0.1079	0.2287	0.0510	100.0000
4199.878 - dins	0.1082	0.2295	0.0515	100.0000
4239.248 - dins	0.1085	0.2303	0.0521	100.0000
4278.618 - dins	0.1088	0.2311	0.0526	100.0000
4317.989 - dins	0.1091	0.2319	0.0532	100.0000
4357.359 - dins	0.1094	0.2327	0.0538	100.0000
4363.448 - dusr	0.1095	0.2328	0.0539	100.0000
4396.729 - dins	0.1097	0.2335	0.0544	100.0000
4436.099 - dins	0.1101	0.2343	0.0550	100.0000
4478.750 - dins	0.1104	0.2351	0.0556	100.0000
4518.120 - dins	0.1107	0.2359	0.0562	100.0000
4557.490 - dins	0.1110	0.2368	0.0569	100.0000
4563.990 - dusr	0.1111	0.2369	0.0570	100.0000
4593.103 - dusr	0.1113	0.2375	0.0574	100.0000
4596.860 - dins	0.1114	0.2376	0.0575	100.0000
4636.230 - dins	0.1117	0.2384	0.0581	100.0000
4675.600 - dins	0.1120	0.2392	0.0588	100.0000
4714.970 - dins	0.1123	0.2400	0.0594	100.0000
4754.340 - dins	0.1126	0.2409	0.0601	100.0000
4793.710 - dins	0.1130	0.2417	0.0607	100.0000
4822.758 - dusr	0.1132	0.2423	0.0612	100.0000
4833.080 - dins	0.1133	0.2425	0.0614	100.0000
4875.731 - dins	0.1136	0.2434	0.0621	100.0000
4915.101 - dins	0.1140	0.2443	0.0628	100.0000
4954.471 - dins	0.1143	0.2451	0.0635	100.0000
4993.842 - dins	0.1146	0.2460	0.0642	100.0000
5033.212 - dins	0.1150	0.2468	0.0649	100.0000
5052.414 - dusr	0.1151	0.2472	0.0653	100.0000
5072.582 - dins	0.1153	0.2477	0.0656	100.0000
5111.952 - dins	0.1156	0.2485	0.0664	100.0000

5151.322 - dins	0.1160	0.2494	0.0671	100.0000
5190.692 - dins	0.1163	0.2502	0.0678	100.0000
5230.062 - dins	0.1166	0.2511	0.0686	100.0000
5272.713 - dins	0.1170	0.2521	0.0694	100.0000
5282.069 - dusr	0.1171	0.2523	0.0696	100.0000
5312.083 - dins	0.1173	0.2529	0.0702	100.0000
5351.453 - dins	0.1177	0.2538	0.0710	100.0000
5390.823 - dins	0.1180	0.2547	0.0718	100.0000
5430.193 - dins	0.1184	0.2556	0.0726	100.0000
5469.563 - dins	0.1187	0.2565	0.0734	100.0000
5508.933 - dins	0.1190	0.2574	0.0742	100.0000
5511.724 - dusr	0.1191	0.2574	0.0742	100.0000
5548.304 - dins	0.1194	0.2583	0.0750	100.0000
5587.674 - dins	0.1197	0.2592	0.0758	100.0000
5595.082 - dusr	0.1198	0.2593	0.0760	100.0000
5627.044 - dins	0.1201	0.2601	0.0767	100.0000
5669.695 - dins	0.1205	0.2611	0.0776	100.0000
5709.065 - dins	0.1208	0.2620	0.0785	100.0000
5741.379 - dusr	0.1211	0.2627	0.0792	100.0000
5748.435 - dins	0.1212	0.2629	0.0794	100.0000
5787.805 - dins	0.1215	0.2638	0.0803	100.0000
5827.175 - dins	0.1219	0.2647	0.0812	100.0000
5866.545 - dins	0.1222	0.2657	0.0821	100.0000
5905.915 - dins	0.1226	0.2666	0.0830	100.0000
5945.285 - dins	0.1229	0.2675	0.0839	100.0000
5971.034 - dusr	0.1232	0.2682	0.0845	100.0000
5984.655 - dins	0.1233	0.2685	0.0849	100.0000
6024.025 - dins	0.1237	0.2694	0.0858	100.0000
6066.676 - dins	0.1241	0.2705	0.0869	100.0000
6106.046 - dins	0.1244	0.2714	0.0878	100.0000
6145.416 - dins	0.1248	0.2724	0.0888	100.0000
6184.786 - dins	0.1252	0.2733	0.0898	100.0000
6200.689 - dusr	0.1253	0.2737	0.0903	100.0000
6220.076 - DGOC	0.1255	0.2742	0.0908	100.0000
6660.105 - DREF	0.4925	1.6930	45.1066	100.0000

A6. Expt SEPS2 : Separators

Peng-Robinson (3-Parm) on ZI with PR corr.
Lohrenz-Bray-Clark Viscosity Correlation

Stage number 1

Specified pressure PSIA	1500.0000
Specified temperature Deg F	150.0000

GOR calc. is Gas Vol at STC/Stage Oil Vol

Feed is wellstream only

Output is 100.0% of liquid to	stage 2	number moles	0.7672
100.0% of vapour to	cumulative	number moles	0.2328

Total number moles output to liquid stream	0.7672
Total number moles output to vapour stream	0.2328
Total liquid volume output BBL	0.4332
Total vapour volume output MSCF	0.0883
Stage Gas-oil ratio (Calculated) MSCF/BBL	0.2039
Vapour mole fraction (Calculated)	23.2796
Stage Oil FVF (Calculated) RB/STB	1.1433

Fluid properties	Liquid		Vapour	
	Observed	Calculated	Observed	Calculated
Mole Weight		148.5005		17.7512
Z-factor		0.7268		0.8862
Viscosity		0.6522		0.0144
Density LB/FT3		46.8413		4.5924
Molar Vol CF/LB-ML		3.1703		3.8653

Molar Distributions Components		Fluid, Z	K-Values	Liquid,X	Vapour,Y
Mnemonic	Number	Calculated	Calculated	Calculated	Calculated
CO2	1	0.2873	1.6087	0.2516	0.4048
N2	2	0.3078	6.5923	0.1337	0.8815
C1	3	42.6014	3.2837	27.8144	91.3332
C2	4	5.2328	1.0471	5.1760	5.4201
C3	5	1.9392	0.5079	2.1901	1.1123

IC4	6	0.8208	0.2879	0.9839	0.2833
NC4	7	0.9747	0.2290	1.1880	0.2721
IC5	8	0.5438	0.1367	0.6806	0.0930
NC5	9	0.4925	0.1159	0.6201	0.0719
C6	10	1.6930	0.0576	2.1687	0.1250
C7+	11	45.1066	4.6481E-05	58.7927	0.0027
Composition Total		100.0000		100.0000	100.0000

Stage number 2

```
Specified pressure PSIA                                       800.0000
Specified temperature Deg F                                   100.0000

GOR calc. is Gas Vol at STC/Stage Oil Vol

Feed   is 100.0% of liquid from stage  1      number moles      0.7672

Output is 100.0% of liquid to   stage  3      number moles      0.6696
          100.0% of vapour to   cumulative    number moles      0.0976

Total number moles output to liquid stream                      0.6696
Total number moles output to vapour stream                      0.0976

Total liquid volume output BBL                                  0.4060
Total vapour volume output MSCF                                 0.0370

Stage Gas-oil ratio (Calculated) MSCF/BBL                       0.0912

Vapour mole fraction (Calculated)                              12.7214

Stage Oil FVF       (Calculated) RB/STB                         1.0714
```

Fluid properties	Liquid		Vapour	
	Observed	Calculated	Observed	Calculated
Mole Weight		167.5816		17.5892
Z-factor		0.4534		0.8962
Viscosity		0.9875		0.0124
Density LB/FT3		49.2291		2.6141
Molar Vol CF/LB-ML		3.4041		6.7285

Molar Distributions Components	Fluid, Z	K-Values	Liquid,X	Vapour,Y

Mnemonic	Number	Calculated	Calculated	Calculated	Calculated
CO2	1	0.2516	1.9476	0.2246	0.4374
N2	2	0.1337	12.0769	0.0555	0.6703
C1	3	27.8144	4.9511	18.5105	91.6466
C2	4	5.1760	1.1137	5.1022	5.6825
C3	5	2.1901	0.4220	2.3640	0.9975
IC4	6	0.9839	0.1968	1.0959	0.2157
NC4	7	1.1880	0.1466	1.3326	0.1953
IC5	8	0.6806	0.0729	0.7716	0.0562
NC5	9	0.6201	0.0582	0.7045	0.0410
C6	10	2.1687	0.0232	2.4765	0.0573
C7+	11	58.7927	1.4532E-06	67.3621	9.7890E-05
Composition Total		100.0000		100.0000	100.0000

Stage number 3

Specified pressure PSIA	200.0000
Specified temperature Deg F	100.0000

GOR calc. is Gas Vol at STC/Stage Oil Vol

Feed is 100.0% of liquid from stage 2	number moles	0.6696
Output is 100.0% of liquid to cumulative	number moles	0.5526
100.0% of vapour to cumulative	number moles	0.1170

Total number moles output to liquid stream	0.5526
Total number moles output to vapour stream	0.1170
Total liquid volume output BBL	0.3877
Total vapour volume output MSCF	0.0444
Stage Gas-oil ratio (Calculated) MSCF/BBL	0.1145
Vapour mole fraction (Calculated)	17.4751
Stage Oil FVF (Calculated) RB/STB	1.0232

Fluid properties	Liquid		Vapour	
	Observed	Calculated	Observed	Calculated
Mole Weight		198.9970		19.2242
Z-factor		0.1312		0.9647
Viscosity		1.1140		0.0114
Density LB/FT3		50.5164		0.6636

Molar Vol	CF/LB-ML		3.9393	28.9697

Molar Distributions Components Mnemonic	Number	Fluid, Z Calculated	K-Values Calculated	Liquid,X Calculated	Vapour,Y Calculated
CO2	1	0.2246	6.3139	0.1164	0.7352
N2	2	0.0555	47.8737	0.0060	0.2891
C1	3	18.5105	17.5027	4.7660	83.4180
C2	4	5.1022	3.2201	3.6760	11.8371
C3	5	2.3640	1.0357	2.3493	2.4331
IC4	6	1.0959	0.4217	1.2191	0.5141
NC4	7	1.3326	0.3044	1.5170	0.4617
IC5	8	0.7716	0.1326	0.9094	0.1206
NC5	9	0.7045	0.1026	0.8356	0.0857
C6	10	2.4765	0.0354	2.9786	0.1054
C7+	11	67.3621	4.0406E-07	81.6264	3.2982E-05
Composition Total		100.0000		100.0000	100.0000

Cumulatives for Separator Train

Standard pressure PSIA	14.6959
Standard temperature Deg F	60.0000
Cumulative liquid mole fraction	0.5526
Cumulative vapour mole fraction	0.4474
Cumulative Surface volume oil BBL	0.3789
Cumulative Surface volume gas MSCF	0.1698
Cumulative GOR (Calculated) MSCF/BBL	0.4379

Fluid properties		Liquid Calculated	Vapour Calculated
Mole Weight		198.9970	18.1011
Z-factor		0.0101	0.9970
Viscosity		1.4536	0.0107
Density	LB/FT3	51.6879	0.0478
Molar Vol	CF/LB-ML	3.8500	378.3528

Molar Distributions Components Mnemonic	Number	Total, Z Measured	Liquid,X Calculated	Vapour,Y Calculated	K-Values Calculated
CO2	1	0.2873	0.1164	0.4983	4.2796
N2	2	0.3078	0.0060	0.6805	112.6874
C1	3	42.6014	4.7660	89.3314	18.7434
C2	4	5.2328	3.6760	7.1556	1.9465
C3	5	1.9392	2.3493	1.4327	0.6098
IC4	6	0.8208	1.2191	0.3289	0.2698
NC4	7	0.9747	1.5170	0.3049	0.2010
IC5	8	0.5438	0.9094	0.0922	0.1014
NC5	9	0.4925	0.8356	0.0688	0.0823
C6	10	1.6930	2.9786	0.1051	0.0353
C7+	11	45.1066	81.6264	0.0015	1.7787E-05
Composition Total		100.0000	100.0000	100.0000	

```
A7.ECHO
-- DENSITY created by PVTi
-- Units: lb /ft^3     lb /ft^3     lb /ft^3
DENSITY
--
-- Fluid Densities at Surface Conditions
--
         52.4390     62.4280      0.0537
/

-- Created from a Differential Liberation Experiment.
-- Using the method of Whitson and Torp.
--PVTi--Please do not alter these lines
--PVTi--as PVTi can use them to re-create the fluid model
--PVTiMODSPEC
========================================================
--PVTiTITLE
--PVTiModified System: From Automatically created during keyword export
--PVTiVERSION
--PVTi  2010.1          /
--PVTiFPE
--PVTiNCOMPS
--PVTi       11 /
--PVTiEOS
--PVTi PR3  /
--PVTiPRCORR
--PVTiLBC
--PVTiOPTIONS
--PVTi  0  0  0  2  0  0  0  0  0  0  0  0  0  0  0  0  0  0  0  0
--PVTi/
--PVTiNOECHO
--PVTiMODSYS
========================================================
--PVTiUNITS
--PVTi   FIELD       ABSOL         PERCENT      /
--PVTiDEGREES
--PVTi   Fahrenheit /
--PVTiSTCOND
--PVTi      60.0000      14.6959 /
--PVTiLNAMES
--PVTi CO2
--PVTi N2
--PVTi C1
--PVTi C2
--PVTi C3
--PVTi IC4
--PVTi NC4
--PVTi IC5
--PVTi NC5
--PVTi C6
--PVTi 1*
--PVTi /
--PVTiCNAMES
--PVTi 1*
```

```
--PVTi 1*
--PVTi 1*
--PVTi 1*
--PVTi 1*
--PVTi 1*
--PVTi 1*
--PVTi 1*
--PVTi 1*
--PVTi 1*
--PVTi C7+
--PVTi /
--PVTiTCRIT
--PVTi  8.878998547E+01 -2.325100060E+02 -1.165900091E+02
9.010398544E+01
--PVTi  2.059699824E+02  2.749099805E+02  3.056899797E+02
3.690499780E+02
--PVTi  3.856099776E+02  4.538299758E+02  8.987542687E+02
/
--PVTiPCRIT
--PVTi  1.071331110E+03  4.923126500E+02  6.677816960E+02
7.083423800E+02
--PVTi  6.157582100E+02  5.290524000E+02  5.506553730E+02
4.915778550E+02
--PVTi  4.887856340E+02  4.366151890E+02  2.238690294E+02
/
--PVTiVCRIT
--PVTi  1.505735240E+00  1.441661400E+00  1.569809080E+00
2.370732080E+00
--PVTi  3.203692000E+00  4.212854980E+00  4.084707300E+00
4.933685680E+00
--PVTi  4.981741060E+00  5.622479460E+00  1.473824770E+01
/
--PVTiZCRIT
--PVTi  2.740777974E-01  2.911514044E-01  2.847294766E-01  2.846347951E-
01
--PVTi  2.761646200E-01  2.827369588E-01  2.738555491E-01  2.727108716E-
01
--PVTi  2.684389142E-01  2.504174849E-01  2.263345781E-01
/
--PVTiVCRITVIS
--PVTi  1.505735240E+00  1.441661400E+00  1.569809080E+00
2.370732080E+00
--PVTi  3.203692000E+00  4.212854980E+00  4.084707300E+00
4.933685680E+00
--PVTi  4.981741060E+00  5.622479460E+00  1.473824770E+01
/
--PVTiZCRITVIS
--PVTi  2.740777974E-01  2.911514044E-01  2.847294766E-01  2.846347951E-
01
--PVTi  2.761646200E-01  2.827369588E-01  2.738555491E-01  2.727108716E-
01
--PVTi  2.684389142E-01  2.504174849E-01  2.263345781E-01
/
--PVTiSSHIFT
```

```
--PVTi -4.273033674E-02 -1.313342386E-01 -1.442656189E-01 -1.032683540E-
01
--PVTi -7.750138148E-02 -6.198372515E-02 -5.422489699E-02 -4.177245672E-
02
--PVTi -3.027789648E-02 -7.288775999E-03  1.876010146E-01
/
--PVTiACF
--PVTi  2.250000000E-01  4.000000000E-02  1.300000000E-02  9.860000000E-
02
--PVTi  1.524000000E-01  1.848000000E-01  2.010000000E-01  2.270000000E-
01
--PVTi  2.510000000E-01  2.990000000E-01  7.593494718E-01
/
--PVTiMW
--PVTi  4.401000000E+01  2.801300000E+01  1.604300000E+01
3.007000000E+01
--PVTi  4.409700000E+01  5.812400000E+01  5.812400000E+01
7.215100000E+01
--PVTi  7.215100000E+01  8.400000000E+01  2.336092000E+02
/
--PVTiZI
--PVTi  2.872923555E-01  3.078132381E-01  4.260135215E+01
5.232825047E+00
--PVTi  1.939223400E+00  8.208353015E-01  9.747419205E-01  5.438033872E-
01
--PVTi  4.925011809E-01  1.692972809E+00  4.510663921E+01
/
--PVTiTBOIL
--PVTi -1.092100093E+02 -3.203500037E+02 -2.587900053E+02 -
1.273900088E+02
--PVTi -4.369001102E+01  1.066998754E+01  3.118998700E+01
8.212998565E+01
--PVTi  9.688998526E+01  1.470199839E+02  5.897725201E+02
/
--PVTiTREF
--PVTi  6.772998603E+01 -3.190900037E+02 -2.586100053E+02 -
1.302700087E+02
--PVTi -4.387001101E+01  6.772998603E+01  6.772998603E+01
6.772998603E+01
--PVTi  6.772998603E+01  6.052998622E+01  6.000000000E+01
/
--PVTiDREF
--PVTi  4.850653269E+01  5.019208788E+01  2.653188725E+01
3.421052756E+01
--PVTi  3.633307854E+01  3.477237929E+01  3.614579463E+01
3.870534140E+01
--PVTi  3.907990922E+01  4.276315945E+01  5.276412024E+01
/
--PVTiPARACHOR
--PVTi  7.800000000E+01  4.100000000E+01  7.700000000E+01
1.080000000E+02
--PVTi  1.503000000E+02  1.815000000E+02  1.899000000E+02
2.250000000E+02
```

```
--PVTi  2.315000000E+02  2.710000000E+02  6.029028054E+02
/
--PVTiHYDRO
--PVTi  N N H H H H H H H H H
--PVTi /
--PVTiTHERMX
--PVTi    0.0002778 /
--PVTiBIC
--PVTi  -1.200000000E-02
--PVTi   1.000000000E-01  1.000000000E-01
--PVTi   1.000000000E-01  1.000000000E-01  0.000000000E+00
--PVTi   1.000000000E-01  1.000000000E-01  0.000000000E+00
0.000000000E+00
--PVTi   1.000000000E-01  1.000000000E-01  0.000000000E+00
0.000000000E+00
--PVTi   0.000000000E+00
--PVTi   1.000000000E-01  1.000000000E-01  0.000000000E+00
0.000000000E+00
--PVTi   0.000000000E+00  0.000000000E+00
--PVTi   1.000000000E-01  1.000000000E-01  0.000000000E+00
0.000000000E+00
--PVTi   0.000000000E+00  0.000000000E+00  0.000000000E+00
--PVTi   1.000000000E-01  1.000000000E-01  0.000000000E+00
0.000000000E+00
--PVTi   0.000000000E+00  0.000000000E+00  0.000000000E+00
0.000000000E+00
--PVTi   1.000000000E-01  1.000000000E-01  2.790000000E-02  1.000000000E-
02
--PVTi   1.000000000E-02  0.000000000E+00  0.000000000E+00
0.000000000E+00
--PVTi   0.000000000E+00
--PVTi   1.000000000E-01  1.000000000E-01  5.147000002E-02  1.000000000E-
02
--PVTi   1.000000000E-02  0.000000000E+00  0.000000000E+00
0.000000000E+00
--PVTi   0.000000000E+00  0.000000000E+00
--PVTi /
--PVTiSPECHA
--PVTi  4.729150800E+00  7.440052900E+00  4.597785500E+00
1.291918014E+00
--PVTi -1.008885504E+00 -3.319959400E-01  2.265932002E+00 -
2.275008150E+00
--PVTi -8.661081421E-01 -1.054027398E+00  2.138848987E+00
/
--PVTiSPECHB
--PVTi  9.744900480E-03 -1.800630440E-03  6.915907040E-03  2.363244520E-
02
--PVTi  4.064355960E-02  5.104661240E-02  4.419970520E-02  6.722176720E-
02
--PVTi  6.466081160E-02  7.722674400E-02  1.755949990E-01
/
--PVTiSPECHC
--PVTi -4.129676758E-06  1.975639720E-06  8.824032630E-07 -5.114547902E-
06
```

```
--PVTi -1.169165894E-05 -1.360832434E-05 -8.167943320E-06 -2.011761491E-
05
--PVTi -1.901921820E-05 -2.299261301E-05 -3.889710939E-05
/
--PVTiSPECHD
--PVTi  7.023679600E-10 -4.783473920E-10 -4.636038080E-10  3.568356872E-
10
--PVTi  1.316683960E-09  1.185629880E-09 -1.155733168E-10  2.343820312E-
09
--PVTi  2.172630920E-09  2.659578736E-09  0.000000000E+00
/
--PVTiHEATVAPS
--PVTi  1.802570424E+04  0.000000000E+00  0.000000000E+00
1.650621600E+04
--PVTi  3.603408601E+04  4.586099659E+04  6.166418764E+04
5.938211357E+04
--PVTi  6.289700021E+04  7.462523487E+04  1.786112137E+05
/
--PVTiCALVAL
--PVTi  0.000000000E+00  0.000000000E+00  1.891038000E+03
3.323854000E+03
--PVTi  4.754344000E+03  6.184834000E+03  6.184834000E+03
7.615324000E+03
--PVTi  7.615324000E+03  9.045814000E+03  2.192487600E+04
/
--PVTiSIMULATE
========================================================
--PVTiUNITS
--PVTi   FIELD       ABSOL         PERCENT      /
--PVTiDEGREES
--PVTi   Fahrenheit /
--PVTiSTCOND
--PVTi      60.0000      14.6959 /
--PVTiEXP
--PVTi   1  ZI       DL         220.0000
--PVTi                     2692.4670    2394.9370    2097.4070
1799.8770
--PVTi                     1502.3460    1204.8160     907.2860
609.7560
--PVTi                      312.2260      14.6959
/
--PVTi   2  ZI       SEPS        60.0000      14.6959  0  0 /
--PVTi /
--PVTi--End of PVTi generated section--
-- Column Properties are:
--       'Oil GOR'    'PSAT'    'Oil FVF'    'Oil Visc'
-- Units: Mscf /stb     psia     rb /stb     cp
PVTO
--
-- Live Oil PVT Properties (Dissolved Gas)
--
          0.0000     14.6959      1.0934      1.5170
                    312.2260      1.0920      1.5421
                    609.7560      1.0905      1.5668
```

	907.2860	1.0892	1.5909	
	1204.8160	1.0879	1.6145	
	1502.3460	1.0866	1.6377	
	1799.8770	1.0854	1.6605	
	2097.4070	1.0843	1.6828	
	2394.9370	1.0831	1.7046	
	2692.4670	1.0820	1.7261	
	2990.0849	1.0810	1.7472	/
0.0512	312.2260	1.1220	0.5427	
	609.7560	1.1185	0.5593	
	907.2860	1.1152	0.5755	
	1204.8160	1.1120	0.5914	
	1502.3460	1.1090	0.6070	
	1799.8770	1.1062	0.6223	
	2097.4070	1.1035	0.6373	
	2394.9370	1.1010	0.6521	
	2692.4670	1.0986	0.6666	
	2990.0849	1.0963	0.6808	/
0.1017	609.7560	1.1471	0.5220	
	907.2860	1.1433	0.5383	
	1204.8160	1.1397	0.5544	
	1502.3460	1.1364	0.5701	
	1799.8770	1.1332	0.5856	
	2097.4070	1.1301	0.6008	
	2394.9370	1.1273	0.6157	
	2692.4670	1.1245	0.6304	
	2990.0849	1.1219	0.6448	/
0.1510	907.2860	1.1708	0.4994	
	1204.8160	1.1667	0.5153	
	1502.3460	1.1629	0.5310	
	1799.8770	1.1593	0.5464	
	2097.4070	1.1559	0.5615	
	2394.9370	1.1527	0.5764	
	2692.4670	1.1497	0.5911	
	2990.0849	1.1468	0.6055	/
0.2008	1204.8160	1.1942	0.4758	
	1502.3460	1.1899	0.4913	
	1799.8770	1.1859	0.5065	
	2097.4070	1.1821	0.5214	
	2394.9370	1.1785	0.5361	
	2692.4670	1.1751	0.5506	
	2990.0849	1.1718	0.5648	/
0.2519	1502.3460	1.2178	0.4522	
	1799.8770	1.2132	0.4670	
	2097.4070	1.2090	0.4817	
	2394.9370	1.2050	0.4961	
	2692.4670	1.2012	0.5102	
	2990.0849	1.1976	0.5242	/
0.3045	1799.8770	1.2417	0.4290	
	2097.4070	1.2370	0.4432	
	2394.9370	1.2325	0.4572	
	2692.4670	1.2283	0.4710	
	2990.0849	1.2243	0.4846	/
0.3589	2097.4070	1.2663	0.4064	

```
                 2394.9370      1.2613      0.4200
                 2692.4670      1.2566      0.4333
                 2990.0849      1.2522      0.4465 /
          0.4155   2394.9370      1.2915      0.3848
                 2692.4670      1.2863      0.3976
                 2990.0849      1.2814      0.4103 /
          0.4744   2692.4670      1.3176      0.3641
                 2990.0849      1.3121      0.3763 /
          0.5360   2990.0849      1.3446      0.3444
                 3092.9562      1.3427      0.3486 /
/

-- Created from a Differential Liberation Experiment.
-- Using the method of Whitson and Torp.
--PVTi--Please do not alter these lines
--PVTi--as PVTi can use them to re-create the fluid model
--PVTiMODSPEC
========================================================
--PVTiTITLE
--PVTiModified System: From Automatically created during keyword export
--PVTiVERSION
--PVTi  2010.1          /
--PVTiFPE
--PVTiNCOMPS
--PVTi       11 /
--PVTiEOS
--PVTi PR3  /
--PVTiPRCORR
--PVTiLBC
--PVTiOPTIONS
--PVTi  0  0  0  2  0  0  0  0  0  0  0  0  0  0  0  0  0  0  0  0
--PVTi/
--PVTiNOECHO
--PVTiMODSYS
========================================================
--PVTiUNITS
--PVTi   FIELD       ABSOL         PERCENT      /
--PVTiDEGREES
--PVTi   Fahrenheit /
--PVTiSTCOND
--PVTi      60.0000      14.6959 /
--PVTiLNAMES
--PVTi CO2
--PVTi N2
--PVTi C1
--PVTi C2
--PVTi C3
--PVTi IC4
--PVTi NC4
--PVTi IC5
--PVTi NC5
--PVTi C6
--PVTi 1*
--PVTi /
```

```
--PVTiCNAMES
--PVTi 1*
--PVTi 1*
--PVTi 1*
--PVTi 1*
--PVTi 1*
--PVTi 1*
--PVTi 1*
--PVTi 1*
--PVTi 1*
--PVTi 1*
--PVTi C7+
--PVTi /
--PVTiTCRIT
--PVTi  8.878998547E+01 -2.325100060E+02 -1.165900091E+02
9.010398544E+01
--PVTi  2.059699824E+02  2.749099805E+02  3.056899797E+02
3.690499780E+02
--PVTi  3.856099776E+02  4.538299758E+02  8.987542687E+02
/
--PVTiPCRIT
--PVTi  1.071331110E+03  4.923126500E+02  6.677816960E+02
7.083423800E+02
--PVTi  6.157582100E+02  5.290524000E+02  5.506553730E+02
4.915778550E+02
--PVTi  4.887856340E+02  4.366151890E+02  2.238690294E+02
/
--PVTiVCRIT
--PVTi  1.505735240E+00  1.441661400E+00  1.569809080E+00
2.370732080E+00
--PVTi  3.203692000E+00  4.212854980E+00  4.084707300E+00
4.933685680E+00
--PVTi  4.981741060E+00  5.622479460E+00  1.473824770E+01
/
--PVTiZCRIT
--PVTi  2.740777974E-01  2.911514044E-01  2.847294766E-01  2.846347951E-
01
--PVTi  2.761646200E-01  2.827369588E-01  2.738555491E-01  2.727108716E-
01
--PVTi  2.684389142E-01  2.504174849E-01  2.263345781E-01
/
--PVTiVCRITVIS
--PVTi  1.505735240E+00  1.441661400E+00  1.569809080E+00
2.370732080E+00
--PVTi  3.203692000E+00  4.212854980E+00  4.084707300E+00
4.933685680E+00
--PVTi  4.981741060E+00  5.622479460E+00  1.473824770E+01
/
--PVTiZCRITVIS
--PVTi  2.740777974E-01  2.911514044E-01  2.847294766E-01  2.846347951E-
01
--PVTi  2.761646200E-01  2.827369588E-01  2.738555491E-01  2.727108716E-
01
```

```
--PVTi  2.684389142E-01  2.504174849E-01  2.263345781E-01
/
--PVTiSSHIFT
--PVTi -4.273033674E-02 -1.313342386E-01 -1.442656189E-01 -1.032683540E-
01
--PVTi -7.750138148E-02 -6.198372515E-02 -5.422489699E-02 -4.177245672E-
02
--PVTi -3.027789648E-02 -7.288775999E-03  1.876010146E-01
/
--PVTiACF
--PVTi  2.250000000E-01  4.000000000E-02  1.300000000E-02  9.860000000E-
02
--PVTi  1.524000000E-01  1.848000000E-01  2.010000000E-01  2.270000000E-
01
--PVTi  2.510000000E-01  2.990000000E-01  7.593494718E-01
/
--PVTiMW
--PVTi  4.401000000E+01  2.801300000E+01  1.604300000E+01
3.007000000E+01
--PVTi  4.409700000E+01  5.812400000E+01  5.812400000E+01
7.215100000E+01
--PVTi  7.215100000E+01  8.400000000E+01  2.336092000E+02
/
--PVTiZI
--PVTi  2.872923555E-01  3.078132381E-01  4.260135215E+01
5.232825047E+00
--PVTi  1.939223400E+00  8.208353015E-01  9.747419205E-01  5.438033872E-
01
--PVTi  4.925011809E-01  1.692972809E+00  4.510663921E+01
/
--PVTiTBOIL
--PVTi -1.092100093E+02 -3.203500037E+02 -2.587900053E+02 -
1.273900088E+02
--PVTi -4.369001102E+01  1.066998754E+01  3.118998700E+01
8.212998565E+01
--PVTi  9.688998526E+01  1.470199839E+02  5.897725201E+02
/
--PVTiTREF
--PVTi  6.772998603E+01 -3.190900037E+02 -2.586100053E+02 -
1.302700087E+02
--PVTi -4.387001101E+01  6.772998603E+01  6.772998603E+01
6.772998603E+01
--PVTi  6.772998603E+01  6.052998622E+01  6.000000000E+01
/
--PVTiDREF
--PVTi  4.850653269E+01  5.019208788E+01  2.653188725E+01
3.421052756E+01
--PVTi  3.633307854E+01  3.477237929E+01  3.614579463E+01
3.870534140E+01
--PVTi  3.907990922E+01  4.276315945E+01  5.276412024E+01
/
--PVTiPARACHOR
--PVTi  7.800000000E+01  4.100000000E+01  7.700000000E+01
1.080000000E+02
```

```
--PVTi  1.503000000E+02  1.815000000E+02  1.899000000E+02
2.250000000E+02
--PVTi  2.315000000E+02  2.710000000E+02  6.029028054E+02
/
--PVTiHYDRO
--PVTi  N N H H H H H H H H H
--PVTi /
--PVTiTHERMX
--PVTi    0.0002778 /
--PVTiBIC
--PVTi  -1.200000000E-02
--PVTi   1.000000000E-01  1.000000000E-01
--PVTi   1.000000000E-01  1.000000000E-01  0.000000000E+00
--PVTi   1.000000000E-01  1.000000000E-01  0.000000000E+00
0.000000000E+00
--PVTi   1.000000000E-01  1.000000000E-01  0.000000000E+00
0.000000000E+00
--PVTi   0.000000000E+00
--PVTi   1.000000000E-01  1.000000000E-01  0.000000000E+00
0.000000000E+00
--PVTi   0.000000000E+00  0.000000000E+00
--PVTi   1.000000000E-01  1.000000000E-01  0.000000000E+00
0.000000000E+00
--PVTi   0.000000000E+00  0.000000000E+00  0.000000000E+00
--PVTi   1.000000000E-01  1.000000000E-01  0.000000000E+00
0.000000000E+00
--PVTi   0.000000000E+00  0.000000000E+00  0.000000000E+00
0.000000000E+00
--PVTi   1.000000000E-01  1.000000000E-01  2.790000000E-02  1.000000000E-
02
--PVTi   1.000000000E-02  0.000000000E+00  0.000000000E+00
0.000000000E+00
--PVTi   0.000000000E+00
--PVTi   1.000000000E-01  1.000000000E-01  5.147000002E-02  1.000000000E-
02
--PVTi   1.000000000E-02  0.000000000E+00  0.000000000E+00
0.000000000E+00
--PVTi   0.000000000E+00  0.000000000E+00
--PVTi /
--PVTiSPECHA
--PVTi  4.729150800E+00  7.440052900E+00  4.597785500E+00
1.291918014E+00
--PVTi -1.008885504E+00 -3.319959400E-01  2.265932002E+00 -
2.275008150E+00
--PVTi -8.661081421E-01 -1.054027398E+00  2.138848987E+00
/
--PVTiSPECHB
--PVTi  9.744900480E-03 -1.800630440E-03  6.915907040E-03  2.363244520E-
02
--PVTi  4.064355960E-02  5.104661240E-02  4.419970520E-02  6.722176720E-
02
--PVTi  6.466081160E-02  7.722674400E-02  1.755949990E-01
/
--PVTiSPECHC
```

```
--PVTi -4.129676758E-06  1.975639720E-06  8.824032630E-07 -5.114547902E-
06
--PVTi -1.169165894E-05 -1.360832434E-05 -8.167943320E-06 -2.011761491E-
05
--PVTi -1.901921820E-05 -2.299261301E-05 -3.889710939E-05
/
--PVTiSPECHD
--PVTi  7.023679600E-10 -4.783473920E-10 -4.636038080E-10  3.568356872E-
10
--PVTi  1.316683960E-09  1.185629880E-09 -1.155733168E-10  2.343820312E-
09
--PVTi  2.172630920E-09  2.659578736E-09  0.000000000E+00
/
--PVTiHEATVAPS
--PVTi  1.802570424E+04  0.000000000E+00  0.000000000E+00
1.650621600E+04
--PVTi  3.603408601E+04  4.586099659E+04  6.166418764E+04
5.938211357E+04
--PVTi  6.289700021E+04  7.462523487E+04  1.786112137E+05
/
--PVTiCALVAL
--PVTi  0.000000000E+00  0.000000000E+00  1.891038000E+03
3.323854000E+03
--PVTi  4.754344000E+03  6.184834000E+03  6.184834000E+03
7.615324000E+03
--PVTi  7.615324000E+03  9.045814000E+03  2.192487600E+04
/
--PVTiSIMULATE
========================================================
--PVTiUNITS
--PVTi   FIELD       ABSOL         PERCENT      /
--PVTiDEGREES
--PVTi   Fahrenheit /
--PVTiSTCOND
--PVTi      60.0000      14.6959 /
--PVTiEXP
--PVTi   1  ZI       DL         220.0000
--PVTi                     2692.4670    2394.9370    2097.4070
1799.8770
--PVTi                     1502.3460    1204.8160     907.2860
609.7560
--PVTi                      312.2260      14.6959
/
--PVTi   2  ZI       SEPS        60.0000      14.6959  0  0 /
--PVTi /
--PVTi--End of PVTi generated section--
-- Column Properties are:
--   'Gas Pressure'  'Gas OGR'   'Gas FVF'    'Gas Visc'
-- Units: psia     stb /Mscf     rb /Mscf     cp
PVTG
--
-- Wet Gas PVT Properties (Vapourised Oil)
--
         14.6959    0.001643    231.9987     0.01127
```

	0.001285	231.9371	0.008939
	0.0009189	231.8742	0.00894
	0.000643	231.8267	0.008942
	0.0004415	231.7921	0.008942
	0.0002995	231.7676	0.008943
	0.0002032	231.7511	0.008944
	0.0001413	231.7404	0.008944
	0.0001062	231.7344	0.008944
	0.0001016	231.7336	0.008944
	0	231.7161	0.01128 /
312.2260	0.0001016	10.6107	0.01307
	0	10.6105	0.01307 /
609.7560	0.0001062	5.3463	0.01355
	0	5.3464	0.01356 /
907.2860	0.0001413	3.5485	0.01399
	0	3.5487	0.01399 /
1204.8160	0.0002032	2.6479	0.01447
	0	2.6482	0.01447 /
1502.3460	0.0002995	2.1112	0.01501
	0.0001062	2.1115	0.01501
	0.0001016	2.1115	0.01501
	0	2.1116	0.01501 /
1799.8770	0.0004415	1.7577	0.01563
	0.0002032	1.7580	0.01563
	0.0001413	1.7581	0.01563
	0.0001062	1.7582	0.01563
	0.0001016	1.7582	0.01563
	0	1.7583	0.01563 /
2097.4070	0.000643	1.5092	0.01633
	0.0004415	1.5094	0.01632
	0.0002995	1.5096	0.01632
	0.0002032	1.5097	0.01632
	0.0001413	1.5098	0.01632
	0.0001062	1.5099	0.01632
	0.0001016	1.5099	0.01632
	0	1.5100	0.01631 /
2394.9370	0.0009189	1.3263	0.01709
	0.000643	1.3266	0.01708
	0.0004415	1.3268	0.01708
	0.0002995	1.3270	0.01707
	0.0002032	1.3271	0.01707
	0.0001413	1.3271	0.01707
	0.0001062	1.3272	0.01707
	0.0001016	1.3272	0.01707
	0	1.3273	0.01706 /
2692.4670	0.001285	1.1869	0.01792
	0.0009189	1.1873	0.01791
	0.000643	1.1875	0.0179
	0.0004415	1.1877	0.01789
	0.0002995	1.1879	0.01788
	0.0002032	1.1880	0.01788
	0.0001413	1.1880	0.01788
	0.0001062	1.1880	0.01787
	0.0001016	1.1881	0.01787

```
                          0       1.1882     0.01787 /
      2990.0849    0.001756       1.0778     0.01881
                   0.001285       1.0782     0.01878
                  0.0009189       1.0785     0.01877
                   0.000643       1.0787     0.01875
                  0.0004415       1.0789     0.01874
                  0.0002995       1.0790     0.01873
                  0.0002032       1.0791     0.01873
                  0.0001413       1.0791     0.01873
                  0.0001062       1.0792     0.01873
                  0.0001016       1.0792     0.01873
                          0       1.0793     0.01872 /
/
```

APPENDIX B

PVT Properties Reports of KTL Oil Sample

B1. Report on Saturation Pressure Calculation
B2. Report on Bubble Point Pressure Calculation
B3. Report on Constant Composition Expansion
B4. Report on Differential Liberation
B5. Report on Separators Test
B6. Oil PVT Properties Report and Gas PVT Properties Report

B1. Expt PSAT1 : Saturation Pressure Calculation

Peng-Robinson (3-Parm) on ZI with PR corr.
Lohrenz-Bray-Clark Viscosity Correlation

Specified temperature	Deg F	220.0000
Calculated bubble point pressure	PSIA	5762.2564
Observed bubble point pressure	PSIA	5420.0000

Fluid properties	Liquid	Vapour
	Calculated	Calculated
Mole Weight	70.7463	21.6349
Z-factor	1.4950	1.4950
Viscosity	0.1872	0.0318
Density LB/FT3	37.3857	15.9823
Molar Vol CF/LB-ML	1.8923	1.3537

Molar Distributions Components Mnemonic	Number	Total, Z Measured	Liquid,X Calculated	Vapour,Y Calculated	K-Values Calculated
CO2	1	0.9649	0.9649	1.0201	1.0572
N2	2	0.2179	0.2179	0.3715	1.7049
C1	3	60.9747	60.9747	83.7508	1.3735
C2	4	7.8540	7.8540	7.3943	0.9415
C3	5	4.2434	4.2434	3.2570	0.7675
IC4	6	0.9441	0.9441	0.6141	0.6504
NC4	7	2.1684	2.1684	1.3035	0.6011
IC5	8	0.7989	0.7989	0.4183	0.5236
NC5	9	1.1931	1.1931	0.5952	0.4988
C6	10	1.8156	1.8156	0.7111	0.3916
C7+	11	18.8249	18.8249	0.5643	0.0300
Composition Total		100.0000	100.0000	100.0000	

B2. Expt BUBBLE1 : Bubble Point Pressure Calculation

Peng-Robinson (3-Parm) on ZI with PR corr.
Lohrenz-Bray-Clark Viscosity Correlation

Specified temperature	Deg F	220.0000
Calculated bubble point pressure	PSIA	5762.2564
Observed bubble point pressure	PSIA	5420.0000

Fluid properties	Liquid		Vapour
	Observed	Calculated	Calculated
Mole Weight		70.7463	21.6349
Z-factor		1.4950	1.0694
Viscosity		0.1872	0.0318
Density LB/FT3	36.8931	37.3857	15.9823
Molar Vol CF/LB-ML		1.8923	1.3537

Molar Distributions Components		Total, Z	Liquid,X	Vapour,Y	K-Values
Mnemonic	Number	Measured	Calculated	Calculated	Calculated
CO2	1	0.9649	0.9649	1.0201	1.0572
N2	2	0.2179	0.2179	0.3715	1.7049
C1	3	60.9747	60.9747	83.7508	1.3735
C2	4	7.8540	7.8540	7.3943	0.9415
C3	5	4.2434	4.2434	3.2570	0.7675
IC4	6	0.9441	0.9441	0.6141	0.6504
NC4	7	2.1684	2.1684	1.3035	0.6011
IC5	8	0.7989	0.7989	0.4183	0.5236
NC5	9	1.1931	1.1931	0.5952	0.4988
C6	10	1.8156	1.8156	0.7111	0.3916
C7+	11	18.8249	18.8249	0.5643	0.0300
Composition Total		100.0000	100.0000	100.0000	

B3. Expt CCE1 : Constant Composition Expansion

```
Peng-Robinson         (3-Parm)  on ZI       with PR corr.
Lohrenz-Bray-Clark Viscosity Correlation
Density units are               LB/FT3
Specific volume units are       CF/LB-ML
Viscosity units are             CPOISE
Surface Tension units are       DYNES/CM

Specified temperature           Deg F               220.0000

Liq Sat calc. is Vol oil/Vol Fluid at Sat. Vol
```

Pressure PSIA	Inserted Point	Rel Volume Calculated	Vap Mole Frn Calculated	Liq Density Calculated	Vap Density Calculated
7000.000		0.9785		38.2077	
6841.986		0.9810		38.1110	
6683.973		0.9835		38.0121	
6525.960		0.9861		37.9108	
6367.947		0.9889		37.8072	
6209.934		0.9916		37.7010	
6051.921		0.9945		37.5923	
5893.908		0.9975		37.4808	
5762.256	- Psat	1.0000		37.3857	15.9823
5735.895		1.0013	0.0065	37.4371	15.9220
5577.882		1.0093	0.0438	37.7421	15.5611
4879.352		1.0527	0.1868	39.0456	13.9543
4338.834		1.0983	0.2788	40.0183	12.6727
3798.317		1.1602	0.3593	40.9725	11.3305
3257.799		1.2482	0.4310	41.9195	9.9062
2717.282		1.3805	0.4959	42.8718	8.3852
2176.765		1.5944	0.5558	43.8464	6.7692
1636.247		1.9789	0.6124	44.8687	5.0843
1095.730		2.8010	0.6678	45.9819	3.3790
555.213		5.3852	0.7262	47.2844	1.7034

Pressure PSIA	Inserted Point	Liq Z-Fac Calculated	Vap Z-Fac Calculated	Surf Tension Calculated	Liq Sat Calculated
7000.000		1.7770			1.0000
6841.986		1.7413			1.0000
6683.973		1.7056			1.0000
6525.960		1.6697			1.0000
6367.947		1.6337			1.0000
6209.934		1.5977			1.0000
6051.921		1.5615			1.0000
5893.908		1.5253			1.0000
5762.256	- Psat	1.4950	1.0694	0.2555	1.0000

5735.895		1.4928	1.0673	0.2621	0.9967
5577.882		1.4793	1.0549	0.3044	0.9774
4879.352		1.4081	1.0039	0.5644	0.9045
4338.834		1.3396	0.9692	0.8780	0.8582
3798.317		1.2578	0.9393	1.3381	0.8177
3257.799		1.1610	0.9152	2.0098	0.7816
2717.282		1.0467	0.8985	2.9838	0.7484
2176.765		0.9119	0.8913	4.3765	0.7172
1636.247		0.7522	0.8957	6.3176	0.6868
1095.730		0.5609	0.9133	8.9278	0.6554
555.213		0.3256	0.9455	12.3227	0.6190

Pressure PSIA	Inserted Point	Liq Visc Calculated	Vap Visc Calculated	Liq Mole Wt Calculated	Vap Mole Wt Calculated
7000.000		0.2132		70.7463	
6841.986		0.2099		70.7463	
6683.973		0.2065		70.7463	
6525.960		0.2032		70.7463	
6367.947		0.1999		70.7463	
6209.934		0.1966		70.7463	
6051.921		0.1933		70.7463	
5893.908		0.1899		70.7463	
5762.256	- Psat	0.1872	0.0318	70.7463	21.6349
5735.895		0.1883	0.0317	71.0656	21.6097
5577.882		0.1951	0.0310	73.0053	21.4647
4879.352		0.2280	0.0278	82.1879	20.9412
4338.834		0.2570	0.0255	90.1179	20.6481
3798.317		0.2899	0.0232	98.9617	20.4370
3257.799		0.3274	0.0210	108.9577	20.2975
2717.282		0.3705	0.0189	120.4483	20.2234
2176.765		0.4206	0.0171	133.9699	20.2169
1636.247		0.4795	0.0155	150.4465	20.3004
1095.730		0.5498	0.0143	171.6869	20.5429
555.213		0.6334	0.0134	202.2527	21.1566

Pressure PSIA	Inserted Point	Liq Mol Vol Calculated	Vap Mol Vol Calculated
7000.000		1.8516	
6841.986		1.8563	
6683.973		1.8612	
6525.960		1.8661	
6367.947		1.8712	
6209.934		1.8765	
6051.921		1.8819	
5893.908		1.8875	
5762.256	- Psat	1.8923	1.3537

5735.895	1.8983	1.3572
5577.882	1.9343	1.3794
4879.352	2.1049	1.5007
4338.834	2.2519	1.6293
3798.317	2.4153	1.8037
3257.799	2.5992	2.0490
2717.282	2.8095	2.4118
2176.765	3.0554	2.9866
1636.247	3.3530	3.9928
1095.730	3.7338	6.0795
555.213	4.2774	12.4203

Molar Distributions K-Values Inserted Point	Com(1 ,CO2) Calculated	Com(2 ,N2) Calculated	Com(3 ,C1) Calculated	Com(4 ,C2) Calculated
7000.000	1.0000	1.0000	1.0000	1.0000
6841.986	1.0000	1.0000	1.0000	1.0000
6683.973	1.0000	1.0000	1.0000	1.0000
6525.960	1.0000	1.0000	1.0000	1.0000
6367.947	1.0000	1.0000	1.0000	1.0000
6209.934	1.0000	1.0000	1.0000	1.0000
6051.921	1.0000	1.0000	1.0000	1.0000
5893.908	1.0000	1.0000	1.0000	1.0000
5762.256 - Psat	1.0572	1.7049	1.3735	0.9415
5735.895	1.0583	1.7118	1.3770	0.9416
5577.882	1.0654	1.7549	1.3983	0.9425
4879.352	1.1039	1.9759	1.5067	0.9503
4338.834	1.1446	2.1943	1.6119	0.9618
3798.317	1.1995	2.4756	1.7453	0.9800
3257.799	1.2754	2.8535	1.9219	1.0083
2717.282	1.3857	3.3884	2.1684	1.0537
2176.765	1.5571	4.1998	2.5383	1.1305
1636.247	1.8528	5.5624	3.1566	1.2740
1095.730	2.4610	8.2881	4.3949	1.5898
555.213	4.3045	16.3583	8.0791	2.5927

Molar Distributions K-Values Inserted Point	Com(5 ,C3) Calculated	Com(6 ,IC4) Calculated	Com(7 ,NC4) Calculated	Com(8 ,IC5) Calculated
7000.000	1.0000	1.0000	1.0000	1.0000
6841.986	1.0000	1.0000	1.0000	1.0000
6683.973	1.0000	1.0000	1.0000	1.0000
6525.960	1.0000	1.0000	1.0000	1.0000
6367.947	1.0000	1.0000	1.0000	1.0000
6209.934	1.0000	1.0000	1.0000	1.0000
6051.921	1.0000	1.0000	1.0000	1.0000
5893.908	1.0000	1.0000	1.0000	1.0000

5762.256 - Psat	0.7675	0.6504	0.6011	0.5236
5735.895	0.7665	0.6488	0.5993	0.5215
5577.882	0.7604	0.6392	0.5888	0.5091
4879.352	0.7349	0.5982	0.5435	0.4561
4338.834	0.7169	0.5673	0.5099	0.4166
3798.317	0.7006	0.5371	0.4770	0.3780
3257.799	0.6872	0.5077	0.4451	0.3404
2717.282	0.6791	0.4805	0.4152	0.3044
2176.765	0.6827	0.4588	0.3904	0.2722
1636.247	0.7134	0.4513	0.3776	0.2482
1095.730	0.8172	0.4821	0.3962	0.2433
555.213	1.2117	0.6606	0.5327	0.3030

Molar Distributions K-Values Inserted Point	Com(9 ,NC5) Calculated	Com(10,C6) Calculated	Com(11,C7+) Calculated
7000.000	1.0000	1.0000	1.0000
6841.986	1.0000	1.0000	1.0000
6683.973	1.0000	1.0000	1.0000
6525.960	1.0000	1.0000	1.0000
6367.947	1.0000	1.0000	1.0000
6209.934	1.0000	1.0000	1.0000
6051.921	1.0000	1.0000	1.0000
5893.908	1.0000	1.0000	1.0000
5762.256 - Psat	0.4988	0.3916	0.0300
5735.895	0.4967	0.3894	0.0293
5577.882	0.4839	0.3763	0.0254
4879.352	0.4295	0.3217	0.0132
4338.834	0.3892	0.2826	0.0075
3798.317	0.3501	0.2456	0.0039
3257.799	0.3122	0.2105	0.0019
2717.282	0.2761	0.1779	0.0008
2176.765	0.2437	0.1488	0.0003
1636.247	0.2190	0.1255	9.1390E-05
1095.730	0.2111	0.1124	2.6219E-05
555.213	0.2583	0.1265	8.0906E-06

Molar Distributions Liquid, X Inserted Point	Com(1 ,CO2) Calculated	Com(2 ,N2) Calculated	Com(3 ,C1) Calculated	Com(4 ,C2) Calculated
7000.000	0.9649	0.2179	60.9747	7.8540
6841.986	0.9649	0.2179	60.9747	7.8540
6683.973	0.9649	0.2179	60.9747	7.8540
6525.960	0.9649	0.2179	60.9747	7.8540
6367.947	0.9649	0.2179	60.9747	7.8540
6209.934	0.9649	0.2179	60.9747	7.8540
6051.921	0.9649	0.2179	60.9747	7.8540

5893.908	0.9649	0.2179	60.9747	7.8540
5762.256 - Psat	0.9649	0.2179	60.9747	7.8540
5735.895	0.9645	0.2169	60.8267	7.8569
5577.882	0.9621	0.2109	59.9284	7.8738
4879.352	0.9465	0.1843	55.7023	7.9276
4338.834	0.9275	0.1634	52.0871	7.9386
3798.317	0.9004	0.1424	48.0943	7.9109
3257.799	0.8625	0.1211	43.6368	7.8259
2717.282	0.8100	0.0997	38.6065	7.6503
2176.765	0.7367	0.0784	32.8703	7.3228
1636.247	0.6339	0.0574	26.2744	6.7255
1095.730	0.4884	0.0371	18.6622	5.6345
555.213	0.2838	0.0179	9.9297	3.6419

Molar Distributions Liquid, X Inserted Point	Com(5 ,C3) Calculated	Com(6 ,IC4) Calculated	Com(7 ,NC4) Calculated	Com(8 ,IC5) Calculated
7000.000	4.2434	0.9441	2.1684	0.7989
6841.986	4.2434	0.9441	2.1684	0.7989
6683.973	4.2434	0.9441	2.1684	0.7989
6525.960	4.2434	0.9441	2.1684	0.7989
6367.947	4.2434	0.9441	2.1684	0.7989
6209.934	4.2434	0.9441	2.1684	0.7989
6051.921	4.2434	0.9441	2.1684	0.7989
5893.908	4.2434	0.9441	2.1684	0.7989
5762.256 - Psat	4.2434	0.9441	2.1684	0.7989
5735.895	4.2498	0.9463	2.1740	0.8014
5577.882	4.2885	0.9593	2.2082	0.8165
4879.352	4.4645	1.0208	2.3705	0.8892
4338.834	4.6072	1.0737	2.5117	0.9541
3798.317	4.7549	1.1325	2.6702	1.0288
3257.799	4.9046	1.1984	2.8500	1.1162
2717.282	5.0464	1.2718	3.0540	1.2195
2176.765	5.1521	1.3503	3.2796	1.3415
1636.247	5.1467	1.4219	3.5039	1.4805
1095.730	4.8337	1.4434	3.6338	1.6151
555.213	3.6781	1.2530	3.2821	1.6176

Molar Distributions Liquid, X Inserted Point	Com(9 ,NC5) Calculated	Com(10,C6) Calculated	Com(11,C7+) Calculated	Total Calculated
7000.000	1.1931	1.8156	18.8249	100.0000
6841.986	1.1931	1.8156	18.8249	100.0000
6683.973	1.1931	1.8156	18.8249	100.0000
6525.960	1.1931	1.8156	18.8249	100.0000
6367.947	1.1931	1.8156	18.8249	100.0000
6209.934	1.1931	1.8156	18.8249	100.0000
6051.921	1.1931	1.8156	18.8249	100.0000

5893.908	1.1931	1.8156	18.8249	100.0000
5762.256 - Psat	1.1931	1.8156	18.8249	100.0000
5735.895	1.1970	1.8228	18.9436	100.0000
5577.882	1.2208	1.8667	19.6649	100.0000
4879.352	1.3355	2.0791	23.0797	100.0000
4338.834	1.4381	2.2697	26.0290	100.0000
3798.317	1.5566	2.4909	29.3181	100.0000
3257.799	1.6959	2.7520	33.0366	100.0000
2717.282	1.8614	3.0654	37.3149	100.0000
2176.765	2.0584	3.4460	42.3638	100.0000
1636.247	2.2870	3.9093	48.5596	100.0000
1095.730	2.5216	4.4585	56.6718	100.0000
555.213	2.5859	4.9651	68.7450	100.0000

Molar Distributions Vapour, Y Inserted Point	Com(1 ,CO2) Calculated	Com(2 ,N2) Calculated	Com(3 ,C1) Calculated	Com(4 ,C2) Calculated
7000.000				
6841.986				
6683.973				
6525.960				
6367.947				
6209.934				
6051.921				
5893.908				
5762.256 - Psat	1.0201	0.3715	83.7508	7.3943
5735.895	1.0208	0.3713	83.7584	7.3980
5577.882	1.0250	0.3701	83.8007	7.4209
4879.352	1.0448	0.3641	83.9255	7.5336
4338.834	1.0616	0.3587	83.9594	7.6351
3798.317	1.0799	0.3525	83.9411	7.7524
3257.799	1.1001	0.3456	83.8652	7.8911
2717.282	1.1224	0.3380	83.7123	8.0610
2176.765	1.1472	0.3293	83.4362	8.2785
1636.247	1.1744	0.3194	82.9381	8.5683
1095.730	1.2019	0.3078	82.0191	8.9579
555.213	1.2217	0.2933	80.2233	9.4423

Molar Distributions Vapour, Y Inserted Point	Com(5 ,C3) Calculated	Com(6 ,IC4) Calculated	Com(7 ,NC4) Calculated	Com(8 ,IC5) Calculated
7000.000				
6841.986				
6683.973				
6525.960				
6367.947				
6209.934				

6051.921				
5893.908				
5762.256 - Psat	3.2570	0.6141	1.3035	0.4183
5735.895	3.2575	0.6139	1.3030	0.4179
5577.882	3.2609	0.6132	1.3001	0.4157
4879.352	3.2810	0.6106	1.2885	0.4056
4338.834	3.3028	0.6091	1.2806	0.3975
3798.317	3.3315	0.6083	1.2736	0.3889
3257.799	3.3705	0.6085	1.2685	0.3799
2717.282	3.4272	0.6111	1.2682	0.3713
2176.765	3.5172	0.6195	1.2803	0.3652
1636.247	3.6717	0.6417	1.3231	0.3675
1095.730	3.9499	0.6958	1.4396	0.3930
555.213	4.4566	0.8277	1.7484	0.4902

Molar Distributions Vapour, Y Inserted Point	Com(9 ,NC5) Calculated	Com(10,C6) Calculated	Com(11,C7+) Calculated	Total Calculated
7000.000				
6841.986				
6683.973				
6525.960				
6367.947				
6209.934				
6051.921				
5893.908				
5762.256 - Psat	0.5952	0.7111	0.5643	100.0000
5735.895	0.5945	0.7098	0.5548	100.0000
5577.882	0.5907	0.7024	0.5004	100.0000
4879.352	0.5736	0.6689	0.3039	100.0000
4338.834	0.5597	0.6414	0.1941	100.0000
3798.317	0.5450	0.6117	0.1150	100.0000
3257.799	0.5294	0.5794	0.0619	100.0000
2717.282	0.5139	0.5452	0.0295	100.0000
2176.765	0.5016	0.5127	0.0122	100.0000
1636.247	0.5008	0.4905	0.0044	100.0000
1095.730	0.5324	0.5012	0.0015	100.0000
555.213	0.6680	0.6280	0.0006	100.0000

B4. Expt DL1 : Differential Liberation

Peng-Robinson (3-Parm) on ZI with PR corr.
Lohrenz-Bray-Clark Viscosity Correlation

Density units are	LB/FT3
Specific volume units are	CF/LB-ML
Viscosity units are	CPOISE
Surface Tension units are	DYNES/CM
Gas-Oil Ratio units are	MSCF/STB
Relative Volume units are	RB/STB
Gas FVF units are	RB/MSCF
Extracted Gas Volume units are	FT3
Oil Relative Volume units are	BBL/STB

Specified temperature Deg F 220.0000

Relative Oil Saturated Volume (Bo(Pbub)) 1.8451

GOR calc. is Gas Vol at STC/Stock Tank Oil Vol
Oil Rel Vol calc. is Stage Vol oil/Stock Tank Oil Vol

Pressure PSIA	Inserted Point	GOR Calculated	Total RelVol Calculated	Oil RelVol Calculated	Liq Dens Calculated
7000.000		1.5962	1.8054	1.8054	38.2077
6841.986		1.5962	1.8100	1.8100	38.1110
6683.973		1.5962	1.8147	1.8147	38.0121
6525.960		1.5962	1.8196	1.8196	37.9108
6367.947		1.5962	1.8246	1.8246	37.8072
6209.934		1.5962	1.8297	1.8297	37.7010
6051.921		1.5962	1.8350	1.8350	37.5923
5893.908		1.5962	1.8405	1.8405	37.4808
5762.256	- Psat	1.5962	1.8451	1.8451	37.3857
5735.895		1.5828	1.8475	1.8390	37.4371
5577.882		1.5051	1.8624	1.8034	37.7420
4879.352		1.2075	1.9421	1.6683	39.0448
4338.834		1.0152	2.0256	1.5813	40.0144
3798.317		0.8473	2.1391	1.5053	40.9640
3257.799		0.6984	2.3005	1.4376	41.9036
2717.282		0.5646	2.5426	1.3764	42.8430
2176.765		0.4429	2.9325	1.3200	43.7923
1636.247		0.3307	3.6272	1.2672	44.7623
1095.730		0.2256	5.0934	1.2165	45.7689
555.213	@ Tres	0.1227	9.6295	1.1644	46.8603
14.695	@ Tstd	2.3366E-16	282.7906	1.0000	52.7808

Pressure PSIA	Inserted Point	Vap Dens Calculated	Gas Grav Calculated	Vap Z-Fac Calculated	Liq Z-Fac Calculated

7000.000					1.7770
6841.986					1.7413
6683.973					1.7056
6525.960					1.6697
6367.947					1.6337
6209.934					1.5977
6051.921					1.5615
5893.908					1.5253
5762.256	- Psat	15.9823	0.7468	1.0694	1.4950
5735.895		15.9220	0.7459	1.0673	1.4928
5577.882		15.5611	0.7409	1.0549	1.4793
4879.352		13.9553	0.7229	1.0039	1.4081
4338.834		12.6773	0.7129	0.9692	1.3393
3798.317		11.3415	0.7059	0.9390	1.2571
3257.799		9.9271	0.7017	0.9146	1.1597
2717.282		8.4215	0.7002	0.8973	1.0446
2176.765		6.8287	0.7022	0.8890	0.9082
1636.247		5.1770	0.7100	0.8913	0.7460
1095.730		3.5147	0.7312	0.9054	0.5509
555.213	@ Tres	1.8842	0.7960	0.9317	0.3127
14.695	@ Tstd	0.0823	1.0689	0.9912	0.0117

Pressure PSIA	Inserted Point	Surf Tension Calculated	Gas FVF Calculated	Liq Visc Calculated	Vap Visc Calculated
7000.000			0.5729	0.2132	
6841.986			0.5795	0.2099	
6683.973			0.5864	0.2065	
6525.960			0.5937	0.2032	
6367.947			0.6014	0.1999	
6209.934			0.6095	0.1966	
6051.921			0.6181	0.1933	
5893.908			0.6273	0.1899	
5762.256	- Psat	0.2555	0.6354	0.1872	0.0318
5735.895		0.2621	0.6370	0.1883	0.0317
5577.882		0.3044	0.6474	0.1951	0.0310
4879.352		0.5642	0.7043	0.2279	0.0278
4338.834		0.8769	0.7647	0.2569	0.0255
3798.317		1.3344	0.8463	0.2895	0.0232
3257.799		2.0001	0.9611	0.3266	0.0210
2717.282		2.9607	1.1305	0.3690	0.0190
2176.765		4.3242	1.3981	0.4174	0.0171
1636.247		6.2038	1.8648	0.4726	0.0155
1095.730		8.6925	2.8285	0.5347	0.0143
555.213	@ Tres	11.8691	5.7447	0.6032	0.0132
14.695	@ Tstd	23.1698	176.5363	1.8353	0.0094

Pressure	Inserted	Moles Extrac	GasVol Extrc	Liquid Sat	Vapour Sat

PSIA	Point	Calculated	Calculated	Calculated	Calculated
7000.000				1.0000	
6841.986				1.0000	
6683.973				1.0000	
6525.960				1.0000	
6367.947				1.0000	
6209.934				1.0000	
6051.921				1.0000	
5893.908				1.0000	
5762.256	- Psat			1.0000	
5735.895		0.0065	5.4008	0.9954	0.0046
5577.882		0.0438	36.6809	0.9729	0.0271
4879.352		0.1871	156.5545	0.8884	0.1116
4338.834		0.2797	233.9954	0.9149	0.0851
3798.317		0.3605	301.5965	0.9138	0.0862
3257.799		0.4322	361.5404	0.9095	0.0905
2717.282		0.4966	415.4188	0.9010	0.0990
2176.765		0.5552	464.4500	0.8858	0.1142
1636.247		0.6092	509.6309	0.8583	0.1417
1095.730		0.6598	551.9593	0.8036	0.1964
555.213	@ Tres	0.7093	593.4090	0.6632	0.3368
14.695	@ Tstd	0.7683	642.8018	0.0441	0.9559

Pressure PSIA	Inserted Point	Liq Mol Wt Calculated	Vap Mol Wt Calculated	Liq Visc Calculated	Vap Visc Calculated
7000.000		70.7463		0.2132	
6841.986		70.7463		0.2099	
6683.973		70.7463		0.2065	
6525.960		70.7463		0.2032	
6367.947		70.7463		0.1999	
6209.934		70.7463		0.1966	
6051.921		70.7463		0.1933	
5893.908		70.7463		0.1899	
5762.256	- Psat	70.7463	21.6349	0.1872	0.0318
5735.895		71.0656	21.6097	0.1883	0.0317
5577.882		73.0051	21.4648	0.1951	0.0310
4879.352		82.1824	20.9423	0.2279	0.0278
4338.834		90.0894	20.6537	0.2569	0.0255
3798.317		98.8886	20.4511	0.2895	0.0232
3257.799		108.8016	20.3274	0.3266	0.0210
2717.282		120.1249	20.2840	0.3690	0.0190
2176.765		133.2713	20.3414	0.4174	0.0171
1636.247		148.8445	20.5693	0.4726	0.0155
1095.730		167.8288	21.1817	0.5347	0.0143
555.213	@ Tres	192.5028	23.0616	0.6032	0.0132
14.695	@ Tstd	233.6726	30.9663	1.8353	0.0094

Pressure PSIA	Inserted Point	Liq Mol Vol Calculated	Vap Mol Vol Calculated
7000.000		1.8516	
6841.986		1.8563	
6683.973		1.8612	
6525.960		1.8661	
6367.947		1.8712	
6209.934		1.8765	
6051.921		1.8819	
5893.908		1.8875	
5762.256	- Psat	1.8923	1.3537
5735.895		1.8983	1.3572
5577.882		1.9343	1.3794
4879.352		2.1048	1.5007
4338.834		2.2514	1.6292
3798.317		2.4140	1.8032
3257.799		2.5965	2.0477
2717.282		2.8038	2.4086
2176.765		3.0433	2.9788
1636.247		3.3252	3.9732
1095.730		3.6669	6.0265
555.213	@ Tres	4.1080	12.2396
14.695	@ Tstd	4.4272	376.1288

Molar Distributions K-Values	Inserted Point	Com(1 ,CO2) Calculated	Com(2 ,N2) Calculated	Com(3 ,C1) Calculated	Com(4 ,C2) Calculated
7000.000		1.0000	1.0000	1.0000	1.0000
6841.986		1.0000	1.0000	1.0000	1.0000
6683.973		1.0000	1.0000	1.0000	1.0000
6525.960		1.0000	1.0000	1.0000	1.0000
6367.947		1.0000	1.0000	1.0000	1.0000
6209.934		1.0000	1.0000	1.0000	1.0000
6051.921		1.0000	1.0000	1.0000	1.0000
5893.908		1.0000	1.0000	1.0000	1.0000
5762.256	- Psat	1.0572	1.7049	1.3735	0.9415
5735.895		1.0583	1.7118	1.3770	0.9416
5577.882		1.0654	1.7549	1.3983	0.9425
4879.352		1.1039	1.9758	1.5066	0.9503
4338.834		1.1446	2.1938	1.6117	0.9618
3798.317		1.1995	2.4742	1.7449	0.9802
3257.799		1.2755	2.8503	1.9209	1.0088
2717.282		1.3857	3.3815	2.1663	1.0545
2176.765		1.5570	4.1846	2.5340	1.1321
1636.247		1.8518	5.5274	3.1464	1.2767
1095.730		2.4570	8.1992	4.3681	1.5941
555.213	@ Tres	4.2850	16.0688	7.9854	2.5976
14.695	@ Tstd	58.8115	592.9568	191.7877	27.3157

Molar Distributions K-Values Inserted Point	Com(5 ,C3) Calculated	Com(6 ,IC4) Calculated	Com(7 ,NC4) Calculated	Com(8 ,IC5) Calculated
7000.000	1.0000	1.0000	1.0000	1.0000
6841.986	1.0000	1.0000	1.0000	1.0000
6683.973	1.0000	1.0000	1.0000	1.0000
6525.960	1.0000	1.0000	1.0000	1.0000
6367.947	1.0000	1.0000	1.0000	1.0000
6209.934	1.0000	1.0000	1.0000	1.0000
6051.921	1.0000	1.0000	1.0000	1.0000
5893.908	1.0000	1.0000	1.0000	1.0000
5762.256 - Psat	0.7675	0.6504	0.6011	0.5236
5735.895	0.7665	0.6488	0.5993	0.5215
5577.882	0.7604	0.6392	0.5888	0.5091
4879.352	0.7349	0.5982	0.5436	0.4561
4338.834	0.7170	0.5675	0.5100	0.4168
3798.317	0.7010	0.5375	0.4774	0.3784
3257.799	0.6880	0.5086	0.4459	0.3412
2717.282	0.6806	0.4819	0.4167	0.3058
2176.765	0.6852	0.4613	0.3928	0.2744
1636.247	0.7177	0.4555	0.3815	0.2515
1095.730	0.8246	0.4891	0.4025	0.2485
555.213 @ Tres	1.2255	0.6738	0.5446	0.3121
14.695 @ Tstd	7.2650	2.5328	1.7481	0.6588

Molar Distributions K-Values Inserted Point	Com(9 ,NC5) Calculated	Com(10,C6) Calculated	Com(11,C7+) Calculated
7000.000	1.0000	1.0000	1.0000
6841.986	1.0000	1.0000	1.0000
6683.973	1.0000	1.0000	1.0000
6525.960	1.0000	1.0000	1.0000
6367.947	1.0000	1.0000	1.0000
6209.934	1.0000	1.0000	1.0000
6051.921	1.0000	1.0000	1.0000
5893.908	1.0000	1.0000	1.0000
5762.256 - Psat	0.4988	0.3916	0.0300
5735.895	0.4967	0.3894	0.0293
5577.882	0.4839	0.3763	0.0254
4879.352	0.4295	0.3218	0.0132
4338.834	0.3894	0.2828	0.0075
3798.317	0.3505	0.2460	0.0039
3257.799	0.3129	0.2112	0.0019
2717.282	0.2774	0.1789	0.0008
2176.765	0.2457	0.1504	0.0003
1636.247	0.2221	0.1278	9.8363E-05
1095.730	0.2159	0.1157	2.9592E-05

555.213 @ Tres	0.2666	0.1319	9.7003E-06
14.695 @ Tstd	0.4865	0.1393	3.4808E-09

Molar Distributions Fluid, Z Inserted Point	Com(1 ,CO2) Calculated	Com(2 ,N2) Calculated	Com(3 ,C1) Calculated	Com(4 ,C2) Calculated
7000.000	0.9649	0.2179	60.9747	7.8540
6841.986	0.9649	0.2179	60.9747	7.8540
6683.973	0.9649	0.2179	60.9747	7.8540
6525.960	0.9649	0.2179	60.9747	7.8540
6367.947	0.9649	0.2179	60.9747	7.8540
6209.934	0.9649	0.2179	60.9747	7.8540
6051.921	0.9649	0.2179	60.9747	7.8540
5893.908	0.9649	0.2179	60.9747	7.8540
5762.256 - Psat	0.9649	0.2179	60.9747	7.8540
5735.895	0.9649	0.2179	60.9747	7.8540
5577.882	0.9645	0.2169	60.8267	7.8569
4879.352	0.9622	0.2109	59.9283	7.8740
4338.834	0.9474	0.1840	55.6994	7.9331
3798.317	0.9321	0.1620	52.0720	7.9677
3257.799	0.9117	0.1390	48.0563	7.9854
2717.282	0.8844	0.1151	43.5614	7.9776
2176.765	0.8473	0.0906	38.4723	7.9285
1636.247	0.7957	0.0661	32.6431	7.8085
1095.730	0.7211	0.0427	25.8952	7.5547
555.213 @ Tres	0.6067	0.0221	18.0327	7.0152
14.695 @ Tstd	0.4104	0.0069	8.9394	5.6912

Molar Distributions Fluid, Z Inserted Point	Com(5 ,C3) Calculated	Com(6 ,IC4) Calculated	Com(7 ,NC4) Calculated	Com(8 ,IC5) Calculated
7000.000	4.2434	0.9441	2.1684	0.7989
6841.986	4.2434	0.9441	2.1684	0.7989
6683.973	4.2434	0.9441	2.1684	0.7989
6525.960	4.2434	0.9441	2.1684	0.7989
6367.947	4.2434	0.9441	2.1684	0.7989
6209.934	4.2434	0.9441	2.1684	0.7989
6051.921	4.2434	0.9441	2.1684	0.7989
5893.908	4.2434	0.9441	2.1684	0.7989
5762.256 - Psat	4.2434	0.9441	2.1684	0.7989
5735.895	4.2434	0.9441	2.1684	0.7989
5577.882	4.2498	0.9463	2.1740	0.8014
4879.352	4.2885	0.9593	2.2082	0.8164
4338.834	4.4659	1.0208	2.3703	0.8889
3798.317	4.6146	1.0736	2.5104	0.9521
3257.799	4.7747	1.1324	2.6667	1.0235
2717.282	4.9477	1.1984	2.8432	1.1051

2176.765	5.1337	1.2732	3.0447	1.1995
1636.247	5.3290	1.3584	3.2763	1.3102
1095.730	5.5181	1.4545	3.5423	1.4411
555.213 @ Tres	5.6463	1.5575	3.8392	1.5964
14.695 @ Tstd	5.4668	1.6352	4.1119	1.7742

Molar Distributions Fluid, Z Inserted Point	Com(9 ,NC5) Calculated	Com(10,C6) Calculated	Com(11,C7+) Calculated	Total Calculated
7000.000	1.1931	1.8156	18.8249	100.0000
6841.986	1.1931	1.8156	18.8249	100.0000
6683.973	1.1931	1.8156	18.8249	100.0000
6525.960	1.1931	1.8156	18.8249	100.0000
6367.947	1.1931	1.8156	18.8249	100.0000
6209.934	1.1931	1.8156	18.8249	100.0000
6051.921	1.1931	1.8156	18.8249	100.0000
5893.908	1.1931	1.8156	18.8249	100.0000
5762.256 - Psat	1.1931	1.8156	18.8249	100.0000
5735.895	1.1931	1.8156	18.8249	100.0000
5577.882	1.1970	1.8228	18.9436	100.0000
4879.352	1.2207	1.8666	19.6648	100.0000
4338.834	1.3349	2.0778	23.0776	100.0000
3798.317	1.4346	2.2626	26.0183	100.0000
3257.799	1.5473	2.4717	29.2913	100.0000
2717.282	1.6764	2.7114	32.9794	100.0000
2176.765	1.8261	2.9898	37.1943	100.0000
1636.247	2.0018	3.3179	42.0930	100.0000
1095.730	2.2106	3.7109	47.9087	100.0000
555.213 @ Tres	2.4604	4.1906	55.0328	100.0000
14.695 @ Tstd	2.7545	4.7970	64.4125	100.0000

Molar Distributions Liquid, X Inserted Point	Com(1 ,CO2) Calculated	Com(2 ,N2) Calculated	Com(3 ,C1) Calculated	Com(4 ,C2) Calculated
7000.000	0.9649	0.2179	60.9747	7.8540
6841.986	0.9649	0.2179	60.9747	7.8540
6683.973	0.9649	0.2179	60.9747	7.8540
6525.960	0.9649	0.2179	60.9747	7.8540
6367.947	0.9649	0.2179	60.9747	7.8540
6209.934	0.9649	0.2179	60.9747	7.8540
6051.921	0.9649	0.2179	60.9747	7.8540
5893.908	0.9649	0.2179	60.9747	7.8540
5762.256 - Psat	0.9649	0.2179	60.9747	7.8540
5735.895	0.9645	0.2169	60.8267	7.8569
5577.882	0.9622	0.2109	59.9283	7.8740
4879.352	0.9474	0.1840	55.6994	7.9331
4338.834	0.9321	0.1620	52.0720	7.9677

3798.317	0.9117	0.1390	48.0563	7.9854
3257.799	0.8844	0.1151	43.5614	7.9776
2717.282	0.8473	0.0906	38.4723	7.9285
2176.765	0.7957	0.0661	32.6431	7.8085
1636.247	0.7211	0.0427	25.8952	7.5547
1095.730	0.6067	0.0221	18.0327	7.0152
555.213 @ Tres	0.4104	0.0069	8.9394	5.6912
14.695 @ Tstd	0.0322	5.7034E-05	0.2249	0.8970

Molar Distributions Liquid, X Inserted Point	Com(5 ,C3) Calculated	Com(6 ,IC4) Calculated	Com(7 ,NC4) Calculated	Com(8 ,IC5) Calculated
7000.000	4.2434	0.9441	2.1684	0.7989
6841.986	4.2434	0.9441	2.1684	0.7989
6683.973	4.2434	0.9441	2.1684	0.7989
6525.960	4.2434	0.9441	2.1684	0.7989
6367.947	4.2434	0.9441	2.1684	0.7989
6209.934	4.2434	0.9441	2.1684	0.7989
6051.921	4.2434	0.9441	2.1684	0.7989
5893.908	4.2434	0.9441	2.1684	0.7989
5762.256 - Psat	4.2434	0.9441	2.1684	0.7989
5735.895	4.2498	0.9463	2.1740	0.8014
5577.882	4.2885	0.9593	2.2082	0.8164
4879.352	4.4659	1.0208	2.3703	0.8889
4338.834	4.6146	1.0736	2.5104	0.9521
3798.317	4.7747	1.1324	2.6667	1.0235
3257.799	4.9477	1.1984	2.8432	1.1051
2717.282	5.1337	1.2732	3.0447	1.1995
2176.765	5.3290	1.3584	3.2763	1.3102
1636.247	5.5181	1.4545	3.5423	1.4411
1095.730	5.6463	1.5575	3.8392	1.5964
555.213 @ Tres	5.4668	1.6352	4.1119	1.7742
14.695 @ Tstd	2.4057	1.2470	3.5696	1.9063

Molar Distributions Liquid, X Inserted Point	Com(9 ,NC5) Calculated	Com(10,C6) Calculated	Com(11,C7+) Calculated	Total Calculated
7000.000	1.1931	1.8156	18.8249	100.0000
6841.986	1.1931	1.8156	18.8249	100.0000
6683.973	1.1931	1.8156	18.8249	100.0000
6525.960	1.1931	1.8156	18.8249	100.0000
6367.947	1.1931	1.8156	18.8249	100.0000
6209.934	1.1931	1.8156	18.8249	100.0000
6051.921	1.1931	1.8156	18.8249	100.0000
5893.908	1.1931	1.8156	18.8249	100.0000
5762.256 - Psat	1.1931	1.8156	18.8249	100.0000
5735.895	1.1970	1.8228	18.9436	100.0000
5577.882	1.2207	1.8666	19.6648	100.0000

4879.352	1.3349	2.0778	23.0776	100.0000
4338.834	1.4346	2.2626	26.0183	100.0000
3798.317	1.5473	2.4717	29.2913	100.0000
3257.799	1.6764	2.7114	32.9794	100.0000
2717.282	1.8261	2.9898	37.1943	100.0000
2176.765	2.0018	3.3179	42.0930	100.0000
1636.247	2.2106	3.7109	47.9087	100.0000
1095.730	2.4604	4.1906	55.0328	100.0000
555.213 @ Tres	2.7545	4.7970	64.4125	100.0000
14.695 @ Tstd	3.0753	5.8131	80.8289	100.0000

Molar Distributions Vapour, Y Inserted Point	Com(1 ,CO2) Calculated	Com(2 ,N2) Calculated	Com(3 ,C1) Calculated	Com(4 ,C2) Calculated
7000.000				
6841.986				
6683.973				
6525.960				
6367.947				
6209.934				
6051.921				
5893.908				
5762.256 - Psat	1.0201	0.3715	83.7508	7.3943
5735.895	1.0208	0.3713	83.7584	7.3980
5577.882	1.0250	0.3701	83.8005	7.4211
4879.352	1.0458	0.3635	83.9192	7.5389
4338.834	1.0669	0.3553	83.9258	7.6637
3798.317	1.0935	0.3439	83.8533	7.8271
3257.799	1.1280	0.3281	83.6783	8.0477
2717.282	1.1741	0.3065	83.3442	8.3610
2176.765	1.2389	0.2767	82.7170	8.8398
1636.247	1.3354	0.2358	81.4772	9.6451
1095.730	1.4907	0.1811	78.7679	11.1827
555.213 @ Tres	1.7585	0.1111	71.3850	14.7833
14.695 @ Tstd	1.8942	0.0338	43.1321	24.5020

Molar Distributions Vapour, Y Inserted Point	Com(5 ,C3) Calculated	Com(6 ,IC4) Calculated	Com(7 ,NC4) Calculated	Com(8 ,IC5) Calculated
7000.000				
6841.986				
6683.973				
6525.960				
6367.947				
6209.934				
6051.921				
5893.908				

5762.256 - Psat	3.2570	0.6141	1.3035	0.4183
5735.895	3.2575	0.6139	1.3030	0.4179
5577.882	3.2609	0.6132	1.3001	0.4157
4879.352	3.2822	0.6106	1.2885	0.4054
4338.834	3.3088	0.6093	1.2804	0.3968
3798.317	3.3472	0.6087	1.2731	0.3873
3257.799	3.4039	0.6095	1.2678	0.3770
2717.282	3.4938	0.6136	1.2686	0.3668
2176.765	3.6514	0.6266	1.2868	0.3595
1636.247	3.9605	0.6626	1.3513	0.3625
1095.730	4.6558	0.7619	1.5454	0.3967
555.213 @ Tres	6.6995	1.1018	2.2392	0.5538
14.695 @ Tstd	17.4776	3.1584	6.2399	1.2558

Molar Distributions Vapour, Y Inserted Point	Com(9 ,NC5) Calculated	Com(10,C6) Calculated	Com(11,C7+) Calculated	Total Calculated
7000.000				
6841.986				
6683.973				
6525.960				
6367.947				
6209.934				
6051.921				
5893.908				
5762.256 - Psat	0.5952	0.7111	0.5643	100.0000
5735.895	0.5945	0.7098	0.5548	100.0000
5577.882	0.5907	0.7024	0.5004	100.0000
4879.352	0.5734	0.6686	0.3040	100.0000
4338.834	0.5587	0.6398	0.1944	100.0000
3798.317	0.5424	0.6079	0.1156	100.0000
3257.799	0.5246	0.5726	0.0625	100.0000
2717.282	0.5065	0.5349	0.0301	100.0000
2176.765	0.4919	0.4989	0.0127	100.0000
1636.247	0.4909	0.4741	0.0047	100.0000
1095.730	0.5312	0.4851	0.0016	100.0000
555.213 @ Tres	0.7343	0.6329	0.0006	100.0000
14.695 @ Tstd	1.4962	0.8100	2.8135E-07	100.0000

B5. Expt SEPS1 : Separators

Peng-Robinson (3-Parm) on ZI with PR corr.
Lohrenz-Bray-Clark Viscosity Correlation

Stage number 1

Specified pressure PSIA	1297.6480
Specified temperature Deg F	204.0000

GOR calc. is Gas Vol at STC/Stage Oil Vol

Feed is wellstream only

Output is	100.0% of liquid to	stage 2	number moles	0.3611
	100.0% of vapour to	cumulative	number moles	0.6389

Total number moles output to liquid stream	0.3611
Total number moles output to vapour stream	0.6389
Total liquid volume output BBL	0.2231
Total vapour volume output MSCF	0.2425
Stage Gas-oil ratio (Calculated) MSCF/BBL	1.0870
Vapour mole fraction (Calculated)	63.8939
Stage Oil FVF (Calculated) RB/STB	1.2221

Fluid properties	Liquid		Vapour	
	Observed	Calculated	Observed	Calculated
Mole Weight		160.1309		20.2355
Z-factor		0.6320		0.8935
Viscosity		0.5963		0.0145
Density LB/FT3		46.1660		4.1262
Molar Vol CF/LB-ML		3.4686		4.9041

Molar Distributions Components		Fluid, Z	K-Values	Liquid,X	Vapour,Y
Mnemonic	Number	Calculated	Calculated	Calculated	Calculated
CO2	1	0.9649	2.0773	0.5715	1.1872
N2	2	0.2179	7.0121	0.0450	0.3156
C1	3	60.9747	3.7472	22.1302	82.9255
C2	4	7.8540	1.3665	6.3637	8.6961
C3	5	4.2434	0.7112	5.2035	3.7009

IC4	6	0.9441	0.4245	1.4931	0.6339
NC4	7	2.1684	0.3487	3.7141	1.2949
IC5	8	0.7989	0.2169	1.5989	0.3468
NC5	9	1.1931	0.1883	2.4787	0.4667
C6	10	1.8156	0.1010	4.2660	0.4310
C7+	11	18.8249	2.7796E-05	52.1352	0.0014
Composition Total		100.0000		100.0000	100.0000

Stage number 2

Specified pressure PSIA		14.6959
Specified temperature Deg F		60.0000
GOR calc. is Gas Vol at STC/Stage Oil Vol		
Feed is 100.0% of liquid from stage 1	number moles	0.3611
Output is 100.0% of liquid to cumulative	number moles	0.2282
100.0% of vapour to cumulative	number moles	0.1329
Total number moles output to liquid stream		0.2282
Total number moles output to vapour stream		0.1329
Total liquid volume output BBL		0.1825
Total vapour volume output MSCF		0.0504
Stage Gas-oil ratio (Calculated) MSCF/BBL		0.2763
Vapour mole fraction (Calculated)		36.8000
Stage Oil FVF (Calculated) RB/STB		1.0000

Fluid properties	Liquid		Vapour	
	Observed	Calculated	Observed	Calculated
Mole Weight		237.5192		27.2249
Z-factor		0.0118		0.9932
Viscosity		1.8448		0.0097
Density LB/FT3		52.8895		0.0722
Molar Vol CF/LB-ML		4.4909		376.9024

Molar Distributions Components	Fluid, Z	K-Values	Liquid,X	Vapour,Y

Mnemonic	Number	Calculated	Calculated	Calculated	Calculated
CO2	1	0.5715	58.8701	0.0256	1.5090
N2	2	0.0450	594.2940	0.0002	0.1219
C1	3	22.1302	192.2525	0.3100	59.6040
C2	4	6.3637	27.3355	0.5952	16.2705
C3	5	5.2035	7.2645	1.5743	11.4364
IC4	6	1.4931	2.5297	0.9553	2.4167
NC4	7	3.7141	1.7456	2.9145	5.0874
IC5	8	1.5989	0.6574	1.8296	1.2027
NC5	9	2.4787	0.4854	3.0578	1.4843
C6	10	4.2660	0.1388	6.2451	0.8671
C7+	11	52.1352	3.4205E-09	82.4924	2.8216E-07
Composition Total		100.0000		100.0000	100.0000

Cumulatives for Separator Train

Standard pressure PSIA	14.6959
Standard temperature Deg F	60.0000
Cumulative liquid mole fraction	0.2282
Cumulative vapour mole fraction	0.7718
Cumulative Surface volume oil BBL	0.1825
Cumulative Surface volume gas MSCF	0.2929
Cumulative GOR (Calculated) MSCF/BBL	1.6047

Fluid properties		Liquid	Vapour
		Calculated	Calculated
Mole Weight		237.5192	21.4388
Z-factor		0.0118	0.9958
Viscosity		1.8448	0.0103
Density	LB/FT3	52.8895	0.0567
Molar Vol	CF/LB-ML	4.4909	377.8917

Molar Distributions Components		Total, Z	Liquid,X	Vapour,Y	K-Values
Mnemonic	Number	Measured	Calculated	Calculated	Calculated
CO2	1	0.9649	0.0256	1.2426	48.4780
N2	2	0.2179	0.0002	0.2822	1375.5185

C1	3	60.9747	0.3100	78.9106	254.5260
C2	4	7.8540	0.5952	10.0001	16.8008
C3	5	4.2434	1.5743	5.0326	3.1968
IC4	6	0.9441	0.9553	0.9408	0.9848
NC4	7	2.1684	2.9145	1.9478	0.6683
IC5	8	0.7989	1.8296	0.4942	0.2701
NC5	9	1.1931	3.0578	0.6418	0.2099
C6	10	1.8156	6.2451	0.5061	0.0810
C7+	11	18.8249	82.4924	0.0012	1.4544E-05
Composition Total		100.0000	100.0000	100.0000	

```
B6.ECHO
-- DENSITY created by PVTi
-- Units: lb /ft^3     lb /ft^3     lb /ft^3
DENSITY
--
-- Fluid Densities at Surface Conditions
--
         53.2002     62.4280      0.0588
/

-- Created from a Differential Liberation Experiment.
-- Using the method of Whitson and Torp.
--PVTi--Please do not alter these lines
--PVTi--as PVTi can use them to re-create the fluid model
--PVTiMODSPEC
========================================================
--PVTiTITLE
--PVTiModified System: From Automatically created during keyword export
--PVTiVERSION
--PVTi  2010.1          /
--PVTiFPE
--PVTiNCOMPS
--PVTi       11 /
--PVTiEOS
--PVTi PR3  /
--PVTiPRCORR
--PVTiLBC
--PVTiOPTIONS
--PVTi  0  0  0  2  0  0  0  0  0  0  0  0  0  0  0  0  0  0  0  0
--PVTi/
--PVTiNOECHO
--PVTiMODSYS
========================================================
--PVTiUNITS
--PVTi   FIELD       ABSOL         PERCENT      /
--PVTiDEGREES
--PVTi   Fahrenheit /
--PVTiSTCOND
--PVTi      60.0000      14.6959 /
--PVTiLNAMES
--PVTi CO2
--PVTi N2
--PVTi C1
--PVTi C2
--PVTi C3
--PVTi IC4
--PVTi NC4
--PVTi IC5
--PVTi NC5
--PVTi C6
--PVTi 1*
--PVTi /
--PVTiCNAMES
--PVTi 1*
```

```
--PVTi 1*
--PVTi 1*
--PVTi 1*
--PVTi 1*
--PVTi 1*
--PVTi 1*
--PVTi 1*
--PVTi 1*
--PVTi 1*
--PVTi C7+
--PVTi /
--PVTiTCRIT
--PVTi  8.878998547E+01 -2.325100060E+02 -1.165900091E+02
9.010398544E+01
--PVTi  2.059699824E+02  2.749099805E+02  3.056899797E+02
3.690499780E+02
--PVTi  3.856099776E+02  4.538299758E+02  9.722702451E+02
/
--PVTiPCRIT
--PVTi  1.071331110E+03  4.923126500E+02  6.677816960E+02
7.083423800E+02
--PVTi  6.157582100E+02  5.290524000E+02  5.506553730E+02
4.915778550E+02
--PVTi  4.887856340E+02  4.366151890E+02  1.883081031E+02
/
--PVTiVCRIT
--PVTi  1.505735240E+00  1.441661400E+00  1.569809080E+00
2.370732080E+00
--PVTi  3.203692000E+00  4.212854980E+00  4.084707300E+00
4.933685680E+00
--PVTi  4.981741060E+00  5.622479460E+00  1.729198542E+01
/
--PVTiZCRIT
--PVTi  2.740777974E-01  2.911514044E-01  2.847294766E-01  2.846347951E-
01
--PVTi  2.761646200E-01  2.827369588E-01  2.738555491E-01  2.727108716E-
01
--PVTi  2.684389142E-01  2.504174849E-01  2.119021905E-01
/
--PVTiVCRITVIS
--PVTi  1.505735240E+00  1.441661400E+00  1.569809080E+00
2.370732080E+00
--PVTi  3.203692000E+00  4.212854980E+00  4.084707300E+00
4.933685680E+00
--PVTi  4.981741060E+00  5.622479460E+00  1.729198542E+01
/
--PVTiZCRITVIS
--PVTi  2.740777974E-01  2.911514044E-01  2.847294766E-01  2.846347951E-
01
--PVTi  2.761646200E-01  2.827369588E-01  2.738555491E-01  2.727108716E-
01
--PVTi  2.684389142E-01  2.504174849E-01  2.119021905E-01
/
--PVTiSSHIFT
```

```
--PVTi -4.273033674E-02 -1.313342386E-01 -1.442656189E-01 -1.032683540E-
01
--PVTi -7.750138148E-02 -6.198372515E-02 -5.422489699E-02 -4.177245672E-
02
--PVTi -3.027789648E-02 -7.288775999E-03  2.504144839E-01
/
--PVTiACF
--PVTi  2.250000000E-01  4.000000000E-02  1.300000000E-02  9.860000000E-
02
--PVTi  1.524000000E-01  1.848000000E-01  2.010000000E-01  2.270000000E-
01
--PVTi  2.510000000E-01  2.990000000E-01  8.871406414E-01
/
--PVTiMW
--PVTi  4.401000000E+01  2.801300000E+01  1.604300000E+01
3.007000000E+01
--PVTi  4.409700000E+01  5.812400000E+01  5.812400000E+01
7.215100000E+01
--PVTi  7.215100000E+01  8.400000000E+01  2.734355626E+02
/
--PVTiZI
--PVTi  9.648880529E-01  2.178779474E-01  6.097469986E+01
7.853981248E+00
--PVTi  4.243432405E+00  9.441377722E-01  2.168404334E+00  7.988858073E-
01
--PVTi  1.193141141E+00  1.815649562E+00  1.882490187E+01
/
--PVTiTBOIL
--PVTi -1.092100093E+02 -3.203500037E+02 -2.587900053E+02 -
1.273900088E+02
--PVTi -4.369001102E+01  1.066998754E+01  3.118998700E+01
8.212998565E+01
--PVTi  9.688998526E+01  1.470199839E+02  6.776743824E+02
/
--PVTiTREF
--PVTi  6.772998603E+01 -3.190900037E+02 -2.586100053E+02 -
1.302700087E+02
--PVTi -4.387001101E+01  6.772998603E+01  6.772998603E+01
6.772998603E+01
--PVTi  6.772998603E+01  6.052998622E+01  5.999998631E+01
/
--PVTiDREF
--PVTi  4.850653269E+01  5.019208788E+01  2.653188725E+01
3.421052756E+01
--PVTi  3.633307854E+01  3.477237929E+01  3.614579463E+01
3.870534140E+01
--PVTi  3.907990922E+01  4.276315945E+01  5.377221654E+01
/
--PVTiPARACHOR
--PVTi  7.800000000E+01  4.100000000E+01  7.700000000E+01
1.080000000E+02
--PVTi  1.503000000E+02  1.815000000E+02  1.899000000E+02
2.250000000E+02
```

```
--PVTi  2.315000000E+02  2.710000000E+02  7.011412992E+02
/
--PVTiHYDRO
--PVTi  N N H H H H H H H H H
--PVTi /
--PVTiTHERMX
--PVTi    0.0002778 /
--PVTiBIC
--PVTi  -1.200000000E-02
--PVTi   1.000000000E-01  1.000000000E-01
--PVTi   1.000000000E-01  1.000000000E-01  0.000000000E+00
--PVTi   1.000000000E-01  1.000000000E-01  0.000000000E+00
0.000000000E+00
--PVTi   1.000000000E-01  1.000000000E-01  0.000000000E+00
0.000000000E+00
--PVTi   0.000000000E+00
--PVTi   1.000000000E-01  1.000000000E-01  0.000000000E+00
0.000000000E+00
--PVTi   0.000000000E+00  0.000000000E+00
--PVTi   1.000000000E-01  1.000000000E-01  0.000000000E+00
0.000000000E+00
--PVTi   0.000000000E+00  0.000000000E+00  0.000000000E+00
--PVTi   1.000000000E-01  1.000000000E-01  0.000000000E+00
0.000000000E+00
--PVTi   0.000000000E+00  0.000000000E+00  0.000000000E+00
0.000000000E+00
--PVTi   1.000000000E-01  1.000000000E-01  2.790000000E-02  1.000000000E-
02
--PVTi   1.000000000E-02  0.000000000E+00  0.000000000E+00
0.000000000E+00
--PVTi   0.000000000E+00
--PVTi   1.000000000E-01  1.000000000E-01  5.212000000E-02  1.000000000E-
02
--PVTi   1.000000000E-02  0.000000000E+00  0.000000000E+00
0.000000000E+00
--PVTi   0.000000000E+00  0.000000000E+00
--PVTi /
--PVTiSPECHA
--PVTi  4.729150800E+00  7.440052900E+00  4.597785500E+00
1.291918014E+00
--PVTi -1.008885504E+00 -3.319959400E-01  2.265932002E+00 -
2.275008150E+00
--PVTi -8.661081421E-01 -1.054027398E+00  2.941612848E+00
/
--PVTiSPECHB
--PVTi  9.744900480E-03 -1.800630440E-03  6.915907040E-03  2.363244520E-
02
--PVTi  4.064355960E-02  5.104661240E-02  4.419970520E-02  6.722176720E-
02
--PVTi  6.466081160E-02  7.722674400E-02  2.065250198E-01
/
--PVTiSPECHC
--PVTi -4.129676758E-06  1.975639720E-06  8.824032630E-07 -5.114547902E-
06
```

```
--PVTi -1.169165894E-05 -1.360832434E-05 -8.167943320E-06 -2.011761491E-
05
--PVTi -1.901921820E-05 -2.299261301E-05 -4.559941183E-05
/
--PVTiSPECHD
--PVTi  7.023679600E-10 -4.783473920E-10 -4.636038080E-10  3.568356872E-
10
--PVTi  1.316683960E-09  1.185629880E-09 -1.155733168E-10  2.343820312E-
09
--PVTi  2.172630920E-09  2.659578736E-09  0.000000000E+00
/
--PVTiHEATVAPS
--PVTi  1.802570424E+04  0.000000000E+00  0.000000000E+00
1.650621600E+04
--PVTi  3.603408601E+04  4.586099659E+04  6.166418764E+04
5.938211357E+04
--PVTi  6.289700021E+04  7.462523487E+04  2.295458080E+05
/
--PVTiCALVAL
--PVTi  0.000000000E+00  0.000000000E+00  1.891038000E+03
3.323854000E+03
--PVTi  4.754344000E+03  6.184834000E+03  6.184834000E+03
7.615324000E+03
--PVTi  7.615324000E+03  9.045814000E+03  2.889083333E+04
/
--PVTiSIMULATE
========================================================
--PVTiUNITS
--PVTi   FIELD       ABSOL         PERCENT      /
--PVTiDEGREES
--PVTi   Fahrenheit /
--PVTiSTCOND
--PVTi      60.0000      14.6959 /
--PVTiEXP
--PVTi   1  ZI       DL         220.0000
--PVTi                       7000.0000    6841.9869    6683.9739
6525.9608
--PVTi                       6367.9477    6209.9346    6051.9216
5893.9085
--PVTi                       5735.8954    5577.8824    4879.3520
4338.8346
--PVTi                       3798.3173    3257.7999    2717.2826
2176.7653
--PVTi                       1636.2479    1095.7306     555.2132
14.6959 /
--PVTi   2  ZI       SEPS        60.0000      14.6959  0  0 /
--PVTi /
--PVTi--End of PVTi generated section--
-- Column Properties are:
--       'Oil GOR'    'PSAT'    'Oil FVF'    'Oil Visc'
-- Units: Mscf /stb     psia     rb /stb     cp
PVTO
--
-- Live Oil PVT Properties (Dissolved Gas)
```

--

0.0000	14.6959	1.0889	1.9056
	555.2132	1.0865	1.9619
	1095.7306	1.0842	2.0160
	1636.2479	1.0820	2.0681
	2176.7653	1.0800	2.1183
	2717.2826	1.0781	2.1666
	3257.7999	1.0763	2.2133
	3798.3173	1.0747	2.2583
	4338.8346	1.0731	2.3018
	4879.3520	1.0716	2.3439
	5577.8824	1.0698	2.3963
	5735.8954	1.0694	2.4078
	5762.2564	1.0694	2.4097
	5893.9085	1.0691	2.4193
	6051.9216	1.0687	2.4306
	6209.9346	1.0683	2.4418
	6367.9477	1.0679	2.4529
	6525.9608	1.0676	2.4639
	6683.9739	1.0672	2.4748
	6841.9869	1.0669	2.4857
	7005.2657	1.0665	2.4967 /
0.1226	555.2132	1.1644	0.6032
	1095.7306	1.1572	0.6403
	1636.2479	1.1507	0.6762
	2176.7653	1.1449	0.7111
	2717.2826	1.1396	0.7450
	3257.7999	1.1347	0.7778
	3798.3173	1.1303	0.8098
	4338.8346	1.1262	0.8408
	4879.3520	1.1224	0.8710
	5577.8824	1.1179	0.9089
	5735.8954	1.1169	0.9172
	5762.2564	1.1167	0.9186
	5893.9085	1.1160	0.9256
	6051.9216	1.1150	0.9338
	6209.9346	1.1141	0.9420
	6367.9477	1.1132	0.9501
	6525.9608	1.1124	0.9582
	6683.9739	1.1115	0.9662
	6841.9869	1.1107	0.9741
	7005.2657	1.1098	0.9822 /
0.2362	1095.7306	1.2242	0.5347
	1636.2479	1.2159	0.5691
	2176.7653	1.2084	0.6026
	2717.2826	1.2017	0.6353
	3257.7999	1.1956	0.6671
	3798.3173	1.1901	0.6982
	4338.8346	1.1850	0.7285
	4879.3520	1.1802	0.7580
	5577.8824	1.1747	0.7952
	5735.8954	1.1735	0.8034
	5762.2564	1.1733	0.8048
	5893.9085	1.1723	0.8116

	6051.9216	1.1712	0.8198
	6209.9346	1.1700	0.8278
	6367.9477	1.1689	0.8359
	6525.9608	1.1679	0.8438
	6683.9739	1.1668	0.8518
	6841.9869	1.1658	0.8596
	7005.2657	1.1647	0.8677 /
0.3504	1636.2479	1.2814	0.4726
	2176.7653	1.2721	0.5038
	2717.2826	1.2637	0.5343
	3257.7999	1.2562	0.5641
	3798.3173	1.2493	0.5933
	4338.8346	1.2431	0.6219
	4879.3520	1.2373	0.6499
	5577.8824	1.2306	0.6852
	5735.8954	1.2291	0.6931
	5762.2564	1.2289	0.6944
	5893.9085	1.2277	0.7009
	6051.9216	1.2263	0.7086
	6209.9346	1.2250	0.7164
	6367.9477	1.2236	0.7240
	6525.9608	1.2223	0.7316
	6683.9739	1.2211	0.7392
	6841.9869	1.2198	0.7468
	7005.2657	1.2186	0.7545 /
0.4709	2176.7653	1.3399	0.4174
	2717.2826	1.3295	0.4453
	3257.7999	1.3203	0.4727
	3798.3173	1.3119	0.4995
	4338.8346	1.3043	0.5259
	4879.3520	1.2973	0.5519
	5577.8824	1.2892	0.5847
	5735.8954	1.2875	0.5920
	5762.2564	1.2872	0.5933
	5893.9085	1.2858	0.5993
	6051.9216	1.2841	0.6066
	6209.9346	1.2825	0.6138
	6367.9477	1.2809	0.6210
	6525.9608	1.2794	0.6281
	6683.9739	1.2778	0.6352
	6841.9869	1.2764	0.6422
	7005.2657	1.2748	0.6495 /
0.6005	2717.2826	1.4014	0.3690
	3257.7999	1.3900	0.3937
	3798.3173	1.3798	0.4181
	4338.8346	1.3706	0.4421
	4879.3520	1.3622	0.4657
	5577.8824	1.3524	0.4957
	5735.8954	1.3504	0.5025
	5762.2564	1.3500	0.5036
	5893.9085	1.3483	0.5091
	6051.9216	1.3464	0.5158
	6209.9346	1.3444	0.5224
	6367.9477	1.3425	0.5290

	6525.9608	1.3407	0.5356
	6683.9739	1.3389	0.5421
	6841.9869	1.3371	0.5486
	7005.2657	1.3353	0.5553 /
0.7419	3257.7999	1.4674	0.3266
	3798.3173	1.4549	0.3484
	4338.8346	1.4438	0.3699
	4879.3520	1.4337	0.3912
	5577.8824	1.4219	0.4183
	5735.8954	1.4195	0.4244
	5762.2564	1.4191	0.4254
	5893.9085	1.4170	0.4305
	6051.9216	1.4147	0.4365
	6209.9346	1.4124	0.4425
	6367.9477	1.4102	0.4485
	6525.9608	1.4080	0.4545
	6683.9739	1.4058	0.4604
	6841.9869	1.4037	0.4664
	7005.2657	1.4016	0.4725 /
0.8984	3798.3173	1.5394	0.2895
	4338.8346	1.5259	0.3086
	4879.3520	1.5136	0.3276
	5577.8824	1.4996	0.3518
	5735.8954	1.4966	0.3572
	5762.2564	1.4961	0.3581
	5893.9085	1.4937	0.3626
	6051.9216	1.4909	0.3680
	6209.9346	1.4882	0.3734
	6367.9477	1.4855	0.3788
	6525.9608	1.4829	0.3842
	6683.9739	1.4804	0.3895
	6841.9869	1.4779	0.3948
	7005.2657	1.4754	0.4003 /
1.0739	4338.8346	1.6194	0.2569
	4879.3520	1.6046	0.2735
	5577.8824	1.5876	0.2949
	5735.8954	1.5841	0.2997
	5762.2564	1.5835	0.3005
	5893.9085	1.5806	0.3045
	6051.9216	1.5773	0.3093
	6209.9346	1.5740	0.3141
	6367.9477	1.5708	0.3189
	6525.9608	1.5677	0.3236
	6683.9739	1.5646	0.3284
	6841.9869	1.5617	0.3331
	7005.2657	1.5587	0.3380 /
1.2735	4879.3520	1.7097	0.2279
	5577.8824	1.6891	0.2466
	5735.8954	1.6849	0.2509
	5762.2564	1.6842	0.2516
	5893.9085	1.6807	0.2551
	6051.9216	1.6766	0.2593
	6209.9346	1.6727	0.2635
	6367.9477	1.6689	0.2677

	6525.9608	1.6652	0.2719
	6683.9739	1.6615	0.2760
	6841.9869	1.6580	0.2802
	7005.2657	1.6544	0.2845 /
1.5794	5577.8824	1.8475	0.1951
	5735.8954	1.8419	0.1986
	5762.2564	1.8410	0.1992
	5893.9085	1.8366	0.2021
	6051.9216	1.8314	0.2056
	6209.9346	1.8263	0.2091
	6367.9477	1.8214	0.2126
	6525.9608	1.8166	0.2161
	6683.9739	1.8120	0.2196
	6841.9869	1.8075	0.2231
	7005.2657	1.8029	0.2267 /
1.6580	5735.8954	1.8828	0.1883
	5762.2564	1.8819	0.1889
	5893.9085	1.8771	0.1916
	6051.9216	1.8716	0.1950
	6209.9346	1.8662	0.1983
	6367.9477	1.8610	0.2017
	6525.9608	1.8560	0.2050
	6683.9739	1.8510	0.2084
	6841.9869	1.8463	0.2117
	7005.2657	1.8415	0.2152 /
1.6716	5762.2564	1.8889	0.1872
	5893.9085	1.8841	0.1899
	6051.9216	1.8785	0.1933
	6209.9346	1.8731	0.1966
	6367.9477	1.8678	0.1999
	6525.9608	1.8627	0.2032
	6683.9739	1.8578	0.2065
	6841.9869	1.8530	0.2099
	7005.2657	1.8481	0.2133 /
1.7409	5893.9085	1.9201	0.1817
	6051.9216	1.9142	0.1849
	6209.9346	1.9085	0.1881
	6367.9477	1.9030	0.1913
	6525.9608	1.8976	0.1945
	6683.9739	1.8924	0.1977
	6841.9869	1.8873	0.2009
	7005.2657	1.8822	0.2042 /
1.8285	6051.9216	1.9594	0.1753
	6209.9346	1.9534	0.1783
	6367.9477	1.9475	0.1814
	6525.9608	1.9418	0.1844
	6683.9739	1.9362	0.1875
	6841.9869	1.9309	0.1905
	7005.2657	1.9255	0.1937 /
1.9214	6209.9346	2.0011	0.1690
	6367.9477	1.9949	0.1719
	6525.9608	1.9888	0.1748
	6683.9739	1.9829	0.1777
	6841.9869	1.9772	0.1807

```
                7005.2657      1.9715      0.1837 /
       2.0200   6367.9477      2.0454      0.1629
                6525.9608      2.0390      0.1657
                6683.9739      2.0327      0.1685
                6841.9869      2.0266      0.1713
                7005.2657      2.0205      0.1741 /
       2.1252   6525.9608      2.0928      0.1570
                6683.9739      2.0861      0.1596
                6841.9869      2.0796      0.1623
                7005.2657      2.0731      0.1650 /
       2.2378   6683.9739      2.1434      0.1512
                6841.9869      2.1365      0.1537
                7005.2657      2.1296      0.1563 /
       2.3588   6841.9869      2.1980      0.1455
                7005.2657      2.1905      0.1480 /
/

-- Created from a Differential Liberation Experiment.
-- Using the method of Whitson and Torp.
--PVTi--Please do not alter these lines
--PVTi--as PVTi can use them to re-create the fluid model
--PVTiMODSPEC
========================================================
--PVTiTITLE
--PVTiModified System: From Automatically created during keyword export
--PVTiVERSION
--PVTi  2010.1          /
--PVTiFPE
--PVTiNCOMPS
--PVTi       11 /
--PVTiEOS
--PVTi PR3  /
--PVTiPRCORR
--PVTiLBC
--PVTiOPTIONS
--PVTi  0  0  0  2  0  0  0  0  0  0  0  0  0  0  0  0  0  0  0  0
--PVTi/
--PVTiNOECHO
--PVTiMODSYS
========================================================
--PVTiUNITS
--PVTi   FIELD       ABSOL         PERCENT      /
--PVTiDEGREES
--PVTi   Fahrenheit /
--PVTiSTCOND
--PVTi      60.0000      14.6959 /
--PVTiLNAMES
--PVTi CO2
--PVTi N2
--PVTi C1
--PVTi C2
--PVTi C3
--PVTi IC4
--PVTi NC4
```

```
--PVTi IC5
--PVTi NC5
--PVTi C6
--PVTi 1*
--PVTi /
--PVTiCNAMES
--PVTi 1*
--PVTi 1*
--PVTi 1*
--PVTi 1*
--PVTi 1*
--PVTi 1*
--PVTi 1*
--PVTi 1*
--PVTi 1*
--PVTi 1*
--PVTi C7+
--PVTi /
--PVTiTCRIT
--PVTi  8.878998547E+01 -2.325100060E+02 -1.165900091E+02
9.010398544E+01
--PVTi  2.059699824E+02  2.749099805E+02  3.056899797E+02
3.690499780E+02
--PVTi  3.856099776E+02  4.538299758E+02  9.722702451E+02
/
--PVTiPCRIT
--PVTi  1.071331110E+03  4.923126500E+02  6.677816960E+02
7.083423800E+02
--PVTi  6.157582100E+02  5.290524000E+02  5.506553730E+02
4.915778550E+02
--PVTi  4.887856340E+02  4.366151890E+02  1.883081031E+02
/
--PVTiVCRIT
--PVTi  1.505735240E+00  1.441661400E+00  1.569809080E+00
2.370732080E+00
--PVTi  3.203692000E+00  4.212854980E+00  4.084707300E+00
4.933685680E+00
--PVTi  4.981741060E+00  5.622479460E+00  1.729198542E+01
/
--PVTiZCRIT
--PVTi  2.740777974E-01  2.911514044E-01  2.847294766E-01  2.846347951E-
01
--PVTi  2.761646200E-01  2.827369588E-01  2.738555491E-01  2.727108716E-
01
--PVTi  2.684389142E-01  2.504174849E-01  2.119021905E-01
/
--PVTiVCRITVIS
--PVTi  1.505735240E+00  1.441661400E+00  1.569809080E+00
2.370732080E+00
--PVTi  3.203692000E+00  4.212854980E+00  4.084707300E+00
4.933685680E+00
--PVTi  4.981741060E+00  5.622479460E+00  1.729198542E+01
/
--PVTiZCRITVIS
```

```
--PVTi  2.740777974E-01  2.911514044E-01  2.847294766E-01  2.846347951E-
01
--PVTi  2.761646200E-01  2.827369588E-01  2.738555491E-01  2.727108716E-
01
--PVTi  2.684389142E-01  2.504174849E-01  2.119021905E-01
/
--PVTiSSHIFT
--PVTi -4.273033674E-02 -1.313342386E-01 -1.442656189E-01 -1.032683540E-
01
--PVTi -7.750138148E-02 -6.198372515E-02 -5.422489699E-02 -4.177245672E-
02
--PVTi -3.027789648E-02 -7.288775999E-03  2.504144839E-01
/
--PVTiACF
--PVTi  2.250000000E-01  4.000000000E-02  1.300000000E-02  9.860000000E-
02
--PVTi  1.524000000E-01  1.848000000E-01  2.010000000E-01  2.270000000E-
01
--PVTi  2.510000000E-01  2.990000000E-01  8.871406414E-01
/
--PVTiMW
--PVTi  4.401000000E+01  2.801300000E+01  1.604300000E+01
3.007000000E+01
--PVTi  4.409700000E+01  5.812400000E+01  5.812400000E+01
7.215100000E+01
--PVTi  7.215100000E+01  8.400000000E+01  2.734355626E+02
/
--PVTiZI
--PVTi  9.648880529E-01  2.178779474E-01  6.097469986E+01
7.853981248E+00
--PVTi  4.243432405E+00  9.441377722E-01  2.168404334E+00  7.988858073E-
01
--PVTi  1.193141141E+00  1.815649562E+00  1.882490187E+01
/
--PVTiTBOIL
--PVTi -1.092100093E+02 -3.203500037E+02 -2.587900053E+02 -
1.273900088E+02
--PVTi -4.369001102E+01  1.066998754E+01  3.118998700E+01
8.212998565E+01
--PVTi  9.688998526E+01  1.470199839E+02  6.776743824E+02
/
--PVTiTREF
--PVTi  6.772998603E+01 -3.190900037E+02 -2.586100053E+02 -
1.302700087E+02
--PVTi -4.387001101E+01  6.772998603E+01  6.772998603E+01
6.772998603E+01
--PVTi  6.772998603E+01  6.052998622E+01  5.999998631E+01
/
--PVTiDREF
--PVTi  4.850653269E+01  5.019208788E+01  2.653188725E+01
3.421052756E+01
--PVTi  3.633307854E+01  3.477237929E+01  3.614579463E+01
3.870534140E+01
```

```
--PVTi  3.907990922E+01  4.276315945E+01  5.377221654E+01
/
--PVTiPARACHOR
--PVTi  7.800000000E+01  4.100000000E+01  7.700000000E+01
1.080000000E+02
--PVTi  1.503000000E+02  1.815000000E+02  1.899000000E+02
2.250000000E+02
--PVTi  2.315000000E+02  2.710000000E+02  7.011412992E+02
/
--PVTiHYDRO
--PVTi  N N H H H H H H H H H
--PVTi /
--PVTiTHERMX
--PVTi    0.0002778 /
--PVTiBIC
--PVTi  -1.200000000E-02
--PVTi   1.000000000E-01  1.000000000E-01
--PVTi   1.000000000E-01  1.000000000E-01  0.000000000E+00
--PVTi   1.000000000E-01  1.000000000E-01  0.000000000E+00
0.000000000E+00
--PVTi   1.000000000E-01  1.000000000E-01  0.000000000E+00
0.000000000E+00
--PVTi   0.000000000E+00
--PVTi   1.000000000E-01  1.000000000E-01  0.000000000E+00
0.000000000E+00
--PVTi   0.000000000E+00  0.000000000E+00
--PVTi   1.000000000E-01  1.000000000E-01  0.000000000E+00
0.000000000E+00
--PVTi   0.000000000E+00  0.000000000E+00  0.000000000E+00
--PVTi   1.000000000E-01  1.000000000E-01  0.000000000E+00
0.000000000E+00
--PVTi   0.000000000E+00  0.000000000E+00  0.000000000E+00
0.000000000E+00
--PVTi   1.000000000E-01  1.000000000E-01  2.790000000E-02  1.000000000E-
02
--PVTi   1.000000000E-02  0.000000000E+00  0.000000000E+00
0.000000000E+00
--PVTi   0.000000000E+00
--PVTi   1.000000000E-01  1.000000000E-01  5.212000000E-02  1.000000000E-
02
--PVTi   1.000000000E-02  0.000000000E+00  0.000000000E+00
0.000000000E+00
--PVTi   0.000000000E+00  0.000000000E+00
--PVTi /
--PVTiSPECHA
--PVTi  4.729150800E+00  7.440052900E+00  4.597785500E+00
1.291918014E+00
--PVTi -1.008885504E+00 -3.319959400E-01  2.265932002E+00 -
2.275008150E+00
--PVTi -8.661081421E-01 -1.054027398E+00  2.941612848E+00
/
--PVTiSPECHB
--PVTi  9.744900480E-03 -1.800630440E-03  6.915907040E-03  2.363244520E-
02
```

```
--PVTi  4.064355960E-02  5.104661240E-02  4.419970520E-02  6.722176720E-
02
--PVTi  6.466081160E-02  7.722674400E-02  2.065250198E-01
/
--PVTiSPECHC
--PVTi -4.129676758E-06  1.975639720E-06  8.824032630E-07 -5.114547902E-
06
--PVTi -1.169165894E-05 -1.360832434E-05 -8.167943320E-06 -2.011761491E-
05
--PVTi -1.901921820E-05 -2.299261301E-05 -4.559941183E-05
/
--PVTiSPECHD
--PVTi  7.023679600E-10 -4.783473920E-10 -4.636038080E-10  3.568356872E-
10
--PVTi  1.316683960E-09  1.185629880E-09 -1.155733168E-10  2.343820312E-
09
--PVTi  2.172630920E-09  2.659578736E-09  0.000000000E+00
/
--PVTiHEATVAPS
--PVTi  1.802570424E+04  0.000000000E+00  0.000000000E+00
1.650621600E+04
--PVTi  3.603408601E+04  4.586099659E+04  6.166418764E+04
5.938211357E+04
--PVTi  6.289700021E+04  7.462523487E+04  2.295458080E+05
/
--PVTiCALVAL
--PVTi  0.000000000E+00  0.000000000E+00  1.891038000E+03
3.323854000E+03
--PVTi  4.754344000E+03  6.184834000E+03  6.184834000E+03
7.615324000E+03
--PVTi  7.615324000E+03  9.045814000E+03  2.889083333E+04
/
--PVTiSIMULATE
=========================================================
--PVTiUNITS
--PVTi   FIELD       ABSOL         PERCENT      /
--PVTiDEGREES
--PVTi   Fahrenheit /
--PVTiSTCOND
--PVTi      60.0000      14.6959 /
--PVTiEXP
--PVTi   1  ZI       DL         220.0000
--PVTi                     7000.0000    6841.9869    6683.9739
6525.9608
--PVTi                     6367.9477    6209.9346    6051.9216
5893.9085
--PVTi                     5735.8954    5577.8824    4879.3520
4338.8346
--PVTi                     3798.3173    3257.7999    2717.2826
2176.7653
--PVTi                     1636.2479    1095.7306     555.2132
14.6959 /
--PVTi   2  ZI       SEPS        60.0000      14.6959  0  0 /
--PVTi /
```

```
--PVTi--End of PVTi generated section--
-- Column Properties are:
--   'Gas Pressure'  'Gas OGR'   'Gas FVF'    'Gas Visc'
-- Units: psia     stb /Mscf     rb /Mscf     cp
PVTG
--
-- Wet Gas PVT Properties (Vapourised Oil)
--
        14.6959   0.0004413    231.3357     0.01082
                  0.0001154    231.2610    0.008561
                 3.996e-005    231.2437    0.008561
                 1.549e-005    231.2381    0.008561
                          0    231.2345     0.01083 /
       555.2132  1.549e-005      5.7448     0.01324
                          0      5.7448     0.01324 /
      1095.7306  3.996e-005      2.8286     0.01428
                          0      2.8287     0.01428 /
      1636.2479   0.0001154      1.8649     0.01553
                          0      1.8652     0.01553 /
      2176.7653   0.0003108      1.3983     0.01711
                  0.0001154      1.3987      0.0171
                 3.996e-005      1.3988      0.0171
                 1.549e-005      1.3988      0.0171
                          0      1.3989      0.0171 /
      2717.2826   0.0007384      1.1309     0.01897
                  0.0004413      1.1312     0.01896
                  0.0003108      1.1314     0.01895
                  0.0001154      1.1316     0.01894
                 3.996e-005      1.1317     0.01893
                 1.549e-005      1.1318     0.01893
                          0      1.1318     0.01893 /
      3257.7999    0.001537      0.9617     0.02104
                  0.0007384      0.9624     0.02098
                  0.0004413      0.9627     0.02096
                  0.0003108      0.9628     0.02095
                  0.0001154      0.9629     0.02093
                 3.996e-005      0.9630     0.02093
                 1.549e-005      0.9630     0.02092
                          0      0.9630     0.02092 /
      3798.3173    0.002846      0.8474     0.02323
                   0.001537      0.8481      0.0231
                  0.0007384      0.8485     0.02303
                  0.0004413      0.8486       0.023
                  0.0003108      0.8487     0.02299
                  0.0001154      0.8488     0.02297
                 3.996e-005      0.8488     0.02296
                 1.549e-005      0.8488     0.02296
                          0      0.8488     0.02296 /
      4338.8346    0.004797      0.7663      0.0255
                   0.002846      0.7667     0.02528
                   0.001537      0.7670     0.02513
                  0.0007384      0.7672     0.02505
                  0.0004413      0.7672     0.02501
                  0.0003108      0.7673       0.025
```

	0.0001154	0.7673	0.02498	
	3.996e-005	0.7673	0.02497	
	1.549e-005	0.7673	0.02497	
	0	0.7673	0.02497	/
4879.3520	0.007515	0.7067	0.02783	
	0.004797	0.7067	0.02749	
	0.002846	0.7067	0.02725	
	0.001537	0.7067	0.02709	
	0.0007384	0.7067	0.02699	
	0.0004413	0.7067	0.02696	
	0.0003108	0.7067	0.02694	
	0.0001154	0.7067	0.02692	
	3.996e-005	0.7067	0.02691	
	1.549e-005	0.7067	0.02691	
	0	0.7067	0.0269	/
5577.8824	0.01241	0.6510	0.03098	
	0.007515	0.6499	0.03029	
	0.004797	0.6493	0.02992	
	0.002846	0.6488	0.02966	
	0.001537	0.6485	0.02949	
	0.0007384	0.6483	0.02938	
	0.0004413	0.6483	0.02934	
	0.0003108	0.6482	0.02932	
	0.0001154	0.6482	0.0293	
	3.996e-005	0.6482	0.02929	
	1.549e-005	0.6482	0.02928	
	0	0.6482	0.02928	/
5735.8954	0.01377	0.6409	0.03172	
	0.01241	0.6406	0.03152	
	0.007515	0.6392	0.03083	
	0.004797	0.6385	0.03045	
	0.002846	0.6380	0.03019	
	0.001537	0.6376	0.03001	
	0.0007384	0.6374	0.0299	
	0.0004413	0.6373	0.02986	
	0.0003108	0.6373	0.02984	
	0.0001154	0.6372	0.02981	
	3.996e-005	0.6372	0.0298	
	1.549e-005	0.6372	0.0298	
	0	0.6372	0.0298	/
5762.2564	0.01401	0.6393	0.03185	
	0.01377	0.6393	0.0318	
	0.01241	0.6389	0.03161	
	0.007515	0.6375	0.03092	
	0.004797	0.6368	0.03054	
	0.002846	0.6362	0.03027	
	0.001537	0.6359	0.03009	
	0.0007384	0.6357	0.02998	
	0.0004413	0.6356	0.02994	
	0.0003108	0.6355	0.02993	
	0.0001154	0.6355	0.0299	
	3.996e-005	0.6355	0.02989	
	1.549e-005	0.6355	0.02989	
	0	0.6355	0.02988	/

5893.9085	0.01524	0.6316	0.03248	
	0.01401	0.6312	0.03229	
	0.01377	0.6312	0.03225	
	0.01241	0.6308	0.03206	
	0.007515	0.6292	0.03136	
	0.004797	0.6284	0.03098	
	0.002846	0.6278	0.0307	
	0.001537	0.6274	0.03052	
	0.0007384	0.6271	0.03041	
	0.0004413	0.6271	0.03037	
	0.0003108	0.6270	0.03035	
	0.0001154	0.6270	0.03033	
	3.996e-005	0.6269	0.03032	
	1.549e-005	0.6269	0.03031	
	0	0.6269	0.03031	/
6051.9216	0.01682	0.6231	0.03326	
	0.01524	0.6225	0.03301	
	0.01401	0.6221	0.03283	
	0.01377	0.6220	0.03279	
	0.01241	0.6215	0.03259	
	0.007515	0.6198	0.03188	
	0.004797	0.6189	0.03149	
	0.002846	0.6182	0.03122	
	0.001537	0.6178	0.03103	
	0.0007384	0.6175	0.03092	
	0.0004413	0.6174	0.03088	
	0.0003108	0.6174	0.03086	
	0.0001154	0.6173	0.03083	
	3.996e-005	0.6173	0.03082	
	1.549e-005	0.6172	0.03082	
	0	0.6172	0.03081	/
6209.9346	0.01853	0.6152	0.03406	
	0.01682	0.6145	0.03378	
	0.01524	0.6139	0.03354	
	0.01401	0.6135	0.03336	
	0.01377	0.6134	0.03332	
	0.01241	0.6129	0.03312	
	0.007515	0.6110	0.0324	
	0.004797	0.6100	0.032	
	0.002846	0.6092	0.03172	
	0.001537	0.6087	0.03153	
	0.0007384	0.6084	0.03142	
	0.0004413	0.6083	0.03138	
	0.0003108	0.6082	0.03136	
	0.0001154	0.6082	0.03133	
	3.996e-005	0.6081	0.03132	
	1.549e-005	0.6081	0.03132	
	0	0.6081	0.03131	/
6367.9477	0.02038	0.6080	0.03488	
	0.01853	0.6072	0.03457	
	0.01682	0.6065	0.03431	
	0.01524	0.6058	0.03407	
	0.01401	0.6053	0.03388	
	0.01377	0.6052	0.03385	

	0.01241	0.6047	0.03364	
	0.007515	0.6026	0.03291	
	0.004797	0.6015	0.03251	
	0.002846	0.6007	0.03222	
	0.001537	0.6002	0.03203	
	0.0007384	0.5998	0.03191	
	0.0004413	0.5997	0.03187	
	0.0003108	0.5996	0.03185	
	0.0001154	0.5996	0.03182	
	3.996e-005	0.5995	0.03181	
	1.549e-005	0.5995	0.03181	
	0	0.5995	0.03181	/
6525.9608	0.02238	0.6013	0.03573	
	0.02038	0.6005	0.03539	
	0.01853	0.5996	0.0351	
	0.01682	0.5989	0.03484	
	0.01524	0.5982	0.03459	
	0.01401	0.5976	0.0344	
	0.01377	0.5975	0.03437	
	0.01241	0.5969	0.03416	
	0.007515	0.5947	0.03342	
	0.004797	0.5935	0.03301	
	0.002846	0.5927	0.03272	
	0.001537	0.5921	0.03252	
	0.0007384	0.5917	0.0324	
	0.0004413	0.5916	0.03236	
	0.0003108	0.5915	0.03234	
	0.0001154	0.5914	0.03231	
	3.996e-005	0.5914	0.0323	
	1.549e-005	0.5914	0.0323	
	0	0.5914	0.0323	/
6683.9739	0.02454	0.5953	0.03662	
	0.02238	0.5943	0.03623	
	0.02038	0.5934	0.03592	
	0.01853	0.5925	0.03563	
	0.01682	0.5917	0.03536	
	0.01524	0.5909	0.03511	
	0.01401	0.5903	0.03492	
	0.01377	0.5902	0.03488	
	0.01241	0.5896	0.03467	
	0.007515	0.5873	0.03392	
	0.004797	0.5860	0.0335	
	0.002846	0.5850	0.03321	
	0.001537	0.5844	0.03301	
	0.0007384	0.5840	0.03289	
	0.0004413	0.5839	0.03285	
	0.0003108	0.5838	0.03283	
	0.0001154	0.5837	0.0328	
	3.996e-005	0.5837	0.03279	
	1.549e-005	0.5837	0.03278	
	0	0.5837	0.03278	/
6841.9869	0.02689	0.5899	0.03755	
	0.02454	0.5887	0.03711	
	0.02238	0.5876	0.03676	

	0.02038	0.5866	0.03644
	0.01853	0.5857	0.03615
	0.01682	0.5848	0.03587
	0.01524	0.5840	0.03562
	0.01401	0.5834	0.03543
	0.01377	0.5833	0.03539
	0.01241	0.5826	0.03518
	0.007515	0.5802	0.03441
	0.004797	0.5788	0.03399
	0.002846	0.5778	0.03369
	0.001537	0.5772	0.03349
	0.0007384	0.5768	0.03337
	0.0004413	0.5766	0.03333
	0.0003108	0.5765	0.03331
	0.0001154	0.5764	0.03328
	3.996e-005	0.5764	0.03326
	1.549e-005	0.5764	0.03326
	0	0.5764	0.03326 /
7005.2657	0.02953	0.5849	0.03855
	0.02689	0.5835	0.03805
	0.02454	0.5822	0.03766
	0.02238	0.5811	0.0373
	0.02038	0.5800	0.03698
	0.01853	0.5791	0.03668
	0.01682	0.5781	0.0364
	0.01524	0.5773	0.03615
	0.01401	0.5767	0.03595
	0.01377	0.5765	0.03591
	0.01241	0.5758	0.0357
	0.007515	0.5732	0.03492
	0.004797	0.5718	0.03449
	0.002846	0.5707	0.03419
	0.001537	0.5700	0.03399
	0.0007384	0.5696	0.03386
	0.0004413	0.5695	0.03382
	0.0003108	0.5694	0.0338
	0.0001154	0.5693	0.03377
	3.996e-005	0.5693	0.03376
	1.549e-005	0.5692	0.03375
	0	0.5692	0.03375 /

/

APPENDIX C

Table C: Oil production data of Haripur field

Date	Oil	Water	Gas	THP	Date	Oil	Water	Gas	THP
	BBL/D	BBL/D	MSCF/D	PSIG		BBL/D	BBL/D	MSCF/D	PSIG
12/1/1987	300.43	0.1	292.56	690	4/1/1991	263.78	4.84	313.37	395
1/1/1988	306.09	0.06	243.65	725	5/1/1991	242.86	1.53	296.75	415
2/1/1988	0	0	0	0	6/1/1991	167.39	3.41	138.83	240
3/1/1988	0	0	0	0	7/1/1991	232.36	4.76	282.29	445
4/1/1988	270.23	0.09	220.15	630	8/1/1991	257.98	0	429.36	425
5/1/1988	254.11	0.13	239.31	575	9/1/1991	248.48	8.67	376.7	415
6/1/1988	319.48	0.05	272.67	580	10/1/1991	308.96	6.57	363.45	390
7/1/1988	218.37	0.05	313.68	575	11/1/1991	195.07	4.79	330.23	300
8/1/1988	218.87	0.06	313.68	220	12/1/1991	178.99	6.41	303.74	290
9/1/1988	286.84	0.05	309.87	555	1/1/1992	178.46	7.81	287.84	300
10/1/1988	313.98	0.09	341.7	750	2/1/1992	214.86	11.53	349.31	330
11/1/1988	308.19	0.06	306.33	640	3/1/1992	196.59	15.89	279.23	275
12/1/1988	236.52	0.04	313.73	590	4/1/1992	225.05	14.53	267.2	275
1/1/1989	0	0	0	0	5/1/1992	181.42	14.32	247.65	270
2/1/1989	0	0	0	0	6/1/1992	172.47	15.23	241.77	260
3/1/1989	0	0	0	0	7/1/1992	163.05	15.84	214.58	250
4/1/1989	157.07	0.12	92	350	8/1/1992	270.2	15.73	238	240
5/1/1989	380.31	0.28	283.04	590	9/1/1992	203.29	21.72	261.67	240
6/1/1989	383.92	0.07	563.73	380	10/1/1992	136.82	15.41	243.03	220
7/1/1989	368.38	0.58	629.55	580	11/1/1992	171.27	14.8	242.83	215
8/1/1989	363.11	0.25	533.23	595	12/1/1992	137.89	15.37	244.26	220
9/1/1989	359.41	0.28	556.33	575	1/1/1993	140.18	17.33	235.94	240
10/1/1989	346.66	0.14	529.03	515	2/1/1993	169.1	18.01	224.35	240
11/1/1989	264.19	0.1	432.33	685	3/1/1993	147.26	24.84	250.52	240
12/1/1989	305.34	0.15	548.19	595	4/1/1993	135.57	19.32	234.73	250
1/1/1990	356.34	0.1	563.55	540	5/1/1993	137.89	18.67	211.61	240
2/1/1990	344.98	0.13	482.71	565	6/1/1993	151.51	18.54	202.27	215
3/1/1990	405.48	0.17	408.97	520	7/1/1993	134.48	17.6	190.26	230
4/1/1990	319.4	0.17	374.57	485	8/1/1993	126.11	17.6	181.61	230
5/1/1990	312.12	0.16	341.69	545	9/1/1993	119.91	17.6	172.2	230
6/1/1990	348.5	0.25	498.83	495	10/1/1993	124.52	17.15	172.97	225
7/1/1990	336.42	0.3	477.74	500	11/1/1993	118.15	17.32	177.03	230
8/1/1990	334.08	0.67	465.36	500	12/1/1993	110.59	20.23	175.42	215
9/1/1990	317.27	1.11	429.17	500	1/1/1994	97.27	19.44	166.74	200
10/1/1990	301.63	1.52	385.3	465	2/1/1994	102.23	0	159.64	200
11/1/1990	393	2	381.93	465	3/1/1994	95.68	20.21	164.9	200
12/1/1990	313.23	3.45	363.68	465	4/1/1994	96.08	0.75	162.53	215
1/1/1991	299.21	4.16	367.29	455	5/1/1994	104.2	21.11	234.19	215
2/1/1991	284.99	4.5	365.89	430	6/1/1994	83.82	17.91	154.87	115
3/1/1991	272.98	5.07	342.87	415	7/1/1994	9.11	2.59	94.79	62

APPENDIX D

Table D: Oil reserve calculation in Haripur field

Bhubon Formation Oil Zone	Bulk volume[*10^6 ft3]	Net volume[*10^6 ft3]	Pore volume[*10^6 RB]	HCPV oil[*10^6 RB]	STOIIP (in oil)[*10^6 STB]	STOIIP[*10^6 STB]	GIIP (in oil)[*10^6 MSCF]
Zone 69	1066	1066	31	13	10	10	5
Zone 70	995	995	24	11	9	9	4
Zone 71	920	920	23	8	6	6	3
Zone 72	847	847	23	5	4	4	2
Zone 73	776	776	17	4	3	3	1
Zone 74	707	707	15	2	1	1	1
Total (Zone 69-74)	5311	5311	133	43	33	33	16

APPENDIX E

Table E1: Break even analysis (Haripur oil field)

Year	Oil Production, STB (800 STB/D)	Revenue, USD	Variable Cost, USD	Total Cost, USD	Revenue-Cost, USD
2026	0	0	0	9.00E+07	-9.00E+07
2027	292000	14600000	657000	9.07E+07	-7.61E+07
2028	584000	29200000	1314000	9.13E+07	-6.21E+07
2029	876000	43800000	1971000	9.20E+07	-4.82E+07
2030	1168000	58400000	2628000	9.26E+07	-3.42E+07
2031	1460000	73000000	3285000	9.33E+07	-2.03E+07
2032	1752000	87600000	3942000	9.39E+07	-6.34E+06
2033	2044000	102200000	4599000	9.46E+07	7.60E+06
2034	2336000	116800000	5256000	9.53E+07	2.15E+07
2035	2628000	131400000	5913000	9.59E+07	3.55E+07
2036	2920000	146000000	6570000	9.66E+07	4.94E+07
2037	3212000	160600000	7227000	9.72E+07	6.34E+07
2038	3504000	175200000	7884000	9.79E+07	7.73E+07
2039	3796000	189800000	8541000	9.85E+07	9.13E+07
2040	4088000	204400000	9198000	9.92E+07	1.05E+08
2041	4380000	219000000	9855000	9.99E+07	1.19E+08
2042	4672000	233600000	10512000	1.01E+08	1.33E+08
2043	4964000	248200000	11169000	1.01E+08	1.47E+08
2044	5256000	262800000	11826000	1.02E+08	1.61E+08
2045	5548000	277400000	12483000	1.02E+08	1.75E+08
2046	5840000	292000000	13140000	1.03E+08	1.89E+08
2047	6132000	306600000	13797000	1.04E+08	2.03E+08

Table E2: Financial analysis (Haripur oil field)

Year	2022	2023	2024	2025	2026
k	0	1	2	3	4
Discount Rate, i%	10	10	10	10	10
Discount Factor	1	1.1	1.21	1.331	1.4641
Capital Expenditure	-2.00E+07	-2.00E+07	-2.00E+07	-2.00E+07	-1.00E+07
Sale Revenue	0	0	0	0	0
Operating Cost	0	0	0	0	0
Net Cash Flow, NCF	-2.00E+07	-2.00E+07	-2.00E+07	-2.00E+07	-1.00E+07
Discounted NCF	-2.00E+07	-1.82E+07	-1.65E+07	-1.50E+07	-6.83E+06

Table E2: Financial analysis (Cont.) (Haripur oil field)

Year	2027	2028	2029	2030	2031
k	5	6	7	8	9
Discount Rate, i%	10	10	10	10	10
Discount Factor	1.61051	1.771561	1.9487171	2.14358881	2.357947691
Capital Expenditure	0	0	0	0	0
Sale Revenue	1.46E+07	1.46E+07	1.46E+07	1.46E+07	1.46E+07
Operating Cost	-6.57E+05	-6.57E+05	-6.57E+05	-6.57E+05	-6.57E+05
Net Cash Flow, NCF	1.39E+07	1.39E+07	1.39E+07	1.39E+07	1.39E+07
Discounted NCF	8.66E+06	7.87E+06	7.15E+06	6.50E+06	5.91E+06

Table E2: Financial analysis (Cont.) (Haripur oil field)

Year	2032	2033	2034	2035	2036
k	10	11	12	13	14
Discount Rate, i%	10	10	10	10	10
Discount Factor	2.59374246	2.853116706	3.138428377	3.452271214	3.797498336
Capital Expenditure	0	0	0	0	0
Sale Revenue	1.46E+07	1.46E+07	1.46E+07	1.46E+07	1.46E+07
Operating Cost	-6.57E+05	-6.57E+05	-6.57E+05	-6.57E+05	-6.57E+05
Net Cash Flow, NCF	1.39E+07	1.39E+07	1.39E+07	1.39E+07	1.39E+07
Discounted NCF	5.38E+06	4.89E+06	4.44E+06	4.04E+06	3.67E+06

Table E2: Financial analysis (Cont.) (Haripur oil field)

Year	2037	2038	2039	2040	2041
k	15	16	17	18	19
Discount Rate, i%	10	10	10	10	10
Discount Factor	4.177248169	4.594972986	5.054470285	5.559917313	6.115909045
Capital Expenditure	0	0	0	0	0
Sale Revenue	1.46E+07	1.46E+07	1.46E+07	1.46E+07	1.46E+07
Operating Cost	-6.57E+05	-6.57E+05	-6.57E+05	-6.57E+05	-6.57E+05
Net Cash Flow, NCF	1.39E+07	1.39E+07	1.39E+07	1.39E+07	1.39E+07
Discounted NCF	3.34E+06	3.03E+06	2.76E+06	2.51E+06	2.28E+06

Table E2: Financial analysis (Cont.) (Haripur oil field)

Year	2042	2043	2044	2045	2046	2047
k	20	21	22	23	24	25
Discount Rate, i%	10	10	10	10	10	10
Discount Factor	6.7274999 49	7.4002499 44	8.1402749 39	8.9543024 33	9.8497326 76	10.834705 94
Capital Expenditure	0	0	0	0	0	0
Sale Revenue	1.46E+07	1.46E+07	1.46E+07	1.46E+07	1.46E+07	1.46E+07
Operating Cost	-6.57E+05	-6.57E+05	-6.57E+05	-6.57E+05	-6.57E+05	-6.57E+05
Net Cash Flow, NCF	1.39E+07	1.39E+07	1.39E+07	1.39E+07	1.39E+07	1.39E+07
Discounted NCF	2.07E+06	1.88E+06	1.71E+06	1.56E+06	1.42E+06	1.29E+06

Table E3: Break even analysis (Kailashtila oil field)

Year	Cumulative Oil Production, STB (800 STB/D)	Revenue, USD	Variable Cost, USD	Total Cost, USD	Revenue-Cost, USD
2024	0	0	0	3.00E+07	-3.00E+07
2025	292000	14600000	0	3.00E+07	-1.54E+07
2026	584000	29200000	0	3.00E+07	-8.00E+05
2027	876000	43800000	0	3.00E+07	1.38E+07
2028	1168000	58400000	0	3.00E+07	2.84E+07
2029	1460000	73000000	0	3.00E+07	4.30E+07
2030	1752000	87600000	0	3.00E+07	5.76E+07
2031	2044000	102200000	0	3.00E+07	7.22E+07
2032	2336000	116800000	0	3.00E+07	8.68E+07
2033	2628000	131400000	0	3.00E+07	1.01E+08
2034	2920000	146000000	0	3.00E+07	1.16E+08
2035	3212000	160600000	0	3.00E+07	1.31E+08
2036	3504000	175200000	0	3.00E+07	1.45E+08
2037	3796000	189800000	0	3.00E+07	1.60E+08
2038	4088000	204400000	0	3.00E+07	1.74E+08
2039	4380000	219000000	0	3.00E+07	1.89E+08
2040	4672000	233600000	0	3.00E+07	2.04E+08
2041	4964000	248200000	0	3.00E+07	2.18E+08
2042	5256000	262800000	0	3.00E+07	2.33E+08
2043	5548000	277400000	0	3.00E+07	2.47E+08
2044	5840000	292000000	0	3.00E+07	2.62E+08
2045	6132000	306600000	0	3.00E+07	2.77E+08

Table E4: Financial analysis (Kailashtila oil field)

Year	2022	2023	2024	2025	2026
k	0	1	2	3	4
Discount Rate, i%	10	10	10	10	10
Discount Factor	1	1.1	1.21	1.331	1.4641
Capital Expenditure	-1.00E+07	-1.00E+07	-1.00E+07	0	0
Sale Revenue	0	0	0	1.46E+07	1.46E+07
Operating Cost	0	0	0	0	0
Net Cash Flow, NCF	-1.00E+07	-1.00E+07	-1.00E+07	1.46E+07	1.46E+07
Discounted NCF	-1.00E+07	-9.09E+06	-8.26E+06	1.10E+07	9.97E+06

Table E4: Financial analysis (Cont.) (Kailashtila oil field)

Year	2027	2028	2029	2030	2031
k	5	6	7	8	9
Discount Rate, i%	10	10	10	10	10
Discount Factor	1.61051	1.771561	1.948717	2.143589	2.357948
Capital Expenditure	0	0	0	0	0
Sale Revenue	1.46E+07	1.46E+07	1.46E+07	1.46E+07	1.46E+07
Operating Cost	0.00E+00	0.00E+00	0.00E+00	0.00E+00	0.00E+00
Net Cash Flow, NCF	1.46E+07	1.46E+07	1.46E+07	1.46E+07	1.46E+07
Discounted NCF	9.07E+06	8.24E+06	7.49E+06	6.81E+06	6.19E+06

Table E4: Financial analysis (Cont.) (Kailashtila oil field)

Year	2032	2033	2034	2035	2036
k	10	11	12	13	14
Discount Rate, i%	10	10	10	10	10
Discount Factor	2.593742	2.853117	3.138428	3.452271	3.797498
Capital Expenditure	0	0	0	0	0
Sale Revenue	1.46E+07	1.46E+07	1.46E+07	1.46E+07	1.46E+07
Operating Cost	0.00E+00	0.00E+00	0.00E+00	0.00E+00	0.00E+00
Net Cash Flow, NCF	1.46E+07	1.46E+07	1.46E+07	1.46E+07	1.46E+07
Discounted NCF	5.63E+06	5.12E+06	4.65E+06	4.23E+06	3.84E+06

Table E4: Financial analysis (Cont.) (Kailashtila oil field)

Year	2037	2038	2039	2040	2041
k	15	16	17	18	19
Discount Rate, i%	10	10	10	10	10
Discount Factor	4.177248	4.594973	5.05447	5.5599173	6.115909
Capital Expenditure	0	0	0	0	0
Sale Revenue	1.46E+07	1.46E+07	1.46E+07	1.46E+07	1.46E+07
Operating Cost	0.00E+00	0.00E+00	0.00E+00	0.00E+00	0.00E+00
Net Cash Flow, NCF	1.46E+07	1.46E+07	1.46E+07	1.46E+07	1.46E+07
Discounted NCF	3.50E+06	3.18E+06	2.89E+06	2.63E+06	2.39E+06

Table E4: Financial analysis (Cont.) (Kailashtila oil field)

Year	2042	2043	2044	2045
k	20	21	22	23
Discount Rate, i%	10	10	10	10
Discount Factor	6.727499949	7.400249944	8.140274939	8.954302433
Capital Expenditure	0	0	0	0
Sale Revenue	1.46E+07	1.46E+07	1.46E+07	1.46E+07
Operating Cost	0.00E+00	0.00E+00	0.00E+00	0.00E+00
Net Cash Flow, NCF	1.46E+07	1.46E+07	1.46E+07	1.46E+07
Discounted NCF	2.17E+06	1.97E+06	1.79E+06	1.63E+06

APPENDIX F

Two Phase Flash Calculation Algorithm

Followings steps are performed sequentially using oil composition and pure components propertied.

1. Calculate Reduce Pressure (Pri)
2. Calculate Reduce Temperature (Tri)
3. Calculate Equilibrium Constant ki by Wilson equation.
4. Calculate Vapor and liquid fraction (V,L)
5. Calculate Vapor and liquid Composition (xi,yi)
6. Calculate Z- Factor for vapor and liquid from EOS (ZV,ZL)
7. Calculate Components fugacities for vapor and liquid from EOS (fiL,fiV)
8. Check the equal fugacity constraints.
9. If convergence is not reached then update Equilibrium Constant ki.
10. Repeat the whole procedure from step (4) with updated ki.

Calculation Basis: 1 lbmole oil sample

Standard Condition: P=14.7 psia, T=60 oF.

Gas Constant R=10.73 (psia.ft3/lbm-mol.oR)

CF: 1 lbm/ft3=16.01x10-3 gm/cm3

1) Reduce Pressure, $P_{ri}= \dfrac{P}{P_{ci}}$

2) Reduce Temperature $T_{ri}=\dfrac{T}{T_{ci}}$

3) Estimate k_i values from Wilson Equation

$$k_i = \frac{\exp\left[5.37(1+\omega_i)(1-{}^{1}\!/\!_{T_{ri}})\right]}{P_{ri}}$$

4) Material Balance to estimate V,L,x_i,y_i

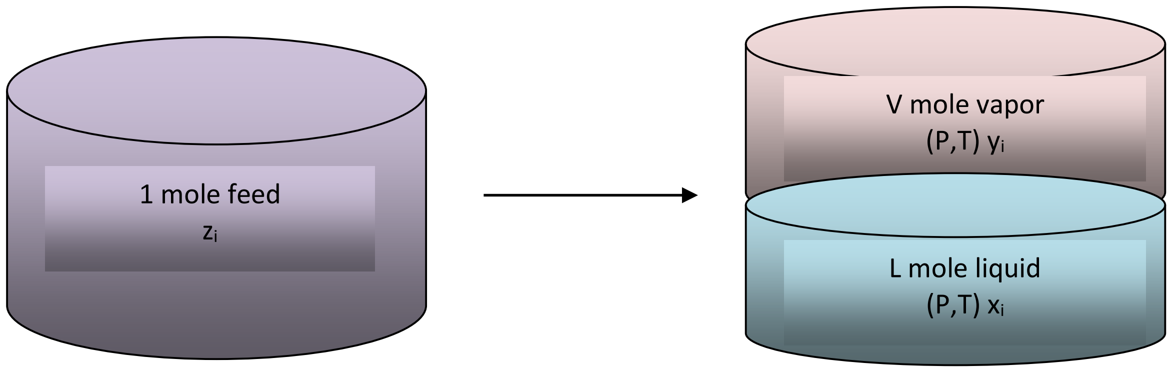

Figure F-1: Separation process

Basis 1 mole feed

z_i= component mole fraction in feed.

V=Vapor mole fraction

L= Liquid mole fraction

y_i= component mole fraction in vapor

x_i= component mole fraction in liquid

L+V=1 or L=1-V

$Lx_i+Vy_i=z_i$

$\sum x_i+\sum y_i=\sum z_i=1$

Equilibrium Constant, $k_i=y_i/x_i$ or $yi=k_ix_i$

$Lx_i+Vy_i=z_i$

$(1-V)x_i+Vk_ix_i=z_i$

$$x_i = \frac{z_i}{[V(k_i-1)+1]}$$

$$y_i = k_i x_i = \frac{k_i z_i}{[V(k_i-1)+1]}$$

Rachford-Rice equation

$$\sum_{i=1}^{n} (y_i - x_i) = 0$$

$$\sum_{i=1}^{n} \frac{z_i(k_i - 1)}{[V(k_i - 1) + 1]} = 0$$ (z_i,k_i known and unknown V)

$$f(V) = 0$$

$$f'(V) = -\sum_{i=1}^{n} \frac{z_i(k_i - 1)^2}{[V(k_i - 1) + 1]^2} = 0$$

Newton-Raphson Algorithms to solve for V

$$V_{n+1} = V_n - \frac{f(V_n)}{f'(V_n)}$$

Initial value of V is 0.5 and convergence criterion is $\left|\frac{V_{n+1} - V_n}{V_{n+1}}\right| \leq 1x10^{-6}$

5) Calculate vapor and liquid composition, x_i,y_i

L=1-V

$$x_i = \frac{z_i}{[V(k_i - 1) + 1]}$$

$$y_i = k_i x_i$$

6) Z- Factor for vapor and liquid from EOS (Z_V,Z_L)

<u>EOS Constants :</u> Ω_{Ao}, Ω_{Bo}

$$\Omega_{Ao} = 0.457235529$$

$$\Omega_{Bo} = 0.077796074$$

<u>EOS Variables set 1(F(Tri,Ωi)):</u> Ω_{Ai}, Ω_{Bi}

$$\Omega_{Ai} = \Omega_{Ao}\left[1 + (0.37464 + 1.54226\omega_i - 0.2669\omega_i^2)(1 - T_{ri}^{0.5})\right]^2$$

$$\Omega_{Bi} = \Omega_{Bo}$$

<u>EOS Variables set2(F(Pri,Tri)):</u> A_i, B_i

$$A_i = \Omega_{Ai} \frac{P_{ri}}{T_{ri}^2},$$

$$B_i = \Omega_{Bi} \frac{P_{ri}}{T_{ri}}$$

EOS Variables set3 for Liquid(F(x_i,$k_{i,j}$)): S_{iL} A_L, B_L

$$S_{iL} = \sum_{j=1}^{n} x_j (1-k_{i,j})\sqrt{A_i A_j}$$

$$A_L = \sum_{i=1}^{n} \sum_{j=1}^{n} x_i x_j (1-k_{i,j})\sqrt{A_i A_j}$$

$$B_L = \sum_{i=1}^{n} x_i B_i$$

Where $k_{i,j}$ are binary interaction coefficients

EOS Variables set4 for Vapor (F(y_i,$K_{i,j}$)): S_{iV} A_V, B_V

$$S_{iV} = \sum_{j=1}^{n} y_j (1-k_{i,j})\sqrt{A_i A_j}$$

$$A_V = \sum_{i=1}^{n} \sum_{j=1}^{n} y_i y_j (1-k_{i,j})\sqrt{A_i A_j}$$

$$B_V = \sum_{i=1}^{n} y_i B_i$$

EOS Coefficients set1

$$m_1 = 1+\sqrt{2}$$
$$m_2 = 1-\sqrt{2}$$

EOS Coefficients set2 for Liquid

$$E_{oL} = -\left[A_L B_L + m_1 m_2 B_L^2 (B_L + 1)\right]$$
$$E_{1L} = A_L - (2(m_1 + m_2) - 1)B_L^2 - (m_1 + m_2)B_L$$
$$E_{2L} = (m_1 + m_2 - 1)B_L - 1$$

EOS Coefficients set3 for Vapor

$$E_{oV} = -\left[A_V B_V + m_1 m_2 B_V^2 (B_V + 1)\right]$$
$$E_{1V} = A_V - (2(m_1 + m_2) - 1)B_V^2 - (m_1 + m_2)B_V$$
$$E_{2V} = (m_1 + m_2 - 1)B_V - 1$$

<u>Cubic Equation for Liquid</u>

$$Z_L^3 + E_{2L} Z_L^2 + E_{1L} Z_L + E_{oL} = 0$$
$$F(Z_L) = Z_L^3 + E_{2L} Z_L^2 + E_{1L} Z_L + E_{oL} = 0$$
$$F'(Z_L) = 3Z_L^2 + 2E_{2L} Z_L + E_{1L}$$

Newton-Raphson Algorithms to solve for Z_L

$$Z_{L\,n+1} = Z_{L\,n} - \frac{F(Z_{L\,n})}{F'(Z_{L\,n})}$$

Initial value of Z_L is 0.1 and convergence criterion is $\left|\dfrac{Z_{L\,n+1} - Z_{L\,n}}{Z_{L\,n+1}}\right| \leq 1x10^{-6}$

The Equation of State

$PV_L = Z_L n_L RT$

<u>Cubic Equation (Vapor)</u>

$$Z_V^3 + E_{2V} Z_V^2 + E_{1V} Z_V + E_{oV} = 0$$
$$F(Z_V) = Z_V^3 + E_{2V} Z_V^2 + E_{1V} Z_V + E_{oV} = 0$$
$$F'(Z_V) = 3Z_V^2 + 2E_{2V} Z_V + E_{1V}$$

Newton-Raphson Algorithms to solve for Z_V

$$Z_{V\,n+1} = Z_{V\,n} - \frac{F(Z_{V\,n})}{F'(Z_{V\,n})}$$

Initial value of Z_V is 0.5 and convergence criterion is $\left|\dfrac{Z_{V\,n+1} - Z_{V\,n}}{Z_{V\,n+1}}\right| \leq 1x10^{-6}$

The Equation of State

$PV_V = Z_V n_V RT$

7) Fugacity (fi_V,fi_L)

Fugacity Coefficients for Liquid

$$\ln\left(\frac{f_{iL}}{Px_i}\right) = -\ln(Z_L - B_L) + \frac{A_L}{(m_1 - m_2)B_L}\left[\frac{2S_{iL}}{A_L} - \frac{B_i}{B_L}\right]\ln\left[\frac{Z_L + m_2 B_L}{Z_L + m_1 B_L}\right] + \frac{B_i}{B_L}(Z_L - 1) = \Theta_L$$

$$f_{iL} = Px_i \exp(\Theta_L)$$

Fugacity Coefficients for Vapor

$$\ln\left(\frac{f_{iV}}{Py_i}\right) = -\ln(Z_V - B_V) + \frac{A_V}{(m_1 - m_2)B_V}\left[\frac{2S_{iV}}{A_V} - \frac{B_i}{B_V}\right]\ln\left[\frac{Z_V + m_2 B_V}{Z_V + m_1 B_V}\right] + \frac{B_i}{B_V}(Z_V - 1) = \Theta_V$$

$$f_{iV} = Py_i \exp(\Theta_V)$$

8) Fugacity Constraint, FC and convergence criterion is 1×10^{-13}

$$FC = \sum_{i=1}^{n}\left(\frac{f_{iL}}{f_{iV}} - 1\right)^2 < 1x10^{-13}$$

9) If converge is reached then stop or if converge is not reach then update k_i

$$k_i^{n+1} = k_i^n \frac{f_{iL}^n}{f_{iV}^n}$$

10) Repeat the whole procedure from Material Balance (4), use updated value of V and ki.